LUMINESCENCE DATING OF SCOTTISH BURNT MOUNDS:

NEW INVESTIGATIONS IN ORKNEY AND SHETLAND

IONA MARY CAMPBELL ANTHONY

SCOTTISH UNIVERSITIES RESEARCH AND REACTOR CENTRE

Presented as a thesis for the degree of Doctor of Philosophy in the University of Glasgow

September 2003

For George and Helen

Abstract

This thesis presents new research on the luminescence dating of burnt mounds in the Orkney and Shetland Islands. Through an examination of available evidence for Scottish burnt mounds, a number of key problematic areas have been identified in relation to our understanding of these sites and their place within the archaeological record. Previous chronological investigations of burnt mounds have so far provided little information on the likely duration of individual sites. Site formation processes are likewise poorly understood.

Luminescence dating has been outlined as a method suited to determining the age of both excavated and unexcavated sites, and to tackling issues of site formation. A combination of stratigraphic and surface sampling at sites on the island of Eday, Orkney, and at coastally eroding sites across Shetland has provided suitable material for study. In addition, detailed sampling during excavation of Cruester burnt mound, on Bressay, Shetland has enabled the collection of a series of samples directly linked with the formation of the mound and structures at the site. Fieldwork is reported together with detailed characterization of the external and internal dose rates of samples collected.

Additive dose thermoluminescence dating techniques have been applied to extracted feldspar grains. A procedure for correcting temperature-shifts due to thermal contact variation has been developed and implemented, leading to improvements in data processing. Problems have been identified relating to unequal sensitization at different stages of equal-predose additive dose run which cause normalization errors leading to incorrect dose estimates. Whilst the underlying physical origins of such changes are not yet firmly understood, a correction method based on modeling of the sensitization behaviour has been applied. When both sets of corrections are applied satisfactory plateau responses are obtained , and data from controlled experiments are consistent with external controls.

Quartz single aliquot regenerative procedures for optically stimulated luminescence dating, normally applied to unheated material, have also been investigated. Controlled laboratory experiments have confirmed that known laboratory doses can be recovered. Sample sensitivity, sensitivity changes and dependence of results on preheating temperatures have

been studied and all appear to be satisfactory. A surprisingly broad distribution in the estimated stored dose of a number of samples has been noted, which may imply microdosimetric heterogeneity in some cases. Evidence has been presented from hearthstone results which suggests that the OSL signals comprise a complex mixture of components with varying thermal stability. This finding is consistent with recent fundamental studies of quartz OSL behaviour, but to some extent contradicts the conventional description of OSL being primarily associated with a single TL trap at 325°C. Methods employed in the identification of incomplete zeroing of the optical signal in unheated sediments were also investigated. Correlation between samples identified as poorly zeroed through this method, and through analysis of the temperature dependence of the dose estimate in feldspar TL work, indicated the technique to be applicable to heated material in this case.

Results from feldspar and quartz investigations, together with available ^{14}C data suggest evidence on Eday for both age distribution within individual monuments, and also a geographical and chronological progression of formation and utilization of burnt mounds on the island. At the site of Cruester, Shetland, consistency between all three sources of chronological information is seen, allowing for detailed interpretation of the archaeological evidence, and definition of the four chronological phases of the site identified during excavation. Whilst this work has illustrated the additional information that may be obtained through combined excavation and sampling strategies, results from vertical sections elsewhere on Shetland are also promising.

It has been established that luminescence approaches coupled to appropriate sampling strategies can provide important information with regards to the formation of individual sites, their relationships to each other and to other monuments within their cultural landscape. Given the presence of more than 1900 burnt mounds in Scotland, many of which are currently threatened by coastal erosion and other destructive processes, this provides a way forward to studying the broader national and regional distributions of sites.

Acknowledgements

This research was funded by an EPSRC studentship and by Historic Scotland. Thanks also go to SURRC, LED2002 and the Department of Archaeology, University of Glasgow for their contributions towards attending conferences.

I would like to thank my supervisors, Dr David Sanderson, Dr Rupert Housley and Dr Gordon Cook for their continued support and advise throughout my post-graduate studies. Also members past and present of the Physics Group, SURRC, East Kilbride. Dr Lorna Carmichael, Dr Alan Cresswell, Dr David Smith, Dr Anne Sommerville, Simon Murphy, Colin Kerr and Joyce Lang contributed a great deal in terms of technical advice, support and biscuits.

Thanks are also due to the following people in other institutions and organizations who gave invaluable assistance and advise during laboratory and fieldwork. Drs Martin Lee, Alan Hall and John Gillece, University of Glasgow for their help with mineral preparation and analysis. Everyone at the Radiocarbon Laboratory, SURRC for their help and advice with samples. Hazel Moore and Graeme Wilson have provided invaluable help, advice and moral support with regards to burnt mounds in Orkney and Shetland. Jane Downes, Julie Gibson, Judith Robertson, Mary Harris and Val Turner also contributed much time and effort whilst sampling in Orkney and Shetland and Olly Davis gave up much of his time in order to help edit and proof read earlier versions of this thesis.

Thanks also go to the staff of Historic Scotland for their prompt and helpful responses to requests for permission to sample scheduled burnt mound sites and to the staff at the RCAHMS who facilitated a database survey of burnt mounds within their catalogues. Special thanks to Dr Rod McCullagh of Historic Scotland for his continued help and advise throughout the project.

A final thanks goes to my family and friends. To my parents, brother, grandparents and Auntie Mattie for their lifelong encouragement of my education and interests. Without their continued support this work would not have been possible. And to Graeme, Ann, Stephanie and Danny Forsyth, who have put up with me over the four years of this research - sorry about the mess.

Glossary of Abreviations and Luminescence Terminology

Types of Luminescence measurements

TL	Thermoluminescence – stimulation by heat
PSL/OSL	Photo/Optically-Stimulated Luminescence, of which there are many forms
	Blue OSL – Blue light Stimulated Luminescence
	GSL - Green light Stimulated Luminescence
	IRSL Infra-red Stimulated Luminescence (A form of OSL)
LM-OSL	Linearly Modulated Optically Stimulated Luminescence

Common luminescence abbreviations

SAR	Single Aliquot Regenerative procedure
SAAD	Single Aliquot Additive Dose procedure
MAAD	Multiple Aliquot Additive Dose procedure
ED/ D_e	Equivalent Dose (usually used in OSL dating to denote the measured stored dose)

Common terminology for TL MAAD measurements

First glow	Measurement of natural + beta signal
Second glow	Measurement of beta signal administered after first glow
Third glow	Measurement of beta normalisation signal administered after second glow
Fourth glow	Measurement of Fading rate
ED	Equivalent Dose
I	Intercept measurement related to supralinearity of growth curve
P	Palaeodose (usually used in TL dating to denote the measured stored dose P=ED+I)

Common terminology for OSL SAR measurements

Test Dose	Small dose administered after each dose point, used to correct data for sensitivity changes between readout cycles
Recycling Ratio	Comparison of two repeated dose points, usually at the beginning and end of a SAR run, used to express effectiveness of the test dose correction

Units

a	year
ka	1000 years
Gy	Used to express stored dose
$mGya^{-1}$	Used to express annual dose rate

CONTENTS

LIST OF FIGURES

Chapter 6 – Optically Stimulated Luminescence Investigations

Chapter 7 – Discussion of Results

LIST OF TABLES

CHAPTER 1 INTRODUCTION

1.1 Background

British burnt mounds, Irish fulachta fiadh, Swedish skärvstenshögar and many other local names describe heaps of fire cracked stones that are found across much of north-western Europe (fig 1.1). Often found associated with hearths and water troughs, they have traditionally been interpreted in terms of cooking sites from the Bronze Age period (~2500-650BC) where hot stones would be used to heat water for cooking. Once cooking was complete, the trough would be cleaned out and the stones removed. With continued use, the resulting debris pile of used stones would form a mound.

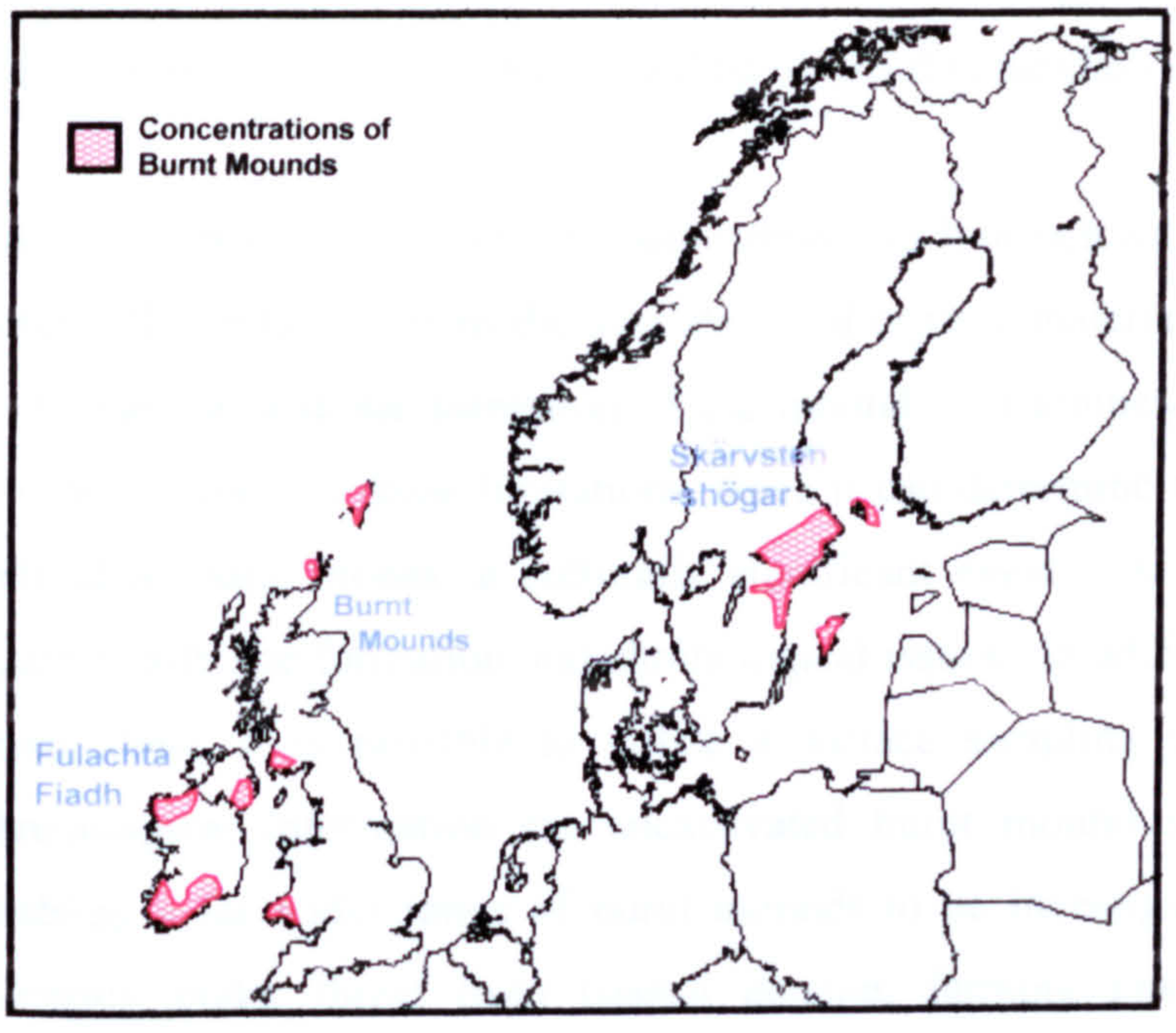

Fig 1.1 Distribution of Burnt Mounds in North-Western Europe (After Larsson, 1989)

Within Scotland, over 1900 burnt mound sites are listed in the National Monument Records (NMR). However, they have suffered from an underestimation in the amount of information they may contain about the past. There has been a tendency for many years to concentrate on mapping their extent (Barber and Russell-White, 1990). Such efforts are of limited usefulness as attempts to analyse distribution patterns assume continuity in both the period of use and function of burnt mounds (e.g. Canter, 1998). Over recent years a growing body of evidence has suggested contradictions in both such assumptions.

Other functional hypotheses have been proposed, ranging from prehistoric saunas (Barfield and Hodder, 1987) to sites for the production of textiles (Jeffrey, 1991). Examination of available dating evidence indicates that burnt mounds were in use over a far wider chronological period than the Bronze Age alone, with examples existing from the Neolithic through to Medieval times (Anthony et al, 2001). Whilst these provide important chronological indicators, the construction of detailed local, regional and national patterns is hampered by the limited number of sites for which chronological information is available and by the unknown variable of duration of use of sites.

Many questions still remain as to function and chronology. Detailed and widespread excavation may be required to fully understand functional aspects of these sites, however additional information on the formation and chronology of individual burnt mound sites may contribute to a wider understanding of this diverse class of monuments.

Sites have been dated both by radiocarbon and luminescence methods, the former being potentially limited by both the availability of organic material and the association between such material and the formation of the mound. Luminescence dating has potential to overcome some of these limitations, since it can determine the age of the last heating of individual burnt stones, a culturally significant event. As such it may be possible to address both site formation and chronological issues. In addition, due to the abundance of burnt stone, it is possible to utilize a surface sampling strategy in order to provide chronological information for unexcavated burnt mound sites (Huxtable et al, 1976) enabling a far wider range of burnt mounds to be investigated. As many mounds are currently under threat from coastal erosion, farming practices and other potentially destructive processes this may prove to be a useful investigative tool for future management plans.

Previous luminescence studies of burnt mounds include early work in Orkney (Huxtable et al, 1976), work in Scandinavia (eg Mejdahl, 1983), studies at the Scottish Universites Research and Reactor Centre (SURRC) of Shelly Knowe, in Sanday (discussed by Hunter & Dockrill, 1990), mounds near Crawford in Lanarkshire (discussed by Spencer, 1996) and in the Kilmartin Valley (Anthony et al , 2001). Whilst these were successful, questions remain as to the most appropriate sampling techniques to use, and whether the

archaeological questions associated with individual mounds, or groups of mounds, can be resolved with the precision available from current techniques.

1.2 Research Aims and Objectives

The aims of this research are twofold. Broadly, to provide an assessment of the chronological information that may be obtained through luminescence investigations of Scottish burnt stone mounds. Specifically, to provide opportunities for comparing age variation within individual sites, with age variation within a group of monuments. By detailed sampling and recording it is hoped that such information may lead to a wider understanding of this group of monuments.

In addition to archaeological outputs, it is hoped that this study will provide important information with regards to luminescence dating of heated stone, both in terms of sampling strategies and luminescence measurements. A key element of this work is to expand on previous work relating to optically stimulated luminescence (OSL) dating of heated stone. Whilst previous studies have compared different optical measurement readouts (Murray and Mejdahl, 1999), it is hoped that a comparison of optical and thermal techniques may further enhance understanding of the luminescence properties of heated stone.

Key objectives of the work include:

- A review of luminescence dating literature in order to formulate an appropriate sampling strategy, and establish the most suitable methods for collection and dating of heated stone samples.

- A summary of current information on the burnt mounds of Scotland allowing for detailed analysis of regional variation within the national group of mounds.

- Identification of suitable areas for sampling. Specifically, geographically linked sites that have the potential to facilitate detailed chronological investigation of age variation both within and between sites. In addition, sampling of more dispersed

sites with varied regional geology to provide the opportunity to study variability in luminescence behaviour.

- Reporting of fieldwork, including location of sampling positions, measurement of background gamma dose rates and comments on the state of preservation of sites visited.

- Detailed assessment of the annual dose rate of samples collected, including external and internal components of the annual dose.

- A comparative study of thermoluminescence (TL) and OSL dating methods addressing issues of sensitization and stability of the luminescence signal, zeroing of the geological signal and continuity between the two datasets.

- An archaeological assessment of the information obtained from luminescence studies, including discussion of evidence for the duration of use of burnt mounds sampled and the construction of local chronological patterns of burnt mound use.

1.3 Thesis Outline

In terms of the structure of this study, a summary of the main principles of luminescence dating is given in chapter 2, covering such aspects as environmental background dosimetry and various methods for determining the stored dose in minerals. Potential problems that may be encountered are also highlighted. Based on a review of current methodologies and past applications of the technique to burnt stones, a luminescence strategy for dealing with samples is formulated.

Building on the review of information on Scottish burnt mounds, chapter 3 highlights potential study areas within the national group of mounds, focusing on Orkney and Shetland clusters as suitable candidates for further investigation. Both regions are discussed in greater detail and sites within these clusters identified for sampling within the research framework.

Chapter 4 documents sampling at each site, together with detailed background dosimetry readings and notes on the state of preservation of each site. Material obtained during fieldwork is described and samples selected for further analysis. Mineral preparation procedures to extract both quartz and feldspars of varying size fractions are detailed, together with mineral yields for each sample. Components of the annual dose contributions to each sample are also quantified and calculations of annual dose rates based on different mineral types presented.

Chapter 5 investigates additive-dose TL methods of determining the stored dose in feldspar minerals. The measurement procedure was validated through use of international standard material, irradiated to a known dose. Developments were introduced to improve precision and investigate the relationship between the level of replication and overall error to optimise the procedure. The run characteristics of each sample were examined, and dose distributions investigated for signs of heterogeneity. Consideration was also given to evidence for a dose dependent sensitivity change within samples. A strong relationship between sensitivity change and estimated dose (ED) was identified, and sensitisation models were constructed to help to understand the cause of such an effect. In light of such research, correction procedures were suggested and implemented. After fading corrections were applied, age calculations for each sample were tabulated.

Chapter 6 documents investigations of single aliquot OSL methods for determining the stored dose in quartz minerals. The accuracy of the technique was investigated by dose recovery experiments, and sensitisation issues examined through the development of an expanded procedure. Relationships between intensity, sensitivity change, recycling ratio, IR response, preheat temperature and the observed distribution of EDs are investigated for each sample, and general trends within the entire dataset observed. Further analysis of results, based on the scatter observed in EDs from individual samples, considers zeroing and microdosimetric effects, with suspect samples highlighted prior to age calculations.

Chapter 7 compares results of both feldspar and quartz methods, supplementing chronological information with radiocarbon dates, where available. Individual sites are analysed for evidence of prolonged use, before local and regional patterns are discussed.

In light of this new chronological information, a more informed discussion of the relationship between the burnt mounds and their archaeological landscape is presented.

A wider consideration of the implications of the research is documented in chapter 8, together with suggested directions for future work including aspects of sampling and luminescence methodology. The benefits of such research are assessed in terms of the contribution they may make to a larger scale interpretation of Scottish and European burnt mounds.

CHAPTER 2 Luminescence Dating Background

2.1 Introduction

This chapter outlines the basic principles that underlie luminescence dating techniques. A brief account of the characteristics of the main 'luminescence dating minerals' is given. Current methodologies for the measurement of stored dose are summarized. Specific components that contribute to the annual dose rate are considered, and methods of measurement outlined. A review of past applications of luminescence dating to heated stone is given before a research strategy for tackling both sampling and laboratory work is developed in light of this review.

2.2 Basic Principles

2.2.1 Introduction

Luminescence dating was first applied in an archaeological context in the 1960s, developing techniques for the dating of fired pottery using thermoluminescence (TL) (Kennedy and Knopff, 1960, Aitken et al, 1964). Over the following 30 years, the technique was applied to an increasingly varied range of heated materials, including burnt flint (Göksu et al, 1974) and heated stones from a variety of sources (Huxtable et al, 1976, Mejdahl, 1983). During the 1980's and 1990's, techniques were developed allowing the further expansion of the technique to unheated materials such as sediments (Wintle and Huntley, 1982, Hutt and Smirnov, 1983, Huntley et al, 1985), greatly increasing application based publications, especially applied geology/geography.

All luminescence dating techniques are based on the principles of an accumulation of stored energy trapped in the crystal lattice of certain minerals, built up as a result of exposure to background ionizing radiation. Optical or thermal stimulation of the mineral produces a measurable quantity of light proportional to the accumulated exposure dose. If the environmental dose rate the mineral has been exposed to can be reconstructed, the age of the material may be calculated:

$$Age(a) = \frac{StoredDose(Gy)}{AnnualDose(Gya^{-1})} \qquad (2.1)$$

The majority of application based luminescence work relies upon a 'zeroing' event that releases the energy built up as a result of past exposure of the particular mineral during distant geological history. Before the advent of more advanced optical techniques, this entailed significant heat exposure to zero the TL traps. However, optical techniques are now able to utilize more easily bleached traps that may be zeroed by exposure to varying quantities of light as opposed to heat.

Sampling strategies must clearly take into account the relationship between the zeroing event and the particular geological/archaeological event being studied. In practice there are many other complications relating to the measurement of stored dose, annual dose and both the significance of the zeroing event and its effectiveness at removing previous accumulated signals.

2.2.2 Trapping mechanisms

As stated above, luminescence occurs when electrons trapped in crystal defects are raised to an excited state and recombine at luminescent centers, giving off a small amount of light. Both insulators and semiconductors exhibit luminescence properties. The process by which such electrons become trapped is thought to relate to defects that produce a local deficit of negative charge in the crystal lattice (fig 2.1). The number and type of defects present within a particular mineral will depend on the type of mineral, the amount of impurities within it, and its formation process (Aitken, 1985).

Interaction of alpha, beta and gamma radiations with matter result in ionization and some of the ejected electrons are attracted to these 'electron traps'. A mineral exposed to a radiation source will thus build up a population of trapped electrons that will be proportional to the radiation dose received. Once trapped, electrons can be released by vibration of the crystal lattice. As temperature increases, so do the vibrations and the probability of eviction. Some traps are more able to 'shield' electrons from such vibration, and are termed 'deep' traps as the energy required to evict

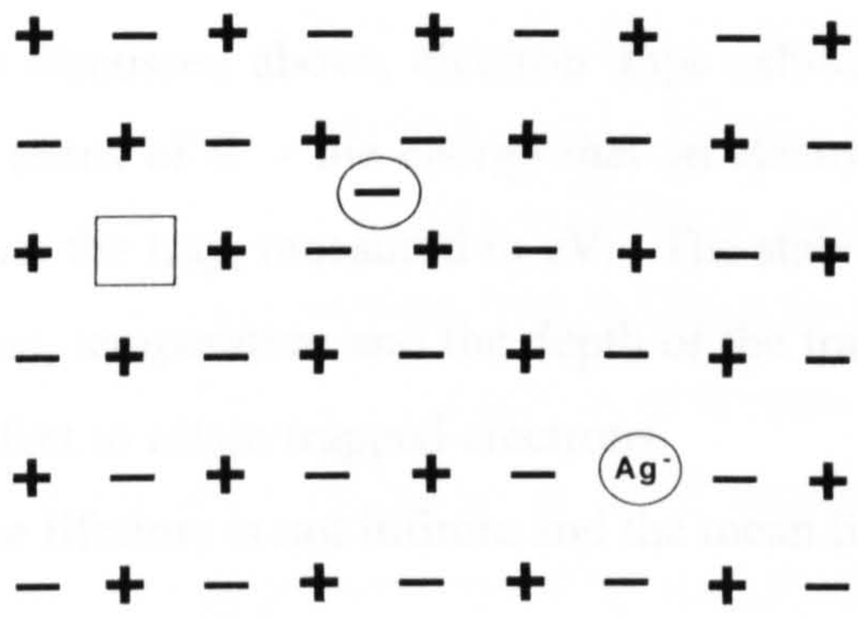

Figure 2. 1: Simple types of defect in the crystal lattice structure of an ionic crystal. From left to right: negative-ion vacancy, negative-ion interstitial, substitutional impurity centre. (From Aitken, 1985)

the electron is greater. Once evicted, electrons may be captured by other empty traps, or recombine with an ion. If this recombination is radiative, luminescence is given off. Consideration of an energy level representation of the luminescence process (fig 2.2) illustrates the mechanisms graphically.

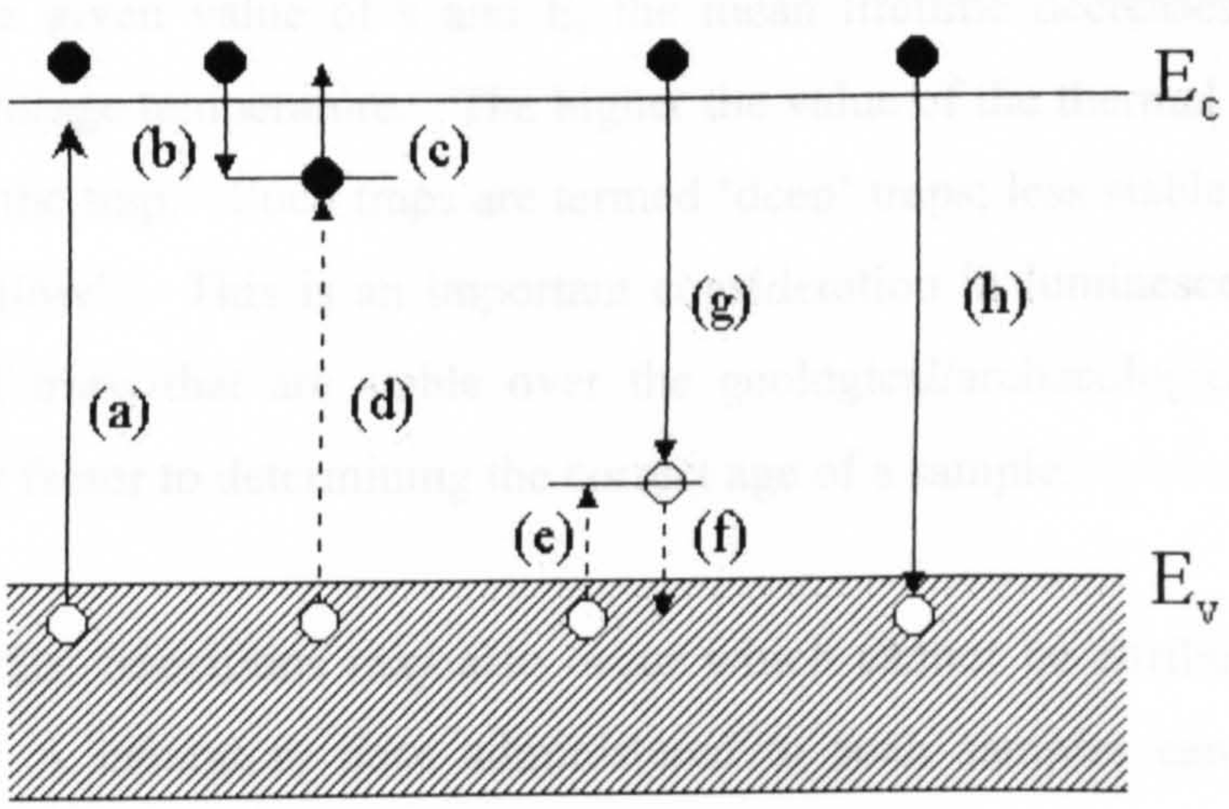

Fig 2.2 Common electronic transitions in (crystalline) semiconductors and insulators: (a) ionization; (b) and (e) electron and hole trapping respectively; (c) and (f) electron and hole release; (d) and (g) indirect recombination; (h) direct recombination. Electrons, solid circles; electron transitions, solid arrows; holes, open circles; hole transitions, dashed arrows (from McKeever, 1985).

2.2.3 Trap stability

As discussed above, electron traps exhibit varying degrees of stability generally described in terms of E - the energy that an electron must acquire from lattice vibrations to escape from the trap, measured in eV. The stability of a trap is dependent on a number of factors: time, temperature and the depth of the trap all play an important role in the ability of each defect to retain trapped electrons.

The lifetime is not infinite and the mean lifetime can be expressed by the exponential:

$$\tau = s^{-1} \exp^{\left(\frac{E}{kT}\right)} \qquad (2.2)$$

where τ is the mean life of the trap (s),

s is a frequency factor dependent on the type of trap (s^{-1}),

E is the activation energy, or trap depth (EV),

k is Boltzmann's constant ($eV\ K^{-1}$)

T is the storage temperature (K).

For traps with a given value of s and E, the mean lifetime decreases exponentially in relation to the storage temperature. The higher the value of the thermal activation energy, the more stable the trap. Such traps are termed 'deep' traps; less stable lower value traps are termed 'shallow'. This is an important consideration in luminescence dating as the identification of traps that are stable over the geological/archaeological time period in question is a key factor to determining the correct age of a sample.

In certain minerals, transitions may also occur which cannot be attributed to the kinetic model above. A laboratory dose administered to such samples can be shown to be depleted (or 'fade') over a short time period. Such short term fading was first noted by Wintle (1973) in volcanic feldspars, with samples showing loss of TL of more than 10% overnight. In the most extreme case, a labradorite sample showed 40% loss of signal over a 4 hr period (Wintle, 1977, Visocekas, 1985). Archaeological samples have also been reported to fade by up to 30% (Mejdahl, 1985). However, other studies of archaeological material report little or no fading (Mejdahl, 1983, Sanderson, 1988) and it is clear that no assumptions as to the likelihood of fading should be made.

The most common explanation for observed short term fading is in terms of quantum mechanical tunnelling from trap to nearby centre, whether athermal, or thermally assisted (Garlick and Robinson, 1972, Wintle, 1973, Visocekas et al, 1976). Templer (1985) demonstrated an increase in fading in zircons at elevated temperatures. He postulated that where traps and centres were sufficiently close, localised transitions could occur. As such, local transitions are thought to contribute to fading at higher temperatures, with tunnelling the dominant mechanism at lower temperatures (Templer, 1986). One consequence of quantum mechanical tunnelling models of fading (Visocekas et al, 1976), is that due to a decrease in the probability of electron escape with increasing trap/hole separation, for a random spatial distribution of traps and centres, there will be a exponential decrease in tunnelling with time.

The t^{-1} relationship assumes a random distribution of defects. Sanderson (1988a) observed that the luminescence intensity of samples studied suggested charge carriers in the region of 10^7-10^8 in samples containing c. 10^{20} atoms. Thus, a random distribution of traps and centres would give a mean separation $> 10^4$ atoms, a distance too great for tunnelling. Whilst he acknowledged the possibility of clustering of defects to reduce lattice strain, he reasoned that such clustering would lead to fading, which could not continue on a t^{-1} timescale. Indeed subsequent work by Smith (1998) reported behaviour which did not replicate t^{-1} decay in a series of volcanic feldspars. Laser spectroscopy measurements indicated defect clustering, and Smith suggested such clustering would produce a stepped decay curve that could lead to a stable signal being isolated.

2.2.4 Zeroing of the Geological Signal

Effective zeroing of the geological signal is a vital component to successful luminescence dating. Residual geological signal will result in an erroneously old date for a sample. There are a number of mechanisms by which a geological signal, or part of it may be 'zeroed'.

Consideration of equation (2.2) shows a trap lifetime dependence on storage temperature. Thus, when a sample is heated, the lifetime of the trap is dramatically reduced. It is this process which luminescence read-outs are based on. If heated sufficiently, traps will be

effectively emptied (although high temperature geological TL in the 700°C region may remain).

Exposure to light may also reset the optical luminescence signal. Again trap response is varied, with some more easily bleached than others. The effectiveness of the bleaching will depend on the wavelength and intensity of the light, exposure time, and mineralogy of the material. In general, a TL residual will remain however samples may be dated by means of optical methods that do not stimulate these traps. There has been much success in recent years in utilizing this zeroing mechanism with respect to sediment dating. This method of zeroing is also of relevance to laboratory safelight considerations.

Clearly insufficient heat or light may not fully reset the luminescence signal. Where minimal resetting has taken place, there may be obvious overestimation in the age of the sample. However, where only a small residual signal remains (of the order of ~1-2Gy) detection may be more problematic.

With regard to TL dating, it is possible to utilize the kinetic equation (2.2) to identify partial zeroing. If ED is calculated at different temperature integrals, a plot of ED against temperature will show a rising slope at higher temperatures where zeroing has not been complete as deeper traps will have retained successively more charge.

With quartz optical readout, a similar method has been proposed. When ED is calculated at different stimulation time integrals, a plot of ED against stimulation time may show a rise with time, indicating incomplete resetting of the harder to bleach medium and slow components of the OSL signal (Bailey, 2003). It is not clear whether this method is also sensitive to the detection of incomplete zeroing by heating.

2.2.5 Selection of minerals for dating

A considerable variety of minerals exhibit luminescence. In the 17th century Boyle (1664) noted " a diamond that shines in the dark". Many other geological specimens were subsequently noted to exhibit luminescence. The luminescent properties of minerals have been utilized in a wide variety of fields, from dosimeters in health physics, to glow-in-the-dark light sticks. However, only a small number of minerals have so far proved suitable

for luminescence dating. Whilst zircons (Zimmerman et al, 1974, Sutton and Zimmerman, 1976), calcite (Debenham and Aitken, 1984) and flint (Göksu et al, 1974, Valladas, 1978) have been studied the predominant minerals used in luminescence dating are quartz and feldspars.

2.2.5.1 Characterization of Quartz

Quartz is a relatively simple mineral that makes up approximately 13% of the earth's crust, and is the most abundant and widely distributed of all minerals. It has a hardness of 7 on the Mohs scale, and a specific gravity of c. 2.65gcm^{-3}. Whilst there are several types of quartz, the most common forms are trigonal α and hexagonal β quartz. α quartz forms at temperatures below 575°C and is composed of $[SiO_4]^{4-}$ tetrahedra. Above 575°C, α quartz transforms to β, marked by a change in the bonding angle of the oxygen molecules. Quartz is comparatively free of internal radioactivity.

Two visible luminescence emission bands have been observed within natural quartz; one around 450nm and one at 650 nm – blue and red respectively (Krbetschek et al, 1997). The blue band has been shown to consist of at least four overlapping peaks at 390nm, 420nm, 450nm and 500nm.

Spectral studies of quartz TL have identified a number of emission bands (fig 2.3), the three main bands being in the near UV to ultraviolet, blue and orange. The near UV to ultraviolet emission at 360-440nm is attributed to a Si vacancy (Nuttall and Weil, 1980). Franklin et al (1995) list the main TL peaks as 376nm 95-110°C, 392nm 150-180°C, 410nm 200-220°C and 430nm 305-325°C, the latter being strongly linked to OSL in quartz. The blue emission band at 460-500nm is characterized by the 375°C TL peak. The red TL emission (600-650nm) is characteristic of volcanic quartz and has been found to have a far higher saturation dose than for the blue band (Krbetschek et al, 1997).

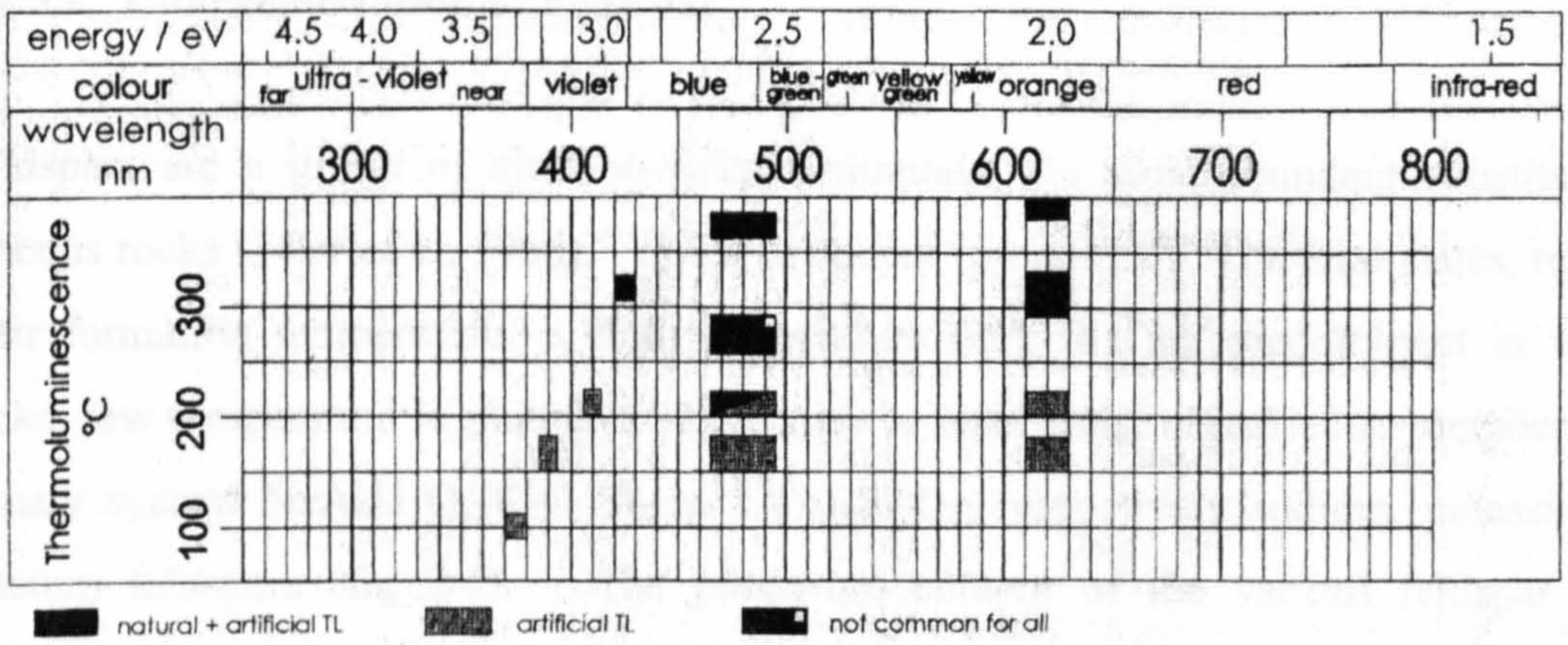

Fig 2.3 Main TL emission bands of quartz (From Krbetschek et al, 1997)

Thermoluminescence dating of quartz is traditionally focused on the 325°C and 375°C peaks (Fleming, 1970). The 325°C peak tends to suffer from large sensitivity changes on second glow and was thus termed the "malign" peak (Aitken, 1985). Both are estimated to have theoretical stability over the period of 10^8 years at 15°C and are thus well suited to the dating of archaeological material.

The 110°C peak has also been utilized in TL dating, in the form of pre-dose (Fleming, 1973) and phototransfer (Bowman, 1979) techniques. The former is limited in applicable age range to c.1000-2000 years by the relatively short lifetime of the 110°C trap. The latter technique uses UV to evict traps from the 370°C region. A proportion of the evicted electrons are then re-trapped in the 110°C region and may be accurately measured for a short period thereafter.

Recent years have seen advances in quartz OSL dating, using both green and blue light to stimulate luminescence from what is commonly attributed to be the 325°C peak. However, recent LMOSL work by Bailey (1997) and Singarayer and Bailey (2003) has shown the quartz optical signal to be derived from at least five different traps, labelled as fast, medium, and slow 1-3 as a reflection of their decay rates. The slow component is seen to be stable at temperatures up to 650°C and would therefore seem associated with a deeper trap than that of the 325°C TL peak.

2.2.5.2 Characterization of Feldspar

Feldspars are a group of alumino-silicate minerals, the most abundant constituents of igneous rocks (Deer et al, 1966). Feldspars occur in two main structural states, related to their formation temperature. High temperature feldspars are predominant in volcanic rocks, low temperature in plutonic. They may be chemically classified as members of the ternary system $NaAlSi_3O_8$-KAl Si_3O_8- $CaAl_2Si_2O_8$, respectively sodium, potassium and calcium feldspars (fig 2.4). The potassium content of the various feldspar groups dominates the internal radiation component (the potassium rich feldspars containing 10-13% K, sodium rich c. 4-6% K, Aitken, 1985). Potassium feldspars vary in specific density from 2.5-2.58gcm^{-3}, with sodium feldspars found in the 2.58-2.62gcm^{-3} region, and plagioclase feldspars in the heavier 2.62-2.74gcm^{-3} fraction.

Fig 2.4 Ternary diagram showing the relationship between alkali and plagioclase feldspars

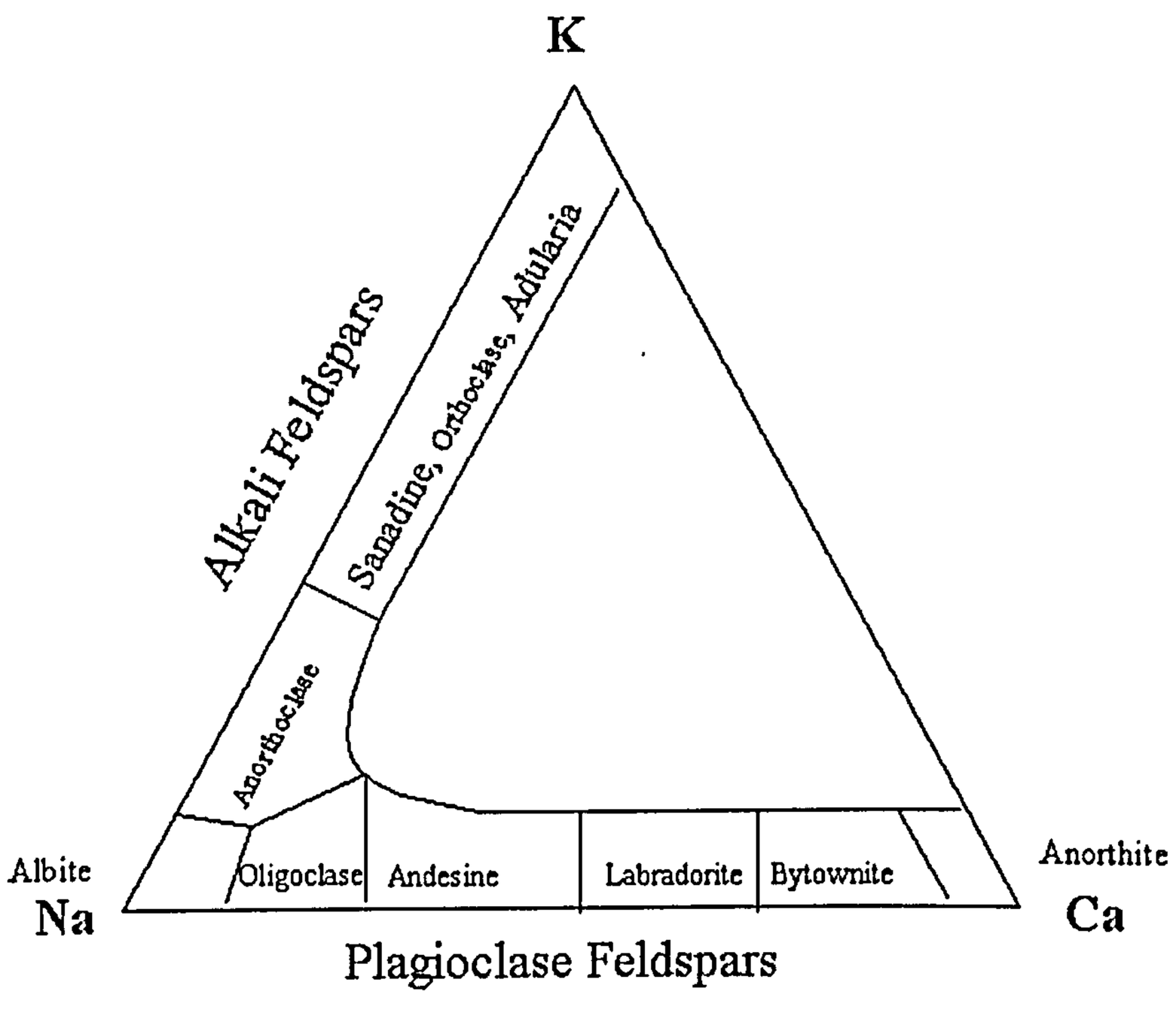

The TL signals derived from feldspars are typically 10-100 times brighter than quartz (Mejdahl, 1985, Sanderson, 1987) and are thus suited to the measurement of small doses. In addition, the internal contribution to the dose rate may help to minimize overall errors.

Existing spectral information with regards to feldspar emissions is limited, and is summarized in Krbetschek et al (1997). The differences in feldspar composition led to great variation in the emission spectra seen. However, in the case of TL emissions, a number of 'type spectra' are available for various materials. Some common features identified within feldspar studies are summarised below (fig 2.5).

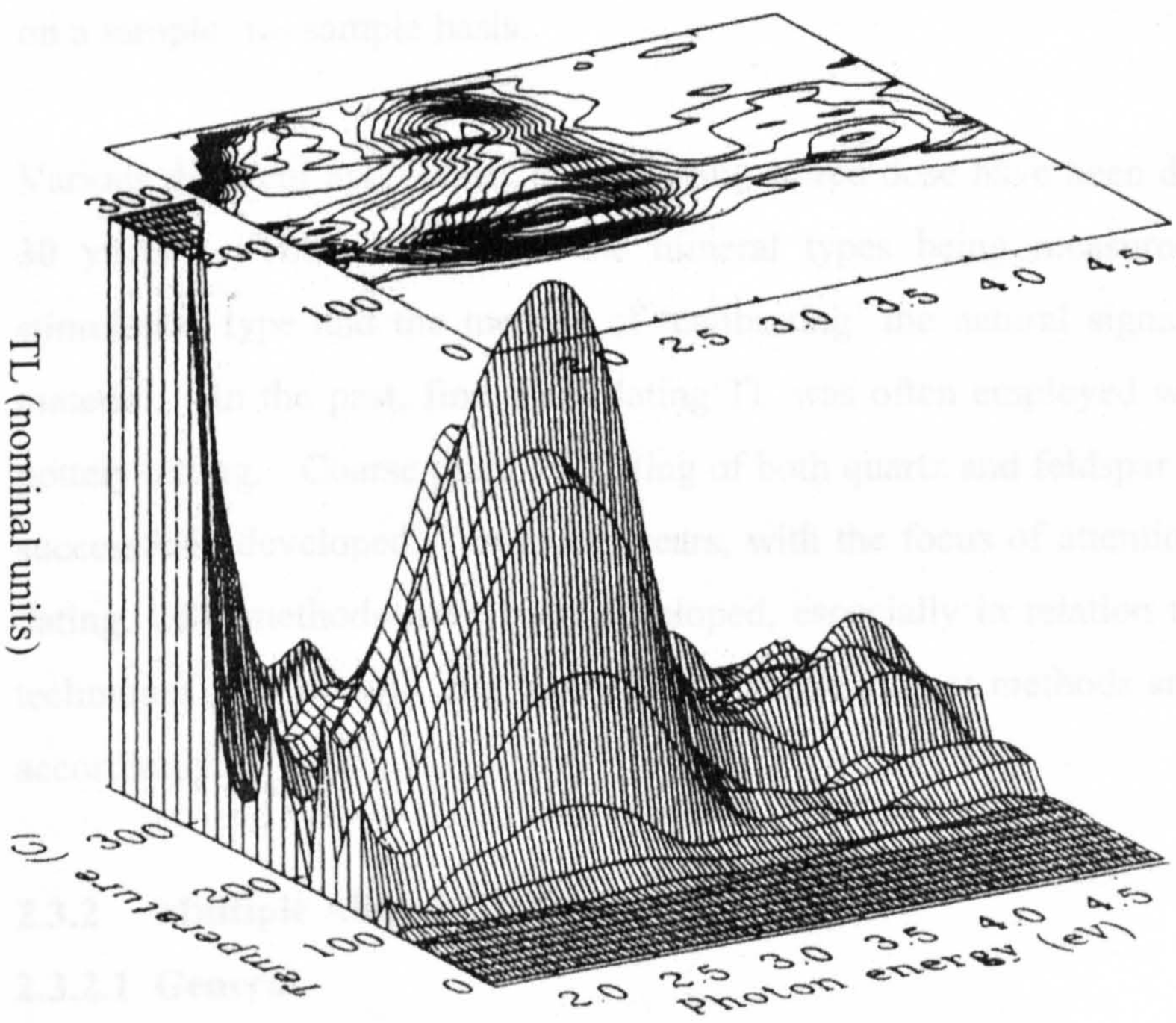

Fig 2.5 "Type spectrum" for high orthoclase feldspars, showing emission in the range 2-3.5 eV (after Prescott and Fox, 1993; from Krbetscheck et al, 1997)

Nine main emission bands have been identified: 275-290 nm, 320-340nm, 390-440nm, 450-490nm, 500-540nm, 560-570nm, 580-600nm, 700-760nm, and emissions >800nm. The most common signal measured in TL dating studies is the violet-blue 390-440nm wavelength. The majority of feldspars show a double peaked glow curve, with peaks centred on 280°C and 350°C at a heating rate of 5 $^{o}Cs^{-1}$. The mean lifetime of these traps is in the region of $2.5x10^{4}$ and $2.8x10^{6}$ ka respectively (Strickertsson, 1985). The

proximity of these emission bands make effective isolation of single bands using combinations of filters problematic. Within OSL dating, the main IR peak utilized is at c. 855nm, which Clark and Sanderson (1994) have shown to be a broad stimulation peak.

2.3 Stored Dose Estimate

2.3.1 Introduction

The natural luminescence signal of a sample is a reflection of the age of the sample and the strength of the radiation field it has been subjected to, combined with the specific sensitivity of the material. This is dependent on both thermal history and the amount of impurities within each mineral. As such, calibration of the natural glow curve is required on a sample- to- sample basis.

Various different approaches to measuring stored dose have been developed over the past 30 years. These vary with the mineral types being measured, the grain size, the stimulation type and the method of 'calibrating' the natural signal for sensitivity of the material. In the past, fine grain dating TL was often employed where the focus was on pottery dating. Coarse grain TL dating of both quartz and feldspar minerals has also been successfully developed. In recent years, with the focus of attention shifting to sediment dating, OSL methods have been developed, especially in relation to quartz. In general, techniques may be split into multiple and single aliquot methods and are discussed below accordingly.

2.3.2 Multiple Aliquot Methods

2.3.2.1 General

Multiple aliquot techniques are many and varied. They are based on the principle of determining estimated dose (ED) based on a number of measurements of different portions of a sample. The main problem encountered in such techniques is one of normalization. In order to relate the portions or aliquots of the sample to one another, a scaling factor is required. A number of different solutions have been developed to overcome this.

The most basic is that of mass normalization, whereby differences in the weight of each aliquot are negated by expressing the luminescence signal as a function of mass. In practice, weight normalization is problematic due to heterogeneity of the TL response per

unit mass from coarse-grained separates, leading to significant scatter and poor precision. A large number of discs are therefore required for accurate measurement of ED to take place.

Normalization of all discs to a 'known' dose can overcome such problems. Expressing the luminescence signal in relation to a common dose point will effectively take account of both mass difference and inhomogeneity in sample response. However, this technique may likewise encounter problems. By irradiating and/or stimulating a sample, whether by heat or light, it is possible to change its sensitivity. Therefore a direct conversion of the ratio of natural to known signal could give an incorrect ED. In addition, irradiation of aliquots to varying degrees during first glow may cause a dose dependent sensitivity change, which would adversely affect normalization. As such, procedures have been developed to account for changes in sensitivity.

A technique particular to the dating of quartz has also been developed whereby the natural signal is normalized to a low temperature component of the glow curve. The 110°C peak has a half-life of a few hours at room temperature. Consequently in a 'natural' sample this signal is not present due to its short lifetime. Due to the sensitivity of this peak, it is possible when using a negligible radiation dose, to measure the intensity of the low temperature peak without adversely affecting the sensitivity of the higher peaks. This signal may then be used as a normalization method for subsequent irradiation of aliquots (Aitken, 1985). This procedure is also relevant to single aliquot dating (see below).

2.3.2.2 Multiple Aliquot Added Dose Protocol (MAAD)

Multiple aliquot additive dose methods of determining ED utilize the gradient of the slope formed when a known dose is added to that of the natural to produce an estimate for the natural ED. As outlined above, there are many techniques of normalization that may be utilized. After normalization, a plot of luminescence intensity against additive dose gives a value for the equivalent dose **Q** (fig 2.6).

However, this equivalent dose is not always equal to the stored dose, as some minerals exhibit supralinearity of growth of luminescence at low doses. If samples from which the

natural signal has been drained are irradiated, read out and plotted as before, I may be measured (fig 2.6) and the palaeodose calculated (P=Q+I).

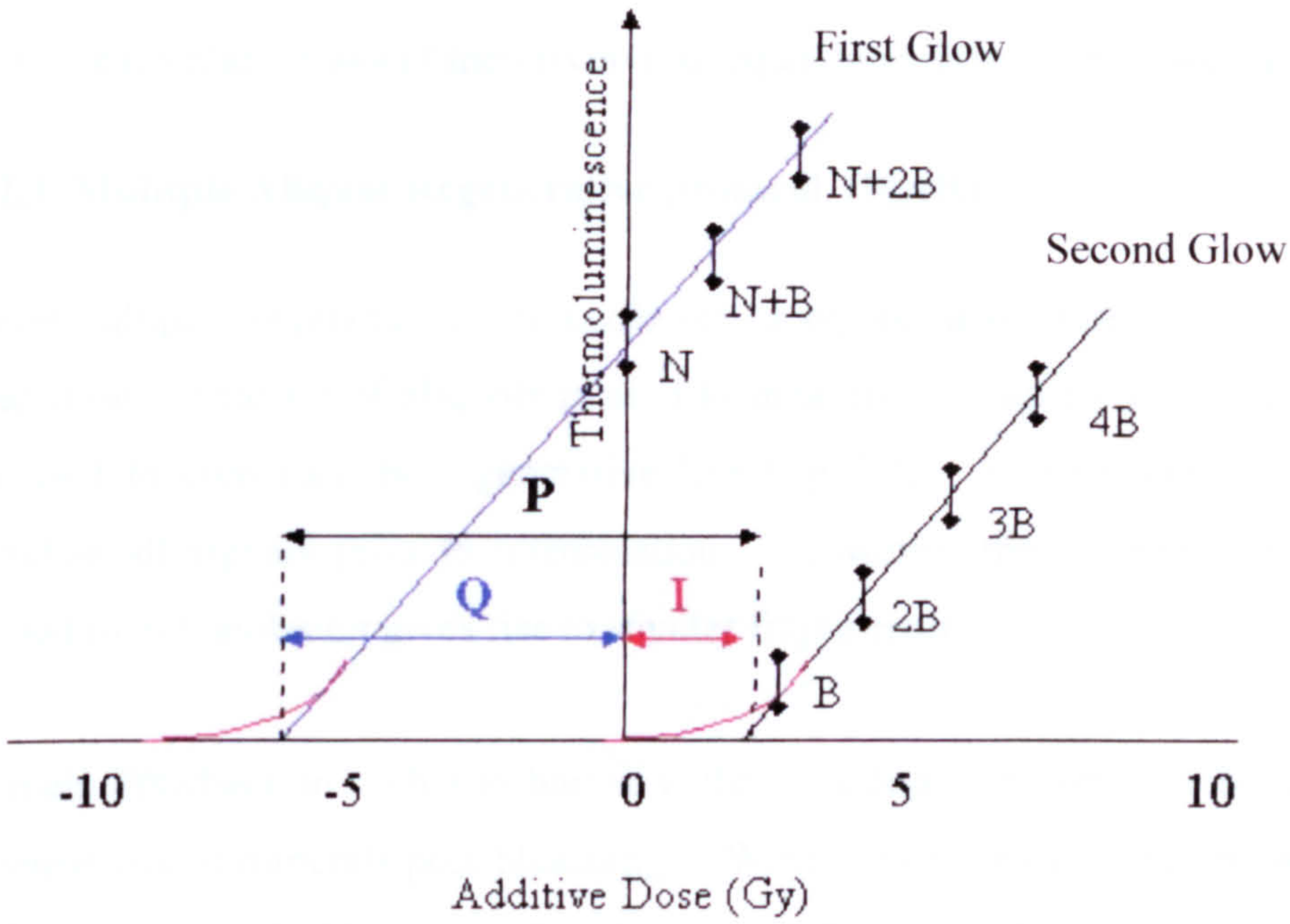

Fig 2.6 Schematic representation of multiple aliquot additive dose protocol. Blue line shows first glow linear regression of natural (N) plus beta (B) dose points, giving a value for Q. Black line shows the second glow linear regression of B dose points, giving a value for I, the supralinearity correction. Red lines indicate the true path of each regression line, with supralinearity at low doses. The palaeodose, P is calculated as the sum of Q and I.

Methods for measuring intercept lines vary. One method is to use the second glow of the original aliquots to reconstruct the line prior to third glow normalization. The disadvantage is that, due to heating on glow 1, it is possible to experience changes in the sensitivity of the material (shown by a change in the gradient of the slope) making interpretation of non-zero intercept values problematic.

Second glow intercept lines can be reconstructed by first bleaching a portion of material that contains the natural dose, then following the palaeodose protocol. Again however, there may be sensitivity changes related to bleaching and residual signal components which must be addressed. With regards to TL, 'unbleachable' residuals in the region of 10% of the total signal have been recorded, attributed in part to electron transfer from other traps (Aitken, 1985).

With regard to dose dependent sensitivity changes during first glow, it may be necessary to give additional doses to aliquots prior to normalization to cancel any dose dependent affects - each aliquot would then receive an equal total dose prior to normalization.

2.3.2.3 Mulitple Aliquot Regenerative protocol (MAR)

Multiple aliquot regenerative protocols use a regenerative dose line to interpolate the stored dose. One set of aliquots is used to measure the natural signal, another bleached then used to construct the regenerative line (fig 2.7). Clearly there is still a need to normalize all signals prior to interpolation. However, the method of interpolation, as opposed to extrapolation gives rise to smaller fitting errors.

The main drawback in such a technique is that it is dependent on there being no change in the sensitivity of minerals post-bleaching. Where sensitivity change has taken place there will be an unquantifiable over/underestimation in the stored dose.

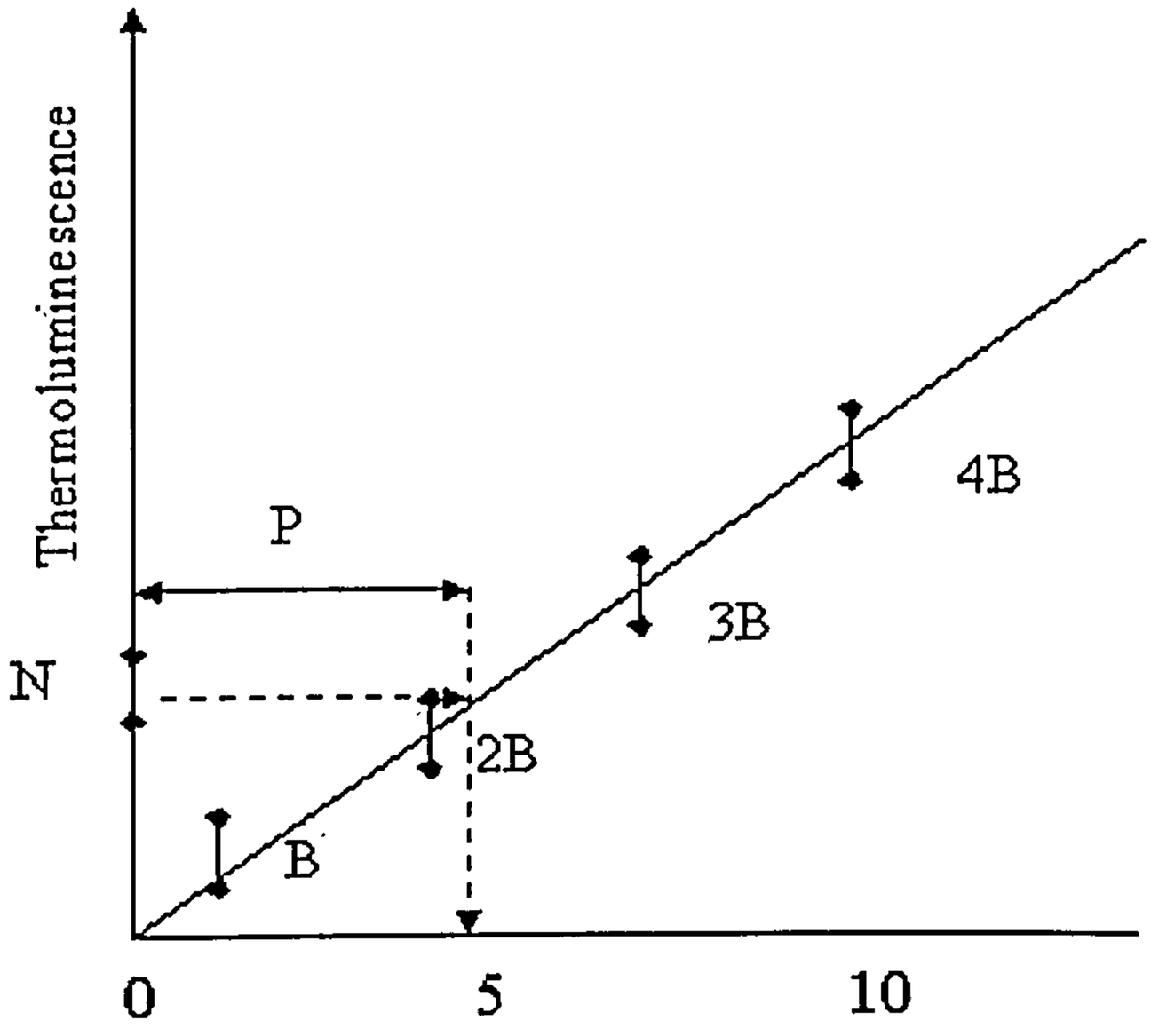

Fig 2.7 Schematic representation of Multiple Aliquot Regenerative protocol. Black line shows the reconstructed regeneration curve, derived from measurements where known doses (B) have been added to a bleached out portion of the sample. The value of the natural signal (N) is then compared to the regeneration curve and a value for P determined.

2.3.2.4 Single Aliquot Regenerative Additive Protocol (SARA)

Despite the implications of the name, this technique is also a multiple aliquot procedure. Introduced by Mejdahl and Bøtter-Jensen (1994), the SARA protocol attempted to overcome problems associated with earlier regenerative methods (see section 2.3.2.3).

Increasing beta doses are added to aliquots containing their natural dose. These are then read out and a regeneration curve constructed for each sample. A value for B_o, B_1, B_2, B_3 etc is calculated from the regeneration curve and plotted as a function of the added dose. The regression line through these points intercepts the additive dose axis, giving the 'true' ED, irrespective of sensitivity change induced during the regeneration readouts (fig 2.8*)* (Mejdahl and Bøtter-Jensen, 1994, 1997).

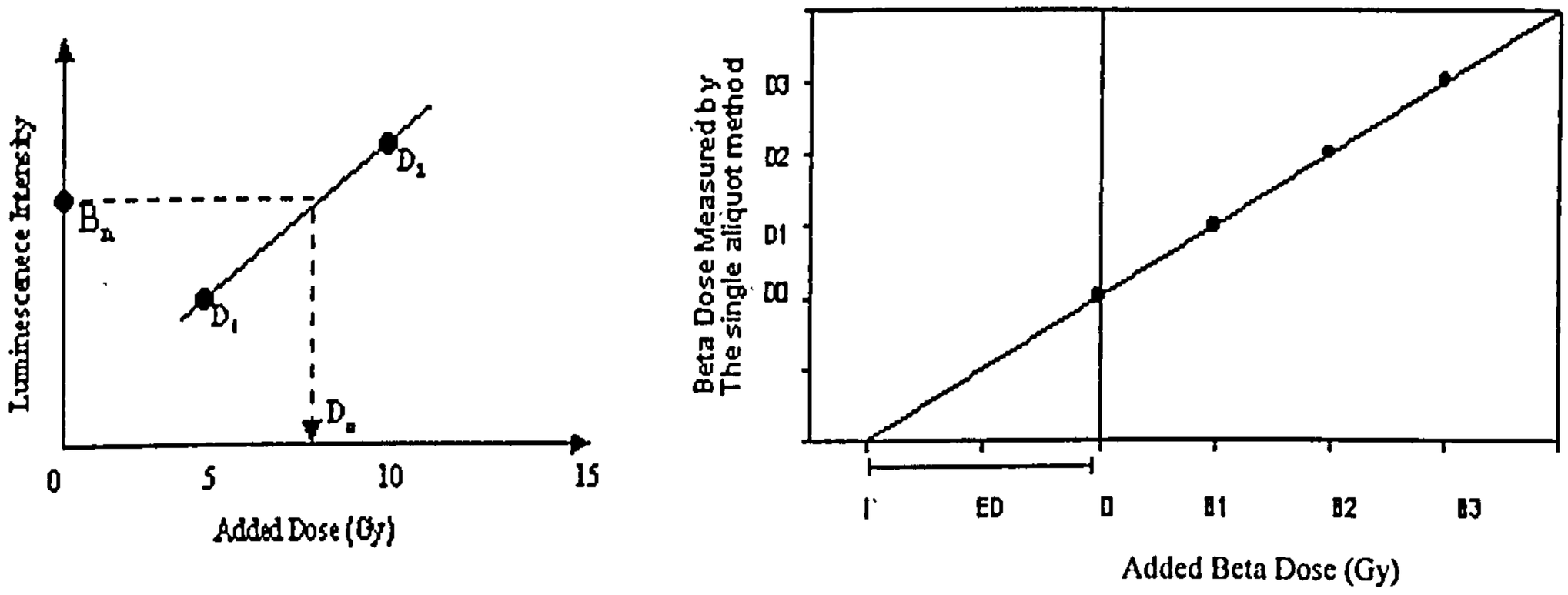

Figure 2.8: Principle of the SARA Method (After Mejdahl and Botter-Jensen, 1997) Portions of sample containing natural signal are given added beta doses (B_n) and their luminescence signal measured. A beta dose below the assumed value of the natural is then given to the now zeroed sample and read out (D_1). This is repeated with a higher beta dose rate (D_2) and a regeneration value for each set of B_n determined (D_n). These values are plotted against their original added beta dose values (B_n) and a regression line constructed to estimate the natural dose (ED).

It is necessary however to verify that the sensitivity change is the same for doses Do-D_n independent of the initial B dose added. Mejdahl and Botter-Jensen (1997) suggested the following expressions should agree within 3% for this condition to be satisfied:

$$\frac{D_0}{ED} = \frac{D_3}{ED+B_3} \qquad (2.3)$$

Whilst a number of additional modifications to the technique were suggested by Murray (1996) and Duller et al. (1999) the reliance on extrapolation of the final ED is still a limiting factor on the precision with which EDs can be measured.

2.3.3 Single Aliquot Methods

2.3.3.1 General

Single aliquot protocols were developed in an attempt to correct for sensitivity changes from cycle to cycle in quartz OSL regenerative protocols. The advantage of such a technique is two-fold. Not only are errors reduced as ED calculations are no longer reliant on extrapolation techniques, but individual EDs can be calculated for each disc, allowing information regarding dose distribution to be easily collected. Increasing automation of luminescence readers made the construction of multiple cycle runs possible.

2.3.3.2 Single Aliquot Additive Dose (SAAD) Protocol

Duller (1991) first proposed a single aliquot additive dose (SAAD) protocol based on IRSL measurements of feldspars. After preheating, a short shine of 0.5s was used to quantify the natural signal. This was followed by successive irradiations, preheats and short shines to construct a dataset for N, $N+\beta_1$, $N+\beta_2$.....$N+\beta_n$. Whilst the short IR readout did not significantly affect the strength of the following signal, the preheat was shown to have an effect on sensitivity, thus correction at each stage was required. Duller proposed correction by means of a second disc, which would be given identical preheat and readout cycles to the first, but with no additional irradiations.

Galloway (1996) later proposed a single aliquot procedure based on only one disc. After added dose measurements were made, repeated cycles of preheat and readout were measured and the decay curve measured as a result of this used to correct the initial signal. He showed that, for the samples studied, the decay took the form:

$$f(n) = 1 - a\ln n \qquad (2.4)$$

Where the initial signal, f(n), is expressed in terms of the number of times *n* an aliquot has been used and a constant *a*, derived from repeat measurements.

2.3.3.3 Single Aliquot Regenerative Protocol (SAR)

Murray and Roberts (1998) introduced the single aliquot regeneration (SAR) method which attempted to correct for sensitivity changes from cycle to cycle to enable EDs to be calculated from the regeneration curve alone.

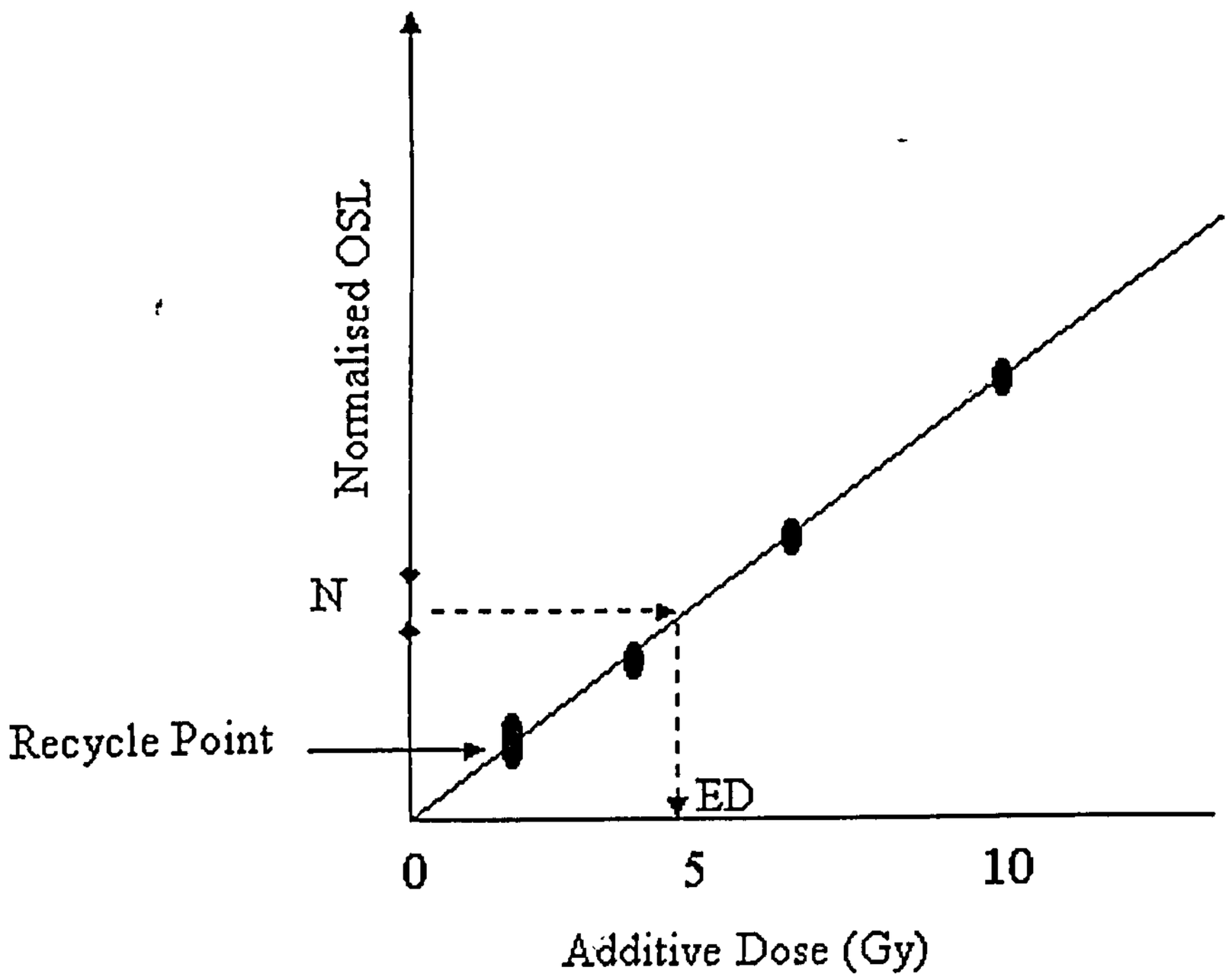

Fig 2.9 Schematic Representation of Single Aliquot Regenerative Protocol

The natural signal (N) is read out and successive beta doses added and read out. Each dose point is normalized to correct for sensitivity changes and a regeneration curve constructed. The normalized natural signal is compared to this curve and ED determined. A recycle point, usually a low dose point performed near to the beginning and end of the measurement cycle, is used to check the effectiveness of sensitivity corrections.

Sensitivity corrections were first made by utilizing the relationship between the 110°C and 325°C peak. If thermoluminescence is recorded during preheating of the sample, the 110^0C peak can be integrated, and used to correct for sensitivity change from cycle to

cycle. A recycle point, repeated at the beginning and end of each run, allows a check on sensitivity corrections to be made (fig 2.9).

Later developments (Murray and Wintle, 2000) removed the need to measure TL by introducing a small test dose cycle between dose points by which sensitivity could be monitored.

Whilst the technique is predominantly used within the quartz dating field, investigations into feldspar SAR protocols have also begun. Strickertsson et al (2001) reported good agreement between quartz and feldspar SAR results from Danish late Pleistocene deposits. Wallinga and Duller (2000) and Wallinga et al (2000) reported good agreement between feldspar SAAD and SAR results, but indicated an overall underestimation in age compared to quartz SAR ages obtained from the same fluvial sediments.

Whilst now widely used within the sediment dating field, there is an underlying weakness in the technique. The success of sensitivity corrections may be monitored by repeat points on the regeneration line, however there is no way to evaluate whether the test dose adequately corrects for changes in the natural readout cycle.

2.3.4 Other Considerations

2.3.4.1 Preheating

During any luminescence run, it is necessary to preheat samples prior to readout to remove unstable components of the signal present due to laboratory irradiation. The temperature and duration of preheat vary from mineral to mineral and technique to technique.

Consideration of equation (2.2) shows a time dependent relationship to trap stability. Traps which are unstable over a period of several hundred or thousand years (depending on the sample age) will not be fully represented in the natural TL glow curve. After artificial irradiation, these unstable traps will again be filled and contribute to the net luminescence signal. In order to remove these components it is necessary to preheat samples prior to readout.

A large degree of variation in preheat treatment is noted throughout luminescence literature with variability in both temperature and time applied (table 2.1). The move to highly automated irradiation and readout systems had encouraged the use of short preheats as samples are heated individually, whereas older manual systems enabled longer bulk preheating to occur.

The advent of SAR OSL dating of quartz has helped to focus attention on the importance of preheating. Evidence from a number of samples has shown a dependence on the preheating temperature of the ED obtained, leading to a recommendation to conduct measurements at a variety of preheat temperatures in order to validate results (Murray and Wintle, 2000).

With regard to OSL of feldspars, considerable variation in the treatment of preheat temperatures is seen. Radtke et al (2001) reported results using no preheat, while others use short high temperature preheats to flush out unstable components (e.g 1 minute preheats at 230°C Engelmenn et al, 2001). At the other end of the spectrum are longer preheats more akin to that seen in feldspar TL dating of upwards of 16 hours at lower temperatures ranging from 130-160°C. In addition, a storage period of several weeks prior to readout has also been used on occassion (Frechen et al, 2001). The effect of such variations in preheating is to a certain extent unquantifiable and likely to be sample dependent. Certainly, longer lower temperature preheats are more effective at removing unstable components from the consideration of the kinetics of trap parameters.

2.3.4.2 Irradiation

The dose rate experienced by a sample in nature is generally in the region of 2-3mGya^{-1}. Laboratory irradiation delivers a dose several million times higher than in nature. For low dose rates, thermal decay of competing traps will provide competition where traps are no longer full. In a high dose rate environment, this competition will cease when one or more of the traps fill, prompting a greater rate of filling of the traps (Aitken, 1985). Intrinsic dose rate effects may also be present in some materials, though Bowman (1978) reports only minimal effect in natural fluoride irradiated from 0.3 mGya^{-1} to 3 Gymin^{-1}.

A temperature dependence has also been noted where the efficiency of trapping decreases with temperature. This is thought to relate to the stability of traps at elevated temperature, producing more competition, and to the increased velocity of ionized electrons reducing the trapping probability (Aitken et al, 1975). This may be relevant where the temperature in nature is significantly different to the laboratory temperature.

Table 2.1 Comparison of preheats utilized in quartz and feldspar protocols

Mineral	Preheat	Method	Reference
Quartz	33hrs @ 160°C	TL MAAD	Huntley and Prescott, 2001
	120s @ 220°C	TL MAAD	Bateman and Herrero, 2001
	300s @ 220°C	TL MAR	Fehrentz and Radke, 2001
	300s @ 220°C	OSL MAR/ MAA	Hilgers et al, 2001
	120s @220°C	OSL SAAD	Bateman and Herrero, 2001
	10s @ 260°C	OSL SAR	Strickertsson et al, 2001
	10s @ 160-300°C	OSL SAR	Bailey et al, 2001
	10s @ 170-300°C	OSL SAR	Radtke et al, 2001
Feldspar	2 weeks storage + 16 hrs @ 160°C + 6 weeks storage	TL/IRSL MAAD	Frechen et al, 2001
	16 hrs @135°C	TL MAAD	Anthony et al, 2001
	600s @ 220°C	IRSL SAAD	Clarke and Kayhko, 1997 and Porat et al, 1997
	300s @ 220°C	IRSL MAR	Fehrentz and Radtke, 2001
	60s @ 230°C	TL MAAD/MAR	Radtke et al, 2001
	60s @ 220°C	TL/ IRSL MAAD	Engelmann et al, 2001
	10s @ 290°C	IRSL SAR	Strickertsson et al, 2001
	None	IRSL MAAD/ MAR	Radtke et al, 2001

2.4 Annual Dose Estimate

2.4.1 Introduction

Within the natural environment, a combination of α, β and γ radiation, from a variety of naturally occurring long-lived radionuclides gives rise to an effectively constant annual dose rate. Natural radiation is present within the burial environment, but also within the sample itself, thus assessment of the annual dose rate is complex. The penetration of these different components of the annual dose varies (fig 2.10). Whilst alpha (α) radiation is highly ionising, its penetration is very limited, generally between 20-30μm in range in solids. Thus, the contribution of α radiation comes entirely from the sample, and not the burial environment. Beta (β) radiation has a penetration range of a few mm in solids

therefore only the outer portion of a sample is affected by external sources of β radiation Gamma (γ) radiation has an much larger penetration range, the majority coming from a 30cm sphere around the sample. In addition, cosmic rays are also external contributors.

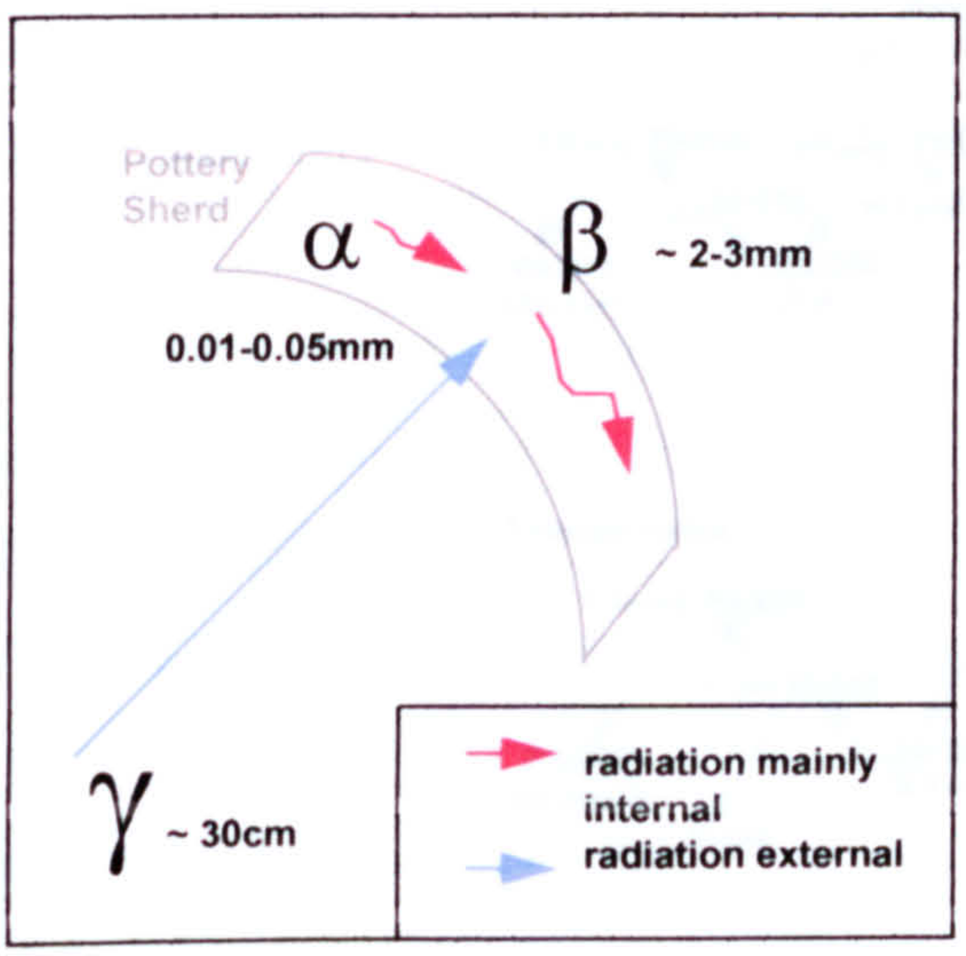

Fig 2.10 Penetration of different types of Radiation (From Aitken, 1990)

Cosmic rays consist of electrons and totally ionised nuclei of atoms. They are composed of a 'soft' component, consisting mainly of electrons, and a 'hard' component made up mainly of muons. The soft component is absorbed in the first 0.5m of soil and as such has little contribution to the annual dose of buried material. The hard component however, can penetrate deep underground. Low lying and equatorial regions are shaded by the Earth's magnetic field, hence the strength of the hard component is dependent on latitude. Altitude and atmospheric pressure also affect the strength due to the different absorption rates of varying thickness of atmosphere (Prescott & Stephan, 1982).

2.4.2 Sources of External Radiation

The vast majority of this radiation is derived from the uranium and thorium decay series (fig 2.11), emitting α, β and γ radiation, and ^{40}K, the radioisotope of potassium, emitting β and γ radiation (fig 2.12). In addition, a small contribution is made from rubidium 87 (fig 2.13) and from cosmic rays. Sanderson (1987) demonstrated that other naturally occurring nuclides did not make a significant contribution to the overall external dose rate.

Fig 2. 11 Radioactive Decay series for U and Th (Hore-Lacy, 2003)

Fig 2.12 ^{40}K decay Scheme (From Fleming, 1979)

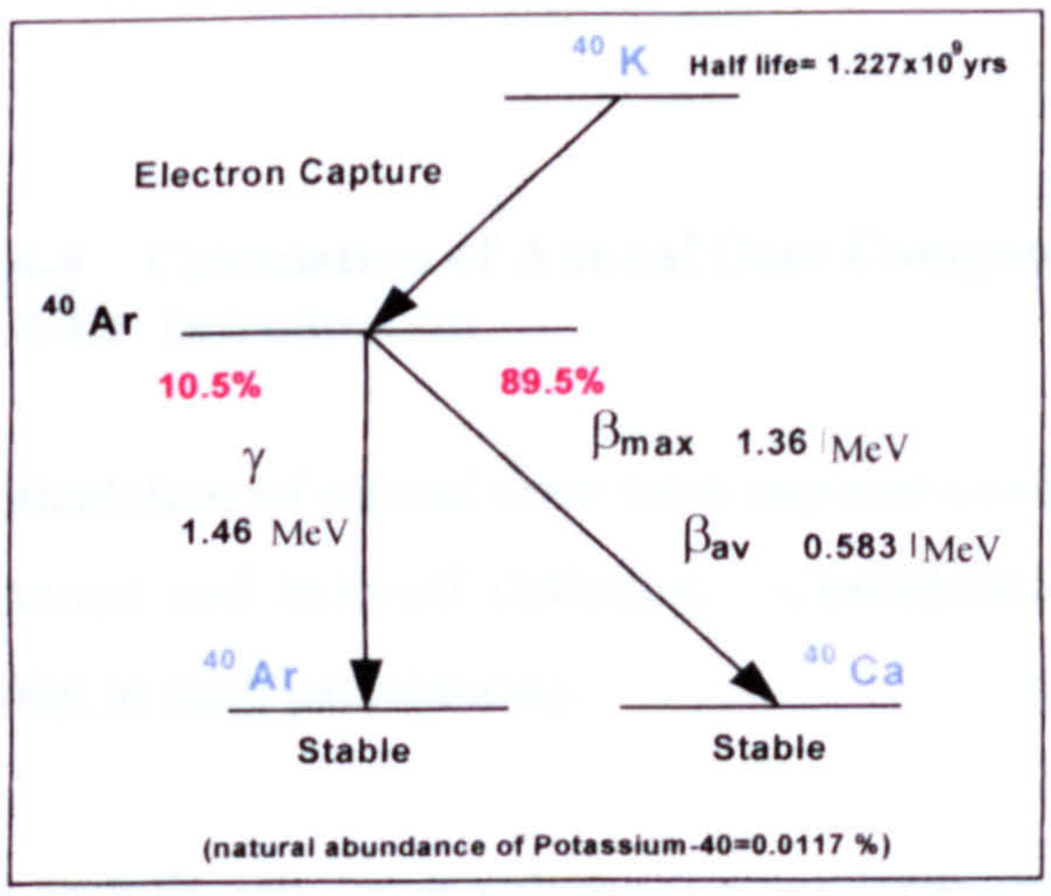

Fig 2.13 ^{87}Rb decay Scheme (From Fleming, 1979)

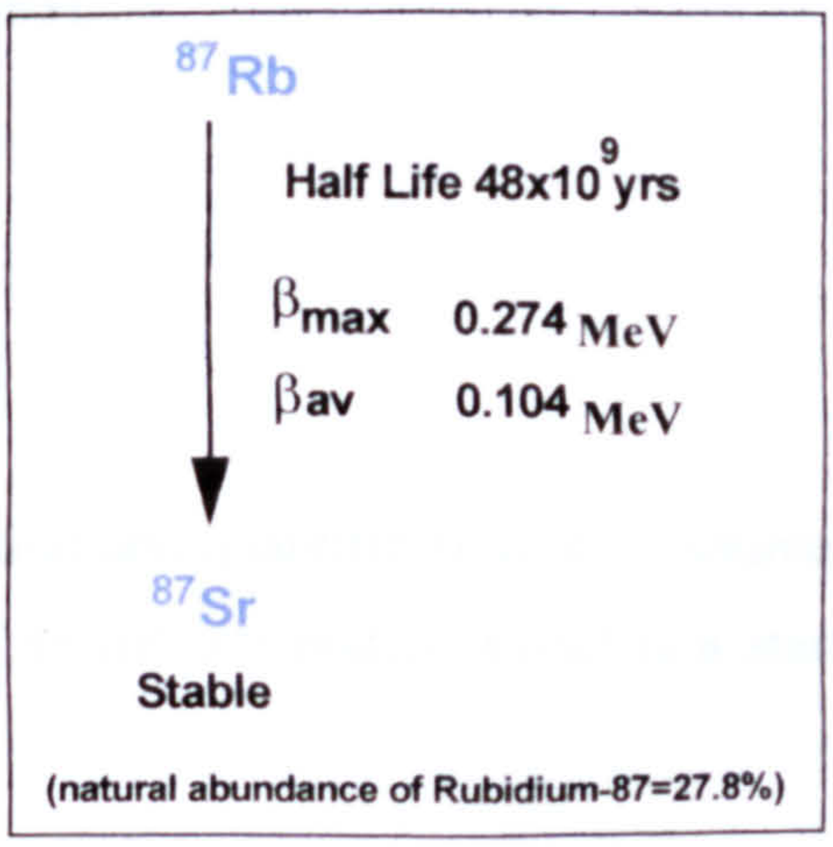

Given the penetration ranges discussed above, it is clear that for the majority of samples, only β and γ and cosmic ray radiation will have a significant effect on the sample. Indeed for 'solid' samples such as pottery and stone, removal of the outer 3mm of the sample will also negate the β dose rate contribution.

2.4.3 Sources of Internal Radiation

The sources of internal radiation which must be considered as part of annual dose calculcations are strongly dependent on both the sample type and the mineral phase extracted. For any sample, whether it be pottery, stone or sediment, there will be contribution from α, β and γ radiation from radionuclides within the matrix of the material. Minerals extracted from this matrix will have been exposed to this radiation field. In the case of coarse grained material, only the surface of grains will have been exposed to α radiation from the surrounding matrix. Etching of the surface of the material will negate this contribution. The matrix beta dose is strongly dependent on water content of the material due to absorbtion, thus correction needs to be made for this measurement.

Specific minerals may contribute significantly to the internal dose rate. The contribution to dose rate from radionuclides within quartz is generally thought to be negligible, due to low radionuclide concentration (Fleming, 1970), however the potassium content of certain feldspars may contribute significantly (Mejdahl, 1983). To a lesser extent, U and Th within feldspars may also have an effect (Aitken, 1985).

2.4.4 Calculation of Annual Dose Components

2.4.4.1 Introduction

Calculation of annual dose rates requires consideration and quantification of all sources of internal and external radiation. Consideration of an infinite matrix model is a starting point to such calculations.

In an infinitely large volume (i.e one large enough that the dimensions are far greater than the radiation range within a homogenous material) energy absorbed should be comparable

to energy released, thus dose rate will be proportional to the sum of individual radionuclide concentrations. Given a known concentration of parent nuclides, infinite matrix dose rates may be calculated by summing the energy released down the decay chain. Dose rate conversion factors were first calculated for U, Th and K by Bell (1976) with later refinement in 1977 and 1979. Additional calculations were made by Warren (1978) for Rb, and recalculations by Nambi and Aitken (1986) and Sanderson (1987). Table 2.2 shows typical conversion factors.

Radionuclide	Concentration	Alpha	Beta	Gamma
U series				
No Radon Loss	1 ppm ^{238}U	2.779	0.1461	0.1149
100% Radon Loss		1.260	0.0610	0.0055
Th Series				
No thoron loss	1ppm ^{232}Th	0.738	0.0286	0.0514
100% thoron loss		0.308	0.0103	0.0208
Natural Potassium	1% K	-	0.830	0.244
Rubidium	50 ppm	-	0.0230	-

Table 2.2 Dose Rate conversion factors ($mGya^{-1}$) (From Aitken, 1985)

For the uranium and thorium series, some consideration of radioactive equilibrium is required prior to conversion. The effect of minimal and total loss of both radon and thoron within the U and Th decay series can be quantified within annual dose rate calculations. However, a number of microdosimetric effects also require corrections to be taken into account before annual dose rates can be calculated for a given mineral phase.

2.4.4.2 Water Content

α β and γ radiation are all absorbed to a certain degree by water. The water content of both the sample and surrounding soil matrix will affect the amount of radiation received, thus a water content correction is required. Zimmerman (1971) estimated that the absorption coefficient for water compared to a typical pottery matrix was 50% higher for α

particles, 25% for β and 14% for γ radiation. For dose rates measured when a sample is dry, the following corrections should be made (Aitken, 1985):

$$D_\alpha = \frac{D_\alpha, dry}{1+1.50WF'} \qquad (2.5)$$

$$D_\beta = \frac{D_\beta, dry}{1+1.25WF'}$$

$$D_\gamma = \frac{D_\gamma, dry}{1+1.14W_iF'}$$

where W is the saturated content of sample expressed as (weight of water/ dry weight), W_i of the soil and F is the fraction of saturation to which the assumed average water content corresponds.

In the case of α particles, given their short range, it has been suggested that the actual moisture effect may be less than suggested above due to the decreased probability of contact with water being made (Aitken, 1985). This is clearly dependent on the ratio of pore to grain size within any given material.

2.4.4.3 Alpha Attenuation and Efficiency

As discussed above, the mean range of α particles is ~20-30μm in solids. As the particle loses energy, it slows progressively towards the end of its path, spending longer and longer in a particular vicinity. The result is that large radionuclide bearing inclusions will not fully irradiate their surroundings. Conversely, radionuclide free minerals such as quartz will be subject to differential amounts of radiation across the mineral, with only the outer surface exposed to α radiation. A correction to the infinite matrix dose rate calculations in the form of an attenuation factor is therefore required. Clearly, given the mean range of alpha particles, the attenuation factor for individual grains will be strongly dependent on both the mineral size and the concentration of radionuclides within the mineral. Both Fleming (1979) and Bell (1980) calculated attenuation factors for grains of varying sizes, with an 'effective' α dose rate being calculated as the external infinite matrix α dose rate multiplied by the attenuation factor (a) plus the internal matrix α dose rate multiplied by the absorbtion factor (where the absorbtion factor = 1 – a).

A further complication with regards to α radiation exists in its effectiveness at producing luminescence. It is less efficient at producing luminescence than β or γ radiation due to the high ionization density produced by α particles. Luminescence traps in the line of the α particle become saturated and much of the energy imparted by the α particle does not

take part in the trapping process (Zimmerman, 1971). A number of correction models have been proposed that compare the effectiveness of α and β radiation, and derive appropriate correction factors.

Fig 2.14 Alpha attenuation factors (After data from Fleming, 1979)

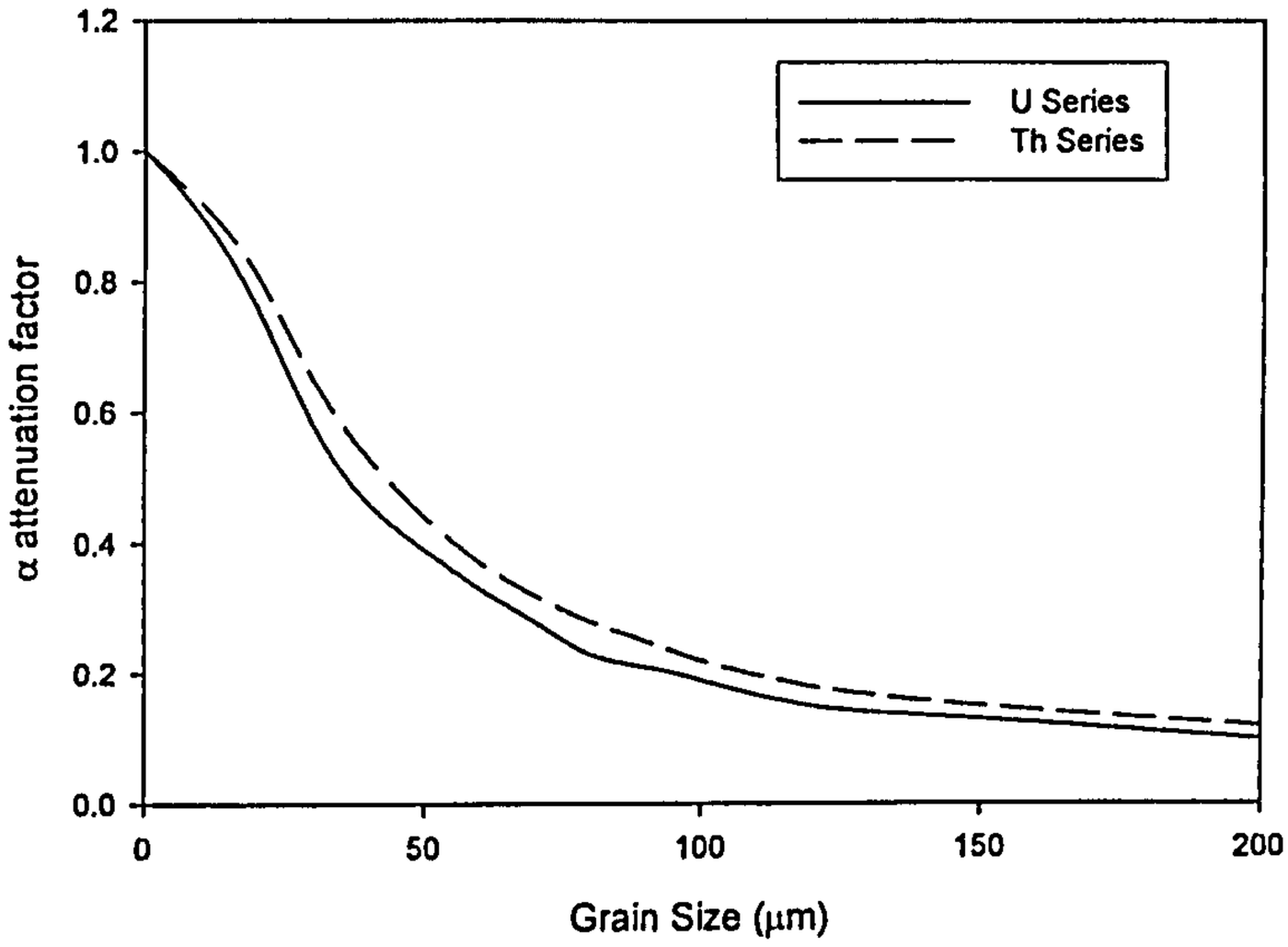

Zimmerman (1971) proposed a 'k-value', defined as the TL per Gy of α radiation divided by the TL per Gy of β radiation. However, further correction was needed to take into account the energy of the alpha source, and an effective k value calculated that compared the alpha source to the natural energy spectrum.

Other approaches involving the comparison of TL per unit α track length (Aitken and Bowman, 1975) and TL per unit α track length per unit volume (Bowman and Huntley, 1984), giving 'a' and 'b' values respectively, were developed in later years reducing the dependance on alpha particle energy. For most dating materials, the relative efficiency is of the order of k=0.15 regardless of the system used. As will be seen in later discussions, etching of quartz grains can all but iradicate the α dose component, however feldspar grains will have an internal component which must be considered.

2.4.4.4 Beta Attenuation

As discussed above, most β radiation is absorbed within 2-3mm of its source in solids. Whilst removal of the outer 3mm of a sample will effectively remove the need for external

β dose rate considerations, attenuation of β radiation by mineral inclusions is an important consideration in the estimate of annual dose rate. Mejdahl (1979) used percentile distances of absorption and scaling procedures to relate attenuation in minerals to calculations made for β dose attenuation in water (Berger, 1971). Mejdahl calculated an absorbed dose factor φ for quartz for a variety of grain sizes, where φ is defined as follows:

$$\phi = \int_0^{t_{max}} [1 - (3/2)(t/t_{max}) + (1/2)(t/t_{max})^3] F(t) dt \qquad (2.6)$$

where $t = x/x_{90}$
x= distance from source
x_{90}= distance within which 90% of radiation absorbed
$t_{max} = D/x_{90}$
D= grain diameter
F(t)= scaled dose distribution

As can be seen from fig 2.15, the attenuation factor is dependent not only on grain diameter, but on relative concentrations of different radionuclides. This is due to the greater attenuation of IC contribution and differences in β energies of U, Th and K products of decay. Where internal β dose rate is not negligible, as in the case of alkali feldspars, self dose fractions can be calculated in a similar manner.

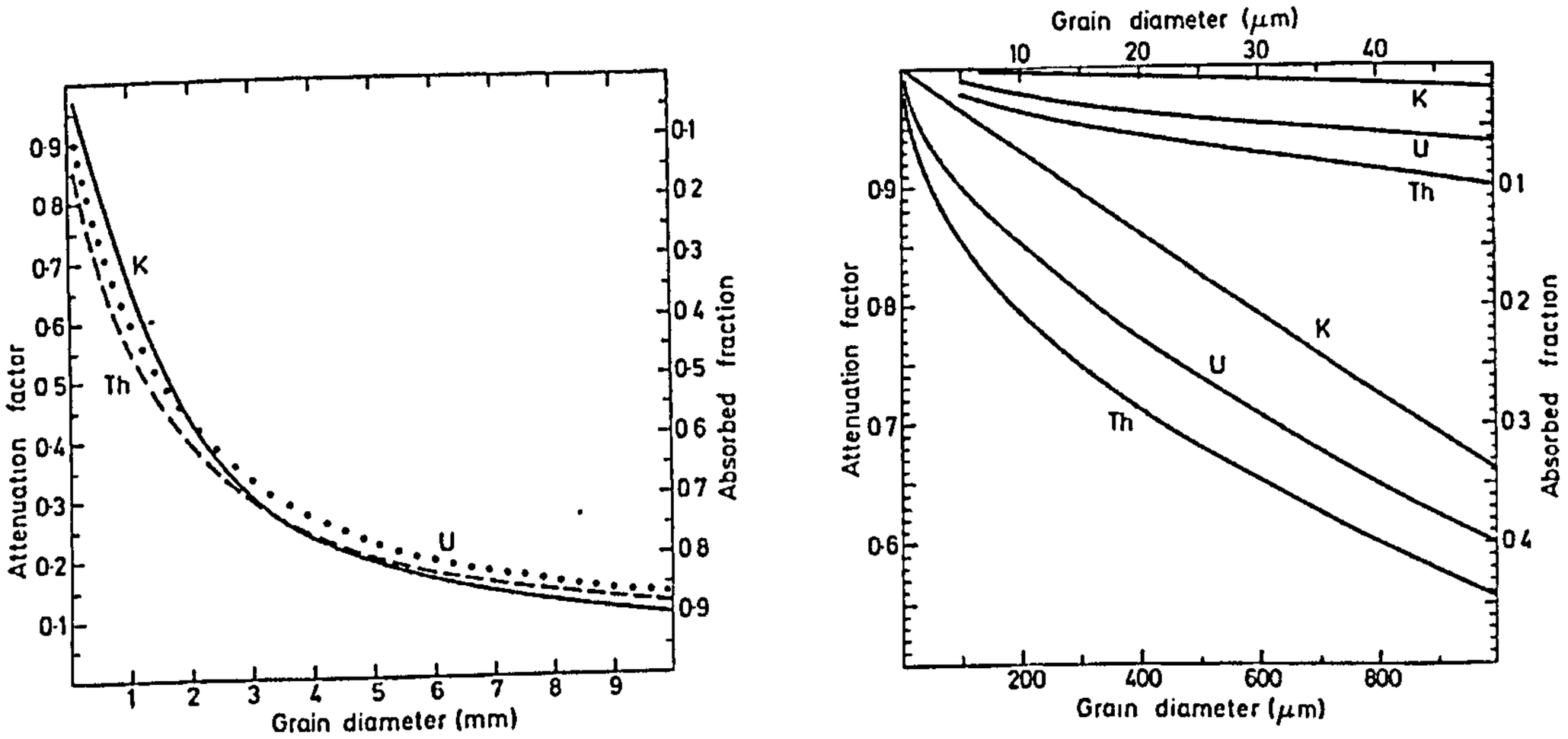

Fig 2.15 Attenuation factors as a function of grain diameter for absorption of β radiation (drawn from tabulated values of Mejdahl, 1979) (from Aitken, 1985).

2.4.4.5 Gamma Attenuation

Due to the larger range of γ radiation, it is not generally subject to the same microdosimetric considerations as differences on this scale are generally negligible. Where the sample and burial context have similar γ dose rates, the external γ dose rate may be used. However, if there is a significant difference between the two dose rates, a grading of gamma dose rates between the two media will occur. The extent to which differences will occur is to a certain extent dependent on the diameter of the sample.

Mejdahl (1983) calculated gamma attenuation factors for stones of varying diameter (fig 2.16). For larger stones the effect may be significant. A similar situation occurs at the boundaries of contexts with varying gamma dose rates (fig 2.17).

Fig 2.16 Gamma attenuation factor variation in stones, for 12ppm Th, 3ppm U & 2%K, stone density 2.6gcm^{-3} (After Data from Mejdahl, 1983)

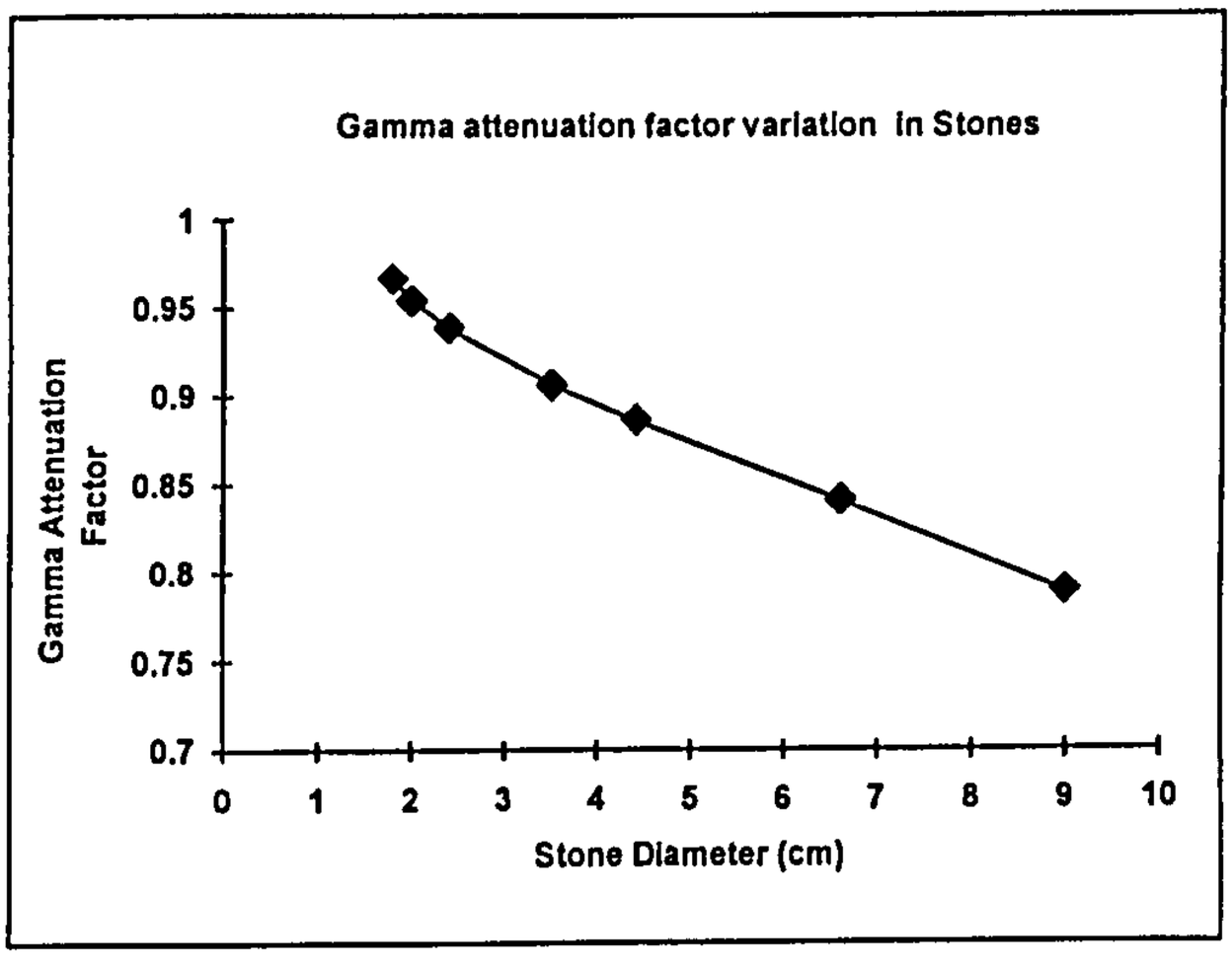

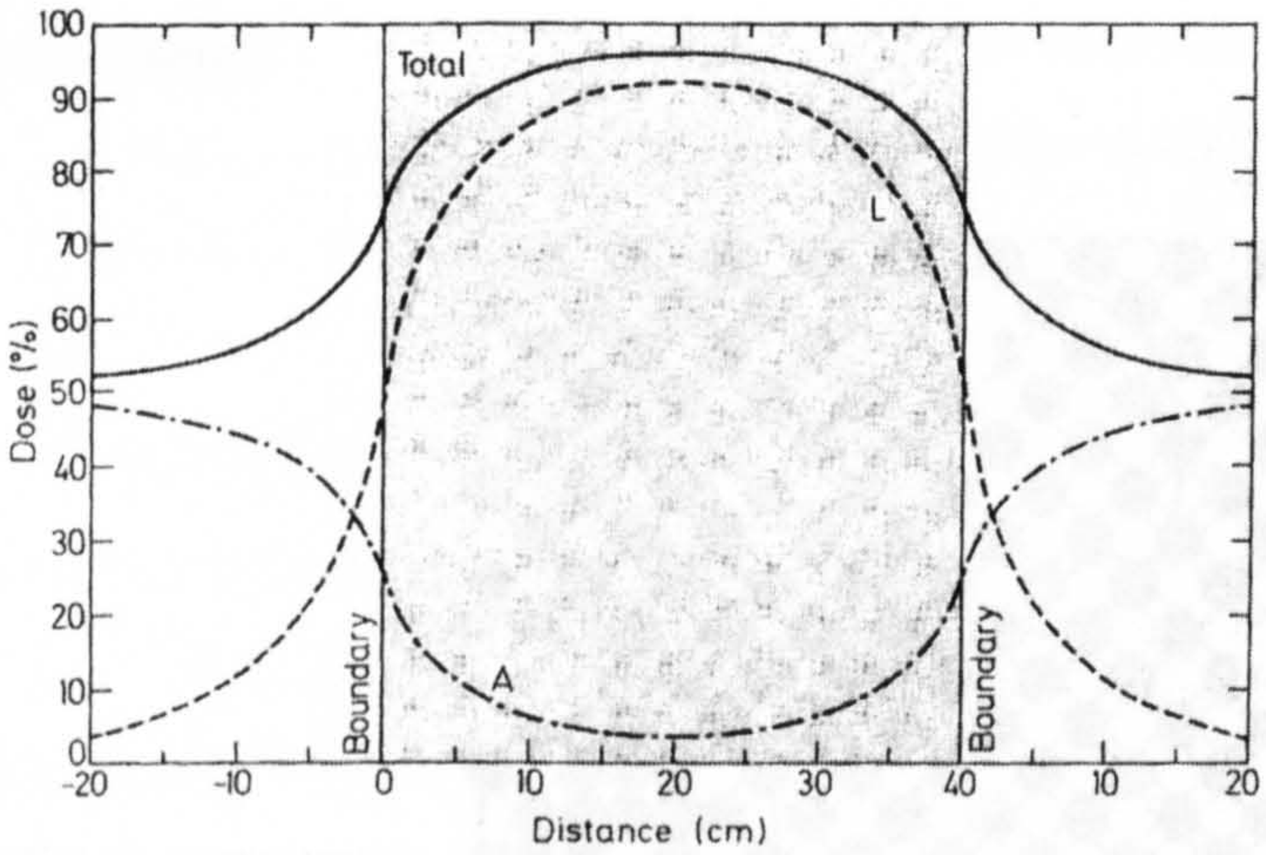

Fig 2.17 Gamma dose for soil layer of thickness 40cm between two soils having half as much radioactivity, expressed as a percentage of the dose in the layer if it was of infinite thickness. Curve L shows the contribution from the layer itself and curve A the contribution from the adjacent solids (From Aitken, 1985).

2.4.4.6 Considerations Specific to Dating Heated Stones

There are a number of microdosimetric considerations relevant to the dating of heated stones which need further consideration. The possibility of gamma attenuation within larger stone samples has already been highlighted as one consideration. On a smaller scale, the distribution of radioactive and non-radioactive minerals may be of issue. Beta dose rate matrix calculations presume a uniform distribution of minerals such that each mineral will receive the 'average' beta dose rate. Clustering of radioactive and non-radioactive minerals such as feldspar and quartz will produce local areas of high and low β radiation (fig 2.18). Such a situation may give rise to a spread in the ED recorded by virtue of the difference in dose rates experienced. The effect will be most pronounced where the majority of the annual dose comes from the matrix β dose rate. Such an effect may also invalidate the age equation (2.1) due to the non-linearity of the beta attenuation equations.

A similar problem may be encountered with regard to the distribution of radionuclides within individual grains. The internal α component of the annual dose again presumes a uniform distribution. If U and Th were for instance located preferentially towards the surface of the mineral, an area which is subsequently removed by etching, the remaining mineral would give an erroneously young age due to overestimation of dose rate. Similarly, feldspar inclusions are known to be present in some quartz. This, if undetected would increase the annual dose received by the mineral, leading to an over-estimation in the age of the material. Again the scale of the effect will be dependent on the percentage

α and β contributions to the total annual dose rate, but should be borne in mind during calculations.

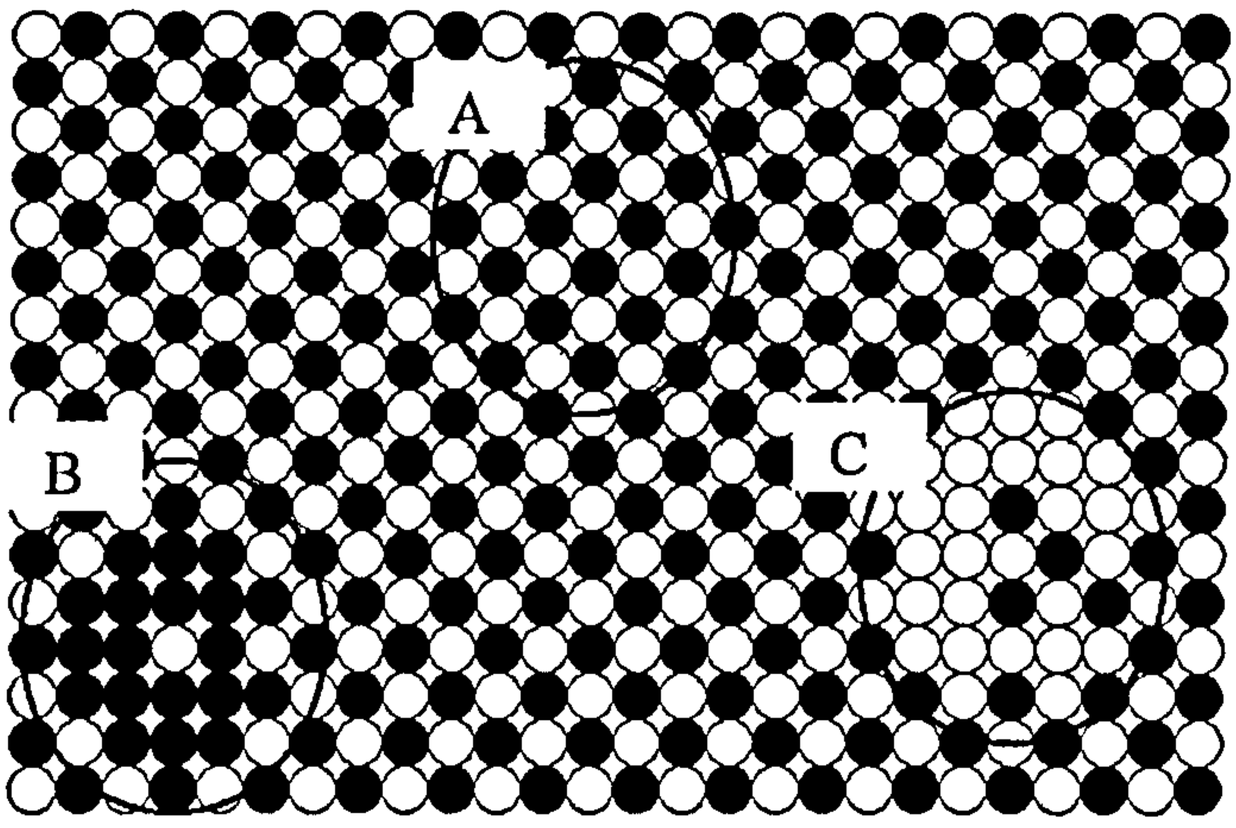

Fig 2.18 Schematic representation of radioactive (black) and non-radioactive (white) mineral distribution within a stone. A represents uniform distribution where the average β dose will be received; B represents clustering of radioactive minerals. The overall β dose in this area will be higher than average, having the greatest affect on the non-radioactive minerals in the vicinity; C represents clustering of non-radioactive minerals where the average β dose rate will be lower.

2.4.5 Measurement of Annual Dose

2.4.5.1 External Contributions

As discussed above, with regard to heated stones, the most significant external contributions to the annual dose are the external gamma and cosmic ray dose.

2.4.5.1.1 Gamma Dose Rates

There are a number of possible methodologies for quantifying the external gamma dose rate. The dose rate may be estimated from samples within the laboratory or from in-situ measurements.

Laboratory based gamma spectrometry is generally a highly accurate way of attaining quantitative data on the relative proportion of radionuclides within a given sample. Where the dating sample is located within a homogenous deposit at least 30cm in spherical volume, such measurements are relatively straight forward though an assessment of the

water content of the particular context is required before information can be converted to effective dose rate. This is potentially problematic due to seasonal variations. The homogeneity of the context may also prove problematic. In the case of burnt stone mounds, it is more convenient to use in-situ gamma spectrometers.

In-situ γ dose rate measurements have the advantage of measuring the dose rate directly, thus requiring no corrections for water content (except in the case where there is reason to believe that the water content in the past has been significantly different from the present day, either through seasonal variation or longer term changes). The requirements of the burial context to be homogenous are also lessened as the measurement is taken from the sample position. In-situ γ dose rate measurement generally takes one of two forms: Gamma thermoluminescence dosimetry (γTLD) capsules that are left in place for a period of time, or gamma spectrometry methods, which give near instant results. There are potential advantages and disadvantages associated with each technique.

γTLD capsules are made from phosphors, generally either fluorite or $CaSO_4$: Dy. They are left in situ over a period of time, generally in the region of a year. Advantages include the ability to compensate for seasonal variations in water content and the relative inexpense of the technique. In addition it is possible to shield the phosphor from the β component of the external sources of radiation. However, due to the different absorption co-efficients for phosphors and dating material, especially in the low energy region, conversion to dose rate can be complex. The long exposure time can also be logistically problematic due to the need to revisit the site and possible disturbance. In addition, modern contributions to the γ spectrum, such as fallout, cannot be isolated so the potential exists for overestimation.

The use of portable gamma spectrometers is a third option in the assessment of the γ dose rate contribution. These are usually NaI crystal scintillators linked either to single or multiple channel counters that can be calibrated to discriminate between different gamma emissions. Where multiple channel counters are used, a spectrum can be recorded and analysed for recent contamination. Careful selection of energy thresholds within single channel models can also identify recent fallout, although this requires two measurements to be taken. The clear advantage in such a system is the rapid measurement time. However,

this does not take account of seasonal water variation. In addition, the detector is generally larger in diameter and therefore requires a larger sampling hole than may be desirable. Careful calibration of the equipment is needed and frequent checks for threshold setting drift is required.

With regards to burnt mound sites, capsules have been successfully used in the past to estimate γ dose rate (Huxtable et al, 1976). In this case the site was under investigation over a number of seasons, thus practical difficulties were not encountered. However, in situations where subsequent visits to sites are not feasible, portable gamma spectrometry would appear the most appropriate method applicable.

2.4.5.1.2 Cosmic Ray Contribution

The cosmic ray dose makes a small but significant contribution to the overall annual dose. As discussed in section 2.4.1, the cosmic ray dose is not constant, but varies with both latitude and altitude. For the majority of Scottish sites however, such effects are minimal.

TLD measurements carried out by Aitken (1969) suggested cosmic ray dose rates to be in the region of 0.28mGya^{-1} at ground level, falling off to around 0.14mGya^{-1} at a depth of 1m below the surface. These calculations were based on measurements within chalk and subsequent revisions have been suggested by Prescott and Stephan (1982) for rock with an average density of 2 gcm^{-3} of 0.185mGya^{-1} at a depth of 0.5m and 0.15 mGya^{-1} at a depth of 1m. In general, a value of 0.185mGya^{-1} is appropriate for most dating samples unless the overburden is greater than 1m in depth.

2.4.5.2 Internal Contribution

2.4.5.2.1 Matrix Dose Rate

For matrix dose rates to be calculated, accurate measurement of water content, and β and γ dose rates are required.

Water content measurements may be made by comparing the dry, saturated and received weight of a sample. For stones, errors are generally small as accurate measurement of each component can be made. Where sediments are concerned, larger errors are involved

due to the difficulties in measuring saturated water content since this is a function of compaction.

The internal beta and gamma components can be determined by a number of direct and indirect methods.

It is possible to measure the beta contribution to the annual dose by means of a thick source beta counter (TSBC) (Sanderson, 1988b). This counter uses a layer of NE102A plastic scintillator to detect β particles, using acetate film to screen out α particles and reference to standards to convert count rates to dose rates. The method is rapid and has proven to be precise. One disadvantage is that no information as to the relative contributions of U, Th and K is given, leading to difficulties in estimating the effects of radon and thoron loss.

High resolution γ spectrometry (HRGS) may be performed on portions of the sample to determine the γ ray contribution. However this requires reference to calibrated standards and counting times may be long for small samples. In addition, to guard against radon loss, samples require sealing for a number of weeks prior to measurement.

β and γ dose rates may also be calculated indirectly by use of alpha counting. The technique uses a zinc sulphide screen which emits light when hit by alpha particles, and the quantity of light emitted measured with a photomultiplier tube (pmt). However, in order to calculate the effective β and γ contributions based on α activity, it is necessary either to assume equal U and Th activities, or to use a 'pair' technique, where the U/Th concentration is assessed by means of identification of the rapidly decaying ^{216}Po component in the Th chain which gives rise, from parent to daughter decay, to two alpha particles in rapid succession. Other methods of ratio estimation have been suggested including energy discrimination (Sanderson, 1979).

2.4.5.2.2 Internal Grain Contribution

The percentage contribution to the annual dose from radionuclides within mineral grains will depend on both the mineral type and on the strength of the external and matrix contributions. In many circumstances the internal contribution will be minimal.

However, in the case of samples where both matrix beta dose rate and external gamma dose are small, the internal contribution may have a significant effect on the age. There are a number of methods which may be used to determine the internal grain contribution to the annual dose.

K content may be estimated by means of flame photometry, X-ray fluorescence and atomic absorption, although the former is by far the least expensive and best established technique (Suhr and Ingamells, 1966). Typical K content of feldspar grains range from 10-13% for K feldspars, to 4-6% for Na feldspars (Aitken, 1985).

Internal U and Th abundance can be measured by a variety of techniques. Neutron activation analysis (NAA) and delayed neutron counting have both been used successfully to determine relative concentrations. Alpha autoradiography may also be used to assess U and Th content if Th/U ratios are assumed. One highly accurate means of determining U and Th content is by use of Inductively Coupled Plasma mass spectrometer (ICPMS) analysis, although in this case cost may be a factor.

2.5 Research Strategy

One of the main aims of this project is to assess the contribution luminescence dating may make to gaining a wider understanding of the chronology of burnt mounds within Scottish archaeology. A summary of current luminescence methodology has highlighted a number of possible avenues of research with regard to the particular techniques that may be employed to date burnt mound sites.

Given the existence of previous luminescence work on burnt mounds in Scotland and elsewhere (Huxtable et al, 1976, Hunter and Dockrill, 1990, Spencer, 1996, Anthony et al, 2001, Eskola et al, 2003, Murray and Medjahl, 1999) it would be wise to take account of procedures used together with any technical difficulties encountered. This would provide a link to past work using well established and validated techniques. These techniques, for the most part, utilized TL multiple aliquot added dose procedures. However, developments in the luminescence field have enabled a number of other approaches to become available which may, if utilized in parallel to these, give added information.

Whilst the original intension of the study by Huxtable et al (1976) had been to pursue coarse grain quartz dating, a lack of suitable material was noted from Orcadian sandstone samples, and consequently a fine grained polymineral MAAD TL approach was adopted. It should be noted that significant fading was reported in a small number of samples.

Anthony et al (2001) used MAAD TL of feldspars in combination with SAR OSL of quartz grains when determining the age of a burnt mound from the Kilmartin Valley. These results agreed well with the one radiocarbon measurement obtained for the site.

Luminescence work outwith Scotland has also focused on OSL dating of heated materials. Eskola et al (2003) used a TL regenerative method for quartz dating where 3 cycles of doses were given after natural readout prior to a fourth repeat point of the first dose. A correction for sensitivity change based on the measured change between repeat points assumed equal steps of sensitivity change at each heating stage. Where sensitivity change was small, Eskola et al reported results in good agreement with other chronological information[1].

Murray and Mejdahl (1999) compared the results obtained from two separate quartz OSL protocols on a group of 16 burnt stone and ceramic samples from 11 sites in Scandinavia and South America. Both SARA and SAR protocols were used, SARA being performed at a single preheat temperature of 220°C for 40s, SAR at a variety of temperatures between 160 and 300°C (though predominantly at 280°C) for 10s. They show no systematic difference in the ED obtained from the two techniques (average ratio of SAR:SARA 1.00±0.02) EDs for SARA measurements were calculated from 2-4 sets of 3 discs per sample. Individual ED determinations on SAR measurements varied in number from 6-39. However, it should be noted that in many cases the error quoted for both techniques is similar in magnitude, suggesting it is not dominated by errors on extrapolation of the SARA line.

[1] The use of TL regenerative methods, as outlined by Eskola et al (2003) was considered, but rejected on the basis that the assumption of equal steps of sensitivity change between heating cycles was likely, in the case of quartz to prove an unreliable method of sensitivity correction.

The use of OSL SAR techniques, may provide new information with regard to the microdosimetric heterogeneity of stones through observed variance of EDs within samples. One key area so far unresolved is the extent to which incomplete zeroing of the geological signal may be identified. Previous comparative work on OSL procedures outlined above (Murray and Medjahl, 1999) did not tackle this issue and any overestimation due to incomplete zeroing is likely to be inherent in both datasets.

S. Barnett (pers. comm.) has previously reported discrepancies in the age estimates of a multiple approach study on c.200 samples of Iron Age Pottery from the British Isles. Whilst quartz MAAD TL results were in good agreement with the expected archaeological age of the sample, SAAD OSL of quartz showed a systematic overestimation of around 25%. In addition, feldspar MAAD IRSL results showed underestimation relative to the quartz TL results in the region of 50-75%.

A multiple procedure methodology, where possible, would seem the wisest approach to this project. A combination of TL and OSL methodologies may together provide valuable information on zeroing issues. In addition, comparison of quartz and feldspar results may shed further light on issues of fading.

By using a combination of different techniques, technical strengths and weaknesses may be explored. In addition, a multiple approach will give wider choice in applicable techniques where varied lithology is encountered.

CHAPTER 3 Background to Burnt Mound Studies and Selection of Sampling Areas

3.1 Introduction

This chapter summarizes current information on the form, function and chronology of burnt mounds in Scotland, documenting possible regional patterns within the existing information. Potential sampling areas are identified with reference to this information.

As outlined in previous chapters, for a sampling strategy to provide useful material for study, the requirements are both demanding and specific. Examination of burnt mounds on the local scale requires a geographically confined area, with a modest density of burnt mounds to provide enough variety, but not one so dense as to render the study unmanageable. Due to the nature of luminescence properties within minerals, itself determined by formation processes and past geological history, such sites should preferably come from an area of simple geology. By attempting to minimize variation of the luminescence response to anthropological activity, differences may be more thoroughly investigated. On a larger regional scale, different issues are encountered. Here, varied geology would be a useful attribute to sampling, as a larger cross-section of material would provide a wider base for technical considerations. At the same time, such sites should be geographically linked if useful archaeological data are to be obtained.

Two study areas are identified within the Orkney and Shetland Islands that conform to these requirements and the distribution of burnt mounds within these areas is examined in greater detail to allow for appropriate site selection.

3.2 Background

> "Burnt mounds are, individually, among the most boring sites with which a field archaeologist must deal. Apart from a new date and a new spot on the distribution map, individual sites have little to contribute to our understanding of the past."
> (Barber and Russell-White, 1990)

Despite being one of the most common types of archaeological sites in Scotland, at first glance burnt mounds appear mundane and predictable in their composition. The lack of artefactual evidence and the general assumption that all represent cooking sites from the Bronze Age period helps to foster this negative image. Yet these apparently 'boring' sites have some remarkable features.

They are widely distributed across much of Northern and Central Europe. Their density in some areas of Scotland exceeds 30 per km^2. Their distinct clusters form patterns along river valleys and coastlines. Their size appears to vary by region. Excavated examples, of which there are relatively few, show large-scale variation in the types of associated features found in their vicinity. Their dating belies a far greater range in age than the Bronze Age period alone. All of these facts suggest burnt mounds to be complex sites that are identified as a group through virtue of their similar appearance yet may have no connection either chronologically or functionally.

3.3 History of Burnt Mound Archaeology

"A most curious class of small cairns" (Anderson, 1873)

Within Britain and Ireland, burnt mounds have been considered as a distinctive type of archaeological site for many years. As early as the 17th century literary references to their purported use can be found.

> "And it was their custom to send their attendants about noon with whatever they had killed in the mornings hunt to an appointed hill, having wood and moorland in the neighbourhood, and to kindle raging fires thereon, and put into them a large number of emery stones; and to dig two pits in the yellow clay of the moorland, and put some of the meat on spits to roast before the fire; and to bind another portion of it with sugans in dry bundles, and set it to boil in the larger of the two pits, and keep plying them with stones that were in the fire, making them seethe often until they were cooked. And these fires were so large that their sites are today in Ireland called Fulachta Fian by the peasantry."
> (From Keating's early 17th Century "History of Ireland"
> Quoted by Ó Drisceóil, 1990)

Whilst it is difficult to assess the value of such detail, it can at least be said that in 17th century Ireland, some were aware of the antiquity and characteristics of Fulachta Fiadh.

In Scotland, antiquarian investigations took place in the mid to late 19th Century (fig 3.1). A number of small-scale excavations were carried out on Shetland in the 1860s, a joint collaboration between the then Earl of Zetland and the Anthropological Society of London. Three sites, Will Houll on Bressay, Harpadale on Yell and Burn, Westerskeld were investigated by J. Hunt, and R. Tate, the results being published in the Memoirs of the

Anthropological Society of London (1866). In the 1870s and 1880s more mounds were investigated. The Rippack on Fair Isle was excavated by Smith around 1883 and reported in the Proceedings of the Society of Antiquaries, Scotland (1882-3). On the mainland, two mounds near Wick were investigated around 1871. An extract from the report of findings is given below:

> "In Caithness there are many examples of a most curious class of small cairns, usually 20 to 30 feet diameter, and 2 to 4 feet high in the centre. They are composed almost entirely of broken stones, a little larger than road metal, say 2 to 3 inches across. These stones are thoroughly burned, and the interstices between them filled with a black unctuous mound, so extremely fine as to be almost impalpable.... We opened two in this neighbourhood at this time; one near Yarhouse Broch, and one near Brounaben Broch, but failed to find any clues to their purpose. Towards the bottom were layers of flat stones, pretty evenly laid above each other, and in the centre of the Brounnaben one was what might have been a short cist, with the sides driven in, but, with the exception of charcoal, cinders, vitrified stones, and a few bits of bones,...we found nothing." (Anderson, 1873, p295-6)

By the end of the 19th century parallels were being drawn between these sites and the fulachta fiadh of Ireland, with the presence of 'cist like' structures sparking debate as to their function (Anderson, 1873).

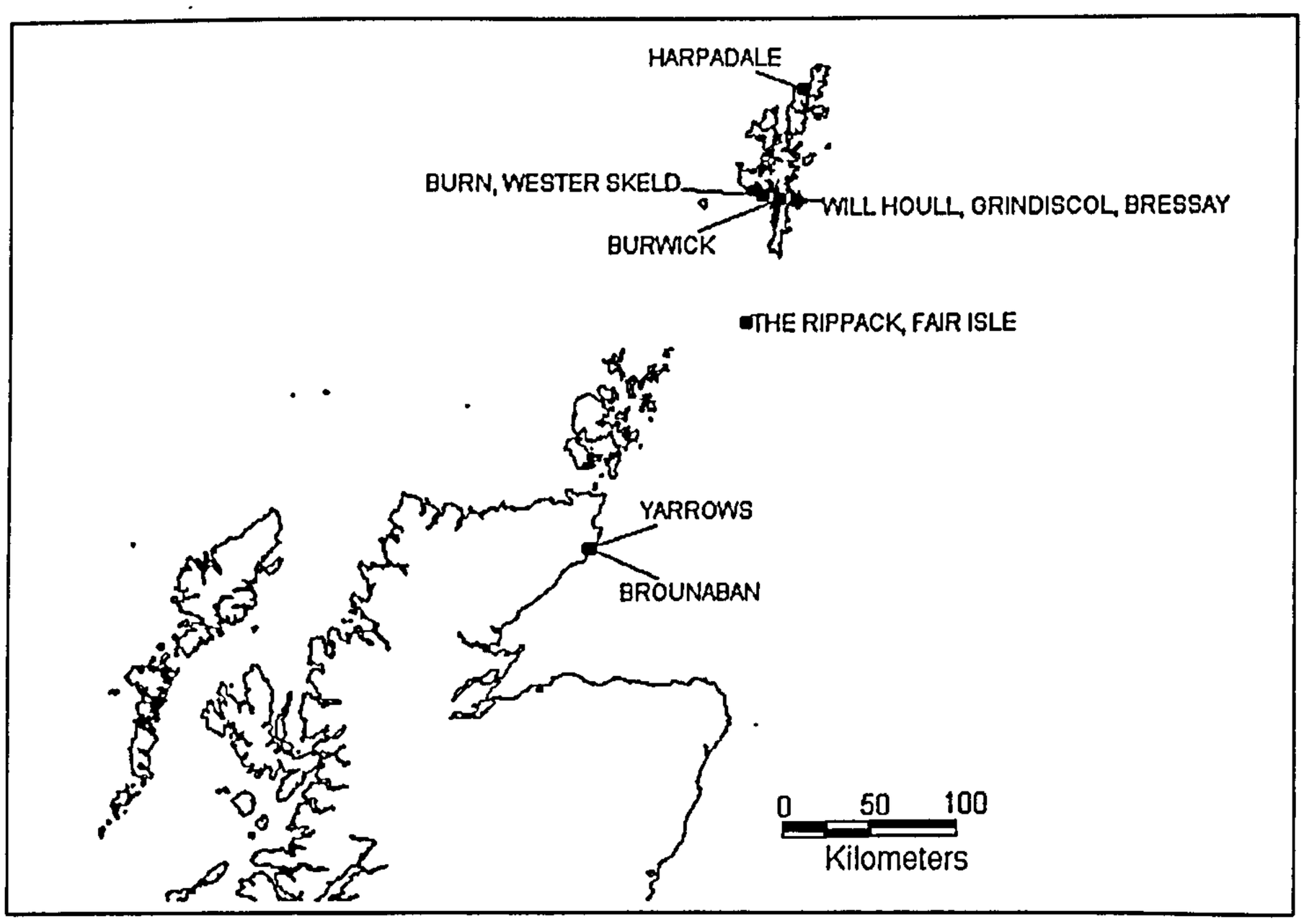

FIGURE 3.1: Location of 19th Century Excavations

From the late 1960s, a number of more wide ranging excavations took place, employing scientific methods of environmental sampling, dating and analysis. Interestingly these raised more questions than answers with regard to the function of burnt mound sites. At the same time, an increasing number of field surveys by the Royal Commission and others greatly expanded the number of known burnt mound. Their records, when examined in detail, show discrete regional differences between the characteristics observed.

3.4 The Burnt Mounds of Scotland

3.4.1 Sources of Information

There are two main sources of information on burnt mounds in Scotland – excavation and survey reports. Fewer than 3% of burnt mounds in Scotland have been examined in detail. Whilst levels of excavation have varied, these reports provide important and detailed information about this class of site. However, the information collected through survey is often the only recorded details available for other burnt mound sites. Again such information is of highly variable quality leading to difficulty in the interpretation of the dataset as a whole. Whilst a valuable source for consultation, a degree of wariness is required when comparing information on different mounds.

Types of information recorded in the sites and monuments records (SMR) include name, location, (varying from 4-8 figure precision) and description. Some confusion has arisen over mis-located mounds from earlier surveys, however it is in the description of the sites that the most variation in the quality and quantity of information is seen. Some sites have no recorded details other than a name and location. Others have varying combinations of size, shape, damage, disturbance, associated features and finds.

The level of preservation of the site may affect the amount of information recorded. A ploughed down site for instance may have little information recorded against it as dimensions and shape are obscured, whereas a site which has been truncated, or damaged so as to expose a section of the mound may have far more detailed description of composition.

The date when individual surveys took place can also be seen to influence the type of data recorded. Some early surveys appear not to comment on the shape of mounds, and only mention upstanding features such as slab built troughs. It is noticeable that in early entries

slab built features tend to be referred to as 'cist like'. Recent surveys often describe such features as troughs, a reflection of current perceptions of burnt mound sites.

However, perhaps the overriding variable is that of the surveyors themselves. The subjectiveness of the description should be borne in mind with regard to mound shape and size. When examining the NMR, it is clear that some surveyors refer to mounds as crescentic, others horseshoe, C, U or banana shaped. All in effect amount to a similar geometry. The measurement of distance across a mound is also subjective. The break of slope is in many cases difficult to ascertain from turf-covered mounds, thus there may be a certain element of over/under estimation in the rough measurements taken (see later section).

In many cases the main purpose of the field survey was not to make a detailed record of archaeological features, rather to record their position within the landscape. As such, any information is, in effect, a bonus.

Further caution is needed when looking at distribution patterns of known mounds within Scotland. Clear evidence for regional clustering of mounds exists. The difficulty in interpreting such data is in the bias folded into such distributional analysis. The vast majority of burnt mounds have been identified through field surveys. Within Scotland therefore it is no surprise that clusters appear in Orkney, Shetland and Dumfriesshire, all areas extensively surveyed by the Royal Commission over the past few decades. The absence of mounds elsewhere may be a true reflection of the original distribution as asserted by Hedges (1977):

> "It is felt that, although this distribution may be filled out to a certain extent by further fieldwork, it is none the less a real one" (p61)

Figure 3.2 shows the known distribution of burnt mounds in Scotland c. 1970. However, a large number of mounds have since been noted in other parts of the country (cf. fig 3.3).

One explanation for the apparent distributional gaps may be that in these areas mounds have been partially destroyed, or covered by sediment or peat. It is noticeable that the majority of mounds recorded on the west coast of Scotland were identified as a result of soil stripping prior to construction work or pipe line extensions, rather than through field survey.

A secondary problem relates to the variable standards of reporting of burnt mounds within survey areas. Halliday (1990) notes of the RCAHMS East Rhins survey in 1987 :

> "The northern field section of the OS had alerted us to the burnt mounds in the north, but we gained little experience in locating or recognizing them until the survey of the East Rhins in Wigtownshire. The survey was conducted over a period of about eighteen months between March 1985 and October 1986. Over the next few months we identified a total of 75, about 60 of them in the last 50 square kilometers to be surveyed. The uneven distribution, with its cluster in the lower reaches of the Luce valley, is unlikely to reflect anything other than the pattern of survey" (p61).

Despite the obvious bias that clearly exists within the collective survey data for Scottish burnt mounds, it is worthwhile examining both the distribution and characteristics of mounds recorded in an effort to identify broad similarities and differences between the groups of sites.

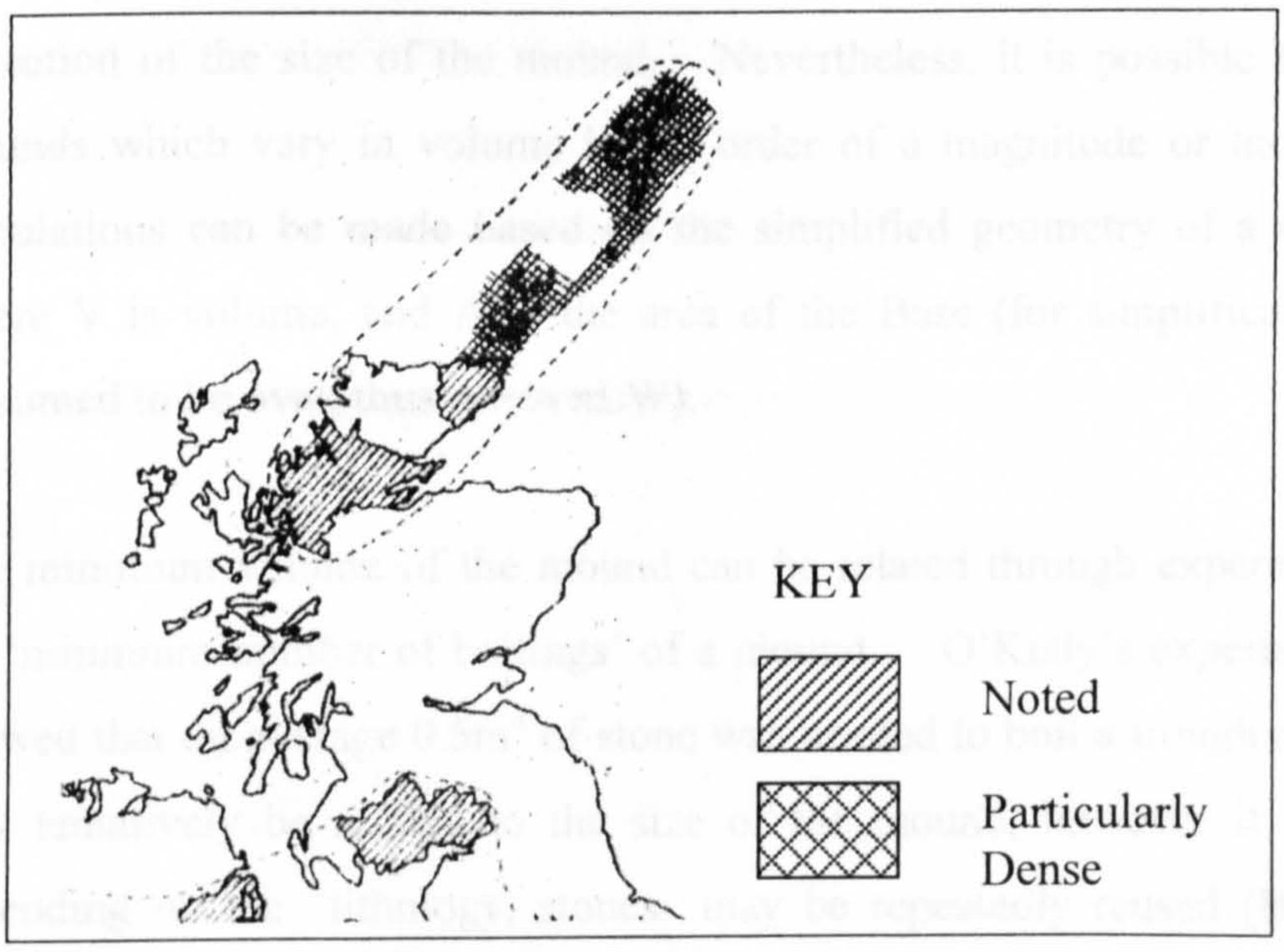

FIGURE 3.2 Distribution of Burnt Mounds in Scotland c. 1975 (from Hedges, 1977)

3.4.2 Overview of Scottish Distribution and Characterization

As outlined above, there are four main clusters of mounds in Scotland in Orkney, Shetland, Dumfriesshire and Galloway and the Borders and Southern Uplands (fig 3.3). The known distribution of burnt mounds shows variable concentrations (fig 3.4). Notable absences occur along the western coast of Scotland, with only a few examples so far recorded (see Appendix A for regional distribution and density maps).

Of the 1900 recorded mounds in Scotland, over half have associated comments regarding their shape. Fig 3.5 shows the relative proportions of mounds of varying shape. By far the most common geometry is the crescentic mound[2]. Circular and oval shaped mounds are the only other common shapes reported. Others, such as pear-shaped and triangular individually form less than 1% of the total. The significance of the shape of the mound is somewhat uncertain. The crescentic form is often thought to arise as a result of the discard pattern of clearing out the trough – a crescent forms around the trough, with its opening lying in line with the firing area. Whether oval and/or circular mounds represent a developed form of the crescent towards the end of a site's use, or reflect a differing function, is unclear.

Calculation of the overall volume of material in recorded mounds is problematic. Around 65% of mounds have associated height (H), width (W) and length (L) measurements. As discussed, the accuracy of such measurements is unlikely to be high as a result of the difficulty in estimating sub-surface dimensions, and should not be thought as a true reflection of the size of the mound. Nevertheless, it is possible to distinguish between mounds which vary in volume by an order of a magnitude or more. Rough volumetric calculations can be made based on the simplified geometry of a cone, where $V=\frac{1}{3}HA$, where V is volume, and A is the area of the Base (for simplification purposes, base is presumed to be oval, thus $A= \frac{1}{4} \pi LW$).

The minimum volume of the mound can be related through experimental archaeology to the 'minimum number of boilings' of a mound. O'Kelly's experiments (O'Kelly, 1954) showed that on average $0.5m^3$ of stone was needed to boil a trough of water. This figure may tentatively be related to the size of the mound, however it has been shown that, depending on the lithology, stones may be repeatedly reused (Buckley, 1990). This, combined with assumptions relating to volumetric calculations is likely to provide significant underestimation. Nevertheless, the results are informative (fig 3.6). They show the vast majority of mounds to be $<20m^3$. A small but significant number of mounds do however appear far greater in volume, the largest, Vassetter on Fair Isle, calculated at over 900 m^3.

---

[2] For the purposes of this discussion, all mounds described as crescentic, C, U, horseshoe or banana shaped have been grouped together.

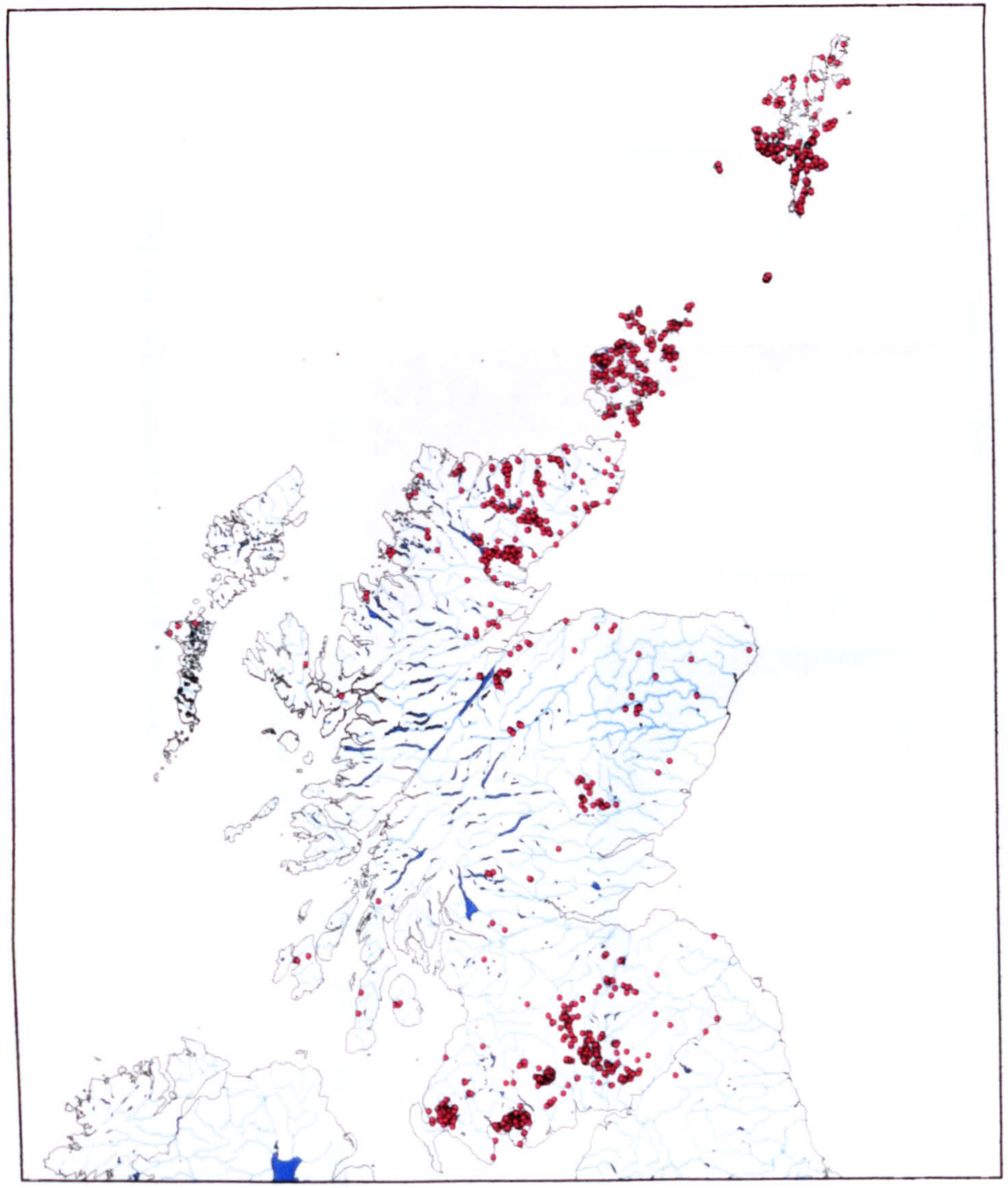

Figure 3.3: Distribution of Burnt Mounds, Scotland (Data from RCAHMS CANMORE Database)

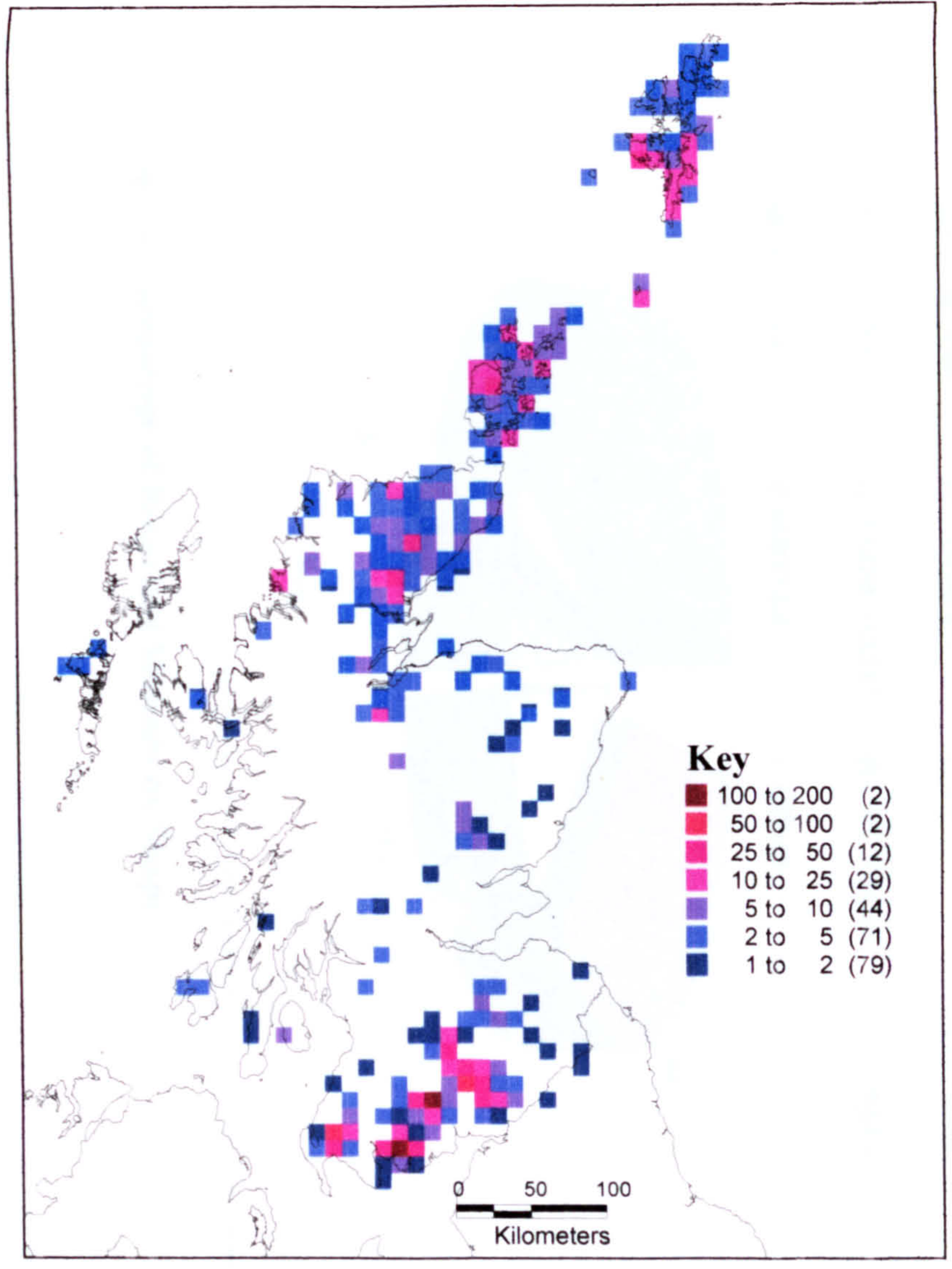

Figure 3.4 Density of Burnt Mounds in Scotland per 100km^2

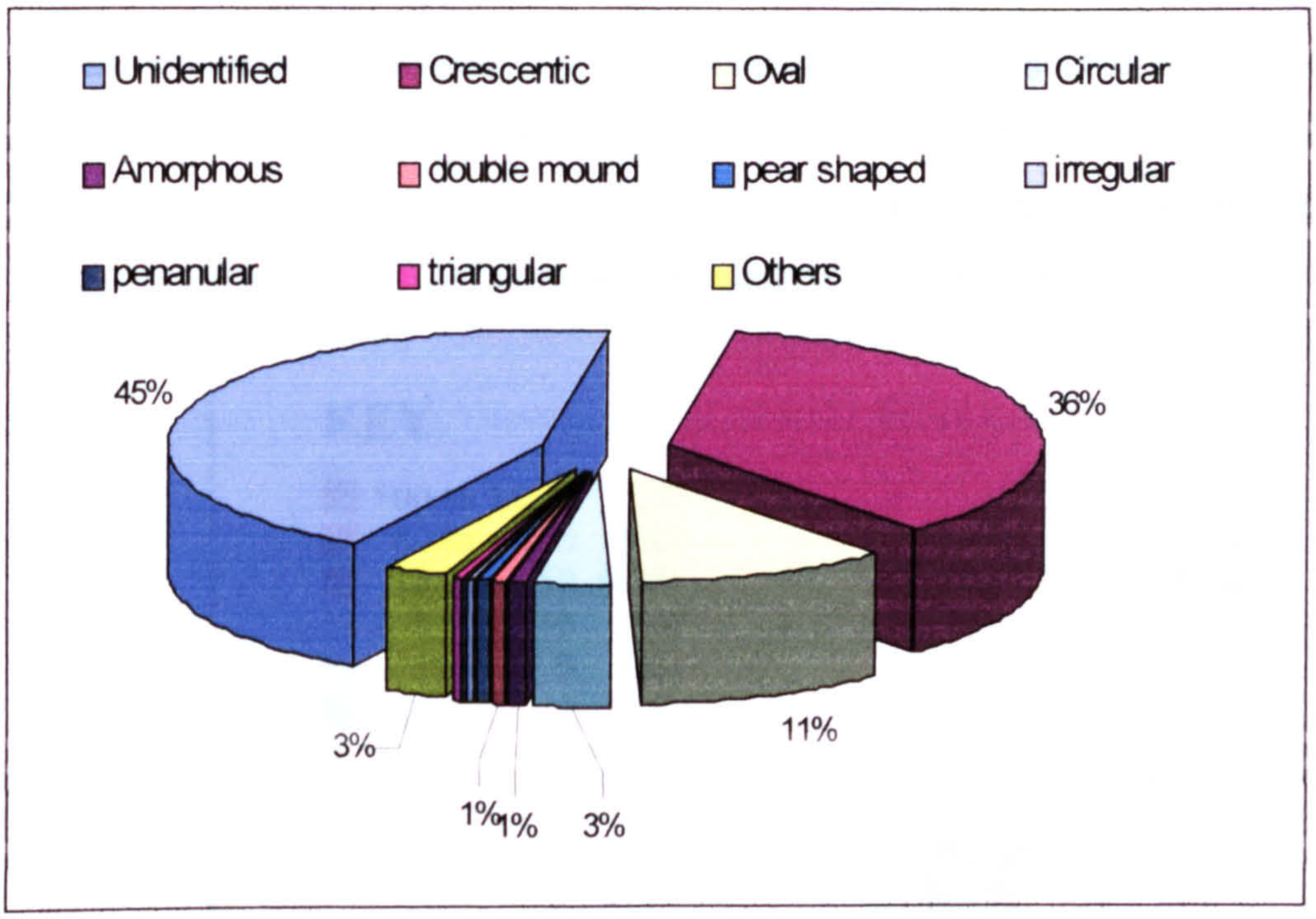

Fig 3.5 Percentage of Recorded Mounds by Shape

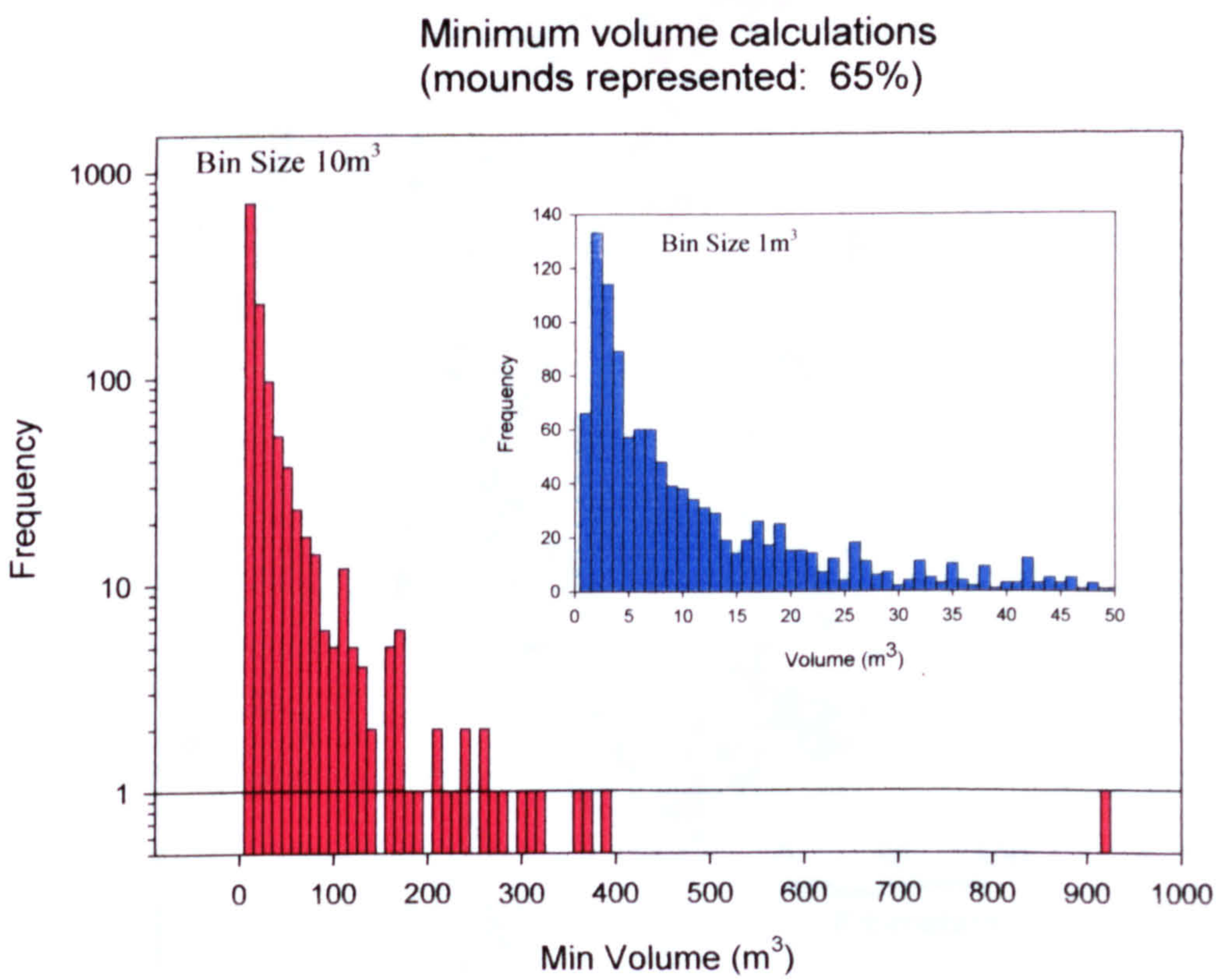

Fig 3.6 Minimum Volume Histogram

When viewed geographically, a general trend in the size of mounds can be seen, with smaller mounds located in the south and larger mounds in the north of Scotland and Northern and Western isles (fig 3.7). The smaller mounds appear more densely concentrated and it possible that these reflect short- lived sites, with mounds in the north being used over a longer time.

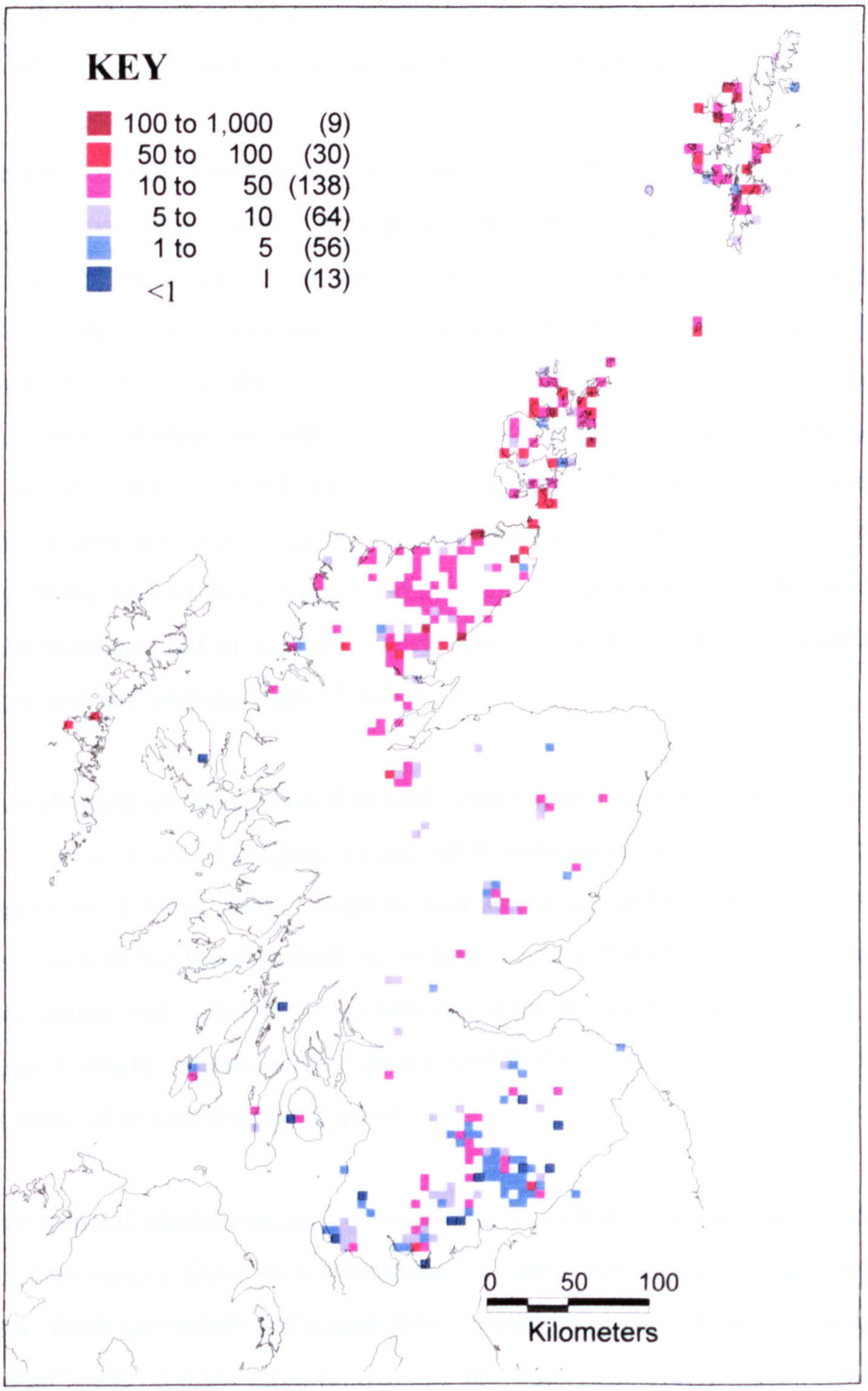

Fig 3.7 Average Volume (m^3) of mound per 25km^2

Further differences can also be found within unexcavated sites in the SMR. Fig 3.8 shows the distribution of unexcavated sites where structural features have been noted. These are closely confined to the far north of Scotland. Sites where hollows thought to be pits[3] have been identified are more widespread, but concentrated further south (fig 3.9). Whilst it is possible that this observation reflects differences in the collection of survey information, examination of the records from excavated mounds shows a similar pattern.

Excavated mounds on the Northern and Western Isles and North of Scotland (fig 3.10) show broad similarities with one another, with predominant features of stone built structures and slab lined troughs (table 3.1). The site of Tangwick, Eshaness is a good example of the complexity with which some sites have been constructed (fig 3.11). Here excavation revealed several phases of activity on the site, with a multi-cellular structure partially built into the mound and evidence of repair and replacement of paved areas and hearth stones noted (Moore and Wilson, 1999). Burnt mounds excavated at Lairg contrast with this situation. Whilst a number of associated pits were located, no clear structural evidence was found (McCullagh and Tipping, 1998). Indeed this group of mounds appear similar in nature to excavated burnt mounds in the southern half of Scotland, where there is far less evidence of permanent stone built structures and site phasing (fig3.12/ table 3.2).

Clearly the small numbers of excavated mounds make interpretation of these regional patterns problematic. Barber (1990) suggests a fourfold classification for burnt mounds based on the relative proportion of burnt mound material and settlement debris. Here traditional 'burnt mound' sites, such as the fulachta fiadh of Ireland would fall into class 1. These sites have no direct association with settlements. Class two occur in clusters of mounds. Class three refers to mounds where structures have been found in direct association, and class four sites where burnt material is found within deposits.

Whilst Barber himself admits that such classification is at best "arbitrarily selected points on a continuum which ranges from sites which are all burnt mound material and no settlement debris to sites which are mainly settlement debris containing relatively small amounts of burnt mound material" (p99) it does serve to illustrate the wide variety of situations in which burnt stone deposits are found.

---

[3] These hollows may also be the result of stone robbing in some areas.

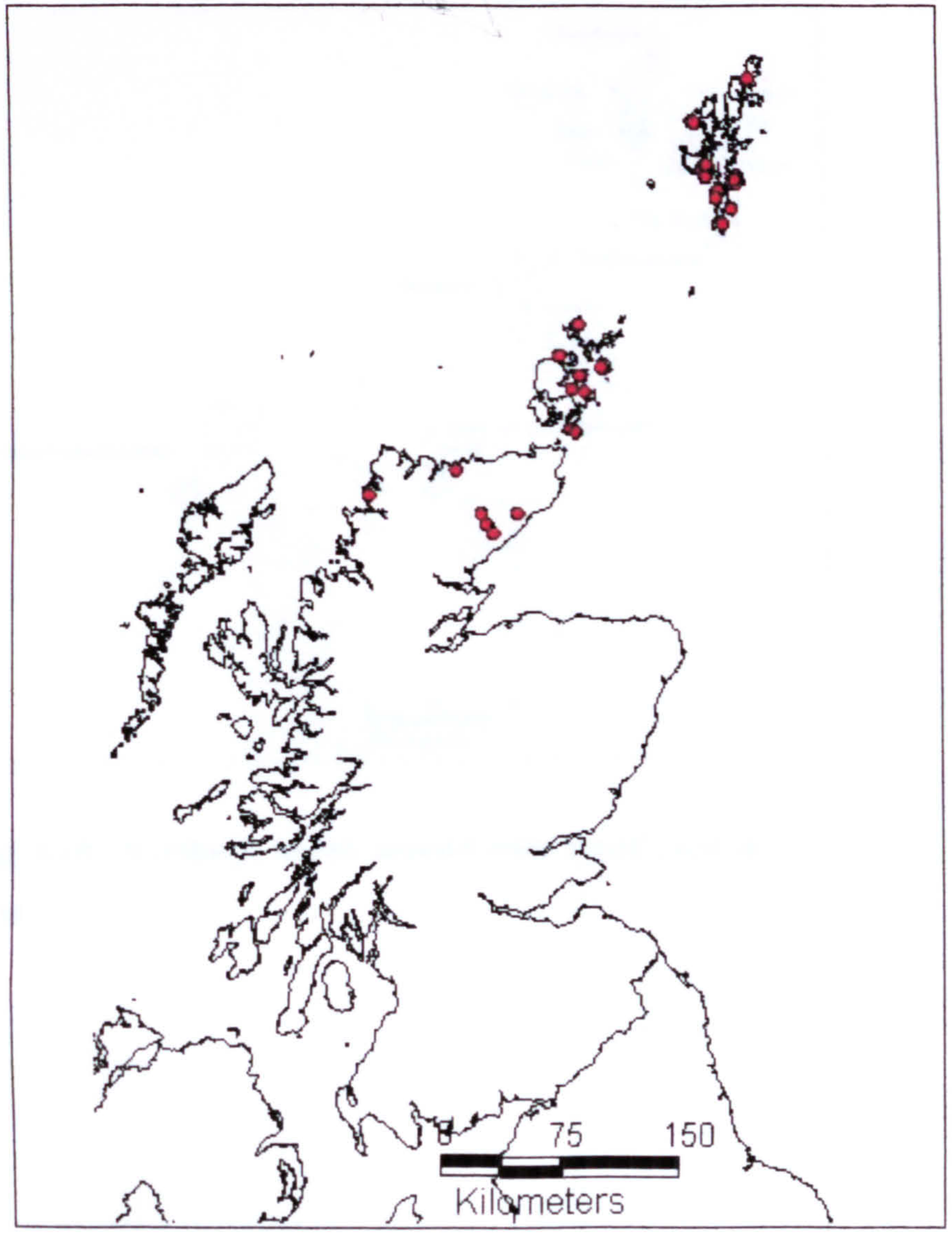

Fig 3.8 Distribution of unexcavated mounds with noted structural features (Data from RCAHMS CANMORE Database)

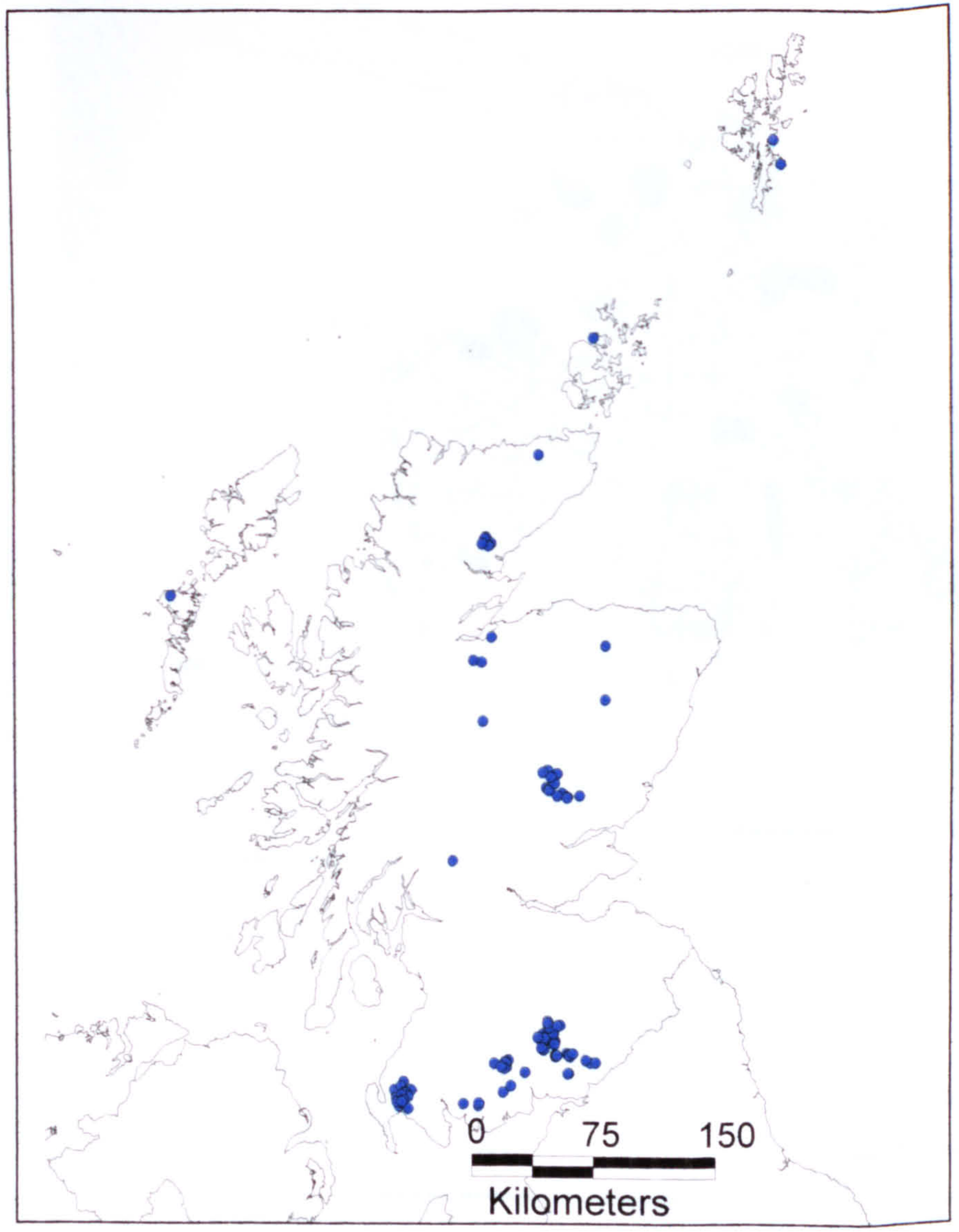

Fig 3.9 Distribution of unexcavated mounds with noted 'hollows' (Data from RCAHMS CANMORE Database)

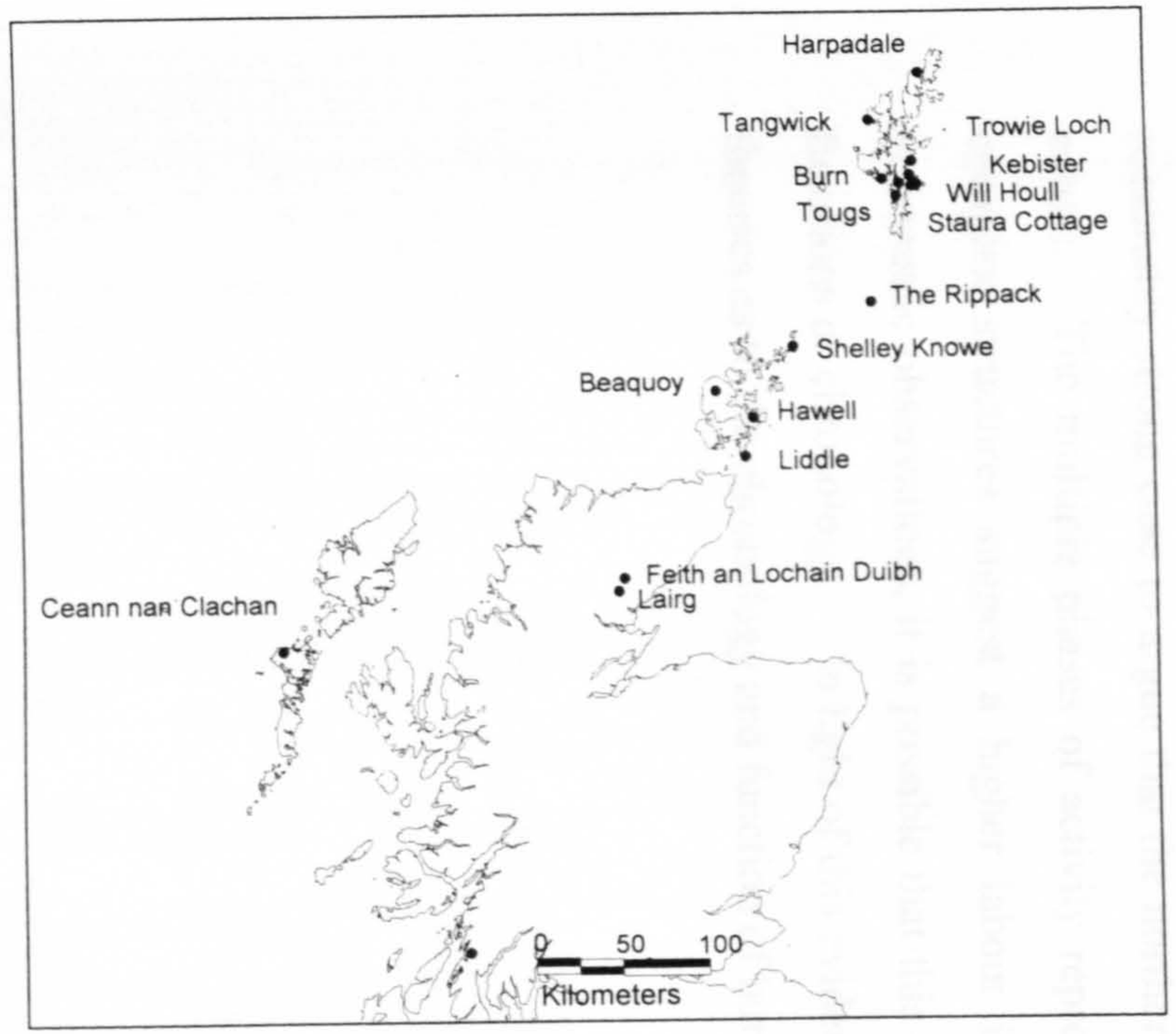

Fig 3.10 Northern burnt mound sites mentioned in text

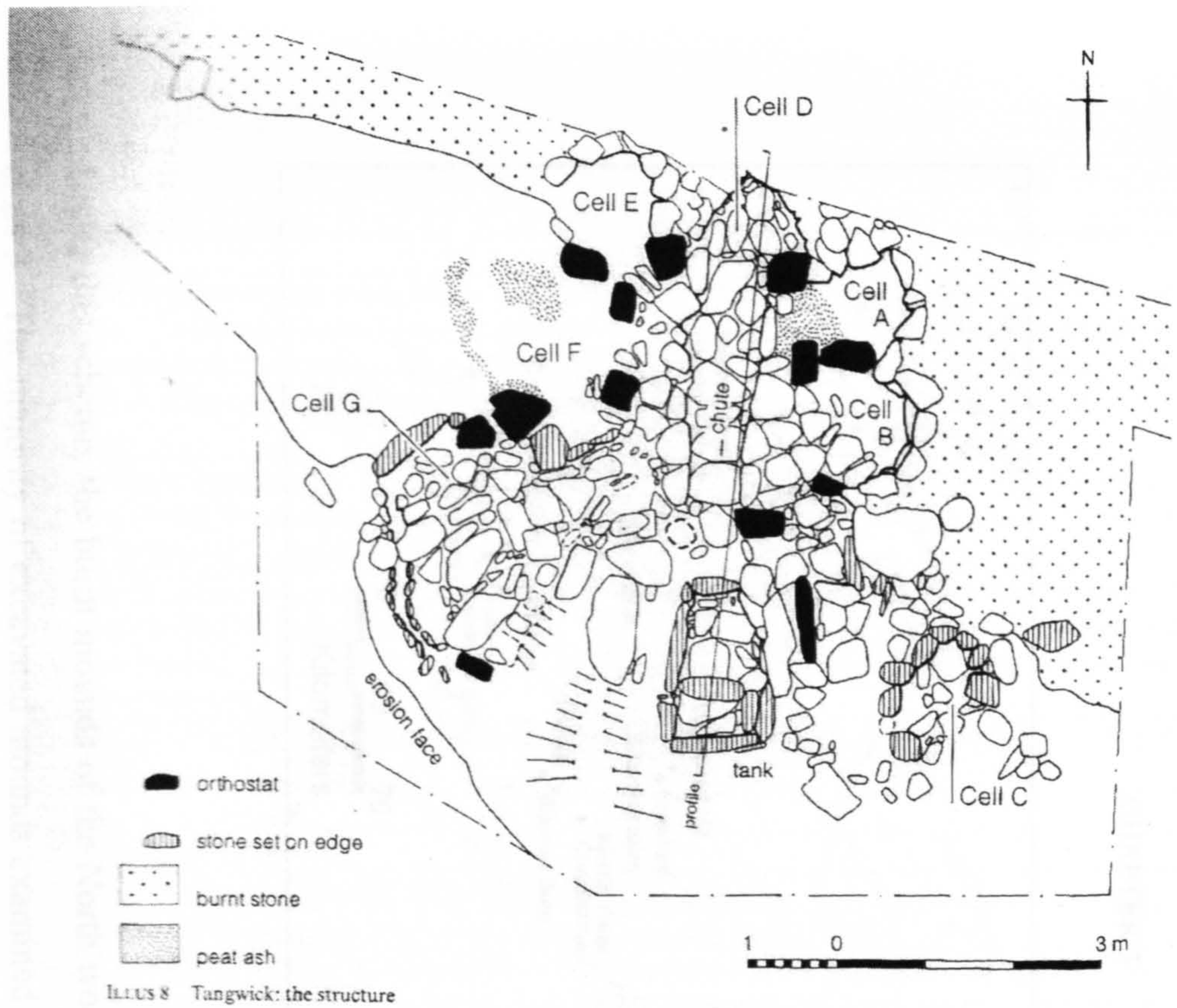

ILLUS 8 Tangwick: the structure

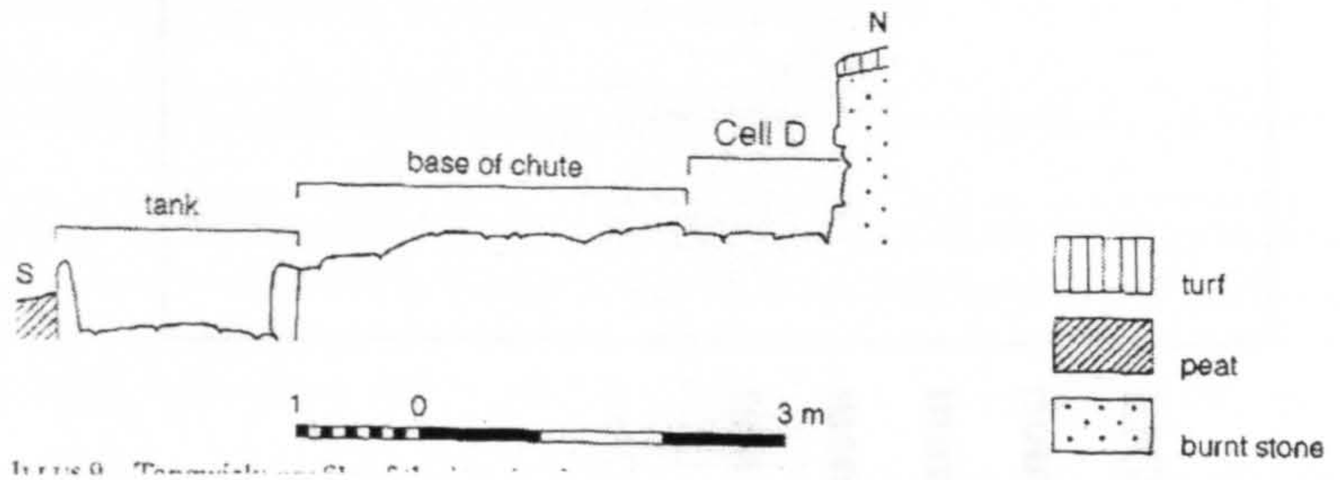

Fig 3.11 General site plan of Tangwick Burnt Mound, Eshaness, Shetland (From Moore and Wilson, 1999).

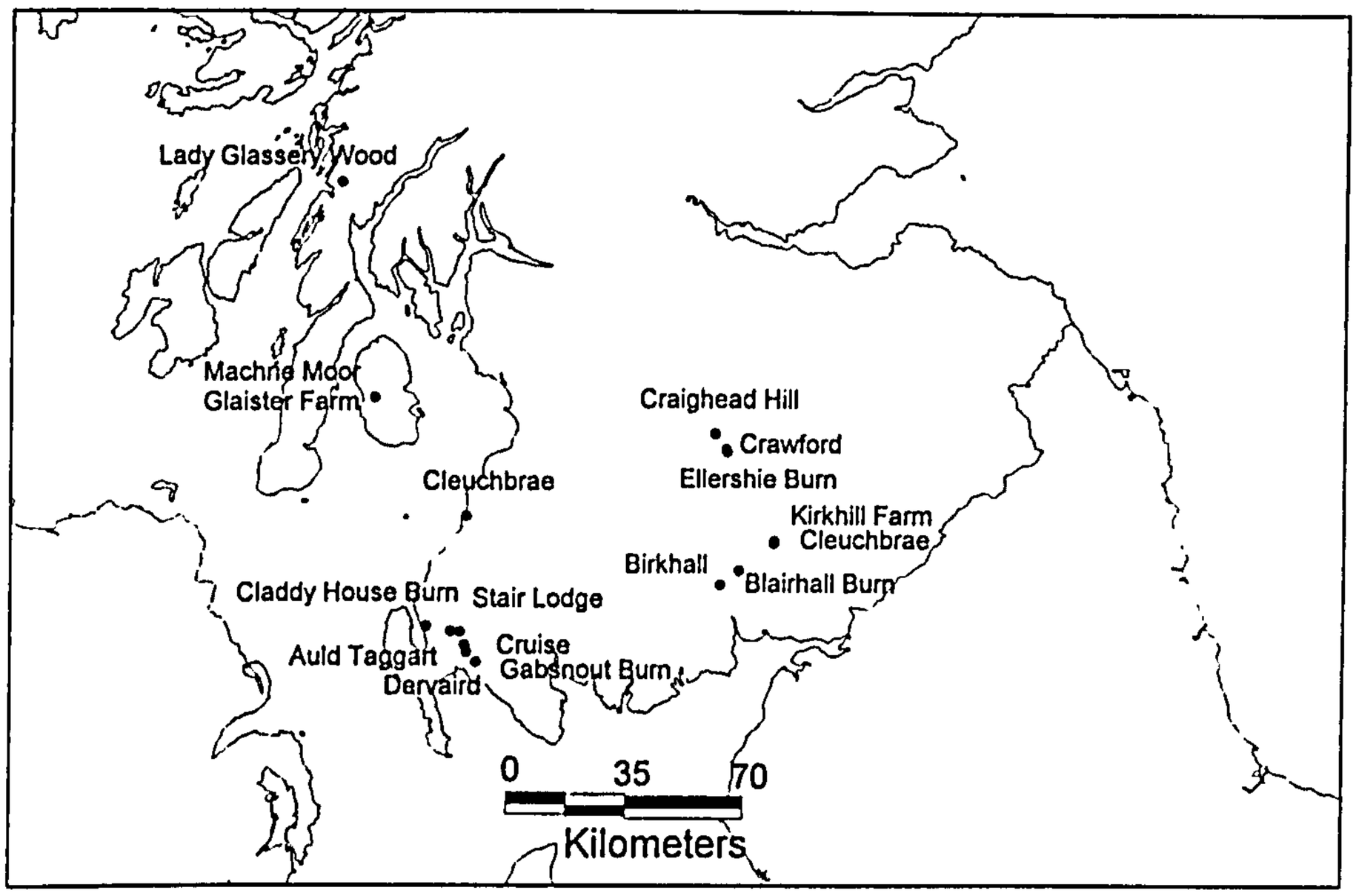

FIG 3.12 Southern burnt mound sites mentioned in text

Under this scheme, the burnt mounds of the North would appear to fall, at least in part, into class 3. The majority of excavated mounds examined elsewhere in Scotland are more likely class 1 and 2. Whilst an interesting observation, such classification does little to explain the observed differences noted. Not withstanding the fact that there may have been differences in local building traditions and availability of durable material, there would appear to be a reasonably strong case to argue that the northern mounds appear in general different in their nature. The multiple phases of activity represented at many of the sites, combined with complex structures suggest a higher labour input and permanence. Coupled with volumetric observations, it is possible that this group of monuments may represent differing functions or chronology. In light of this evidence, it would be prudent to summarize current theories as to the chronology and function of burnt mounds.

Table 3.1 Summary of investigated sites in Northern Scotland

Site	Reference	Summary/Details
Tangwick, Eshaness, Shetland	Moore and Wilson, 1999	Investigation revealed complex structures hidden below the present day storm beach (fig 3.10). Two phases of activity were identified within the mound. The primary mound deposit formed phase 1, with a secondary mound deposit and structures partly overlying to form phase 2. The structure had been partially built into the burnt mound and comprised a central paved floor linking a hearth cell to a stone lined tank at the southern end. Six further cells were also found. Evidence of repair to the paved area and to the hearth was also noted. Finds from the site included a large quantity of pottery and stone objects.
Tougs, Burra Isle, Shetland	Hedges, 1986	Remains of a building, rectangular in shape, on the southern extremity of the mound. Double skinned walls over 1m thick enclosed a space of approximately 6.4m x 5.6m. Within this space was found the remains of a hearth and trough. Both were slab lined and covered with burnt stones. A number of cattle bones found within the trough, together with cereal grain.
Tougs, South Nesting, Shetland	Dockrill et al, 1998	Both a hearth and rubble-filled pit were found between the arms of a crescentic mound. Stratigraphic evidence suggested the site may have had several phases of use. The located hearth was itself sealed by upcast from the nearby pit, leading the excavators to suggest a secondary hearth may be present in an unexcavated area of the mound. A central depression in the mound was found to be the remains of "a substantial structure" composed of flagging and upright orthostats.
Will Houll, Shetland	Hunt, 1866	Form of structure near to the base of the mound, formed of large stone slabs, possibly representing the remains of a trough. A "handled stone implement" was also found in the deposit
Westerskeld, Shetland	Hunt, 1866	Evidence of slab built structures.
The Rippack, Fair Isle	Smith, 1833	A 'cist like' structure formed from slabs found associated with the mound
Kebister, Shetland	Lowe, 1990	Two burnt mounds were partially excavated at Kebister. Hints as to possible structures were seen.
Liddle, Orkney	Hedges, 1977	Evidence of a hearth and several small cells, together with a drainage gully were found alongside a slab built trough.
Beaquoy, Orkney	Hedges, 1977	At Beaquoy, disturbance from later buildings produced a certain amount of ambiguity. Two 'houses' were identified. The primary 'house' was the most disturbed however remains of a flagstone floor and hearth were found, together with an infill of burnt stone. The secondary 'house' appeared to be built on top of the existing mound of burnt stone, with a clay lined trough and well like structure identified.
Shelley Knowe, Sanday, Orkney	Hunter and Dockrill, 1990	Results of the magnetometer survey suggested structural remains to be present to the south-west of the mound.
Hawell, Deernes, Orkney	RCAHMS, 1946	Reports of a slab built structure with several compartments, close to a slab built trough. Past owner also reported encountering a drain running in the direction of the trough.
Ceann nan Clachan, North Uist	Armit and Braby, 1995, 1996, 1997	Multi-phased site – Phase 1: an oval building with hearth, paved area and covered drain. A large amount of burnt stone was found to have accumulated around this structure. A small amount of pottery was also recovered. Phase 2: A structure composed of 3 connecting cells, the most easterly containing a hearth together with evidence of a timber partition. Later modification and reuse of this building formed phase three. However, the extent to which phases 2 and 3 involved 'burnt mound' activity is unclear.
Feith an Lochain Duibh, Clyne	RCAHMS, 1995	A large stone lined trough, together with a stone lined water channel has been recorded. Traces of stone structures within the body of the mound also hint at further structures.
Lairg, Sutherland	McCullagh and Tipping, 1998	A number of mounds were excavated Many were found associated with pits, however no clear structural evidence of the sort seen elsewhere was identified.

Table 3.2 Summary of investigated sites in Southern Scotland

Site	Reference	Summary/Details
Machrie Moor, Arran	Lehane, 1990	A number of mounds on Machrie Moor, Arran were investigated in the late 1980s. An unlined trough was found within the arms of the crescentic mound at NGR 8997 3438 (mound 8). Despite excavation of several areas around the mound, no associated structures were found. A similar situation was encountered at three other mounds on Machrie Moor, though clay lining was present in the trough in some cases.
Glaister Farm, Arran	Lehane, 1990	Three burnt mounds visible in stream section, one of which was positively identified as having a trough
Lady Glassary Wood, Kilmartin	Abernethy, 1998 Anthony et al, 2001	A small burnt mound in the Kilmartin Valley, Lady Glassary Wood, was found to be crescentic in shape, forming a shallow deposit. No associated structures were found, though the extent of excavation was limited.
Dervaid, East Rhins, Dumfries & Galloway	Russell-White, 1990	Large crescentic mound with 'cooking pit' was located between the arms of the mound. The pit was partially lined with stone and had utilized a large oak timber on the base to preserve the boulder clay lining beneath. No other structures were found, though the extent of excavation was limited.
Auld Taggart, East Rhins, Dumfries & Galloway	Russell-White, 1990	Crescentic shaped mound with associated trough between the arms. Evidence of a platform and some kerbing. No other structures or finds were located.
Other mounds in East Rhins area, Dumfrie & Galloway	Russell-White, 1990	Hints of a trough were seen at Cruise. Stair Lodge, Gabsnout Burn and Claddy House Burn were recorded in section and sampled, but due to the limited nature of the investigation, no associated features were found.
Chapeldonan, Dumfries & Galloway	Speller et al, 1997	A number of watching briefs revealed 5 ploughed down burnt mounds. Despite the level of damage, a trough with associated post holes was found at one, and a pit, possibly the remains of a trough, at another.
Birkhall, Dumfries & Galloway	Maynard, 1993	Two pits were located amongst the oval mound at Birkhall. Both were filled with burnt stone and charcoal.
Crawford, South Lanarkshire	Banks, 1999	Two mounds were excavated in advance of motorway construction at Crawford. At the northern mound, a sub-rectangular trough was found between the arms of the crescent. No lining was apparent although the excavators noted the trough held water during rain. A large dump of material appeared to have accumulated over the trough, suggesting it may have gone out of use during the later activity on the site. A small deposit of unheated stones, larger than average, was found close to the trough, possibly a dump of unused heating stones. A similar trough was found at the southern mound, together with a line of stake holes, tentatively interpreted as a possible screen or windbreak. Other than a few pieces of indistinct pottery, no finds were made.
Kirkhill Farm, Dumfries & Galloway	Pollard, 1993	The remains of a truncated burnt mound were found close to a Mesolithic flint scatter and possible settlement. Though badly disturbed by a modern pit, the remains of a trough was located on the southern side. A number of lithics were found within the matrix of the mound, though the excavator now believes these to represent residual material from an earlier site.
Cleuchbrae, Dumfries & Galloway	Duncan and Halliday, 1997	A large oak baulk was recovered from the base of the trough found associated with this mound.
Ellershie Burn, South Lanarkshire	Ward, 1992	Possible evidence of kerbing recorded.
Craighead Hill, South Lanarkshire	Ward, 1992	Two boulders protruding from the summit of the mound are suggestive of some form of structure.

3.5 Existing Chronology

3.5.1 Assumptions and the nature of available evidence

The overriding assumption with regard to the chronology of burnt mounds is that they represent features that date to the Bronze Age period. A lack of artefactual evidence and site stratigraphy has led to reliance upon this assumption. In addition, duration and site formation are not often considered, unless structures with obvious phasing are present. In many cases the only way to accurately date burnt mound sites is through radiometric methods. There are potentially two techniques that can and have been utilized; luminescence and radiocarbon dating.

Luminescence dating is not widely utilized in the field of burnt mound archaeology. With the exception of two burnt mound sites on Mainland Scotland, the technique has been confined to use on the Orkney Islands, most notably by Huxtable et al (1976). The more commonly applied technique is that of radiocarbon dating.

^{14}C is a rare carbon isotope produced in the upper atmosphere by the interaction of cosmic ray neutrons with ^{14}N. It is radioactive, hence decays with time. Entering plants through the uptake of carbon dioxide in photosynthesis, it then passes into the food chain hence is present in all organic matter. Carbon dating operates on two main principles: that over time there has been a constant level of ^{14}C in the atmosphere which mixes instantaneously on production; and that the carbon exchange with the biosphere ceases at the point of death. At this time, carbon begins to decay, hence measurements can be taken by 'counting' the remaining ^{14}C. However, during the past, the level of ^{14}C production has not remained constant due partly to changes in earth's magnetic field and so reference to a calibration curve is needed.

In relation to the ^{14}C dating of burnt mounds, wood in the form of charcoal and seeds are utilized. Whilst an abundance of material is often present, there are major concerns relating to the security of the sampling context. The 'old wood' problem is common to the dating of all types of archaeological sites. This is where, when wood or charcoal is dated, the age obtained is the date at which the particular section of tree rings was laid down. In long lived species there may be a considerable time lag between this age and the date at which the material was utilized as a fuel source or lining material. In some cases this may amount to several hundred years. Due to this, there has been a movement away from bulk charcoal

dating to that of single entity AMS dates on short lived identified material (Ashmore, 1999). Whilst this enables long-lived species to be avoided, it arguably contributes greatly to a secondary problem more specific to burnt mounds, relating to large voids formed due to the clast size of the stone deposits. This enables the filtration of small charcoal and seeds down through the deposits (Hedges and Gowlett, 1986). As such, the positioning of particular entities may bear no relation to the time of original deposition. This should be borne in mind when interpreting radiocarbon dates from specific areas of a site.

3.5.2 Existing Radiocarbon and Luminescence dates for Scottish burnt mounds

3.5.2.1 Overview of the Data

The body of existing radiometric dates for burnt mounds in Scotland can be split into two categories: those for which single 'spot dates' are available, and those for which a more comprehensive dating strategy was followed. The importance of this distinction is evident when considering the volumetric calculations of the previous section. It is clear that, in a significant number of cases, mounds may have been used several hundred times. Due to the lack of secure stratigraphic contexts, it is not possible to distinguish between the frequency and duration of use of a mound. Larger mounds may represent sites that have been used sporadically over a long period, or merely used more frequently than their smaller neighbours. If the duration of use is significant, chronological patterns may be falsely identified by virtue of the samples dated. It is therefore necessary to consider the range of ages obtained from sites for which more than one date has been obtained before looking at the broader picture.

3.5.2.2 Multiple Dates

A number of burnt mound sites have more than one radiometric date associated with them (fig 3.13). (A number of sites which have more than one associated date for the same deposit, or dates from material which pre/post date mound activity have been excluded from this discussion, and included within section 3.5.2.3 as they offer no 'durational' information).

Within Orkney the site of Liddle has been extensively dated using luminescence methods. In addition, two radiocarbon dates are also available (Huxtable et al, 1976). Luminescence dates from a total of eight stones and three pottery fragments range in age from 1300 BC to 200 BC. A radiocarbon date from a peat deposit overlying a structural stone (SRR 525)

suggests a terminus ante quem of 1290-1070 cal BC for that part of the site. In addition, a further date from organic material found at the bottom of the trough (SRR 701) was dated to 1175-955 cal BC. Overall, the data suggest prolonged use of the site from around the 14th to the 3rd century BC, however it is interesting to note that both radiocarbon dates are slightly at odds with the luminescence dates. It is unlikely that this can be explained solely in terms of the old wood effect.

Other sites within the same study show a variety of age ranges. All sites have upwards of 5 associated dates. At Liddle 2, Barswick, Beaquoy, Fan Knowe and Knowe of Scorn a spread of between 500-800 years is seen. Only Graemshall shows relatively little spread in age (fig 3.14).

In the north of Scotland, Kilearnan Hill has five associated radiocarbon dates from charcoal deposits (McIntyre, 1998). The earliest material dated comes from the second phase of activity. Charcoal from a deposit associated with this activity, together with charcoal from material washed into a central phase 2 pit give dates of 1260-810 cal BC and 1150-830 cal BC (GU1921/GU1914) respectively. Charcoal from the fill of the central pit in phase 3, and from a layer dumped around the same time give further dates of 1050-400 cal BC and 1130-790 cal BC (GU1912/ GU 1913). A fifth date from charcoal associated with a hearth on the top of the mound of cal AD 1300-1490 (GU 1915) would appear to represent re-utilization of the site at a later date, probably unrelated to the mound activity.

At Lairg, a number of excavated burnt mounds have multiple ^{14}C dates (McCullagh and Tipping, 1998). At mound 1, charcoal from the base of the mound gave a date of 1610-1120 cal BC (GU3135). Two dates from differing contexts on the summit of the mound gave ages of 1410-1110 cal BC and 1150-830 cal BC (GU 3136/ GU 2821) respectively. Given the error on these determinations it would be unwise to read too much into apparent variations, though again a duration of a few centuries may be indicated. Mound 2 would appear to provide stronger evidence in support of an extended use. A charcoal deposit from the main body of the mound (GU 3134) was determined to be between 1600-1310 cal BC. This is supported by an age determination from charcoal found within the lower fill of a large pit which underlay the mound of 2020-1680 cal BC (GU 3133). A further sample from the

Fig 3.13 Multi-date burnt mound sites in Scotland

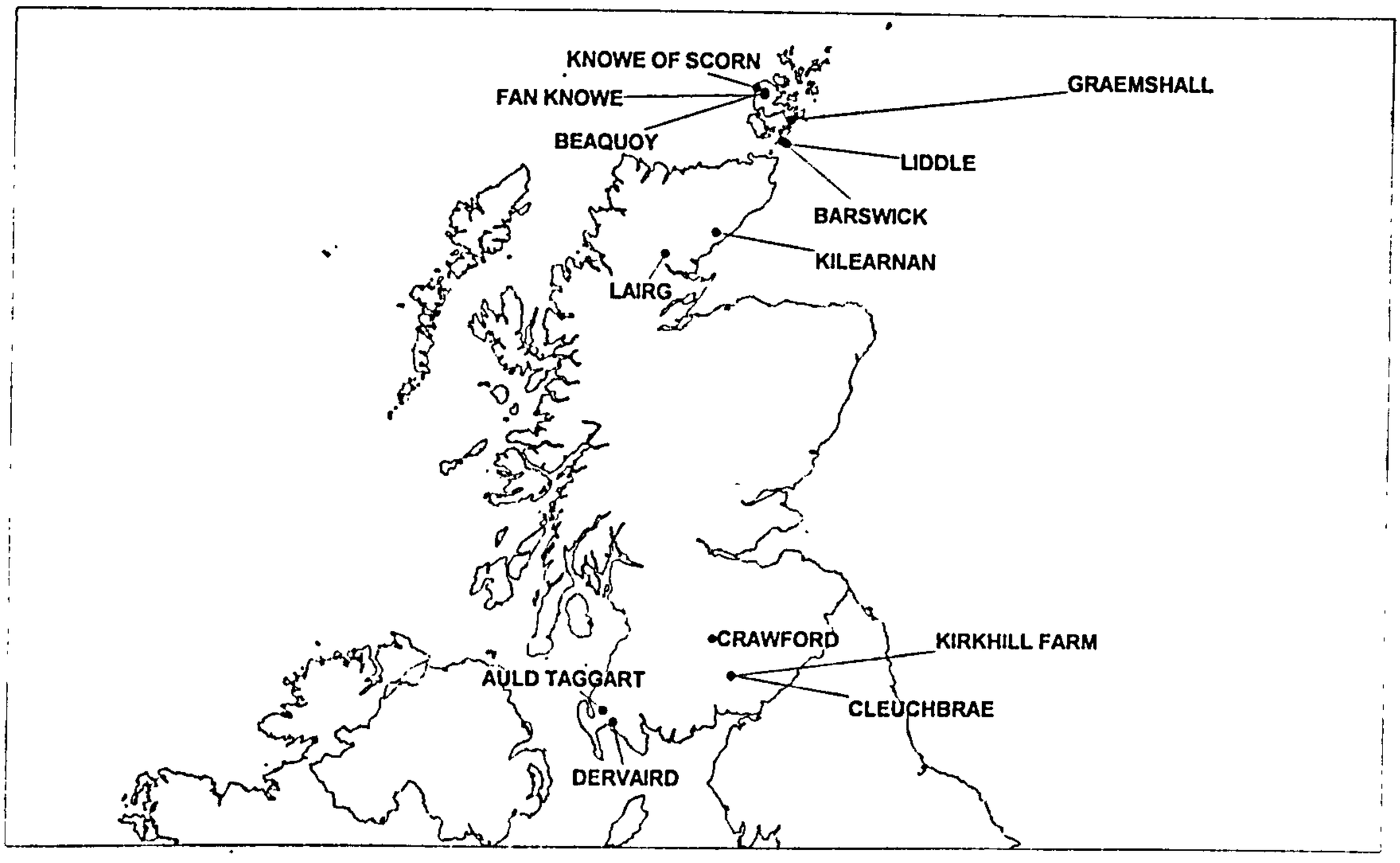

uppermost part of the mound showed an age of 1050-820 cal BC (GU 2822). This would suggest a duration of at least 3-4 centuries.

In Dumfries and Galloway the site of Dervaird (Russell-White, 1990) shows little variation in the dates obtained from the oak baulk recovered from the base of the trough, and also from oak and birch charcoal from the matrix of the mound: 1620-1400 cal BC and 1530-1300 cal BC (GU 2330/2331) respectively. The nearby site of Auld Taggart burnt mound has surprisingly late, but coherent dates (Russell-White, 1990). Identified charcoal from a layer associated with the initial use of the site (GU 2417) dates to cal AD 1020-1250. Charcoal from around the stones of the mound gives a similar date - cal AD 1060-1300 (GU 2414). A further date from a charcoal and stone deposit on the surface of a possible hearth area is also indistinguishable – cal AD 1000-1210 (GU 2413). Both sites would appear to have been short lived, despite being around 25m^3 in volume.

In the South of Scotland a number of mounds have been sufficiently well dated to allow for comparison. At Crawford North (Banks, 1999) deposits from the trough date to 2140-1860 cal BC, compared with material from the matrix of the mound which gives a date of 1680-1390 cal BC (AA12591/12590). Kirkhill Farm has some of the oldest dated deposits (Pollard, 1993). Five radiocarbon dates from various parts of the mound all centre on the

period 3000-2600 cal BC. However, given the evidence of residual lithics within the deposit, it is possible that the charcoal dated may also be residual in nature. The nearby site of Cleuchbrae shows some variation in the four dates obtained from various parts of the mound (Duncan, 1999). Charcoal from a context below the wood lining of the trough dates to 1770-1520 cal BC (OxA-8833). The oak plank forming the lining was dated to 1430-1130 cal BC, and fragments of charcoal from the matrix of the mound above the trough to 1500-1260 cal BC (OxA-8832/8801). In addition, a birch stake found in-situ near to the trough gave a later date of 1260-920 cal BC (OxA-8880). The interpretation of this site is somewhat dependent on the interpretation of the stake-holes found in association with the trough. If roughly contemporary, they suggest a period of use of two to four hundred years.

A summary graph of the above data illustrates the variation in age spread seen (fig 3.14). It is evident that whilst not all mounds appear long-lived, no assumptions in this regard can yet be made. Whilst volumetric data are not available for all of the above mentioned mounds, the small number that do have data show no relationship between size and spread in age. As such, volume should not necessarily be taken as an indication of short/ long duration.

3.5.2.3 Synthesis of results – the search for chronological and regional patterns

3.5.2.3.1 An overall chronology for Scottish Burnt mounds

Using the existing age dataset (see appendix B for summary of radiocarbon dates), it is possible to combine the results from each available date to produce a probability density function (PDF) that describes the probability of Scottish burnt mounds being of a certain date[4]. The density function is produced in 50-year bins. Where multiple dates are present, the normalized sum has been used. Each site is therefore given equal weighting, with the PDFs summed and normalized to 1 (fig 3.15a).

Whilst it is easy to identify the larger peaks in the distribution, one of the weaknesses in this type of analysis is that finer details tend to be lost. In addition, sites with only single dates tend to be over-represented in that their individual PDFs are much sharper due to the unknown spread in ages associated with the site. However, within this analysis, the finer detail is perhaps less relevant than the overall picture.

---

[4] A gaussian distribution has been assumed for all data. In the case of radiocarbon dating this is a simplification that does not account for wiggles in the calibration curve.

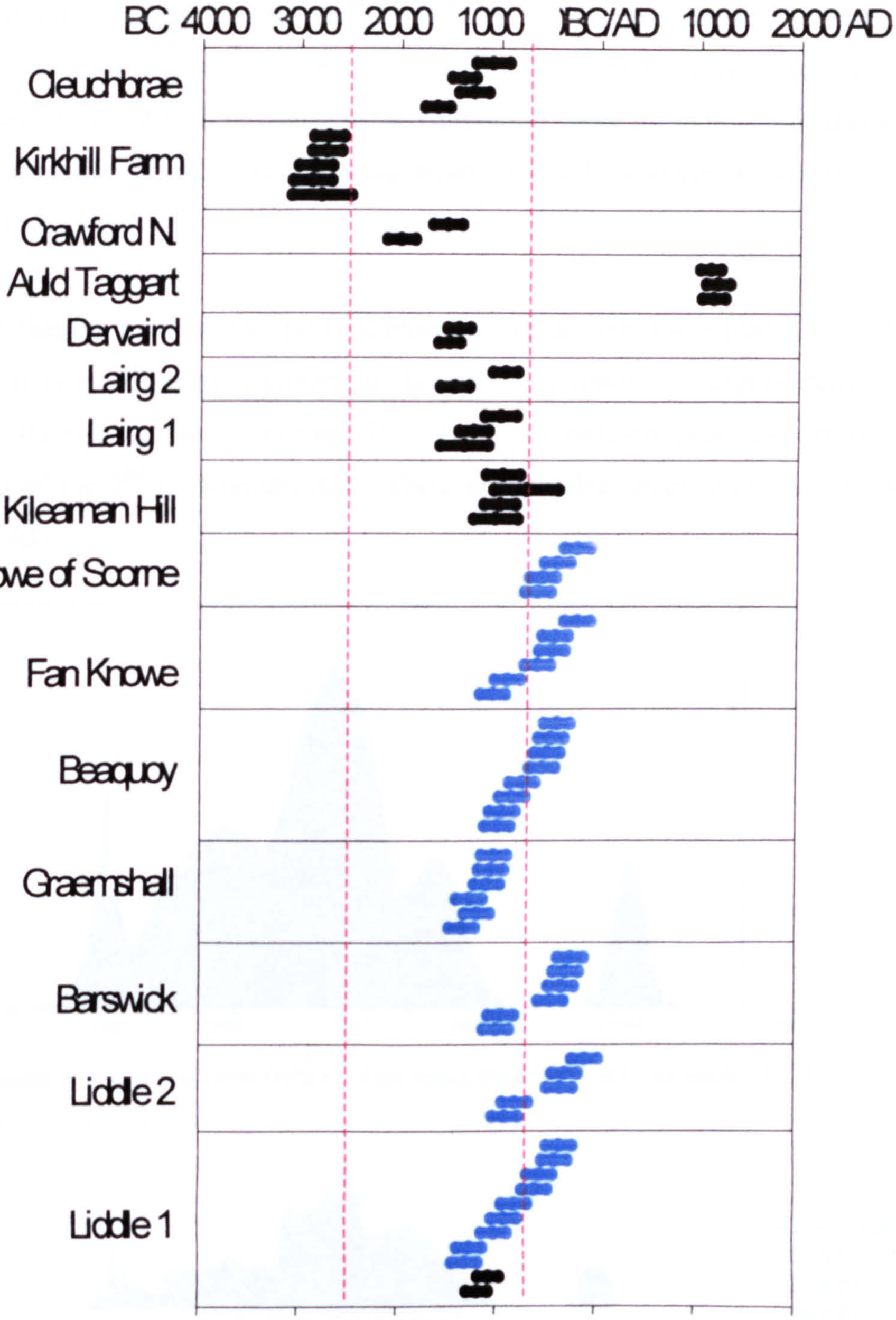

Fig 3.14 Summary of multi-date sites: Blue indicates luminescence dates, black radiocarbon dates Red lines indicates the ~2500-700 BC limits of the Bronze Age with which burnt mounds have traditionally been associated.

A similar plot produced using the Oxcal v.3.0 programme shows the sum of all date distributions assuming a gaussian distribution for luminescence dates and using the distribution produced with reference to the calibration curve for radiocarbon dates (fig 3.15b). No total summing of individual sites has been enforced, however the results are similar to those in fig 3.15a.

It is clear that the predominant peak of burnt mound activity takes place in the Bronze Age. However it is in no means confined to this period in time. Examples exist from the late Neolithic through to the 1st century BC/AD. An isolated peak also exists around the beginning of the 2nd millennium AD. There is a notable absence of sites in the first five centuries AD.

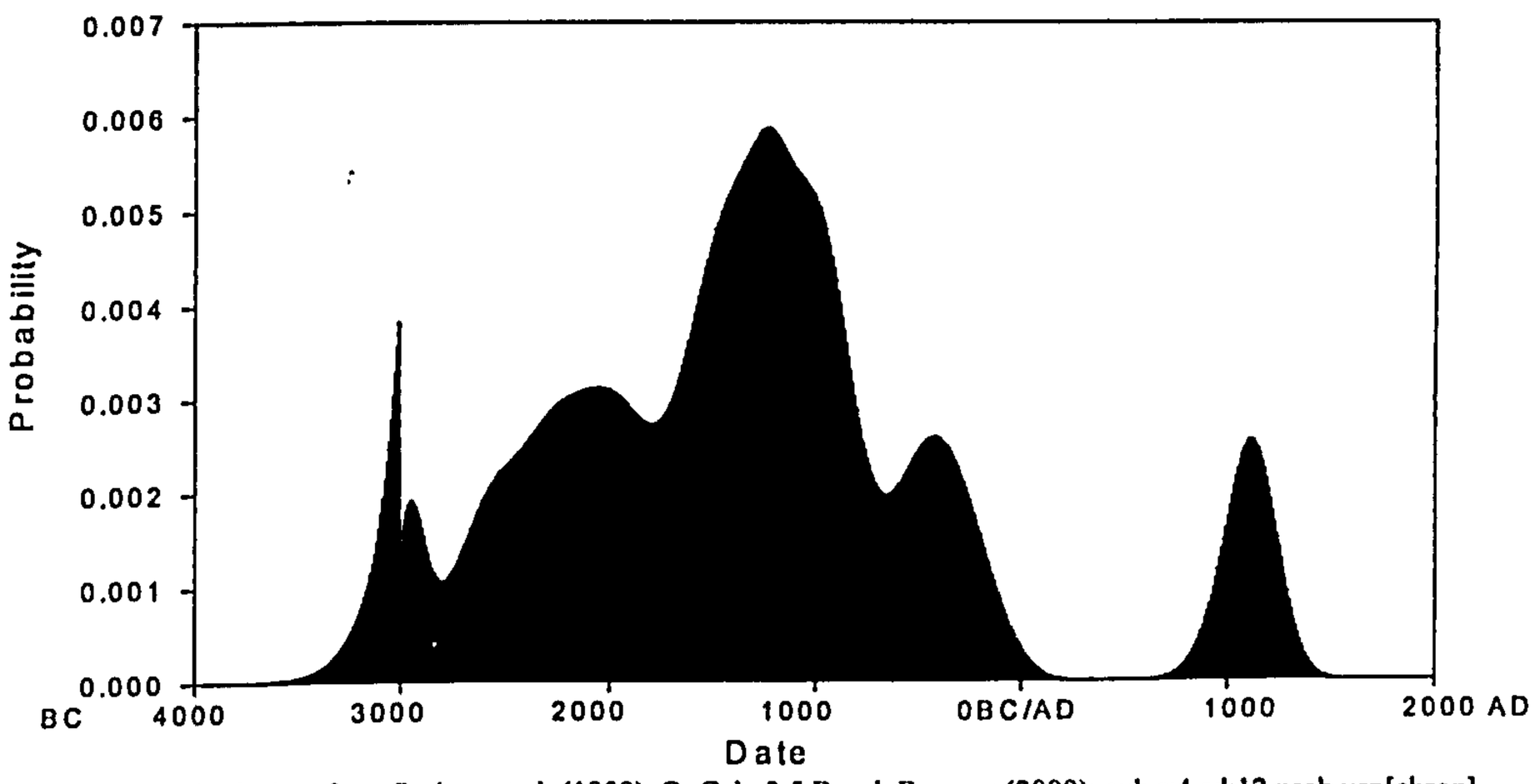

Fig 3.15 (a) Probability Density Function for dated Burnt Mound sites in Scotland (gaussian distribution) (b) Oxcal Sum plot for all radiocarbon and luminescence dates from burnt mounds in Scotland

3.5.2.3.2 Regional Chronological Patterns

By categorizing dates within set time periods it is possible to view the data on a geographic basis. Arbitrary 500-year time blocks have been used to produce progressive distribution maps from 3500 BC to AD 1500 (fig 3.16). Again however problems with regard to assumed duration are encountered. For the purposes of this analysis, it has only been possible to take account of prolonged duration where evidence exists to support it. Spot dates have therefore been represented only within one period.

With a dataset that represents only 2% of the known mounds in Scotland, it would be unwise to read too much into the apparent patterns seen in fig 3.16. However, it is clear that the earliest dated sites are confined to the Borders region and the Western Isles. By 2000 BC a wider distribution is seen, which includes sites from the Northern Isles cluster. Around 1000 BC-500 BC sites in the south of Scotland disappear, with the majority of remaining sites focused in the Orkney Islands. Later medieval activity is confined to two sites in the Glenluce cluster of Dumfries and Galloway.

3.5.3 Summary of Chronological Information

A number of significant problems have been highlighted with regard to the assumed age of Scottish burnt mounds. It has been demonstrated through the existing radiometric data that a number of sites may have had a prolonged duration of use. This in turn has led to uncertainty in the way in which 'spot' dates should be interpreted. Nevertheless, it has been clearly shown that burnt mounds can no longer confidently be thought of as solely a Bronze Age feature. There is evidence for a four millennia span in their distribution. Apparent regional patterns are also identifiable, with possible hints of a tradition that appears first in the South of Scotland, before spreading up the West coast to the North. However, given the small percentage of sites for which dates are available, it in not possible to say whether such patterns are reflective of an overall pattern, or merely represent a bias in sampling.

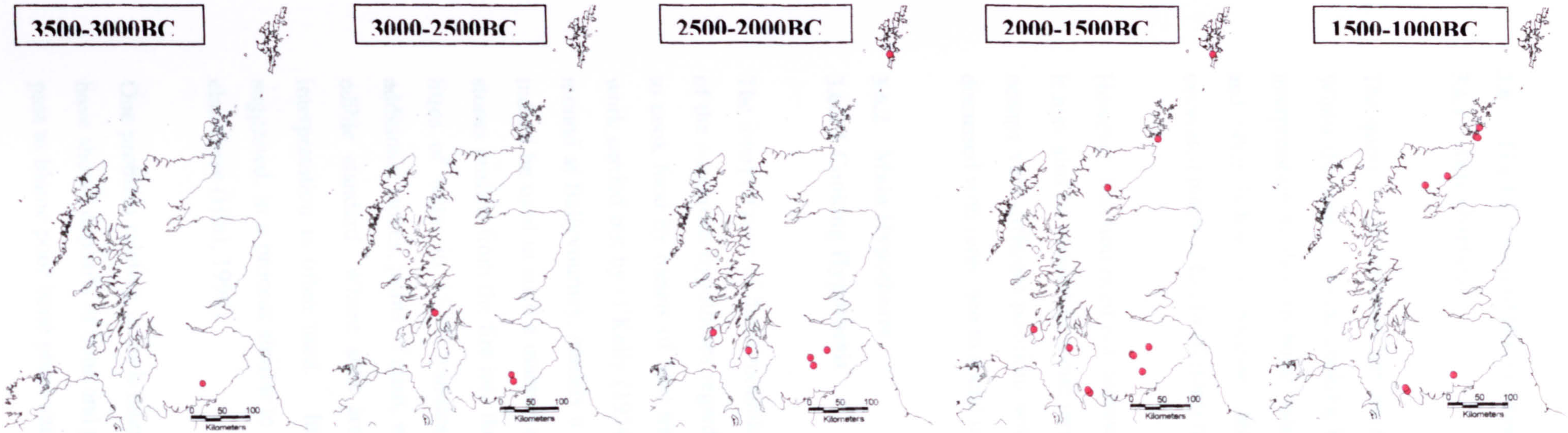

Fig 3.16 Regional Chronological Patterns

3.6 The Function of Burnt Mounds

3.6.1 Introduction

The question of function has been widely debated within the archaeological literature. Whilst the more popular cooking hypothesis continues to be quoted as the conventional interpretation applied to burnt mounds, theories of prehistoric saunas, textile production and other industrial processes are gaining more popularity as a growing number of excavated mounds fail to conform to typical 'fulachta fiadh' type sites.

However, function need not necessarily be seen in terms of the primary purpose of the site. It may also be viewed in social terms. Two sites may have the same primary purpose but occupy very different positions within the community. As such, function should also be discussed with reference to social use.

3.6.2 Main Hypotheses

3.6.2.1 Cooking Hypothesis

The interpretation of burnt mounds as sites for cooking are perhaps the most 'mainstream' of the numerous hypotheses regarding function. Here the primary purpose of the site was to cook food by means of heat transfer from hot stones to water. Indeed, experimental work carried out by O'Kelly (1954) confirmed that the components of an excavated burnt mound at Ballyvourney, namely a timber lined trough, hearth and the mound itself, could indeed be used in such a manner as described by Keating to boil joints of meat. Heated stones pushed from the fire into the re-lined, water filled trough were found to boil the 454 litres of water in 35-40 minutes. With continued supplementing of the trough with additional stones, joints of meat, wrapped in straw and bound with rope were cooked to an edible standard. Where sites are found without a watertight trough, a slant on this interpretation is often used. Instead of boiling as the means of cooking, roasting is suggested, in a process similar to ethnographic examples of 'mu-mu' in New Guinea and elsewhere (Hurl, 1990).

One problem relating to such interpretation is the lack of cooking debris. Occasional sites have shown deposits of bone and pot but these are very few. There was a tendency in the past to blame poor bone preservation on the level of pH of the soil (Huxtable et al, 1976).

Whilst it is true that a number of mounds have acidic soils, which would not favour bone preservation (Máté, 1990), not all fall into this category. Indeed excavations at Crawford (Banks, 1999) revealed bone at a wide variety of sites in the vicinity of the two burnt mounds, yet no bone was found during the excavation of the two. At Cobb Lane, total sieving of large proportions of material produced no finds, yet not only was the soil pH neutral, but bone was found in pre-mound layers (Barfield and Hodder, 1987). The lack of bone would therefore appear to be a real phenomenon. It is important to look at the likely role particular sites would have played in the community in order to determine whether one would expect bone and other 'cooking' debris to be present.

The interpretation of burnt mounds as cooking sites may be split into several categories. Early theories tended to favour the 'hunting camp hypothesis', an interpretation which originated in Early Irish literature. The term 'fulachta fiadh' literally translates as a deer-roasting pit. Vague references within early laws and documents hint at such sites being used for cooking during hunting season (O'Drisceoil, 1988, 1990). As early as 1871 Anderson, in his investigation of two burnt mounds at Wick made the connection between Scottish and Irish sites:

> "Similar cairns, described as 'ancient heaps of burnt stones, usually consisting of small stones broken to the size of road metal', and known in the county of Cork as 'Folach Fia', in Tipperary as 'Deer Roasts', and in Ulster as 'Giants cinders', are common in Ireland.... A culinary purpose has been suggested for these troughs"
> (Anderson, 1873, 296).

The mainstay of the argument was that such sites represented seasonal hunting camps re-used over a number of years. If this were the case these sites may be viewed in isolation from permanent settlement. As such, one would expect to find evidence of butchery and cooking debris associated with the site (though not necessarily within the mound itself). It would be unwise to rule out the 'hunting camp' theory on the grounds of negative evidence alone. However, for many years it has been clear that such interpretation sits uncomfortably with a number of excavated sites which seem far better established than one would expect for a site occupied sporadically for a few days at a time. Indeed the density of sites in some areas would seem to preclude such an interpretation. Hunter, for example in his study of burnt mounds on the small island of Fair Isle, Shetland, is of the view that:

> "...it would be difficult to explain the burnt mounds on Fair Isle as being anything other than component elements of a larger settlement infrastructure. It is not realistic to consider them as belonging to Barber's class 1 – the 'hunting' fulachta, ... On an island as small as Fair Isle this interpretation lacks credibility" (Hunter, 1996, 61).

This link with a more complex settlement pattern is echoed in a number of reports, but most prominently at Liddle, Orkney. The site of Liddle was excavated during the 1970s and revealed a 'house like structure' associated with a burnt mound. The interpretation of this structure as a settlement led Huxtable et al (1976) to conclude that burnt mounds may be used as settlement indicators within the landscape.

Were burnt mounds to represent domestic settlement sites, as was suggested by the excavators of Liddle and Beaquoy, one would expect to find every day domestic refuse associated with the structures found. There is a surprising lack of this at Liddle. Indeed the 'house' is situated on boggy ground not ideal for habitation.

Within the northern isles it is true that there is a correlation between the distribution of burnt mounds and that of agriculturally viable land (see chapter 4 for detail). However, this correlation need not necessarily indicate a direct link between burnt mound and settlement. Dockrill et al (1998) make the observation that:

> "The major flaw in the argument that many burnt mounds represent settlement sites in the Northern isles is that of the position of the site at a local level. The location of Burnt Mounds examined on a large scale may coincide with good land, but the position of these sites at the local scale suggests that many of them occur at places which would have been unfavorable for domestic occupation"
> (Dockrill et al, 1998, 61-2).

An alternative to the settlement theory is that burnt mounds were on the periphery of settlements, rather than the focus of them. In this case, the absence of cooking debris is less problematic. Barber (1990) notes that in such situations, butchery and eating may have taken place elsewhere within the settlement complex. If this were to be accepted, burnt mounds of these types would therefore be seen not in terms of a feasting site, but more the barbeque where the food was cooked.

At Tangwick (Moore and Wilson, 1999) the presence of serving vessels within the pottery assembledge is taken as an indication that food was being consumed and prepared on site.

However, the excavators point out that the size and layout of the structure appears to have been specifically designed to facilitate 'hot stone technology'. As such "when hot stone was being processed, the effects of heat, steam and shattering stone would have rendered a large part of the structure inhospitable and movement within the structure must have been severely restricted" (p230). Thus it would seem that Tangwick represented a highly specialized site related in some way to cooking, but not of a domestic nature; possibly some type of 'seasonal feasting area'.

Some attempt has been made to provide positive evidence of cooking through residue analysis. Isaksson (1996) carried out preliminary investigations on the application of lipid analysis in the identification of food remains within cooking pits in an attempt to resolve such dilemmas. Initial results showed some promise, with clear distinctions between cooking and forging pit signatures identified. However, a number of issues which remain unresolved, as regards to reference ratios and the degradation and/or contamination of samples, may prevent wide-scale application of this technique without controlled sampling.

3.6.2.2 Saunas and Bathing

The notion that burnt mounds may represent sites of prehistoric saunas was most notably publicized by Barfield and Hodder in 1987. Such a concept represents a fundamental change not only in the function of the site, but also in the technology used. The objective switches from one of heating water, to the production of steam. Rather than stones being heated then placed in water with the intension of dissipating heat into the water, water would be placed on the stones for the purpose of steam production. Ó Driscéoil (1990) argued that the presence of a trough, and absence of associated settlement structures posed a major problem with regard to this hypothesis. However, as stated above, not all sites are associated with troughs and the 'roasting pits' may easily be re-interpreted as areas for the collection of heated stones, onto which water may be tossed to produce steam. The absence of associated settlement structures may also be overlooked, if flimsily constructed structures which leave little archaeological evidence behind are proposed. Banks (1999) in a defense of this theory also notes that the percentage of stones which would be subjected to thermal shock and thus liable to cracking would be far greater in the case of a sauna, than in conventional cooking scenarios. Thus, the build up of the mound could conceivably have taken place over a far shorter time period.

References to bathing at burnt mound sites can be found in the late 18th century story of "The romance of Mis and Dubh Ruis" (O'Drisceol, 1990). The overall size of slab lined troughs on the northern isles in many cases would appear sufficient for bathing. However, the smaller, unlined troughs found to the south are perhaps less suited to such an activity. Experimental reconstructions have also shown that the trough rapidly fills with burnt stone whilst being heated, therefore it may have been necessary to partially empty the trough of stone prior to bathing.

3.6.2.3 Other Non Domestic Functions

A number of other 'non-domestic' functions have been suggested as functions for burnt mounds. Jeffery (1991) argued for the suitability of these sites to the production of textiles in that containers of heated water are required for dying etc. Likewise the trough would also have been suitable for brewing, and other industrial processes. One suggestion, based on similar mounds in Sweden, is that burnt mounds may in some cases have been used in relation to the processing of seal blubber (Eskola et al, 2003). As with other hypotheses, lack of positive evidence is the major downfall in each theory.

3.6.3 Summary

It is unlikely, given the variation in size, characteristics and chronology of burnt mounds in Scotland, that all monuments of this type represent one singular function. Some functions would appear to sit better with evidence from sites in particular areas. There is however no a priori reason why burnt mounds could not have performed multiple functions within a particular society. Hot stones and heated water could clearly have been utilized in a variety of ways, not all of which may leave behind traces of evidence. One can say with certainty that stones were being heated at these sites, but the true functions for the moment remains elusive.

3.7 A Way Forward?

A number of unresolved issues have been raised in the preceding sections. It seems clear that there is great variety in the size, shape and associated features recorded with burnt

mound sites in Scotland. Whilst they have been collectively grouped together under the 'burnt mound' heading, there is evidence to suggest multiple functions and chronologies within this classification. As such no single research strategy could hope to untangle the intricacies of problems surrounding burnt mound archaeology.

Additional field surveys will add to the growing distribution of burnt mounds and may at a later date provide important information with regard to the spread of technology. With so many known sites it is clearly unrealistic to expect large- scale excavation of significant numbers of them. Excavation of known burnt mounds may provide hints as to function, but this is likely to be site specific. Whilst both survey and excavation are worthwhile undertakings, as a means to furthering our understanding of burnt mounds on a larger scale, they can provide little aid. However, it is important to catalogue as much information about each mound as is practically possible to enable an informed decision to be taken as to which mounds should be prioritised for further study.

As discussed in chapter 1, chronology is one element that may be tackled in a more comprehensive manner. As described above, a number of sites have been the subject of more intensive dating and provided important information with regard to probable duration. However, such sites tend to sit in isolation from their neighbours, thus it is difficult to interpret the results on a local or even regional basis. In addition, no single strategy has tackled the issue of the formation processes within the mound itself.

A combination of detailed stratigraphic sampling on a limited selection of sites to address durational issues, combined with surface sampling of surrounding sites might provide appropriate material to build up a detailed picture of intra and inter site age variation, allowing for a far greater understanding of the interaction between burnt mound sites on a local basis. In addition, a larger scale project, combining chronological information from burnt mounds dispersed over a wider area may help to relate local and regional patterns.

3.8 Study Areas

3.8.1 Selection of Study Areas

Two areas were selected for further study and sampling with reference to the specific requirements of the sampling strategy, and observations made above with reference to the distribution, chronology and characterization of burnt mounds in Scotland.

The Orkney and Shetland islands were chosen as suitable areas for a variety of reasons. Both Orkney and Shetland are included within the group of burnt mounds where excavated examples have been identified as having substantial structures associated with them. The evidence for multiple phases of use within sites on both Orkney and Shetland, together with this structural evidence suggests these areas to be ideal locations for studying the duration of use of individual sites. Burnt mounds in the Orkney islands have previously been the subject of successful luminescence investigations (Huxtable et al, 1976, Hunter and Dockrill, 1990), thus some information is known about the luminescence characteristics of the material. In addition, the wealth of small islands provides the opportunity for local sampling in areas with simple geology. In Shetland, the complex geology of the region lends itself to more diverse studies in which more varied luminescence response may be expected.

3.8.2 The Orkney Islands
3.8.2.1 General

The Orkney Islands lie off the northern coast of mainland Scotland. They are thought to have been separated from mainland Scotland at sometime before 10,000 BC (Davidson and Jones, 1985). They are generally described in terms of the Mainland, North and South Isles. Many of the Northern Isles are low lying, with the majority of land below 50m in elevation. Rousay is the notable exception, rising to over 200m in height. The Mainland is likewise relatively flat, with only a few confined areas reaching over 50m in height. This is in contrast with the southern island of Hoy, peaking at around 450m (fig 3.17).

The geology of Orkney is dominated by sandstones, mostly of the Middle Old Red Sandstone (Mykura, 1976). Only in a few places on the south western tip of the mainland and Graemsay are the basement complex of metamorphic and igneous rocks visible. Superficial deposits cover much of the Orkney Islands with peat and boulder clay forming

the majority of the deposits. Around half of the land on Orkney is arable or improved grassland, mostly on the lower ground elevations (Davidson and Jones, 1985).

3.8.2.2 The Archaeology of Orkney

> **"The prehistoric monuments of Orkney are justly famed for the abundantly rich picture which they give of man's early past in this area. They constitute a complex which is not surpassed elsewhere in Britain – not even in Wessex, perhaps not even in continental Europe – for the wealth of evidence which it offers."**
> **(Renfrew, 1985, p1)**

The level of preservation of archaeological monuments on Orkney is unique within the British Isles. It is perhaps therefore no surprise that Orkney has continued to attract the attention of those with an interest in the past. From early antiquarians to present day

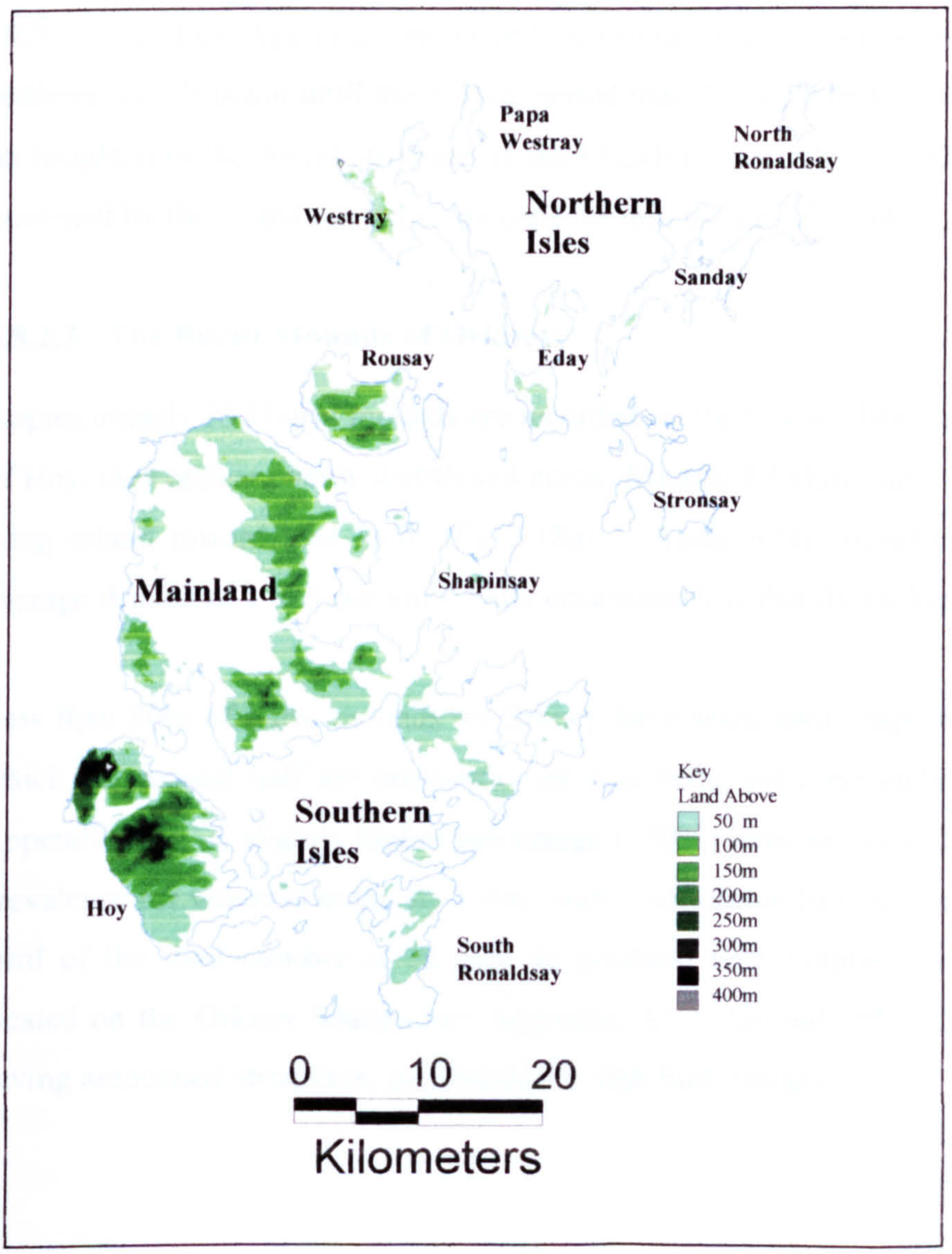

FIG 3.17: Topography of Orkney Islands (based on OS Digimap panorama data)

archaeologists there has been a continual stream of excavation and survey reports from the Orkney Isles. As a result, a large body of information on the environment and habitation of Orkney has accumulated.

The earliest known settlement is that of the Knap of Howar on the small island of Papa Westray dating to between 3700 and 2800 BC (Ritchie, 1984). This, and other later Neolithic houses, like the renowned Skara Brae settlement attest to a well developed farming community populating the Orkney Isles. With these settlements came not only a wealth of material culture, but impressive chambered tombs. A move towards smaller, single use burial sites is seen in later years, with many of Orkney's cists and barrows dating to the Bronze Age period. Convention would dictate that it is within this environment that burnt mounds were utilized. Indeed some go so far as to suggest the burnt mounds of Orkney represent the elusive Bronze Age settlements (Huxtable et al, 1976). The Iron Age is characterized by Orkney's multi-period broch and round house settlements. It is not until the Viking period that Orkney's historical records begin, giving an insight into the social structure of the Orcadian hierarchy. Orkney continued to be governed by the Scandinavian kings until the mid to late 15th century.

3.8.2.3 The Burnt Mounds of Orkney

Approximately 250 burnt mounds are recorded on the Orkney Islands. With the exception of Hoy, they appear evenly distributed across Mainland Orkney and the Islands, with many lying inland towards the lochs (fig 3.18a). Areas where mounds are present have an average density of 1 to 3 per km^2. Only occasionally is this figure higher.

Less than 20% of burnt mounds on Orkney have associated shape information. Of those which do, around half are crescentic, the rest being predominantly circular or oval (see Appendix A). A slightly higher percentage (~30%) have associated dimensions, showing prevalence for volumes in the 10-100m^3 with a noticeable lack of smaller sized mounds. A third of the total number of mounds in Scotland with volumes greater than 100m^3 are located on the Orkney Islands (see Appendix A). Around 10% of mounds are noted as having associated structures, predominantly slab built troughs.

When viewed in terms of elevation, it can be seen that the distribution of burnt mounds on Orkney shows a preference for low lying land (fig 3.18a). Over 90% of mounds are located on land below 50m. However, the 0-50m land banding represents around 70% of the total land area of Orkney thus the relationship is perhaps not as strong as it first appears. Within this banding however, it can be seen that over half the total number of mounds are located on land below 10m (fig 3.18b), an area significantly smaller in proportion to this percentage.

In relation to solid geology, a rough correlation between percentage land mass and number of burnt mounds can be seen with regard to Stromness Flags and Eday beds, however a preferential relationship would seem to exist between Rousay flag areas and the location of burnt mounds, with a little under 60% of the total number being located here. There is a noticeable absence of mounds in areas of Hoy Sandstone. This relationship between Rousay Flags/ Hoy Sandstone and burnt mounds to a certain extent is topography dependent, with the Rousay flags occupying areas of low land and Hoy sandstone areas of high ground (fig 3.19).

When viewed in terms of drift geology, it is apparent that there is a preference for location on boulder clay deposits (fig 3.20). Some 64% of mounds are located on such ground, whilst the area covered by boulder clay represents less than 40% of the total landmass. Burnt mounds located on windblown sand deposits are likewise over-represented, with the total area of sand deposits representing only a few percent land mass. There is a notable absence of mounds on areas of peat, alluvium and glacial silt and gravel.

In many cases, practical factors may govern the positioning of burnt mounds. The apparent avoidance of high ground may be an avoidance of more exposed areas. Likewise, certain solid and drift geological deposits may be avoided/ favored for practical reasons. The preference for siting on boulder clay may reflect an exploitation of the clays natural water collecting attributes. Peat, alluvium and silt may be less suited to such tasks. The location of burnt mounds also appears to correlate closely to areas of improved land (Stamp, 1944), indicating a preference for good farming. However, it should be noted that in many cases, mounds appear at the extremities of such areas. This would seem to re-affirm Hedges' assertion that burnt mounds are in some way linked to agricultural settlements, if somewhat more peripheral in nature.

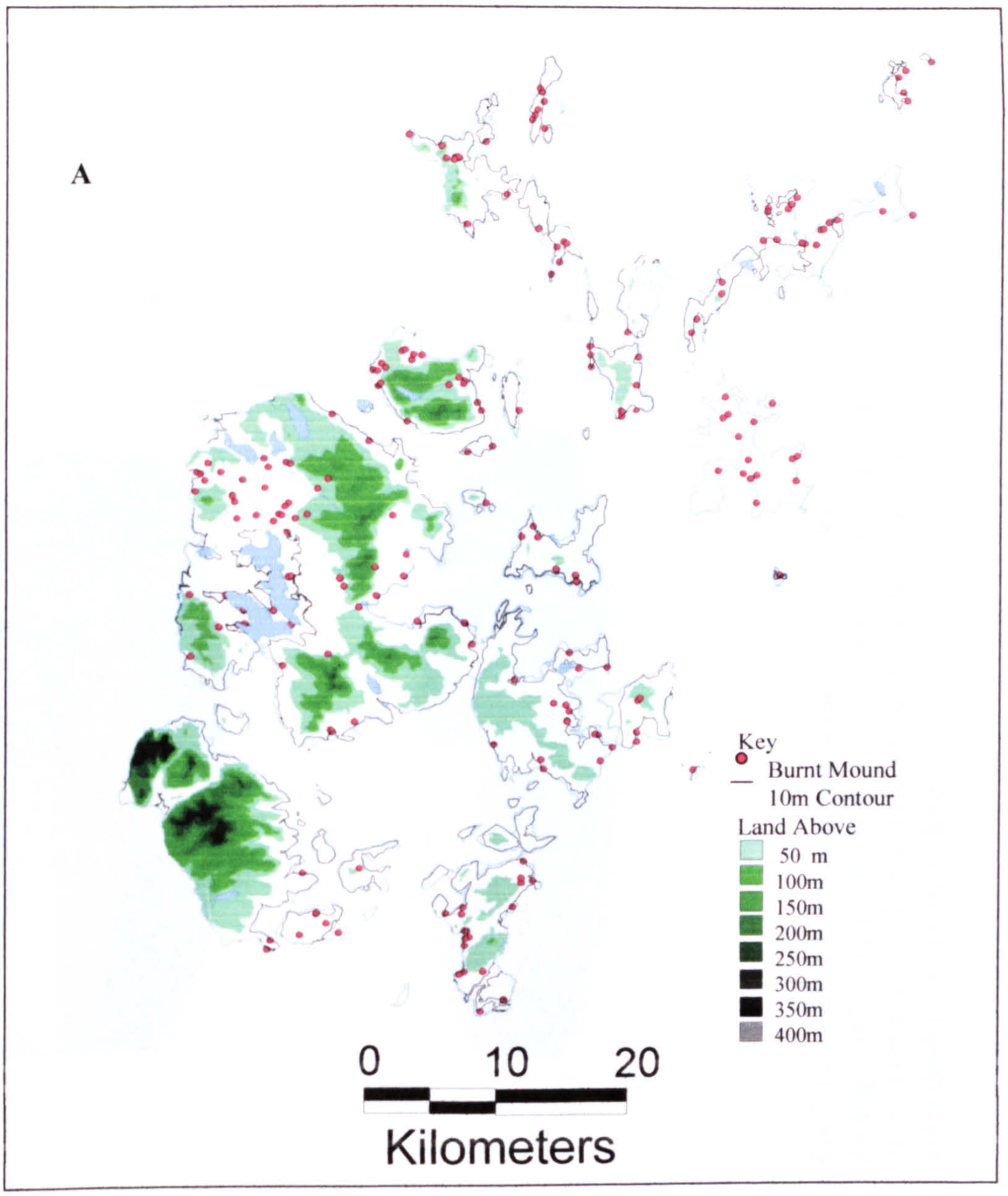

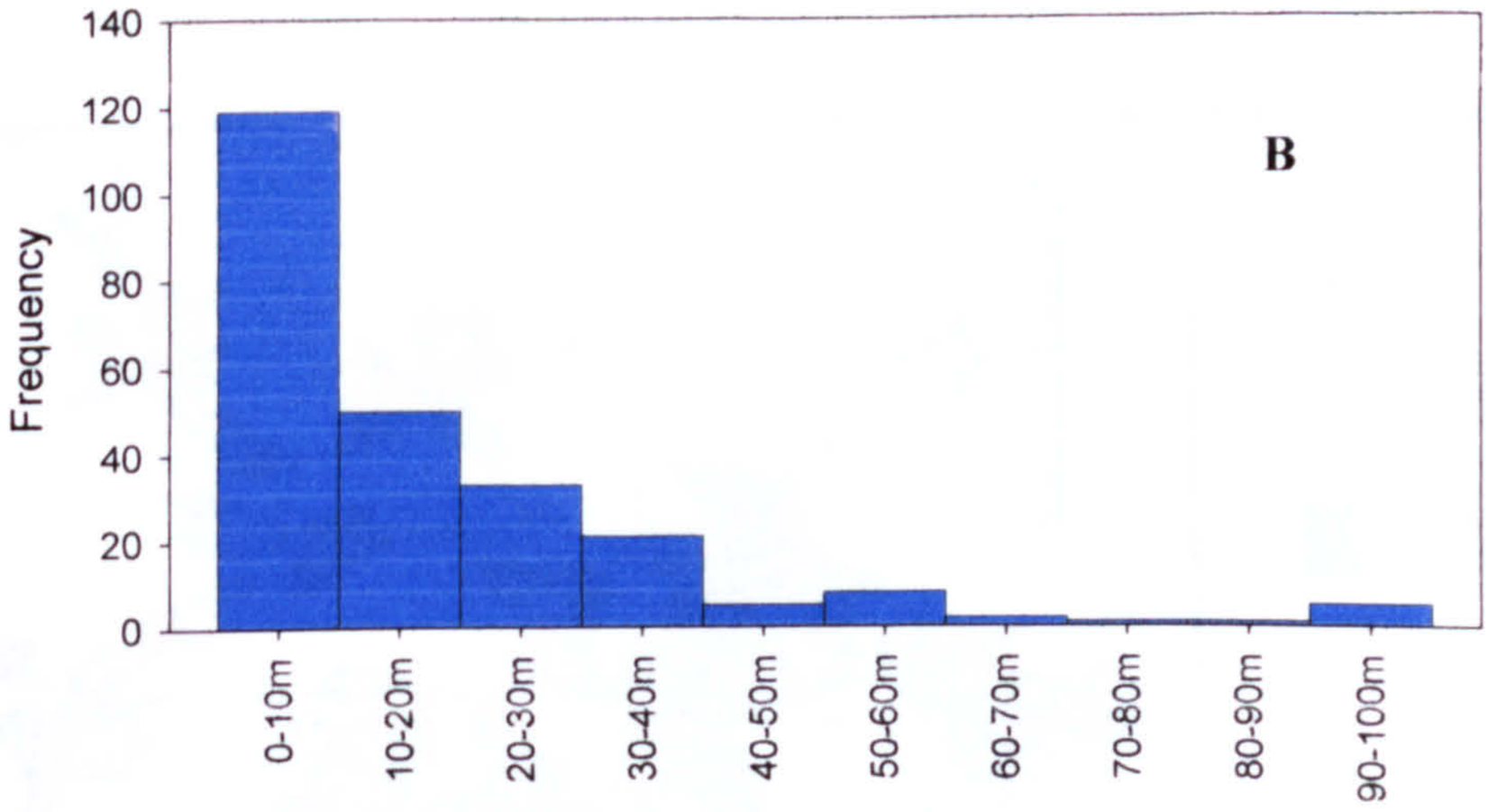

Fig 3.18 A. Distribution of Burnt Mounds in Orkney in relation to topography (based on Ordnance Survey Digimap Panorama data)
B. Number of Burnt Mounds per 10m elevation band

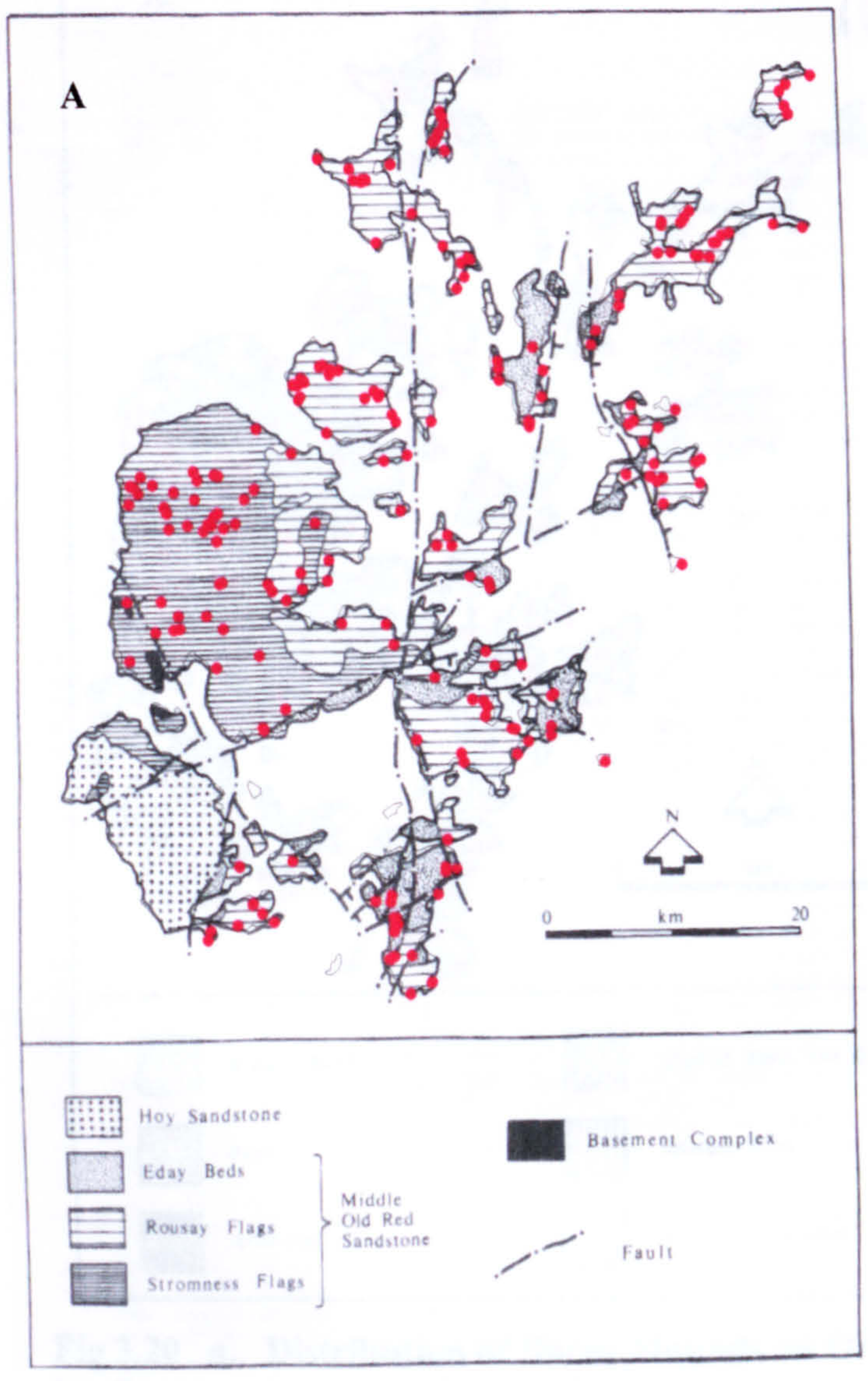

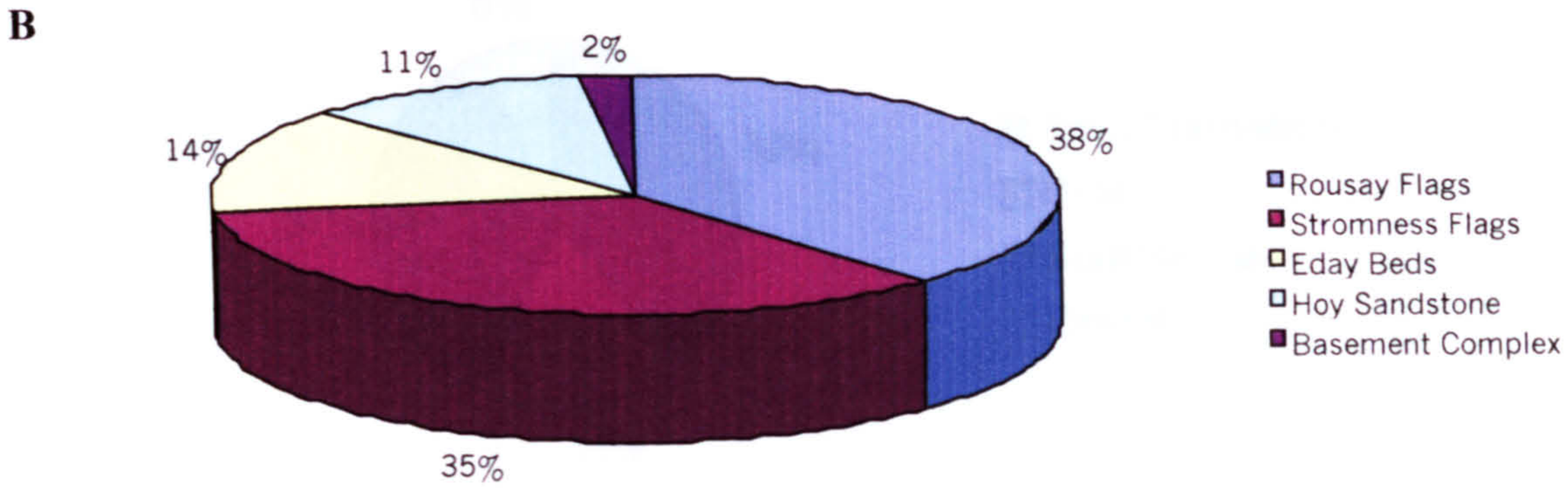

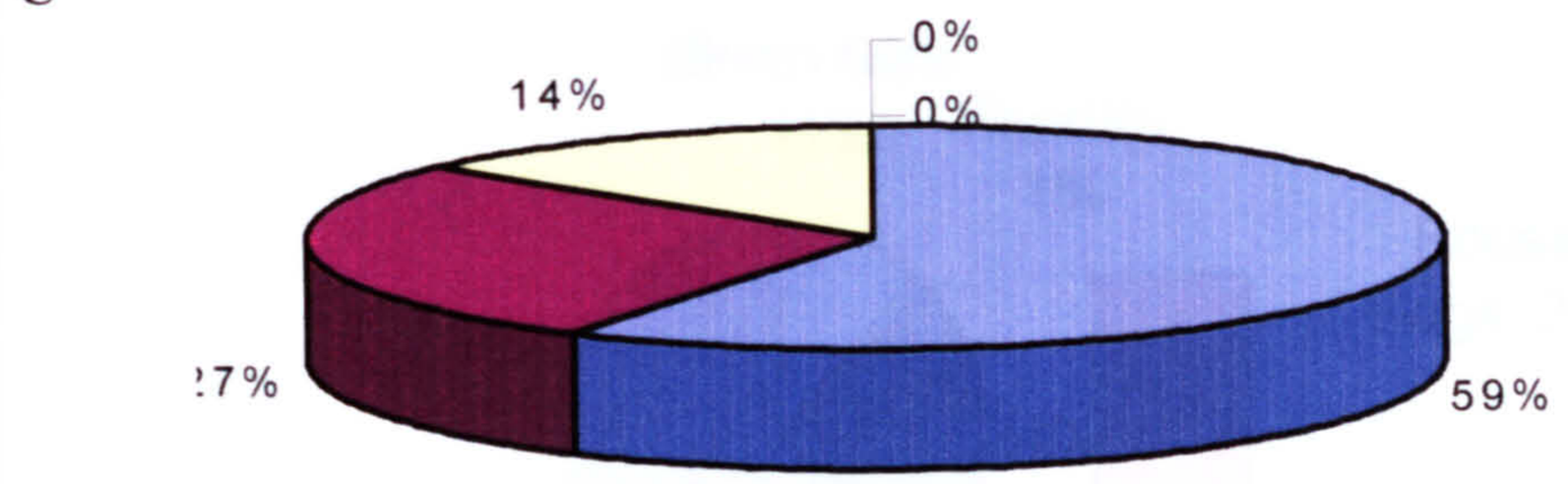

Fig 3.19 a. Distribution of burnt mounds on Orkney in relation to solid geology (after Mykura, 1976) b. Percentage area landmass of main geological units, Orkney c. Percentage of total number of burnt mounds distributed on main geological units, Orkney

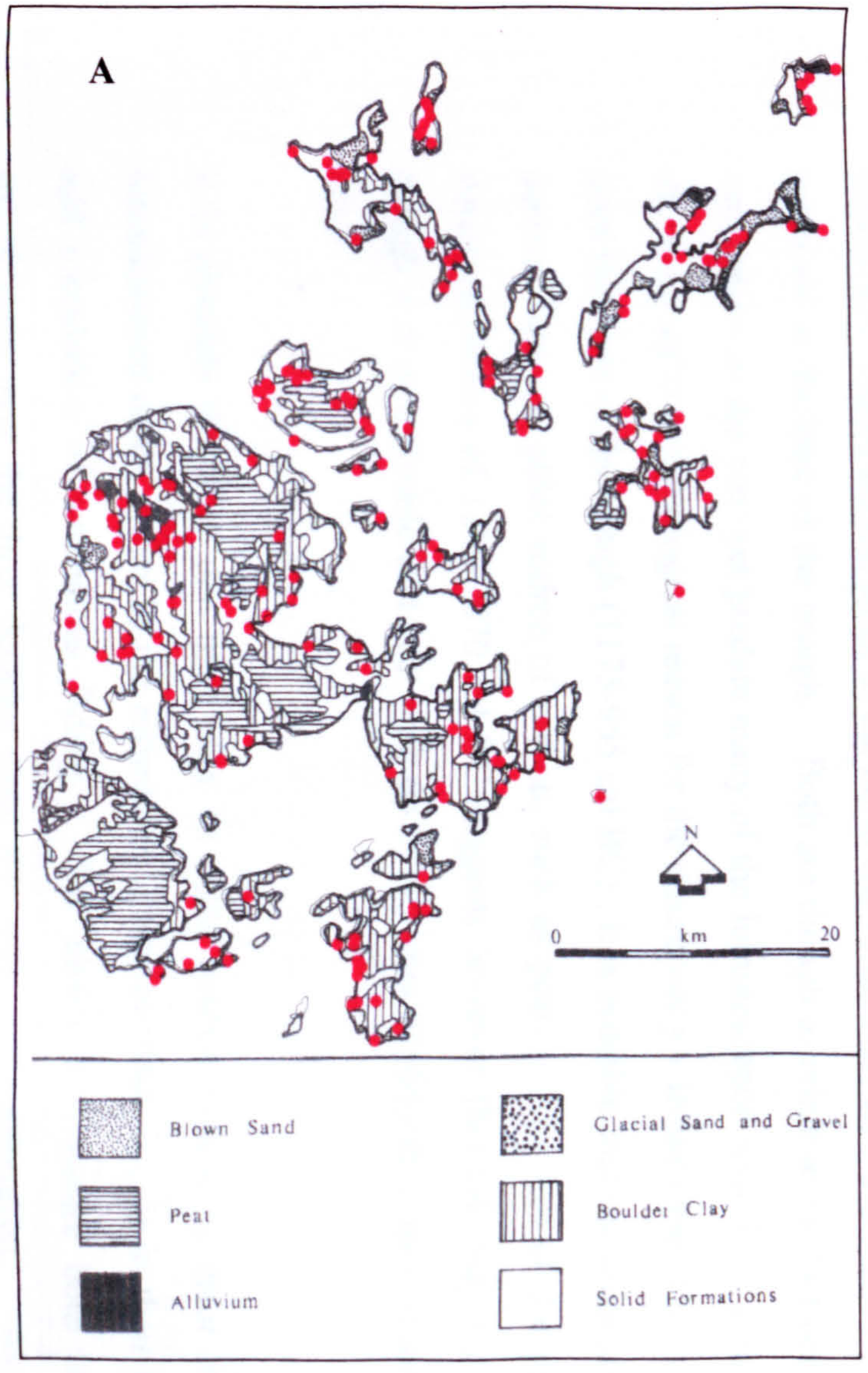

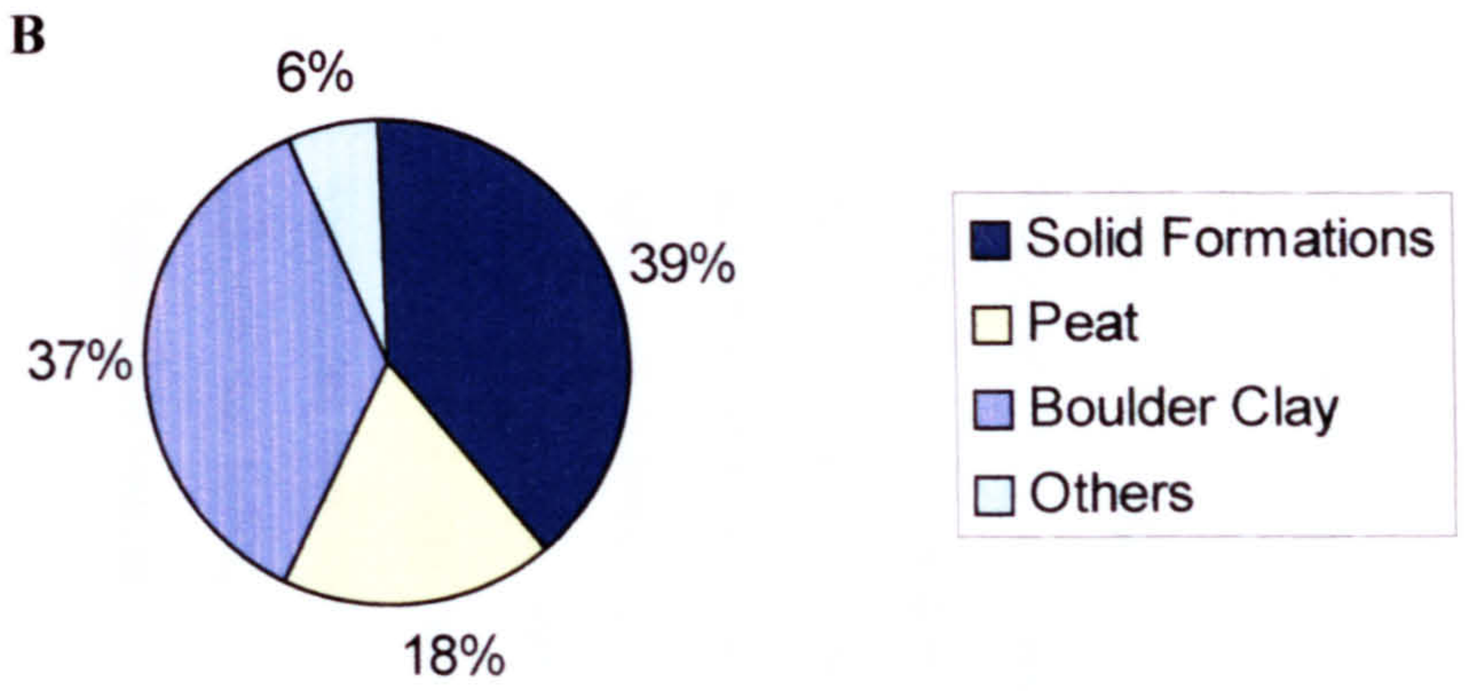

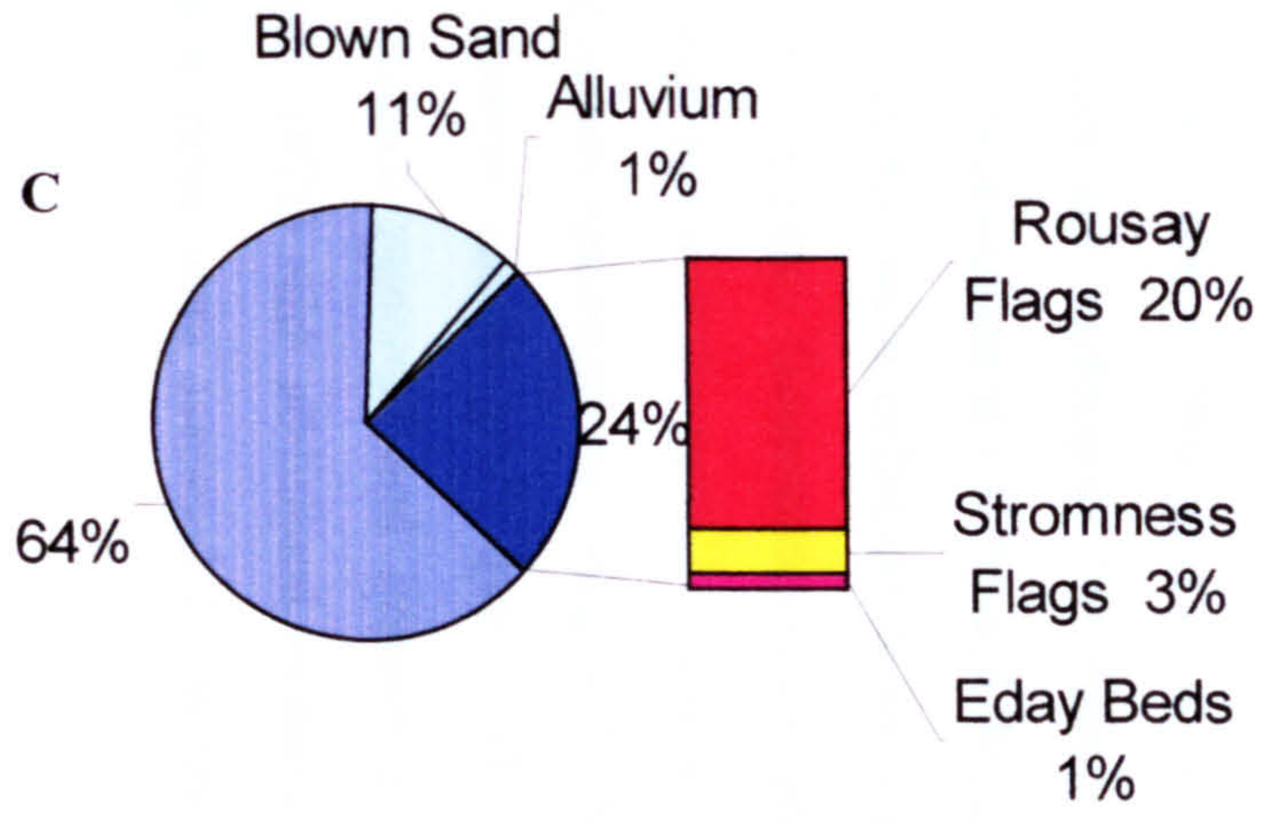

Fig 3.20 a. Distribution of Burnt Mounds on Orkney in Relation to Drift and Solid Geology (After Davidson and Jones, 1985) b. Percentage area landmass of main drift units, Orkney c. Percentage of total number of burnt mounds distributed on main drift units, Orkney

3.8.2.4 Definition of Study Area
3.8.2.4.1 Previous Studies

The Orkney Islands are one of the few areas where previous luminescence studies on burnt mounds have been conducted. The work of Huxtable et al (1976) was the first major attempt to tackle sampling strategies and techniques for dating Scottish burnt mounds. Samples were collected during the excavations at Liddle and Beaquoy from within mound contexts. In addition, surface samples were collected from a number of unexcavated mounds within the mainland Orkney cluster. Gamma dosimetry measurements were made at Liddle with in situ rilsan capsules, left over the period of a year. At other sites, the dose rate was measured with a scintillation spectrometer using a 3" NaI Crystal. Whilst the initial intention had been to perform coarse grain quartz TL dating, problems were encountered due to lack of extracted minerals and instead a fine grain polymineral technique was used (Zimmerman, 1971) with additional measurements to guard against anomalous fading. Internal dose rates were assessed by means of alpha counting and flame photometry.

The results showed great promise, with an interesting spread in ages obtained from site to site. However, in the case of Liddle, where radiocarbon dates were also available, a slight discrepancy was noted. Two carbon dates were obtained, one from a sample of peat overlying a constructional stone at the north end of the site, the other from organic material collected at the base of the trough. Both are though to relate to the last occupation/ post occupation of the site, yet predate many of the luminescence results. It is possible that there is a valid archaeological reason for the discrepancy – In the case of the material dated from the base of the trough (1175-955 cal BC) , it is possible that the unidentified material derived from an older source of carbon, such as peat. The age of the peat overlying structural stones of 1290-1070 cal BC suggests however that this may not be the case, though it is conceivable that peat built up in this area whilst other parts of the site were in use.

It is possible therefore that there may be some hidden systematic error in these early luminescence dates, either in the estimation of annual dose rate or in their measurement and calculation of anomalous fading. The ability to measure both has improved significantly over the three decades since this study was undertaken. As such, it was

deemed a good starting point to resample material at Liddle burnt mound to permit comparisons between old and new techniques to be made.

3.8.2.4.2 Further areas for Research

The Northern Isles of Orkney were considered a suitable area for site investigation on a local level to take place, given the geographical confines of each island. The decision to sample mounds on Eday was taken in consultation with the Orkney Archaeologist, based on consideration of the dating requirements of a site with a readily accessible section, and a small series of other sites in proximity. Whilst it is true that other islands within the Northern Isles cluster offered similar opportunities, the number of mounds on Westray, Sanday and Rousay and Stronsay were felt to be too large for the confines of this project. Whilst North Ronaldsay, Papa Westray and Shapinsay have a similar number of mounds to Eday, they lacked the readily available section found at one of the Eday sites.

Ten burnt mounds have been recorded on Eday, two of which are no longer visible (RCAHMS, 1946, 1980). The scheduled site of Dale, on the West coast of the island, has been truncated by a drainage ditch on the northern side, revealing a large open section. This was considered to be well suited to detailed stratigraphic sampling with a limited excavation. The seven other mounds recorded on the island lie within a 5km radius of Dale. This group of sites was considered well suited to the investigation of local burnt mound chronology.

3.8.2.5 Eday

3.8.2.5.1 Topography, geology, and archaeology of Eday

The island of Eday is located within the centre of the northern Orkney Islands. It is approximately 13km long, varying in width from 1-4km with a total area of approximately 27km^2 and a coastline around 39km in length. Much of the land lies below 50m, with the central area less than 10m in elevation and in danger of sea encroachment. It reaches a maximum height of 101m at Ward Hill on the south of the island, with smaller hills also present in the north (fig 3.21). More prominent cliffs are found on the Westside, and at Red Head in the north.

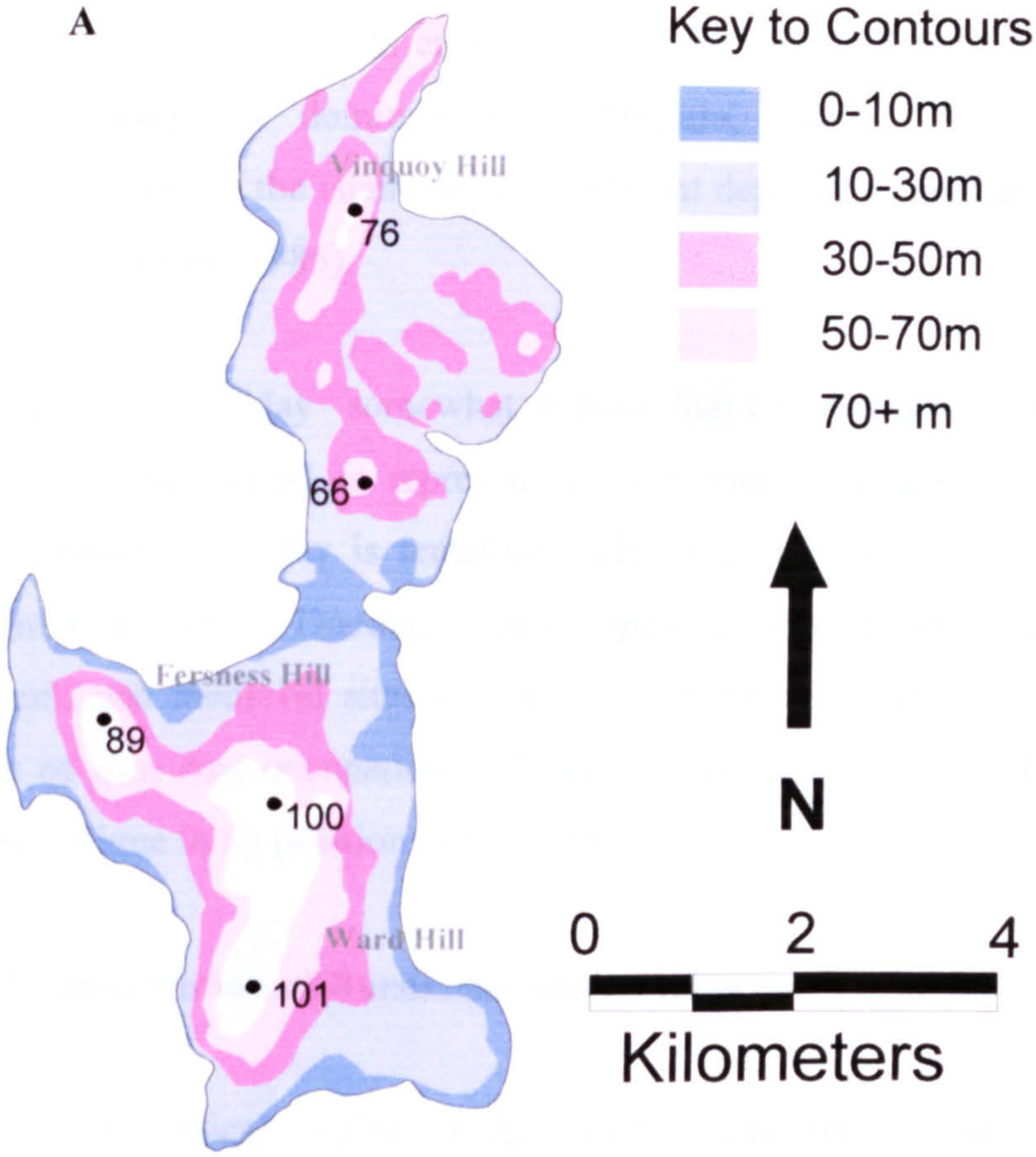

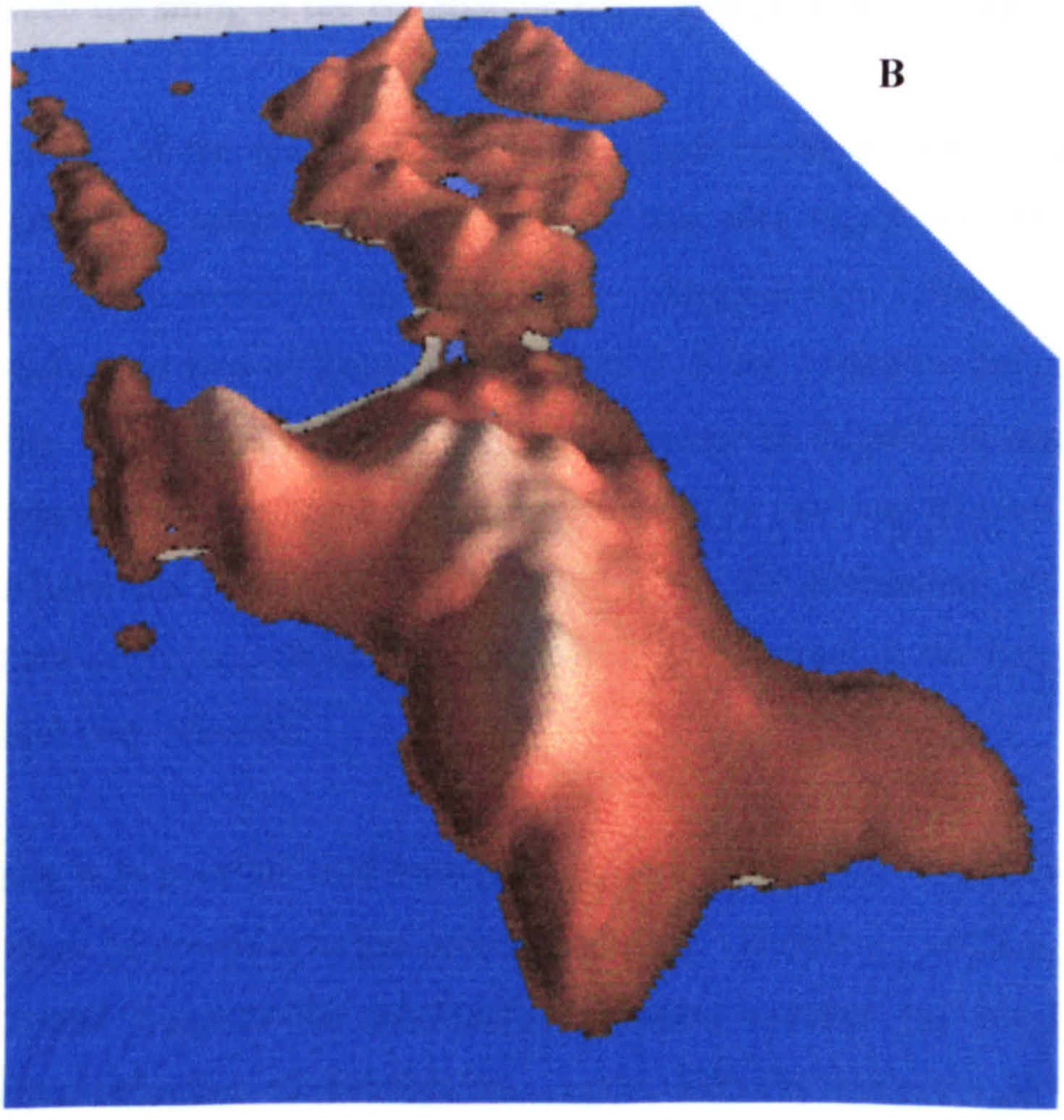

Fig 3.21 a Topography of Eday b. 3D representation of Eday (Contours based on Ordnance Survey Digimap Panorama Data)

The bedrock of Eday consists entirely of Middle Old Red Sandstone deposits, with the Eday beds being the dominant type (Mykura, 1976). Superficial deposits cover approximately half of the island, with significant deposits of peat and boulder clay evident (Davidson and Jones, 1985).

The archaeology of Eday somewhat mirrors that of Mainland Orkney (fig 3.22). The earlier prehistoric period is represented by numerous chambered cairns and standing stones. Bronze age Eday is tentatively identified by its burnt mounds and a possible settlement at the Bay of Doomy. These appear to be restricted to the south of the Island. Later Norse and medieval sites can be found across the island but to date there is little evidence of Iron Age occupation of Eday. Indeed the lack of Broch sites make Eday somewhat unique in its position (RCAHMS, 1946).

3.8.2.5.2 Distribution of Burnt Mounds on Eday

Given the geographical confines of the Island, it is possible to make positive comparisons between the siting of the 10 recorded burnt mound sites on Eday.

Seven out of the ten recorded burnt mounds occur on low lying land less than 10m in elevation, the other 3 lying between 20 and 40m (fig 3.23a). Over 80% of island, some 22.3km^2, is covered by the Eday beds. Despite this, 7 out of the 10 burnt mounds are located on an area of Rousay Flags, with 2 of the 3 others lying close to the boundary (fig 3.23b). Approximately half of Eday is covered by superficial deposits. Around 25% of the island is covered by boulder clay, c. 20% by peat and around 3% by windblown sands (Davidson and Jones, 1985). Fig 3.23c shows the distribution of burnt mounds in relation to these deposits. With the exception of one mound at the Bay of Doomy, all occur on boulder clay deposits.

Clearly it is possible that both the peat and sand deposits post-date the mounds and may therefore be covering as yet unrecorded sites. However, the lack of mounds elsewhere on the island suggests the relationship between boulder clay and burnt mounds to be an accurate reflection of distribution. Again, with the exception of Bay of Doomy, all burnt mounds are located on or at the periphery of areas of arable land.

Fig 3.22 Archaeological Sites on Eday (RCAHMS 1946, 1980)

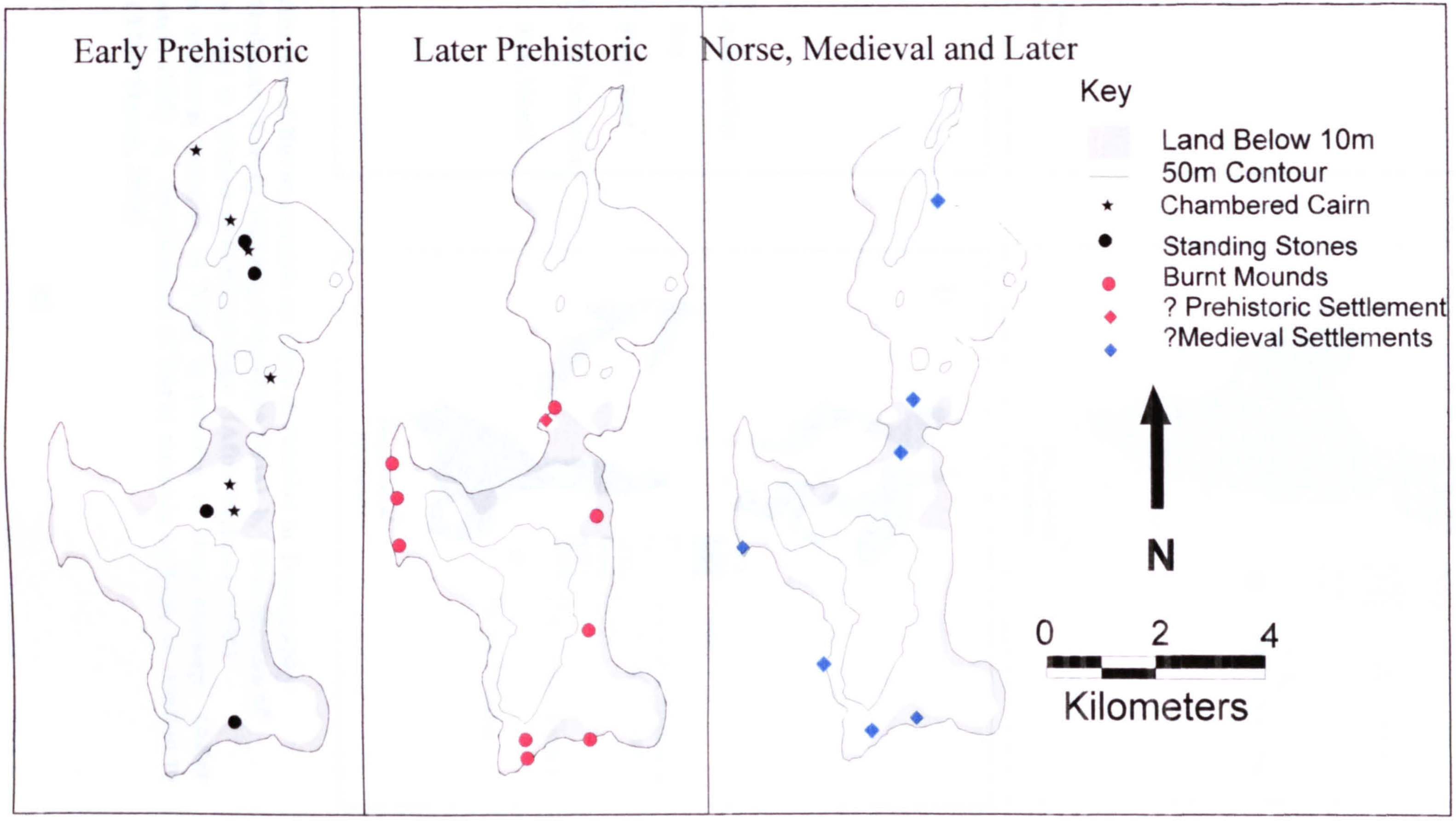

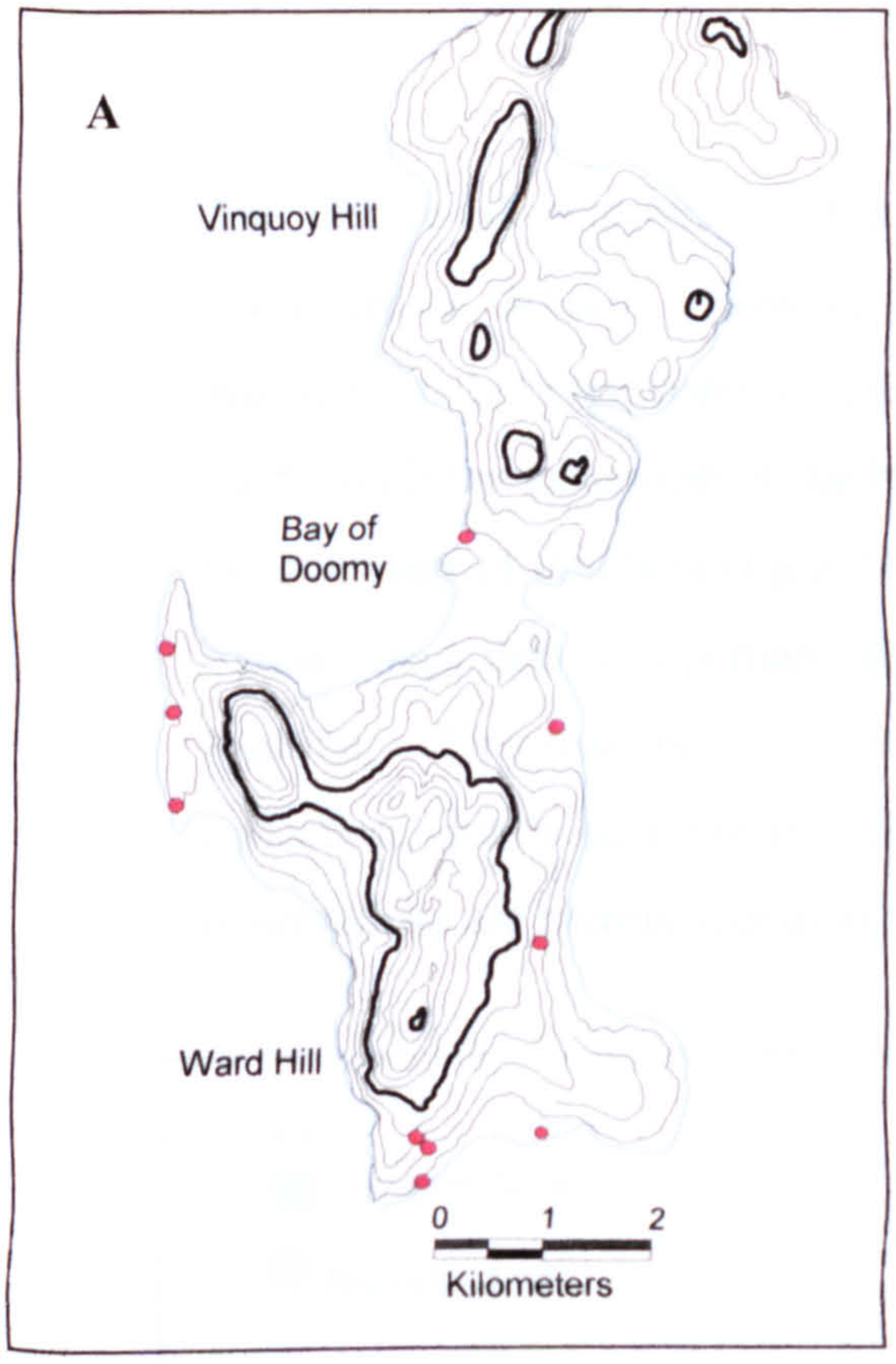

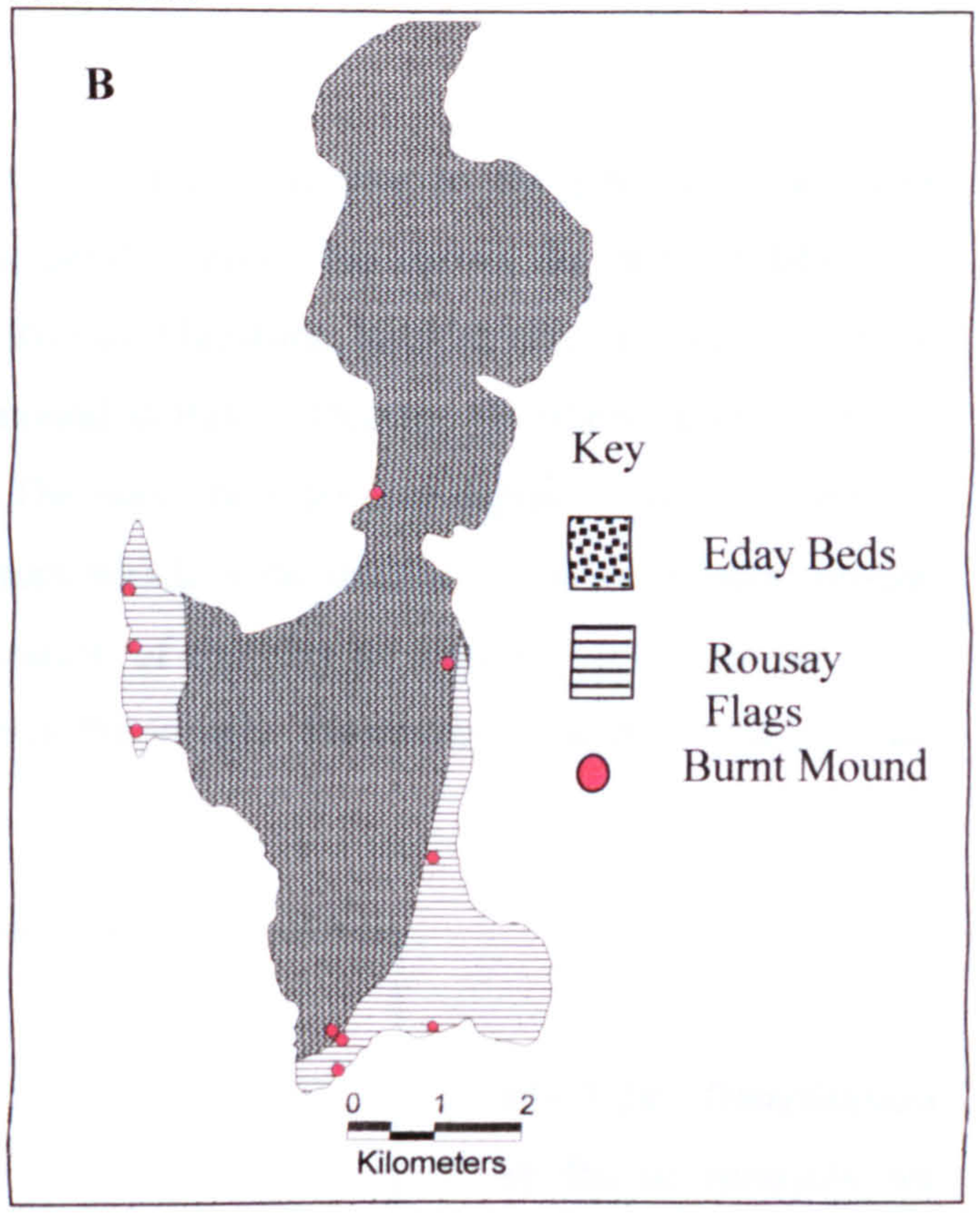

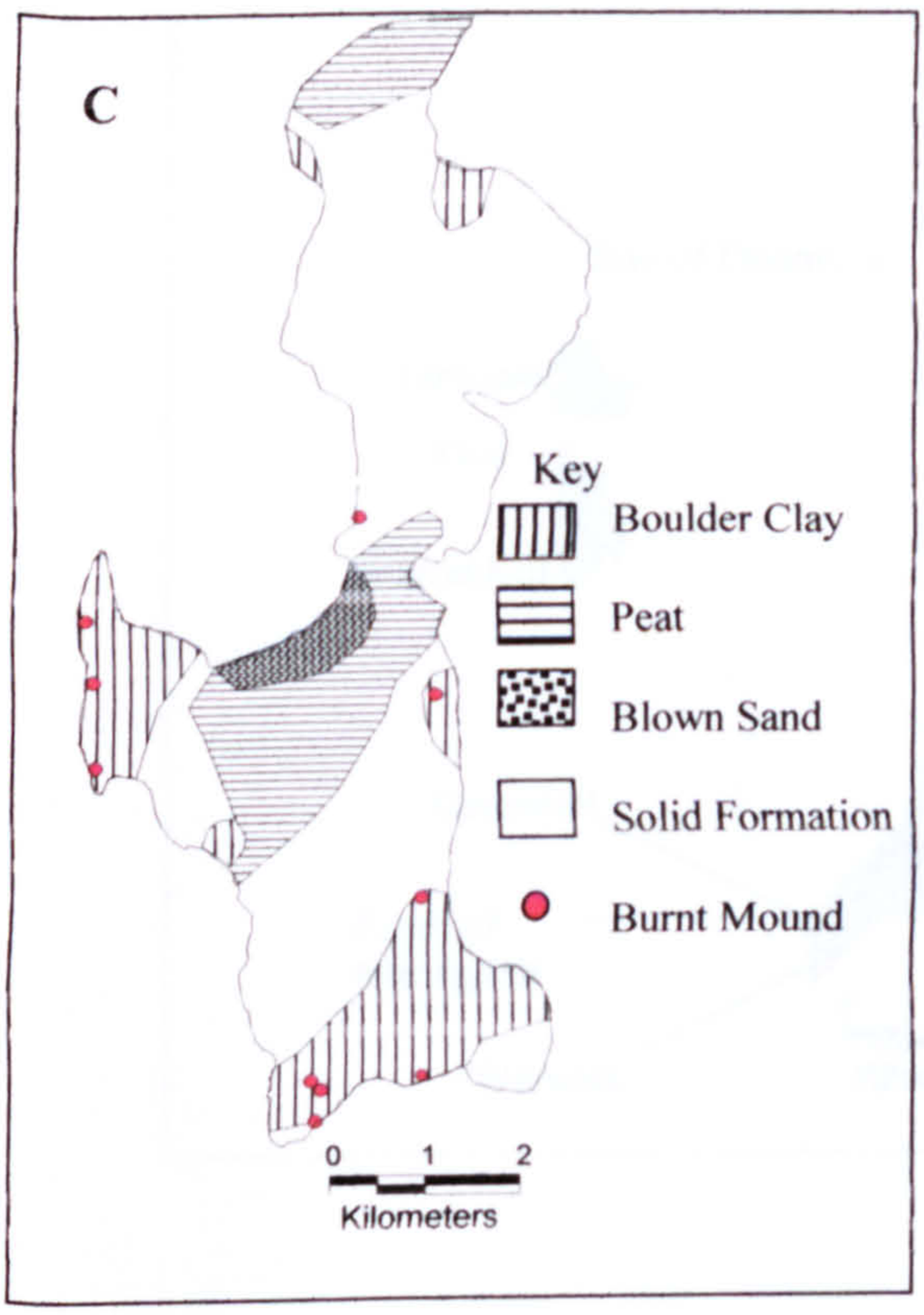

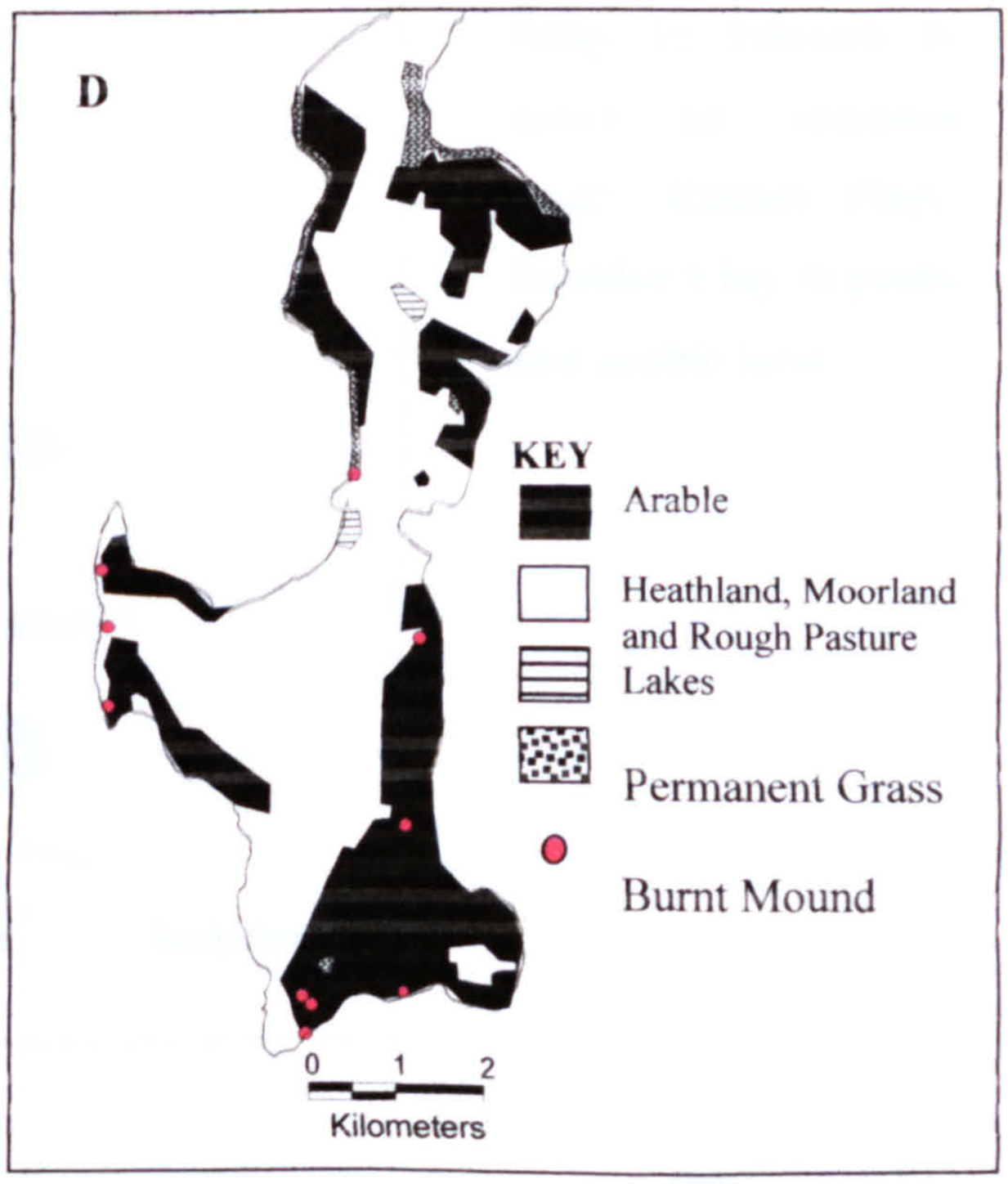

Fig 3.23 a. Distribution of Burnt mounds on Eday in relation to Topography (Contours from Ordnance Survey Digimap Panorama Data) b. Distribution of Burnt mounds on Eday in relation to Solid Geology (After Mykura, 1976) c. Distribution of Burnt mounds on Eday in relation to Drift Geology (After Davidson and Jones, 1985) d. Distribution of Burnt mounds on Eday in relation to Improved Land (After Stamp, 1944)

The picture of distribution of mounds on Eday is similar to the general trends seen elsewhere on Orkney. However this in depth analysis has shown the strong relationship which exists between common areas of Rousay Flagstone, boulder clay deposits and arable land. With the exception of the burnt mound at Bay of Doomy, all others lie on or near to the boundary of this land (fig 3.24). The major boulder clay deposits are all located on Rousay flags thus it is perhaps this feature which is the overriding factor in burnt mound location. This may be linked to utilization of the clay as a natural reservoir for water collection, ideally suited to the situation of the trough. However, without excavation such observations are merely speculation.

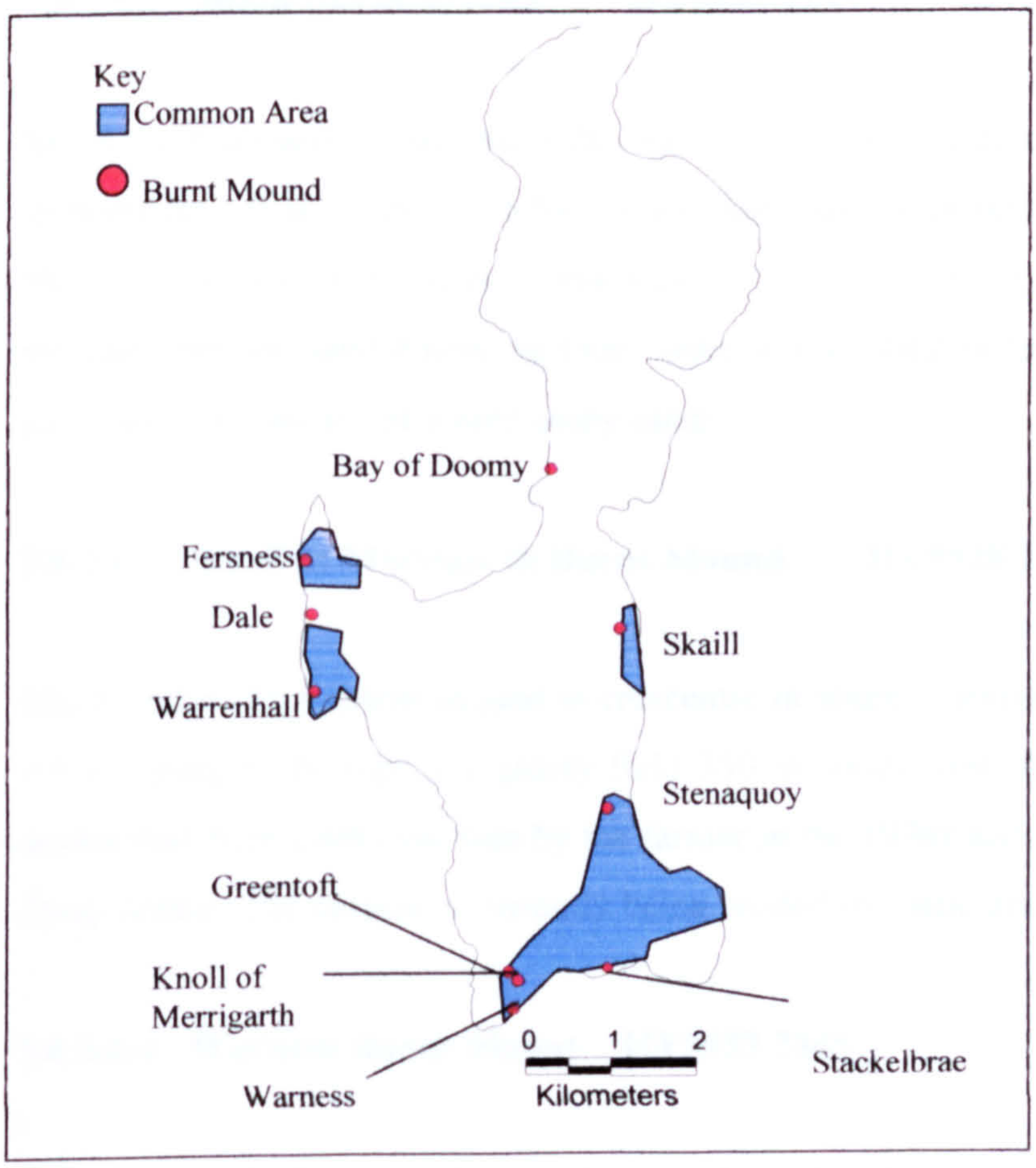

Fig 3.24 Distribution of Burnt mounds on Eday in relation to areas of common land: Rousay Flags, Boulder Clay deposits and arable land.

3.8.2.6 Summary of Burnt Mound Sites

3.8.2.6.1 Dale Burnt Mound HY5297 3312

Dale burnt mound lies close to the shore in a low boggy area to the south of Fersness farm. Measuring approximately 19 m x 10 m x 2 m, the northern third of this mound is greatly disturbed by a large drainage ditch and old boundary wall. The Western half of the mound also appears to be disturbed, with loose rubble and large flags balanced precariously on the top. Rabbit damage and animal erosion is evident.

3.8.2.6.2 Skaill Burnt Mound HY5658 3293

Skaill burnt mound stands nearly 2m high, forming a definite crescentic shape 20 m x 10 m in diameter. It is located in a low peaty heathland approximately 300 m to the north of Skaill farmhouse. The mound comprises two parts and has a great deal of rabbit damage, the east area has sand emerging from some of the rabbit holes and in the west the rabbits have exposed patches of a hard stony earth.

3.8.2.6.3 Knoll of Merrigarth Burnt Mound HY5528 2888

The Knoll of Merrigarth mound is crescentic in shape, surviving to a maximum height of 1.5 m, lying at the top of a grassy field 350 m south west of Greentoft farmhouse. This mound has been partly cut into by the farmer in the 1970s and has also had a modern stone dump added. The mound is currently being eroded by cattle grazing in this field.

3.8.2.6.4 Warness Burnt Mount HY5533 2845

Warness is a badly eroded mound situated on the shore line along a coastal path 800m SSW of Greentoft farm. The mound is being eroded by the sea to the east and by a small stream running west to east, there is also erosion by rat holes, the coastal path and a farm vehicle track. An exposed north south section is visible along the line of the footpath showing burnt mound material at the western end and probable settlement remains towards the east.

3.8.2.6.5 Stackelbrae Burnt Mound HY5641 2884

A large section of eroding coastline has revealed a series of structural deposits of probable medieval/post medieval date, recorded in section by Moore & Wilson (1996). The southern edge of a probable burnt mound can be seen in section extending over 13m, the western edge overlying a deposit of midden material.

3.8.2.6.6 Fersness Burnt Mound HY5290 3375

A badly damaged and eroded mound, now surviving as two separate mounds, located at the point of Fersness 150 m south west of the farm and 100 m from the coast. The north mound is larger, 7.5 m x 5 m, and badly eroding in places with burnt mound material now visible in areas, while the south mound, 5 m x 4 m, has a covering of turf protecting it from erosion.

3.8.2.6.7 Stenaquoy Burnt Mound HY5644 3080

Located to the south of Stenaquoy farm in a cultivated field 200 m east of the school, though reduced in height by ploughing and farm improvements it is still clearly visible. Covering a large oval area 12 m x 10 m and standing to a height of approximately 0.7 m this was identified by a few scatters of burnt stones within the plough soil.

3.8.2.6.8 Greentoft Burnt Mound HY5539 2878

Shown on OS maps as lying approximately 30 m to the East of the Lady Well on Greentoft Farm but no obvious traces of the mound were visible. Perhaps the mound has not survived farm improvements or the map location is incorrect.

3.8.2.6.9 Bay of Doomy Burnt Mound HY5577 3481

The site of a burnt mound at the Bay of Doomy is recorded in the NMR as having been lost through sand encroachment some years ago. A visit to the area failed to locate the mound, though a large sand dune occupying the approximate position of the mound may represent the remains.

3.8.2.6.10 Warrenhall Burnt Mound HY530 322

The burnt mound at Warrenhall is recorded in the NMR as having been completely removed during farm improvements some time around 1927.

3.8.2.7 Sampling Strategy

The selection of surviving burnt mounds on Eday offer a unique opportunity to examine the relationships between a group of mounds within the close confines of a small island. The truncated section at Dale is ideal for detailed stratigraphic sampling allowing questions of duration of use to be addressed. Surface sampling at the remaining mounds will provide important local information with minimal damage to the sites.

The aims of the fieldwork therefore were to conduct detailed sampling at the Dale burnt mound, and minimally invasive sampling at the other sites where possible, Where available, organic material was to be collected for carbon dating, the measurement program thereafter to be aimed at assessing (a) the suitability of the available materials for luminescence and radiocarbon dating, (b) the relationship between ^{14}C and luminescence dating (c) the heterogeneity of dating results within the sectioned site and potential for determining duration of use (d) the implications for minimally invasive sampling of burnt mounds and (e) the chronological relationship between the sectioned sites and their neighbours.

3.8.3 The Shetland Isles

3.8.3.1 General

The Shetland Islands lie approximately 100 miles off the north coast of Scotland, forming a long and narrow chain of land which stretches around 70 miles N-S. The majority of land lies between 0-100m in elevation, with higher regions running down the centre of the Island chain. The highest area, in the Northern Mainland region of Northmaven reaches upwards of 500m in elevation (see fig 3.25).

The geology of the region is complex. There is a dominance of Schist, Gneiss and Phyllites in the central band running North-South. Old Red Sandstone deposits dominate the Western Mainland and the area around Lerwick, Bressay and Sumburgh. Further north a more complex picture of lavas, granites, gabbros and metamorphic rocks is seen. This is admittedly an oversimplified picture of Shetland's solid geology (further detail may be found in Mykura, 1976) Drift geology is less complex with much of Shetland covered by peat, till and morainic drift. Less than 10% of Shetland's land is under plough or improved grass land. The vast majority of land consists of heathland, moorland and rough pasture (Stamp, 1944).

3.8.3.2 The Archaeology of Shetland

The archaeology of the Shetland Isles is in some ways as impressive and complex as that of Orkney. Whilst the geology of the region does not lend itself to the monumental flagstone built structures of the Orkney Islands, vast tracts of high ground have preserved beneath their peat cap a prehistoric landscape rivaled by few other areas of Scotland.

The Neolithic farming community of Shetland would appear from the archaeological record to be well developed and organized. Over 150 probable Neolithic 'oval' houses are identified in the SMR alone. Many of the long moorland boundaries are attributed to this time (Fojut, 1986). Evidence of woodland clearance and the introduction of cattle, sheep and red deer can be charted from the mid 3rd millennium BC onwards (Butler, 1996). Climatic deterioration and the formation of peat in the Bronze Age is thought to have forced a contraction in settlement and land use to lower ground. Pollen evidence from across Shetland indicates a move from arable to pastoral farming around this time (Butler, 1998). The numerous burnt mounds described in detail in Chapter 2 attest (if assumptions as to their chronological placement are correct) to a presence of people along the coastlines of Shetland, a pattern of settlement mirrored to the present day. Excavations such as that at Kebister, Dales Voe (Owen, 1998) show occupation from the early prehistoric period through to present day, interpreted as a sequence of re-occupations of a well situated farming site. Such patterns of re-occupation are repeated elsewhere. At Scatness, evidence of occupation from the Bronze Age through to modern times is being revealed during the excavation of the Old Scatness Broch and its surrounding area (Shetland Amenity Trust). The impressive Iron Age broch is one of many found across

Shetland (RCAHMS, 1946). A number of broch sites are later seen to develop into less defensive wheelhouses in the late Iron Age period.

Late Iron Age Shetland followed a similar path to that of Orkney, with Viking settlement in the 10th century heavily influencing cultural records. It remained in Norse hands until 1469 when Shetland was pledged to Scotland as part of a marriage dowry from the King of Denmark.

3.8.3.3 The Burnt Mounds of Shetland

There are approximately 260 recorded mounds on the Shetland Islands. Most cluster on or near the shoreline, predominantly on the south of the Island (fig 3.25). A density plot of the island shows on average there to be between 1 and 3 mounds per km^2 in these areas (see Appendix A). However several areas show considerably higher densities. The Walls area on western mainland shows an average density of 3-4 mounds per km^2, but reaches as high as 8. Similar intensities are seen on Fair Isle, and smaller 'hotspots' can be found on West Burra, Papa Stour and the area to the north of Lerwick.

Only 27% of the mounds on Shetland have associated geometric information. The vast majority of these are crescentic in form, with only a few isolated examples of oval and circular mounds noted (see Appendix A). Information on size is available for just over 30% of mounds on Shetland. Within this group, the predominant size lies between 10 and $100m^3$. 15 mounds are calculated as being greater than $100m^3$, representing 1/3 of the total mounds of this size in Scotland. Mound volumes less than $1m^3$ are absent (see Appendix A). 12% of mounds on Shetland are known to have associated structures, mainly slab built troughs.

Canter (1998) notes an affinity between burnt mounds and land below 50m, with almost 90% of the known mounds occurring in this region. Breaking these data down into 10m elevation bands, it can be seen that over half the mounds occur in the 0-20m elevation region, a further quarter in the 20-30m region (fig 3.26). The number of mounds occurring in the 0-50m band is vastly over-represented for the amount of area this region covers – approximately 47% of Shetlands land mass- indicating a real and strong correlation.

In relation to solid geology (fig 3.27) it can be seen that burnt mounds are over-represented on areas of old red sandstone and lava, and under-represented on schist, gneiss and phyllite regions. This under-representation cannot be explained solely in terms of topography.

Over half of Shetland's land is covered in peat deposits, and around a sixth by boulder clay and glacial drift. The majority of the rest has no drift deposits, though small isolated wind blown sand and alluvium deposits can be found across much of Shetland. Figure 3.34 shows the relationship between the percentage land cover of drift deposits and burnt mounds occurring on them. It can be seen that there is a preference for mounds to be found on bedrock and boulder clay/drift deposits. There is a close correlation between burnt mounds and areas of arable or permanent grassland and an obvious avoidance of the heathland, moorland and rough pasture which dominates Shetland's landscape. Admittedly this may be more a reflection of survey bias than a true reflection of distribution.

3.8.3.4 Definition of Study Area

3.8.3.4.1 Previous Studies

Despite its wealth of burnt mounds, the Shetland Islands have not yet been the subject of any large scale chronological study. Whilst a number of mounds have been excavated and have associated radiocarbon dates (see above), no luminescence dating has, as yet, been undertaken.

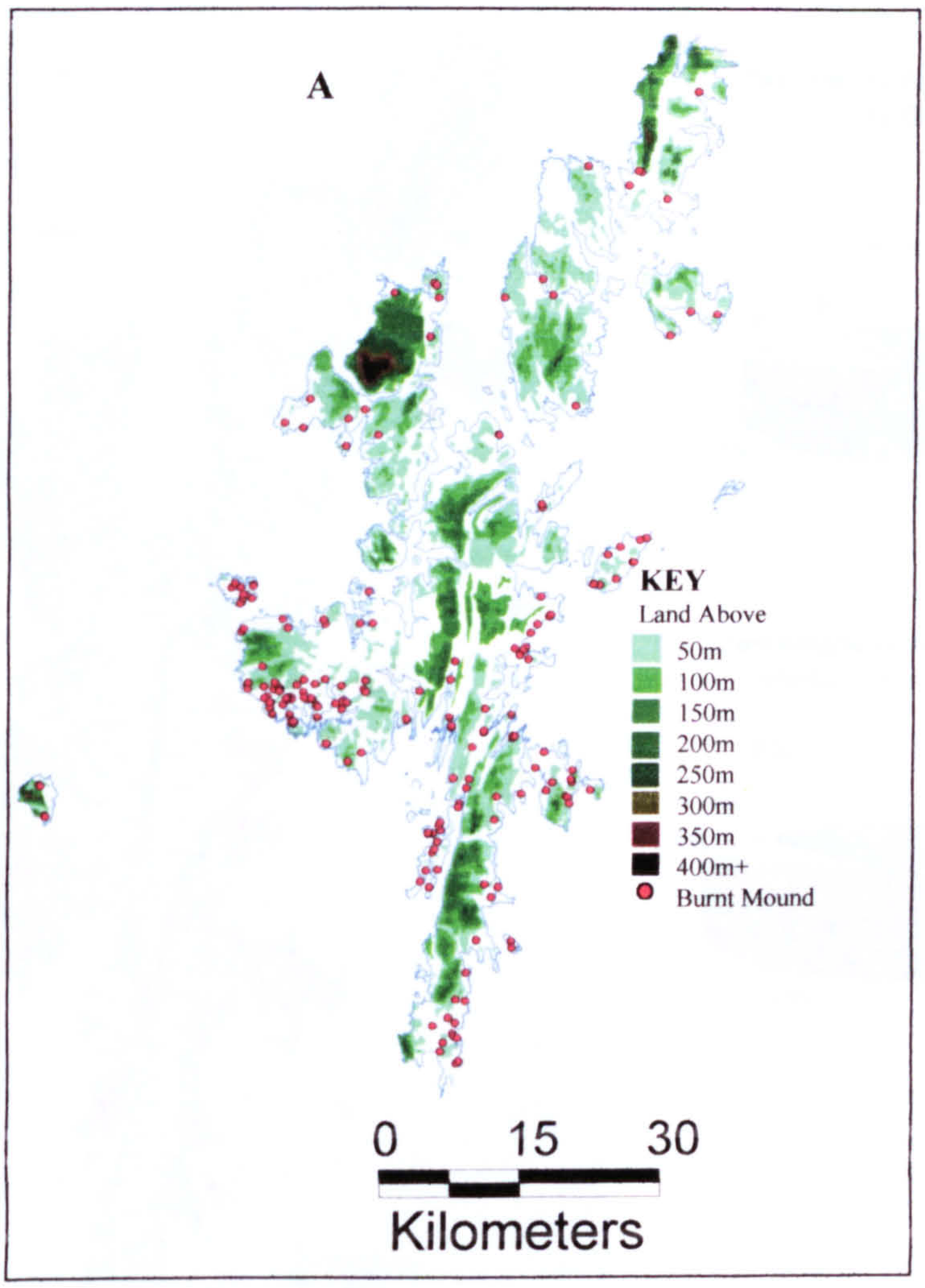

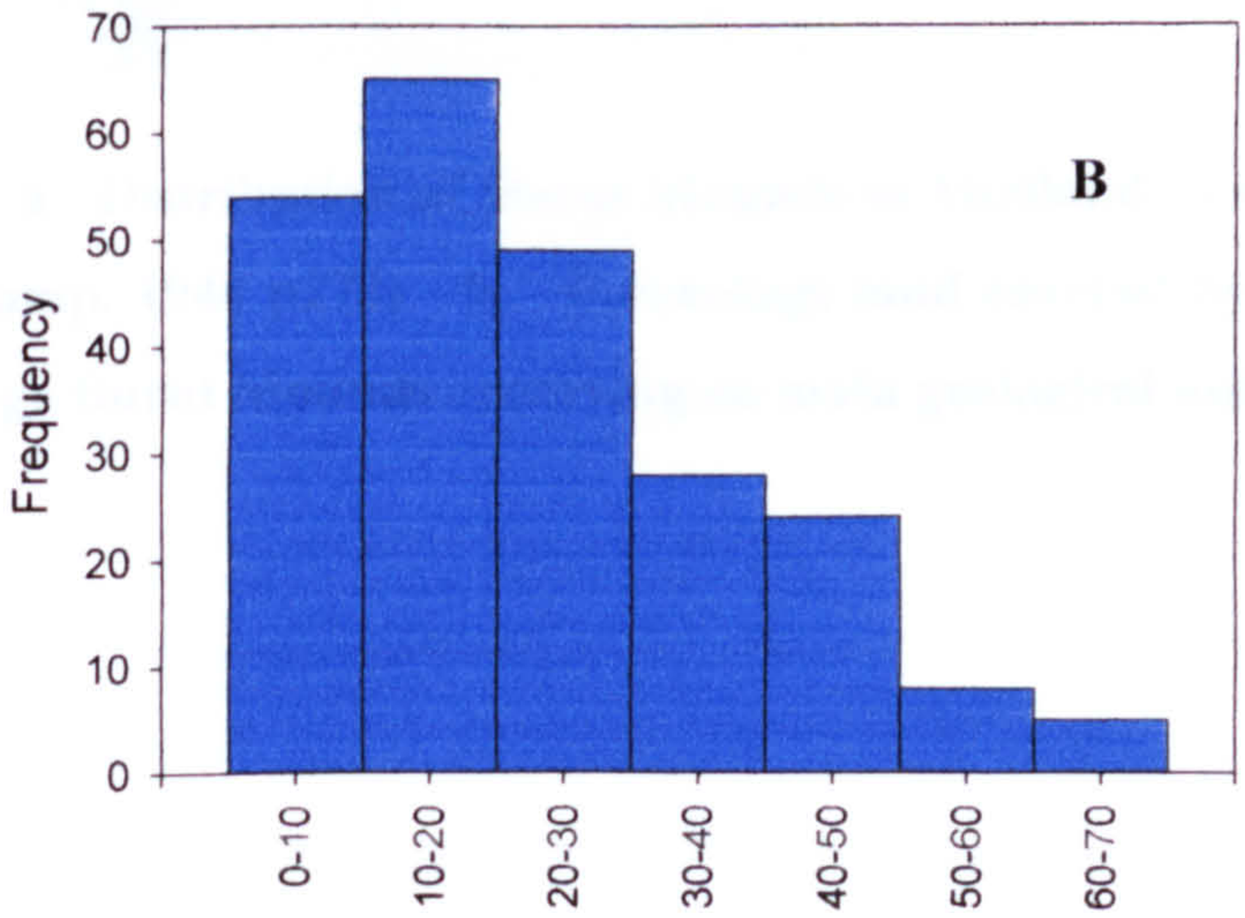

Figure 3.25 a. Distribution of Burnt Mounds in Shetland in relation to Topography (contours based on Ordnance Survey Digimap Panorama data)

b. Histogram of burnt mound distribution in 10m elevation bands

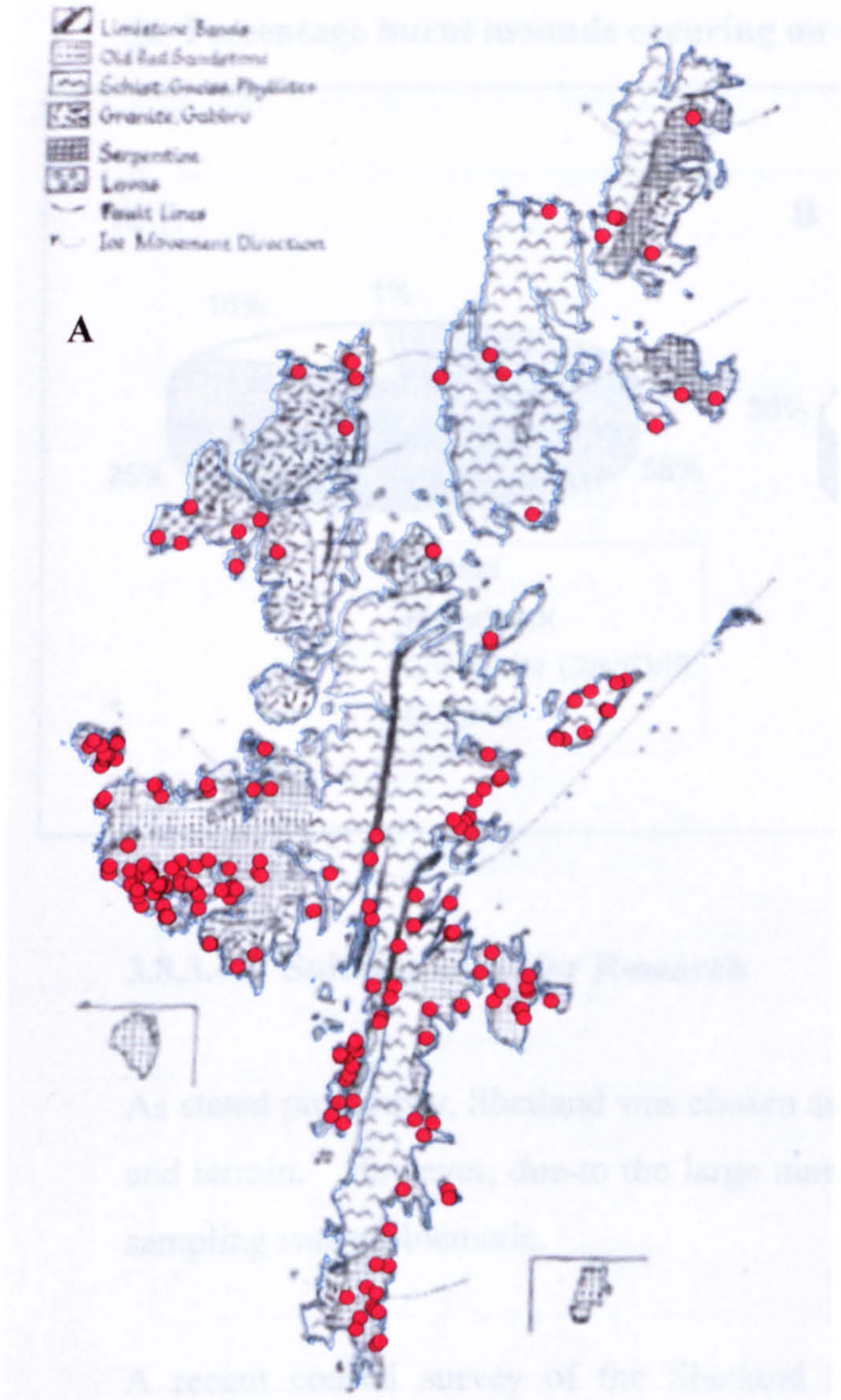

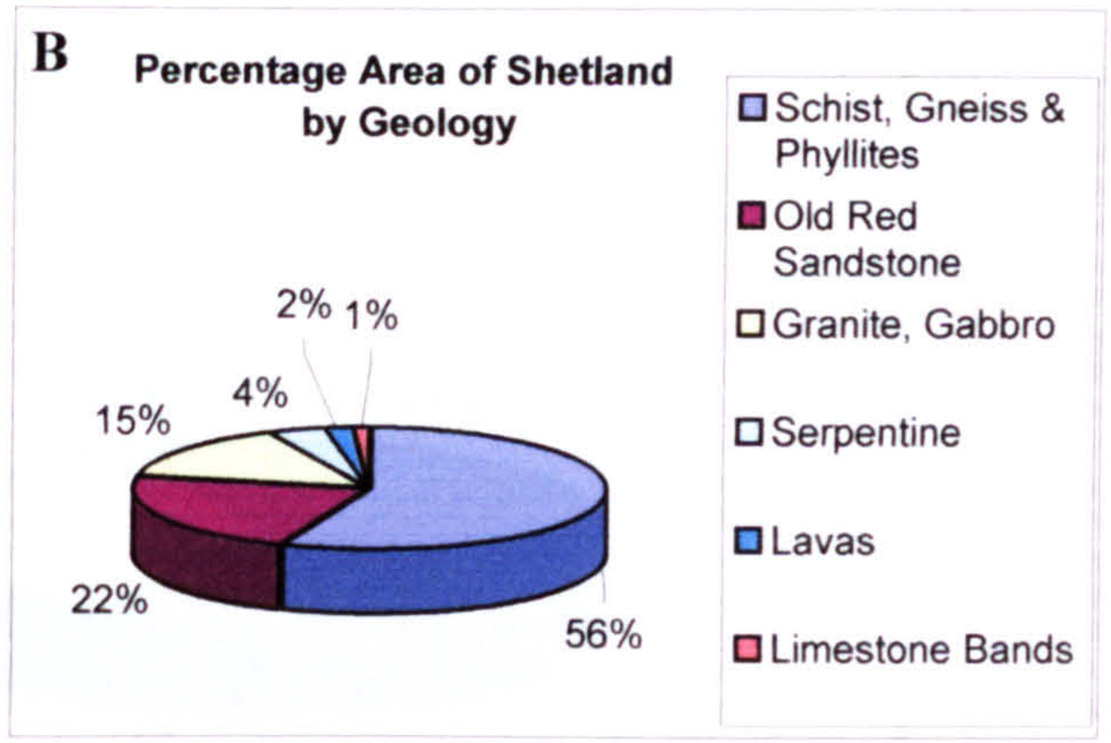

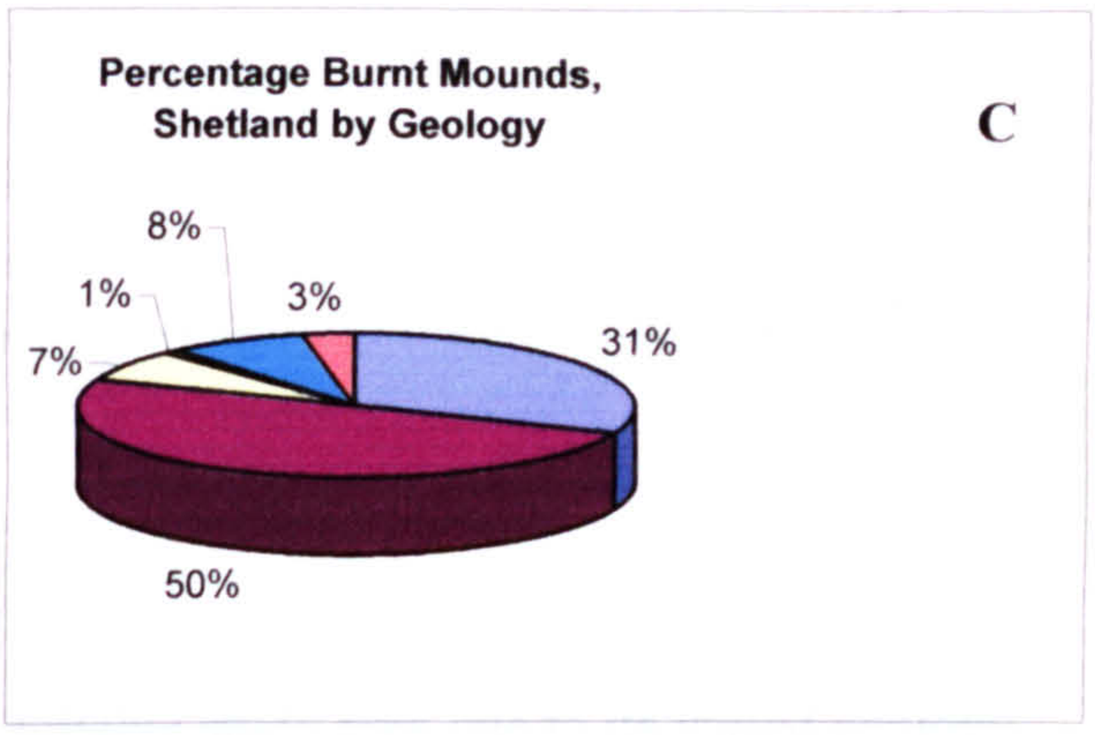

Fig 3.26 a. Distribution of Burnt Mounds in Shetland in relation to Simple Geology (after Stamp, 1944 p272) b. Percentage land covered by main geological units c. Percentage Burnt Mounds occurring on main geological units

Fig 3.27a. Percentage land covered by main drift deposits, Shetland

b. Percentage burnt mounds occuring on main drift deposits, Shetland

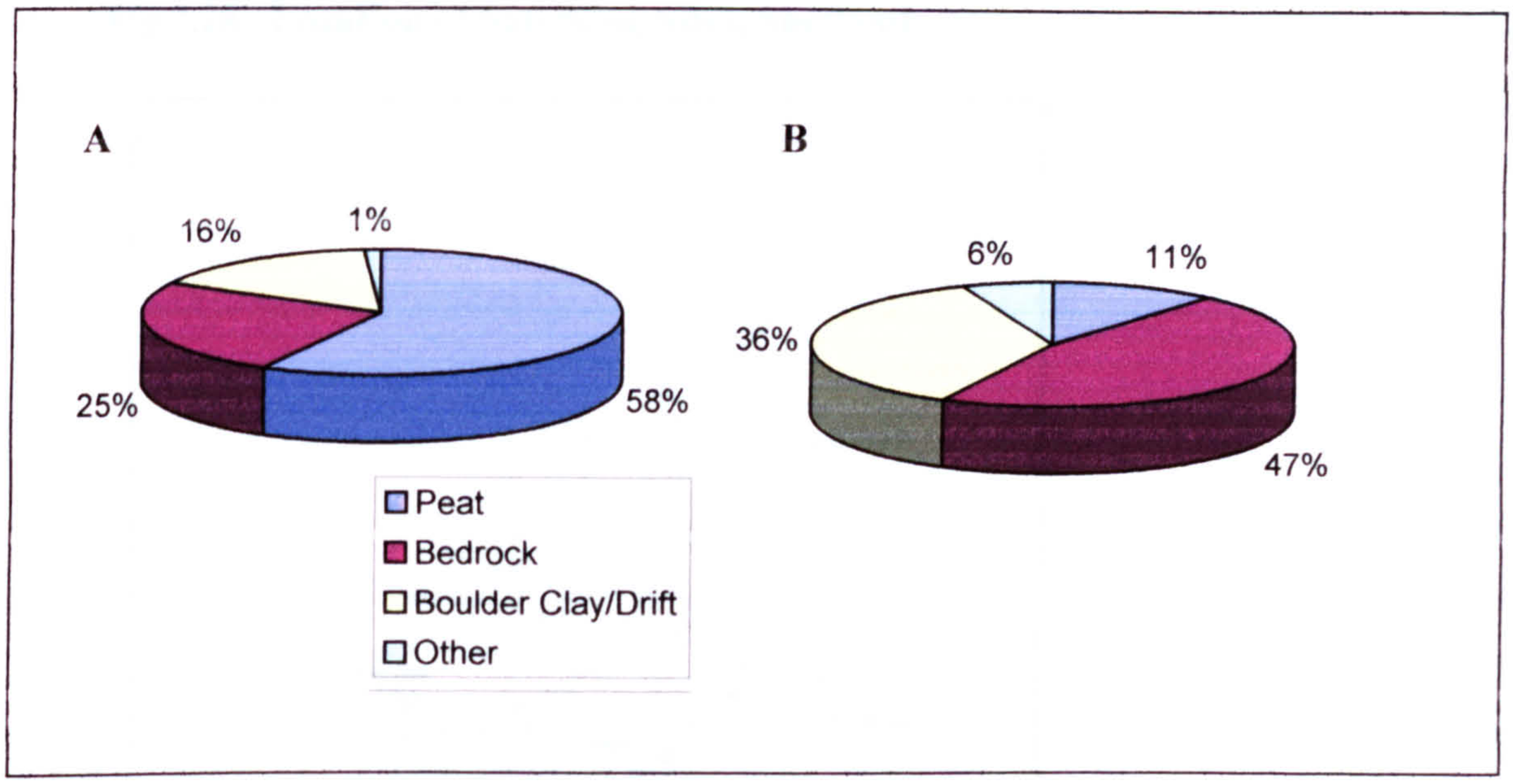

3.8.3.4.2 Suitable areas for Research

As stated previously, Shetland was chosen as a suitable study area due to its varied geology and terrain. However, due to the large number of recorded mounds, selection of sites for sampling was problematic.

A recent coastal survey of the Shetland Islands highlighted a number of mounds in immediate threat (Moore and Wilson, 1996b, 2000). Such mounds were considered appropriate for sampling as the opportunities for further work at these sites may be greatly reduced as coastal erosion increases in future years. After consultation with the Shetland Amenity Trust and Historic Scotland, it was decided that four of these mounds would be sampled in detail. The sites had previously been recorded in summary, and were known to have been truncated and therefore to exhibit existing sections from which samples could readily be retrieved (fig 3.28). Of the four sites chosen one, Cruester, was under excavation at the time of sampling and allowed for a far more varied selection of stones to be collected. Another, Tangwick, had been excavated a number of years previous and the two others had been recorded in summary during the coastal survey.

The four sites were evenly dispersed over the islands, each representing a different geological region of Shetland to enable a large variety of stone types to be collected.

Fig 3.28 Location of Sampling Sites, Shetland

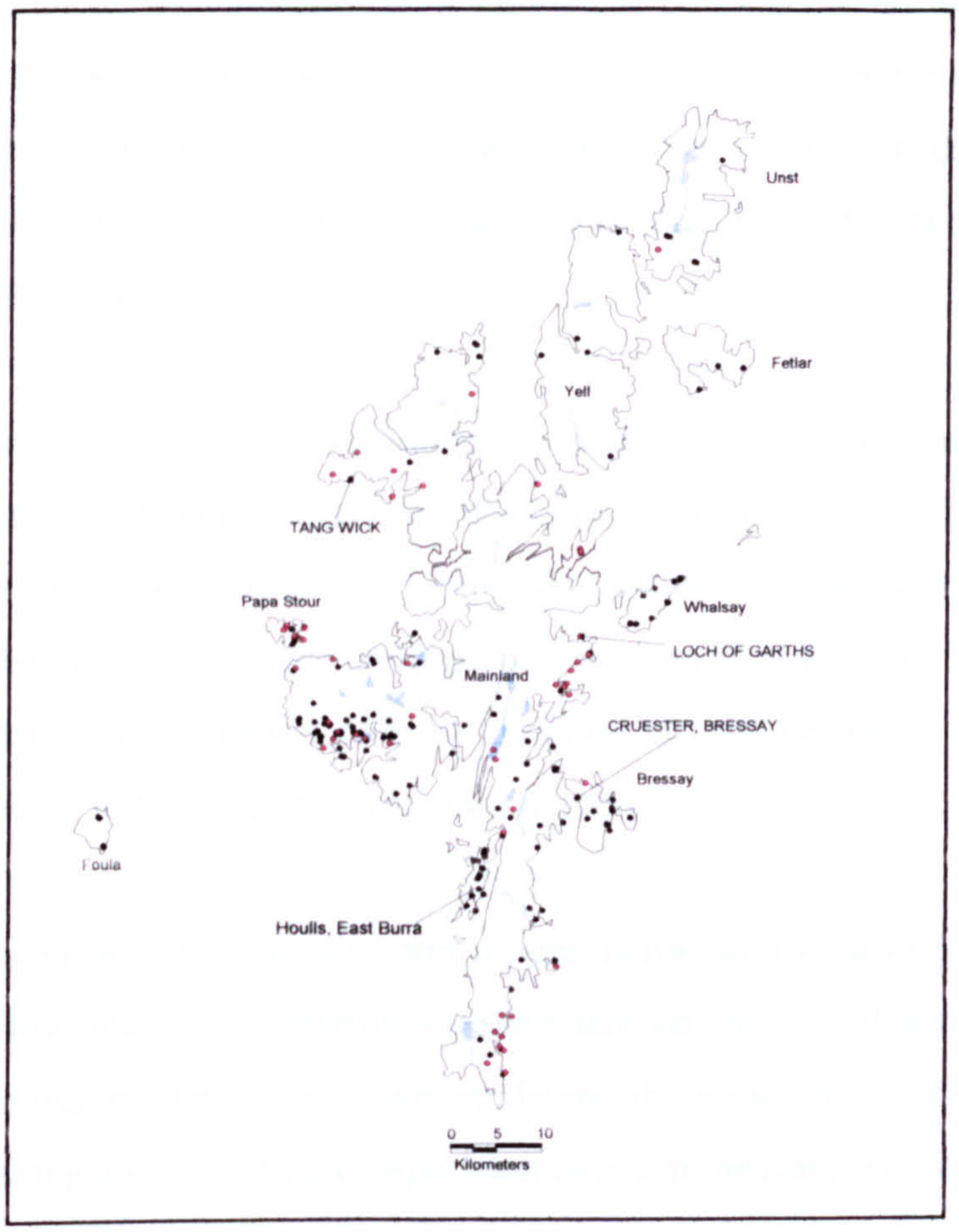

3.8.3.4.3 Cruester, Bressay HU 4815 4232

3.8.3.4.3.1 Topography, Geology and Surrounding Burnt Mounds

(see Appendix C for local area maps)

Cruester burnt mound is located on the Island of Bressay, off the eastern coast of Mainland Shetland. There are ten other burnt mounds recorded on Bressay and the neighbouring Isle of Noss. The topography of both islands is hilly to the south, reaching a maximum height of 210m at Ward Hill. Six of the eleven mounds are located below 20m elevation, the rest occurring between 20 and 60m. This is a fairly typical distribution for Shetland, with the exception of the two mounds on the Eastern coast of Bressay which are located between 50 and 60m, representing some of the highest situated mounds in Shetland.

The geology of Bressay and the Isle of Noss is relatively simple compared to the rest of Shetland. To the north of both islands are bands of cross-bedded sandstone containing pebbly lenses of middle and upper old red sandstone origin. A band of planar-bedded sandstone with subordinate siltstone can be found on the north of Bressay, but the majority of the island, and the north and south of Isle of Noss are covered by flaggy sandstone and siltstone rocks. All but three mounds are located on this deposit, the remainder being found on the cross-bedded sandstone to the north. None is found on the flaggy sandstone and siltstone deposit.

The drift geology is dominated by peat deposits inland, with significant boulder clay and glacial drift deposits around the coast of Bressay. The burnt mounds are found on both boulder clay/glacial drift deposits and on the bedrock. None is located on peat. Examination of areas of improved land on Bressay and Noss show a strong relationship between the location of burnt mounds and the perimeter of permanent grassland, though several in the east are located on moorland.

It is clear that Cruester burnt mound is not unique in its location on Bressay, but tends to follow the same patterns as elsewhere on the island and in Shetland in general. The geology of the island make sandstone the most likely stone type to be encountered, thus making an interesting comparision between the samples from Eday.

3.8.3.4.3.2 Site Summary and Sampling Strategy

Cruester burnt mound is approximately 20m in diameter, standing around 2m in height. It is located on boggy ground, with two water courses running around the northern and southern edge of the mound to the coast. The site has been truncated by coastal erosion and burnt stone deposits are exposed in the coastal section.

The Royal Commission records that in 1933 a small beehive cell was uncovered on the seaward side of the mound. Sherds of steatitic pottery were also recovered (RCAHMS, 1946). By the time of the Ordnance Survey re-examination of the site in 1964 there was no trace of the beehive cell, though a 'short cist' feature was noted .

During the 1996 coastal survey, the erosion face was cleaned and recorded (Moore and Wilson, 1996b). Towards the northern end of the section, layers of ash and soil were noted amongst the burnt stone deposits. A layer of peat was also recorded, appearing to seal a stone lined pit. A column of coursed masonry forming the corner to a wall was also noted extending for over 2m in a southward direction. Substantial structures were observed in the central and southern parts of the section, together with a stone box, thought to be the 'short cist' recorded by the Ordnance Survey.

During the time of sampling, Cruester burnt mound was to be excavated by EASE archaeology as part of ongoing work on coastally eroding sites in the Northern Isles. The sampling strategy was therefore left open to take into account any deposits which might be encountered during excavation. The overriding intention was to collect enough material to allow detailed analysis of the expected duration of use of the site to be carried out. Where possible, such samples should also include radiocarbon dating material.

3.8.3.4.4 Tangwick, Eshaness HU 2335 7751

3.8.3.4.4.1 Topography, Geology and Surrounding Burnt Mounds

(see Appendix C for local area maps)

Tangwick burnt mound is located on the southern coast of the Eshaness peninsula, on the edge of a storm beach. The nearest mound is around 2km to the NW, though there are five others within a 7km radius of Tangwick. The density of mounds in this area is low compared to further south. Much of the Eshaness area lies below 50m in elevation, rising to around 150m to the east. The majority of this group of mounds lie below 30m in elevation.

The geology of the area immediately surrounding Tangwick is dominated by Ryolitic and Andesitic lavas, with larger granite intrusions located to the east. There appears to be no geological preference to the location of burnt mounds in the area. The majority of land in this area is moorland, on which most mounds are situated.

3.8.3.4.4.2 Site Summary and Sampling Strategy

The site of Tangwick was excavated in 1996 as part of the Shetland Burnt Mounds Project (Moore and Wilson, 1996, 2000). Details of the excavation were outlined above in previous sections. Two radiocarbon dates were obtained from the site. A charred cereal grain from a silty layer underlying the primary mound and overlying the peat deposit was dated to 1880-1520 cal BC. Given that no evidence was found for activity which pre-dated the site, the excavators interpreted the date as being representative of activities carried out during the earliest use of the site.

A fragment of charred Iris rhizome found in the ashy layer between primary and secondary stone deposits was also dated. This gave an age of 1100-850 cal BC and was interpreted as being derived from the clearing out of refuse within the structure at an intermediate stage in the use of the burnt mound.

If both interpretations are sound, the dates indicate either a very long period of use, or a hiatus between primary and secondary mound activity. The luminescence sampling strategy was designed to address this uncertainty. By concentrating sampling in the area of strategraphic deposits associated with the radiocarbon dates it was hoped that ambiguities in the interpretation of the dates may be resolved. A decision was also taken to sample the peat lying below the deposit which contained the charred grain. It was hoped that a radiocarbon date for this material may help to clarify the relationship between the two.

3.8.3.4.5 Houlls, East Burra HU 3755 3230

3.8.3.4.5.1 Topography, Geology and Surrounding Burnt Mounds

(see Appendix C for local area maps)

The islands of West Burra, East Burra and Trondra are separated by only a few hundred meters, lying approximately half a kilometer off the western coast of Southern Mainland. They are low lying, less than 50m in elevation. Metamorphic in origin, their solid geology is composed mainly of micaceous psammite and migmatic gneiss (Mykura, 1976). There are relatively few drift deposits, small areas of boulder clay/ glacial drift being the most

significant. These islands are unusual in their absence of significant peat deposits. There is no peat on East Burra and Trondra, and only a small isolated deposit on West Burra.

Twenty two burnt mounds are recorded in this area, the vast majority on West Burra. This is in part due to Gordon Parry's survey of West Burra (Hedges, 1984). Four are known on East Burra, including that of Houlls. All are located below 20m elevation. There would appear to be no evidence of preferential selection of location with regard to either solid or drift geology in this area however most are located on or near to improved land.

3.8.3.4.5.2 Site Summary and Sampling Strategy

During the 1996 coastal survey, the erroded face of the mound at Houlls was straightened and recorded in section. The mound appeared homogenous in composition. A 'roughly built stone structure', probably a tank, was recorded to have been found in front of the erosion face at the northern end of the section. A possible old ground surface was also noted below the mound, sitting above a localised peat deposit. A number of stone tools were found beneath this peat layer.

The length of section exposed was around 12m with a depth of about 1.5m. Such a section proved an ideal opportunity for stratigraphic sampling, both horizontally and vertically. As there appeared to be no obvious stratigraphy to the mound deposit, sampling units from the centre and the extremities seemed most appropriate. In addition, samples of peat from below the mound would provide a terminus post quem for the mound, but may also give a terminus ante quem for the stone tools.

3.8.3.4.6 Loch of Garths, Nesting HU 4843 6026

3.8.3.4.6.1 Topography, Geology and Surrounding Burnt Mounds

(see Appendix C for local area maps)

The Loch of Garths burnt mound is located on the northern extremity of the Nesting region of Shetland, overlooking Dury Voe. The area rises gradually to around 150m in height, though steeper on the southern side of Bellister Hill. Loch of Garths itself lies on a narrow strip of land between a loch and storm beach. Of the 10 burnt mounds located within a 7km radius of Loch of Garths, all lie below 50m in elevation, the majority below

20m. Included within these ten mounds are the two previously discussed sites at Trowie Loch.

The immediate area surrounding the Loch of Garths is underlain by granodiorite. Within a short distance are bands of micaceous gneiss and gneissosse quartzite and granulite. No apparent preference in location was noted. Drift geology is dominated by till and moronic drift and peat deposits. Again no strong preference in location was noted. All mounds do however occur on the margins of arable or permanent grassland.

3.8.3.4.6.2 Site Summary and Sampling Strategy

Loch of Garths burnt mound is sub-rectangular in shape, measuring 18m (E-W) by 7m (N-S); it stands up to 1.5m high. The southern side of the mound is actively eroding into the loch. In 1996 the site was investigated as part of the Shetland Burnt Mounds Project, funded by Historic Scotland and Shetland Amenity Trust (Moore and Wilson, 1996). A plan and profile were recorded and several large stones were noted protruding from the central area of the mound, lying below the water table of the loch, suggesting associated structures may be present. Sections of the mound were actively eroding into the loch at the time of survey.

In order to limit further erosion to the mound, a sampling strategy was formed to take advantage of the present section. As such, sampling units were limited to vertical stratigraphy.

3.9 Summary

Through an examination of both excavation and survey records, regional variation in the size and character of burnt mounds has been noted. Consideration of evidence for both the function and chronology of burnt mounds has highlighted the need for further structured work. The Orkney and Shetland Islands have been identified as promising areas for chronological studies and sites within each area identified for sampling.

CHAPTER 4 – Sample Collection, Characterization and Dosimetry

4.1 Introduction

This chapter summarizes fieldwork carried out in the Orkney and Shetland Islands to enable collection of samples for luminescence investigations. The two study areas have been outlined in detail in chapter 3. Further details are given here of the state of preservation of each site, location of samples taken and associated background dosimetry readings. The recording of sampling locations, background dosimetry and other fieldwork observations is a necessary step in facilitating the interpretation of any chronological information which may be obtained from individual samples.

A larger number of samples than required were collected from each site in order to accommodate the possible need for sub-selection of samples based on attributes observed on closer examination within the laboratory. Selected samples have been catalogued in terms of their overall dimensions and initial weight, together with a brief description of lithology. Detailed internal dosimetric investigations are also required to accurately reconstruct the dose rate environment of each sample and are outlined below.

The decision to investigate both quartz and feldspar methods has been outlined in chapter 2, and extraction procedures for both sets of minerals are outlined, together with mineral yields for each sample. On the basis of these yields, final selection of appropriate material for each dating method can occur, with annual dose rates calculated on this basis.

4.2 Sample Collection

4.2.1 Requirements of Samples

Sampling of heated stone for luminescence dating poses a number of practical issues relating to stone selection, recording and measurement of gamma spectrometry.

The suitability of any one particular stone for luminescence dating will depend on a number of factors. The rock type will determine mineral yield and the homogeneity or otherwise of the internal dose component. Large phenocrysts are prone to shattering during disagregation of the stone, and are as such undesirable.

The size of any particular stone is also important when considering mineral yields. However other factors such as thermal gradients and gamma dose rate gradients must also be considered. A small stone may be sufficiently well heated to negate the possibility of thermal gradients occurring across it. It may be thin enough not to suffer the adverse affects of gamma dose gradient. However, once the outer 3mm are removed there may be insufficient material left for dating. Conversely too large a stone may be insufficiently heated.

For accurate measurement of the gamma dose rate, samples should be in an easily assessed geometry, ideally having a homogenous deposit surrounding the sample for at least 30cm in each direction. This presents practical problems in relation to sites where it is preferable to cause minimal disturbance to the archaeology. A sampling pit at least 30cm must be cut into the mound at each position. Damage can be limited by reducing the surface area of the pit and avoiding areas on the mound that appear unstable. Where erosion has exposed a section face, disturbance due to sampling can be further limited by restricting the horizontal hole made to the diameter of the gamma spectrometer.

4.2.2 Overview of Samples Collected

The collection of samples from Liddle burnt mound was aimed at providing a link between the previous luminescence work on burnt mounds of Huxtable et al (1976) and this project. This link is of significance both scientifically and archaeologically. Whilst it was not possible to sample in the same locations as the previous work, it was hoped that the samples collected would show similar characteristics to those measured previously.

The fieldwork on Eday was primarily aimed at recovering a set of structured samples for use in the dating study of burnt mounds from Orkney and Shetland. The underlying question for the Eday samples is whether there is demonstrable age variation, given the available precision of luminescence dating of burnt stones, within sequences of samples available from Dale. If this is the case the subsequent question is whether this age variation exceeds that found between different sites investigated using minimally invasive approaches.

The fieldwork was successful as the basis for sampling. Moreover, Dale on investigation showed a series of stratified deposits which should in theory be sequential. These provide an excellent opportunity to assess the duration relative to the age resolution available using luminescence methods. At Skaill, an additional opportunity exists to link the formation of the mound with the large scale storm events seen in the windblown sand deposition across the site (Sommerville, 2003). The other sites on Eday provided sampling opportunities ranging from the disturbed site of Stenaquoy, where the material on the ploughed surface most probably belongs to the upper parts of the original mound, to the exposed section at Warness, where lateral sampling was possible. At other sites materials from the tops of mounds was accessible. It will be of interest to determine whether all of these readily accessible samples are suitable for dating, and to examine the extent to which the results obtained can provide a chronological setting for the monuments.

The luminescence samples collected at Cruester offer a number of potential avenues of research. No distinct contexts were identified within the mound itself. However, the horizontal and vertical spread of the samples collected from the coastal section, from the pit at the northern end of the mound and from the top of the mound should enable some assessment as to the duration of use and formation of the mound. In addition, the sequence of paving slabs from the hearth cell, if heated sufficiently in the past, may give valuable insights into the initial building of the cell and subsequent remodelling and renewing of the paving slabs.

At Tangwick, the samples collected from the northern end of the section represent stratified deposits which can be easily linked to the previous excavation. An existing radiocarbon date for the ashy layer between the two stone deposits of 2815 ± 40 BP (OxA-8196) gives a good indication of the expected age of the mound. A combination of TL results from each of the three contexts, combined with this date should give a good indication of the formation process of the mound. If significant age variation between the upper and lower stone layer exists, sample TL4 may clarify further the relationship between these contexts and the unstratified southern part of the mound.

At Houlls it was not possible to sample stratigraphically due to the limited depth of deposit, however the horizontal sampling across the coastal section, and at the pit to the

back of the mound provide the best available opportunity to assess duration of use at this site.

Whilst it was not possible to sample the base of the mound at Loch of Garths due to groundwater levels, dates from the three vertically stratigraphic samples, together with others from around the mound, should enable some conclusion to be drawn as to the formation of the mound.

4.2.3 Excavation and recording methodology

4.2.3.1 Orkney Islands

The excavation at Dale was conducted by Orkney Archaeological Trust (OAT), with samples collected by the author. At the other sites archaeological work was conducted soley by the author. All sites were photographed before and after the work took place to record their condition and to provide a record demonstrating that they had been adequately back-filled. With the exception of sampling at Liddle burnt mound, full details of Orkney fieldwork are given in Robertson et al (2000), Anthony et al, 2000a and Anthony et al (2002).

Archaeological work was undertaken at Dale burnt mound to clean and record archaeological sections. The work involved cleaning back and straightening the section by hand along the line of the drainage ditch that cuts the north side of the mound. This was to allow for the recovery of as much information as possible via recording and sampling with minimum disturbance to the surviving *in situ* deposits. A 1.0 m wide sondage was hand dug into the slope of the mound in the west area, rather than a full section due to the loose nature of the deposit.

Samples were collected for luminescence dating from identified contexts in each site in conjunction with gamma ray dose-rate measurements to quantify the environmental dose rates applicable to luminescence dating. A selection of stone types and sizes was collected where available, the majority of samples being of 5-10cm diameter, and some 50-100g in mass. Sampling and gamma dosimetry records were produced in a series of registered record sheets, which were added to the conventional recording system adopted by OAT.

4.2.3.2 Shetland Islands

All archaeological recording was conducted by EASE Archaeological Consultants, with samples collected by the author. All sites were photographed before and after the work took place to record their condition and to provide a record demonstrating that they had been adequately back-filled. Full details of Shetland fieldwork are given in Moore and Wilson (2001) and Anthony et al (2001).

At the sites of Houlls, Loch of Garths and Tangwick, stone and soil samples were collected from existing sections using minimally invasive approaches. Small test pits were dug where needed to provide additional sampling positions. Sampling at Cruester took place towards the beginning and end of the 2000 excavation whenever sampling opportunities arose. Samples were collected for luminescence dating as detailed above.

4.2.3.3 Gamma Spectrometry

Gamma dosimetry was preformed using an EG7G Ortec Micronomad spectrometer with 75x75mm NaI scintillation detector. Spectra were recorded for 300s each in the sampling locations, integrated and converted to dose rate in $mGya^{-1}$ using calibration factors determined from K, U and Th doped concrete pads at SURRC.

4.2.4 Orkney: Fieldwork and Sampling

4.2.4.1 Introduction

Fieldwork on Orkney was carried out on two separate occasions during July 2000 and August 2001. Scheduled monument consent was granted for work on Dale, Skaill, Knoll of Merrigarth and Stackelbrae burnt mounds prior to sampling.

4.2.4.2 Liddle Burnt Mound

4.2.4.2.1 Excavation and Recording

Since excavation in the 1970s (Hedges, 1977) Liddle burnt mound has been open to the public together with the nearby Tomb of the Eagles. The original excavation sections of

the burnt mound are in a surprisingly good state of preservation and positions for sampling were easily located with reference to original plans. In order to keep disturbance of the section to a minimum, only two positions were sampled.

4.2.4.2.2 Sampling

An area of the original section was sampled at two points, separated by approximately 30cm (fig 4.1). A total of six stones were collected for further analysis.

Table 4.1 Liddle Burnt Mound, Sample Information

Field No.	Context	Description	Assoc γ spec.	Lab Codes (SUTL)
TL1	N/A	4 stones	1	1378-1381
TL2	N/A	2 stones	2	1385-1386

4.2.4.2.3 Gamma Dosimetry

Gamma dosimetry measurements were taken at each of the two sampling positions. Both results are within error of one another, suggesting a mean dose rate of 1.03±0.07mGya^{-1}. This estimate is slightly lower than that reported by Huxtable et al (1976) of 1.35mGya^{-1}.

Table 4.2 Liddle Burnt Mound, Gamma dosimetry measurements

Spectrum No.	Context	Assoc. Samples	Mean 4Π γ dose rate (mGya^{-1})
1	N/A	TL1	0.98±0.08
2	N/A	TL2	1.08±0.11

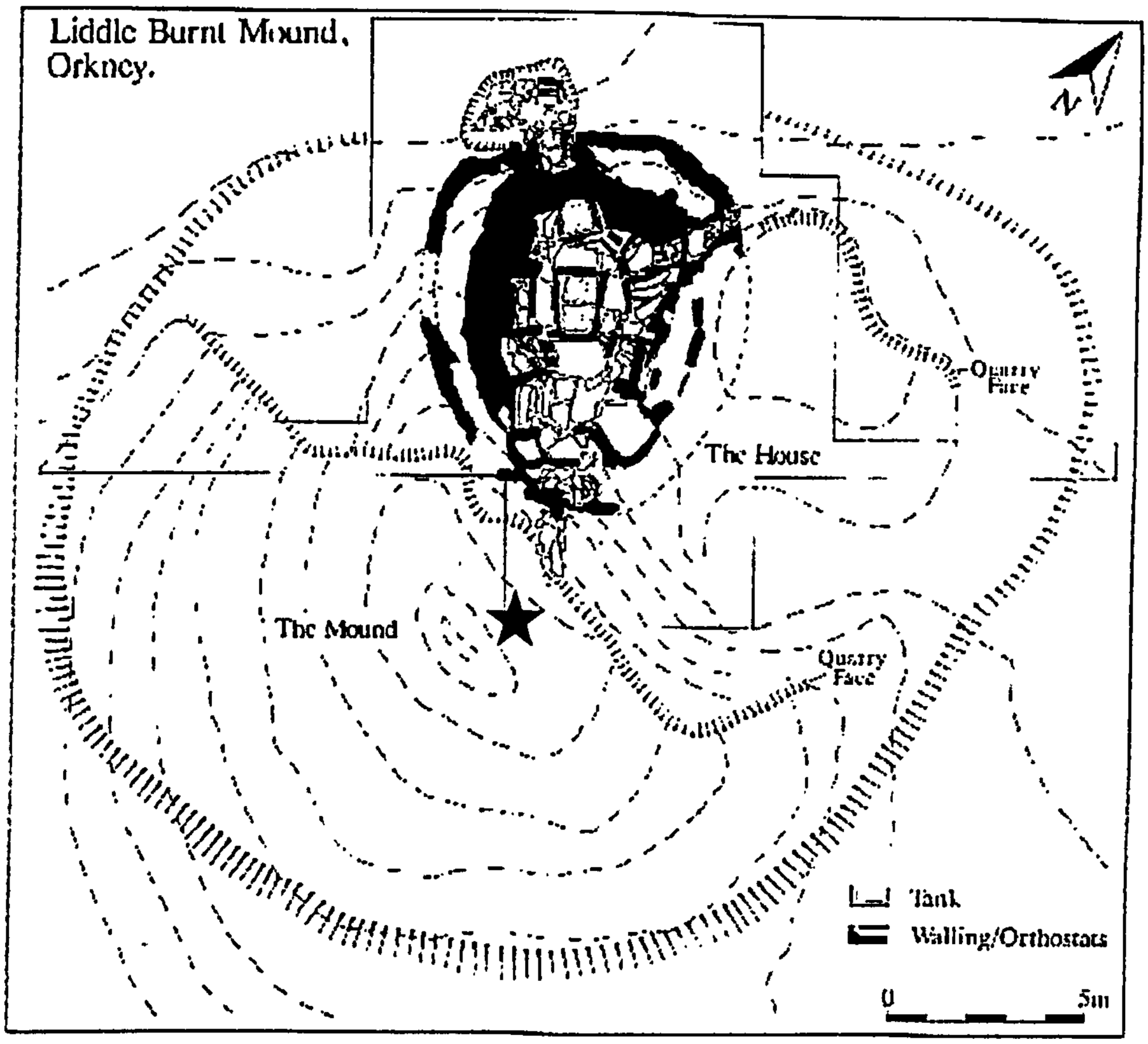

Fig 4.1 ★ Sampling position (Figure of Liddle Burnt Mound from Hedges, 1977)

4.2.4.3 Dale Burnt Mound

4.2.4.3.1 Excavation and Recording

Sections were recorded from the eastern and western side of the northern half of the mound (fig 4.2a).

The east section of the mound comprised a 0.24 m thick turf layer [100] which overlay peat layers [102], 0.16 m deep, and [103], 0.08 m deep, with 0.21 m of a stony peat deposit [106] lying beneath [102] in the east. Due to the angle of the slope and the truncation by a ditch the peat layers did not meet at the top of the section (fig 4.2b)

A thin (0.05 m) root mass indicating a buried turf layer [119] underlay the peat layers and directly overlay 0.19 m of burnt mound material [104], a stony layer with fine dark ash. Beneath [104] lay [105] a 0.18 m deposit of peaty ash with less stones which in turn

overlay [107], 0.36 m of a dark peaty ash with frequent angular stones (maximum 0.18 m). Underlying [107] in the east was [108], a dark peaty ash (0.28 m deep) with pale sandy clay lenses and small stone fragments throughout, while in the west a 0.22 m deep deposit of peaty material with some small stones [109]. The junction of [108] and [109] was truncated by modern rabbit hole disturbance layers.

Peaty deposit [109] overlay a very stony (maximum size 0.18 m) deposit with dark peaty ash [111], 0.26 m deep, which in turn overlay a 0.28 m deposit of splintered and fragmented stone [110], which also underlay [108]. A small lens (0.12 m deep) of yellow stony clay, redeposited natural, [101] underlay [110] and overlay [112] 0.24 m of dark peaty ash with angular stones (maximum size 0.15 m). Ashy deposit [112] was the lowest visible deposit in this section overlying a bright yellow natural clay with angular stones throughout.

On the western sondage, a 0.20 m layer of topsoil [114] comprised turf with a jumble of very large (up to 1.22 m x 0.48 m x 0.15 m) angular and sub-angular flag rubble overlay 0.45 m of burnt mound type material [115], a dark loamy sandy ash with frequent angular stones (fig 4.2c). Deposit [115] did not continue far into the north slope due to disturbance in this area caused by the cutting of the drainage ditch. The finding of a chunk of polystyrene within [115] (where the hole for sampling was dug) indicates the level of disturbance of this area. Underlying [115] was a very large, 0.50 m, deposit of clean, voided angular and sub-angular rubble [116], which in turn overlay 0.60 m of dark peaty ash mixed through angular stones and large slabs (0.5 m x 0.8 m) [117]. The basal deposit in this west area was a clayey ash and stone deposit [118] which lay beneath [117] and was not excavated for fear of flooding due to proximity of the drainage ditch.

General site photographs are located in Appendix I

4.2.4.3.3 Sampling

Samples were taken from 5 contexts within the mound. On the western section, three sequential units were sampled. 11 samples (TL12) were taken from context [112], burnt mound material below redeposited clay. 10 samples (TL13) were take from context [110],

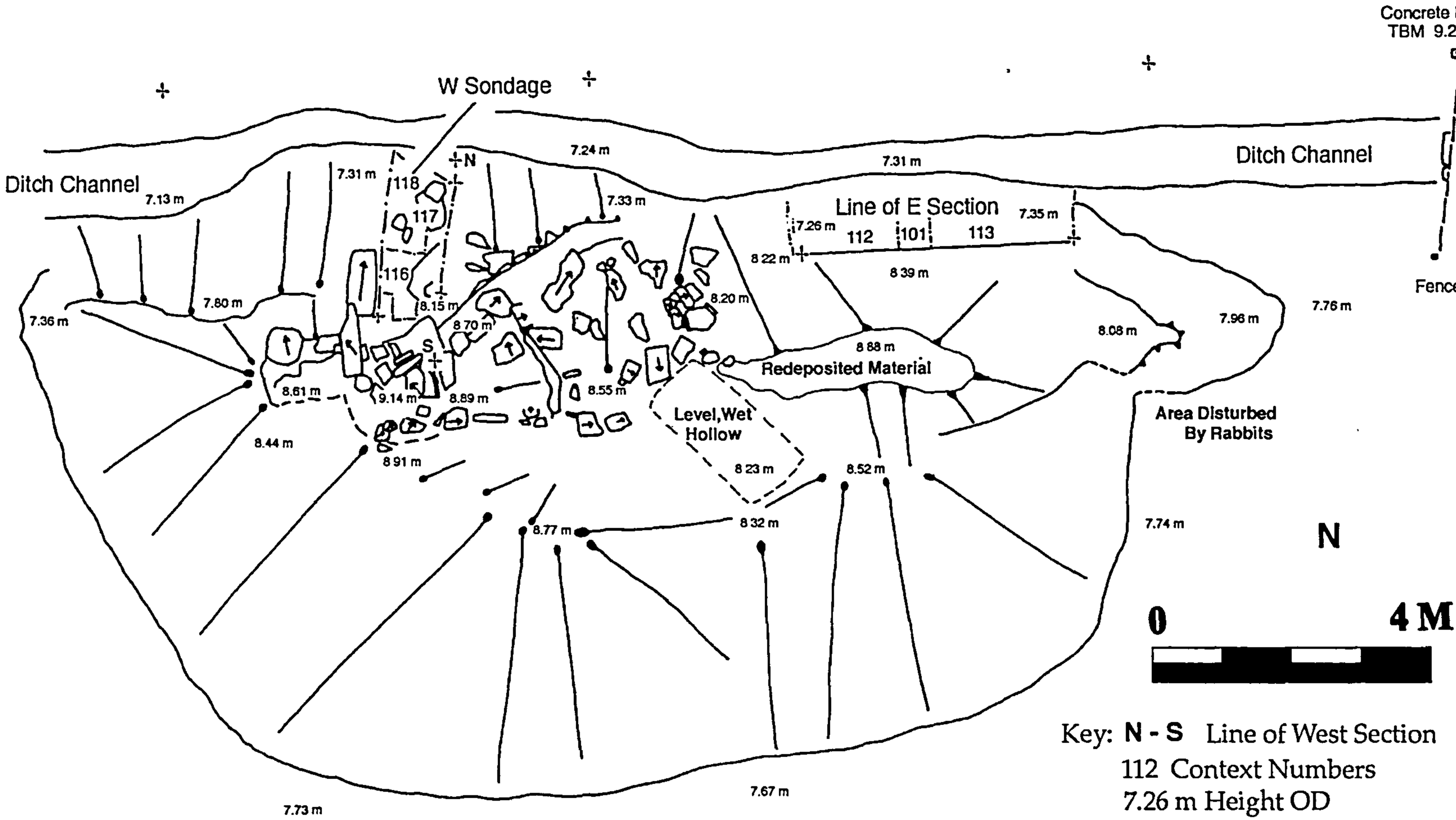

Fig 4.2a General site plan, Dale burnt mound (From Robertson et al, 2000)

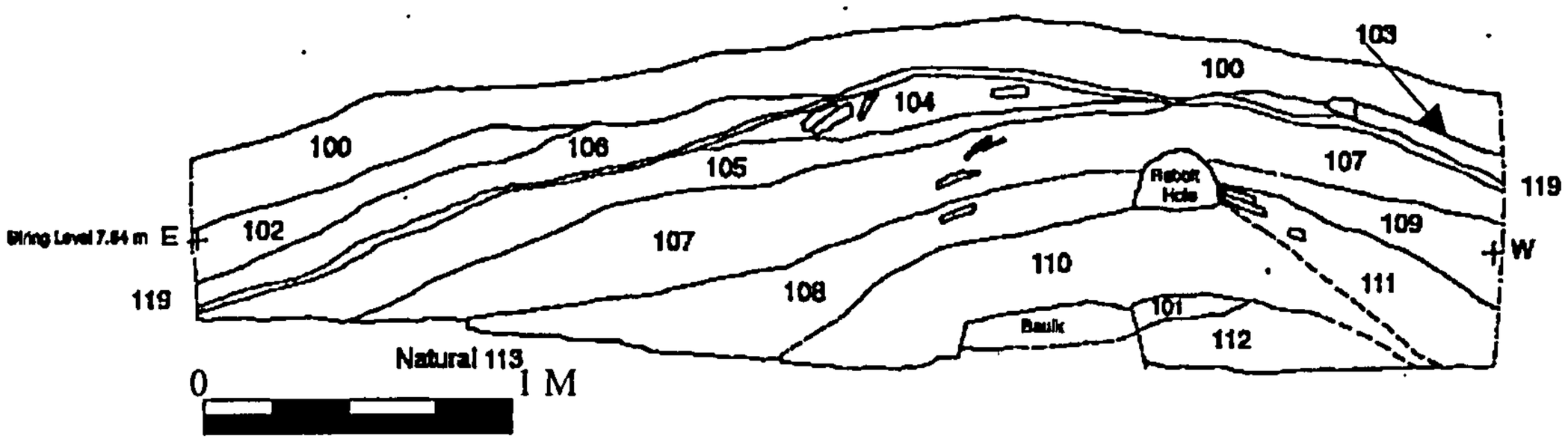

Fig 4.2b Dale Burnt Mound, East Section (From Robertson et al, 2000)

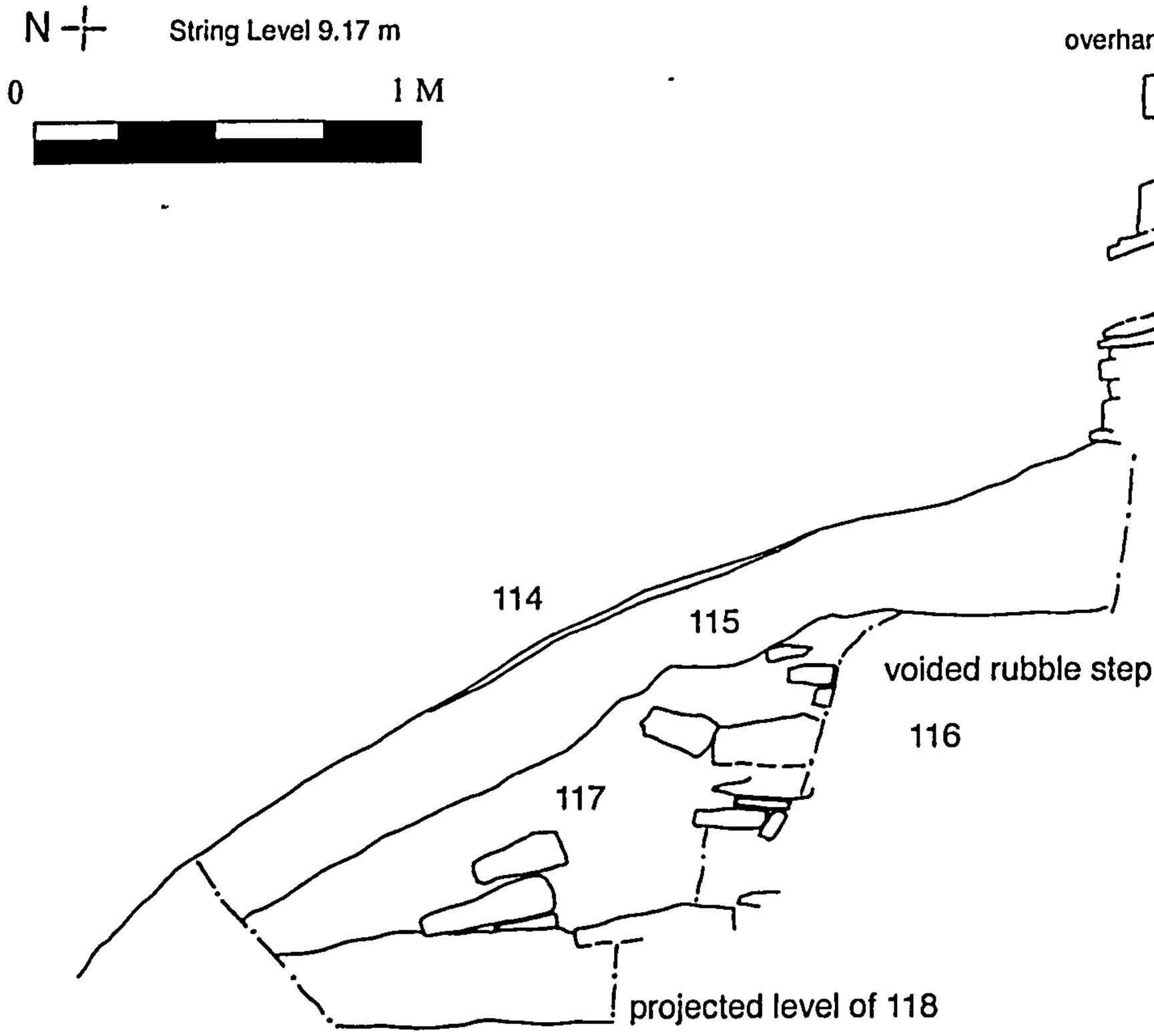

Fig 4.2c West Facing section of West Sondage, Dale Burnt Mound (From Robertson et al, 2000)

material above the redeposited clay lense, and 12 samples (TL14) were taken from context [107], material above a silty ash layer. Soil samples were taken from the above contexts for extraction of organic material for ^{14}C analysis. In addition, a sample of peat from context [102] was also collected for analysis. Gamma dosimetry measurements were made at each sampling position. On the eastern sondage, two positions were sampled. Context [117], material at the base of the mound overlying large flagstones, was sampled and 6 stones (TL15) were collected. 6 samples were also collected from context [115], from stones within a loose deposit stratigraphically higher up in the mound.

Table 4.3: Dale Burnt Mound, Sample information

Field No.	Context	Description	Assoc. γ spec	Lab Codes (SUTL)
TL12	112	11 stones	21	747-757
TL13	110	10 stones	22	758-767
TL14	107	12 stones	23	768-779
TL15	117	6 stones	24	780-785
TL16	115	6 stones	25	786-791

4.2.4.3.3 Gamma Dosimetry

Gamma dosimetry measurements were taken at each sampling position (table 4.2). Results from positions TL12, 13 and 14 are within error, suggesting a mean dose rate for this part of the site of 0.78±0.1mGya^{-1}. At positions TL15 and TL16 the dose rate is in the region of 1-1.1mGya^{-1}. It is probable that this increase is due to the decrease in soil matrix around the disturbed stones. The presence of polystyrene within the stone deposit suggests the disturbance to be modern, thus it may be more appropriate to use the lower dose rates in age calculations.

Table 4.4: Dale Burnt Mound, Gamma Dosimetry Measurements

Spectrum No.	Context	Assoc. Samples	Mean 4Π γ dose rate (mGya^{-1})
21	112	TL12	0.76±0.1
22	110	TL13	0.82±0.1
23	107	TL14	0.76±0.1
24	117	TL15	1.0±0.1
25	115	TL16	1.1±0.1

4.2.4.4 Skaill Burnt Mound

4.2.4.4.1 Excavation and Recording

Samples were collected from Skaill burnt mound on two separate occasions. In July 2000, a small 40cm^2 area located on the southern side of the crescentic mound was deturfed for sampling, revealing a solidly packed stone layer beneath a topsoil/stone mixture (fig 4.3a).

In August 2001, a 1m x 5m trench was positioned on the eastern slope of the mound and hand dug into the slope. A 1.1m baulk was preserved and the trench extended to the East by 2.2m at a reduced width to further investigate the natural deposition history around the mound (fig 4.3a). The trench revealed the extent of the mound below ground surface, and the associated deposits.

The main section (figs 4.3 b & c) composed a turf layer [001] of varying thickness (1-18cm), which overlay a lense of sandy topsoil [002] stretching the full extent of the mound before thinning out to the underlying peat contact. This upper peat layer [003], 40cm at greatest thickness, encroaches approximately 80-90cm up the mound slope. Below both [002] and [003] a series of disjointed sand deposits were found [004 – 008].

Sand deposit [004] was present only in the upper corner of the north-facing section as a 10cm lense, before thinning out. Lense [005] was present in both sections and could be traced for 1.6m. A small area of disturbed sand was noted on the north-facing section around the area of a large boulder. Lense [006] was truncated on the eastern side of the north facing section by an area of disturbed soil, probably representing an old rabbit hole.

The south facing section was also disturbed by recent burrowing thus it is not possible to say definitively that lense [006] and [007] represent the same deposit, though this is likely. Lense [007] thins out to a point on the northern section, though can be traced continuously on the southern section and appears to join lense [008], a thicker more substantial sand deposit.

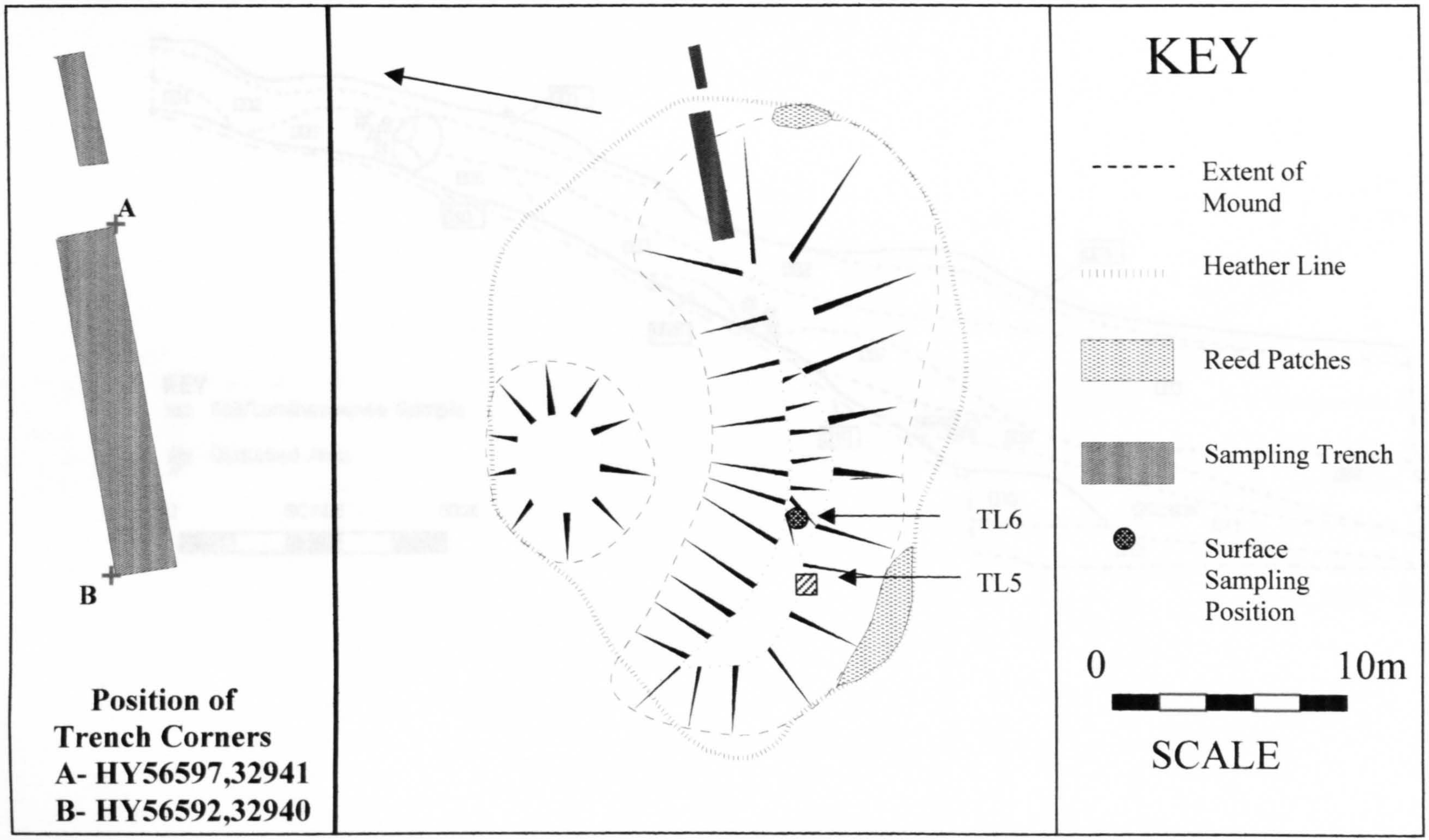

Fig 4.3a General Site Plan, Skaill Burnt Mound

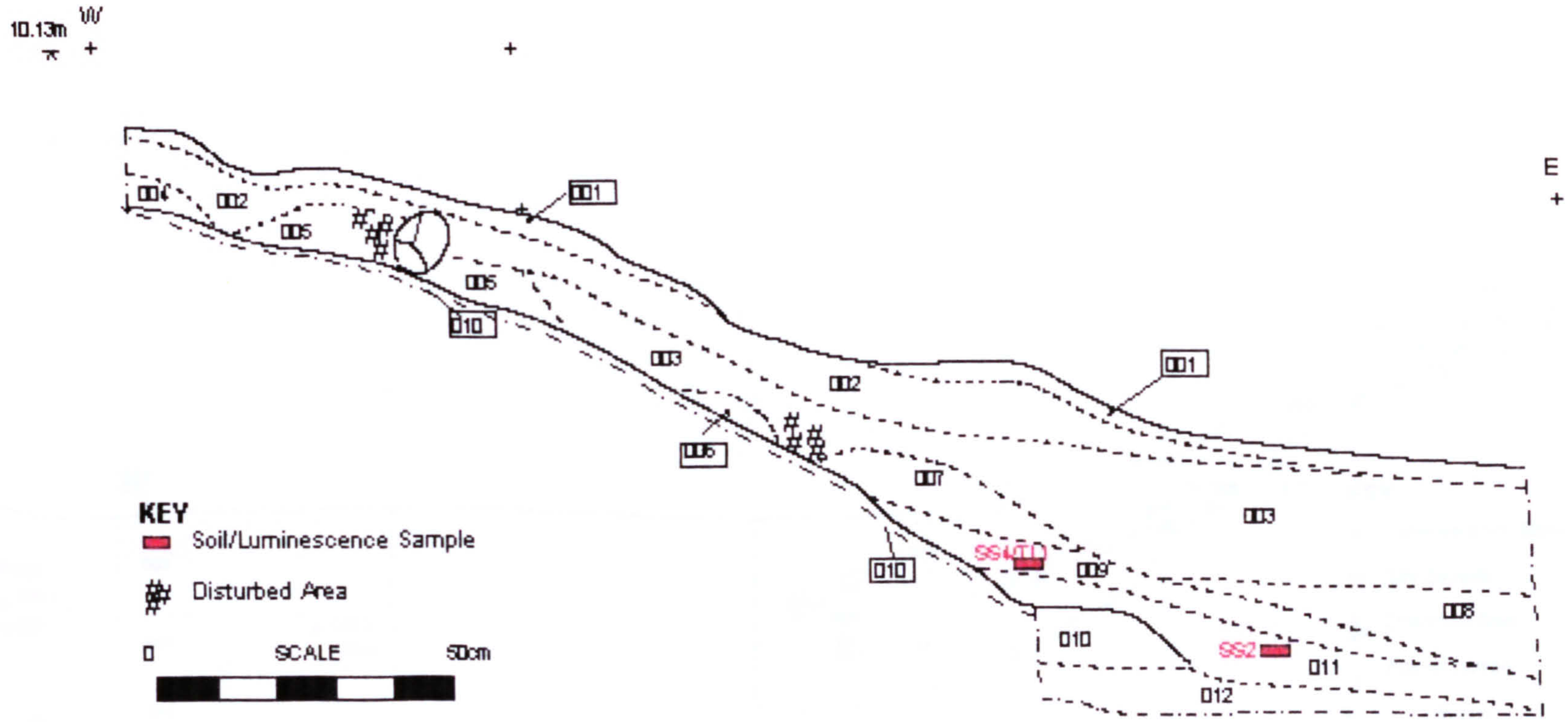

Fig 4.3b Skaill South Facing Section

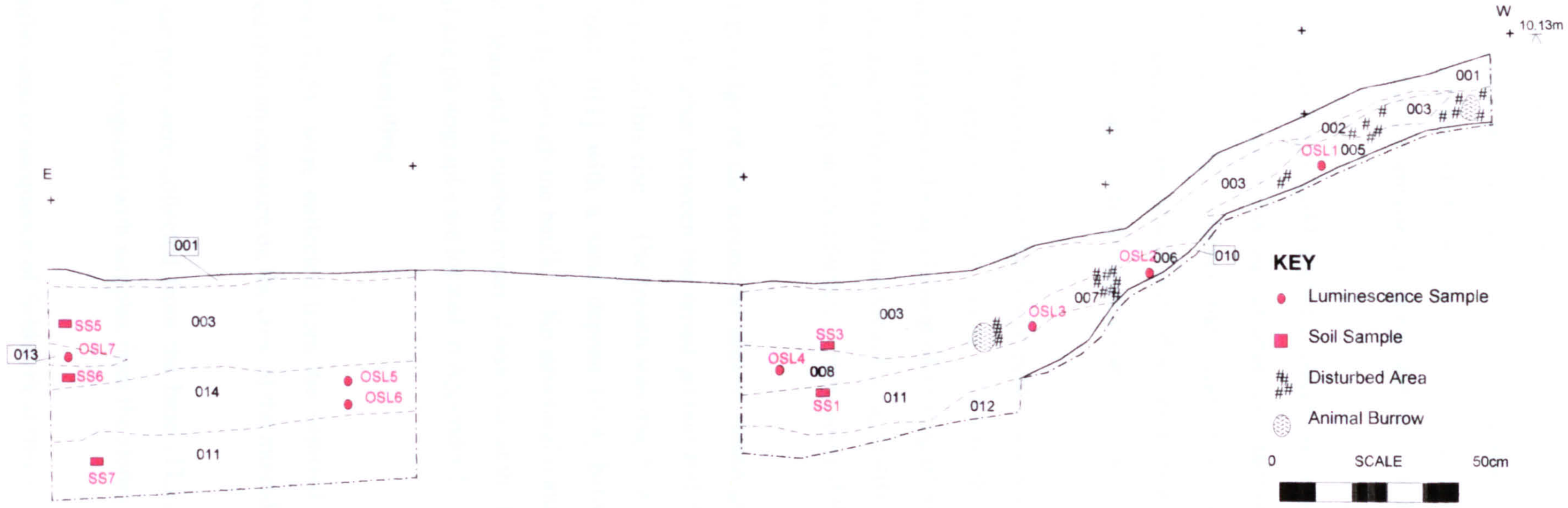

Fig 4.3c North Facing Section, Skaill Burnt Mound

Sand lenses [004,005,006] and part of [007] overlie the main body of the mound [010], a dark ashy matrix with frequent, though not abundant stones. It should be noted that the deposit encountered on the south face of the upper mound during sampling in July 2000 was almost entirely composed of stone, with very little soil matrix between.

Sand lenses [007] and [008] overlie a darker ash deposit with occasional stones [009]. The peat layer that underlies this deposit abuts the main mound deposit, encroaching slightly on the lower edge [011]. Given the build up of peat it is possible that deposit [009] represents later erosion and slump of material or accumulated wash from further up the mound not associated with the primary activity on the site.

Both the main mound and the lower peat overlay a natural greyish clayey subsoil [012] containing frequent weathered stones. Whilst the contact between peat and natural is clear, there appears to be an element of mixing of mound material and natural both under the mound and in the immediate vicinity, suggestive of an element of trample. The level of the water table prohibited further investigation of the natural layers below the mound.

Around the edge of the mound an area of raised ground can be seen, highlighted by an absence of heather between the raised ground and the mound. The extension trench cut through part of this rise. The trench was dug to a depth of 1.05m. The two main peat layers [003, 011] with a sand deposit [014] between were present, appearing to run continuously through the baulk. No structural features were evident, though a small sand lense of clean and disturbed material was seen at the Eastern edge of the section.
General site photographs are located in Appendix I

4.2.4.4.2 Sampling

7 stones (TL5) were collected from the deturfed area. In addition, two stones were collected from an exposure on the crest of the mound (TL6).

Stone samples were collected from the base (TL2) and top of the exposed slope of the mound (TL3), together with samples from the stoney lense above the mound (TL1).

One unforeseen consequence of fieldwork at this site was the identification of one or more windblown sand layers in contact with the burnt mound. Whilst not part of the original

research design, the decision was taken to sample these deposits to investigate the relationship or otherwise of the sand blow event and the termination of activity at the mound. Accordingly OSL samples were collected from the various sand layers. Contexts [005-008] were sampled (OSL1-4 respectively) with material collected in lightproof tubing c.25cm in length. The upper two samples (OSL 1 & 2) seemed limited in extent, with soil present at the inner end of the tubing. Bulk samples were taken from the lower and upper peat layers and from context [009] for possible ^{14}C dating (SS1-4). OSL samples were also collected from the trench extension. An upper and lower sample (OSL 5&6) was collected from the main sand deposit [014] together with one from the sand lense (013-OSL7) which again appeared limited in extent, with soil present at the inner end of the tubing. Bulk samples were collected from the lower peat, and from above and below the sand lense in the upper peat (SS4-6).

Table 4.5: Skaill Burnt Mound, Sample information

Field No.	Context	Description	Assoc. γ spec	Lab Codes (SUTL)
TL1	009	4 stones	1	1343-1346
TL2	010	6 stones	1	1349-1354, 1357
TL3	010	4 stones	1	1347, 1358-1360
TL5	A4	9 stones	A4	810-816
TL6	A4	2 stones	A6	817-818
OSL1	005	Sand	2	1361
OSL2	006	Sand	3	1362
OSL3	007	Sand	4	1363
OSL4	008	Sand	5	1364
OSL5	014	Sand	9	1365
OSL6	014	Sand	10	1366
OSL7	013	Sand	11	1367

4.2.4.4.3 Gamma Dosimetry

Gamma dosimetry measurements were recorded from the deturfed area, and from the surface of the mound, and from various positions within the sampling trenches. At the surface of the mound, and in the small sampling pits, dose rates were in the region of 0.8-0.9mGya^{-1}. Dose rates were lower within the trench, resulting from the overburden of lower activity sand deposits, which were typically in the region of 0.2-0.3mGya^{-1}.

Table 4.6: Skaill Burnt Mound, Gamma Dosimetry Measurements

Spectrum No.	Context	Assoc. Samples	Mean 4Π γ dose rate ($mGya^{-1}$)
A4	A4	TL5	0.92±0.2
A6	A4	TL6	0.83±0.04
1	009	TL1-3	0.539±0.058
2	005	OSL1	0.463±0.051
3	006	OSL2	0.392±0.043
4	007	OSL3	0.335±0.037
5	008	OSL4	0.264±0.030
9	014	OSL5	0.243±0.012
10	014	OSL6	0.255±0.013
11	013	OSL7	0.226±0.015

4.2.4.5 Knoll of Merrigarth

4.2.4.5.1 Excavation and Recording

Disturbed areas several metres in diameter, possibly a result of cattle damage, are visible on the southern side of both mounds. In order to limit further disturbance to the Knoll of Merrigarth burnt mound, samples were taken from the disturbed areas on the S/SE side of each of the mounds. 15x30cm holes were dug into the disturbed area to enable gamma dosimetry measurements. Material was reinstated after sampling. General site photographs are located in Appendix I

4.2.4.5.2 Sampling

8 samples (TL7) were collected from the larger part of the mound, 10 from the smaller (TL8).

Table 4.7: Knoll of Merrigarth Burnt Mound, Sample information

Field No.	Context	Description	Assoc. γ spec	Lab Codes (SUTL)
TL7	6	8 stones	12	802-809
TL8	8	10 stones	13	792-801

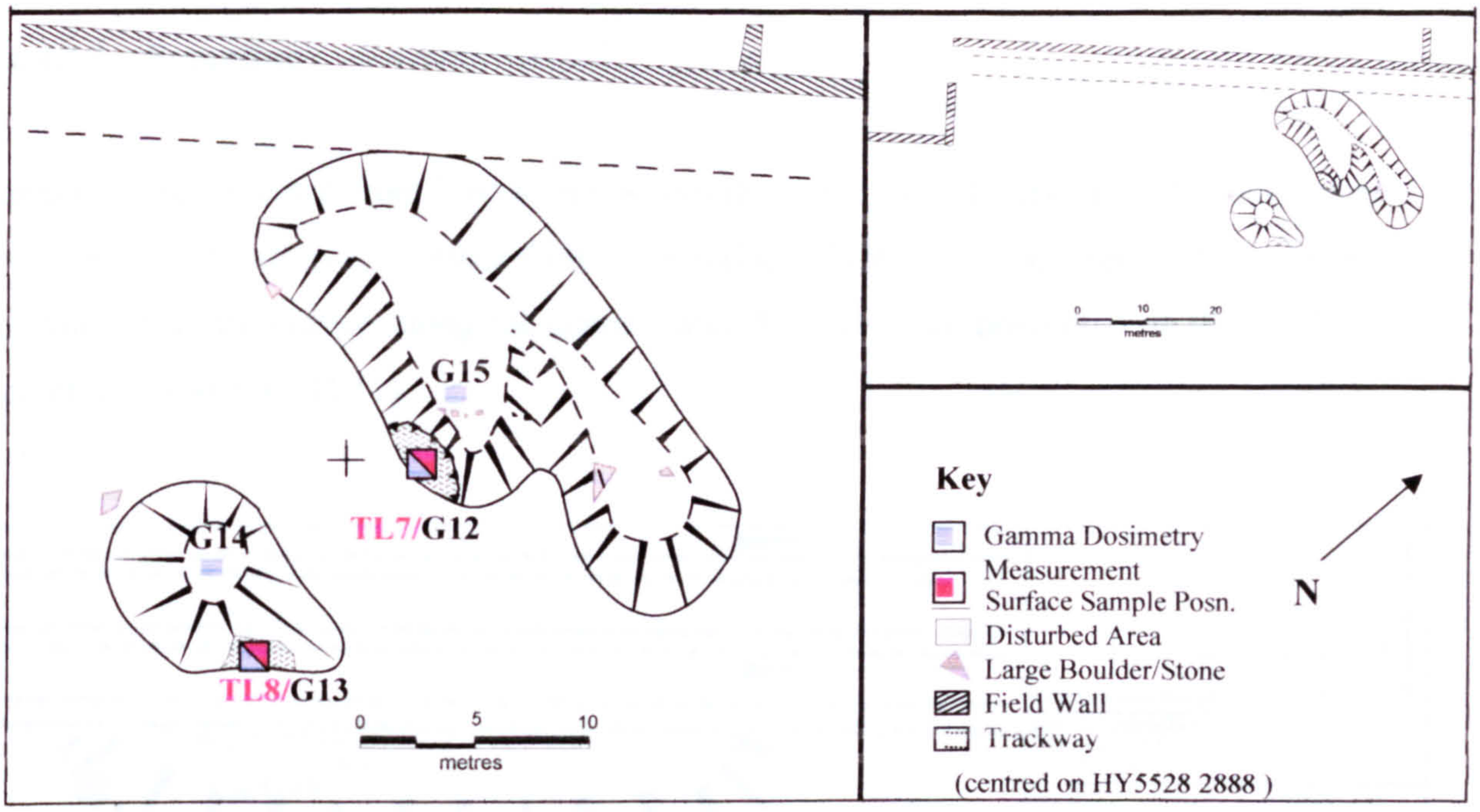

Fig 4.4 General Site Plan, Knoll of Merrigarth Burnt Mound

4.2.4.5.3 Gamma Dosimetry

Gamma dosimetry measurements were recorded both at the sampling positions and on top of each mound.

Table 4.8 Knoll of Merrigarth, Gamma Spectrometry Results

Spectrum No.	Context	Assoc. Samples	Mean 4Π γ dose rate ($mGya^{-1}$)
12	6	TL7	0.9±0.1
13	8	TL8	0.82±0.09
14	7	------	0.98±0.1
15	5	------	1.08±0.1

4.2.4.6 Warness Burnt Mound

4.2.4.6.1 Excavation and Recording

In order to limit further disturbance to Warness mound, samples were taken from the eroding coastal section. 15x30cm holes were dug into the section to enable gamma dosimetry measurements. Material was reinstated after sampling. General site photographs are located in Appendix I

4.2.4.6.2 Sampling

Samples were collected from 3 positions within the burnt mound exposure. 6 stones were collected from position 1, c. 30cm from the interface (TL9). 9 stones were collected from position 2 (TL10) midway along the deposit, and 5 stones from position 3 on the southern face of the exposure (TL11).

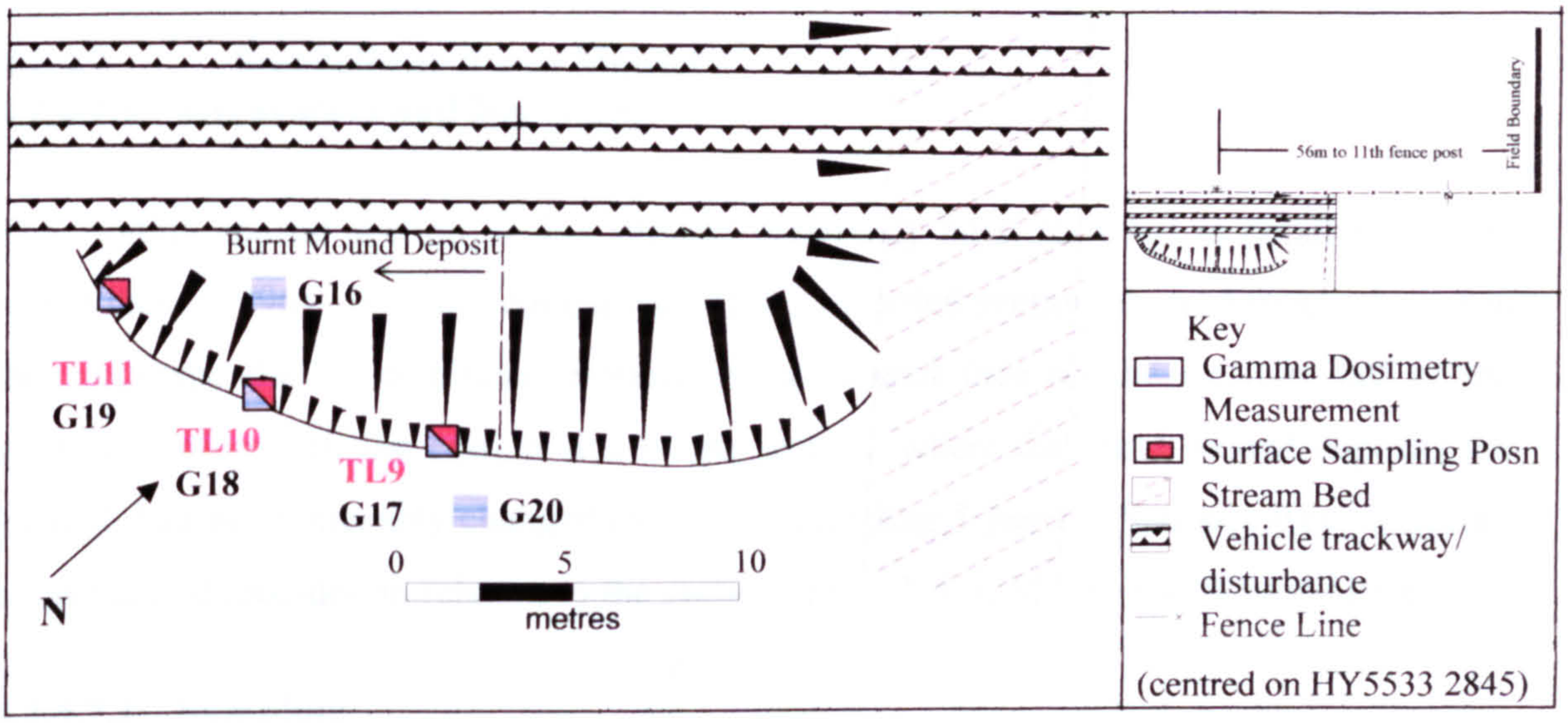

Fig 4.5 General Site Plan, Warness Burnt Mound

Table 4.9: Warness Burnt Mound, Sample information

Field No.	Context	Description	Assoc. γ spec	Lab Codes (SUTL)
TL9	10	6 stones	17	840-845
TL10	10	9 stones	18	851-859
TL11	10	5 stones	19	846-850

4.2.4.6.3 Gamma Dosimetry

Gamma dosimetry measurements were made at each of the three sampling locations, and at a surface position on top of the mound. All measurements were within error of each other, suggesting a relatively uniform dose rate across the site of $0.96 \pm 0.1 mGya^{-1}$.

Table 4.10 Warness , Gamma Spectrometry Results

Spectrum No.	Context	Assoc. Samples	Mean 4Π γ dose rate ($mGya^{-1}$)
16	9	----- Top of Mound	0.96±0.1
17	10	TL9	1.0±0.1
18	10	TL10	0.98±0.1
19	10	TL11	0.91±0.1

4.2.4.7 Stackelbrae Burnt Mound

4.2.4.7.1 Excavation and Recording

The eroding coastal section of this site has previously been recorded in detail by Moore and Wilson (1996). On site comparison of the recorded section showed much change in the landscape due to continued erosion of the coastal face on the western half of the section. However, the eastern side of the section, where the burnt mound deposits are located, had not noticeably changed over the preceeding 5 years. Samples were therefore collected and recorded in relation to the sections provided in Moore and Wilson (1996).

4.2.4.7.2 Sampling

Samples for luminescence dating were collected from two areas within the eroding mound deposit (fig 4.6). Six stones were collected from an area overlying midden material (TL1). A further five stones were collected from a more easterly location where the mound deposit begins to thicken (TL2).

In addition, a soil sample (SS1) containing representative samples of shell and bone was collected from the midden deposit, directly below sample position TL1.

Table 4.11: Stackelbrae Burnt Mound, Sample information

Field No.	Context	Description	Assoc. γ spec	Lab Codes (SUTL)
TL1	60	7 stones	1	1368-1372, 1378-1379
TL2	60	5 stones	2	1373-1377

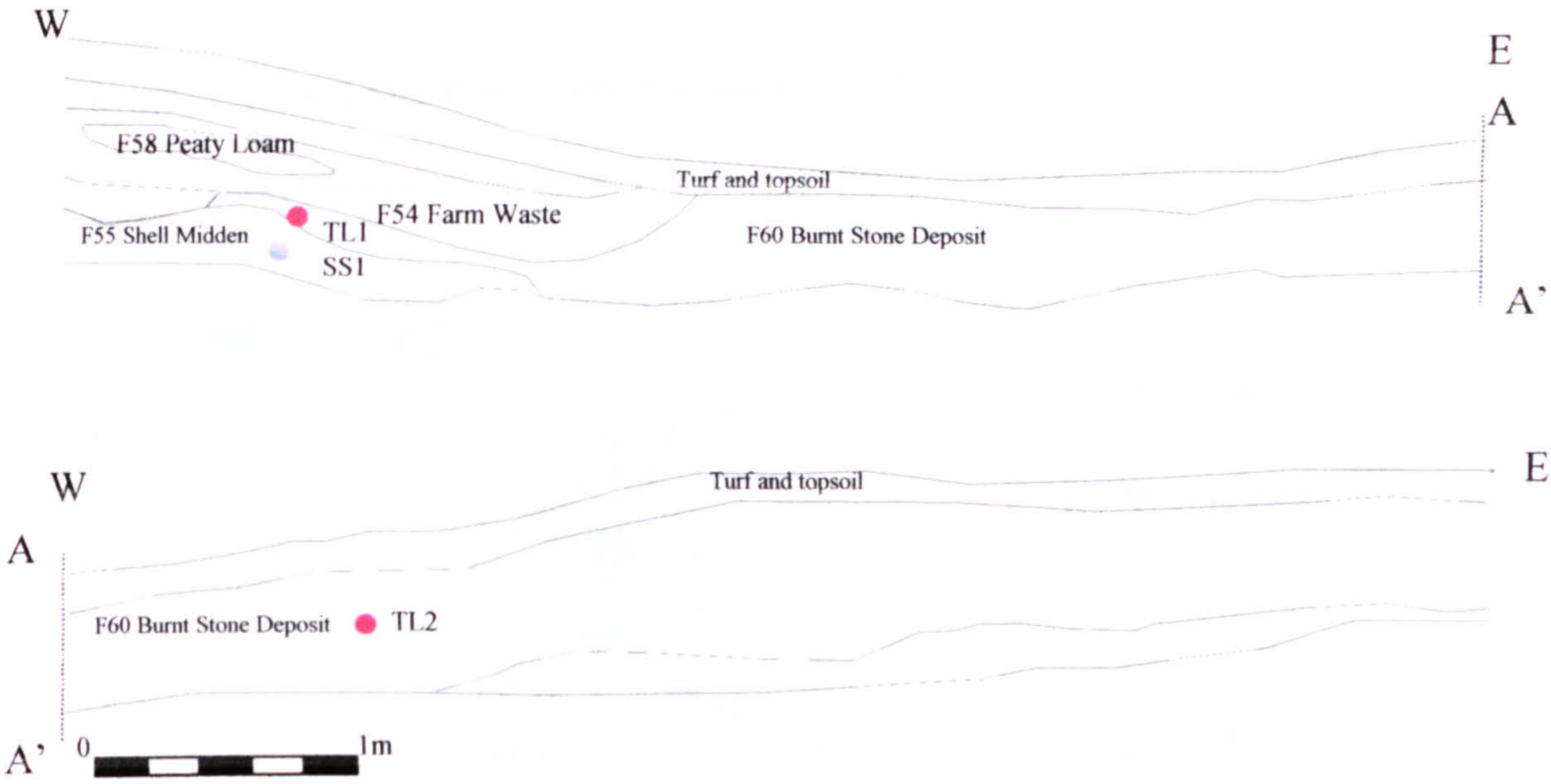

Fig 4.6 Location of Samples, Stackelbrae (section after Moore and Wilson, 1996)

4.2.4.7.3 Gamma Dosimetry

Gamma spectrometry measurements were recorded at each of the two sampling locations. Both measurements were within error of each other, giving an average dose rate of $0.78\pm0.09 mGya^{-1}$.

Table 4.12 Stackelbrae, Gamma Spectrometry Results

Spectrum No.	Context	Assoc. Samples	Mean 4Π γ dose rate ($mGya^{-1}$)
1	60	TL1	0.765±0.084
2	60	TL2	0.795±0.090

4.2.4.8 Fersness

4.2.4.8.1 Excavation and Recording

A small $30cm^2$ area of the southern mound was deturfed and excavated to a depth of 20-30cm for sampling, revealing a loosely packed mixture of topsoil and stones. In order to limit the extent of future erosion on the Northern mound, samples were collected from a small section of visible stones on the easternmost side. A 15x30cm hole was dug into the section to enable gamma dosimetry measurements. Both sampling areas were recorded by photograph and reinstated. General site photographs are located in Appendix I

Fig 4.7 General Site Plan, Fersness Burnt Mound

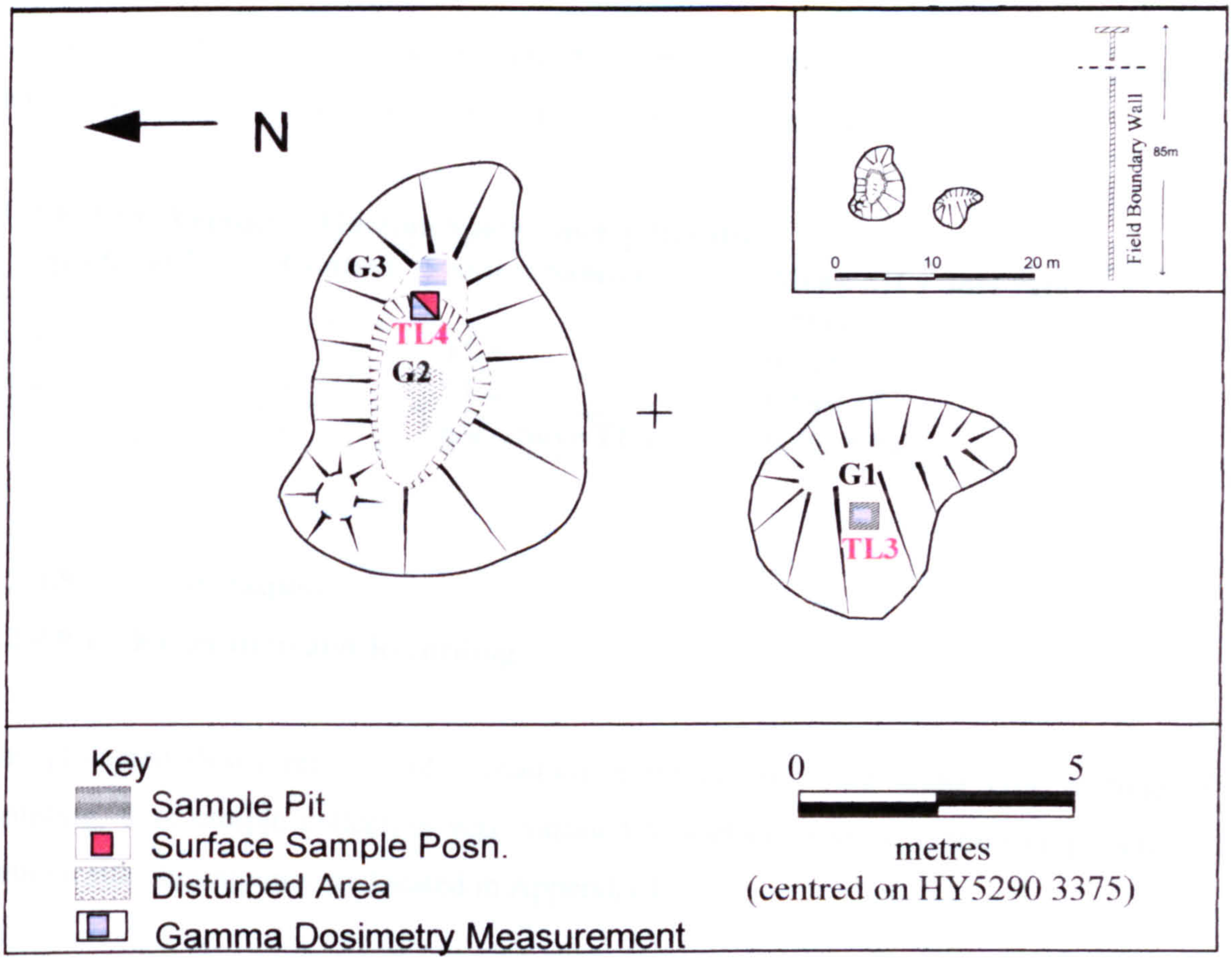

4.2.4.8.2 Sampling

8 stone samples (TL3) and gamma dosimetry measurements were taken from the deturfed area on the southern mound. 7 stone samples were taken from the small section on the northern mound (TL4).

Table 4.13 Fersness Burnt Mound, Sample information

Field No.	Context	Description	Assoc. γ spec	Lab Codes (SUTL)
TL3	2	8 stones	1	819-826
TL4	3	7 stones	2	827-833

4.2.4.8.3 Gamma Dosimetry

Gamma dosimetry measurements were made both on the exposed surface and on the turf/topsoil surface above. Dose rates range from 0.7-0.9mGya^{-1}.

Table 4.14 Fersness , Gamma Spectrometry Results

Spectrum No.	Context	Assoc. Samples	Mean 4Π γ dose rate (mGya^{-1})
1	2	TL3	0.7±0.03
2	3	TL4	0.9±0.15
3	1	n/a above TL4	0.76±0.04

4.2.4.9 Stenaquoy

4.2.4.9.1 Excavation and Recording

The ploughed down remains of Stenaquoy burnt mound were under crop at time of sampling, thus sample collection was confined to surface scatters to limit crop damage. General site photographs are located in Appendix I

4.2.4.9.2 Sampling

Stones were collected from surface scatters of stones at two locations (TL 1 & 2) on the 'top' of the visible mound.

Table 4.15 Stenaquoy Burnt Mound, Sample information

Field No.	Context	Description	Assoc. γ spec	Lab Codes (SUTL)
TL1	1	4 stones	7	834-837
TL2	1	4 stones	8	838,839,860,861

4.2.4.9.3 Gamma Dosimetry

Gamma dosimetry measurements were made across the mound to assess the homogeneity of gamma dose rates. All measurements were within error of each other, suggesting an average dose rate of 0.96±0.1mGya^{-1}.

Table 4.16 Stenaquoy , Gamma Spectrometry Results

Spectrum No.	Context	Assoc. Samples	Mean 4Π γ dose rate ($mGya^{-1}$)
7	1	TL1	0.96±0.1
8	1	TL2	0.96±0.1
9	1	-----	0.90±0.1
10	1	-----	0.94±0.1
11	1	-----	1.04±0.1

4.2.5 Shetland: Fieldwork and sampling

4.2.5.1 Introduction

Fieldwork on Shetland was carried out during October and November 2000. Scheduled monument consent was sought for work on Loch of Garths burnt mound prior to sampling. Full sampling details may be found in Moore and Wilson, 2000 and Anthony et al, 2000b.

4.2.5.2 Cruester

4.2.5.2.1 Excavation and Recording

(From Moore & Wilson, 2000)

A five-week season of investigations was carried out at Cruester in October-November 2000 with funding from Historic Scotland and Shetland Amenity Trust. The work, carried out under the direction of Hazel Moore and Graeme Wilson, EASE, saw the excavation in plan of an 85m^2 area covering the central part of the mound and a representative sample of the mound peripheries.

The site was found to have suffered some damage since it was last seen in 1996. Part of a free-standing wall previously recorded in section had disappeared and elsewhere along the exposure face columns of masonry had collapsed on to the beach.

The excavations revealed a complex stone structure at the centre of the mound, the dominant elements of which were a large enclosed kiln-like hearth (G) and a massive stone lined water tank . It would now appear that the structure previously described as a possible short cist was, in fact, the western end of this tank. These features were linked by a paved floor and surrounded by small paved cells. The external walls of the structure were not free-standing but were revetted into the mound of burnt stone. The building showed signs of numerous phases of alteration and repair: the hearth area alone had been re-paved on no less than eight occasions.

The structure shares similarities with Bronze Age domestic architecture in Shetland but is unlikely to have been used as a primary domestic residence. It is, however, almost identical in plan to a structure found in association with a burnt mound at Tangwick, Eshaness. The current interpretation views the site as a purpose-built structure in which hot stone technology was carried on, generating large amounts of burnt stone. This debris was

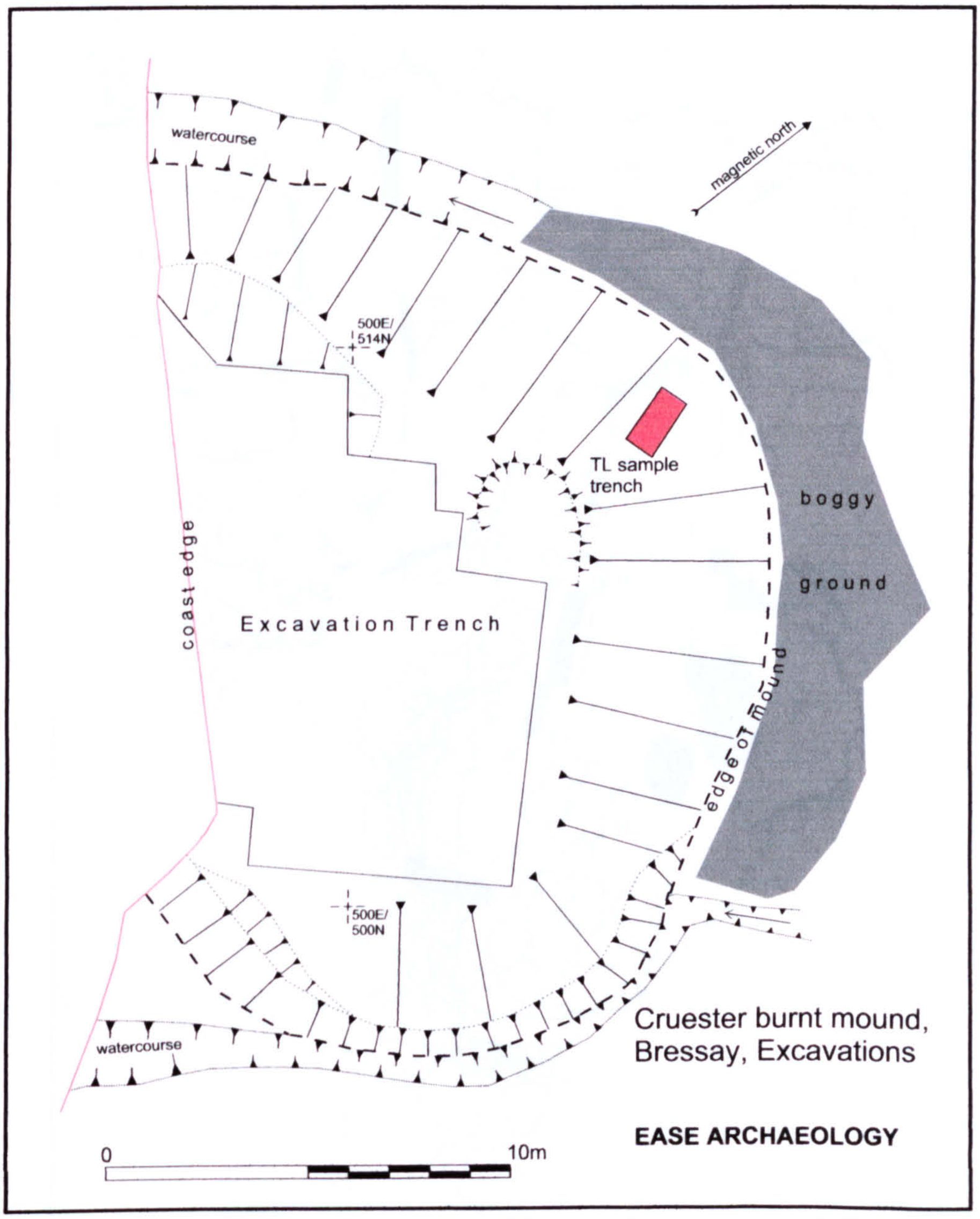

Fig 4.8a General Site Plan, Cruester Burnt Mound

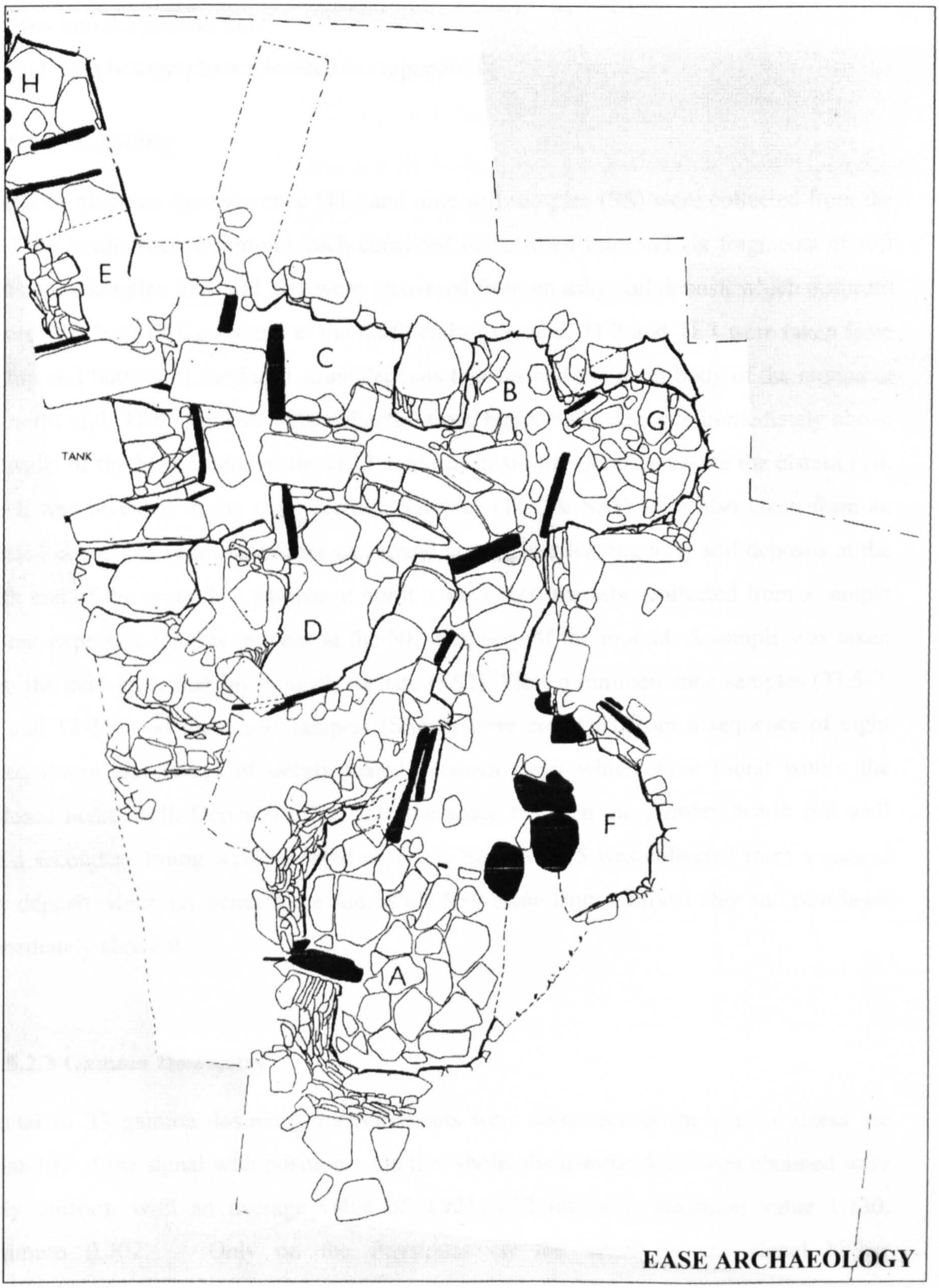

Fig 4.8b Plan of Structures, Cruester Burnt Mound

deposited around the building, eventually accumulating into the large mound which survives into the present time.

General site photographs are located in Appendix I

4.2.5.2.2 Sampling

A total of nineteen luminescence (TL) and nine soil samples (SS) were collected from the site. The luminescence samples each consisted of between four and six fragments of soft sandstone. Samples TL1 and SS1 were recovered from an ashy soil deposit which occurred towards the base of the mound at the north end of the site. TL2 and TL3 were taken from the top and bottom of the burnt stone deposits that formed the main body of the mound at the north end. TL8 and SS4 were collected from burnt stone deposits immediately above the walls of the hearth cell, while TL11 came from similar deposits above the cistern cell, which was revealed in the main section. Samples (TL4 & SS3) were also taken from an isolated deposit of burnt stone that was found among interleaving ashy soil deposits at the south end of the mound. A sample of burnt stone (TL9) was also collected from a sample pit, cut expressly for this purpose at the NE periphery of the mound. A sample was taken from the peat layer that lay beneath the site (SS2). Eleven luminescence samples (TL5-7, 10, and 13-19) and three soil samples (SS6-8) were collected from a sequence of eight paved floors and layers of debris sealed between them which were found within the enclosed hearth cell. Deposits filling into the space between the primary hearth cell wall and a secondary lining were sampled as TL12. Sample SS5 was collected from a natural clay deposit which lay beneath the site, while SS9 came from a mixed clay and peat layer immediately above it.

4.2.5.2.3 Gamma Dosimetry

A total of 33 gamma dosimetry measurements were taken across the site to assess the variability of the signal with position. On the whole, the gamma dose rates obtained were fairly uniform with an average value of $0.921\pm0.125 mGya^{-1}$; maximum value 1.130, minimum 0.702. Only on the flagstones on the beach is the signal higher ($1.62\pm0.16 mGya^{-1}$).

Table 4.17 Cruester Burnt Mound, Sample Information

Samp. Pos	2000 Context	Description	Gamma Dose No.	SUTL No.s
TL1	87	5 stones from ashy soil deposit at base of the mound, in section, N end of site	9	949-953
TL2	51	6 stones from top of burnt stone deposits forming the mound, in section, N end of site	11	954-959
TL3	51	4 stones from lower burnt stone deposits forming the mound, in section, N end	10	960-963
TL4	88	6 stones from isolated deposit of burnt stone, in section, S end of site	-----	964-969
TL5	58	4 stones from accumulation over latest paved floor (floor 8), inside hearth cell	12&13	1050-1053
TL6	55	4 stones from accumulation over floor #7 and beneath floor #8, inside hearth cell	12&13	1054-1057
TL7	57	4 fragments of paving stone from latest paved floor (#8), inside hearth cell	12&13	1058-1061
TL8	15	4 stones from mound material directly above wall head of hearth cell	15	1062-1065
TL9	89	4 stones from sample pit near to base of mound, to NE side of site	28	1066-1069
TL10	59	4 fragments of paving stone from paved floor #7, inside hearth cell	12&13	1070-1073
TL11	51	5 stones from burnt mound deposits immediately above cistern cell, in section	29	1074-1078
TL12	69	2 stones from deposits filling into void between hearth cell wall (068) and secondary re-lining of this wall (061)	12&13	1079-1080
TL13	72	2 stones from accumulation over floor #6 and beneath floor #7, inside hearth cell	12&13	1081-1082
TL14	73	3 fragments of paving stone from paved floor #6, inside hearth cell	12&13	1083-1085
TL15	75	3 fragments of paving stone from paved floor #5, inside hearth cell	12&13	1086-1088
TL16	77	5 fragments of paving stone from paved floor #4, inside hearth cell	12&13	1089-1093
TL17	79	4 fragments of paving stone from paved floor #3, inside hearth cell	12&13	1094-1097
TL18	81	2 fragments of paving stone from paved floor #2, inside hearth cell	12&13	1098-1099
TL19	83	4 fragments of paving stone from paved floor #1, inside hearth cell	12&13	1100-1103
SS1	87	Soil matrix surrounding sample TL1	N/A	N/A
SS2	86	Peat layer underlying site	N/A	N/A
SS3	88	Soil matrix surrounding sample TL4	N/A	N/A
SS4	15	Soil matrix surrounding TL8	N/A	N/A
SS5	85	Clay sample from layer below mound	N/A	N/A
SS6	72	Soil sample from accumulation over floor #6 and beneath floor #7	N/A	N/A
SS7	76	Soil sample from accumulation over floor #4 and beneath floor #5	N/A	N/A
SS8	74	Soil sample from accumulation over floor #5 and beneath floor #6	N/A	N/A
SS9	84	Burnt clay from below earliest paved floor (floor #1)	N/A	N/A

Table 4.18 Cruester Burnt Mound, Gamma Spectrometry Results

Spectrum No	Description/ Associated Samples	Mean 4Π γ dose rate ($mGya^{-1}$)
1	Flagstones	1.62±0.16
2	Clay base	1.03±0.10
3	Rabbit hole above S. burnt mound dep	0.74±0.08
4	Southern cellular structure	1.01±0.12
5	Inner cellular structure, S. side	1.08±0.12
6	Front face of tank	0.90±0.10
7	Inner N cellular structure	1.13±0.15
8	Outer N cellular structure	1.08±0.12
9	Position of TL1	0.76±0.15
10	Position of TL3	0.92±0.10
11	Position of TL2	1.13±0.10
12	055 - Deposit at back of hearth cell	0.89±0.10
13	057/058 corner of hearth cell	0.92±0.10
14	Cell next to hearth	1.05±0.10
15	015 - Upper mound material	0.93±0.10
16	Turf, top of mound	0.70±0.06
17	Southern Cell, next to wall	0.83±0.10
18	SW corner of S. Cell	0.97±0.10
19	NW corner of S cell	1.02±0.10
20	E side of S cell	0.77±0.10
21	S entrace to Eastern Cell	0.76±0.10
22	Centre of eastern Cell	0.76±0.10
23	Middle of Southern Cell	0.95±0.10
24	Middle of Corridor at eastern cell	0.79±0.10
25	N entrace to Eastern Cell	0.80±0.10
26	Middle of corridor N of Eastern Cell	0.86±0.10
27	Corridor in front of hearth cell	1.13±0.15
28	Sample pit North end mound TL9	0.89±0.10
29	Above Cistern TL11	0.99±0.15
30	Between two western cells near tank	1.03±0.10
31	Cell to SE of tank	0.89±0.10
32	Cell to NE of tank	0.92±0.10
33	Easterm cormer of tank	0.98±0.10

4.2.5.3 Tangwick

4.2.5.3.1 Excavation and Recording

(From Moore& Wilson, 2000)

The burnt mound at Tangwick was revisited in October 2000 for the purposes of recovering samples for thermoluminescence dating. It was noted that the site has changed considerably since the 1996 excavation. The excavation trenches had been largely covered over by the storm beach and little of the structure was visible. Samples were taken from the section face and from a trench cut into the mound. The trench measured 1m by 1m and

was cut down to a depth of 1.4m, where upon a layer of mineral soil and peat deposits were encountered.

General site photographs are located in Appendix I

4.2.5.3.2 Sampling

A total of four luminescence (TL), two soil (SS) and five miscellaneous (Misc) samples were collected. The luminescence samples comprised between three and seven burnt stones. They were collected from the upper burnt mound (TL2 and 4), the lower mound (TL1) and from an ashy layer which intervened between (TL3). Three of the miscellaneous samples comprised pot sherds and one was of a slag-like material. Three of these came from the upper burnt mound (Misc 2-4) while two were recovered from the intermediate ashy layer (Misc 1 and 5). Soil samples were collected from peat which lay beneath the site (SS1) and from the ashy layer.

Table 4.19: Tangwick Burnt Mound, Sample Information

Sample	2000 Context	Description	Gamma Dose No	SUTL No.s
TL1	4	5 stones from lower burnt mound deposit, section trench, E end of mound	1	1032-1036
TL2	2	7 stones from upper burnt mound deposit, section trench, E end of mound	2	1037-1043
TL3	3	3 stones from ashy layer, E-W section face, E end of mound	4	1044-1046
TL4	2	3 stones from upper burnt mound deposit, central area	4A	1047-1049
Misc 1	3	Pot sherds from ashy layer, E-W section face, to E end of mound	4	N/A
Misc 2	2	Pot sherds from upper burnt mound deposit, central area	4A	N/A
Misc 3	2	Pot sherds from upper burnt mound deposits, E-W section, above hearth cell	-----	N/A
Misc 4	2	Pot sherds from upper burnt mound deposit, to W of hearth cell	-----	N/A
Misc 5	3	Slag (?) from ashy layer E-W section face, E end of mound	-----	N/A
SS1	5	Peat layer underlying site	-----	N/A
SS2	3	Soil matrix surrounding sample TL3	-----	N/A

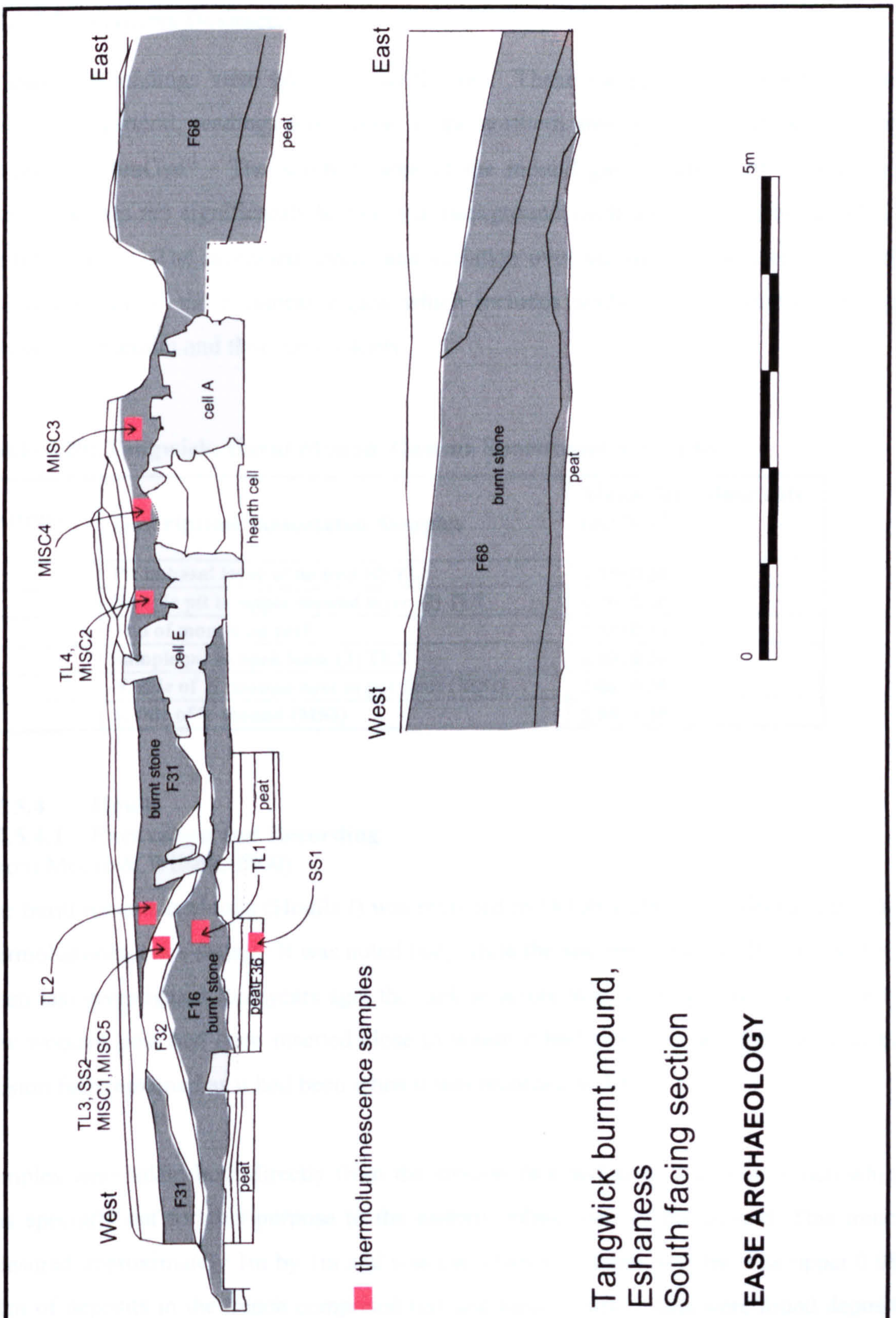

Fig 4.9 General Site Plan, Tangwick Burnt Mound

4.2.5.3.3 Gamma Dosimetry

A total of 6 readings were taken around the site. These varied by around 60% in some places. In general, readings were lower in the northern area of the mound, with average readings c.1.6mGya^{-1}. The southern area of the mound gave readings of 2-2.6mGya^{-1}. These readings are significantly higher than background readings measured at the other 3 Shetland sites. The increased levels, and variation over the site can be attributed to the mixed geology of the Eshaness region which includes acidic volcanic rocks with high potassium, uranium and thorium contents.

Table 4.20: Tangwick, Burnt Mound, Gamma Spectrometry Results

Spectrum No.	Description/ Associated Samples	Mean 4Π γ dose rate (mGya^{-1})
1	Pit in basal layer of mound (4) TL1	1.70±0.20
2	Sample pit in upper mound layer (2) TL2	1.70±0.20
3	Top of mound on turf	1.58±0.15
4	Sample pit in dark lense (3) TL3	1.49±0.20
4A	N. side of S. mound next to pot finds (MS2)	2.06±0.20
5	S. side of S. mound (MS3)	2.58±0.30

4.2.5.4 Houlls

4.2.5.4.1 Excavation and Recording

(From Moore & Wilson, 2000)

The burnt mound at Houlls (Houlls I) was revisited in October 2000 to collect samples for thermoluminescence dating. It was noted that, while the site remained much as it had been when last investigated four years ago, the tank structure was no longer in evidence and a new wooden post had been inserted close to where it had stood. In all other respects the erosion face remained as it had been when it was recorded in 1996.

Samples were taken both directly from the erosion face and from a section trench which was specially cut for this purpose to the eastern, inland side of the mound. This trench measured approximately 1m by 1m and was cut down to a depth of 0.3m. The upper 0.08-0.1m of deposits in the trench comprised turf and topsoil. Below this were found deposits of burnt stone in a silty matrix which were in all respects comparable to the burnt stone deposits seen in the erosion face.

General site photographs are located in Appendix I

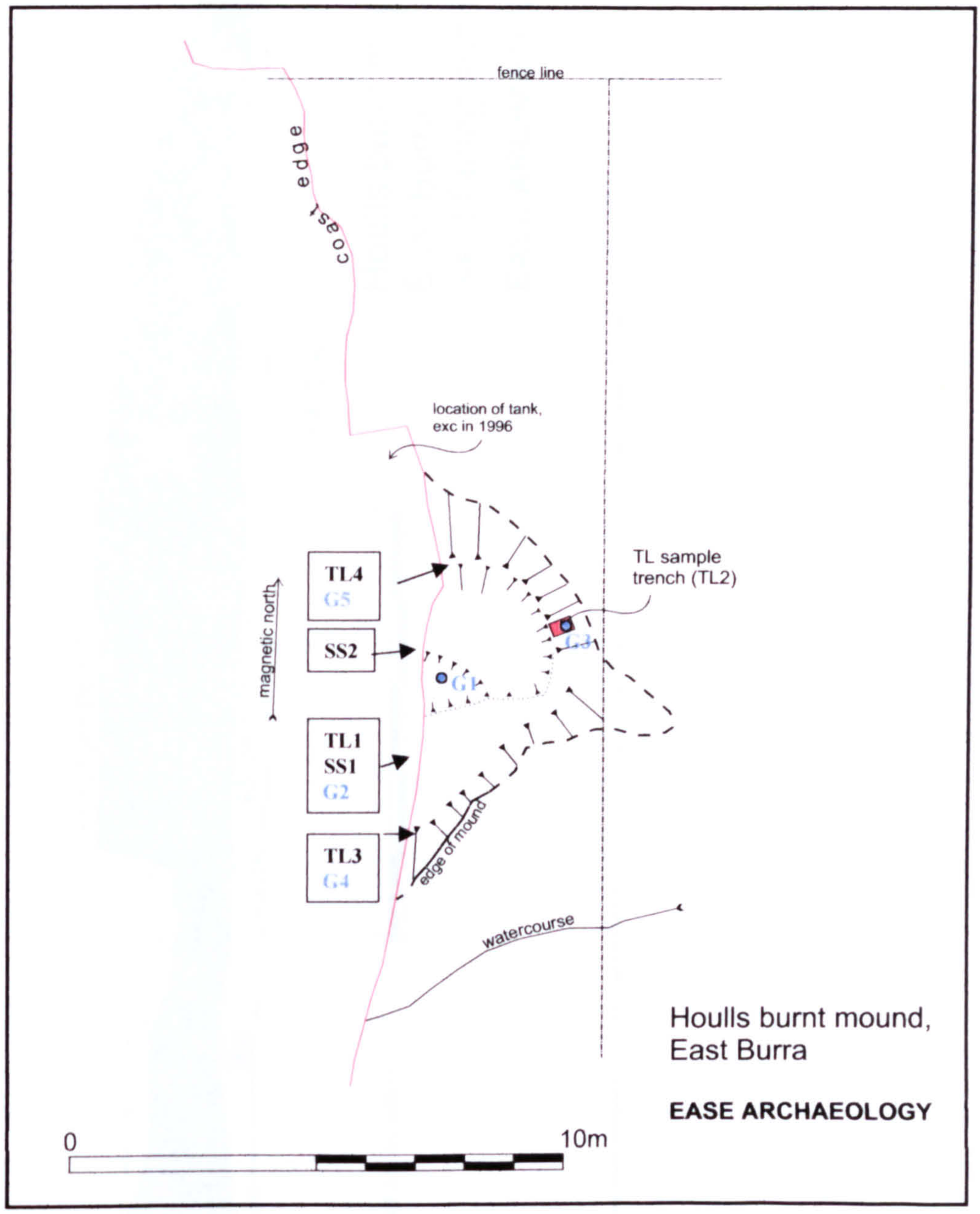

Figure 4.10a: General Site Plan, Houlls Burnt Mound

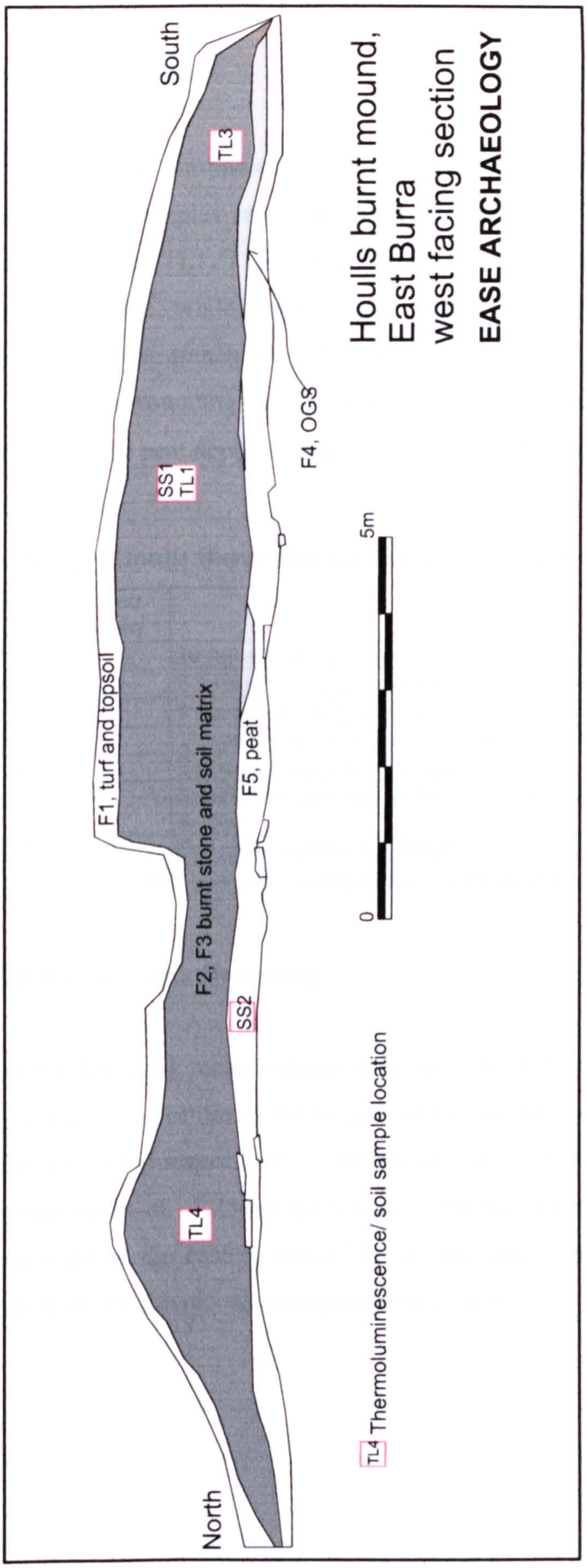

Fig 4.10b. Coastal Section, Houlls Burnt Mound

4.2.5.4.2 Sampling

A total of four luminescence (TL) and three soil samples (SS) were collected. The luminescence samples each comprised between eight and eleven small to medium sized stones. Samples TL1, TL3 and TL4 were collected from burnt stone deposits exposed in the section face, while luminescence sample TL2 was taken from burnt stone deposits uncovered in the trench. Of the three soil samples, SS1 and SS3 were collected from the soil matrix surrounding luminescence samples TL1 and TL3, respectively, while SS2 was taken from the peat deposits underlying the burnt mound.

Table 4.21: Houlls Burnt Mound, Sample Information

Sample No.	2000 Context *	Description	Gamma Dose No.	SUTL No.s
TL1	2	10 stones from body of mound, from centre of section face	2	971-979
TL2	2	8 stones from trench to eastern side of mound	3	980-987
TL3	2	8 stones from body of mound, from S end of section face	4	988-995
TL4	2	11 stones from body of mound, from N end of section face	5	996-1005
SS1	2	Soil matrix surrounding sample TL1	N/A	N/A
SS2	3	Sample from peat deposit beneath mound from N end of section	N/A	N/A
SS3	2	Soil matrix surrounding sample TL3	N/A	N/A

* For context concordance with 1996 recording see Moore & Wilson, 2000.

4.2.5.4.3 Gamma Dosimetry

Gamma dosimetry measurements were taken from 5 positions within the site. G1 on top of the turf at the centre of the mound, and G2-4 from within holes/pits dug for sampling at positions TL1-4 respectively. Whilst all results are within error of each other, giving an average value of 1.254mGya^{-1}, it is noted that lower readings were obtained from the sample pit at the eastern end of the mound and from the top of the mound where the vicinity of the detector to the topsoil was closest.

Table 4.22: Houlls Burnt Mound, Gamma Spectrometry Results

Spectrum No.	Description/ Associated Samples	Mean 4Π γ dose rate ($mGya^{-1}$)
1	Top centre of mound on turf	1.19±0.10
2	Centre of section at position of TL1	1.36±0.10
3	Eastern end of mound in sample pit at position of TL2	1.15±0.10
4	Southern end of section, position of TL3	1.32±0.10
5	Northern end of section, position of TL4	1.26±0.10

4.2.5.5 Loch of Garths Burnt Mound

4.2.5.5.1 Excavation and Recording

(From Moore and Wilson, 2000)

Loch of Garths burnt mound was revisited in October 2000 for the purpose of recovering samples for thermoluminescence dating. Since the site was last visited in 1996, the loch has been drained. This has been effected by means of a channel which runs from the loch side and through the storm beach to the sea. An inspection of the channel found the sides to be near vertical, suggesting that the channel may have been cut by machine. The exposed loch bed is boggy and strewn with debris.

The burnt mound was found to have diminished further since it was last seen. The chief cause of erosion in the recent past has been due to sheep using the existing exposures at the side of the mound as shelters and in doing so, causing further stones to be dislodged. There are now two hollowed 'sheep shelter' areas in the southern side of the mound.

The draining of the loch has exposed further large earthfast stones to the southern side of the mound. These, together with several large stones noted previously within the body of the mound would appear to represent the last remnants of an associated structure.

Samples were collected both from the existing exposure and from a trench. The trench was made by enlarging the easternmost of the two sheep hollows and extending it to an overall depth of 1.4m. In addition to turf and topsoil, three distinct layers were seen in the section. The upper part of the mound was formed of burnt stone in a dry silty soil matrix. Beneath

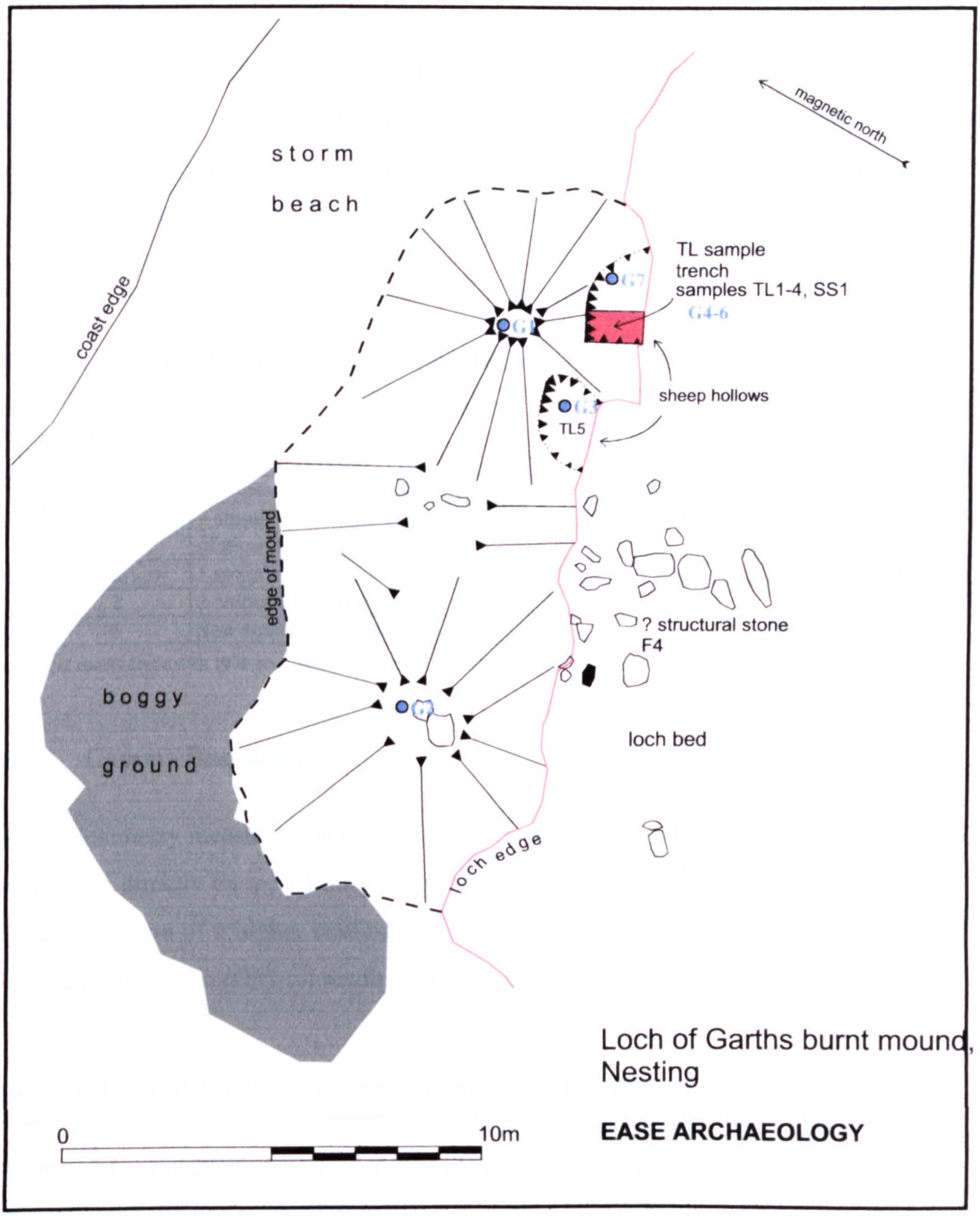

Fig 4.11 General Site Plan, Loch of Garths

this, a lens of sandy soil some 0.3m deep, covered further, waterlogged, deposits of burnt stone in a heavily iron-panned matrix. At this level the trench met the water table and excavation ceased.

General site photographs are located in Appendix I

4.2.5.5.2 Sampling

A total of one soil (SS) and five luminescence (TL) samples were collected. The luminescence samples comprised between one and ten stones, varying in size from small to large. Three samples were taken from the upper deposit of burnt stone, with one sample each collected from the sandy lens and the lower, waterlogged layer. The soil sample was recovered from the sandy lens.

Table 4.23 Loch of Garths, Sample Information

Sample	2000 Context*	Description	Gamma Dose No.	SUTL No.s
TL1	4	10 stones from base of section trench	4	1006-1015
TL2	3	6 stones from sandy lens near base of section trench	5	1016-1021
TL3	2	7 stones from upper burnt stone deposits forming body of mound in section trench	6	1022-1028
TL4	2	1 stone from area close to TL3 sample	---	1029
TL5	2	2 stones from western end of mound	7	1030-1031
SS1	3	Soil matrix surrounding sample TL2	N/A	N/A

* For context concordance with 1996 recording see Moore & Wilson, 2000.

4.2.5.5.3 Gamma Dosimetry

7 gamma dosimetry measurements were made across the site. The lowest readings (G1 & 2) were taken directly on top of the turf where the contribution from the topsoil is greater. With the exception of a higher reading of 1.550mGya^{-1} obtained from within a rabbit hole on the southern section (G3), all readings from sampling positions are ≅1.329mGya^{-1}.

Table 4.24: Loch of Garths, Gamma Spectrometry Results

Spectrum No.	Description/ Associated Samples	Mean 4Π γ dose rate (mGya^{-1})
1	Top centre of mound on turf	1.17±0.10
2	Area to south of mound	1.12 ±0.10
3	Rabbit hole, south section	1.55 ±0.16
4	Base position (TL1) north trench section	1.34±0.15
5	Middle position (TL2) north trench section	1.36±0.14
6	Top position (TL3) north trench section	1.33±0.14
7	Northern wing of mound (TL5)	1.28±0.15

4.3 Sample characterization and selection

4.3.1 Criteria for selection

There are many factors which contribute to appropriate sample selection. The process clearly begins in the field. Context is important both from the point of view of being able to relate any dates to their location within the site, but also in terms of providing an assessable gamma field. Samples located in geometries significantly different from 4Π may incur significant errors in the measurement of external gamma dose rate.

The size of samples collected is balanced between the need for sufficient material for dating, and to collect well zeroed stones not adversely affected by gamma attenuation. Cataloguing of samples collected has highlighted a number of samples that were deemed unsuitable for further analysis due to either a lack of material, or concerns over possible gamma attenuation in larger samples.

Geological identification of cleaned samples has also highlighted a number of potential pitfalls. The main issue being large phenocrysts within a finer grained matrix of some stones which may crack on sample disagregation, causing complications in the internal dose rate estimate for that sample. Where identified, such material was avoided.

Selected samples are detailed in the following section, and basic information with regards to sample weight, approximate dimensions and lithology given.

4.3.2 Orkney Samples

The samples collected from Eday appeared to be of two types. A fine-medium grained reddish sandstone and a fine grained grey mudstone, most probably derived from the Eday beds and Rousay Flags respectively. Samples from Liddle were also identified as Rousay Flags. A sub-section of stones collected from each site were selected for further analysis.

Thin section analysis of a subsection of samples from Eday confirmed initial identification of the material, and highlighted small microstructures within the minerals. The majority of samples showed a highly homogenous material, with no evidence of internal structures. A few however showed cross bedding and, in the case of Rousay Flags, variation in the

colour of the silty layers, probably related to seasonal variations. Evidence of dewatering was seen in one sample.

Small portions of the same samples underwent X-Ray diffraction analysis. All samples showed quartz as a major component, with minor and trace components of feldspar and mica, in keeping with preliminary observations. Trace components of calcite, kaolin and smectite were also found on occasion (fig 4.12). It should be noted that the technique is more sensitive to the detection of quartz, thus no quantitative data should be inferred from the spectra.

4.3.3 Shetland Samples

Samples collected from Shetland were of mixed geology, reflecting the complex geological make up of the Shetland Islands.

At Cruester, a larger selection of samples were identified for analysis, reflecting the complex archaeological information available for the site. A total of 27 samples were selected, representing the main stratigraphic units sampled both from within the mound and the hearth cell structure. The samples selected were of two types. The majority were medium-coarse grained sandstones, often badly weathered and crumbling. However, all stones taken from the floor of the hearth cell were a fine grained siltstone, found further south on the Island of Bressay. Two of these samples were subsequently cut in half or quartered to allow for future investigation of the effectiveness of the zeroing of the hearthstone material (see discussion in Chapter 6).

At Tangwick, the majority of samples collected were identified as Baretchia. Orthoclase feldspars were abundant and often several mm in diameter. Small angular fragments of rock were also noted on examination. Sample selection from Tangwick proved problematic as, in addition to undesirable material, all rocks proved to be extremely hard and difficult to cut and crush.

After an initial clean, samples from Houlls were identified as micaceous psammite and migmatic gneiss. On occasion large phenocrysts were also noted and these samples were subsequently rejected. A subset of nine samples were selected for further analysis. These

Table 4.25 Summary of samples from Orkney selected for analysis

Site	Pos	SUTL No.	Sample Description	Approx Dimensions (cm)	Weight (g)
Liddle	1	1379	RF	15x7x3	430
		1381	RF	8x4x2	95
	2	1386	RF	10x5x2	120
Dale	12	748	EB, iron panning	6x5x2	60
		749	EB	7x6x3	60
		750	EB	6x6x3	95
		751	EB iron panning	7x4x2	100
		753	EB iron panning	10x6x2	180
		754	RF	8x4x1	80
		755	RF	6x5x1	80
	13	760	EB	5x3x2	70
		764	EB	10x7x2	165
		765	RF	6x8x4	335
		767	EB	9x5x2	175
	14	768	RF	15x8x3	440
		769	EB	15x6x3	375
		774	RF	10x8x4	370
		775	EB (very weathered)	8x5x2	75
		777	EB	9x5x1	95
		779	RF	6x7x4	280
	15	782	RF	8x6x3	175
		783	RF	8x4x2	100
		784	EB	6x4x3	80
		785	EB	10x5x2	120
Skaill	1	1343	EB	10x8x3	400
	2	1354	EB	6x5x4	230
	3	1358	RF	5x4x2	50
		1360	EB	6x5x4	200
	5	815	RF	9x9x3	350
	6	817	EB	8x5x3	120
	O-1	1361	Wind blown sand	N/A	100
	O-2	1362	Wind blown sand	N/A	170
	O-3	1363	Wind blown sand	N/A	220
	O-4	1364	Wind blown sand	N/A	300
Knoll of Merrigarth	8	794	RF	8x6x2	205
		795	RF	7x4x3	90
	7	802	EB	10x7x1	150
		803	RF	12x7x2	190
Warness	9	842	RF	7x3x3	75
	10	853	RF	7x5x2	70
		857	EB	6x4x4	170
	11	849	RF	6x5x3	155
Stackelbrae	2	1374	RF	10x4x2	100
Fersness	3	823	RF	5x4x2	70
		824	EB	6x5x2	125
	4	831	RF	5x4x2	75
		833	EB	8x7x3	310
Stenaquoy	1	836	EB	8x6x2	95
	2	838	EB	7x5x5	395
		839	EB	5x4x2	60

RF: Rousay Flagstones, EB Eday Beds

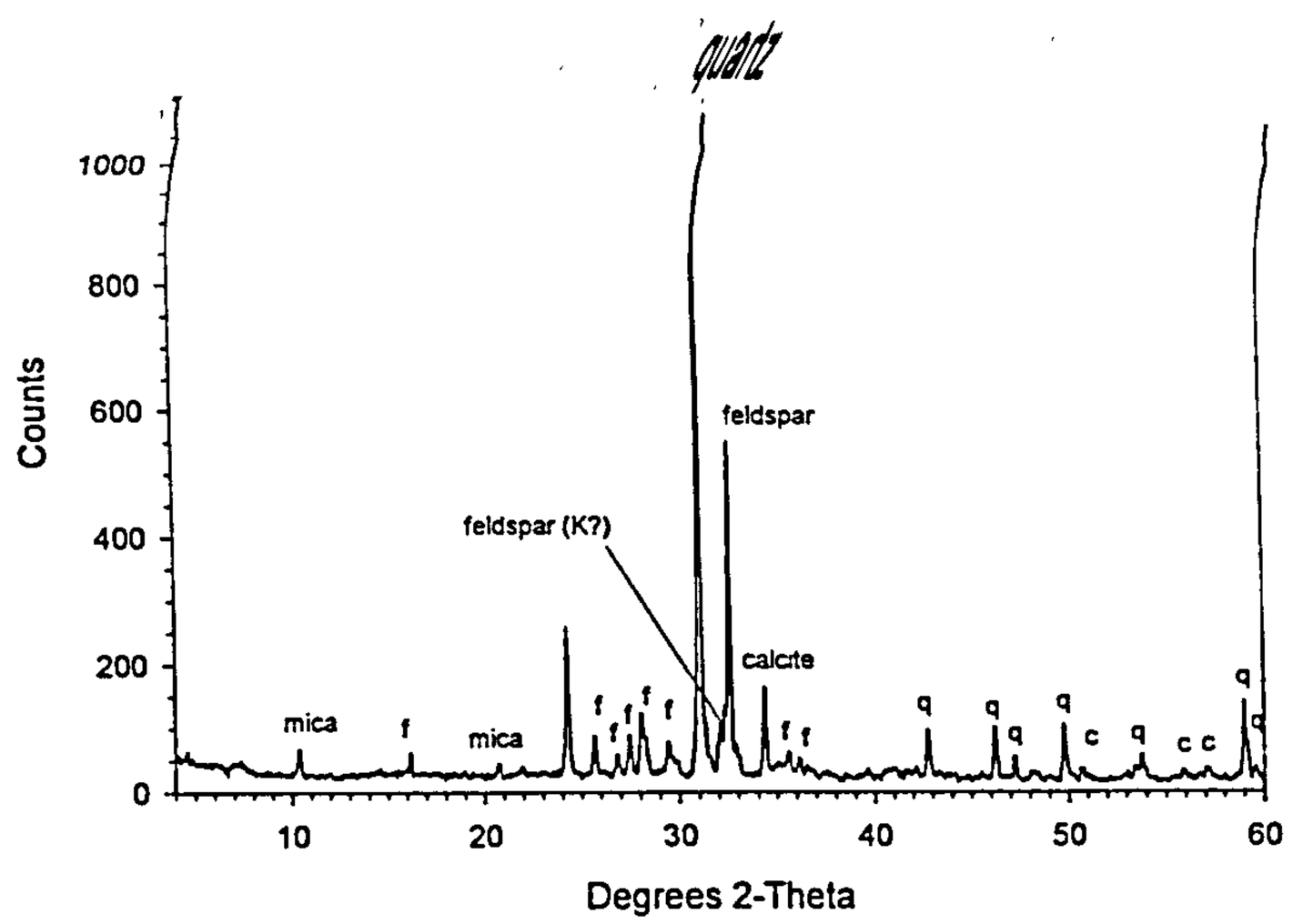

3709: SUTL 802 Knoll of Merrigarth

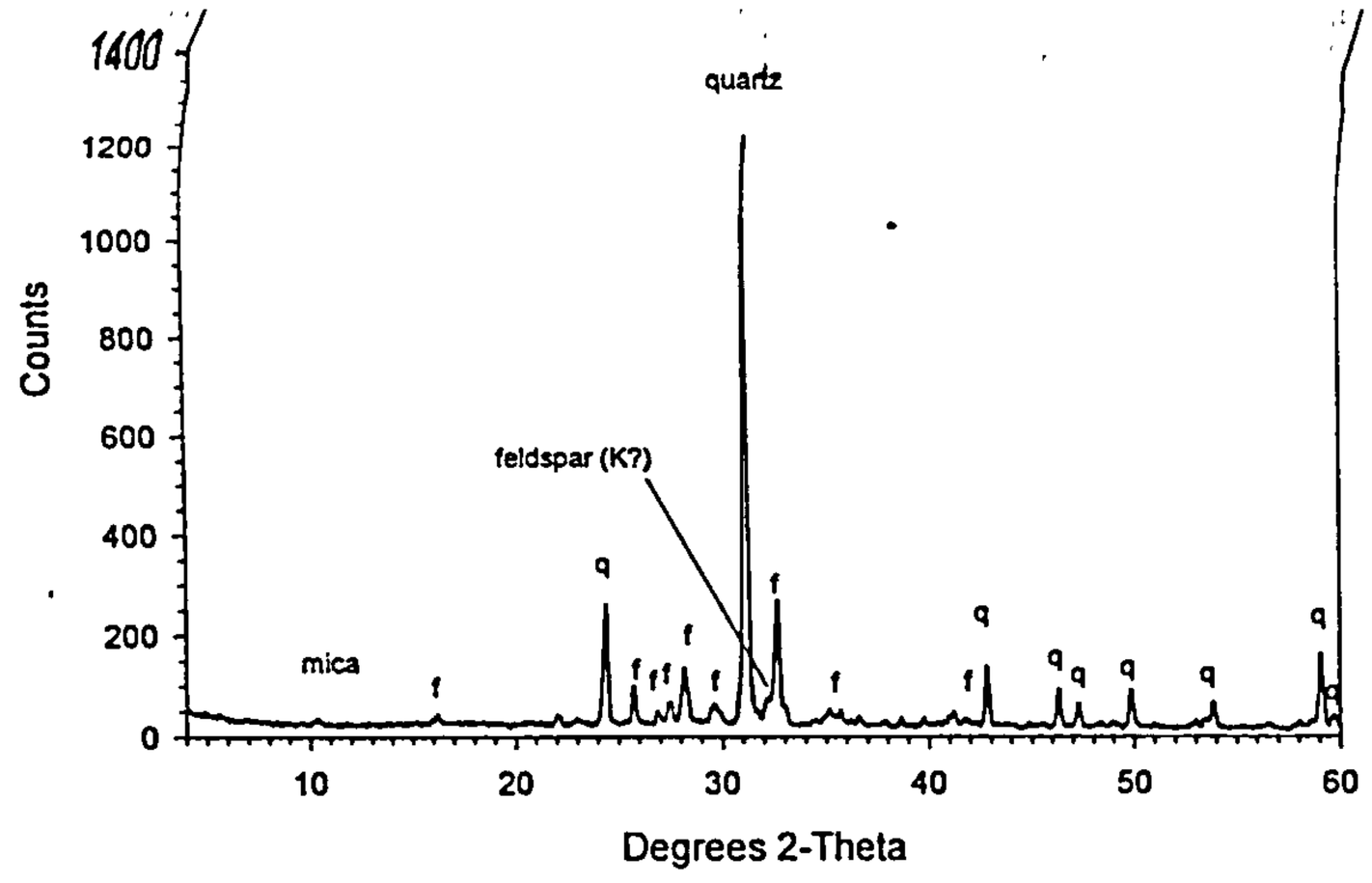

3717: SUTL 857 Warness

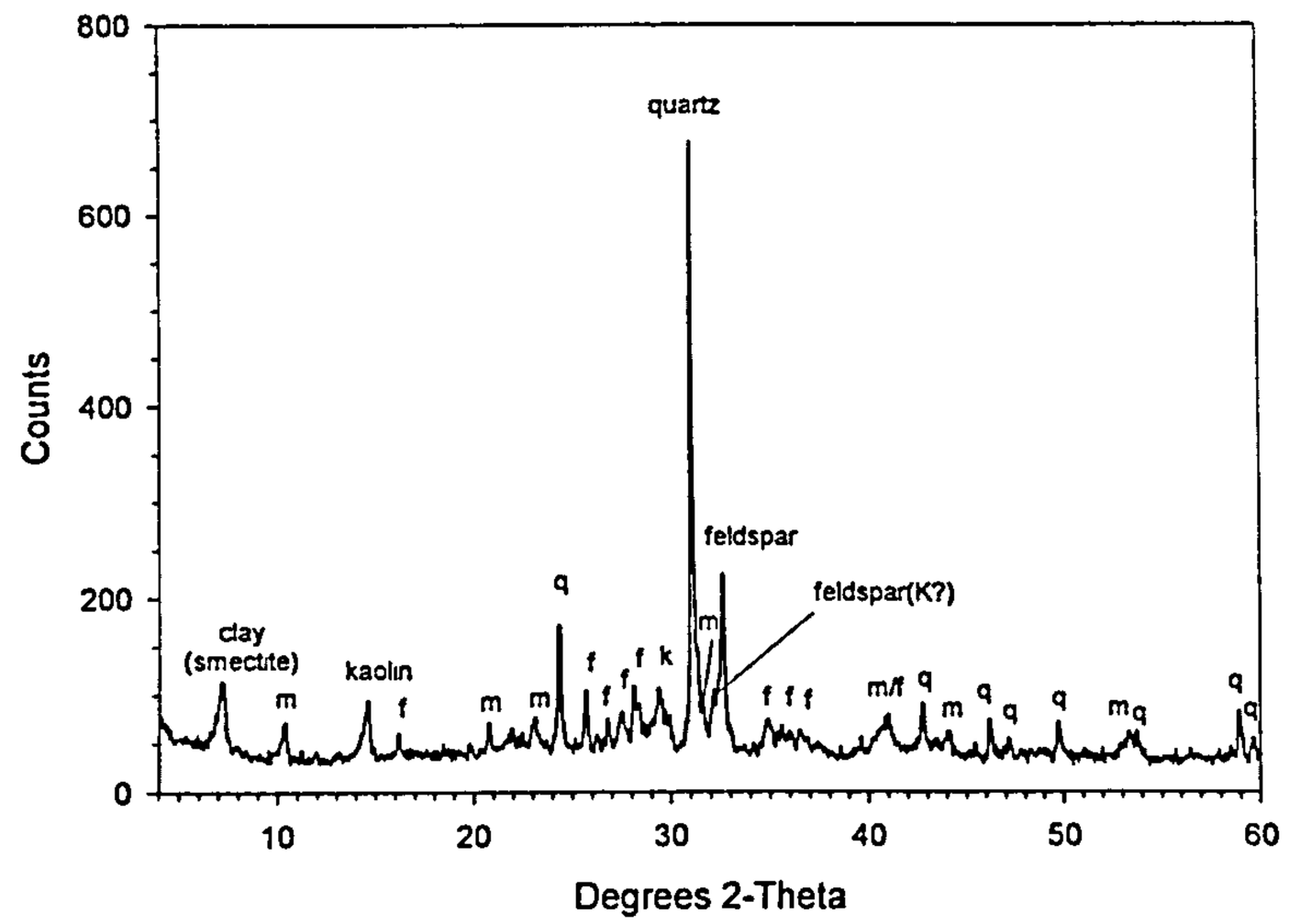

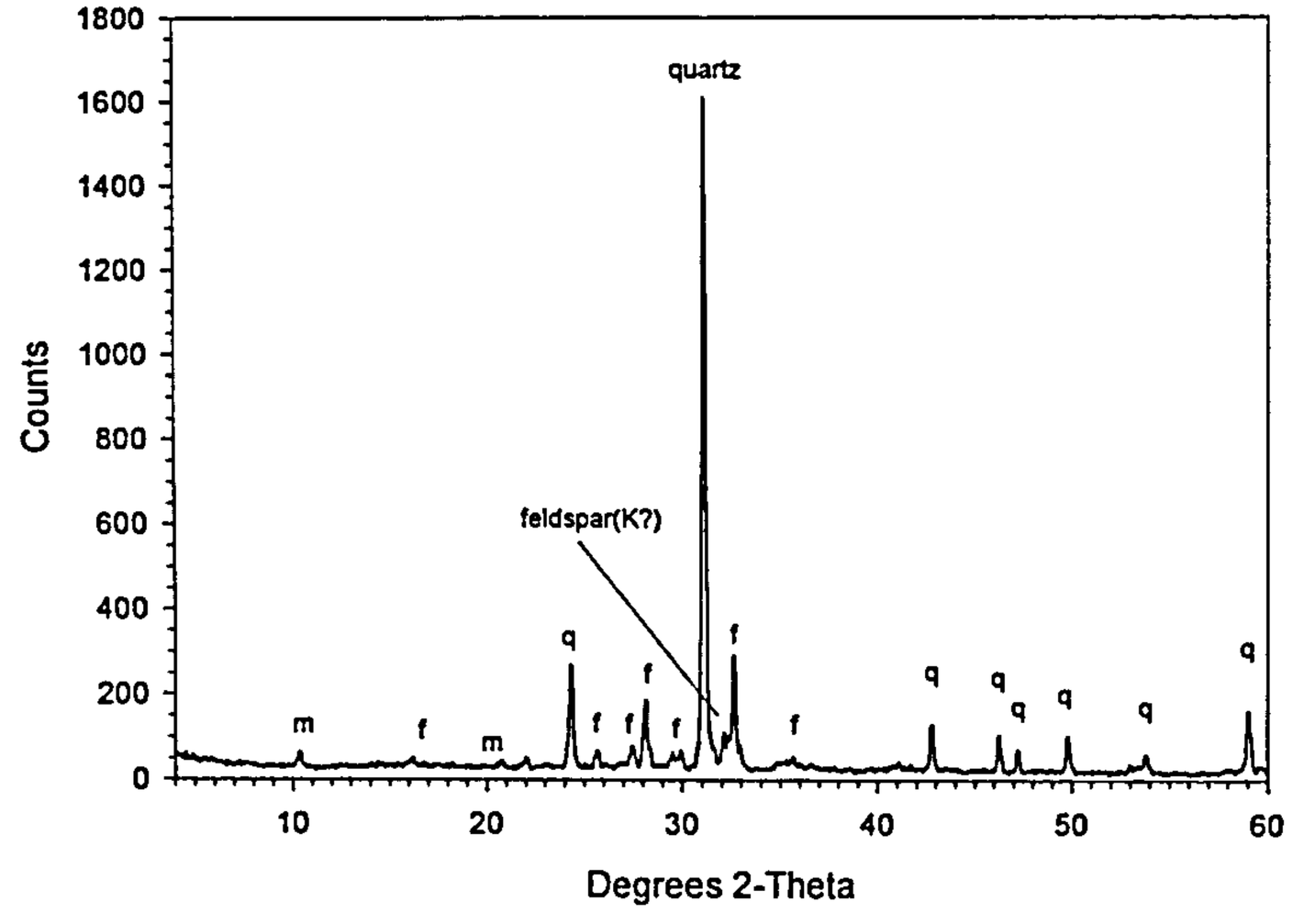

Fig 4.12 Examples of XRD Results: (a) SUTL794 (b) SUTL802 (c) SUTL849 (d) SUTL857

were selected as having the smallest dimensions of the samples collected, and thus less likely to have suffered adverse effects of uneven heating and/or differences in gamma dose rate.

Many of the stones examined from the Loch of Garths were granodioritic, containing large phenocrysts within a finer matrix. On occasion, gneissose quartzite was also noted. The stones selected for further analysis were again the smallest of those collected, and for the most part samples with large phenocrysts were avoided.

4.4 Mineral Preparation

4.4.1 Methodology

As outlined in chapter 2, it was decided to extract both quartz and feldspar minerals from the selected samples for further examination. There are a number of acid and density separation steps which enable isolation of the minerals concerned, however removal of unwanted material and selection of a restricted size fraction are first necessary to enable a more accurate assessment of internal dose rates to be made. The mineral preparation procedure is summarized in table 4.27.

The outer β irradiated 3mm layer of each stone was removed with a water cooled rock saw, the remainder being loosely disaggregated using mortar and pestle. Eskola et al (2003) report that disaggregation can be accomplished by mechanical crushing with no adverse effect on the luminescence properties of the minerals (in terms of the production of spurious luminescence). However, the decision was taken to manually crush each sample due to concerns over potential cracking of larger grains using mechanical methods - whilst cracking may not adversely affect the luminescence signal, it would be problematic in terms of dose rate calculation due to the higher/lower internal dose rate received by the larger grain.

After disaggregation, each sample was separated into size fractions using an automatic siever, with mesh sizes 500μm, 250μm, 125μm, and 90μm. The preferred mineral fraction (90-125μm) was then selected for further separation. Where insufficient material was present in the 90-125μm size fraction, the 125-250μm fraction was also selected.

Table 4.26 Summary of samples from Shetland selected for analysis

Site	Pos	SUTL No.	Sample Description	Approx Dimensions (cm)	Weight (g)
Cruester	1	949	FGSS	7x5x3	205
		951	MGS	7x6x3	170
		953	MGS	7x6x3	190
	2	958	MGS	9x7x4	280
	4	968	MGS	5x4x3	190
		969	MGS	7x5x4	210
	5	1051	MGS	7x5x3	205
		1053	MGS	7x5x4	130
	6	1054	MGS	8x7x2	270
		1055	MGS	7x6x3	400
	7	1059	FGSS	9x9x2	400
	8	1062	MGS	7x5x5	250
		1063	MGS	7x5x4	200
		1064	MGS	8x6x3	350
	9	1068	MGS	7x5x4	200
	11	1075	MGS	7x5x4	200
		1076	MGS	8x4x3	200
		1077	MGS	10x6x4	560
	13	1081	MGS	8x5x4	500
	15	1086	FGSS	8x2x2	380
		1087	FGSS	8x7x2	320
		1088	FGSS	10x6x2	310
	17	1094	FGSS	9x8x3	310
		1095	FGSS	13x7x2	360
		1096	FGSS	10x8x2	400
		1097	FGSS	7x7x3	270
	19	1100	FGSS	7x8x3	300
Tangwick	1	1033	Ba	7x7x5	310
		1034	Ba	6x4x4	155
	2	1040	Ba	8x7x5	305
		1041	Ba	8x5x3	190
		1043	Ba	6x5x4	165
Houlls	1	970	MG	7x4x2	150
		971	MG	8x3x1	170
		976	MG	7x7x3	125
		978	MG	10x5x3	175
	2	983	MG	8x6x4	200
	3	991	MG	7x5x3	150
		993	MG	8x5x4	190
	4	1003	MG	5x4x4	185
		1004	MG	6x7x2	250
Loch of Garths	1	1006	GQ	7x5x3	195
		1007	GD	9x6x3	255
		1008	GD	6x5x5	200
	2	1017	GD large phenocrysts	7x4x3	120
		1018	GD large phenocrysts	7x5x3	155
		1020	GD	6x6x4	190

KEY: FGSS Fine Grained Siltstone; MGS Medium Grained Sandstone; MG=migmatic gneiss; GQ gneissose quartzite; GD granodiorite; Ba=Baretchia

Each selected fraction was treated with 1 molar HCl for 30 minutes to remove carbonates, then for a further 15 minutes with 15% HF to lightly clean the outside of the minerals, followed by a second 30 minute treatment with HCl to remove any insoluble fluorides produced by the HF treatment. Three de-ionised water and acetone washes were then given to remove any residual acids.

Prior to density separation, thick sections from a selection of samples were prepared and examined by SEM. One of the main aims of this work was to determine the likely abundance of heavy minerals such as zircons, which can have an adverse effect on quartz results. Viewing in backscattered light led to easy identification of zircons. In a number of samples, they proved surprisingly abundant, with up to 6 zircon grains being identified within a 0.5mm^2 area (fig 4.13). The presence of zircon necessitated an additional heavy mineral liquid separation to remove such minerals from the quartz fraction.

The samples were sequentially centrifuged in sodium polytungstate solutions of densities of 2.51, 2.58, 2.62, and 2.74 gcm^{-3}. This produced 5 fractions:

<2.51 (discarded)

2.51-2.58, containing potassium feldspars

2.58-2.62, containing sodium feldspars

2.62-2.74, containing plagioclase feldspars and quartz

>2.74, containing heavy minerals which were retained, but not analysed.

Samples were washed three times with de-ionised water and dried with analar acetone.

A portion of the 2.62-2.74 fraction was immersed in 40% HF for 40 minutes to dissolve remaining feldspars and etch the quartz, followed by a 30 minute HCl treatment, and three further water rinses as above.

Table 4.27 Summary of Mineral Preparation Procedure

Step	Description	Reason	Potential Problems	Mitigation
1	Removal of outer 3mm of sample using water cooled rock saw	To remove externally beta irradiated layer and surface contamination	Heating of sample due to rotation of saw, bleaching of outer layer during cutting	Water reservoir kept topped up at all times, Sample transferred to lightproof container immediately after cutting and muddy layer produced with cutting not removed until sample back in lab under safelight conditions
2	Disagregation of Sample with mortar and pestle	To disaggregate sample for sieving	May induce Spurious Luminescence	More compact stones avoided. Only easily disaggregated stones selected which avoided the need for undue force during grinding.
3	Sample sieved to extract various size fractions	To extract minerals of known geometry for dose rate calculations	Incomplete sieving may lead to smaller grains being present in size fractions. This may invalidate internal dose rate assumptions.	Automatic sieve shaker used after sample disagregation, followed by more rigourous shaking by hand to aid seperation
4	Acid treatment : 30 mins with 1M HCl 15 mins with 15% HF 30 mins with 1M HCl	To dissolve carbonates, etch minerals and remove any soluble fluorides produced from the HF etch	Partial etching and/or dissolution due to insufficient exposure of material to acids	Samples stirred throughout acid treatment
5	Density Separation using sodium polytungstate	To isolate specific densities of material related to feldspar/quartz minerals	Failure of density separation due to dilution of tungstate in residual liquid associated with prior density separation or smearing on sides of test tube	As much excess liquid removed from sample at each stage as possible. Excess tungstate solution added to test tubes to minimize effect. Test Tubes rotated during sample extraction to reduce side smearing
			Incomplete removal of tungstate solution from material	3 demineralised water and acetone washes given to each density at end of separation process.
6	Etching of 2.62-2.74μm fraction : 40 mins 40% HF 30 mins 1M HCl	To dissolve plagioclase feldspars and remove any soluble fluorides produced from the HF etch	Fine particles of feldspar adhering to pits in quartz grains	3 demineralised water and acetone washes given at end of acid treatment to aid removal of detrital feldspars.

4.4.2 Results

Percentage yields for each fraction of each sample are detailed in Appendix D[5]. It is clear from figure 4.14 that with the exception of the sand samples from Skaill, and samples from Liddle the <90μm fraction is the most abundant at all sites. All Orkney samples showed a similar pattern, with the 90-125μm fraction in general the least abundant. In the case of samples from Shetland, this fraction represented the second most abundant, with the 125-250μm fraction the least.

Representative fractions of each separate were analysed by SEM to check the efficacy of the separation process. Whilst the majority of samples checked showed a high degree of success in mineral separation, on occasion significant proportions of Na feldspar appeared in the K feldspar fraction, indicating dilution of the 2.58gcm^{-3} density separate.

Quartz on the whole appeared very pure, though on occasion evidence for small amounts of feldspathic material was seen.

On occasion lumps of finer material were also noted (fig 4.15). Whilst these lumps of material appeared on closer examination to be composed of grains of the correct size fraction, it should be noted that beta irradiation of such grains will lead to a higher exposure rate than desired due to their proximity to the source.

Surprisingly, tungstate was also found to be present adhering to the surface of a number of grains, indicating that on occasion the three water washes given after density separation were not enough to remove all residual tungstate from the sample (fig 4.16)

A summary of the mineral yields for each sample can be found in Appendix D.

---

[5] It should be noted that material >500μm was excluded from analysis due to the difficulty in determining whether such material was a product of incomplete disaggregation or truly represented minerals of this size fraction. As such, the % weight yields are not reflective of the overall % distribution of mineral size fractions from samples.

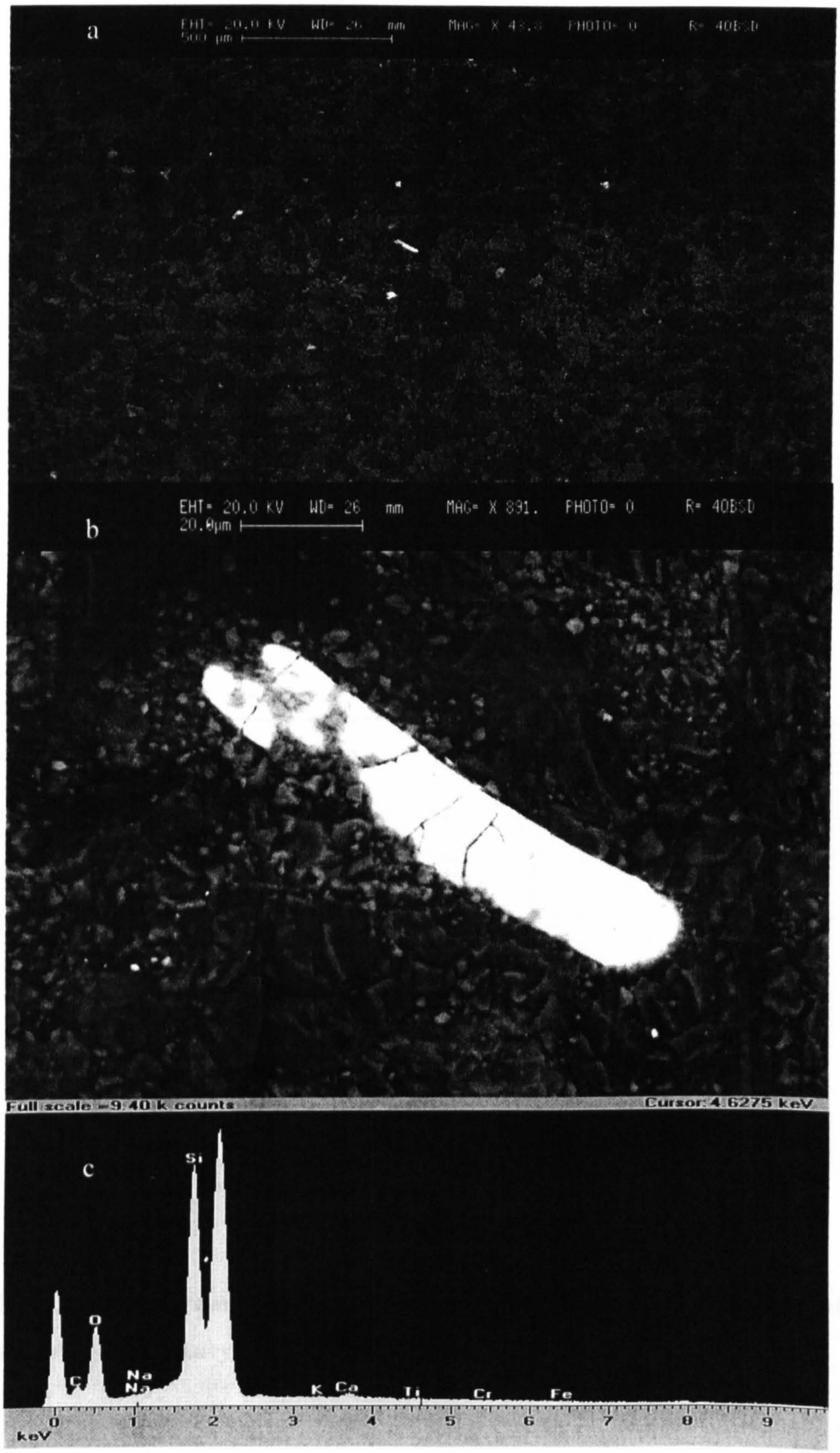

Fig 4.13 a. Backscattered SEM image of thick section SUTL 794. b. Close up of Zircon grain. c. Spectrum confirming presence of zircon (centred on b)

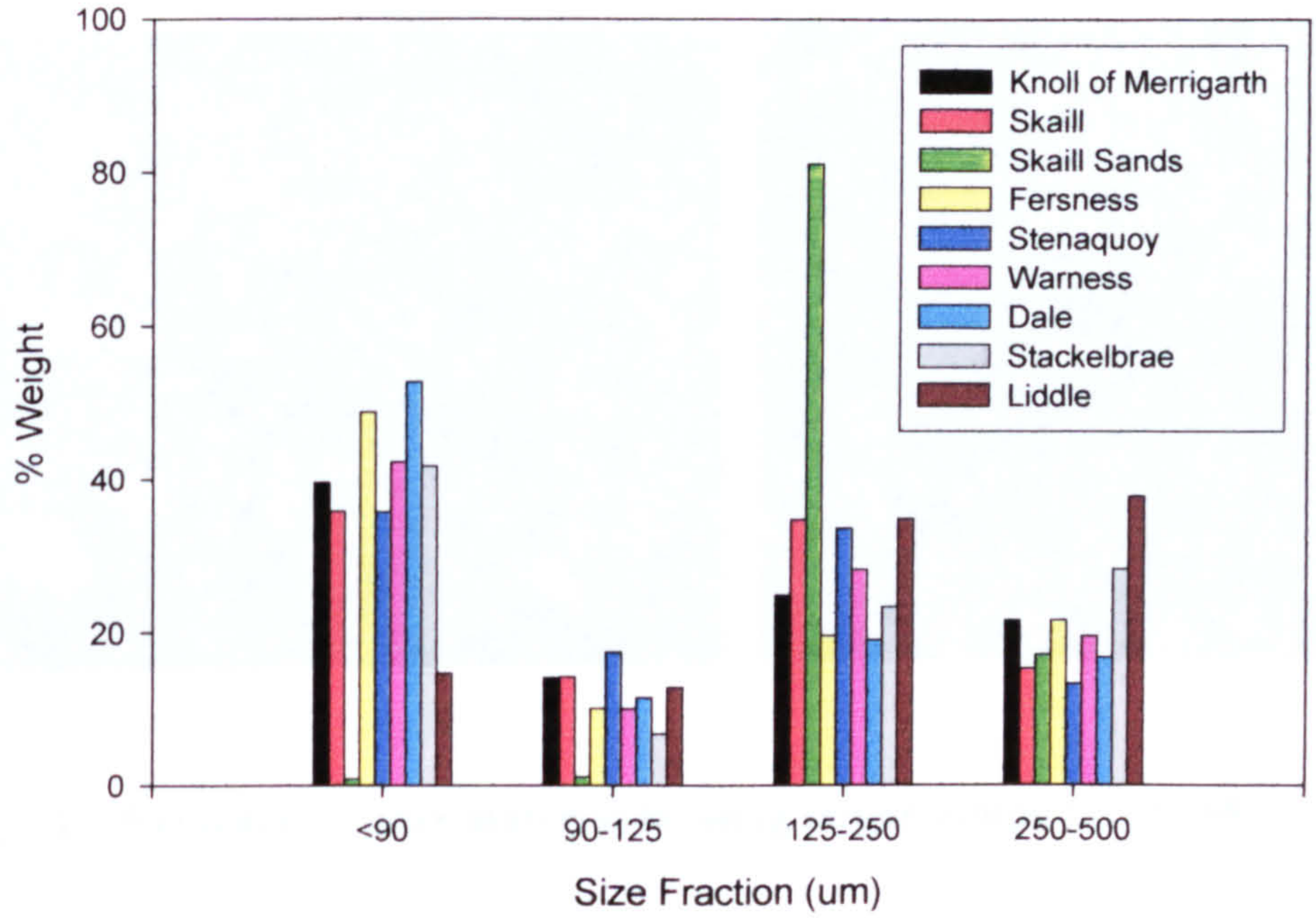

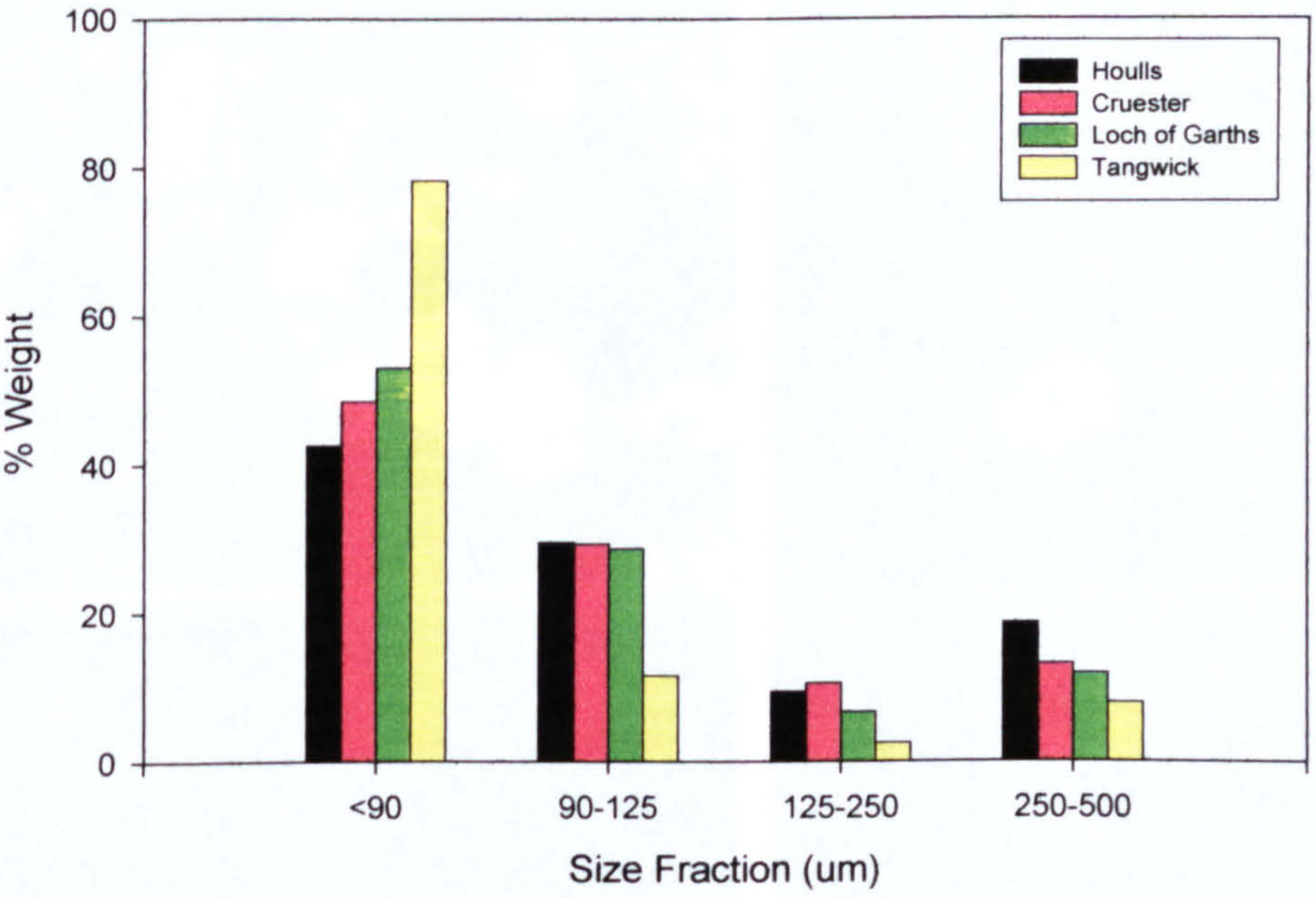

Fig 4.14 Histogram of average %weight values for each sieved size fraction for each site from (a) Orkney and (b) Shetland

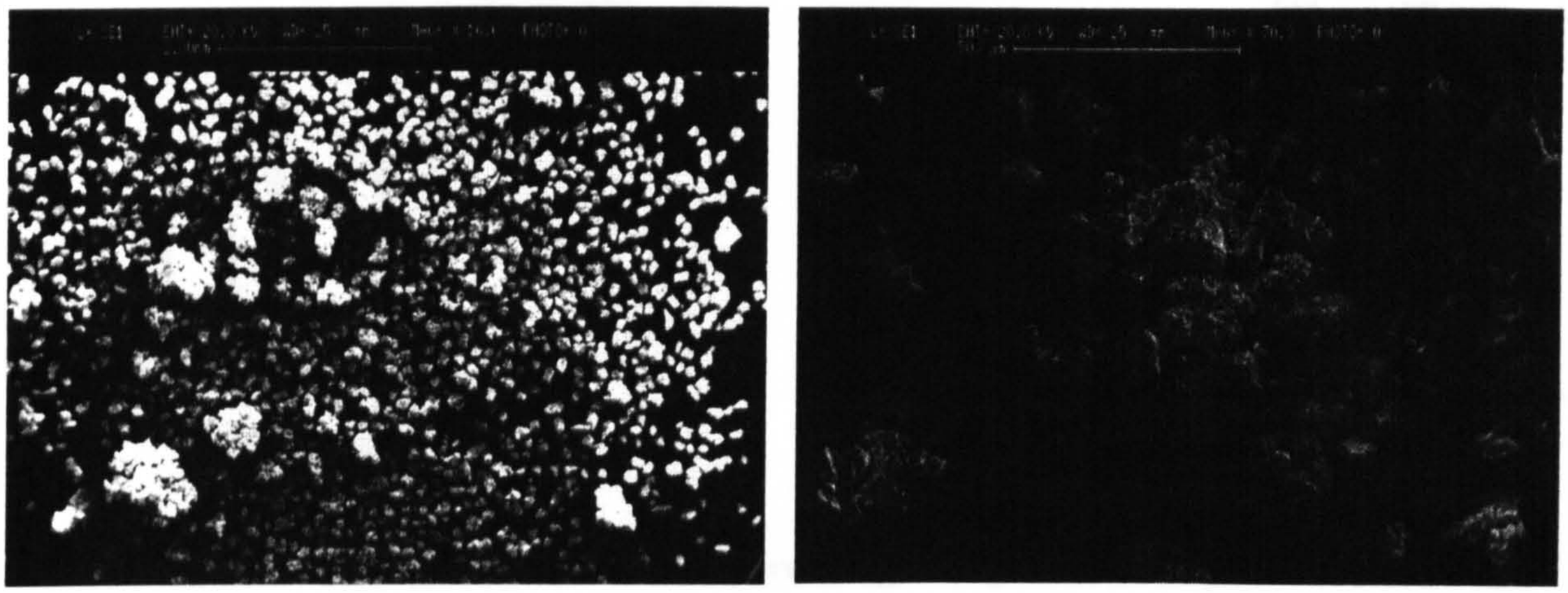

Fig 4.15 Evidence of finer material forming larger lumps SUTL768

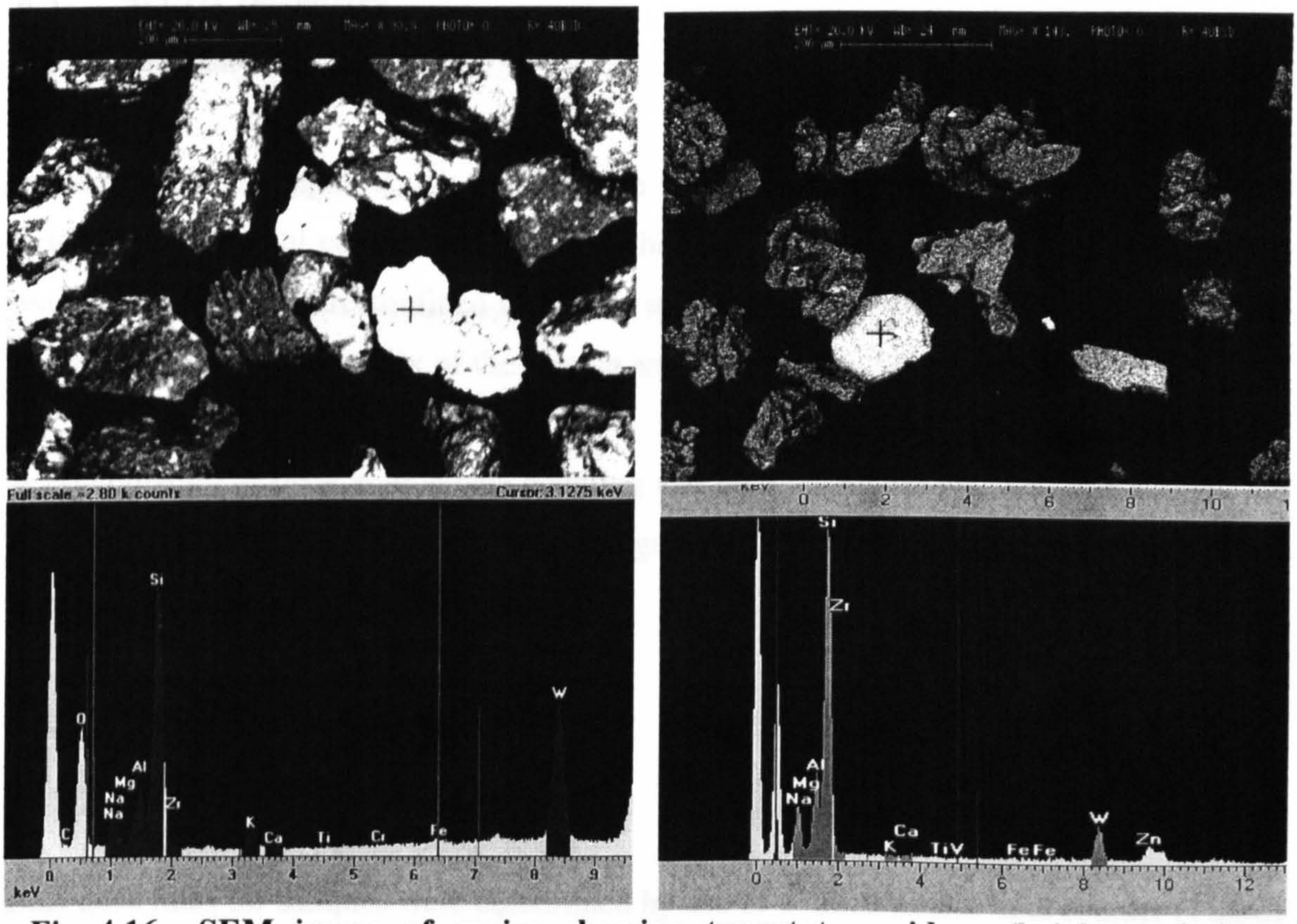

Fig 4.16 SEM image of grains showing tungstate residues (bright grains) and spectrum centred on cross hairs confirming presence of tungstate (w) (a) SUTL969 (b) SUTL 824

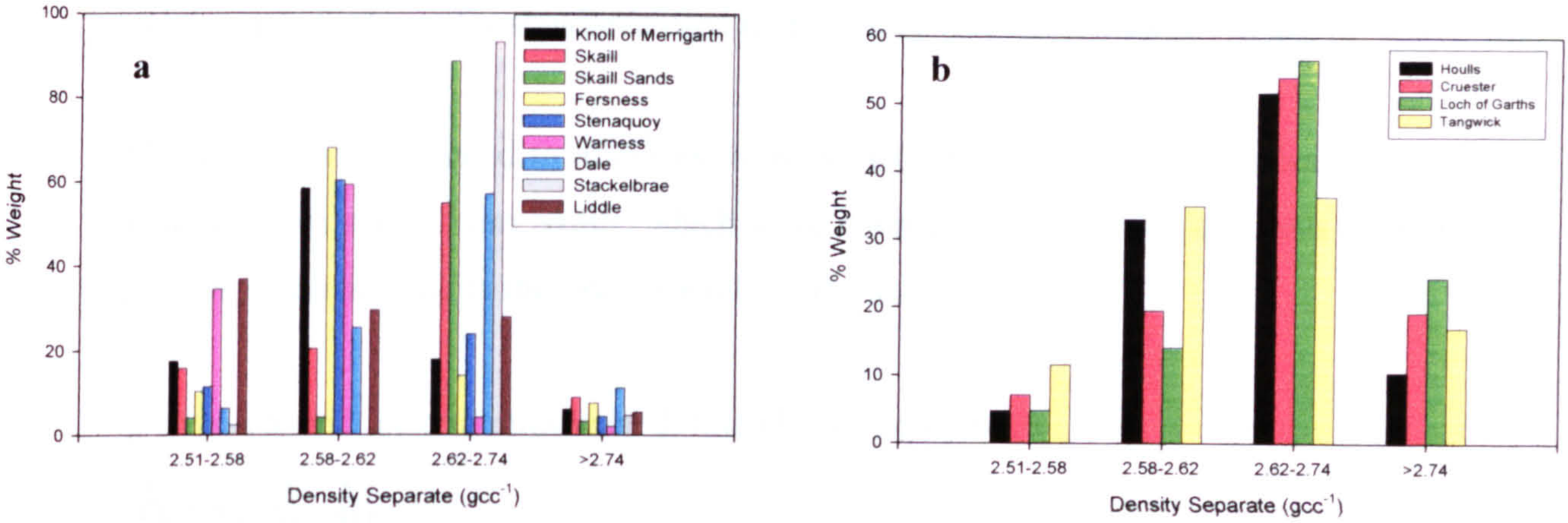

Fig 4.17 Histogram showing average percentage weight mineral yields for each site on (a) Orkney and (b) Shetland.

4.5 Matrix Dosimetry

4.5.1 Introduction

As discussed in chapter 2, the annual dose that a sample receives is combined of both external and internal components. Due to the removal of the outer 3mm of each sample, external components are confined to gamma and cosmic ray. Internal components include contributions from the matrix of the sample and internally within each mineral type.

A combination of thick source beta counting and high resolution gamma spectrometry has been utilized to assess the matrix beta and gamma dose rate. Results are detailed below together with water content measurements.

4.5.2 Thick Source Beta Counting

4.5.2.1 Methodology

Beta dose rates for samples were determined by use of a thick source beta counter (TSBC) (Sanderson, 1988b). The counter uses layers of NE102A plastic scintillator to detect β particles, using acetate film to screen out α particles.

20g crushed and dried samples were counted using standard procedures:

The background was measured in response to international dose rate standard minerals, and the net count rate for standards used to determine conversion values in $mGya^{-1}cps^{-1}$.

All samples were counted for 6 cycles of 300s, with the exception of samples SUTL1361-4, windblown sands from Skaill, which were counted for 10 cycles of 1000s to improve counting statistics due to the low dose rate of the samples.

β dose rate and uncertainties were defined by the equation:

$$\dot{D}_s = \psi\,(\dot{C}_s - \dot{B})$$

$$\text{where}\ \psi = \frac{D_{std}}{C_{std} - \dot{B}}$$

$\dot{B}$ = Background
D_{std} = Dose rate of Standard
C_{std} = Count rate of Standard
ψ = Mean sensitivity
C_s = Count rate of Sample

Uncertainties were calculated by propagation of errors, taking into account the counting state of the measurement and background samples.

4.5.2.2 Results

Samples from Orkney show little variation in the measured beta dose rate. The vast majority of samples have TSBC dose rates in the region of 1.5-3$mGya^{-1}$, with only the windblown sand samples from Skaill giving values below this average.

A different picture is seen in the Shetland samples. Stones from Cruester show a similar TSBC distribution to those in Orkney, reflecting their similar geology. Samples from both Houlls and the Loch of Garths show a wider range of TSBC results, both higher and lower, ranging from 1-4$mGya^{-1}$. Tangwick likewise shows no clear distributional patterns, with samples ranging in value from 3$mGya^{-1}$ to > 8. The higher dose rates in this case are most probably attributed to the high feldspar content of the Tangwick samples and can also be seen reflected in the on site gamma dosimetry values.

Table 4.28 TSBC Results, Orkney Dataset

Site	Pos	SUTL No.	Run No.	TSBC ($mGya^{-1}$)
Liddle	1	1379	626	2.95±0.04
		1381	643	2.14±0.01
	2	1386		2.10±0.11
Dale	12	748	527	2.14±0.12
		749	526	1.98±0.12
		750	520	1.98±0.07
		751	521	1.84±0.08
		753		2.15±0.10
		754	530	2.17±0.08
		755	529	1.81±0.08
	13	760	522	2.55±0.10
		764	523	2.07±0.05
		765	525	2.51±0.14
		767	538	1.72±0.10
	14	768	524	2.50±0.13
		769	532	2.28±0.12
		774	534	2.23±0.10
		775	535	2.13±0.07
		777	536	1.62±0.08
		779		2.01±0.13
	15	782		2.22±0.08
		783		1.87±0.12
		784		1.84±0.08
		785		2.17±0.10
Skaill	1	1343	648	2.28±0.09
	2	1354	640	2.27±0.10
	3	1358	646	2.47±0.12
		1360	639	3.23±0.10
	5	815	499	2.14±0.14
	6	817	500	2.15±0.08
	O-1	1361	605	1.08±0.07
	O-2	1362	604	1.16±0.07
	O-3	1363	606	1.06±0.09
	O-4	1364	603	0.91±0.05
Knoll of Merrigarth	8	794	508	1.48±0.08
		795	495	2.29±0.07
	7	802	497	2.89±0.10
		803	498	2.94±0.09
Warness	9	842		2.41±0.09
	10	853		2.21±0.10
		857	503	2.08±0.07
	11	849	506	1.65±0.08
Stackelbrae	2	1374	642	1.63±0.12
Fersness	3	823	505	1.86±0.08
		824	504	1.96±0.08
	4	831	514	1.65±0.08
		833	515	2.37±0.09
Stenaquoy	1	836	501	2.13±0.08
	2	838	502	2.08±0.10
		839		1.74±0.06

Table 4.29 TSBC Results, Shetland Dataset

Site	Pos	SUTL No.	Run No.	TSBC ($mGya^{-1}$)
Cruester	1	949	598	2.17±0.08
		951	557	2.27±0.09
		953	558	2.17±0.09
	2	958	609	1.53±0.06
	4	968	551	2.22±0.11
		969	550	2.07±0.07
	5	1051	549	2.38±0.12
		1053	608	2.15±0.11
	6	1054	555	2.11±0.07
		1055	553	2.20±0.10
	7	1059		2.06±0.11
	8	1062	600	1.86±0.14
		1063	60	2.07±0.08
		1064	554	2.35±0.12
	9	1068	596	2.05±0.09
	11	1075	--	1.97±0.12
		1076	610	2.01±0.08
		1077	--	2.11±0.14
	13	1081	556	2.45±0.09
	15	1086	611	2.85±0.11
		1087	616	2.78±0.09
		1088	617	2.79±0.11
	17	1094	614	2.27±0.11
		1095	615	2.53±0.11
		1096	618	2.61±0.14
		1097	613	2.27±0.06
	19	1100	607	2.86±0.09
Tangwick	1	1033	595	8.27±0.19
		1034	592	5.31±0.14
	2	1040	594	3.31±0.10
		1041	593	2.98±0.11
		1043	637	6.90±0.15
Houlls	1	970	585	3.16±0.07
		971	584	2.33±0.06
		976	589	1.61±0.07
		978	590	2.73±0.10
	2	983	586	3.86±0.11
	3	991	587	3.86±0.11
		993	582	4.10±0.10
	4	1003		3.56±0.17
		1004	516	3.04±0.14
Loch of Garths	1	1006	560	1.11±0.08
		1007	580	2.69±0.06
		1008	561	2.55±0.09
	2	1017	559	3.20±0.14
		1018	581	3.81±0.12
		1020	597	2.97±0.10

Fig 4.18 TSBC Dose Rates for samples from (A) Orkney and (B) Shetland

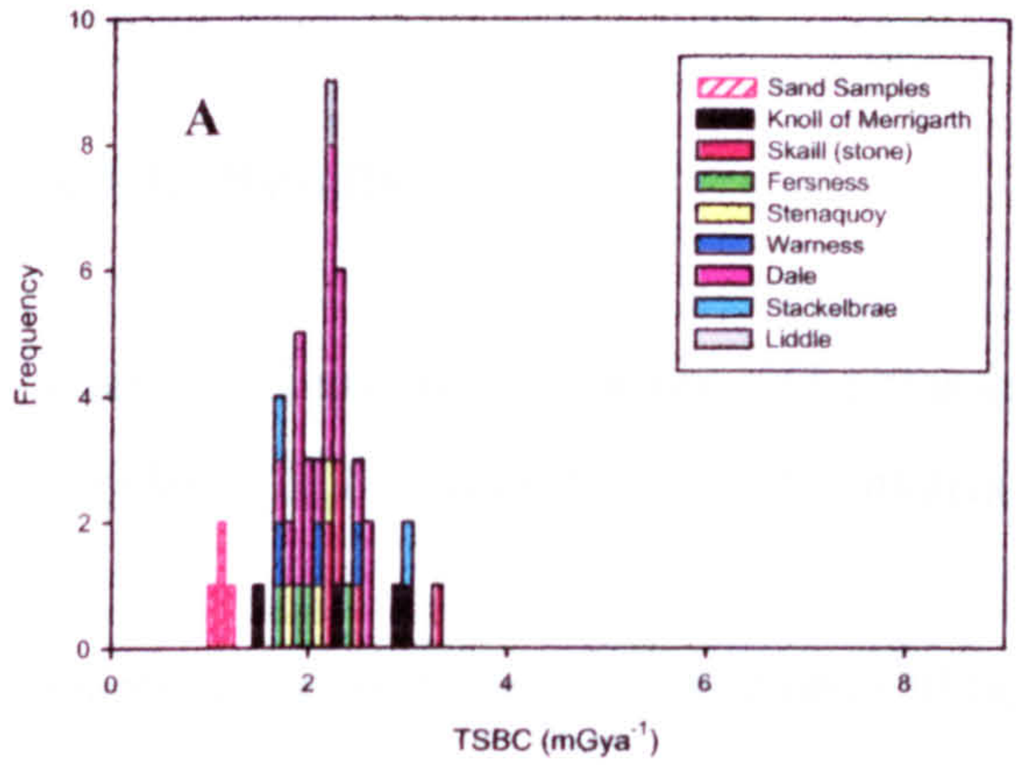

4.5.3 High Resolution Gamma Spectrometry

4.5.3.1 Methodology

High resolution gamma spectrometry was performed using two liquid nitrogen cooled HPGe detectors, linked to a multi-channel analyzer. As outlined in chapter 2, the decay of K, U, Th and their daughter products produces gamma rays of discrete energy bands which can be identified within each spectrum.

Spectrum peaks were integrated and converted to and K, U and Th content estimates with reference to a Shap granite standard. 20g geometries were used throughout for both sample and standard. Samples were crushed and sealed in their counting pots using epoxy resin and stored for a period of not less than 4 weeks to minimize the effect of radon loss. Counting times of 85,000 and 150,000s were needed due to the small geometry of the samples (20g).

The ^{40}K peak at 1460keV was used to estimate K activity ($Bqkg^{-1}$). A combination of ^{234}Th, ^{226}Ra, ^{214}Pb, ^{210}Pb and ^{214}Bi peaks resulting from the decay of ^{235}U and ^{238}U were used to estimate U activity. Th activity was assessed in a similar manner with reference to ^{228}Ac, ^{224}Ra, ^{212}Pb and ^{208}Tl peaks.

K, U and Th activity was converted to % content, or ppm in the case of U and Th, contents were converted to β and γ dose rates using the conversion factors outlined in chapter 2.

Due to a lack of material, it was not possible to obtain γ spectrometry measurements for every sample.

4.5.3.2 Results

Calculated uranium, thorium and potassium contents for each of the samples measured are tabulated below, together with dry matrix beta and gamma dose rates.

Gamma spectrometry results from Orkney and Shetland samples show large variations in the calculated K, U and Th content. The potassium content for all Orkney samples is between 1 –3%, however a much greater range is seen in samples from Shetland, up to a maximum value of 10%, with the two outlying values belonging to samples from Tangwick (table 4.30). Uranium values are similar in both Orkney and Shetland samples, ranging from 0.5-4.5ppm, however thorium values show much greater variation. Whilst all Orkney samples show values lower than 6ppm, samples from Shetland average around 10ppm, with a maximum value of 23ppm in the case of one sample from the Loch of Garths.

The calculated dose rates for a dry matrix show on average a gamma to beta ratio of 0.47±0.02 (fig 4.19). This ratio is slightly lower than the ratio expected for a typical matrix of 2% K, 3ppm U, and 10ppm Th and is a reflection of the lower thorium content of the samples.

Table 4.30 Summary of Gamma Spectrometry Results

Site	Posn	SUTL No	K (%)	U (ppm)	Th (ppm)	β dose rate ($mGya^{-1}$)	γ dose rate ($mGya^{-1}$)
Skaill	5	815	2.82±0.28	0.63±0.78	1.19±0.80	2.47±0.26	0.81±0.11
	6	817	1.95±0.24	1.06±1.08	0.74±0.74	1.80±0.25	0.63±0.14
Knoll of Merrigarth	8	794	1.29±0.20	1.78±0.86	5.43±1.98	1.49±0.22	0.80±0.15
		795	1.73±0.10	1.09±0.26	5.13±1.20	1.74±0.10	0.81±0.07
	7	802	2.32±0.25	4.59±1.65	5.17±1.11	2.74±0.32	1.35±0.21
		803	2.89±0.31	3.73±1.44	2.66±5.51	3.02±0.37	1.26±0.34
Warness	11	849	1.63±0.21	2.26±1.18	3.04±3.32	1.77±0.27	0.81±0.22
	10	857	2.32±0.25	2.46±0.78	3.22±1.70	2.37±0.24	1.01±0.14
Stenaquoy	2	838	2.00±0.23	1.54±1.15	1.79±0.85	1.93±0.26	0.75±0.15
Cruester	1	949	2.03±0.10	0.85±0.34	3.27±0.92	1.90±0.10	0.75±0.06
		951	1.87±0.09	1.36±0.29	4.55±0.93	1.88±0.09	0.84±0.06
	4	968	2.11±0.09	0.95±0.29	3.51±0.93	1.99±0.09	0.80±0.06
		969	1.67±0.24	1.23±0.72	10.41±3.32	1.87±0.23	1.08±0.20
	6	1055	2.21±0.11	0.94±0.21	4.46±0.98	2.10±0.10	0.87±0.06
	8	1062	1.73±0.10	0.59±0.20	4.48±0.94	1.65±0.09	0.71±0.06
		1063	2.58±0.29	1.22±0.90	2.87±1.82	2.40±0.28	0.91±0.16
	9	1068	1.80±0.23	1.25±0.86	10.04±2.51	1.97±0.24	1.09±0.17
Tangwick	1	1033	9.68±0.73	3.57±1.09	12.31±3.90	8.91±0.64	3.38±0.30
		1034	5.31±0.44	3.16±1.13	8.71±1.71	5.11±0.41	2.09±0.19
	2	1041	2.21±0.25	2.30±1.00	10.93±3.38	2.48±0.27	1.36±0.22
Houlls	1	970	2.70±0.10	2.68±0.36	10.03±0.98	2.92±0.10	1.47±0.07
		971	2.56±0.27	2.80±0.80	7.60±3.14	2.75±0.27	1.33±0.20
		976	1.20±0.08	3.30±0.39	9.99±1.04	1.77±0.09	1.18±0.07
		978	2.17±0.09	3.01±0.37	11.93±1.02	2.58±0.09	1.48±0.07
	3	991	3.13±0.36	5.09±2.08	4.93±5.14	3.48±0.45	1.59±0.37
Loch of Garths	1	1007	3.06±0.12	0.62±0.20	9.67±1.06	2.90±0.11	1.31±0.07
		1008	2.60±0.11	1.19±0.22	9.88±1.06	2.62±0.10	1.27±0.07
	2	1020	2.26±0.11	3.93±0.40	22.58±0.91	3.34±0.11	2.23±0.07

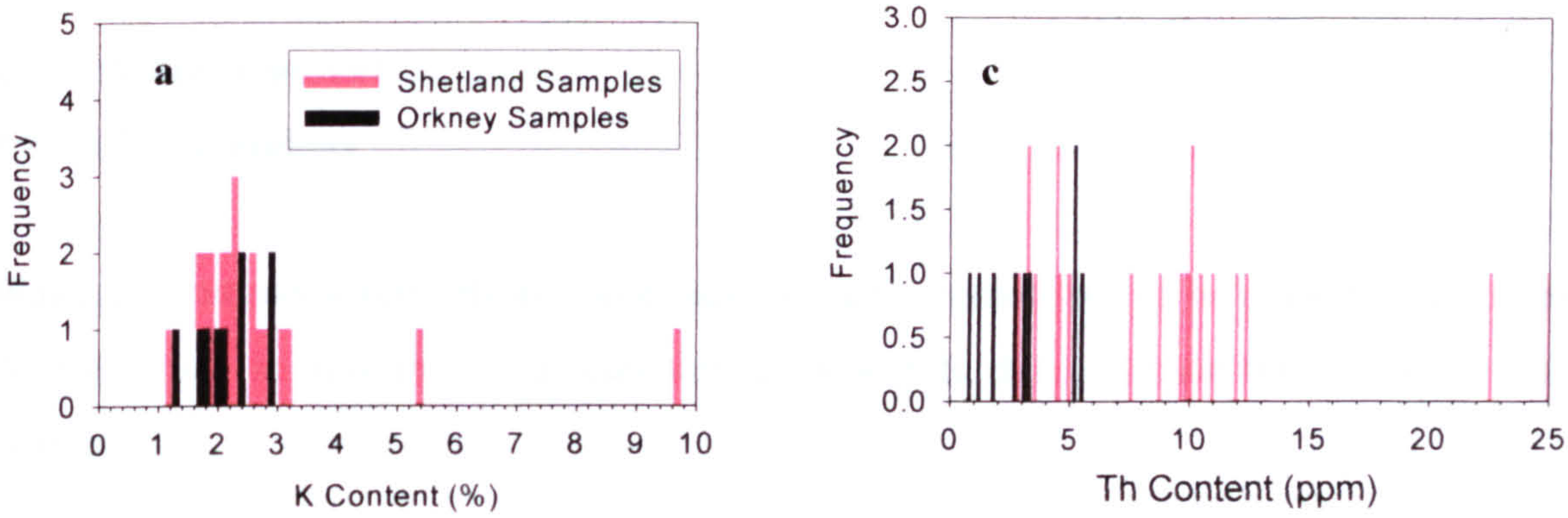

Fig 4.19 Histogram of (a) Potassium Content (b) Uranium Content and (c) Thorium Content for samples from Orkney and Shetland as determined by High Resolution Gamma Spectrometry

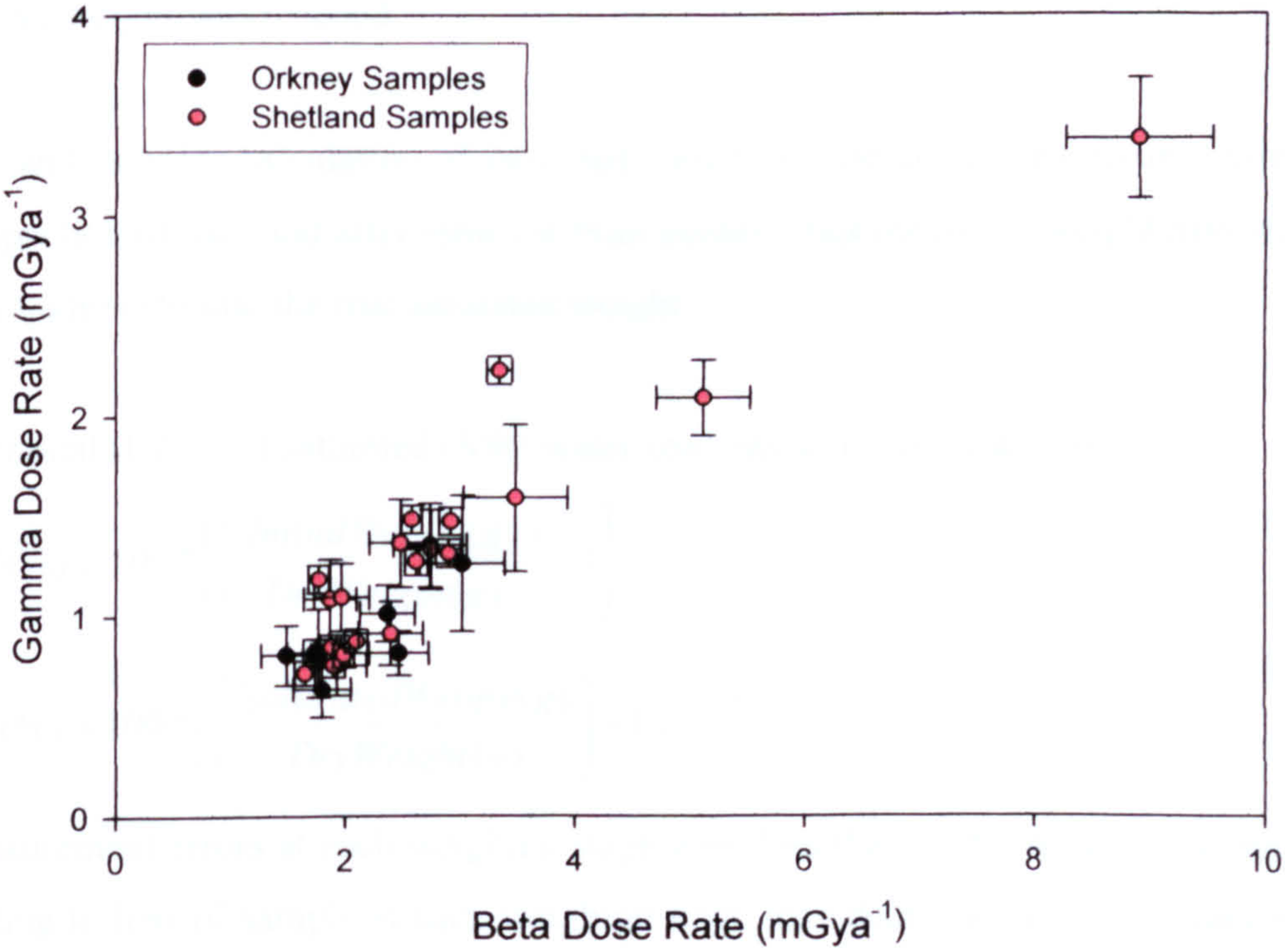

Fig 4.20 Comparison of calculated beta and gamma dose rates from Orkney and Shetland Samples.

content is therefore important as it sets an upper limit on the water content of the sample. A lower limit cannot accurately be defined, but in the majority of cases, the saturated water content of stones is small enough that a midpoint between zero content and saturated may be taken, with errors to reflect the possible range without adversely affecting the precision of the annual dose estimate. As discussed above, water content calculations for sand and sediment samples is far harder to model.

4.5.4.2 Results

Water content measurements for each sample are tabulated in Appendix D. Considerable variation was seen in the fractional and saturated water content of samples both within individual sites, and from site to site.

At Liddle, saturated water contents ranged from 6-17% with all samples within 95-100% of their saturated value. These measurements are in good agreement with observed water content measurements reported from Liddle by Huxtable et al (1976).

At Dale a similar range of saturated water contents was noted, from 5-18%. The majority of samples were at, or near, saturation at time of sampling, ranging from 70-100% of their saturated water content. No obvious differences were seen within the contexts sampled.

Skaill showed much lower saturated water contents in the region of 5-7%, with fractional water content 10-40% of their saturated values. At the Knoll of Merrigarth, measured saturated water contents ranged from 2-10%, with samples 50-70% saturated at the time of sampling. Fersness showed a similar picture to Skaill, with all saturated water content measurements falling between 6 and 9%, though more variation was seen in the water content measurements at the time of sampling – ranging from 20-80% of the saturated value. Stenaquoy, Stackelbrae and Warness likewise showed variation from less than 10% of the saturated value, to 100% in some cases. Saturated water content values from the three sites ranged from 7-12% .

For three of the four Shetland sites (Houlls, Loch of Garths and Tangwick), saturated water content is within 2-5%, with actual water contents ranging from 50-100% of this value. These lowered values are a reflection of the geology of the samples.

At Cruester, a similar picture as that seen in Orkney emerges, with saturated water contents ranging from 2-12%, and fractional water content measurement also showing a wide range of values, from 2-100% of their saturated values. Given the coarser grained nature of these sandstones, the variation seen is to be expected. It is also notable that the hearthstone samples show a more restricted range of saturated water contents ranging from 2-4%. All are at or near saturation. Again this is a reflection of the finer, more compact nature of the stone.

4.5.5 Summary

Matrix beta dose rates have been calculated for samples by two independent means for approximately 30% of samples. Comparison of TSBC and gamma spectrometry results give informative data about the possible effects of radon loss. As TSBC samples were measured immediately after crushing, the effect of any radon loss should be more pronounced within these measurements. However, the effect of any loss is likely to be minimal due to the low percentage contribution of the U series to the beta dose rate.

Figure 4.21 shows there to be good agreement between both methods, suggesting radon loss to be a minor effect if any. The agreement between methods also gives confidence to the measurement of β dose rate in samples for which there was insufficient material to perform both analyses.

γ dose rates determined by laboratory γ spectrometry can likewise be compared to the corresponding in-situ field measurements for the sample concerned. However, before comparison takes place it is first necessary to correct laboratory γ spectrometry results for the effect of water content to enable valid wet-to-wet comparisons to be made.

It is clear from fig 4.22 that there is considerable scatter about the 1:1 line when the results are compared. Whilst it is possible that the discontinuity in results reflect differing sources

of gamma ray contribution, there are a number of other possible explanations which should be investigated further. It is possible that either reading may be in error. In-situ field gamma spectrometry measurements may be inaccurate due to poor calibration of the measurement instrument, and/or inaccurate assessment of the geometry of the sampling position.

The gamma spectrometer used during fieldwork was calibrated before and after each fieldtrip using doped concrete blocks of known activity. No difference was noted in the efficiency of the detector over the fieldwork period. Individual measurements may however be influenced by detector drift caused by variation in temperature and high voltage (HV). Prior to each measurement the ^{40}K peak was centered on a set channel to compensate for such drift. As such, gamma spectrometer calibration was not thought to be a major component in the observed differences between the two methods.

A more likely cause of error within the in-situ measurements is in the need to accurately assess the geometry of the measurement position. Ideally such assessment should not be required as positions greatly differing from 4Π should be avoided. However it was not always possible to collect samples from such areas. Where samples were collected from geometries less than 4Π, geometries were estimated and dose rates corrected accordingly. Fig 4.23 shows some indication of an over-correction in the case of these samples, however evidence from 4Π measurements suggests that additional sources of variation also exist.

Incorrect identification of peaks within the gamma spectra of samples, background and standards may cause errors in the dose rate calculations of the laboratory gamma spectrometry. Uranium and Thorium play a larger role in the overall gamma dose rate compared to beta, however a check for consistency in the calibrated U and Th content for each identified peak with other peaks in the decay chain highlighted any discrepancies.

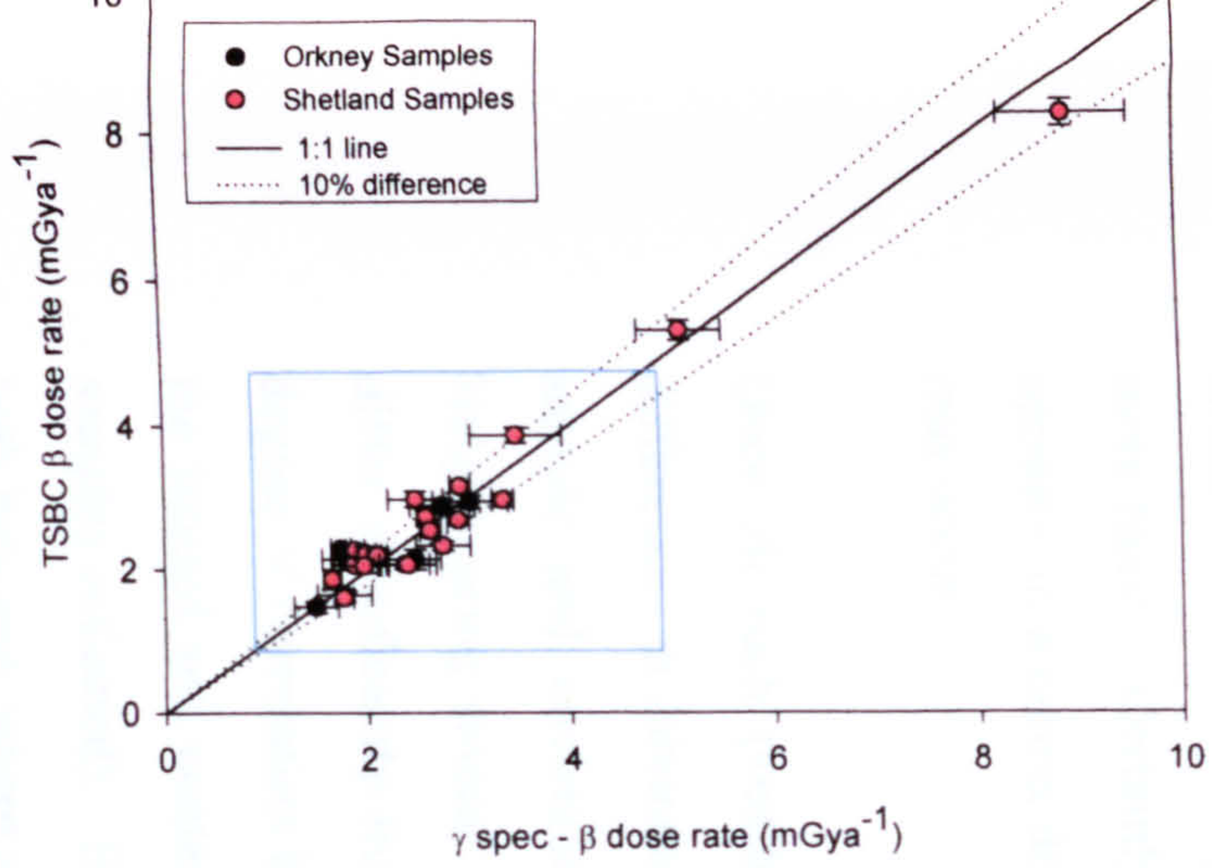

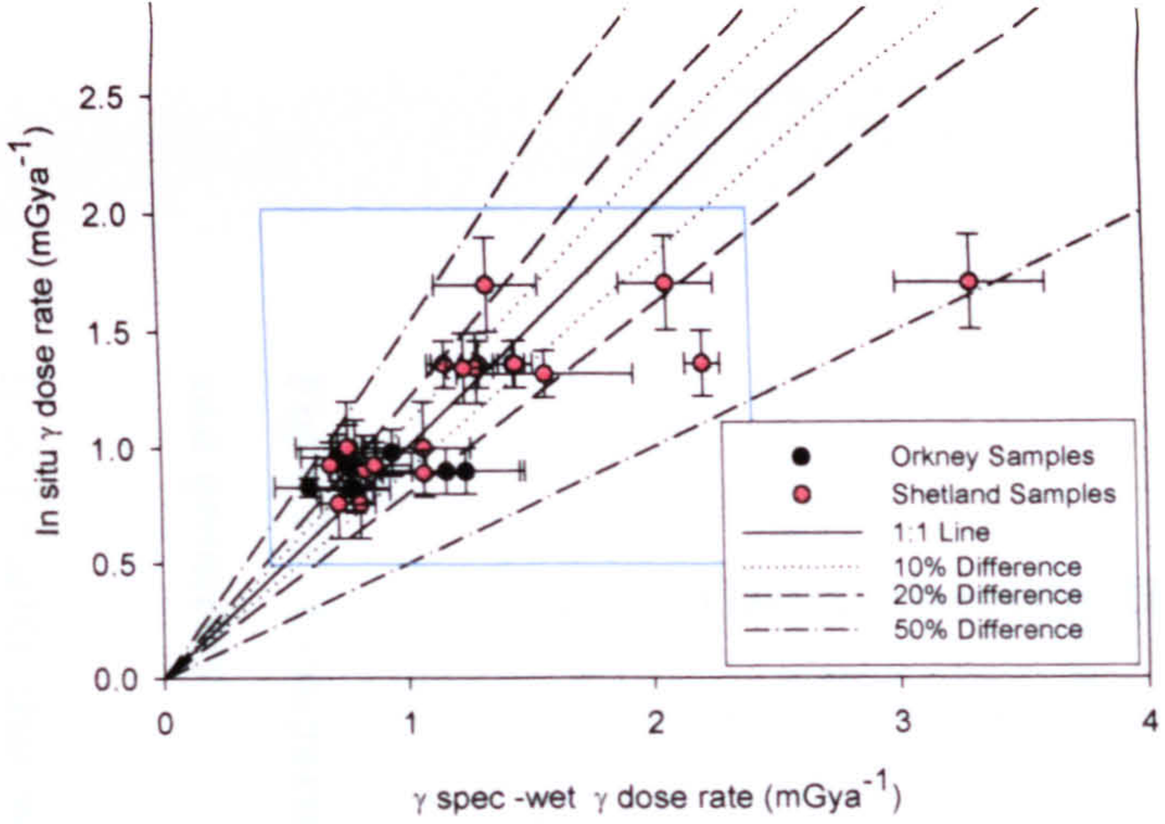

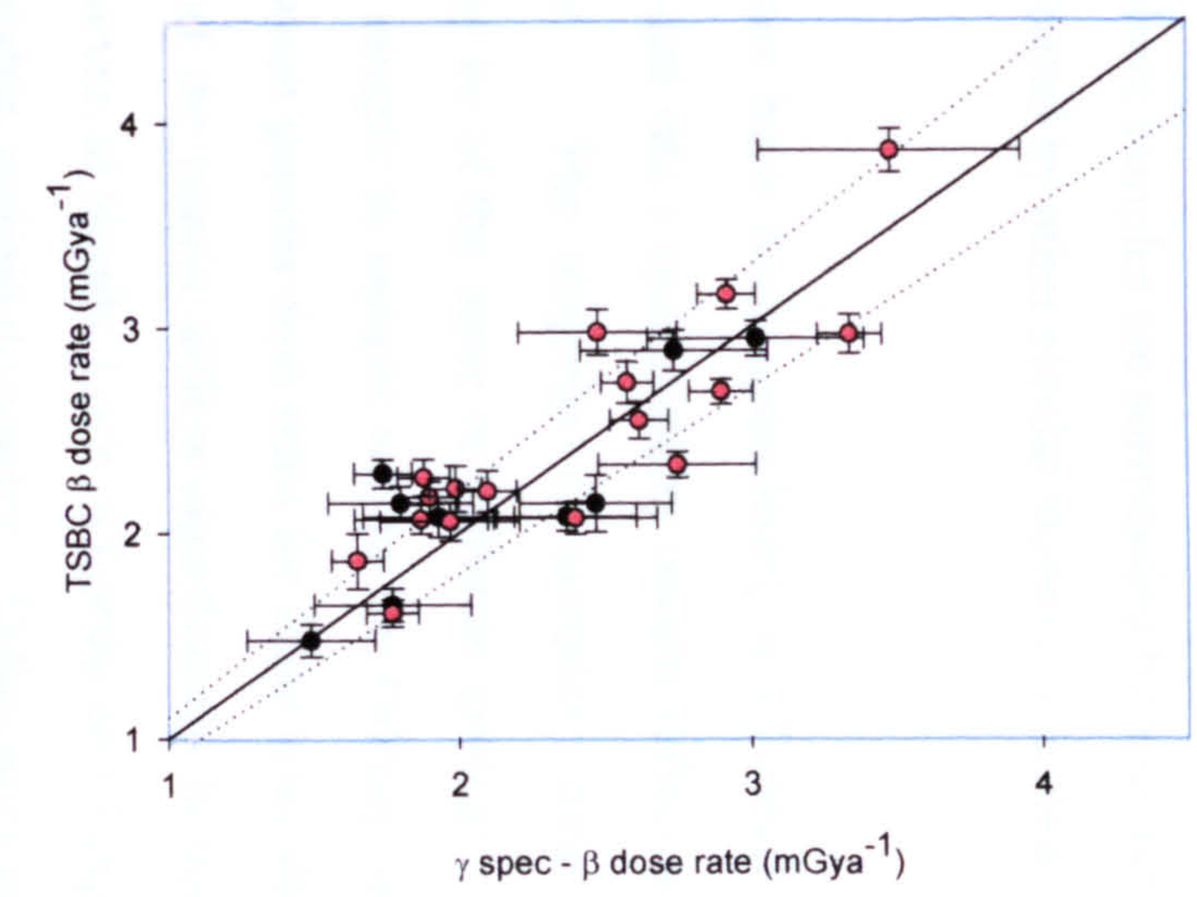

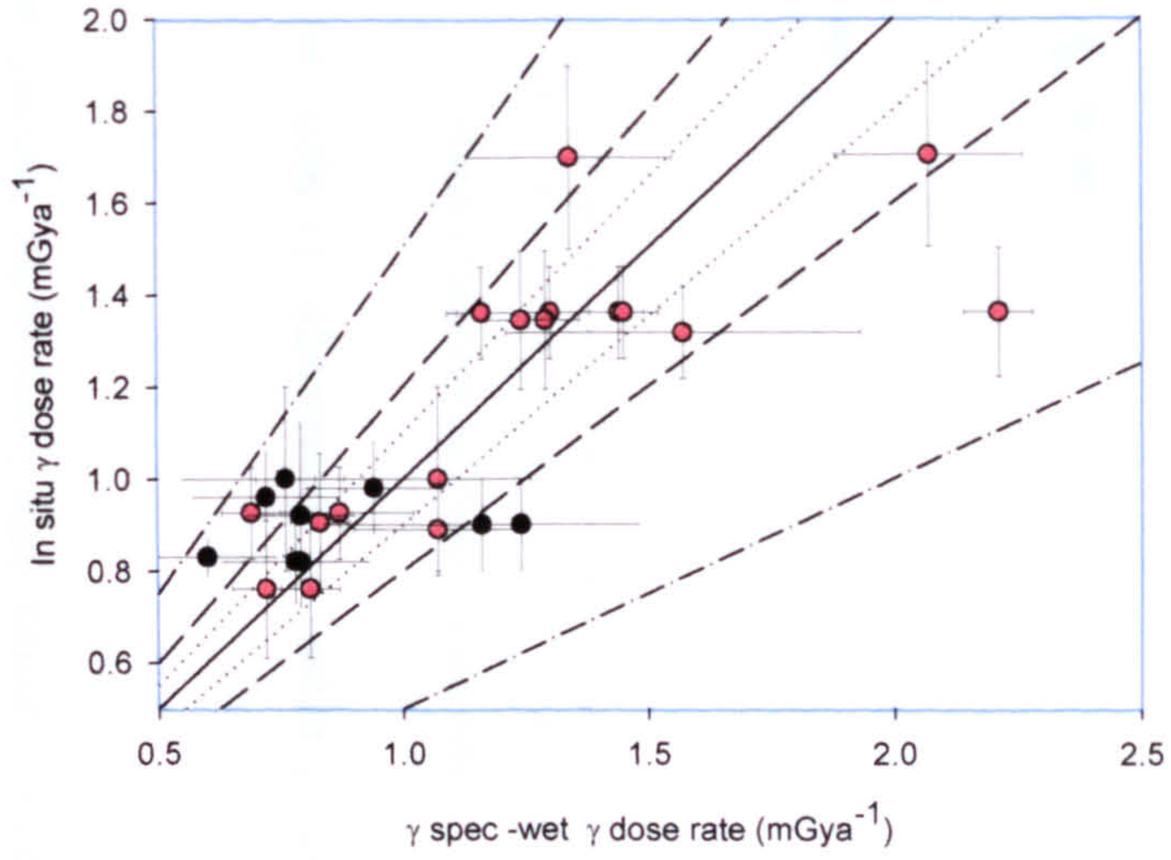

Fig 4.21 Comparison of β dose rates determined by TSBC and γ spectrometry for samples from Orkney and Shetland

Fig 4.22 Comparison of in situ and matrix γ dose rates for samples from Orkney and Shetland

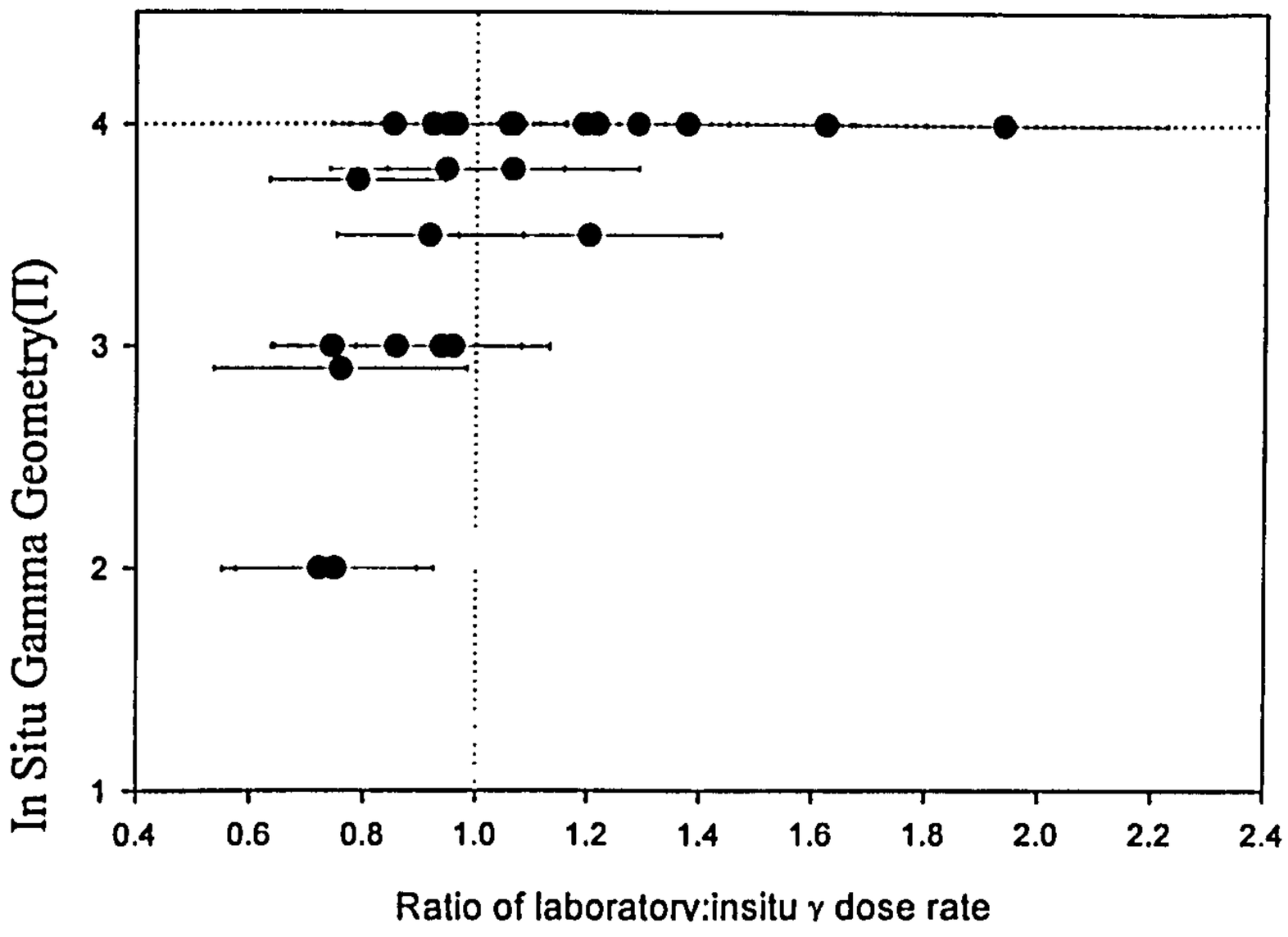

Fig 4.23 Comparison of ratio of laboratory to insitu γ dose rates with estimated in situ geometry.

It is possible that water content corrections may cause discrepancies, either because the measured water content and correction value is in error, or a difference exists between the water content of the sample and field conditions. Given that the majority of samples studied show relatively small fractional and saturated water contents, the latter is perhaps more likely. Certainly where samples are surrounded by a sediment dominated matrix (as opposed to a matrix dominated by other similar stones), it is clear that potential differences may occur.

Once all such possibilities have been considered, it is clearly also possible that the differences in laboratory and site γ spectrometry results reflect a true difference between sample and environment. The majority of samples come from a stoney matrix. Neighbouring stones may be of the same or different geology. Beta dose rates do not differ significantly from sample to sample within the Orkney sites and Cruester, thus a degree of correlation between gamma dose rates for these sites should be expected (unless the limited soil content of the matrix differs significantly in dosimetry from the stone samples collected). However, at Houlls, Loch of Garths and Tangwick variation is seen in both beta and, where available, gamma dosimetry. Differences are generally in the region of a factor of 2 difference between highest and lowest samples, however this variation is enough to cause significant localized variations in the dose rate measured on site, as noted

at Tangwick. Where such differences occur, it would seem appropriate to take in situ gamma dose rate measurements alone as a reflection of the external gamma dose rate field.

4.6 Annual Dose Rate Calculations

Given both matrix and external dose rate information detailed above, it is possible to calculate the annual dose rate for the different mineral fractions and sizes prepared for each sample.

In the case of quartz grains, it is assumed that the internal dose rate within the mineral is of negligible value, thus no further information is required in the calculation of annual dose rates. However, the contribution from internal mineral activity in feldspars is not negligible (as discussed in chapter 2) and requires further clarification prior to dose rate calculations.

For both potassium and sodium feldspars, internal dose rate contributions will depend on the K, U and Th content of the mineral. As discussed in chapter 2, K content in K-Feldspars is generally in the region of 12±3%, while it is typically 5±3% for Na feldspar. The majority of the internal dose can therefore be attributed to β radiation resulting from decay of ^{40}K. However where external gamma dose rate and matrix dose rates are low, the internal α and β dose component from U and Th decay may also be of significance.

ICP-MS studies at SURRC of U and Th content from minerals extracted from a variety of burnt mound samples in the past have shown U and Th content in the region of 0-0.4ppm and 0-1ppm respectively (Spencer, 1996, Anthony et al, 2001). In the majority of samples examined in this study, both β and γ dose rates are such that even when lower and upper limits of these ranges are converted to dose rates, the contribution made to the annual dose is minimal. Assumed values were therefore used in the annual dose calculations which reflected the range of concentrations seen in past studies (0.2±0.2ppm U, 0.5±0.5ppm Th).

Annual dose rates have been calculated for K and Na feldspars, and for quartz at the appropriate size fraction for each sample, and are presented in tables 4.31 and 4.32 below.

Table 4.31 Annual Dose Rate Summary and Calculations, Orkney Samples

Site	Pos	SUTL No.	Size Frac (μm)	Water Content (%)	TSBC ($mGya^{-1}$)	γ spec β dose rate ($mGya^{-1}$)	Effective β dose rate ($mGya^{-1}$)	In Situ γ dose rate ($mGya^{-1}$)	γ spec γ dose rate ($mGya^{-1}$)	γ and cosmic ray dose ($mGya^{-2}$)	K Annual Dose Rate ($mGya^{-1}$)	Na Annual Dose Rate ($mGya^{-1}$)	Quartz Annual Dose Rate ($mGya^{-1}$)
Liddle	1	1379	90-125	4±3	2.95±0.04		2.64±0.10	0.98±0.08		1.165±0.08	4.31±0.21	3.99±0.21	3.62±0.13
		1381	125-250	9±8	2.14±0.10		1.75±0.18	0.98±0.08		1.165±0.08	3.55±0.28	3.16±0.28	2.73±0.20
	2	1386	125-250	6±6	2.10±0.11		1.78±0.16	1.08±0.11		2.345±0.11	3.68±0.28	3.29±0.28	2.86±0.19
Dale	1	748	90-125	5±5	2.14±0.12		1.89±0.15	0.76±0.10		0.945±0.10	3.53±0.25	3.21±0.25	2.83±0.18
	2	749	90-125	7±7	1.98±0.12		1.71±0.17	0.76±0.10		0.945±0.10	3.35±0.26	3.03±0.26	2.65±0.20
		750	90-125	9±9	1.98±0.07		1.67±0.18	0.76±0.10		0.945±0.10	3.31±0.27	2.99±0.27	2.61±0.21
			125-250				1.62±0.17				3.39±0.28	3.00±0.28	2.56±0.20
		751	90-125	7±7	1.84±0.08		1.59±0.15	0.76±0.10		0.945±0.10	3.23±0.25	2.91±0.25	2.53±0.18
			125-250				1.54±0.14				3.31±0.26	2.92±0.26	2.48±0.17
		753	90-125	3±3	2.15±0.10		1.95±0.11	0.76±0.10		0.945±0.10	3.59±0.23	3.27±0.23	2.89±0.15
		754	125-250	5±4	2.17±0.08		1.86±0.11	0.76±0.10		0.945±0.10	3.63±0.25	3.24±0.25	2.80±0.15
		755	90-125	8±7	1.81±0.08		1.55±0.14	0.76±0.10		0.945±0.10	3.19±0.24	2.87±0.24	2.49±0.17
			125-250				1.50±0.14				3.27±0.26	2.88±0.26	2.44±0.17
	1	760	90-125	4±3	2.55±0.10		2.28±0.12	0.82±0.10		1.005±0.10	3.98±0.23	3.66±0.23	3.28±0.16
	3	764	90-125	3±2	2.07±0.05		1.88±0.06	0.82±0.10		1.005±0.10	3.58±0.21	3.26±0.21	2.88±0.12
			125-250				1.82±0.06				3.65±0.23	3.26±0.23	2.82±0.12
		765	90-125	4±3	2.51±0.14		2.25±0.15	0.82±0.10		1.005±0.10	3.95±0.25	3.63±0.25	3.25±0.18
			125-250				2.18±0.14				4.01±0.26	3.62±0.26	3.18±0.17
		767	90-125	5±4	1.72±0.10		1.52±0.11	0.82±0.10		1.005±0.10	3.22±0.23	2.90±0.23	2.52±0.15
	1	768	90-125	7±6	2.50±0.13		2.16±0.19	0.76±0.10		0.945±0.10	3.80±0.27	3.48±0.27	3.10±0.21
	4	769	90-125	5±4	2.28±0.12		2.02±0.14	0.76±0.10		0.945±0.10	3.66±0.24	3.34±0.24	2.96±0.17
			125-250				1.95±0.14				3.72±0.26	3.33±0.26	2.89±0.17
		774	90-125	4±4	2.23±0.10		2.00±0.13	0.76±0.10		0.945±0.10	3.64±0.24	3.32±0.24	2.94±0.16
		775	90-125	6±6	2.13±0.07		1.86±0.14	0.76±0.10		0.945±0.10	3.50±0.24	3.18±0.24	2.80±0.17
		777	90-125	4±3	1.62±0.08		1.45±0.09	0.76±0.10		0.945±0.10	3.09±0.22	2.77±0.22	2.39±0.13
		779	90-125	6±6	2.00±0.13		1.75±0.17	0.76±0.10		0.945±0.10	3.39±0.26	3.07±0.26	2.70±0.20
	1	782	90-125	6±5	2.22±0.08		1.94±0.13	1.00±0.10		1.185±0.10	3.82±0.24	3.50±0.24	3.12±0.16
	5	783	90-125	5±4	1.87±0.12		1.66±0.13	1.00±0.10		1.185±0.10	3.54±0.24	3.22±0.24	2.84±0.16
		784	90-125	7±7	1.84±0.08		1.59±0.15	1.00±0.10		1.185±0.10	3.47±0.25	3.15±0.25	2.77±0.18

Site	Pos	SUTL No.	Size Frac (μm)	Water Content (%)	TSBC ($mGya^{-1}$)	γ spec β dose rate ($mGya^{-1}$)	Effective β dose rate ($mGya^{-1}$)	In Situ γ dose rate ($mGya^{-1}$)	γ spec γ dose rate ($mGya^{-1}$)	γ and cosmic ray dose ($mGya^{-2}$)	K Annual Dose Rate ($mGya^{-1}$)	Na Annual Dose Rate ($mGya^{-1}$)	Quartz Annual Dose Rate ($mGya^{-1}$)
		785	90-125	9±9	2.17±0.10		1.83±0.20	1.00±0.10		1.185±0.10	3.71±0.28	3.39±0.28	3.01±0.22
Skaill	1	1343	90-125	3±2	2.28±0.09		2.07±0.10	0.54±0.06		0.725±0.06	3.49±0.21	3.17±0.21	2.79±0.12
	2	1354	90-125	3±3	2.27±0.10		2.06±0.12	0.54±0.06		0.725±0.06	3.48±0.22	3.16±0.22	2.78±0.13
	3	1358	90-125	3±2	2.47±0.12		2.24±0.12	0.54±0.06		0.725±0.06	3.66±0.22	3.34±0.22	2.96±0.13
		1360	90-125	3±3	3.23±0.10		2.93±0.14	0.54±0.06		0.725±0.06	4.35±0.23	4.03±0.23	3.65±0.15
	5	815	90-125	3±2	2.14±0.14	2.47±0.26	2.09±0.14	0.92±0.20	0.81±0.11	1.039±0.12	3.82±0.25	3.50±0.25	3.13±0.18
	6	817	90-125	4±3	2.15±0.08	1.80±0.25	1.77±0.14	0.83±0.04	0.63±0.14	0.902±0.07	3.36±0.23	3.04±0.23	2.67±0.16
		1361	125-250	20±5	1.08±0.07		0.79±0.06	0.46±0.05		0.645±0.05	2.26±0.21	1.87±0.21	1.43±0.08
		1362	125-250	20±5	1.16±0.07		0.84±0.07	0.39±0.04		0.575±0.04	2.24±0.22	1.85±0.22	1.41±0.08
		1363	125-250	20±5	1.06±0.09		0.77±0.08	0.34±0.04		0.525±0.04	2.12±0.22	1.73±0.22	1.29±0.09
		1364	125-250	20±5	0.91±0.05		0.66±0.05	0.26±0.03		0.445±0.03	1.93±0.21	1.54±0.21	1.10±0.06
Knoll of Merrigarth	8	794	90-125	2±2	1.48±0.08	1.49±0.22	1.36±0.11	0.78±0.15	0.80±0.15	0.984±0.09	3.03±0.22	2.71±0.22	2.34±0.14
		795	90-125	4±3	2.29±0.07	1.74±0.10	1.48±0.07	0.78±0.15	0.81±0.07	0.99±0.06	3.16±0.19	2.84±0.19	2.47±0.09
			125-250				1.43±0.07				3.24±0.22	2.85±0.22	2.42±0.09
	7	802	90-125	8±8	2.89±0.10	2.74±0.32	2.41±0.26	0.79±0.07	1.35±0.21	1.256±0.12	4.36±0.33	4.04±0.33	3.66±0.29
			125-250				2.33±0.25				4.41±0.34	4.02±0.34	3.58±0.28
		803	90-125	8±7	2.94±0.09	3.02±0.37	2.55±0.25	0.79±0.07	1.26±0.34	1.214±0.17	4.45±0.35	4.13±0.35	3.77±0.31
			125-250				2.47±0.19				4.50±0.32	4.11±0.32	3.68±0.30
Warness	9	842	90-125	5±4	2.41±0.09		2.13±0.13	1.0±0.10		1.185±0.10	4.01±0.24	3.69±0.24	3.31±0.16
	10	853	90-125	6±6	2.210±0.10		1.93±0.10	0.98±0.10		1.165±0.10	3.79±0.22	3.47±0.22	3.10±0.14
		857	90-125	6±5	2.08±0.07	2.37±0.24	1.95±0.16	0.98±0.10	1.01±0.14	1.145±0.09	3.79±0.25	3.47±0.25	3.09±0.18
			125-250				1.88±0.15				3.85±0.27	3.46±0.27	3.03±0.18
	11	849	90-125	6±5	1.65±0.08	1.77±0.27	1.50±0.15	0.91±0.10	0.81±0.22	1.02±0.12	3.21±0.26	2.89±0.26	2.52±0.19
			125-250				1.45±0.14				3.29±0.27	2.90±0.27	2.47±0.19
Stackelbrae	2	1374	125-250	5±4	1.63±0.12		1.40±0.12	0.80±0.08		0.985±0.08	3.21±0.25	2.82±0.25	2.38±0.14
Fersness	3	823	90-125	4±3	1.86±0.08		1.67±0.09	0.70±0.03		0.885±0.03	3.25±0.19	2.93±0.19	2.55±0.09
			125-250				1.61±0.09				3.32±0.22	2.93±0.22	2.49±0.09
		824	90-125	5±4	1.96±0.08		1.74±0.11	0.70±0.03		0.885±0.03	3.32±0.20	3.00±0.20	2.62±0.11
			125-250				1.70±0.10				3.41±0.23	3.02±0.23	2.58±0.10
	4	831	90-125	3±2	1.65±0.08		1.50±0.08	0.90±0.15		1.085±0.15	3.28±0.24	2.96±0.24	2.58±0.17
		833	90-125	5±4	2.37±0.09		2.10±0.13	0.90±0.15		1.085±0.15	3.88±0.26	3.56±0.26	3.18±0.20

Site	Pos	SUTL No.	Size Frac (μm)	Water Content (%)	TSBC ($mGya^{-1}$)	γ spec β dose rate ($mGya^{-1}$)	Effective β dose rate ($mGya^{-1}$)	In Situ γ dose rate ($mGya^{-1}$)	γ spec γ dose rate ($mGya^{-1}$)	γ and cosmic ray dose ($mGya^{-2}$)	K Annual Dose Rate ($mGya^{-1}$)	Na Annual Dose Rate ($mGya^{-1}$)	Quartz Annual Dose Rate ($mGya^{-1}$)
Stenaquoy	1	836	90-125	5±5	2.13±0.08		1.89±0.13	0.96±0.10		1.145±0.10	3.73±0.24	3.41±0.24	3.03±0.16
			125-250				1.82±0.13				3.79±0.26	3.40±0.26	2.96±0.16
	2	838	90-125	4±3	2.08±0.10	1.93±0.26	1.80±0.14	0.96±0.10	0.75±0.15	1.024±0.09	3.51±0.24	3.19±0.24	2.82±0.17
		839	90-125	6±6	1.74±0.06		1.52±0.12	0.96±0.10		1.145±0.10	3.36±0.23	3.04±0.23	2.66±0.16

Table 4.32 Annual Dose Rate Summary and Calculations, Shetland Samples

Site	Pos	SUTL No.	Size Frac (μm)	Water Content (%)	TSBC ($mGya^{-1}$)	γ spec β dose rate ($mGya^{-1}$)	Effective β dose rate ($mGya^{-1}$)	In Situ γ dose rate ($mGya^{-1}$)	γ spec γ dose rate ($mGya^{-1}$)	γ and cosmic ray dose ($mGya^{-2}$)	K Annual Dose Rate ($mGya^{-1}$)	Na Annual Dose Rate ($mGya^{-1}$)	Quartz Annual Dose Rate ($mGya^{-1}$)
Cruester	1	949	90-125	4±3	2.174±0.077	1.90±0.10	1.82±0.09	0.76±0.15	0.72±0.07	0.926±0.08	3.44±0.21	3.12±0.21	2.75±0.12
		951	125-250	3±2	2.269±0.090	1.88±0.09	1.82±0.07	0.76±0.15	0.81±0.06	0.971±0.08	3.61±0.23	3.22±0.23	2.79±0.11
		953	125-250	3±2	2.172±0.085		1.97±0.09	0.76±0.15		0.945±0.15	3.74±0.27	3.35±0.27	2.92±0.17
	2	958	90-125	3±3	1.526±0.058		1.38±0.07	1.13±0.10		1.315±0.10	3.39±0.21	3.07±0.21	2.70±0.12
	4	968	125-250	4±3	2.215±0.112	1.99±0.09	1.82±0.09	1.00±0.20	0.76±0.06	1.067±0.11	3.71±0.25	3.32±0.25	2.89±0.14
		969	125-250	1±1	2.065±0.072	1.87±0.23	1.77±0.11	1.00±0.20	1.07±0.19	2.219±0.14	4.81±0.27	4.42±0.27	2.99±0.18
	5	1051	125-250	2±1	2.378±0.123		2.11±0.11	0.910.10		1.095±0.10	4.03±0.25	3.64±0.25	3.21±0.15
		1053	125-250	2±2	2.146±0.110		1.91±0.11	0.910.10		1.095±0.10	3.83±0.25	3.44±0.25	3.01±0.15
	6	1054	90-125	3±2	2.109±0.071		1.91±0.08	0.910.10		1.095±0.10	3.70±0.21	3.38±0.21	3.01±0.13
			125-250				1.85±0.08				3.77±0.24	3.38±0.24	2.95±0.13
		1055	90-125	4±3	2.202±0.103	2.10±0.10	1.93±0.09	0.910.10	0.83±0.06	1.054±0.11	3.67±0.22	3.35±0.22	2.98±0.14
	7	1059	90-125	4±3	2.060±0.107		1.85±0.12	0.910.10		1.095±0.10	3.64±0.23	3.32±0.23	2.95±0.16
	8	1062	90-125	3±3	1.863±0.135	1.65±0.09	1.59±0.09	0.93±0.10	0.69±0.06	0.994±0.10	3.27±0.22	2.95±0.22	2.70±0.14
		1063	90-125	4±4	2.070±0.079	2.40±0.28	2.00±0.16	0.93±0.10	0.87±0.15	1.083±0.09	3.77±0.25	3.45±0.25	3.09±0.19
			125-250				1.94±0.16				3.84±0.27	3.45±0.27	3.02±0.18
		1064	90-125	2±2	2.348±0.122		2.15±0.12	0.93±0.10		1.115±0.10	3.96±0.23	3.64±0.23	3.27±0.16
	9	1068	90-125	2±1	2.054±0.094	1.97±0.24	1.84±0.12	0.89±0.10	1.07±0.17	1.165±0.10	3.70±0.23	3.38±0.23	3.01±0.16
			125-250				1.78±0.12				3.77±0.25	3.38±0.25	2.95±0.15
	11	1075	90-125	2±2	1.968±0.115		1.81±0.11	0.99±0.15		1.175±0.15	3.68±0.25	3.36±0.25	2.99±0.19
		1076	90-125	6±6	2.006±0.084		1.76±0.15	0.99±0.15		1.175±0.15	3.63±0.27	3.31±0.27	2.94±0.21
		1077	90-125	3±2	2.108±0.136		1.91±0.13	0.99±0.15		1.175±0.15	3.78±0.26	3.46±0.26	3.09±0.25
	13	1081	90-125	2±1	2.452±0.087		2.25±0.08	0.910.10		1.095±0.10	4.04±0.21	3.72±0.21	3.35±0.13
			125-250				2.18±0.08				4.10±0.24	3.71±.24	3.28±0.13
	15	1086	90-125	2±1	2.848±0.105		2.61±0.10	0.910.10		1.095±0.10	4.40±0.22	4.08±0.22	3.71±0.14
		1087	90-125	2±1	2.775±0.091		2.55±0.09	0.910.10		1.095±0.10	4.34±0.22	4.02±0.22	3.65±0.13
		1088	90-125	2±2	2.793±0.110		2.56±0.12	0.910.10		1.095±0.10	4.35±0.23	4.03±0.23	3.66±0.16
	17	1094	125-250	1±1	2.267±0.112		2.04±0.10	0.910.10		1.095±0.10	3.96±0.24	3.57±0.24	3.14±0.14
		1095	90-125	2±1	2.532±0.111		2.32±0.11	0.910.10		1.095±0.10	4.11±0.23	3.79±0.23	3.42±0.15

Site	Pos	SUTL No.	Size Frac (μm)	Water Content (%)	TSBC ($mGya^{-1}$)	γ spec β dose rate ($mGya^{-1}$)	Effective β dose rate ($mGya^{-1}$)	In Situ γ dose rate ($mGya^{-1}$)	γ spec γ dose rate ($mGya^{-1}$)	γ and cosmic ray dose ($mGya^{-2}$)	K Annual Dose Rate ($mGya^{-1}$)	Na Annual Dose Rate ($mGya^{-1}$)	Quartz Annual Dose Rate ($mGya^{-1}$)
		1096	90-125	1±1	2.614±0.135		2.43±0.13	0.910.10		1.095±0.10	4.22±0.24	3.90±0.24	3.53±0.16
		1097	125-250	2±2	2.272±0.058		2.02±0.07	0.910.10		1.095±0.10	3.94±0.23	3.55±0.23	3.12±0.12
	19	1100	90-125	3±2	2.863±0.092		2.60±0.11	0.910.10		1.095±0.10	4.39±0.24	4.07±0.23	3.70±015
Tangwick	1	1033	90-125	2±2	8.265±0.188	8.91±0.64	7.88±0.36	1.70±0.20	3.30±0.30	1.888±0.20	10.46±0.45	10.14±0.45	9.77±0.41
		1034	125-250	1±1	5.308±0.137	5.11±0.41	4.69±0.20	1.70±0.20	2.07±0.19	2.07±0.14	7.58±0.32	7.19±0.32	6.76±0.25
	2	1040	125-250	3±2	3.311±0.099		2.91±0.11	1.70±0.20		1.885±0.20	5.62±0.30	5.23±0.30	4.80±0.23
		1041	125-250	1±1	2.976±0.110	2.48±0.27	2.73±0.15	1.70±0.20	1.34±0.21	1.882±0.20	5.43±0.32	5.04±0.32	4.33±0.24
		1043	125-250	2±1	6.897±0.154		6.13±0.16	1.70±0.20		1.885±0.20	8.84±0.32	8.45±0.32	8.02±0.26
Houlls	1	970	90-125	2±2	3.159±0.071	2.92±0.10	2.79±0.08	1.36±0.10	1.44±0.08	1.585±0.06	5.07±0.20	4.75±0.20	4.37±0.11
		971	90-125	2±1	2.331±0.063	2.75±0.27	2.33±0.13	1.36±0.10	1.30±0.19	1.515±0.11	4.54±0.24	4.22±0.24	3.85±0.17
		976	90-125	2±1	1.607±0.066	1.77±0.09	1.55±0.05	1.36±0.10	1.16±0.07	1.443±0.06	3.68±0.19	3.36±0.19	2.99±0.08
			125-250				1.50±0.05				3.76±0.21	3.37±0.21	2.94±0.08
		978	90-125	2±1	2.731±0.103	2.58±0.09	2.44±0.07	1.36±0.10	1.45±0.07	1.59±0.06	4.72±0.19	4.40±0.19	4.03±0.10
	2	983	90-125	2±1	3.858±0.114		3.54±0.11	1.15±0.10		1.335±0.10	5.57±0.23	5.25±0.23	4.88±0.15
			125-250				3.43±0.11				5.59±0.25	5.20±0.25	4.77±0.15
	3	991	90-125	1±1	3.860±0.107	3.48±0.45	3.41±0.22	1.32±0.10	1.57±0.36	1.63±0.19	5.73±0.34	5.41±0.34	5.04±0.29
		993	90-125	2±2	4.098±0.095		3.76±0.13	1.32±0.10		1.505±0.10	5.96±0.24	5.64±0.24	5.27±0.16
			125-250				3.64±0.12				5.97±0.25	5.58±0.25	5.15±0.16
	4	1003	90-125	1±1	3.560±0.169		3.31±0.16	1.26±0.10		1.445±0.10	5.45±0.25	5.13±0.25	4.76±0.19
		1004	90-125	1±1	3.044±0.142		2.83±0.14	1.26±0.10		1.445±0.10	4.97±0.24	4.65±0.24	4.28±0.17
Loch of Garths	1	1006	90-125	1±1	1.107±0.083		1.03±0.08	1.34±0.15		1.525±0.15	3.25±0.24	2.93±0.24	2.56±0.17
		1007	90-125	1±1	2.686±0.061	2.90±0.11	2.60±0.07	1.34±0.15	1.29±0.07	1.502±0.09	4.79±0.20	4.47±0.20	4.10±0.11
		1008	90-125	2±1	2.547±0.090	2.62±0.10	2.37±0.07	1.34±0.15	1.24±0.07	1.479±0.08	4.54±0.20	4.22±0.20	3.85±0.11
			125-250				2.29±0.07				4.59±0.26	4.20±0.23	3.77±0.11
	2	1017	90-125	2±1	3.201±0.137		2.94±0.13	1.36±0.14		1.545±0.14	5.18±0.26	4.86±0.26	4.49±0.19
		1018	90-125	2±1	3.811±0.116		3.50±0.12	1.36±0.14		1.545±0.14	5.74±0.25	5.42±0.25	5.05±0.18
		1020	90-125	1±1	2.965±0.095	3.34±0.11	2.93±08	1.36±0.14	2.21±0.07	1.546±0.14	5.17±0.23	4.85±0.23	4.48±0.16
			125-250				2.84±0.08				5.21±0.26	4.82±0.26	4.38±0.16

4.7 Summary

The two study areas of Orkney and Shetland have been identified using criteria developed within the research strategy as being well placed to investigate issues of age variation and duration of use. On a wider scale, the diverse geologies of the regions offer the additional benefit of more accurately assessing the suitability of luminescence dating with respect to varied lithologies.

Detailed fieldwork records have enabled a wide selection of samples to be placed within their appropriate contexts and chronological framework for each site. As a whole, samples offer the potential to investigate many aspects of site formation and landscape development, from the use of burnt mounds across a geographically confined island, to a wider discussion of burnt mounds in the Northern Isles. In addition, a limited number of samples have been collected for radiocarbon dating in the hope of supplementing any chronological information obtained.

Samples collected during fieldwork have been further selected for analysis on the grounds of their dimensions and geological characteristics. Together with weight, these three categories have been tabulated to provide a record of sample characteristics for future reference.

Samples have been ground, sieved and separated to extract both quartz and feldspar minerals. Each stage of the separation process has been carefully documented and checked to identify any potential problems that may arise from failure of either sieving or density separation steps.

Components of the annual dose have been quantified where material permitted, using TSBC and γ spectrometry methods. Water content of each sample has also been tabulated. Internal dose components have been considered prior to calculation of annual dose rates for each size fraction and extracted minerals for each sample.

The information contained in this chapter will be drawn on in the proceeding two chapters both in terms of age calculation and sample characteristics.

CHAPTER 5 THERMOLUMINESCENCE INVESTIGATIONS

5.1 Introduction

As outlined in previous chapters, one of the aims of utilizing additive dose TL methods in this research was to provide a link between past luminescence work, both within SURRC and elsewhere. Preliminary studies on extracted quartz from a selection of samples indicated poor sensitivity leading to a high degree of scatter amongst which regression analysis was not possible. As such, TL investigations were confined to feldspar minerals, which showed far more promise.

Whilst the additive dose feldspar TL technique has been used successfully in the past to date a variety of material including hearthstones, pottery and burnt stones (Sanderson, 1988, Spencer, 1996, Anthony et al, 2001) a validation of the procedure used was carried out with a bright IAEA feldspar irradiated to a known dose. This served not only to validate the chosen procedure, but also as a system check on both irradiator and TL readers. Potential problems highlighted by these experiments are discussed, and correction procedures outlined where appropriate.

Each sample run is described in terms of its luminescence characteristics, and regression data fully explored. A number of additional relationships related to sensitivity change are noted within the Orkney and Shetland dataset which were not immediately obvious during validation runs. These relationships are fully explored and correction methods developed. The corrected ED estimates are used, together with annual dose rate information documented in chapter 4, to calculated age estimates for each sample.

5.2 Validation of Measurement Procedure

5.2.1 Introduction

In order to preserve an element of continuity between past SURRC laboratory measurements (e.g Sanderson et al, 1988), it was decided to implement standard SURRC protocols for feldspar inclusion dating.

The original protocol was based on one set of 8 discs and followed the procedure outlined by figure 5.1, with reference to table 5.1 for dose data. Glow 1 is a measure of N+ β, Glow 2 β and Glow 3 a normalization dose. Glow 4 is a measure of fading over a set time period.

Disc	Dose 1	Dose 2	Dose 3	Fading Dose-1	Fading Dose -2
1	1.5	12	5	5	
2	3	10.5	5	5	
3	4.5	9	5	5	
4	6	7.5	5	5	
5	7.5	6	5		5
6	9	4.5	5		5
7	10.5	3	5		5
8	12	1.5	5		5

Table 5.1: Dose Information for Discs 1-8 (All doses are in Gy)

A standard preheat of 16 hrs at 135°C was used throughout, with readout to 500°C at a rate of $5°Cs^{-1}$. Each glow curve was integrated into 10°C bands for analysis. In house SURRC software was used to analyze the data. Regression of the G3 normalized integrals produced a plateau plot in 10°C bands from 0-500°C. A temperature range for the plateau was manually selected and the weighted mean across the plateau calculated. Palaeodose was calculated as ED+I, where ED is given by Glow 1 regression, I by Glow 2 regression. Where evidence of short-term fading existed, a correction was performed to take account of it. Fading was first calculated by normalizing the G4 response to G3 for each disc, then comparing the ratio of stored to prompt readout at each 10°C integral. Where the ratio differed significantly from 1, each 10°C regression result was directly corrected by the amount of fading measured and the weighted mean of the plateau re-calculated, thus folding fading errors into the regression analysis.

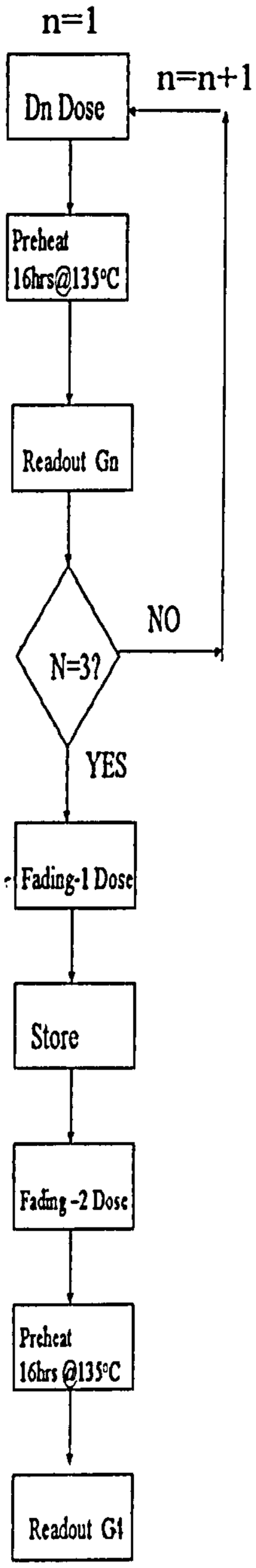

Figure 5.1: Flowchart of Multiple Aliquot Protocol

5.2.2 Protocol Details

Validation of the above multiple aliquot protocol was undertaken using a gamma irradiated 90-150μm IAEA feldspar standard (F1). The experiment was designed in order to test the precision and reproducibility of standard 8 disc TL runs. Two sets of 24 discs (FSP010 and FSP011) were run (as 3 sets of 8 discs) to allow comparisons between 8- disc ED determinations and larger 24 disc datasets.

Approximately 4g of F1 Feldspar was gamma irradiated at the Glasgow vet school to an approximate dose of 4.5 Gy on the 22nd of January 2001 using a Mk 4 hotspot ^{60}Co cell. Approximately 2-3mg of sample was dispensed onto each stainless steel disc using silicone grease as an adhesive. Discs were placed in the irradiator and given stepped doses as indicated in table 5.1 Discs were then removed, and preheated on the irradiator plate overnight as indicated in fig 5.1. Samples were then individually measured on the TL reader, with each disc being placed on the heater plate and heated to 500°C. This cycle was repeated as indicated in fig 5.1 and glows 2-3 measured. After fading dose 1 was administered, samples were stored in a dark drawer for a period of 4 weeks at room temperature prior to G4 readout.

5.2.3 Equipment details

TL readings were carried out on two manual TL readers (PC1 & PC2) and on a SURRC automatic reader. Both manual readers were fitted with a 7-59 and KG1 filter to detect

the near UV and blue spectrum. The heater plate was ramped from 0°C to 500°C at a rate of 5°C per second, unless otherwise stated. At the beginning of each measurement cycle, both dark and light counts were measured: the 'dark count' represents the combined effect of thermal electrons, cosmic radiation, natural radioactivity and afterpulses, generally giving a signal between 20 and 200cps (Spencer, 1996). A ^{14}C doped plastic scintillator, NE102 (peak emissions at 423nm) was used as a low level light source. These two counts provided a check on system settings.

An automatic TL reader, with a capacity to read 24 discs in series, was also utilised. This was fitted with a BG39 3mm filter, detecting a broad spectrum (~ 350nm-600nm), and run from an Apple computer.

An Elsec automatic β irradiator, using a ^{90}Sr source, 1.85 GBq in strength was used for irradiation. This irradiator was commissioned and calibrated in 1997 relative to primary air kerma standards at the National Physical Laboratory. Dose rates are known on the centre of the disc to a precision of ± 2% at the 95% confidence interval.

5.2.4 Basic Run Information

5.2.4.1 Glow curve characteristics

Throughout both runs, glow curves showed a consistently similar shape, characterised by a main peak at around 270°C and several smaller shoulders at higher temperatures. Intensities were typically in the region of 2-4,000,000 counts at peak maxima.
Peak temperatures were tabulated for all glow curves to allow a comparison of reader reproducibility from run to run and disc to disc.

Due to the possibility of ambiguity in the position of T_{max} , caused by system noise and multiple component features, temperature at 50% (T1/2) on the first rise of the glow was also noted. Spencer (1996) identifies this position as the best parameter to measure as "it behaved in a similar manner to a mathematical inflection and the count rate was at a maximum, and therefore the effect of undesirable noise....was far less" (p88). As $T_{½}$ is at a maximum in the first numerical derivative of a glow curve, and zero in the second (fig 5.3), $T_{½}$ can still be determined when T_{max} position is uncertain (Spencer, 1996).

Comparison of values from disc to disc within each glow, and from glow to glow showed significant variation in both peak temperature and $T_{1/2}$ positions (fig 5.4, table 5.2). On average a scatter of 10°C was seen between discs on the same glow, with larger scatters being seen between glows – up to 30°C in some places.

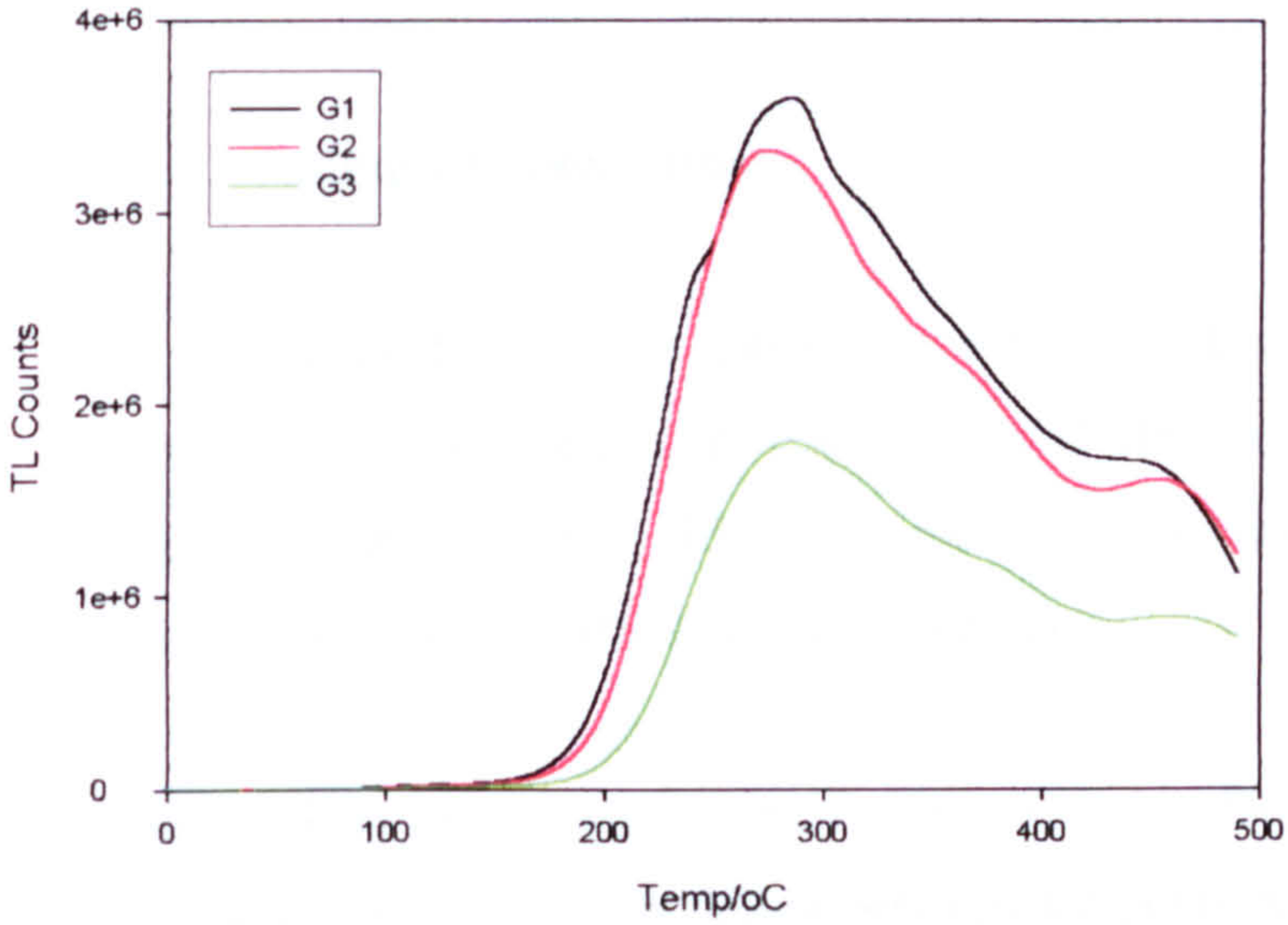

Fig 5.2 FSP010 Typical Glow curves for G1-3

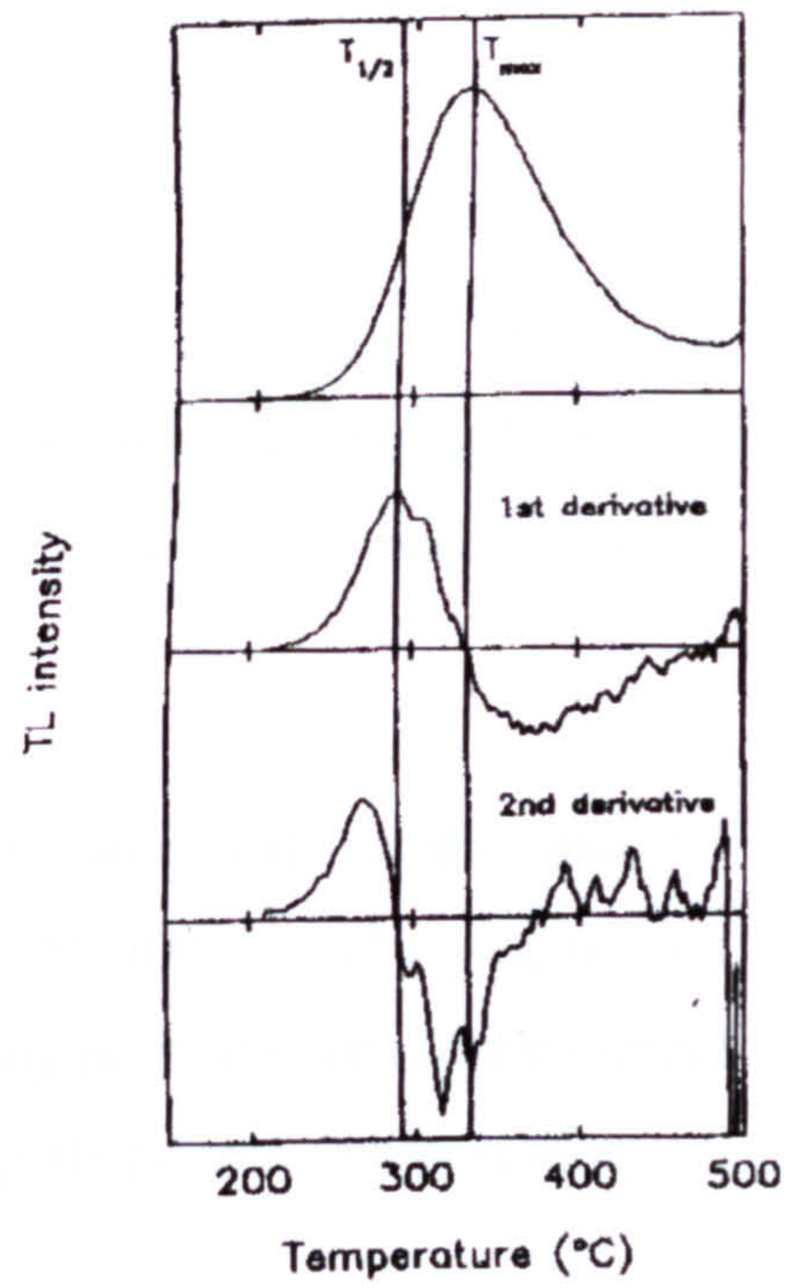

Fig 5.3 $T_{½}$ positions for 1st and 2nd derivatives (From Spencer, 1996, p88)

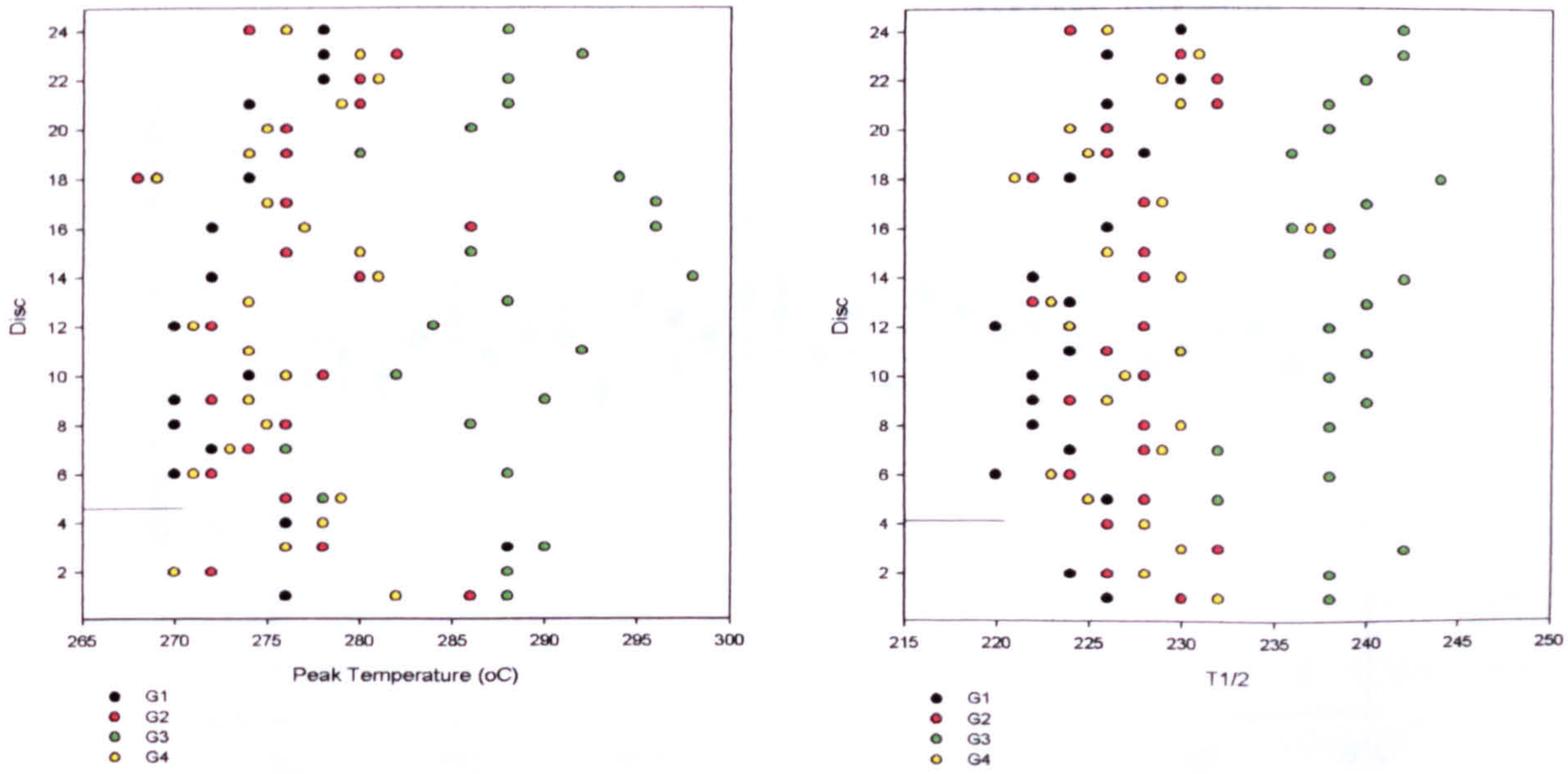

Fig 5.4 (a) Variation in Peak Temperature FSP010 (b) Variation in $T_{1/2}$ Temperature

Table 5.2 T_{max} and $T_{1/2}$ positions for F1 runs

Run (FSP)	Average Peak Temperature Position (°C)				Average $T_{1/2}$ Position (°C)				Peak Temp-$T_{1/2}$ (°C)			
	G 1	G2	G3	G4	G 1	G2	G3	G4	G 1	G2	G3	G4
010	275±4	277±4	288±6	276±5	225±3	227±4	239±3	226±5	50±5	49±6	49±7	50±7
011	274±4	274±5	285±6	277±5	225±3	224±3	236±4	225±4	49±5	50±6	49±7	51±6

Average and standard deviation quoted

5.2.4.2 Fading Characteristics

No significant fading was noted after a four week storage period. Fig 5.5 shows the average ratio of stored:prompt readout for FSP010. At temperatures higher than 170°C the ratio is within error of 1. Identical results were obtained for FSP011. As such no fading corrections were performed on the F1 dataset.

Smith (1998) previously reported more extensive fading measurements on the same F1 feldspars, noting a 5-10% fading between temperatures of 250-400°C, and no significant fading at temperatures over 400°C. It is thought that the long preheat given to the sample on this occasion may have successfully removed unstable signals prior to fading readout.

Fig 5.5 FSP010 Ratio of Stored:Prompt luminescence as function of Temp

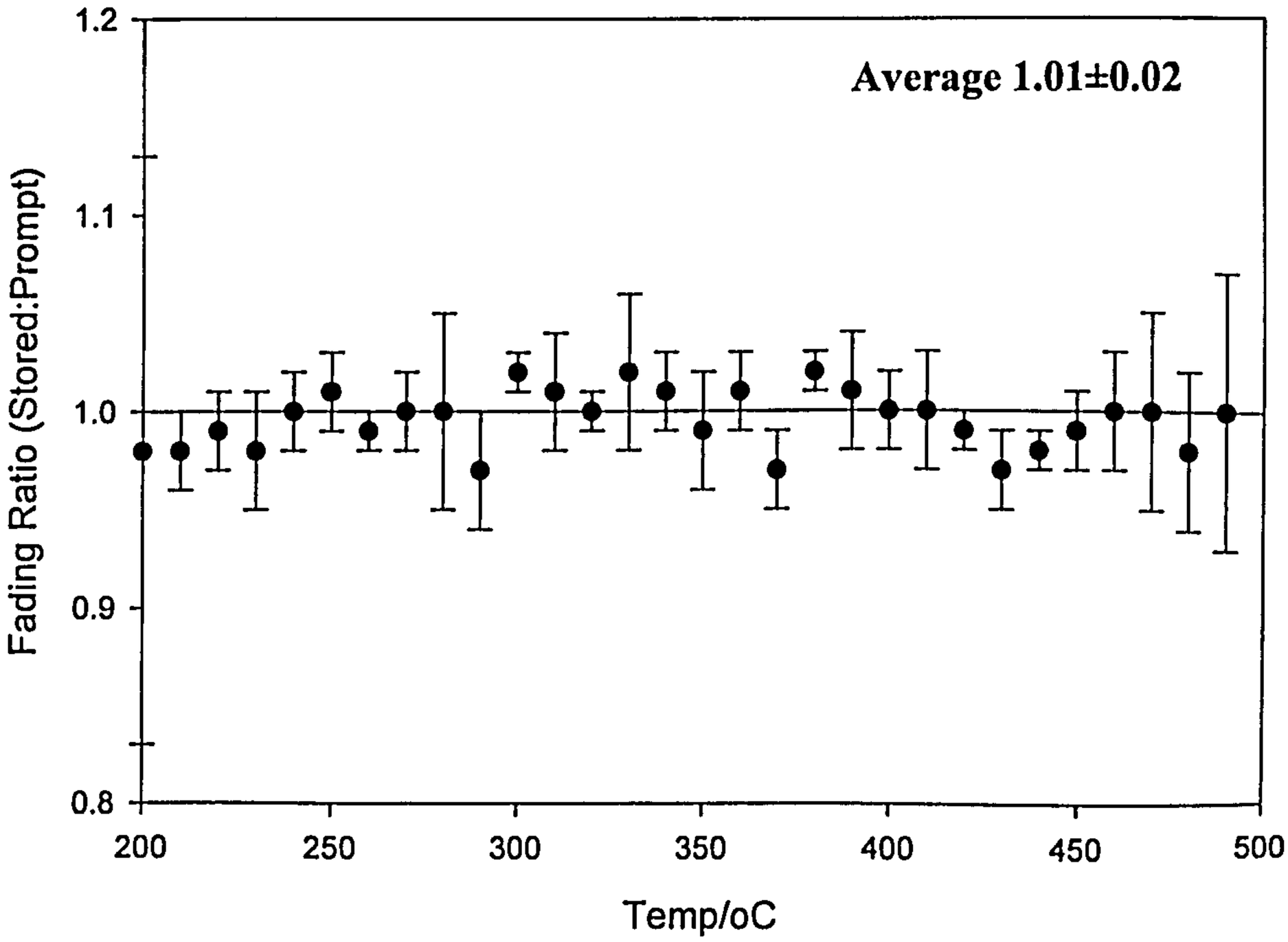

5.2.4.3 Regression Characteristics

As outlined above, regression is automatically calculated over each 10°C integral band. A number of characteristics can be defined based on regression analysis. The sensitivity change between 1st and 2nd glow can be calculated as the ratio of the gradient of the ED to I regression curve. As such, a plot of sensitivity change against temperature produces an informative graph of the relative sensitivity changes at varying points along the glow curve. As can be seen from fig 5.6, some changes in sensitivity appear to have a structure similar to the glow curve shape. On the whole, a sensitivity decrease between G1 and G2 is noted, in the region of 20% for the most part. Likewise, ED plateau plots also show correlated structures with glow curve shape (fig 5.7).

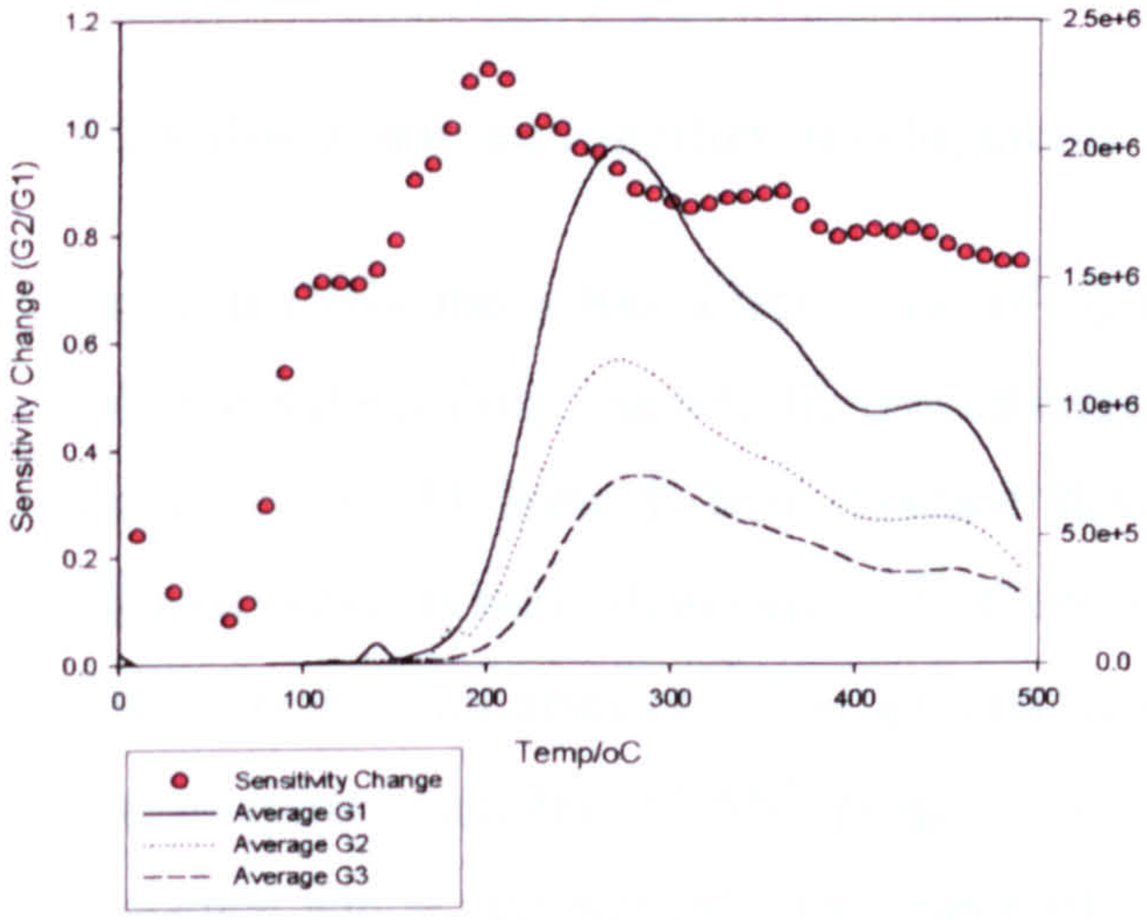

Fig 5.6 FSP010 Sensitivity change as a function of temperature plotted with average glow curve response for each measurement cycle.

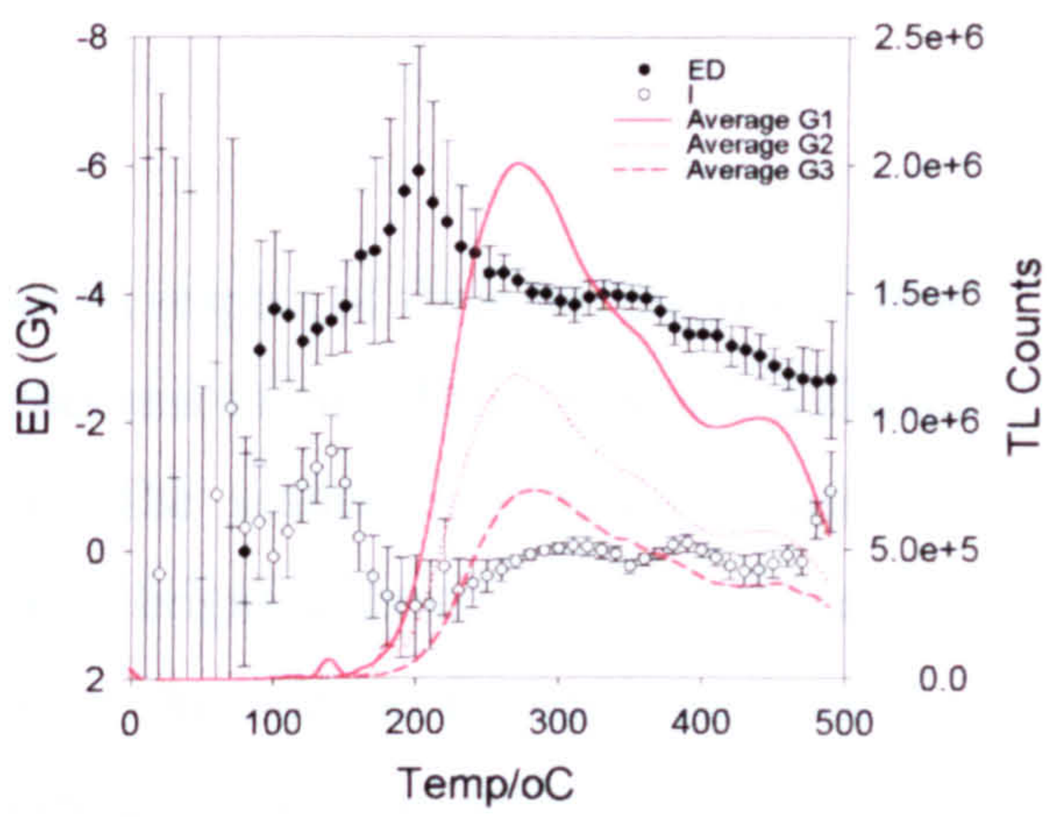

Fig 5.7 FSP010 ED Plateau Plot with averaged glow curve responses for each measurement cycle.

5.2.5 Comparison of ED Results

The results of the TL additive dose runs are shown in table 5.3. Average results from both 24 disc runs give an ED of 3.995±0.061Gy. Average results of all 6, 8 disc runs give an ED of 4.088±0.051Gy with a standard deviation on individual measurements of 0.406. It is notable that a number of intercept values are negative, the largest being –0.59±0.02, the average being -0.075±0.118. This negative intercept effect is more dominant in the

second run (FSP011). The resulting average AD is less than the expected 4.5Gy by approximately 10%.

Table 5.3: TL Results for FSP010 and FSP011 detailing plateau region, ED, I and palaeodose values (ED+I) for sets of 8 discs and combined 24 disc runs

Run	Plateau (oC)	Discs	ED (Gy)	I (Gy)	ED+I (Gy)
FSP010	250-350	24	-4.02±0.04	0.06±0.03	-4.09±0.07
	290-350	1-8	-3.78±0.08	-0.03±0.01	-3.75±0.08
	250-350	9-16	-4.00±0.11	0.08±0.02	-4.07±0.13
	250-350	17-24	-4.26±0.07	0.09±0.04	-4.35±0.12
FSP011	250-350	24	-4.20±0.05	-0.29±0.04	-3.90±0.10
	250-350	1-8	-4.42±0.16	0.21±0.07	-4.64±0.18
	250-350	9-16	-4.40±0.05	-0.21±0.01	-4.20±0.06
	300-350	17-24	-4.03±0.09	-0.59±0.02	-3.52±0.14

5.2.6 Discussion and further developments

Basic analysis above has selected sets of eight discs in respect of their run position – thus the first 8 discs form one set, the second eight another and so on. This analysis has shown variation in ED outwith two standard deviations. The scatter in EDs on 8 disc TL measurements is more than expected of a homogenous bright feldspar. It is possible that this represents an artefact of the gamma irradiation. In order to further investigate the distributions seen, the TLAN[6] program was further developed to include an autoreject sequence which automatically calculated EDs over a set temperature range for all possible combinations of eight discs (6561 combinations in total). The temperature range 250-350°C was selected for analysis as the majority of 8 disc runs showed a plateau within this region. ED was calculated from the total integral of this area as opposed to a weighted mean of all 10°C integrals across the area. It is worth noting at this point that the EDs determined in this way are not independent of one another as data are continually reused to produce the array of ED estimates with each disc used in 1/3 of all ED determinations. However, each individual combination of 8 discs is unique and has value statistically in examining distributional information on the range of EDs obtained.

[6] TLAN is a suite of turbo basic dos based programmes written at SURRC specifically for the analysis of TL results, allowing spectral replay, integration, regression and analysis of regression results.

Plotted as a histogram (fig 5.8(i)), it can be seen that the distribution of FSP010 is gaussian in nature. This would indicate that the spread in ED seen is not related to uneven irradiation of the material. A similar analysis was carried out using sets of 16 discs in the same manner as above (fig 5.8(ii)). A notable increase in precision is seen confirming that much of the scatter in ED is related to precision rather than other systematic errors. It it is interesting to note that the average value of ED+I for the histogram is approximately 4.5Gy, 10% higher than previous estimates –note that the ED distribution peaks at 4.1Gy, but the contribution from I is in the region of 0.3-0.4Gy, increasing ED+I to 4.5Gy. This value is more in line with the expected result, and suggests that there may be a problem relating to calculation of ED over narrow 10°C bands, as opposed to over a larger area.

It is possible that the weighted mean of the ED along the plateau temperature may cause underestimation of the total error. Weighted mean analysis is thought to be valid where measurements are independent of one another. In the case of integral band regression, this may not be an entirely accurate assumption. Feldspar glow curves are generally thought to be the result of many overlapping peaks. As such, neighbouring 10°C integrals are not truly independent of one another. Consideration of figure 5.9 shows that whilst temperature integrals 1, 3 and 5 are independent of one another, integrals 1 and 2 for example have a common trap dependency.

The variability in the value of I, ranging from –0.59 to +0.21 is likewise a cause for concern. Consideration of figure 5.8 shows the most common value for I, based on all possible combinations, to be between +0.2 and +0.4 Gy, with the negative values playing only a minor role in both charts. The fact that the negative I value is not dominant in fig 5.8 also indicates that there may be a problem in relation to the use of 10°C integrals.

Possible evidence of variability in thermal contact and heating rate between runs was a major cause for concern in respect of the 10°C integration method for calculating ED. Certainly the 10°C bands would be far more susceptible to peak misalignment than the wider bands used for multiple regression above. There are a number of possible explanations for the observed behaviour. Thermal lag, caused by poor contact between disc and heater plate, either through poor centering of the disc or due to a slight bevel in the disc itself, may cause misalignment of peak positions. Both would be expected to

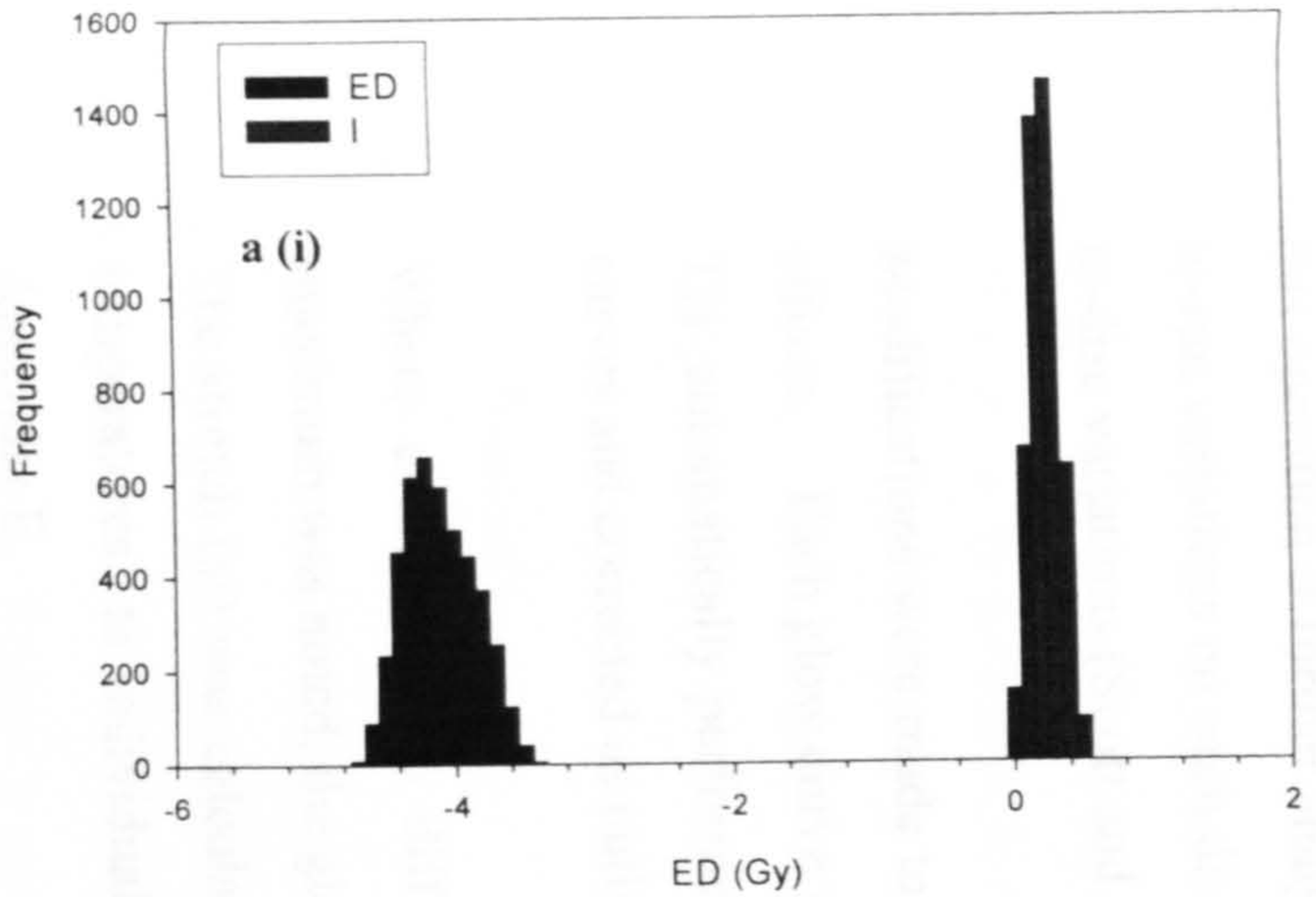

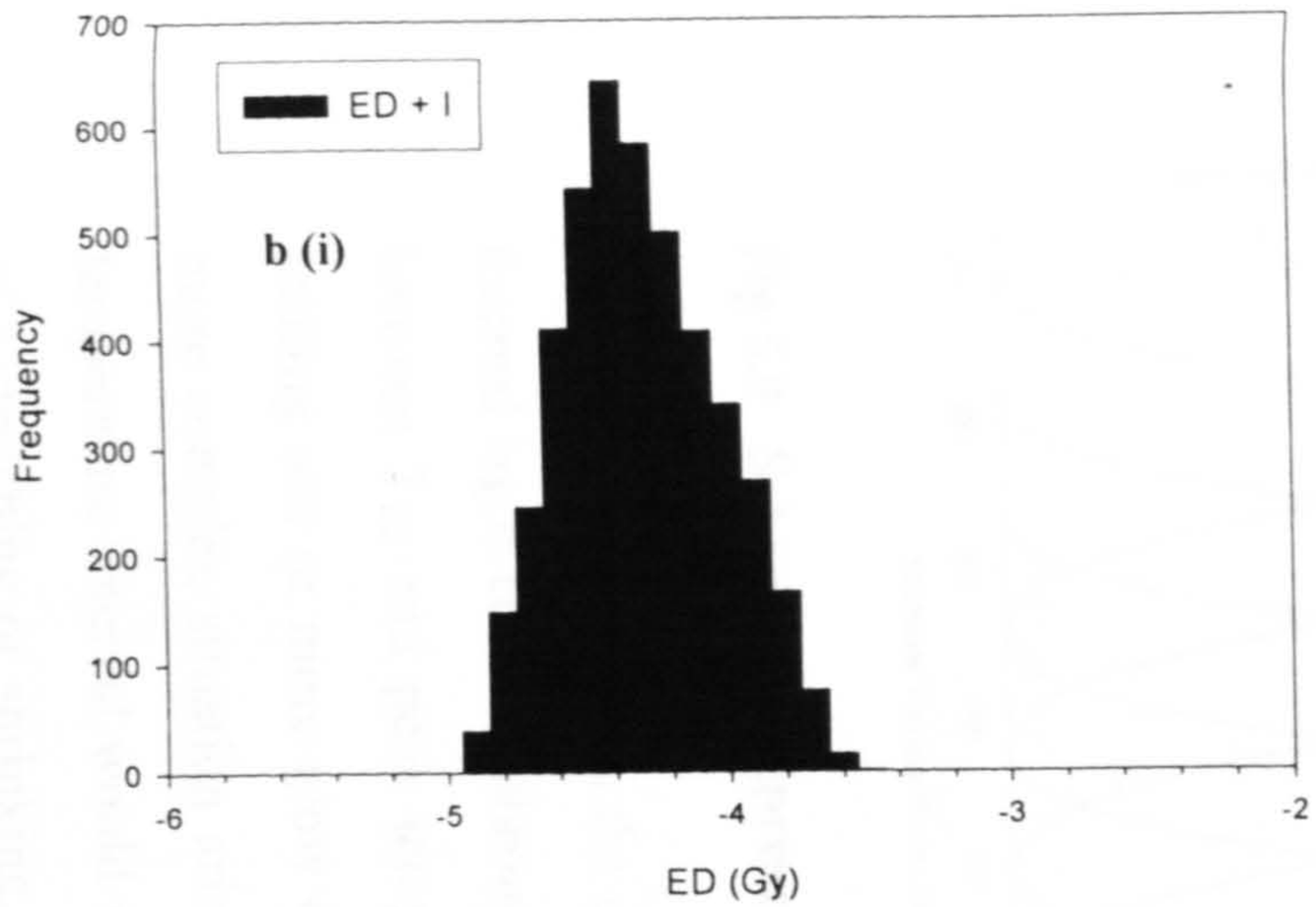

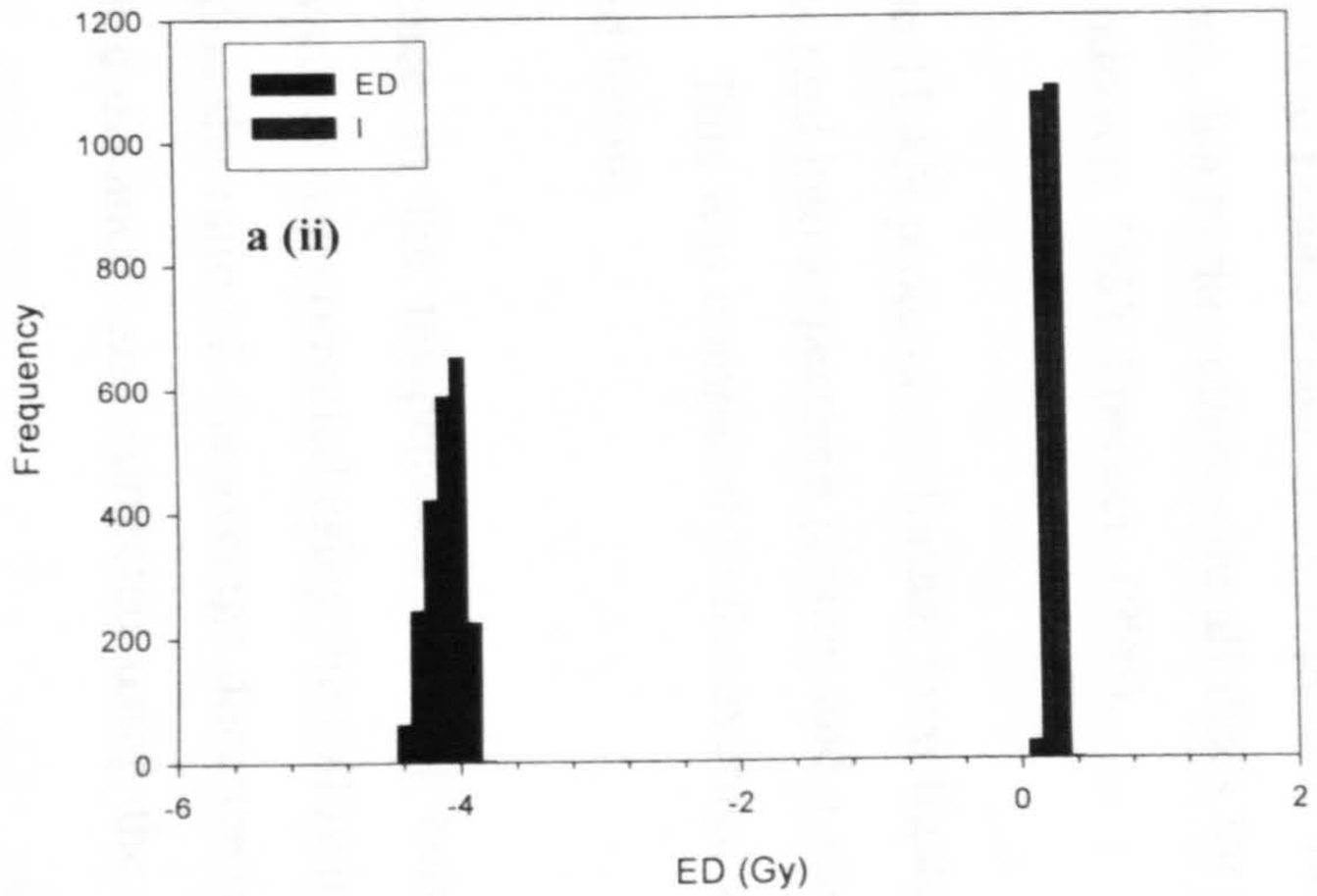

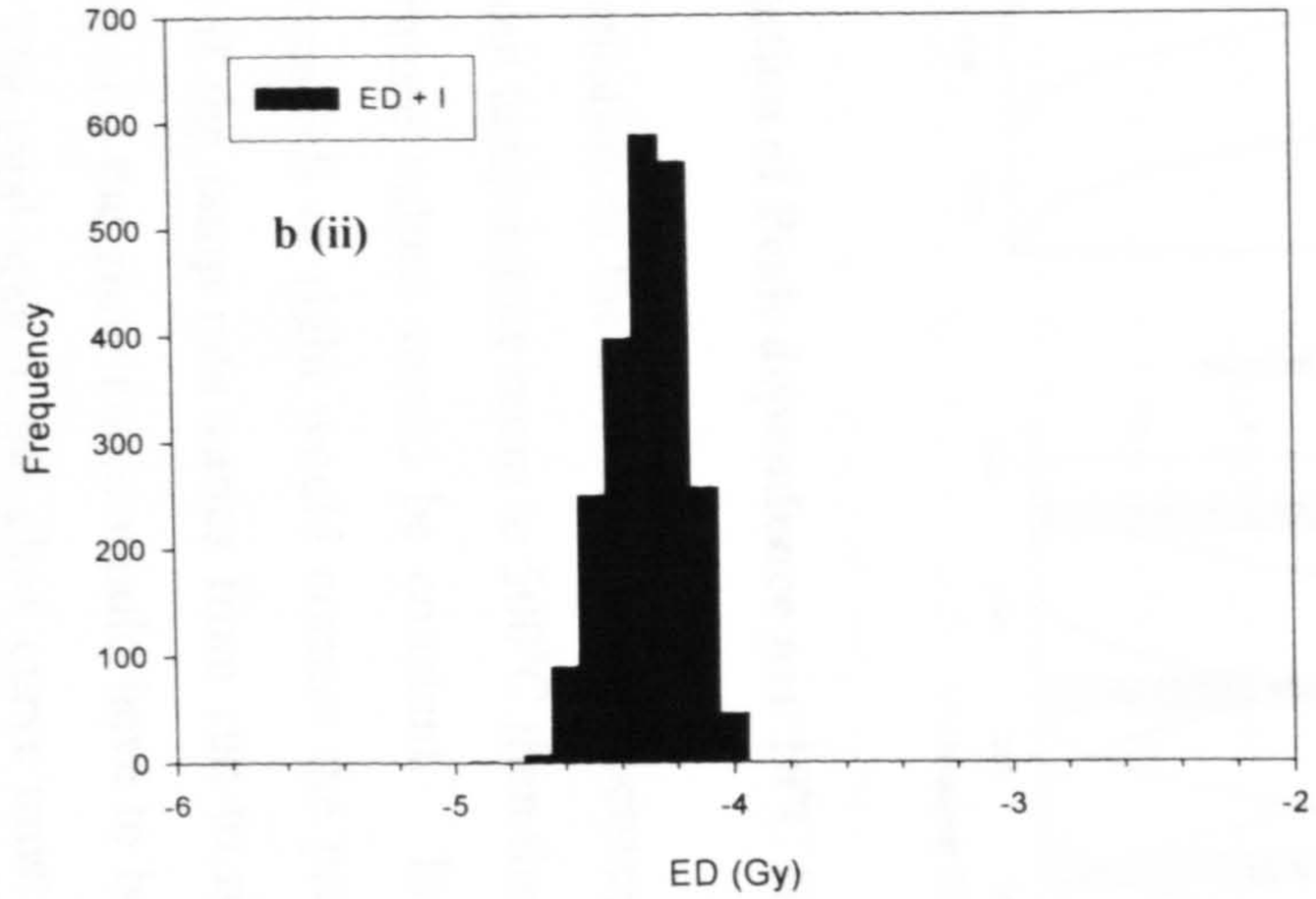

Fig 5.8 a. Histogram of ED and I for FSP010 for (i) 8 disc combinations and (ii) 16 disc combinations
b. Histogram of ED+I for (i) 8 disc combinations and (ii) 16 disc combinations

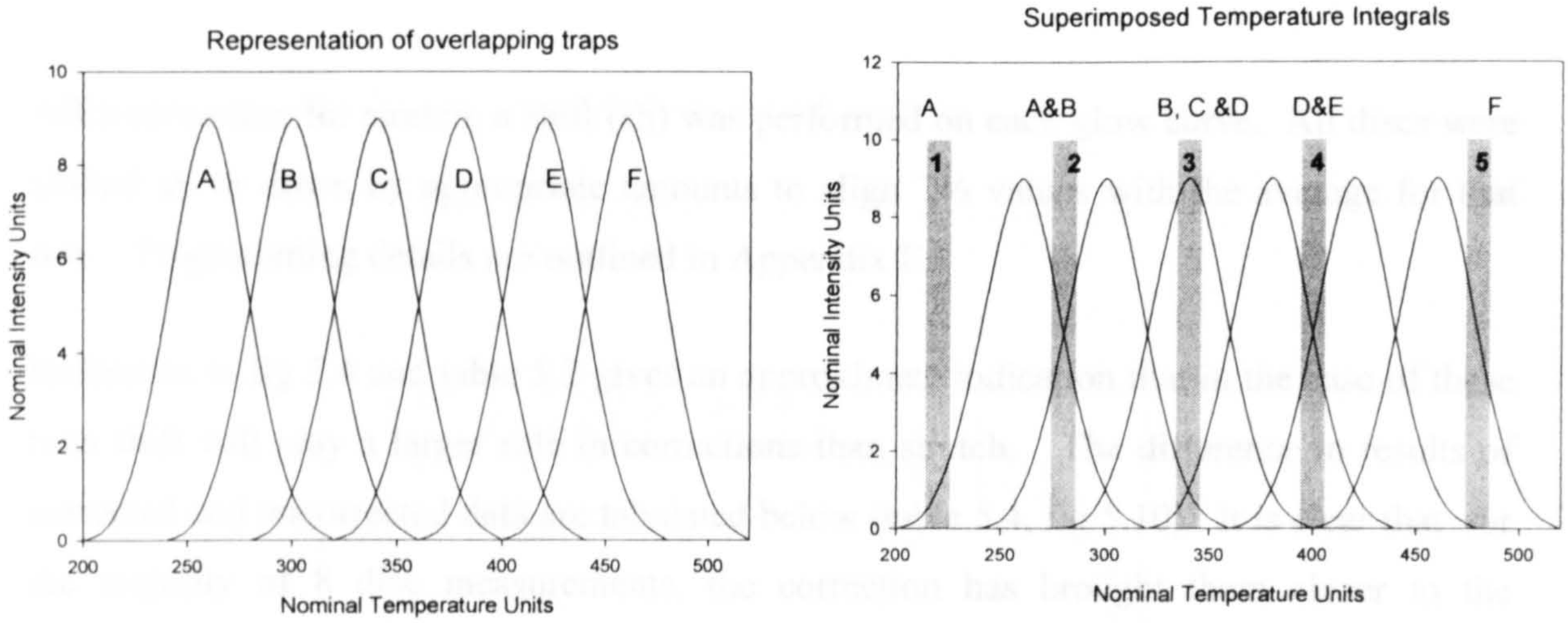

Fig 5.9 Schematic Representation of Peak dependence per 10°C Integral Band

vary from run to run as the orientation of the disc may change between readouts. If the thermal lag is constant throughout temperature ramp to 500°C then the temperature interval between $T_{1/2}$ and peak temperature values would be constant. In this case, manually shifting one or more glow curves left or right would correct the problem. However, a more complex situation arises if the ramp rate varies from run to run. In this case, the temperature interval would vary and the glow curve would have to be corrected by means of a stretching or shrinking. The total area of the glow curve must be conserved during this operation if further analysis is to remain valid. It is important not only to correct run-to-run variations on each disc but, due to the reliance on all discs for regression, also disc-to-disc variations (Scott and Sanderson, 1988, Spencer, 1996).

Modifications were made to the TLAN program to further investigate and correct for such effects. Each glow curve was read into a spectrum plotter, and a search for peak max and T½ automatically performed. This was compared to the average values for all 72 glow curves and corrected as outlined below.

Where evidence of a difference in the temperature interval between T1/2 and peak maximum was noted, the glow curve was corrected using the following sets of equations. The stretch (st) was calculated as the ratio of the average distance between T ½ and Peak temperatures to individual disc distance and corrected using the procedure outlined in Appendix E.

After correction for stretch, a shift (sh) was performed on each glow curve. All discs were shifted up or down by appropriate amounts to align T½ values with the average for that run. Programming details are outlined in Appendix E.

Reference to fig 5.4 and table 5.2 gives an approximate indication that in the case of these runs shift will play a larger role in corrections than stretch. The difference in results of corrected and uncorrected data are tabulated below (table 5.4, fig 5.10). It is clear that for the majority of 8 disc measurements, the correction has brought them closer to the expected result. The corrected average of both 24 disc runs was 4.30±0.15Gy.

Table 5.4 Corrected ED+I Results, FSP010 and FSP011

RUN	Discs	Uncorrected ED+1 (Gy)	Corrected ED+I (Gy)
FSP010	1-24	-4.09±0.07	-4.38±0.13
	1-8	-3.75±0.08	-3.75±0.22
	9-16	-4.07±0.13	-4.39±0.26
	17-24	-4.35±0.12	-4.35±0.15
FSP011	1-24	-3.90±0.10	-4.21±0.19
	1-8	-4.64±0.18	-4.64±0.20
	9-16	-4.20±0.06	-4.35±0.11
	17-24	-3.52±0.14	-3.91±0.21

It was decided to further investigate this using old laboratory data from Crawford Burnt Mound. The thermal properties of this material are investigated in detail by Spencer (1996). It can be seen that in the case of TL219 (fig 5.11a), the ED plateau is significantly improved and, in the case of TL189 (fig 5.11b) both ED and I plateau are greatly improved. In such cases it is clear that peak alignment is of great importance to the plateau integrity.

5.2.7 Summary

Analysis of the F1 dataset shown variation in individual 8 disc ED estimates which are outwith expected 2σ variations. Where possible it would appear preferable to run sets of 24 discs which are in better agreement with the mean. The issue of error calculation is as yet unresolved, though it would seem unwise to use the weighted mean at face value (however in many cases the error on annual dose will be significantly higher than the error on the estimated dose and form the major uncertainty in the date).

Fig 5.10 FSP010 Uncorrected and corrected plateau plots

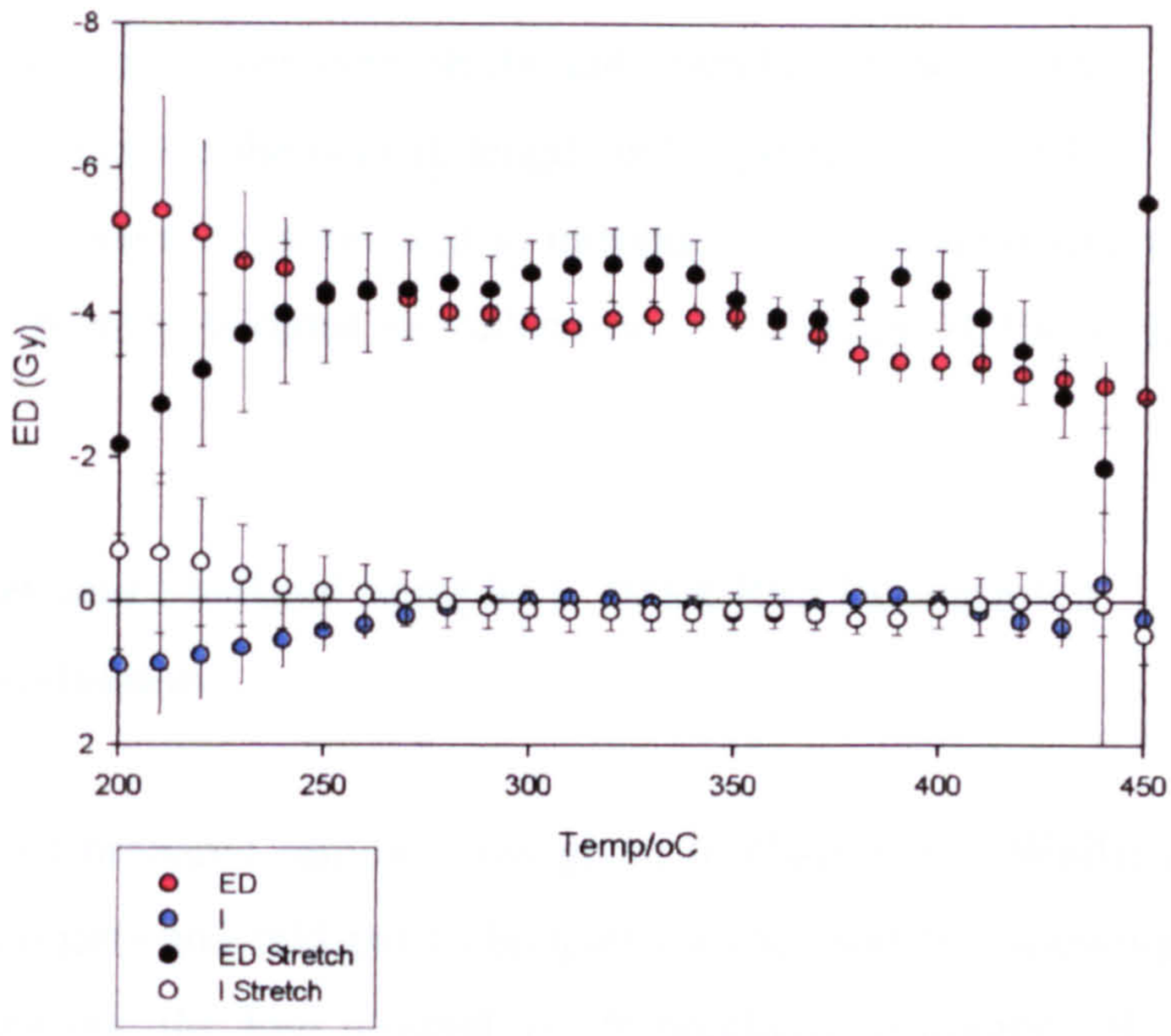

Uncorrected Data
Plateau from 200 - 400 'C
-1.9 % Variation
ED : -3.95 +/- 0.05 +/- 0.05
I : 0.08 +/- 0.03 +/- 0.03
ED + I : -4.03 +/- 0.06 +/- 0.08
1st/2nd Slope : 0.92 +/- 0.08 +/- 0.08
Mean I/AD : -0.06 +/- 0.07

Corrected Data
Plateau from 200 - 400 'C
-2.7 % Variation
ED : -4.23 +/- 0.11 +/- 0.08
I : 0.13 +/- 0.07 +/- 0.03
ED + I : -4.38 +/- 0.13 +/- 0.12
1st/2nd Slope : 0.87 +/- 0.03 +/- 0.03
Mean I/AD : 0.02 +/- 0.09

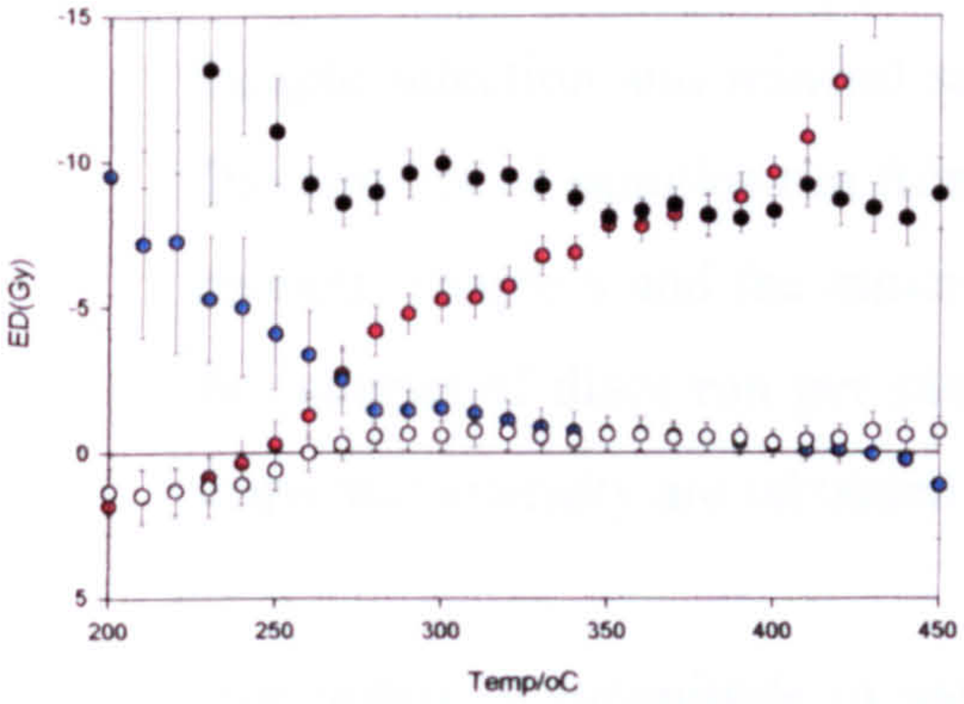

Plateau Region 350-390oC
-1.8% Variation

ED: -7.93±0.17±0.11
I: -0.62±0.07±0.04
ED+I: -7.32±0.19±0.13
2nd/1st: 0.89±0.03
I/AD: 0.07±0.03

Plateau Region 260-450oC
-1.6% Variation

ED: -8.75±0.24±0.14
I: -0.52±0.12±0.04
ED+I: -8.23±0.19±0.13
2nd/1st: 0.96±0.07
I/AD: 0.06±0.02

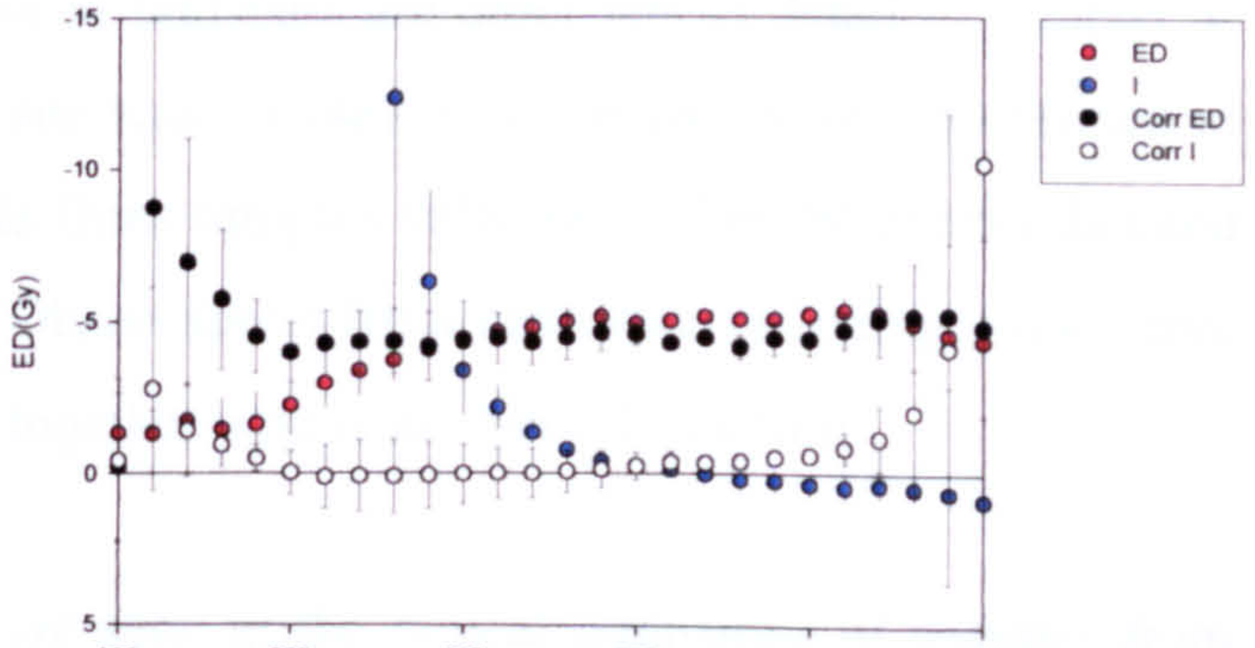

Plateau from 250 - 400 'C
-3.2 % Variation

ED : -4.81 +/- 0.10 +/- 0.14
I : -0.34 +/- 0.06 +/- 0.10
ED + I : -4.68 +/- 0.13 +/- 0.15
1st/2nd Slope : 0.59 +/- 0.43 +/- 0.43
Mean I/AD : 0.36 +/- 0.40

Plateau from 250 - 400 'C
-1.8 % Variation

ED : -4.33 +/- 0.10 +/- 0.03
I : -0.39 +/- 0.09 +/- 0.04
ED + I : -4.06 +/- 0.18 +/- 0.07
1st/2nd Slope : 0.88 +/- 0.08 +/- 0.0
Mean I/AD : 0.02 +/- 0.05

Fig 5.11 Uncorrected and Corrected Plateau Plots (a) TL219 (b)TL189

As suspected in earlier work, there is clear evidence of peak misalignment due to variable thermal contact both in the F-1 dataset and in earlier laboratory runs. A method has been developed to correct for both shifts and stretches in peak area. This would appear to significantly improve the plateau length and expected value of ED. As such, the correction method would seem a useful step to introduce into routine dating runs, though should not be applied blindly without consideration of whether shifts in the dataset are real or apparent.

5.3 Orkney and Shetland Samples : Basic Run Information

5.3.1 Introduction

An outline of prepared samples was given in chapter 4. Whilst it was the intention to utilise both quartz and feldspar techniques for each sample, allowing for a large number of intercomparisons, the low mineral yields precluded a number of samples from feldspar runs. All samples were measured using the same procedure outlined above for F1 experiments.

5.3.2 Glow Curve Characteristics

5.3.2.1 Analysis of samples

Sample selection and mineral separation of feldspars are described in detail in Chapter 4. The number of samples run from each site was dictated by the research design outlined in previous chapters and the mineral yields from samples collected. The latter also dictated the number of discs run per sample. Observations from each run, including glow curve shape and intensity are tabulated below together with basic run information.

Five orders of magnitude of variation are seen in the typical intensities of samples from Orkney and Shetland (fig 5.12). There is no clear evidence to link the variations in intensity observed to the rock type of the sample (fig 5.13).

Table 5.5 Glow curve characteristics, Orkney Dataset

Site	Pos.	Sample / Min	Run No.	No	Fraction (μm)	Glow Curve Characteristics
LIDDLE	1	1379 K	LD001	8	90-125	Twin peaks at 250/320°C . Typical intensity –30-40,000
		1381 K	1381G1 (PC1)	8	90-125	Twin peaks at 250/320°C . Typical intensity –30-40,000
	3	1386 K	1386G1 (PC1)	8	90-125	Single peak at 340°C . Typical intensity –60-70,000
DALE	1 2	748 Na	DAL123 (AUTO)	16	90-125	Twin peak at 330/440. G1 equal intensity – appears as single broad peak; G2 and 3 can distinguish between them. Typical intensity 6-8,000 G1; 2-4000 G2/3
		749 Na	DAL128 (AUTO)	24	90-125	Main peak at 450°C with shoulder at 315°C. Typical intensity 10-20,000.
		750 Na	12D001 (PC2)	24	90-125	Twin peak 280/330°C. Typical intensities 5000 G1 – 2000 G2/3. 330°C peak becomes far less dominant G2/3
		751 Na	12D002 (PC1)	24	90-125	Twin peaks at 285/375°C 375 more dominant in G1. Typical intensity 10-20,000 G1. G2/23 2-3,000 Some noise in G2/3 due to lower intensity.
		753 K	12D007 (PC2)	24	90-125	Twin peaks at 260/340°C 340 becomes less dominant G2/3. Typical intensity –5-10,000 G1. G2/23 1-5,000
		754 Na	DAL124 (AUTO)	24	90-125	Twin peak 320/420°C. 320°C peak more dominant. Typical intensity 5-10,000 G1; 1-2,000 G2/3.
		755 Na	12D008 (AUTO)	24	90-125	Main peak at 450°C with smaller peak at 275°C. Typical intensity 5-10,000.
DALE	1 3	760 K	13D005 (AUTO)	24	90-125	Twin peaks at 300 & 400°C, 300°C slightly more dominant. Typical intensity 25-30,000.
		764 Na	13D001 (AUTO)	24	90-125	Twin peak 250/360°C. Typical intensity 4-5,000
		765 Na	13D002 (AUTO)	24	90-125	Twin peaks at 280/410°C. 410 more dominant in G1, equal in G2/3. Typical intensity 10-30,000 G1; 5-10,000G2/3.
		767 K	13D004 (AUTO)	24	90-125	Twin peaks at 250/340°C. 250 more dominant in some cases. Typical intensity 10-15,000 G1; 1-2,000G2/3.
DALE	1 4	768 Na	DAL146 (AUTO)	24	90-125	Single peak at 320°C. Typical intensity 5,000 G1; 1-2,000 G2/3.
		769 Na	DAL142 (AUTO)	24	90-125	Twin peaks at 310/430°C, 430 slightly more dominant. Typical intensity 6-10,000 counts.
		774 K	14D003 (PC1)	24	90-125	Twin peaks at 280/360°C, 280 becomes more dominant in G2/3 Typical intensity 10-20,000 counts G1; 5-10,000 G2/3.
		775 K	14D004 (PC2)	24	90-125	Main peak at 260°C with two shoulders at 350 and 420°C. Typical intensity 5-10,000 counts.
		777 K	DAL147 (AUTO)	24	90-125	Twin peaks at 300 and 430°C. 430°C peak slightly more dominant. Typical intensity 20-30,000 counts.
		779 K	DAL145 (PC2)	24	90-125	Main peak at 280°C with two shoulders at 350 and 420°C. Typical intensity 15-20,000 counts.

DALE	15	782 K	15D001 (AUTO)	24	90-125	Single peak at 330°C. Typical intensity 2-4,000.
		785 Na	15D004 (PC2)	24	90-125	Single peak at 320°C. Typical intensity 1-2,000.
SKAILL	5	815 K	SKA002 (AUTO)	16	90-125	Main peak @250°C with secondary peak at 350°C. Typical counts at peak max 20-30,000 on G1, 8-15,000 G2 and G3
	5	815 P/Q	SKA008 (PC1)	24	90-125	Single peak @300-320°C Typical counts at peak max 6-10,000. Noise across peak due to low intensity
	6	817 Na	SKA010 (AUTO)	24	90-125	Main peak @370°C with shoulder at 270°C. Typical counts at peak max 4-7000. By G2 shoulder becomes more dominant - change in glow curve shape
	1	1343 K	1343G1 (PC1)	8	90-125	Twin peaks at 320 and 380°C, typical intensity peak max 5-10,000 counts.
	3	1360 K	1360G1 (PC2)	8	90-125	Twin peaks at 310 and 380°C, typical intensity peak max 5-10,000 counts.
K. OF Merrigarth	8	794 Na	MER003 (PC1)	24	90-125	One main peak @350°C, 2 minor peaks @ 295 and 400°C. Typical counts at peak max 2-4,000. Noise across peak due to low intensity
	8	795 Na	MER004 (PC2)	24	90-125	Main peak @320°C, Typical intensity 4-6000.
	7	802 K	MER005 (AUTO)	24	90-125	Main peak @350°C, Typical intensity 3-5000.
	7	803 K	MER006 (AUTO)	24	90-125	Main peak @310°C, Typical intensity 4-6000.
WARNESS	9	842 K	WAR001 (AUTO)	16	90-125	G1 main peak at 350°C with two shoulders at 275 and 420°C, Typical intensity 300-400,000. Change of shape in G2 and 3 with third peak (420°C) more dominant than 350°C peak. Slight decrease in intensity
	10	857 K	WAR004 (AUTO)	16	90-125	Main peak at 250°C with smaller peak at 350°C. Typical intensity 30-60,000 on G1, slightly reduced G2/G3. No shape change.
FERSNESS	3	823 Na	FER001 (PC1	24	90-125	Twin peaks at 310 and 390°C, typical intensity at G1 peak max 7-10,000 counts. Signal level significantly reduced by G2/G3 – no change in shape.
	3	824 K	FER002 (PC2)	24	90-125	Single peak @350°C. Typical counts at peak max c.2-4000.
	4	831 Na	FER003 (AUTO)	24	90-125	Single peak @360°C with low temperature shoulder at 250°C. Typical counts at peak max c.2-4000.
	4	831 K	FER005 (AUTO)	24	90-125	Main peak @ 380°C with minor peak at 250°C. Typical intensity at peak max 10-20,000, reducing to 5,000 by G2/3. Minor peak becomes more pronounced in G2/G3.
STENAQUOY	1	836 Na	STN005 (AUTO)	24	90-125	Main peak @430°C with shoulder at 295°C. Typical intensity 10-15,000. G2 change in shape – shoulder equal or greater intensity than main peak. Total intensity drops to c.3000
	2	838 K	STN003 (PC1)	24	90-125	Twin peaks of equal intensity at 280 and 380°C. Typical intensities of 10-15,000 throughout
	2	839 K	STN004 (PC1)	24	90-125	Twin peaks at 290 and 400°C, lower temp peak slightly more dominant. Typical intensity 15-20000 on G1, 5-10,000 G2 and 3. No change in shape.

Table 5.6 Glow curve characteristics, Shetland Dataset

Site	Pos.	Sample/ Mineral	Run No.	Discs	Frac (μm)	Glow Curve Characteristics
CRUESTER	1	949 K	CRU021 (AUTO)	8	90-125	Single peak @360°C Typical intensity 10-30,000
	1	951 Na	CRU022 (AUTO)	8	125-250	Single peak @360°C Typical intensity 10-20,000
	1	953 K	CRU023 (AUTO)	8	125-250	Single peak @360°C Typical intensity 3-5,000
	2	958 Na	CRU024 (AUTO)	8	90-125	Main peak @320°C with shoulder at 420°C Typical intensity 30-50,000.
	4	968 Na	CRU025 (PC2)	8	125-250	Single peak @360°C Typical intensity 10-30,000
	5	1051 K	CRU006 (AUTO)	24	125-250	Main peak @350°C with shoulder at 300°C Typical intensity 5-10,000.
	5	1051 Na	CRU044 (AUTO)	8	125-250	Main peak @370°C with shoulder at 320°C Typical intensity 5-10,000.
	6	1054 K	CRU029 (AUTO)	8	90-125	Single peak @320°C Typical intensity 10,000
	8	1062 K	CRU031 (AUTO)	8	90-125	Main peak @350°C Typical intensity 10-20,000.
	9	1068 Na	CRU045 (AUTO)	8	90-125	Single peak @320°C Typical intensity 2-5,000
	15	1088 K	CRU034 (AUTO)	8	90-125	Main peak @370°C with shoulder at 300°C Typical intensity 5-10,000.
	19	1100 K	CRU043 (AUTO)	8	90-125	Main peak @330°C with shoulder at 300°C Typical intensity 3-5,000.
Tangwick	1	1033 K	TAN01 (AUTO)	8	90-125	Main peak @360°C with shoulder at 320°C Typical intensity 3-5,000.
	1	1034 Na	TAN02 (AUTO)	8	125-250	Single peak @350°C Typical intensity 2-5,000
	2	1040 Na	TAN03 (PC1)	8	125-250	Single peak @320°C Typical intensity 5-10,000
	2	1041 Na	TAN04 (PC2)	8	125-250	Single peak @340°C Typical intensity 10-15,000
Houlls	1	970 K	HL001	8	90-125	Single peak @350°C small shoulder @300°C Typical intensity 300-500,000
	1	976 K	HL002	8	125-250	Single peak @350°C small shoulder @300°C Typical intensity 3-5,000
L. Garths	1	1008 Na	LG001	16	125-250	Single Peak @330°C Typical Intensity 2-3000
	2	1017	LG002 K	8	125-250	Single Peak @350°C Typical Intensity 5-8000

Fig 5.12 Histogram of Typical sample intensities

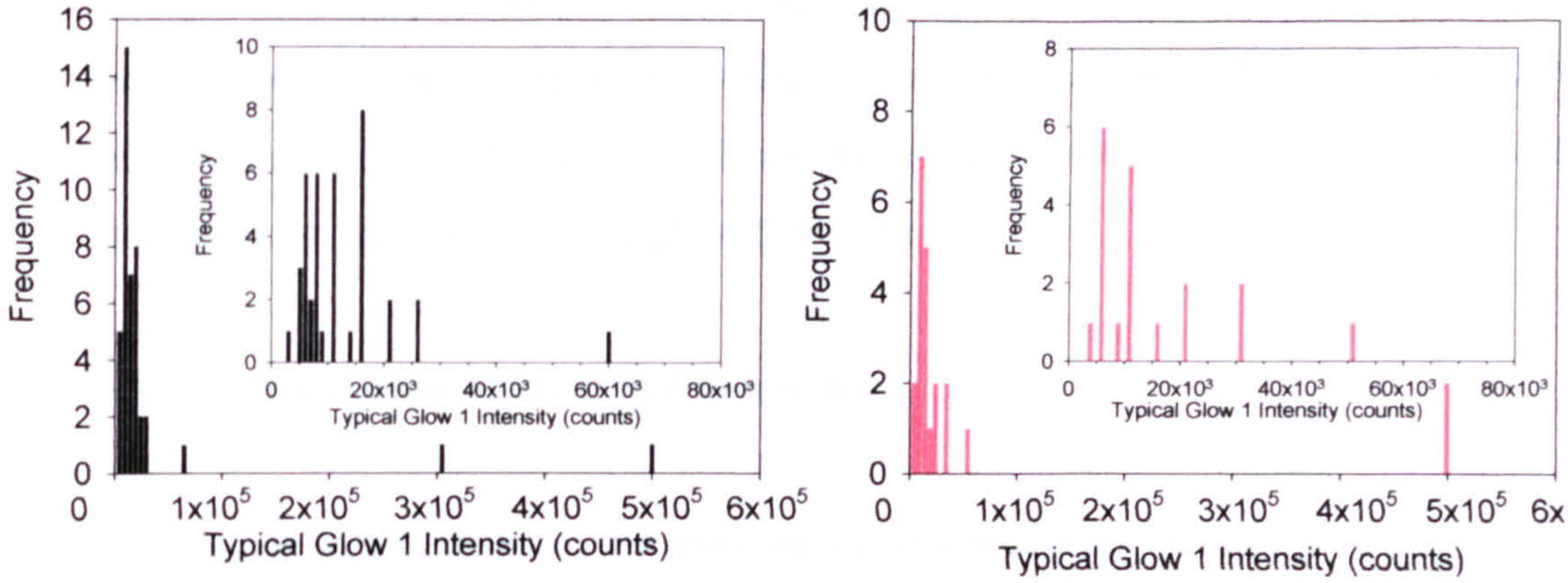

(a) Orkney Samples
Mean 18800±46610±7370

(b) Shetland Samples
Mean 37800±109420±24470

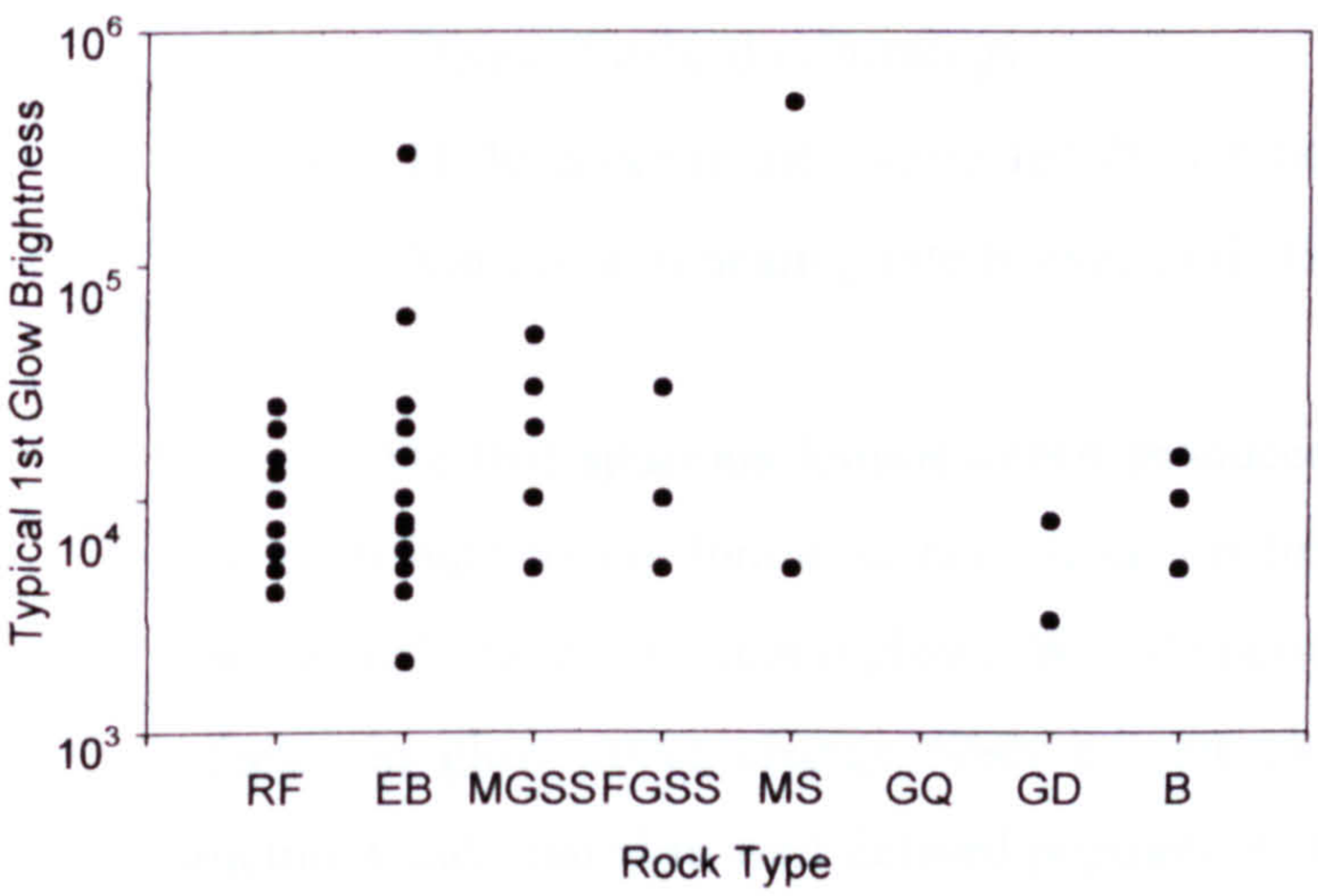

Fig 5.13 Relationship between Intensity and Rock Type (RF=Rousay Flags, EB= Eday Beds, MGSS=Med. Grained Sandstone, FGSS= Fine Grained Sandstone, MG= Migmatic Gneiss, GQ=Gneissose Quartzite, GD=Granodiorite, B=Baretchia)

In general the observed glow curve shapes from the Orkney dataset can be divided into three categories:

(a) single peak dominance (fig 5.14a)

(b) single peak with shoulder/inflection (s) or minor peaks (fig 5.14b)

(c) twin peaks of similar intensity (fig 5.14c).

The glow curves from the Shetland dataset are far less variable than those seen in Orkney. All show a single/main peak, occasionally with a secondary shoulder/inflection (fig 5.15a-c).

On occasion, changes in the shape of the glow curve are observed on second readout. This was confined only to the Orkney dataset and not observed in any run from Shetland

material. In the case of SKA010-SUTL817 the main peak became less dominant (fig 5.16a). Similarly WAR001-SUTL842 showed in increase in dominance of a minor shoulder on second and third glow (fig 5.16b). In the case of STN005-SUTL836 the low temperature shoulder present in G1 became more pronounced and of equal intensity to the main peak on second and third glow (fig 5.16c).

5.3.2.2 Discussion of observed behaviour

The change in the shape of the glow curve observed may be attributed to one of a number of factors:

(i) Spurious luminescence on first glow

(ii) Contamination of disc after first glow

(iii) Discs of mixed mineralogy

(iv) Differences in the charge distribution between natural and β induced TL

(v) Variation in heating rate between G1, G2 and G3

It is possible that spurious luminescence produced as a result of laboratory pre-treatment may contribute to the luminescence signal on first glow. Heating of the sample would remove such traces by second glow. Whilst spurious luminescence cannot be ruled out as a factor in glow curve change observed, the shape of the changes highlighted appear structured and related to well defined populations of traps therefore it is possible that other explanations may be more satisfactory.

It would seem unlikely that the change in shape has occurred as a result of contamination, as there is an equal probability of contamination being picked up after second glow as after first. The change in glow curve seen always takes place between first and second glow. On no instance does it occur between second and third.

Fig 5.14 Examples of glow curves from Orkney Dataset A. DAL146-SUTL 768 Single peak glow curve B. SKA010-SUTL817 Main peak with shoulder/inflection C. DAL147-SUTL777 Two peaks of similar intensity

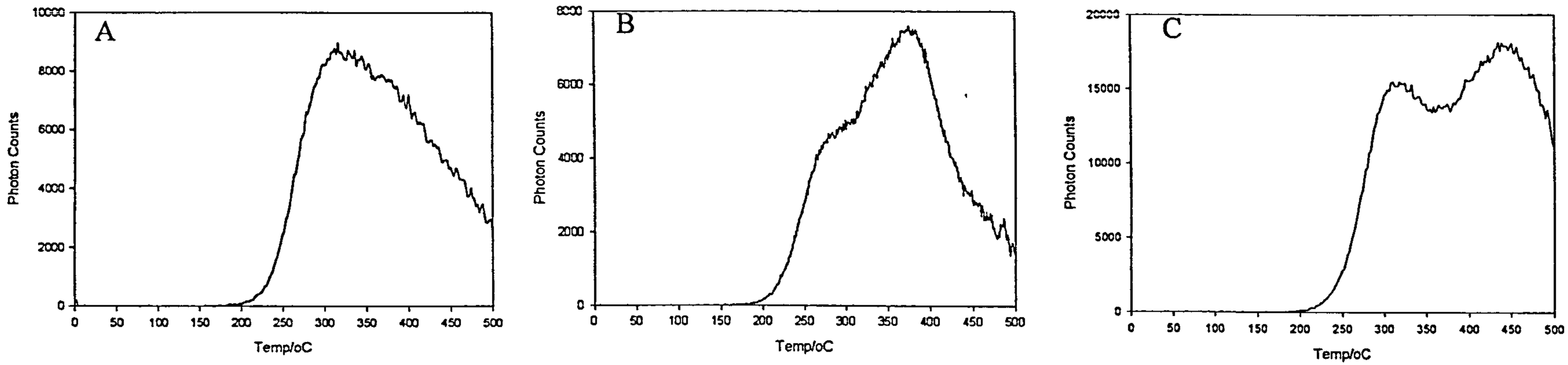

Fig 5.15 Examples of glow curves from Shetland Dataset A & B CRU023-SUTL953 and HL001-SUTL970 respectively, Main peak with slight inflection on low temperature side of peak C. CRU031 –SUTL1062 Single peak.

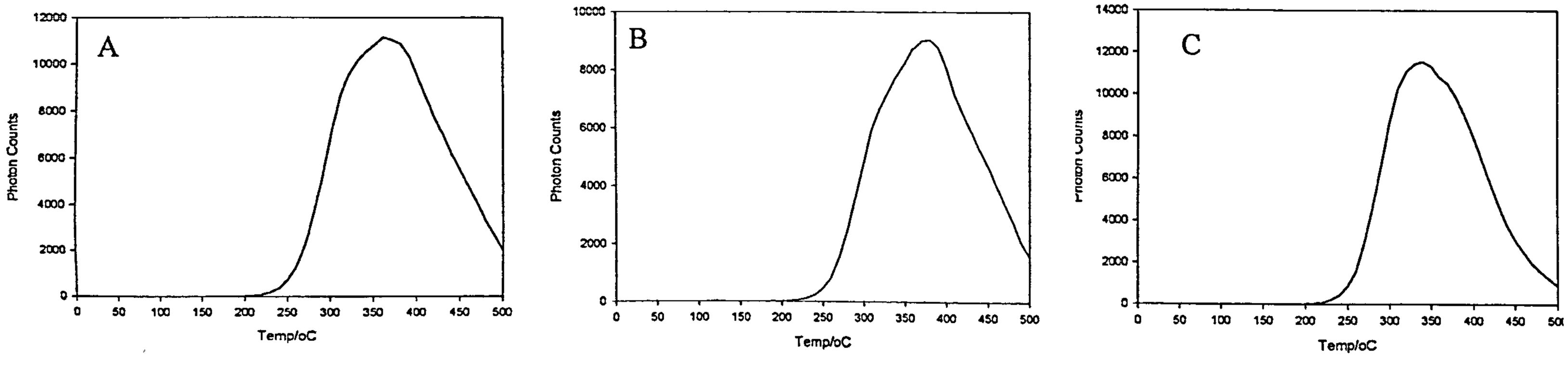

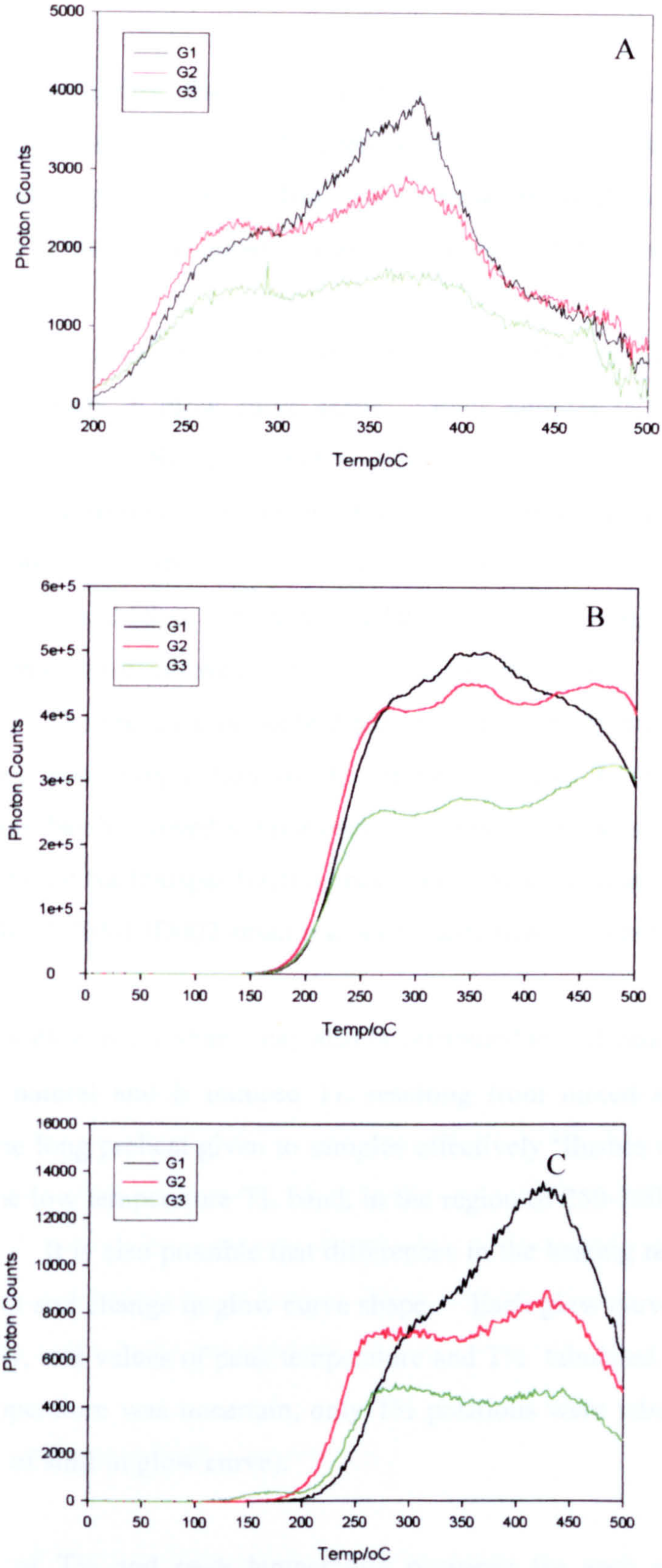

Fig 5.16 Examples of Glow curves where a change in shape occurs A. SKA010-SUTL817 Main peak becomes less dominant in G2&3 suggesting 270°C peak unstable over archaeological timescale. B. WAR001-SUTL842 Minor shoulder more pronounced in G2&3. C. STN005-SUTL836 By G2 low temperature shoulder of equal intensity to main peak.

The third possibility, that the discs of the samples concerned contain material of mixed mineralogy, may be explained in terms of differential sensitivity changes of the two or more minerals present on the disc. Such a situation would occur as a result of a failure on some part of the density separation and acid treatment described in chapter 4.

SEM work was carried out on retained fractions of the density separates of all samples that showed changes in glow curve shape. Four samples (STN005-SUTL836; DAL123 – SUTL748, 13D002-SUTL765 and TAN001-SUTL1033) showed indications of a failure of the density separation. Elemental mapping identified a small but significant potassium feldspar presence within the sodium fraction and vice versa (fig 5.17). It is probable that dilution of the 2.58gcc^{-1} tungstate solution with the remnants of the lighter 2.51gcc^{-1} solution may have allowed the lighter potassium fraction to mix with the sodium rich feldspars. The presence of Na feldspar in the K feldspar fraction is unlikely to have been caused by poor preparation of the density separate as no other samples within the preparation batch showed similar contamination. It is possible that air bubbles within or attached to the Na feldspar fraction may lead to its separation in the lighter fraction. In the case of SUTL765-13D002 small traces of quartz was also present.

Change in glow curve shape may also be attributed to differences in the charge distribution between natural and β induced TL resulting from mixed stable and metastable traps. Whilst the long preheat given to samples effectively 'flushes out' the lower stability traps within the low temperature TL band, in the region of 250-300°C some unstable traps may remain. It is also possible that differences in the heating rate between G1-3 may cause movement and change in glow curve shape. Each glow curve was analysed as discussed previously, and values of peak temperature and T½ tabulated. (Where the position of the peak temperature was uncertain, only T½ positions were tabulated restricting analysis to evidence of shift in glow curve).

Analysis of T½ and peak temperature positions for each run identified a number of samples where a potential problem existed with regard to the reproducibility of thermal contact on the heater plate. In the majority of cases, the shift in peak position would appear to be related to thermal contact between the disc and heater plate, most probably caused by flaws in the stainless steel discs used, as opposed to variability in the reader

itself – the scatter seen cannot be grouped by glow number as in the case of the F1 runs. Instead the variation seen is scattered across all runs (fig 5.18a&b). The only exception to this general trend was in a number of G4 fading runs where reader reproducibility appeared to be the main contributor to the shift in position – most probably a result of a change in the thermal stability of the reader during the prolonged period of storage prior to fading measurements.

On a few occasions however, there is also evidence of variation in the ramp rate of the glow curve – fig 5.18b shows a sample where the variation in the Peak temp-T1/2 values exceed 50°C in individual difference.

The above analysis was not carried out on samples which showed evidence of a change in the shape of the glow curve from first to second/third glow as the probability that changes in the position of peak temperature and T½ was unrelated to thermal contact was high therefore the corrections were deemed inappropriate.

5.3.3 Regression and Fading Characteristics

5.3.3.1 Introduction

Regression was carried out in an identical manner to F1 samples described above, with the additional step of shift/stretch corrections where appropriate. Results of the regression and standard short term fading tests are tabulated in the following sections. For a number of samples (mainly from Tangwick and Loch of Garths) it was not possible to regress the data due to large amounts of scatter. These runs have been excluded from further analysis, but are discussed further in summary section 5.5.

5.3.3.2 Stretch and Shift Corrections

As outlined above, it was decided to perform shift and stretch corrections on a number of runs due to variability in thermal contact. Eight runs were identified as showing signs of poor thermal contact reproducibility. These are tabulated below, together with their uncorrected regression results. Corrections performed on four of these (FER001, SKA002,

A

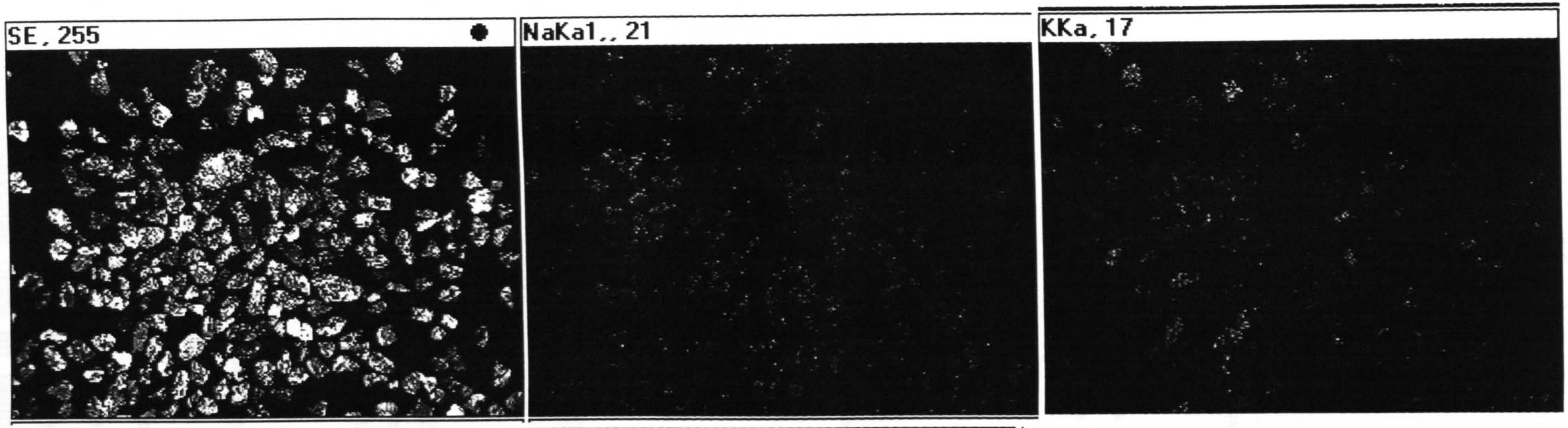

B

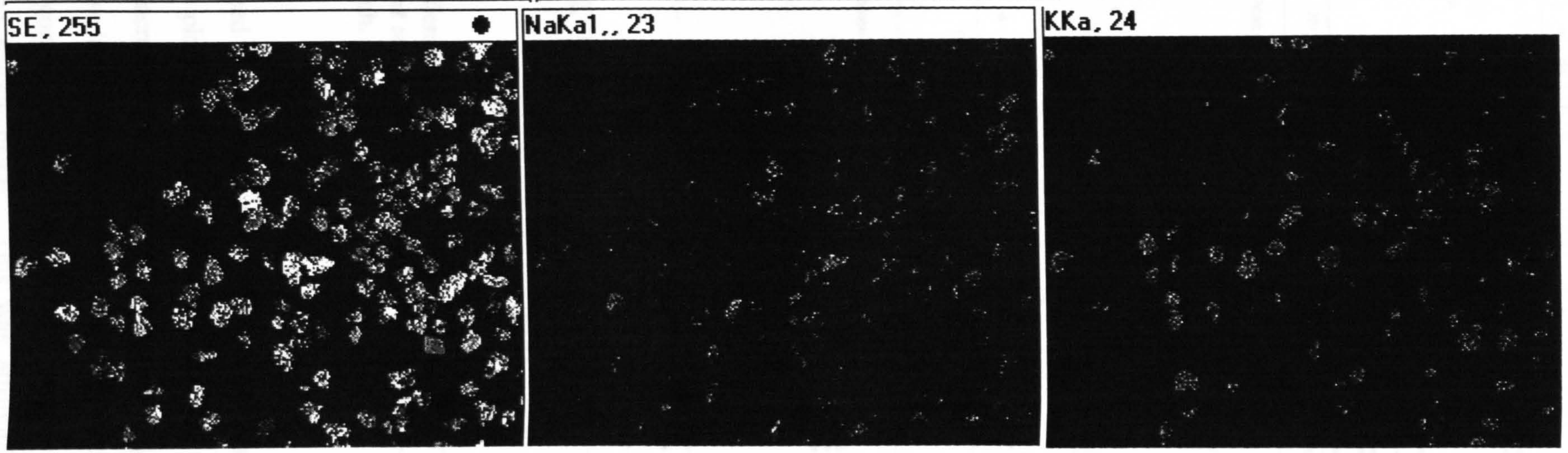

Fig 5.17 Evidence of failure of K/Na feldspar density separation (a) SUTL836-Na feldspar with K feldspar contamination indicated by the detection of K concentrations (Kka) which correlate spacially with grains identified on SEM image (b) SUTL1033 K feldspar with significant Na Feldspar content contamination indicated by the detection of Na concentrations (NaKa) which correlate spacially with grains identified on SEM image.

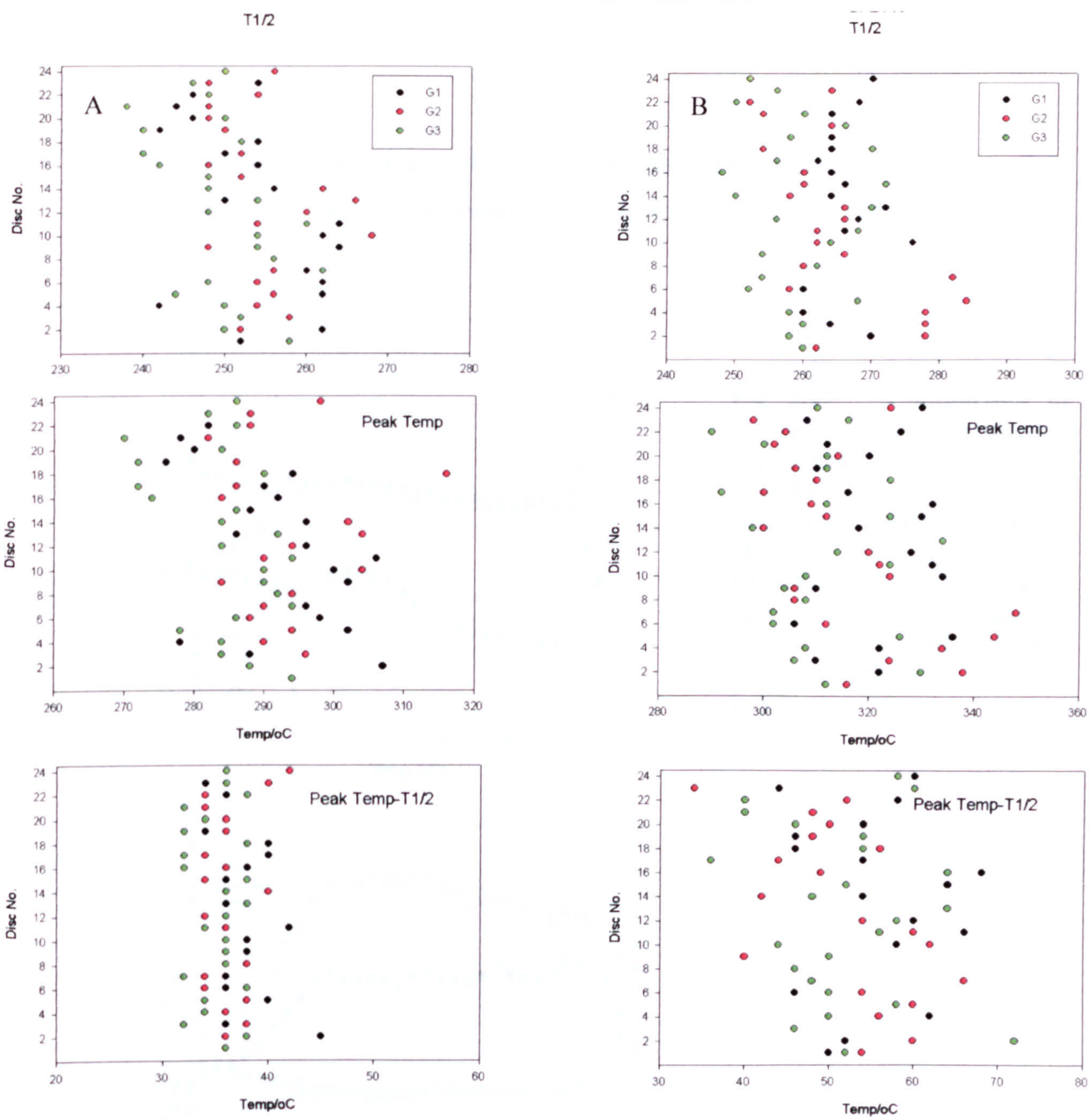

Fig 5.18 Examples of evidence for peak shift and stretch A. STN003 -SUTL838 Evidence of peak shift but no evidence of stretch. B. DAL144-SUTL 775 Evidence of both peak shift and stretch.

12D001, 14D004) produced significant improvement in the plateau length, though the weighted mean across the plateau remained the same (fig 5.19). In the case of 14D003-SUTL774 the correction increased the plateau length, but also significantly decreased the calculated ED. An increase in ED was seen in the remaining three samples.

Perhaps unsurprisingly, corrections also significantly improved agreement between individual discs on fading measurements. This was attributed to the long delay in

measurement between G3 and G4 leading to changes in the thermal characteristics of the reader used. Table 5.8 and 5.9 presents full regression results for all Orkney and Shetland data.

a

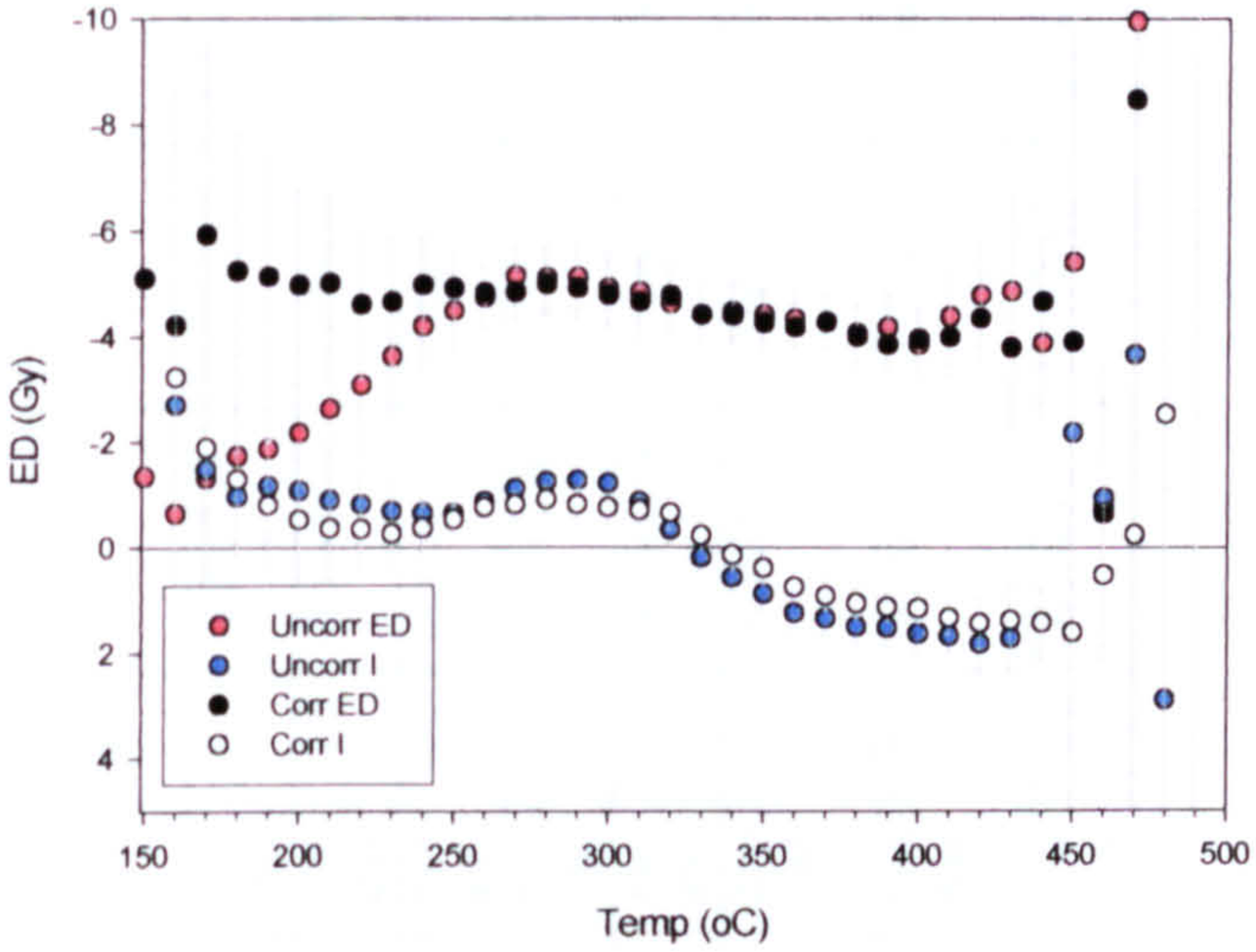

b

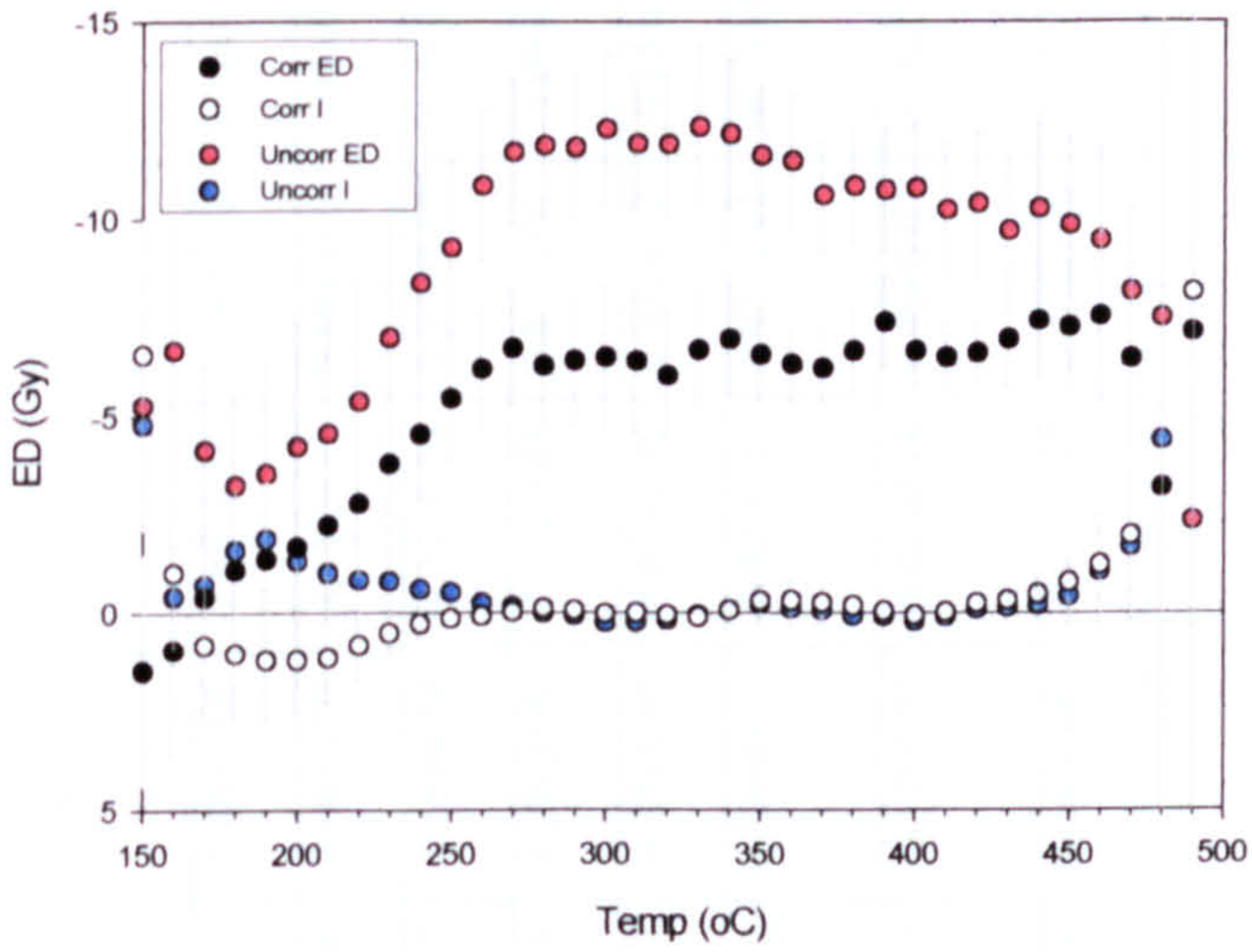

c

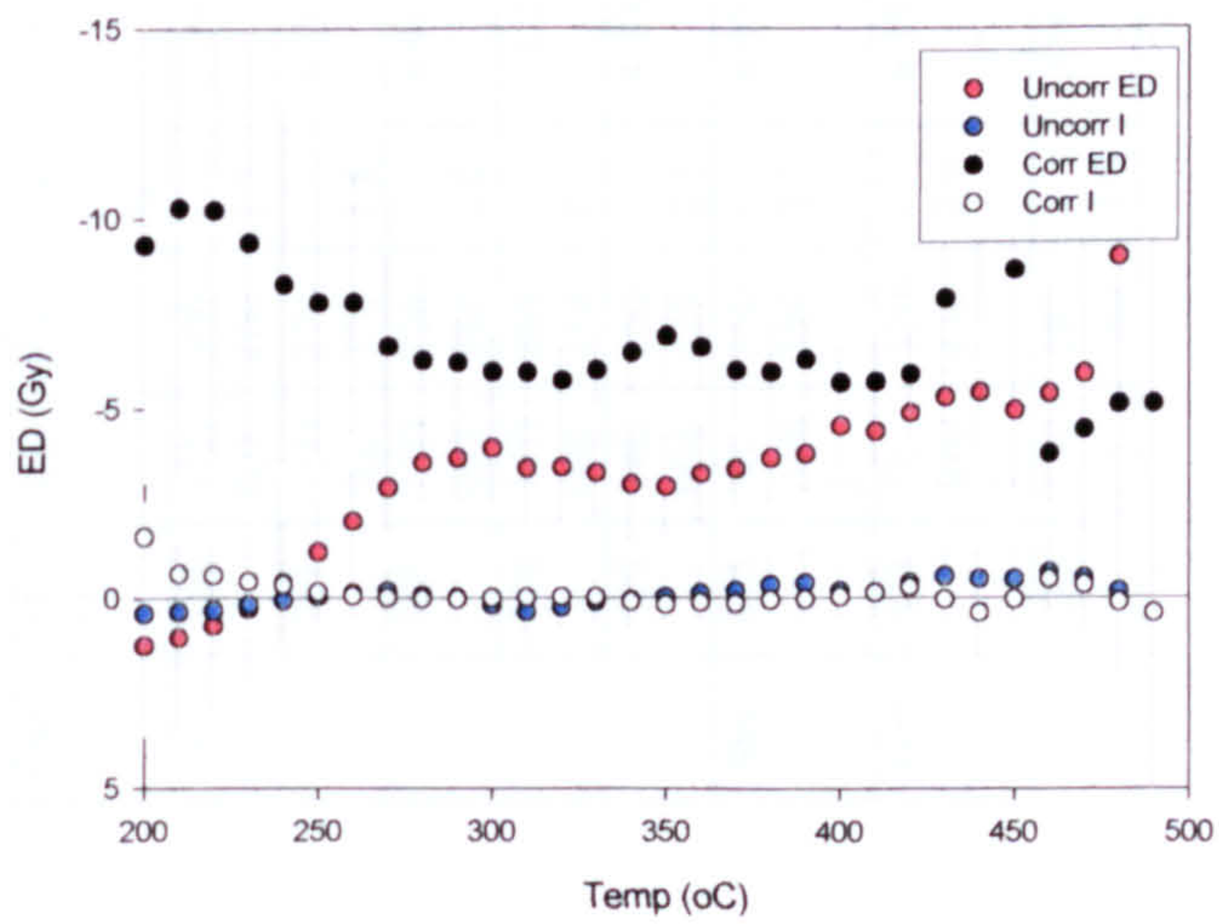

Fig 5.19 Comparison of corrected and uncorrected regression results (a) 14D004 – SUTL775 Improved plateau length, identical ED + I values (b) 14D003 – SUTL774 Similar plateau length, decrease in ED (c) STN003-SUTL838 Improved Plateau, increase in ED

Table 5.7 Uncorrected and Corrected Regression Results from Samples exhibiting peak shift/stretch

			Uncorrected Data							Corrected Data						
Site	SU TL	Run	Plat (°C)	Var %	ED (Gy)	I (Gy)	ED+I (Gy)	$1^{st}/2^{nd}$	I/AD	Plat (°C)	Va %	ED (Gy)	I (Gy)	ED+I (Gy)	$1^{st}/2^{nd}$	I/AD
Dal	750	12D 001	300-400	-1.7	-6.09±0.15	-0.26±0.06	-5.85±0.16	0.84±0.03	0.04±0.02	300-450	-2.7	-6.06±0.24	-0.23±0.04	-5.87±0.24	0.86±0.04	0.07±0.05
	751	12D 002	270-370	-1.8	-4.19±0.16	-0.06±0.07	-4.15±0.17	0.88±0.05	0.01±0.05	270-450	-1.8	-5.13±0.16	-0.03±0.04	-5.16±0.16	0.90±0.06	-0.03±0.07
	765	13D 002	220-380	-3.6	-4.91±0.17	-0.56±0.10	-4.33±0.20	1.07±0.30	0.10±0.06	250-400	-4.0	-6.13±0.33	-0.80±0.10	-5.72±0.35	1.02±0.10	0.06±0.08
	774	14D 003	260-410	-1.5	-11.2±0.44	0.09±0.06	-11.3±0.45	0.87±0.07	-0.00±0.01	250-450	-1.3	-6.15±0.26	0.02±0.03	-6.45±0.27	0.63±0.04	0.01±0.03
	775	14D 004	250-420	-2.3	-4.53±0.14	-0.35±0.06	-4.67±0.16	0.63±0.02	-0.15±0.34	180-400	-1.6	-4.52±0.14	-0.31±0.07	-4.31±0.16	0.61±0.02	0.03±0.19
Ska	815	SK A00 2	260-350	-2.2	-6.65±0.17	0.23±0.07	-6.82±0.22	0.87±0.02	-0.03±0.04	250-500	-2.7	-6.59±0.10	0.35±0.08	-7.03±0.13	0.47±0.05	0.03±0.09
Fers	823	FE R00 1	320-430	-2.9	-6.19±0.17	-0.17±0.07	-6.01±0.18	0.46±0.03	0.03±0.04	260-500	-2.7	-6.23±0.16	-0.12±0.06	-6.10±0.17	0.48±0.17	0.07±0.18
Sten	838	ST0 03	280-380	-3.0	-3.90±0.16	0.04±0.06	-3.93±0.17	0.85±0.09	-0.01±0.02	250-450	-2.2	-6.15±0.25	0.01±0.05	-6.15±0.26	1.04±0.16	-0.00±0.02

Table 5.8 Regression Results Orkney Dataset

Site	SUTL	Run No.	Fad Time (days)	% Fad	Plateau Temp (oC)	Var. (%)	ED (Gy)	I (Gy)	ED+I Gy)	$2^{nd}/1^{st}$ Slope	I/AD	Corrected ED (Gy)
Liddle	1379	LID001	60	0±3	300-450	-1.8	-8.78±0.20	0.10±0.08	-8.76±0.24	0.82±0.14	-0.01±0.07	-8.76±0.24
	1381	1381G1	60	1±2	290-420	-2.0	-9.46±0.34	-0.02±0.07	-9.45±0.35	1.11±0.09	0.0±0.02	-9.54±0.31
	1386	1386G1	60	2±4	300-400	-2.5	-7.69±0.54	-0.54±0.08	-6.96±0.57	0.92±0.08	0.08±0.02	-7.10±0.55
DALE TL12	748	DAL123	60	1±1	350-420	-4.5	-3.87±0.23	-0.01±0.27	-3.86±0.26	0.72±0.04	0.01±0.07	-3.90±0.24
	749	DAL128	30	5±3	300-450	-3.1	-5.99±0.17	1.52±0.35	-7.36±0.30	0.86±0.12	-0.21±0.09	-7.73±0.31
	750	12D001	14	1±2	300-450	-2.7	-6.06±0.24	-0.23±0.04	-5.87±0.24	0.86±0.04	0.07±0.05	-5.91±0.15
	751	12D002	30	5±5	270-450	-1.8	-5.13±0.16	-0.03±0.04	-5.16±0.16	0.90±0.06	-0.03±0.07	-5.36±0.19
	753	12D007	30	5±1	200-400	-3.1	-5.47±0.15	0.17±0.09	-5.62±0.18	0.72±0.17	-0.04±0.05	-5.90±0.22
	754	DAL124	14	5±3	310-430	-1.2	-4.99±0.16	-0.14±0.10	-4.84±0.20	0.65±0.02	0.03±0.05	-5.08±0.25
DALE TL13	760	13D005	120	2±2	320-410	-2.1	-6.10±0.10	0.17±0.09	-6.26±0.07	0.71±0.02	-0.03	-6.40±0.10
	764	13D001	60	0±2	250-400	-2.8	-5.21±0.11	-0.56±0.04	-4.62±0.12	0.69±0.03	0.10±0.07	-4.62±0.12
	765	13D002	30	0±3	250-400	-4.0	-6.13±0.33	-0.80±0.10	-5.72±0.35	1.02±0.10	0.06±0.08	-5.72±0.35
	767	13D004	13	7±2	230-390	-2.4	-4.26±0.15	0.05±0.05	-4.38±0.16	0.41±0.04	-0.02±0.04	-4.69±0.23
DALE TL14	768	DAL146	540	3±4	300-500	-3.4	-4.89±0.14	-0.83±0.08	-4.05±0.16	0.57±0.04	0.17±0.08	-4.17±0.19
	769	DAL142	120	1±1	320-440	-0.3	-4.74±0.12	1.35±0.10	-6.09±0.16	1.12±0.11	-0.40±0.05	-6.15±0.17
	774	14D003	180	0±3	250-450	-1.3	-6.15±0.26	0.02±0.03	-6.45±0.27	0.63±0.04	0.01±0.03	-6.45±0.27
	775	14D004	240	2±2	180-400	-1.6	-4.52±0.14	-0.31±0.07	-4.31±0.16	0.61±0.02	0.03±0.19	-4.36±0.19
	777	DAL147	32	5±3	300-440	-1.7	-4.51±0.13	-0.03±0.04	-4.53±0.15	0.67±0.02	0.01±0.11	-4.76±0.16
	779	779	80	2±1	240-340	-2.0	-6.06±0.13	-0.02±0.09	-6.00±0.16	0.55±0.11	-0.03±0.08	-6.12±0.21
DALE TL15	782	15D001	90	1±2								
	785	15D004	90	1±1	260-410	-1.6	-5.44±0.21	-0.61±0.09	-4.86±0.23	0.82±0.09	0.10±0.02	-4.91±0.25

Site	SUTL	Run No.	Fad Time (days)	% Fad	Plateau Temp (oC)	Var. (%)	ED (Gy)	I (Gy)	ED+I Gy)	$2^{nd}/1^{st}$ Slope	I/AD	Corrected ED (Gy)
Skaill	815	SKA002	240	5±2	250-500	-2.7	-6.59±0.10	0.35±0.08	-7.03±0.13	0.47±0.05	0.03±0.09	-7.32±0.25
	815	SKA008	60	1±1	240-400	-2.1	-5.34±0.33	-0.26±0.06	-5.10±0.34	0.70±0.09	0.06±0.02	-5.15±0.36
	817	SKA010	240	14±6	250-350	-1.1	-6.15±0.16	-0.75±0.08	-5.42±0.21	1.07±0.16	0.14±0.04	-6.18±0.25
	1343	1343G1	60	0±1	240-410	-2.8	-4.04±0.10	-0.15±0.05	-3.94±0.11	0.69±0.11	0.01±0.06	-3.94±0.11
	1360	1360G1	60	1±2	250-340	-4.5	-7.54±0.27	0.05±0.06	-7.59±0.28	0.88±0.05	-0.00±0.01	-7.67±0.30
K. of Mer.	794	MER003	240	7±3	270-380	-2.7	-5.62±0.15	0.14±0.13	-5.74±0.18	0.71±0.04	-0.02±0.04	-6.14±0.16
	795	MER004	240	6 ±1	250-370	-1.7	-6.48±0.14	0.04±0.01	-6.51±0.16	0.79±0.06	0.00±0.02	-6.90±0.15
	802	MER005	30	9±3	300-410	-1.9	-7.77±0.14	-0.10±0.04	-7.68±0.15	0.71±0.14	0.01±0.09	-8.37±0.14
	803	MER006	30	15 ±4	280-450	-1.7	-8.22±0.19	-0.06±0.04	-8.10±0.20	0.80±0.15	0.01±0.02	-9.32±0.20
Warness	842	WAR001	90	-2±3	270-450	-0.7	-9.42±0.13	-0.98±0.05	-8.47±0.17	0.86±0.06	0.12±0.11	-8.30±0.18
	857	WAR004	30	6±2	250-400	-2.7	-5.48±0.18	0.58±0.09	-6.01±0.23	0.69±0.03	-0.10±0.04	-6.37+0.26
Fersness	823	FER001	300	1±2	260-500	-2.7	-6.23±0.16	-0.12±0.06	-6.10±0.17	0.48±0.17	0.07±0.18	-6.14±0.18
	824	FER002	30	8±1	270-400	-3.5	-6.04±0.15	0.08±0.06	-6.10±0.16	0.67±0.05	-0.01±0.03	-6.59±0.21
	831	FER003	90	0±3	240-370	-1.7	-8.52±0.37	-0.08±0.07	-8.50±0.38	0.77±0.06	0.01±0.09	-8.50±0.38
	831	FER005	90	0±2	250-320	-3.5	-5.00±0.50	-0.67±0.07	-4.51±0.53	0.86±0.04	0.15±0.06	-4.51±0.53
Sten.	836	STN005	120	-1±2	270-400	-1.3	-8.64±0.41	-1.50±0.21	-7.70±0.47	0.94±0.14	0.19±0.06	-7.62±0.48
	838	STN003	270	4±3	250-450	-2.2	-6.15±0.25	0.01±0.05	-6.15±0.26	1.04±0.16	-0.00±0.02	-6.40±0.27
	839	STN004	30	1±1	270-450	-4.0	-4.01±0.13	0.11±0.03	-4.10±0.15	0.86±0.11	-0.03±0.03	-4.14±0.16

TABLE 5.9 Regression Results, Shetland Dataset.

Site	SUTL	Run No.	Fad (d)	% Fad	Plateau Temp (oC)	Var (%)	ED (Gy)	I (Gy)	ED+I (Gy)	2nd/1st Slope	I/AD	Corrected ED (Gy)
Cruester	949	CRU021	90	1±2	300-490	-2.0	-7.93±0.15	-0.25±0.04	-7.70±0.17	0.76±0.06	0.05±0.08	-7.78±0.18
	951	CRU022	90	0±2	350-500	-4.2	-6.37±0.18	0.72±0.06	-7.10±0.21	0.64±0.11	-0.09±0.22	-7.10±0.21
	953	CRU023	60	6±3	330-450	-3.1	-8.7±0.68	-0.25±0.17	-8.55±0.70	0.73±0.06	0.04±0.02	-9.06±0.75
	958	CRU024	90	3±1	320-450	-1.6	-7.09±0.21	1.44±0.09	-8.53±0.24	0.85±0.08	-0.24±0.06	-8.79±0.26
	968	CRU025	90	6±3	290-340	-4.5	-6.31±0.82	-0.74±0.28	-5.54±0.88	0.61±0.03	0.11±0.02	-5.87±0.80
	1051	CRU006	120	0±2	270-450	-1.6	-8.55±0.23	1.77±0.33	-10.7±0.42	0.92±0.47	-0.40±0.18	-10.62±0.42
	1051	CRU044	120	0±1	380-440	-1.0	-8.92±0.69	1.76±0.13	-10.7±0.72	0.80±0.02	-0.26±0.03	-10.65±0.72
	1054	CRU029	30	7±5	350-450	-3.5	-5.27±0.29	0.14±0.09	-5.35±0.30	0.65±0.05	-0.01±0.05	-5.72±0.36
	1062	CRU031	90	6±2	350-440	-0.7	-8.15±0.33	1.57±0.14	-9.76±0.37	0.74±0.03	-0.24±0.02	-10.35±0.41
	1068	CRU045	240	0±3	330-500	-1.9	-12.67±1.20	1.70±0.10	-14.2±1.22	0.99±0.08	-0.13±0.04	-14.23±1.22
	1088	CRU034	240	1±4	320-440	-2.2	-8.06±0.35	0.03±0.04	-8.01±0.36	0.81±0.05	-0.01±0.04	-8.09±0.35
	1100	CRU043	240	1±2	220-340	-5.1	-7.55±0.54	-0.22±0.19	-7.30±0.60	0.32±0.13	0.17±0.16	-7.37±0.63
Houlls	970	HL001	60	0±3	320-410	-2.2	-10.94±0.24	-0.55±0.13	-10.4±0.33	0.68±0.04	0.05±0.02	-10.37±0.33

5.3.3.3 Plateau Analysis

The length of the observed plateau varied from sample to sample but was on average between 100-160°C in length (fig 5.20a&b). This variation in plateau length is to be expected due to differences in glow curve shape and past heating. The average plateau region for the Orkney samples is between 270-400°C, with Shetland samples showing higher plateau regions of 320-440°C.

Fig 5.20 Histogram of plateau lengths a. Orkney Dataset, b. Shetland Dataset

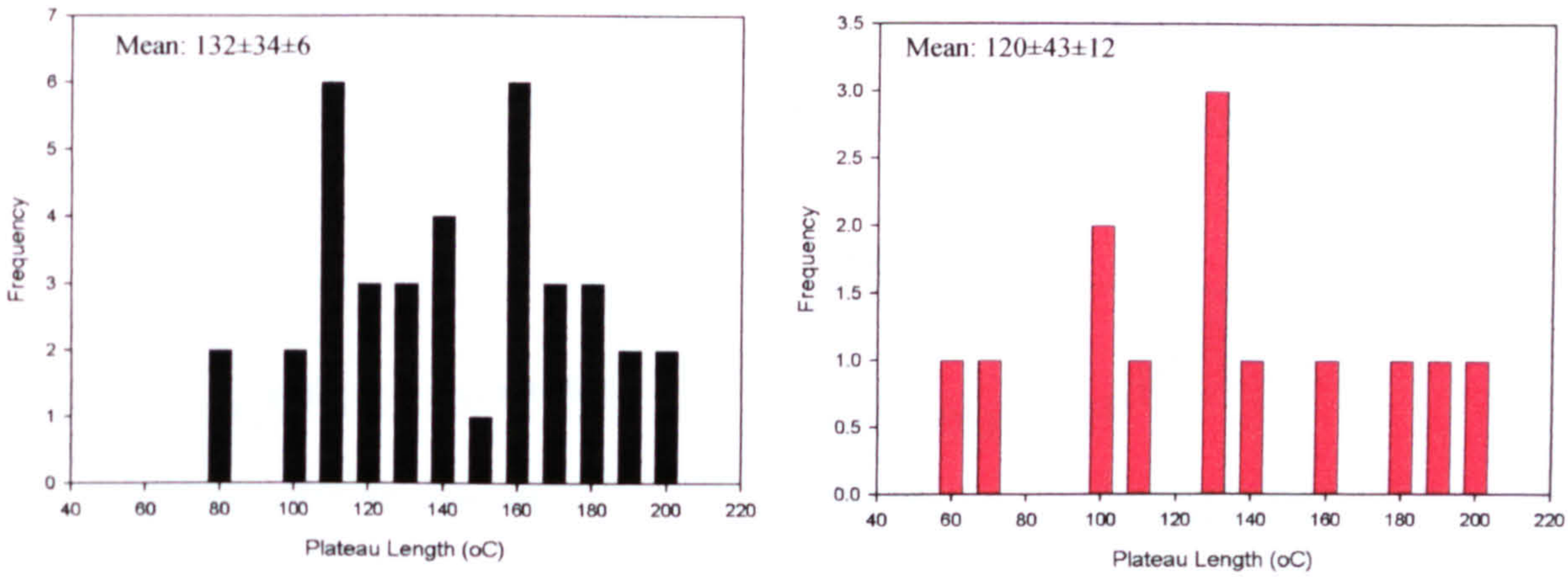

A selection of samples are shown in figs 5.21(i) and 5.22(i) to illustrate the variety in value and plateau shape seen in runs from Orkney and Shetland (full regression plots for samples can be found in Appendix F). In addition, regression lines are shown for ED and I for the integrals over the plateau region, illustrating the sensitivity loss/gain between first and second glow (fig 5.21ii, 5.22ii).

In a number of cases, regression plots show a plateau within the 200-400°C region, with an increase in ED at higher temperatures. This is indicative of poor zeroing of the geological signal during anthropological heating. Samples affected are SUTL 751, 754, 765, 794, 795, 824 and 1100. In such cases, data within the affected area has been rejected from regression analysis and only the stable plateau area used for ED calculation.

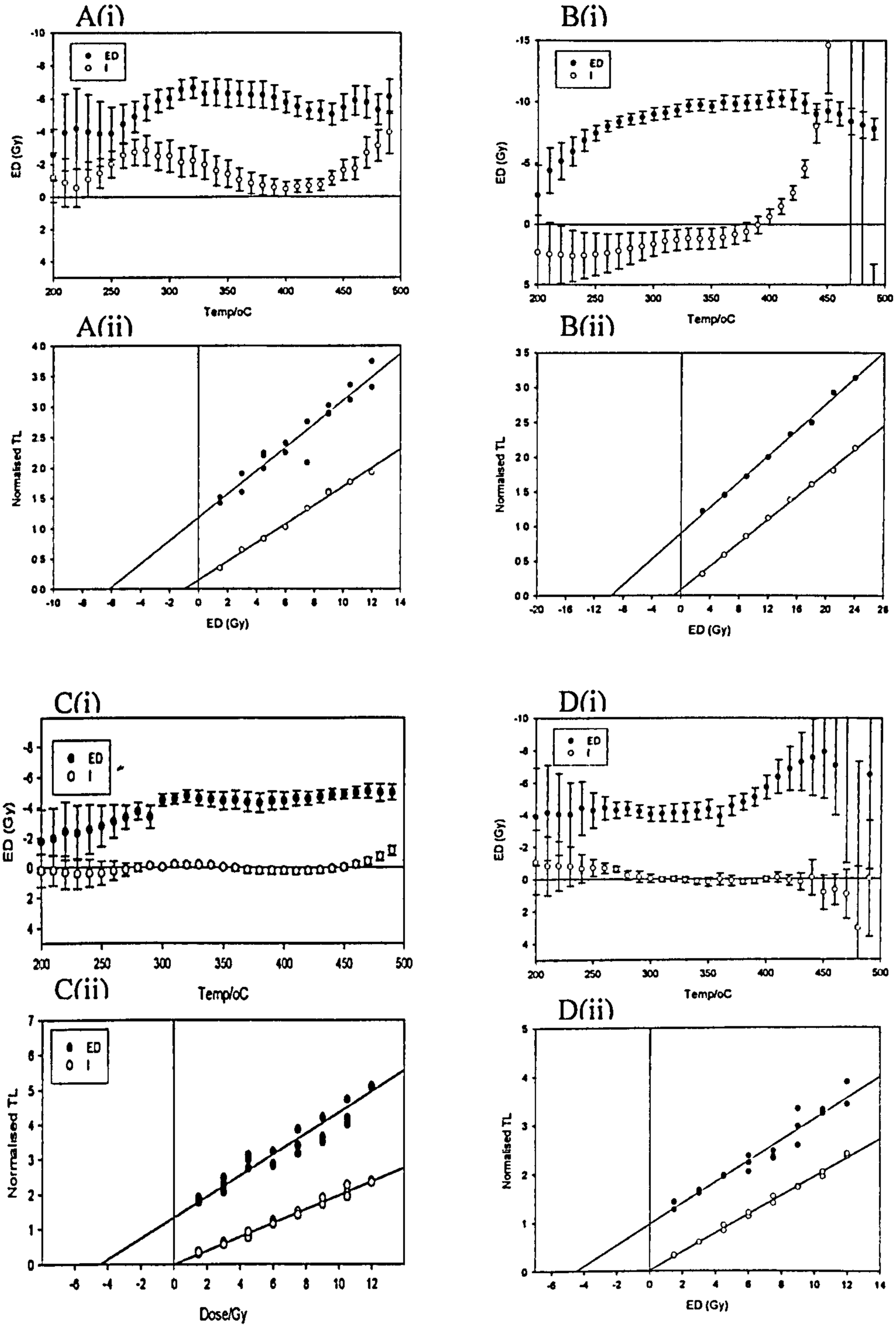

Fig 5.21 Examples of (i) Plateau plots and (ii) regression lines for Orkney Samples (A) STN005-SUTL836 Negative Intercept with poor plateau. Little sensitivity change on second glow. (B) WAR001-SUTL842 Large positive intercept, long ED plateau. (C) DAL147-SUTL777 Zero intercept, good ED and I plateau, 30% decrease in sensitivity from G1 to G2. (D) 12D002-SUTL751 Small negative intercept, ED plateau rises at high temperatures indicating poor zeroing, small loss of sensitivity on third glow.

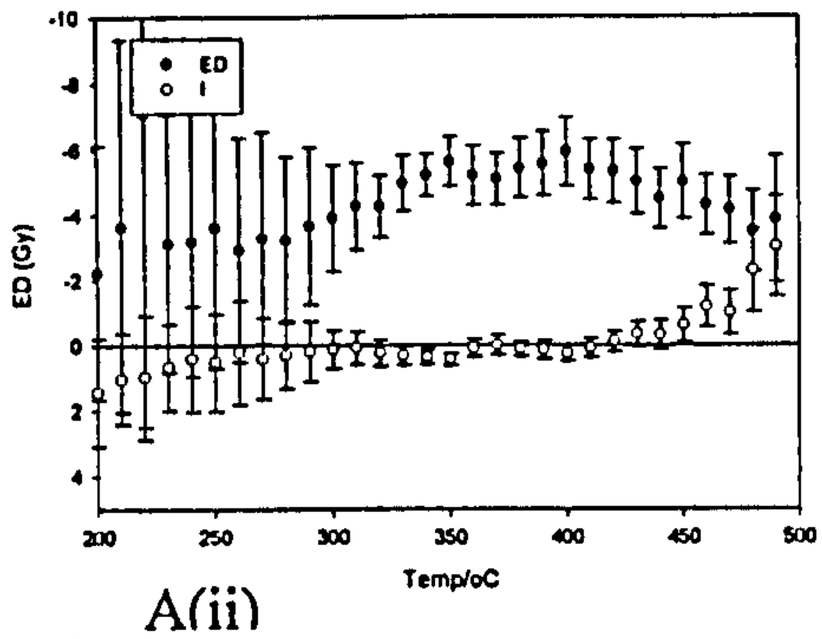

Fig 5.22 Examples of (i) Plateau plots and (ii) regression lines for Shetland Samples (A) CRU029-SUTL1054 small positive intercept, scatter on individual ED regressions, 35% loss in sensitivity between first and second glow. (B) CRU034-SUTL1088 Zero intercept, scatter in precision of ED plateau, loss of sensitivity on second glow. (C) CRU021-SUTL949 Small negative intercept, good ED plateau (D) HL001-SUTL970 Large negative intercept, variable ED plateau, 30% loss of sensitivity between glow 1 and 2.

5.3.2.4 Sensitivity Changes

As outlined above, by comparing the ratio of G2:G1 regression slopes it is possible to investigate the sensitivity change a sample has undergone from first to second glow. Values <1represent a decrease in sensitivity between first and second glow, values >1 an increase.

Fig 5.23a and b show histograms of the sensitivity change over the selected plateau region for each run. It is clear that with two or three exceptions the all samples show a significant loss in sensitivity, up to 70% in some cases.

Fig 5.23 Histogram of Sensitivity change between first and second glow a. Orkney Dataset; b. Shetland Dataset

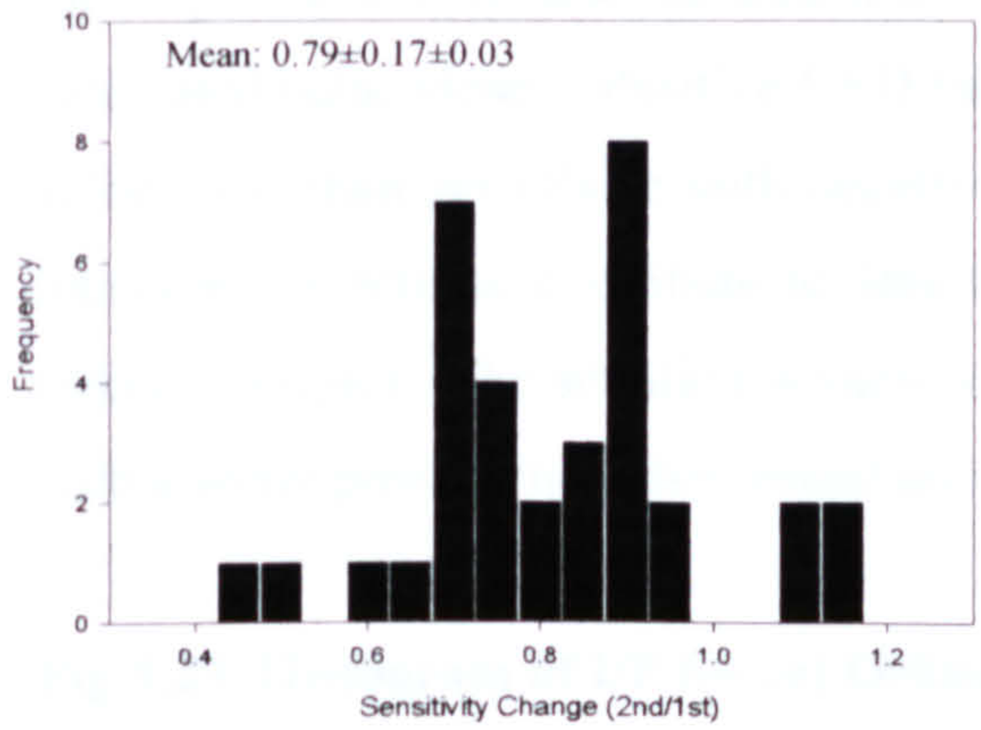

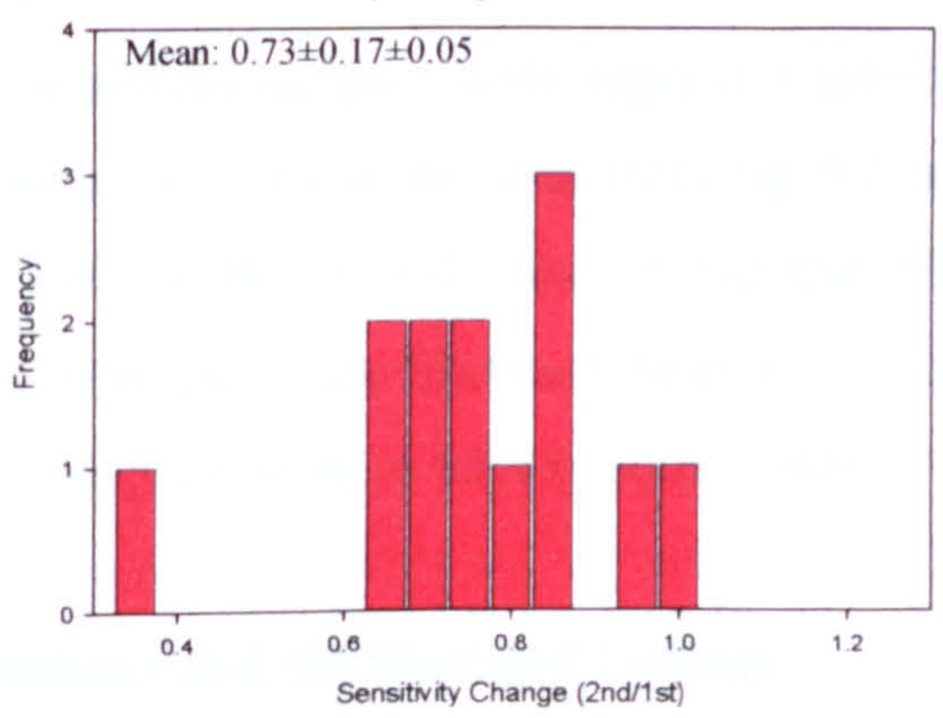

5.3.2.5 Intercept Values

Second glow regression gives an intercept value for each glow curve. In theory this value should be zero, however, as outline in chapter 3 a number of processes may cause positive or negative intercept values such as supralinearity and/or dose dependant sensitivity changes post first glow irradiation.

A histogram of intercept values for the Orkney dataset (fig 5.24a) shows that the majority of values are at or about zero, however there is a significant spread either direction of zero in the values of I obtained. Fig 5.24b shows the intercept values for the Shetland dataset. A large proportion are significantly higher than zero.

Fig 5.24 Histogram of Intercept values for (a) Orkney dataset and (b) Shetland Dataset

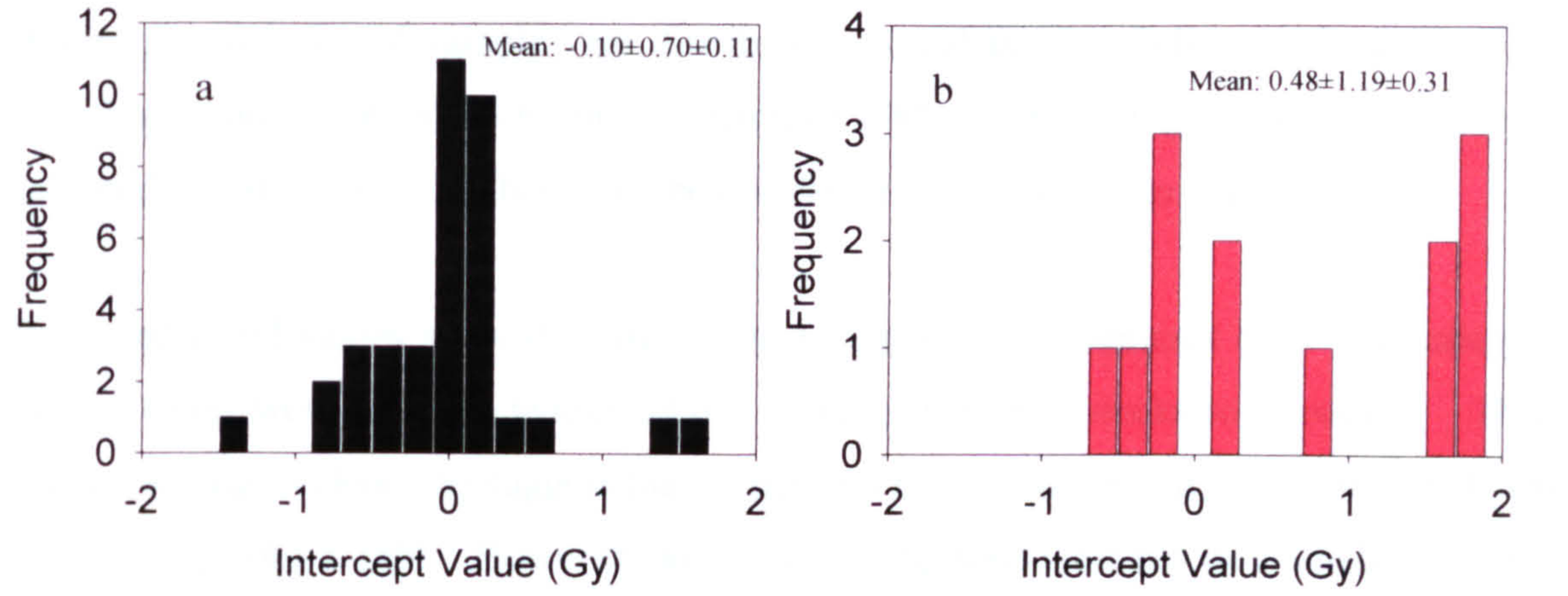

Intercept value may also be examined in terms of the contribution they make to the calculated palaeodose. Positive I/AD values represent samples with negative I intercepts, values less than zero those with negative intercepts. It can be seen from fig 5.25a that intercept corrections contribute to less than 10% of the overall dose in the majority of Orkney samples. The situation is significantly different in the Shetland dataset (fig 5.25b), with a wider positive/negative spread and contributions of up to 40% in some cases

Fig 5.25 Histogram of I/P for (a) Orkney Dataset and (b) Shetland Dataset

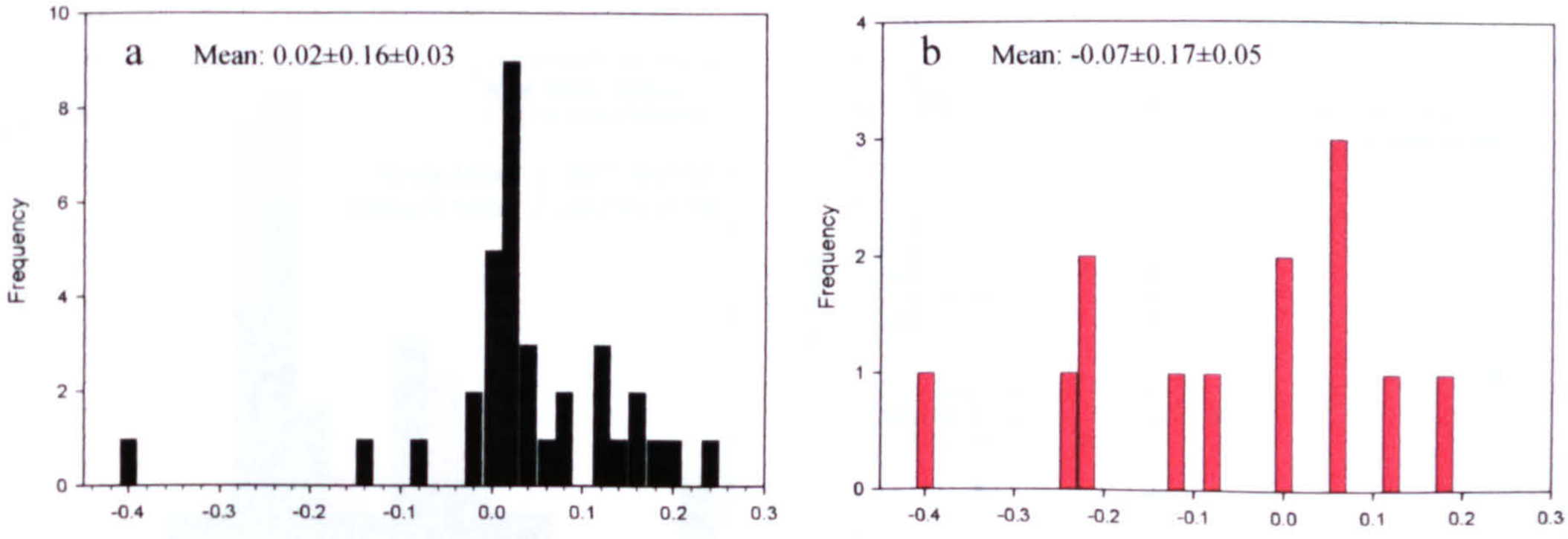

5.3.3.6 Fading

With the exception of three samples, observed fading was less than 10%. However, examination of fig 5.26a shows a bimodal distribution in the distribution of fading results. Whilst the majority of samples are distributed around the 2% fading mark, a small but significant number show fading in the region of 6-8%. This sub-group of samples is not confined to a single site, neither can it be correlated with a particular geology.

Corrected ED+I values showed similar plateau regions to uncorrected data. A variety of storage times were used for fading delays, ranging from two weeks to 8 months. There was no strong evidence to suggest that larger percentages of fading were correlated with longer delays (fig 5.26b). However, additional fading tests were run on a small number of samples to investigate the effect of prolonged storage on the fading ratio obtained.

Six samples were selected from the Orkney dataset and repeat fading measurements of shorter and longer durations carried out (fig 5.27). In only one case (FER002-SUTL824) was a significant increase in fading seen over the extended time period. All other samples with the exception of MER006-SUTL803 showed little or no increase/decrease in measurable fading. In the case of MER006, the percentage fading originally measured (15%) could not be reproduced on repeat measurements, leading to the conclusion that the first set of fading discs may have inadvertently been exposed to light during storage.

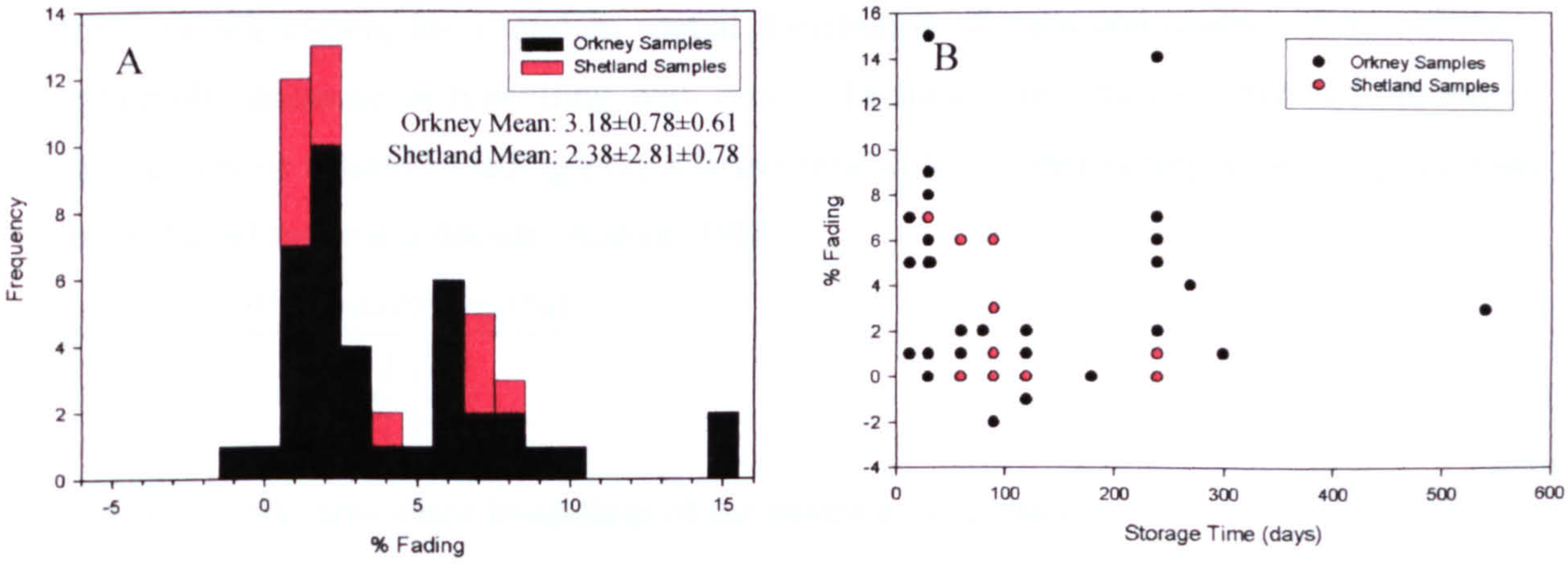

Fig 5.26 A Histogram of Fading results for Orkney and Shetland Dataset. B. Fading results in relation to storage time.

Fig 5.27 Repeat Fading Test Results

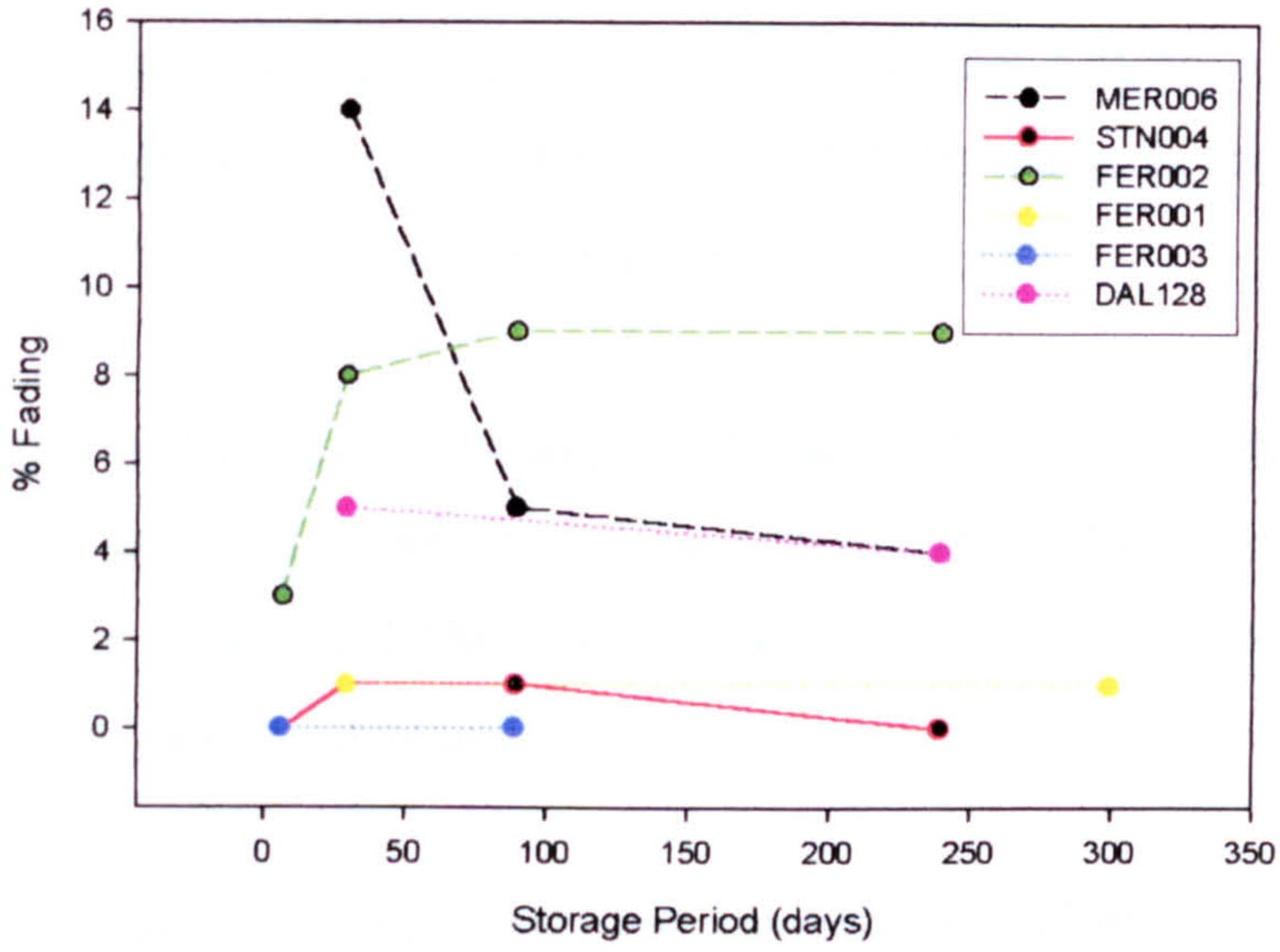

It is clear that the direct short term fading corrections outlined above do not take account of any subsequent fading that may occur over a longer timescale. The difficulty in projecting fading further back than a measurable timescale, is in the determination of the rate of fading with time. Certainly a linear rate could not be sustained.

One consequence of quantum mechanical tunnelling models of fading (Visocekas et al, 1976), is that due to a decrease in the probability of electron escape with increasing trap/hole separation, for a random spatial distribution of traps and centres, there will be a hyperbolic decrease in tunnelling with time. In such a system, the observed laboratory fading may be related to fading over a larger timescale by determining a factor 'g', defined as the % fading over a decade (Aitken, 1985).

g is thus: $\frac{ObservedFading(\%)}{\log\left(\frac{T_s}{T_p}\right)}$,

where T_s is the time since irradiation of the stored measurement

and T_p is the time since irradiation of the prompt measurement.

For each order of magnitude difference in years, the sample should exhibit g% fading. However, the amount of fading observed will also depend on the dose rate administered to the sample. If the magnitude of difference between dose rates encountered in burial environment and in the lab is significant, it can be shown that a sample T years old, irradiated over a long period (T) at low dose rates will exhibit the same % fading as a sample T/2.7 years old irradiated over a laboratory time scale (Aitken, 1985).

As the total amount of fading is dependent on t^{-1}, for archaeological timescales, the total % fading sample to sample will be strongly dependant on g, and be little affected by age variation of several 1000 years. As such, correction for dose rate will have only a small effect on the % fading calculated.

Huntley and Lamothe (2001) and Lamothe et al (2003) have recently developed a correction method based on the above observations, which combines these factors to produce a correction equation for young samples:

$$I_f = I_o\left[1 - g\log\left(\frac{1}{e}\frac{D_{lab}}{D_{soil}}\right)\right]$$

Encouraging results have been reported in both these papers and more recently Balescu et al (2003). However Auclair et al (2003) have highlighted the difficulties in accurately measuring g-values, reporting both over and underestimations, and a dependence on preheating. As Aitken's model does not take account of the likelihood of the rate changing during the extrapolation process such corrections may be unwise.

Whilst it would be possible to calculate g values for the Orkney and Shetland dataset based on the fading results obtained, present evidence suggests that without further detailed measurement the values obtained may be highly inaccurate. As such, short- term fading results were used as a direct correction, with the implication that the ages reported would be minimum ages for the samples.

5.3.4 Further Analysis

5.3.4.1 Dose Distribution

Dose distribution of 24 disc runs was investigated as outlined above for F1. The vast majority of samples conformed to a gaussian distribution about the mean, and were in excellent agreement with 24 disc regression results (fig 5.28). The excess scatter seen in ED regression was reflected in the width of the distribution, the histogram of I results being much more tightly confined. On occasion however multimodal distribution was observed. This could not be attributed to a single contaminated disc. On occasion, where regression results indicated incomplete zeroing of the sample, bimodal distribution in the modelled run was noted (e.g fig 5.28c). In other cases no simple explanation was found. It is possible in these cases that heterogeneity of the sample may be an issue.

5.3.4.2 Dose Dependent Sensitivity Change

The presence of a negative intercept on a number of runs is non-physical and suggestive of a dose dependent sensitivity change (DDSC). A DDSC is known to occur in some samples as a result of prior irradiation. In such a case, discs would have had an uneven prior dose at the time of G2 irradiation. This would in effect change the gradient of any regression line, with D1 in any set being subjected to a smaller change than D8. Depending on whether the sensitivity change is an increase or decrease, this would skew the regression line towards a positive/negative intercept. As can be seen from fig 5.29, although the sensitivity change increases/decreases linearly with disc no/ G1 dose, the effect of reversing doses administered on G2 is to produce an arced G2 response. Regression through all points yields a line with the same gradient, but a higher/lower intercept.

It is presumed that any dose-dependent sensitivity change (DDSC) is cumulative with respect to past radiation exposure received by the sample, thus by Glow 3, all discs should have had equal pre-doses (N+13.5Gy) and therefore exhibit similar sensitivity.

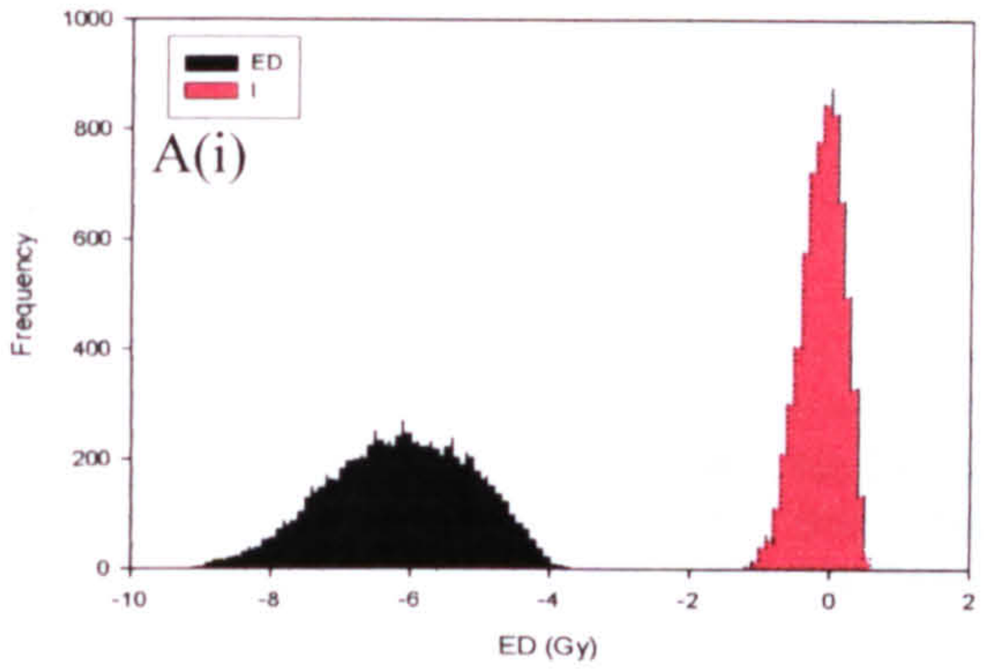

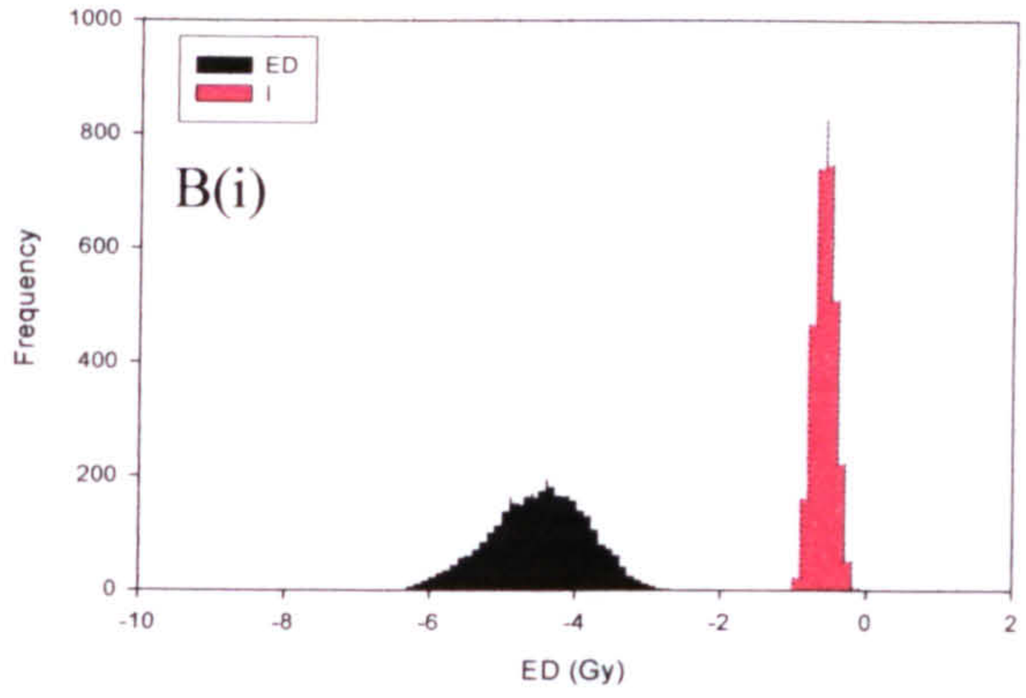

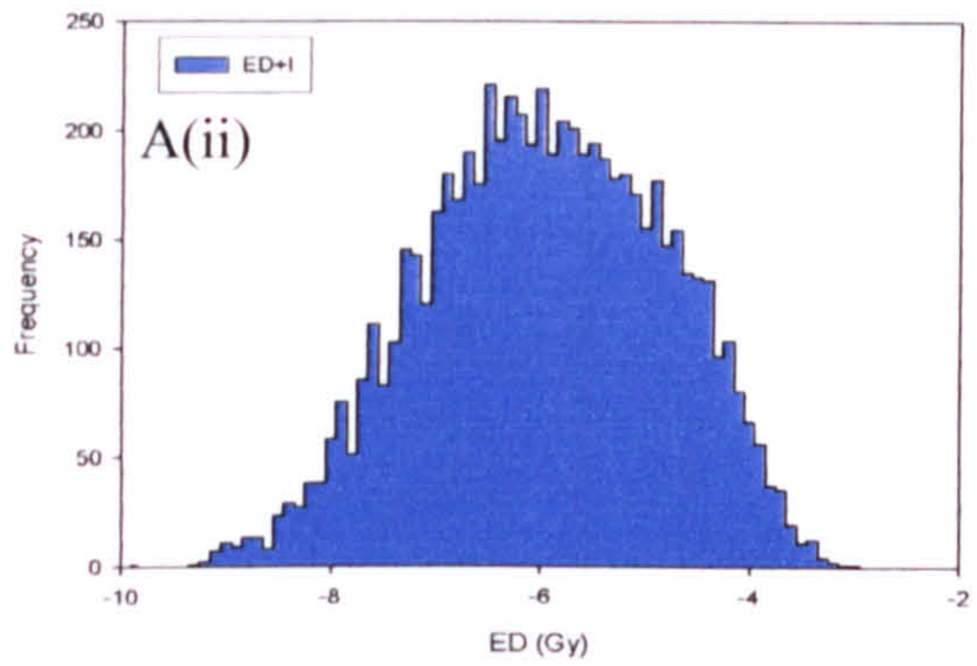

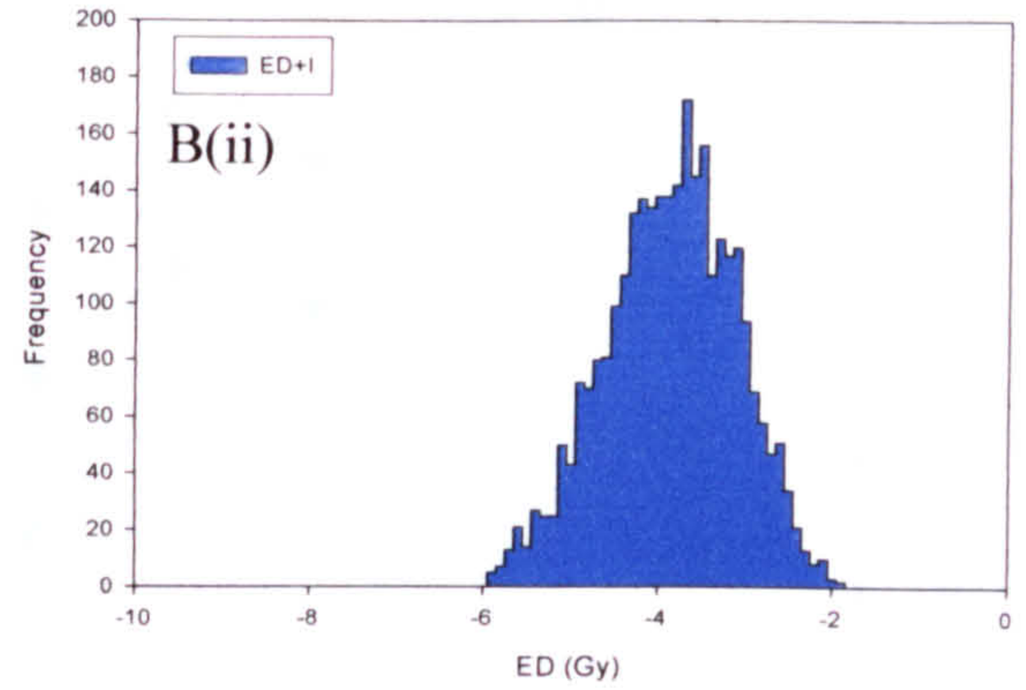

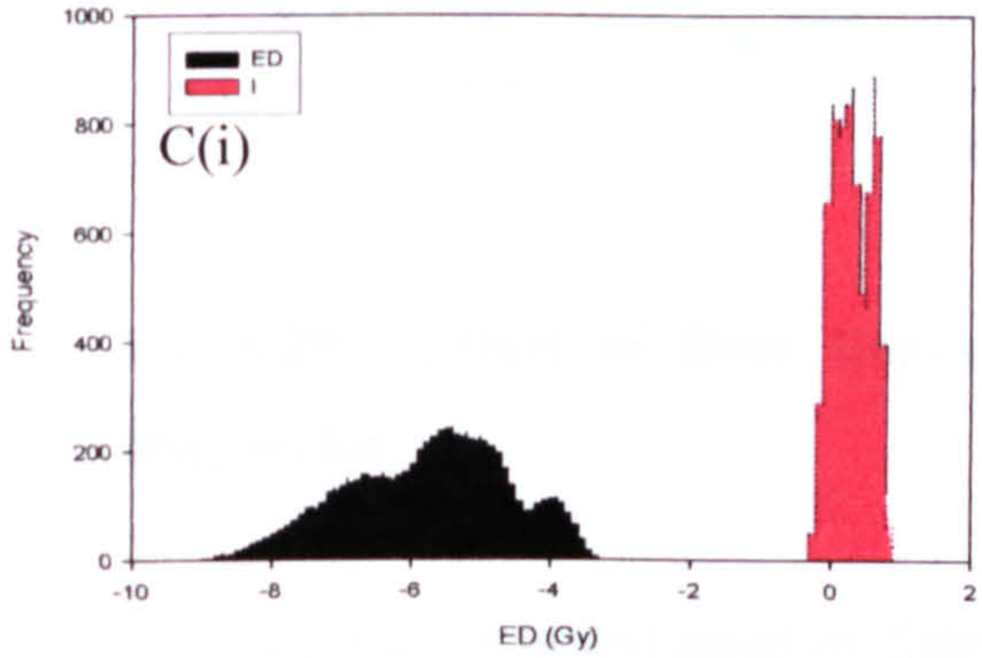

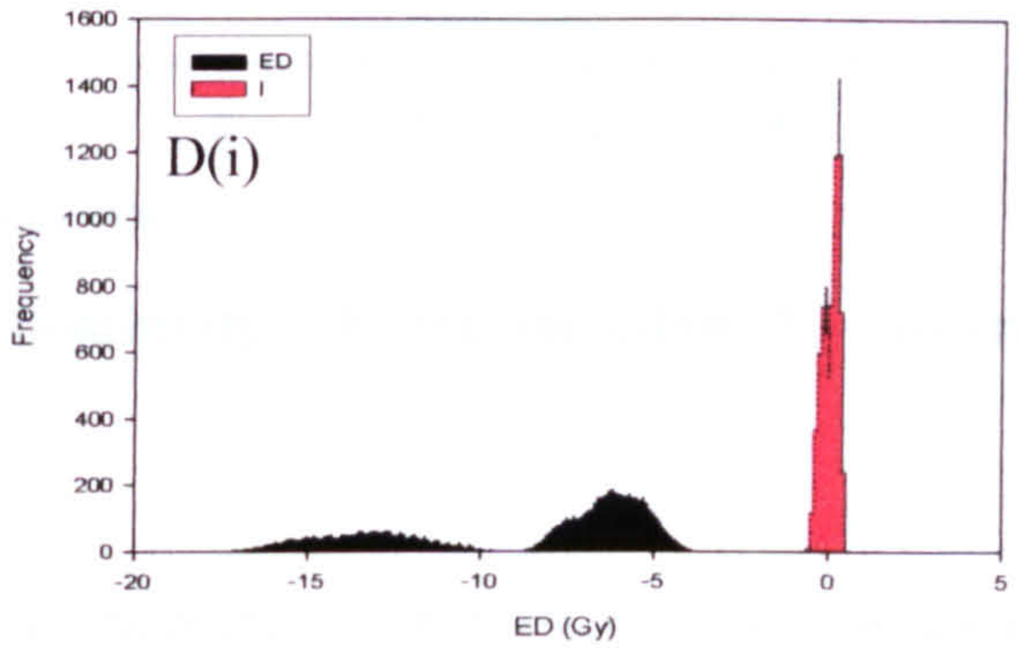

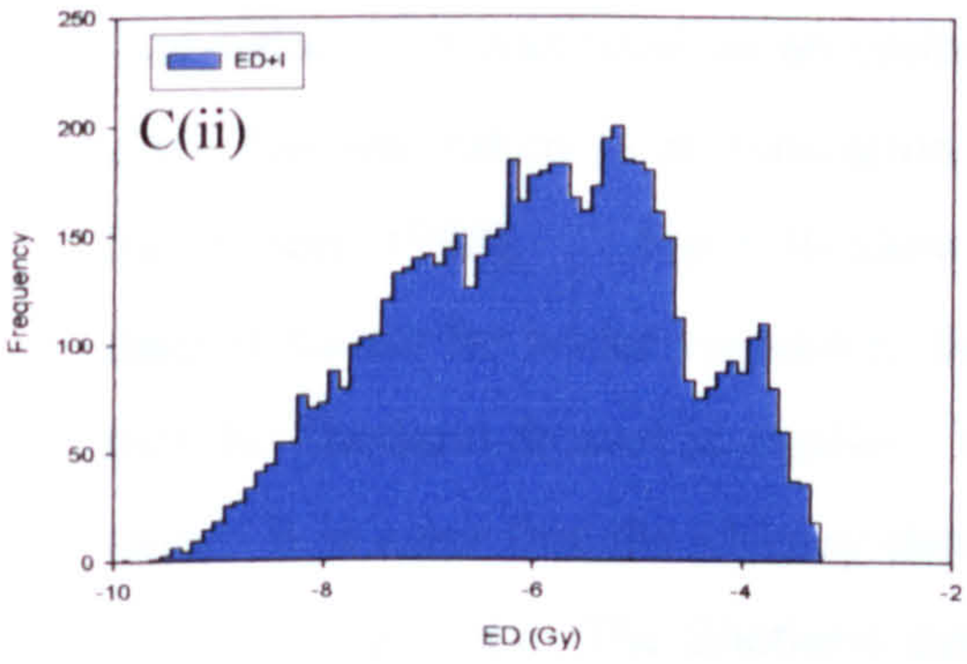

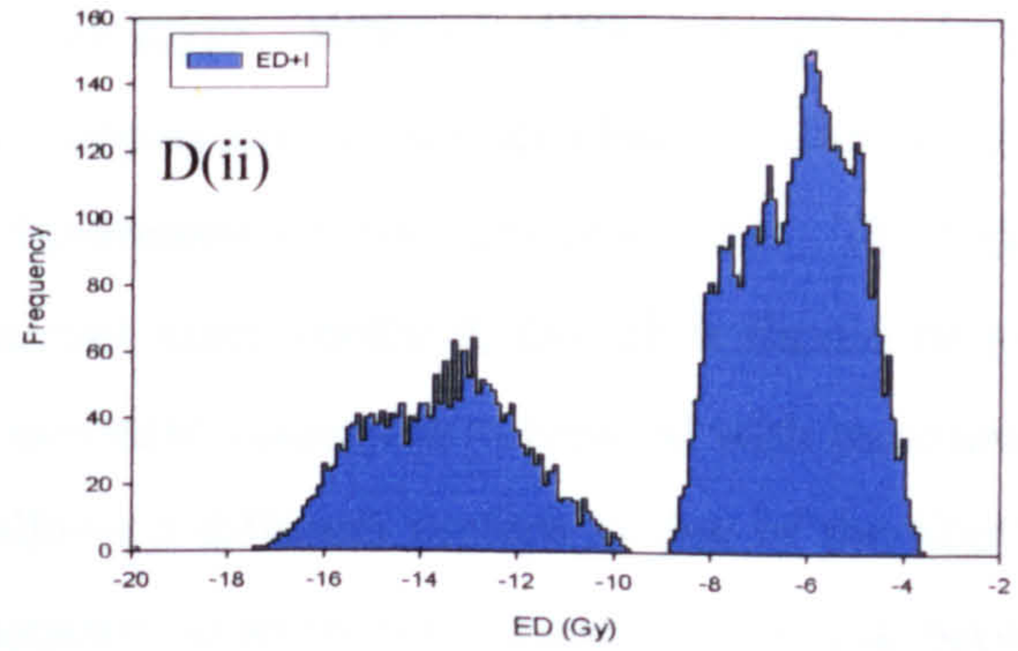

Fig 5.28 Multiple 8 Disc regression results (i) ED and I values (ii) ED+I (A) FER001-SUTL823 Gaussian distribution, Intercept value zero. (B) 13D001-SUTL764 Gaussian Distribution, negative intercept. (C) MER003-SUTL794 Three distinct ED distributions. I values variable, ED+I Three distributions less distinct. (D) FER002-SUTL823 Intercept gaussian distribution centred on zero. ED two distinct distributions, ED+I also 2 distributions.

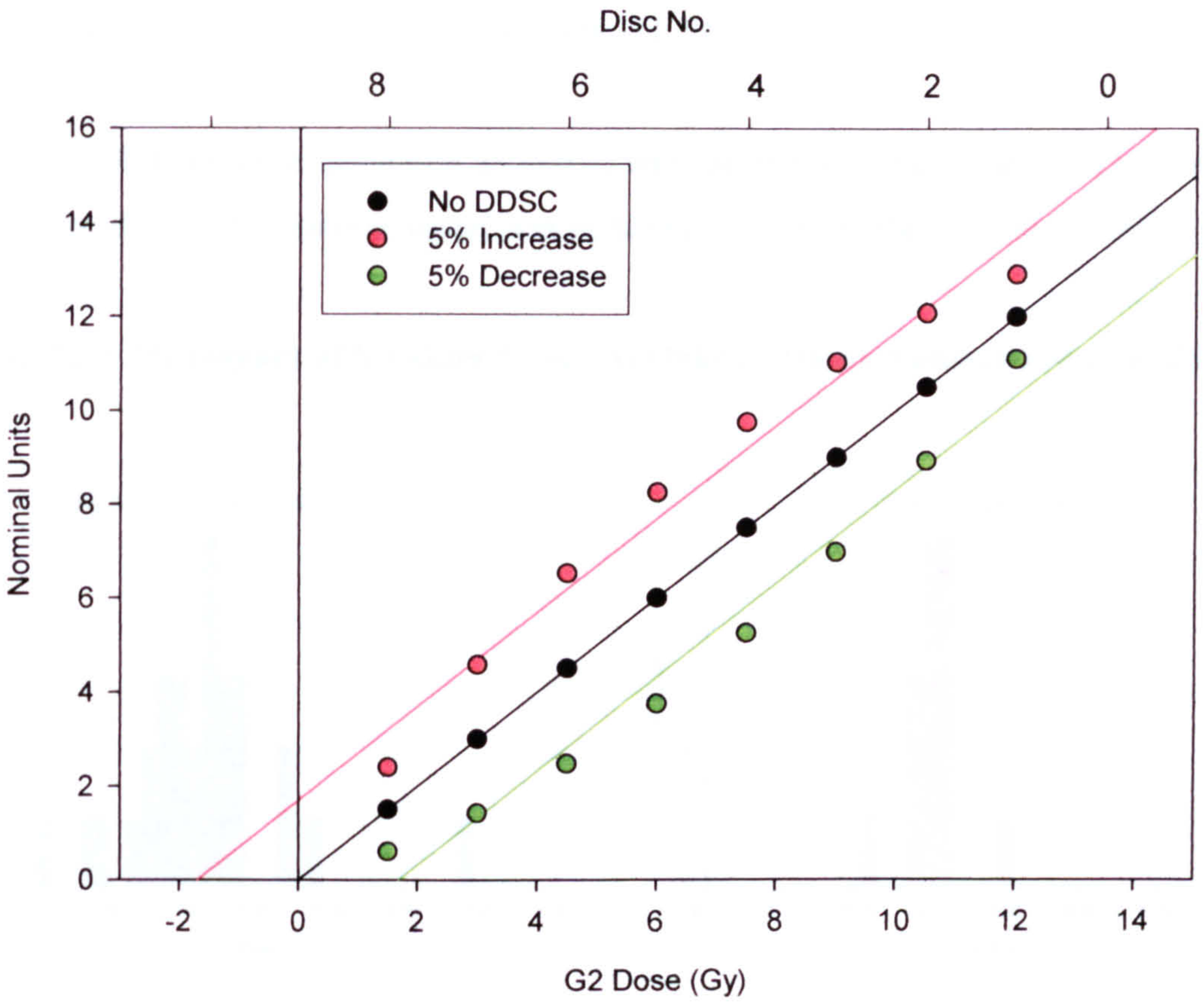

Fig 5.29: Effect of Dose Dependent Sensitivity Change on Glow 2 – Intercept Regression

This was further investigated by fitting a non-linear regression ($y=y_o+ax+bx^2$) to the data. The value of b was used as an estimate of curvature. Where b differs significantly from zero, this was taken as an indication of dose dependent sensitivity change (after Scott and Sanderson, 1988). Fig 5.30 shows the distribution of b-values observed. The Orkney dataset shows far wider variability than samples from Shetland, though it should be noted that the Shetland dataset is smaller. When intercept values are compared with measured b-values it is clear that the Orkney dataset follows a different pattern to that of the Shetland samples (fig 5.31). The Shetland dataset appears to show no indication of a link between curvature and intercept value, indeed no samples show b- values significantly different from zero indicating that the linear fit is appropriate to the regression. Orkney samples on the other hand show evidence of a linear if somewhat scattered relationship between curvature and intercept value, despite the values of b not being significantly different from

zero. It was therefore decided to further investigate a selection of samples from the Orkney dataset by re-measuring intercept values in a way not susceptible to DDSC.

Sets of 8 discs were dispensed as before and run in the same manner. However, prior to first irradiation, the natural signal was removed by heating the sample to 500°C. This in

Fig 5.30 Histogram of b-values from (A) Orkney Dataset and (B) Shetland Dataset

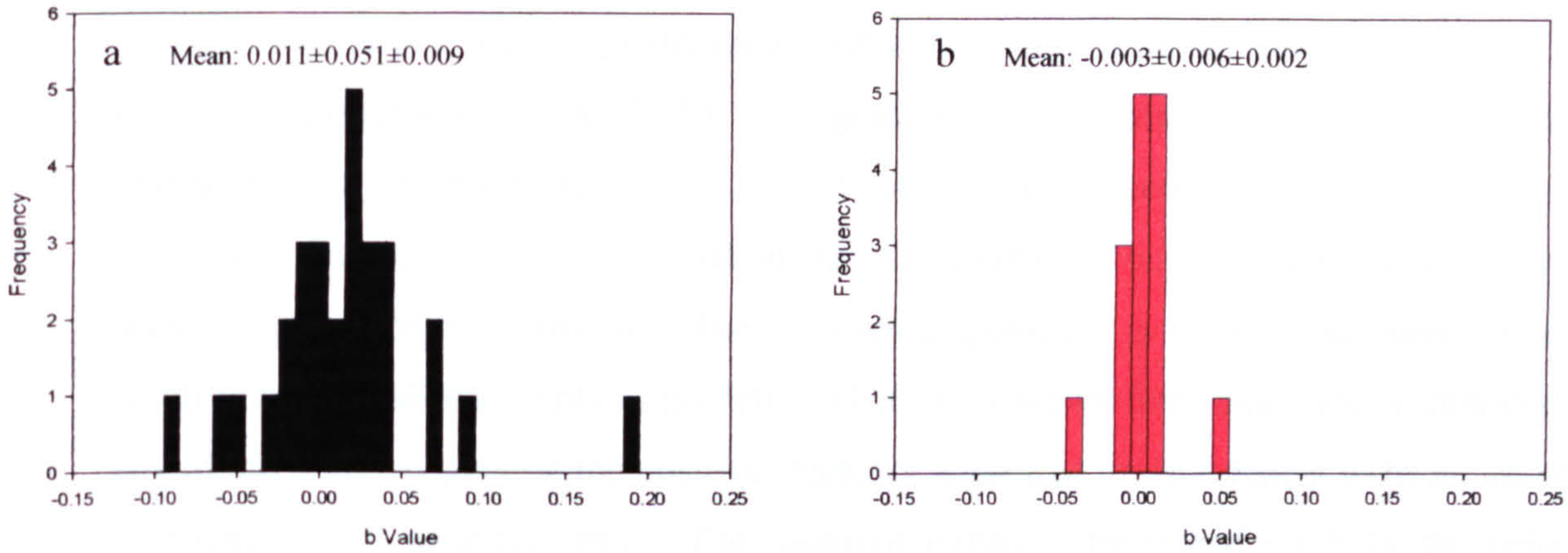

Fig 5.31 Comparison of Intercept values in relation to calculated 'b' values for Orkney and Shetland Dataset

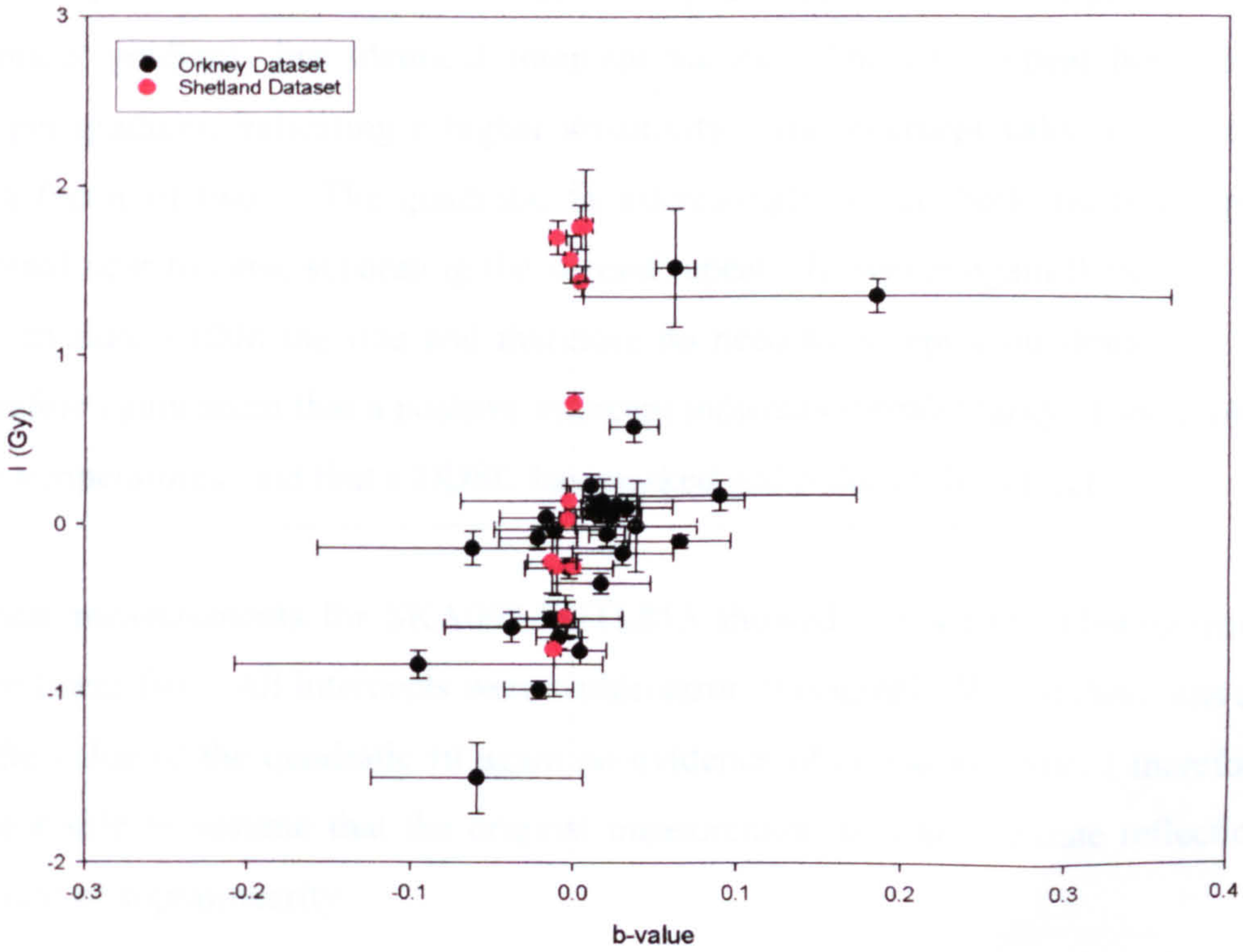

effect produced a run which gave two estimates of intercept value, one which should not be susceptible to DDSC, one which would suffer the same conditions as the normal runs.

Three samples were chosen which reflected the range of intercept values seen within the Orkney dataset, WAR001, WAR004 and SKA002, large negative, positive and near zero intercept respectively. It was expected that the second repeat regression would be in good agreement with the intercept regression from the original runs.

WAR001-SUTL842 was originally measured with a large negative intercept (-0.98±0.05). Repeat measurements showed that the gradient of 2nd and original were identical, indicating similar sensitivities (fig 5.32). However, the intercept value of the 2nd repeat was lower than the first, though within statistical error. The 1st repeat showed a lower sensitivity, but gives a positive value. When a quadratic is fitted to all three lines the result is to shift all intercepts to the left. There is however little evidence of curvature in any of the lines, suggesting the positive intercept measured on first repeat to be an accurate measurement of supralinearity. The negative intercept measured on both the original dataset and second repeat would therefore appear to be attributed to a dose dependant sensitivity change, and follows the predicted similar gradient as discussed above.

For sample WAR004-SUTL857 second repeat regression and original have not only identical gradients but identical intercept values. The first repeat however showed a steeper gradient, indicating a higher sensitivity. The intercept value was likewise higher by a factor of two. The quadratic fit interestingly forced both the first repeat and the original near to zero, separating the second repeat. However again there was no evidence of curvature within the line and therefore no need to accept a quadratic fit. It would therefore again seem that a positive intercept indicates supralinearity of the growth curve at low temperatures, and that a DDSC has masked and reduced this effect.

Repeat measurements for SKA002-SUTL815 showed a gradient indistinguishable on all three linear fits. All intercepts were within error of original. Whilst there was a difference in the value of the quadratic fit again no evidence of curvature existed therefore it would appear safe to assume that the original measurement was an accurate reflection of small amount of supralinearity.

Fig 5.32 Repeat intercept measurements from Orkney samples (a) WAR001-SUTL842 Negative intercept on original and second repeat regression. First Repeat regression positive and near zero with quadratic fit. (b) WAR004-SUTL857 Positive intercept on original and second repeat regression. First regression larger positive with linear fit, near zero with quadratic. (c) SKA002 – SUTL815 Good agreement between all three regressions on linear fit. Original and first regression identical with quadratic fit, second regression negative.

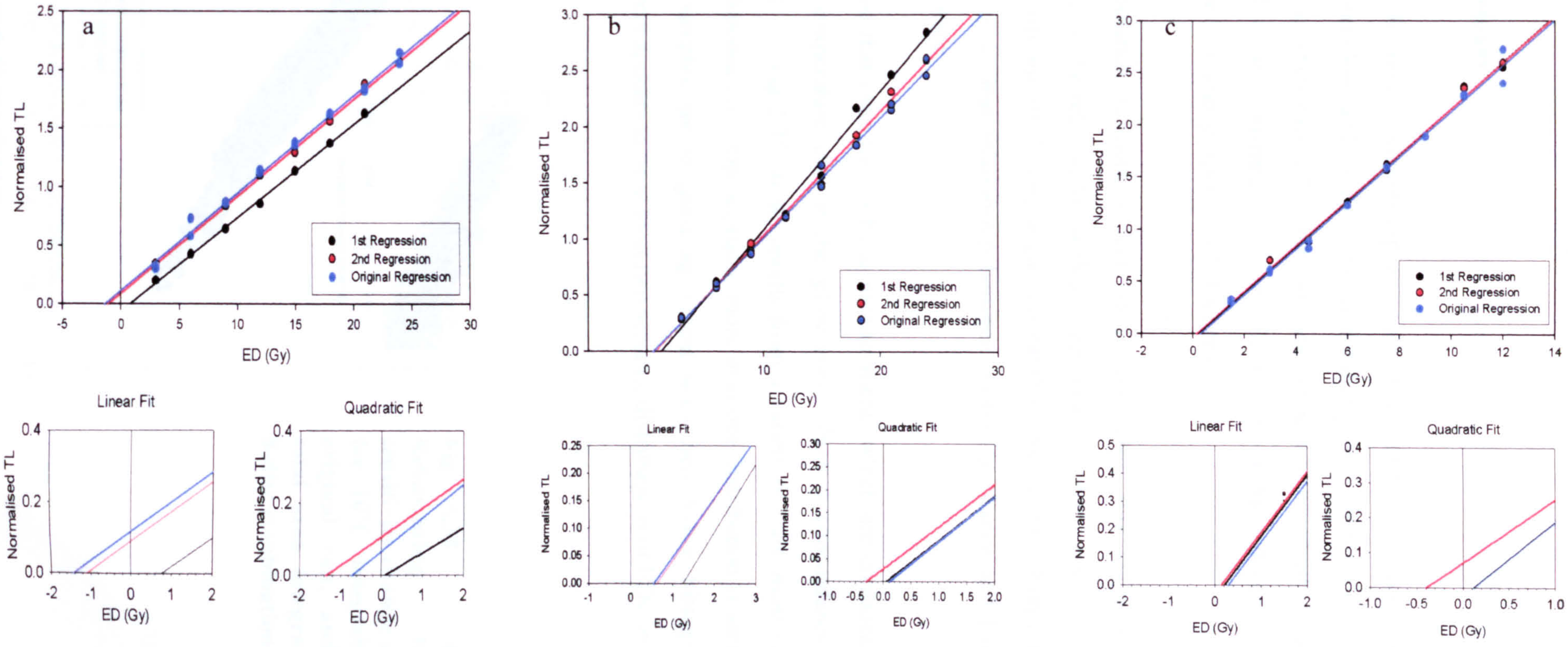

5.3.4.3 Sensitivity changes

During routine data collection, a relationship was noted between the change in sensitivity between first and second glow, and the ED obtained for that glow. This was first noted on individual glow curves, when each 10°C integral measurement of sensitivity change was plotted against ED. It is best illustrated in the F-1 dataset due to the reduced scatter (fig 5.33) but was observed in a large proportion of other runs.

Where 8 disc combination histograms had been constructed, this allowed for the opportunity to investigate the relationship with a larger dataset of 6561 points. Fig 5.34 shows these together with the 10°C integral plot for 14D006 –SUTL768. Both follow the same pattern describing a clear relationship between sensitivity change and ED which appears non-liner in nature.

It is interesting to note that even the outlying measurements which are considerably off plateau at the high temperature end of the glow curve show a concordance in the relationship described. Fig 5.35 shows results from a variety of runs, most of which conform to a single distribution. On occasion, more than one distribution is seen in the scatter plot – such samples are in good agreement with their 8-disc histograms of distribution. Again there appears to be at least two separate distributions of EDs present.

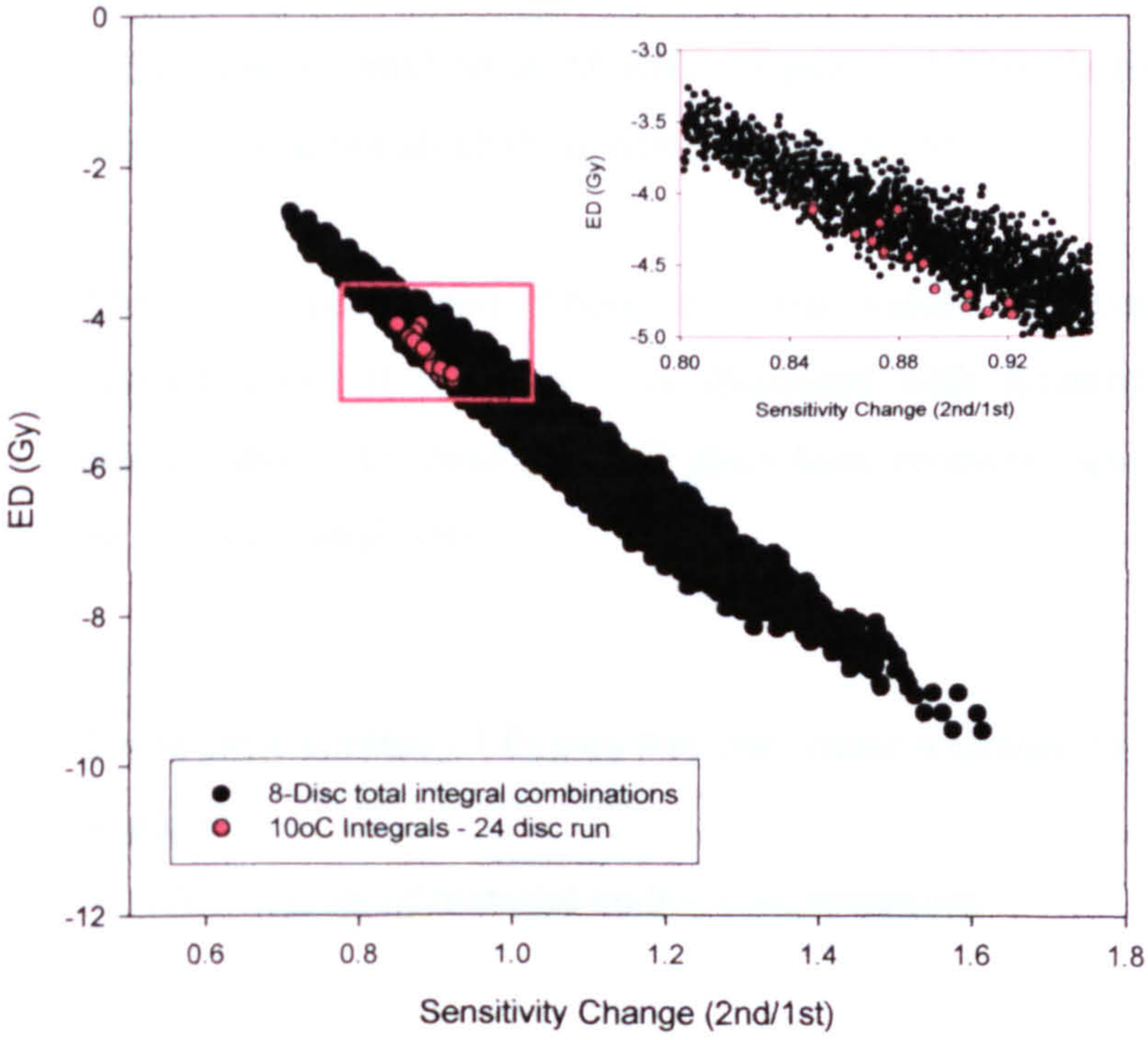

Fig 5.33 FSP010 Relationship between sensitivity change and ED for 10°C integrals from original run, and from total area integration of 8-disc combinations.

Fig 5.34 14d006-SUTL768 Relationship between sensitivity change and ED calculated in 10°C integrals.

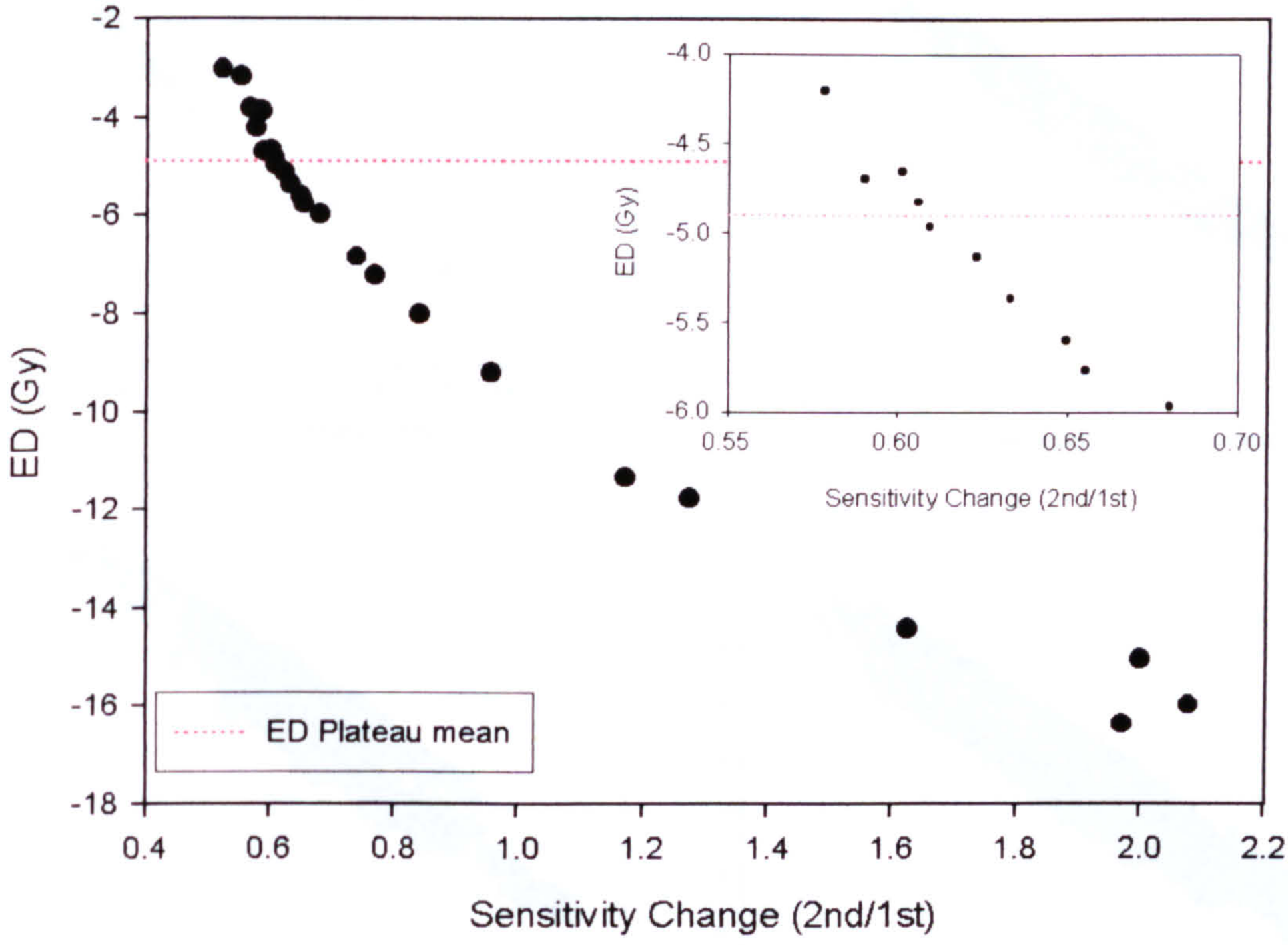

The relationship outlined above is interesting and difficult to interpret at present. The calculated ED value of a sample should be independent of sensitivity change through additive methods. A survey of evidence from similar feldspar dating runs from other burnt mounds studied at SURRC (Spencer, 1996) shows the effect to be present in the majority, but not all of these runs also (fig 5.36).

The only mechanism where the two values are connected is through third glow normalisation of the data. As discussed with reference to dose dependant sensitivity change above, by third glow all discs have received equal predoses, thus are presumed to be of equal sensitivity.

There are a number of factors that may cause a change in sensitivity of a sample from glow to glow:

(i) Loss of material and/or contamination

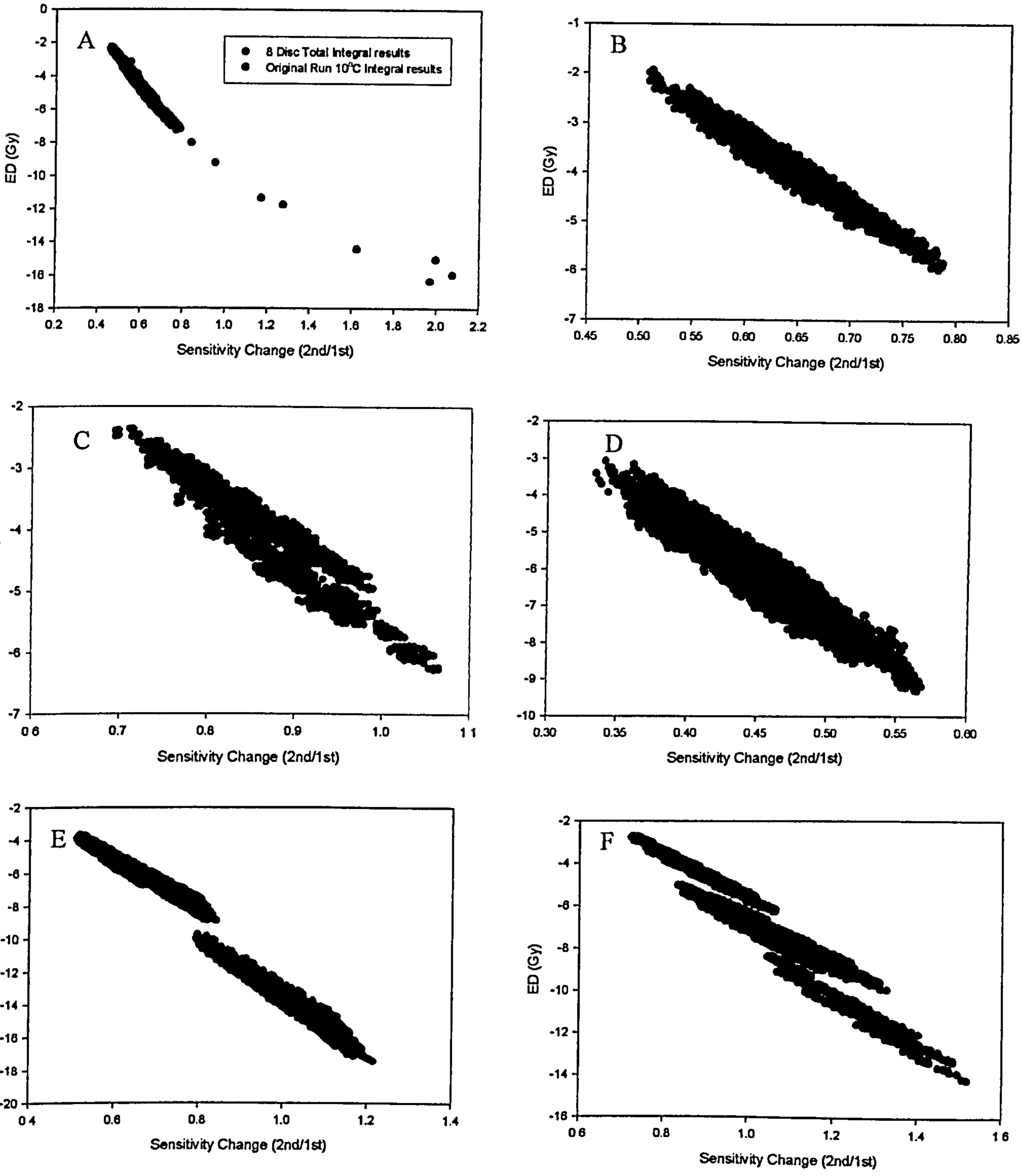

Fig 5.35 Relationship between sensitivity change and ED (A) 14D006-SUTL768 Single distribution in good agreement with 10°C integral values (B) 13D001-SUTL764 Single Distribution (C) 12D002-SUTL751 Possible two distributions (D) FER001-SUTL823 Single distribution more widely scattered (E) FER002-SUTL824 Two distinct distributions (F) STN003-SUTL838 Three separate distributions.

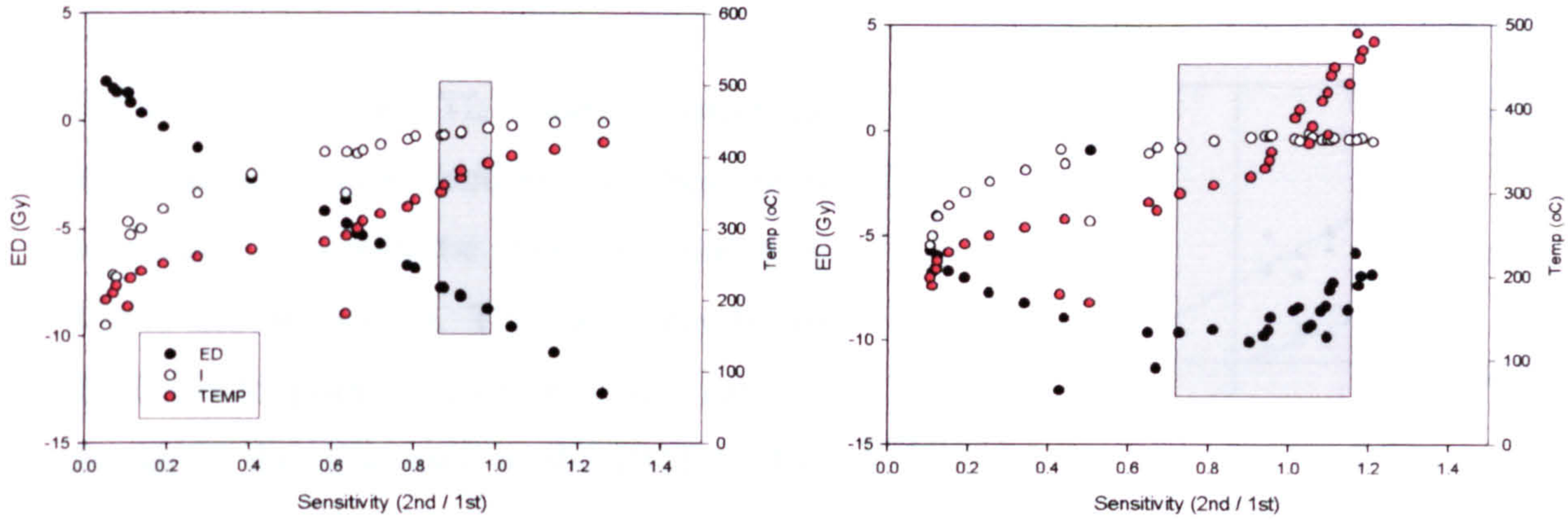

Fig 5.36 Evidence of variable relationship between sensitivity change and ED in other burnt mound samples (Crawford). (a) Near linear relationship in sample SUTL219 (b) No clear relationship Sample SUTL222

(ii) Spurious Luminescence

(iii) Efficiency of TL reader to detect signal

(iv) Prior heating

(v) Prior irradiation

Loss of material is likely to produce increased scatter about the regression line, due to the random nature of such loss. For homogenous samples, the proportion of lost material should also be related to the sensitivity decrease. The scatter in first glow will also be related to microdosimetric effects relating to background radiation and the distribution of radioisotopes within minerals, giving rise to variance not seen on second glow. However, examination of R^2 values for regression fits show no correlation with the proportion of decrease in second glow.

Contamination, as discussed above, is an unlikely cause of the apparent decrease in sensitivity due its confinement to first/second glow response. Spurious thermoluminescence due to crushing and pretreatment could potentially cause an increase in luminescence on first glow. Such spurious luminescence would be confined to thermoluminescence measurements and examination of a number of samples using a

combined IR/TL readout showed similar sensitivity changes on the regression of the optical data (fig 5.37).

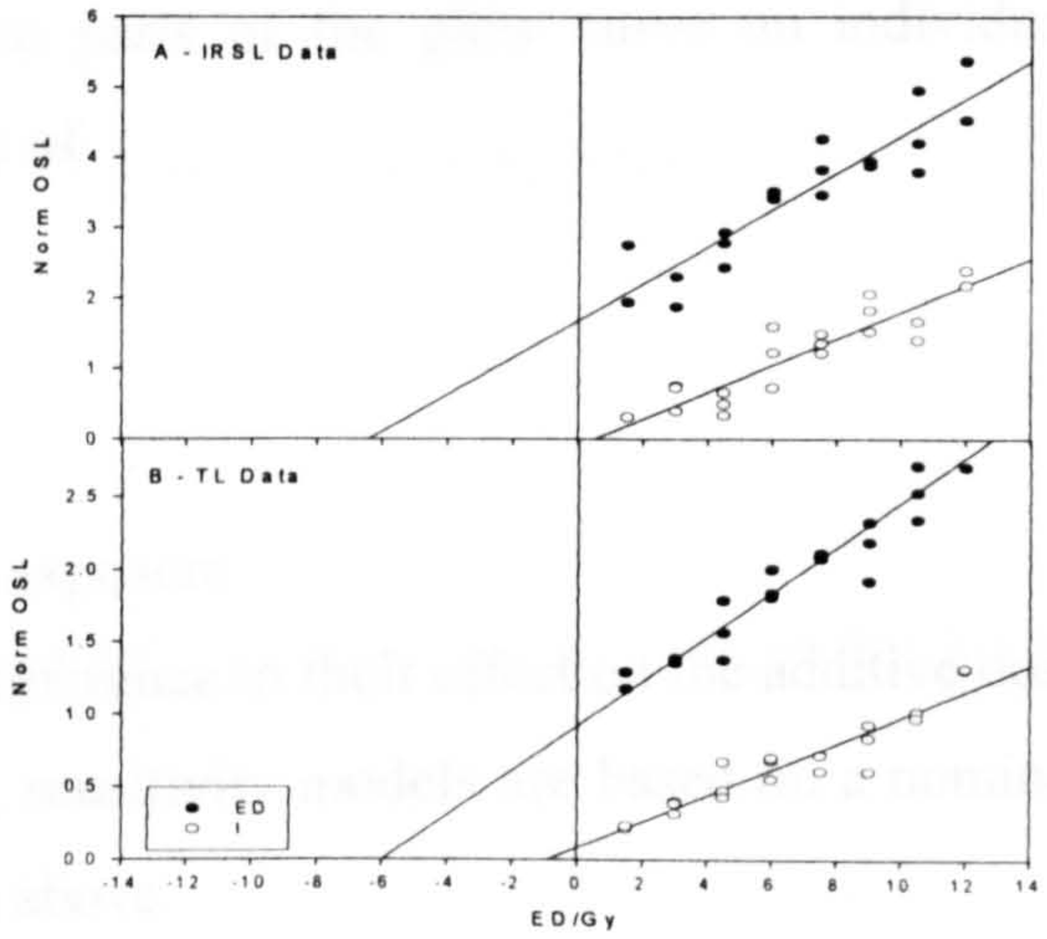

Figure 5.37: A combined additive dose IRSL/TL run for sample SUTL815 shows slope ratios of 0.69±0.11 and 0.59±0.07 for IRSL and TL respectively, indicating that Spurious TL does not play a large role in the sensitivity change seen.

The efficiency of the TL reader to detect the luminescence signal produced by heating is dependent upon both the photomultiplier tube (PMT) and filters used. There are a number of short and long-term factors that may cause a change in the efficiency of the PMT. The PMT can suffer from short-term shock primarily as a result of exposure to light, vibration or electrical surge. The change in efficiency as a result of shock may adversely affect the PMT for up to a day, but is generally not attributed to long-term instability. A change in the background temperature may also affect the efficiency by increasing the dark count. Longer-term problems relate to power supply drift which can send the PMT off plateau. Over longer periods filters may also affect the efficiency as dirt and silicone grease accumulate on the surface of the filter. These long-term effects are routinely monitored by means of light and dark count tests at the beginning of each day and would be unlikely to routinely cause loss on G2 without affecting G1 also. As such it is unlikely that TL reader efficiency plays a role in the loss in sensitivity seen.

Prior heating and previous exposure to radiation are both known to affect the sensitivity of a sample. Quartz is well known for exhibiting increased sensitivity after heating. Likewise sensitivity changes related to past irradiation, outlined in chapter 3 may also contribute. Sensitisation models will now be examined in detail in order to investigate whether a theoretical link can be established between ED and sensitivity change is similar to the relationship observed within the majority of samples.

5.3.4.4 Sensitisation models

There are a number of different possible scenarios for sensitivity change that may take place from sample to sample, and at different parts of the glow curve on individual samples. These may crudely be viewed in terms of

(i) No sensitivity change

(ii) Change due to heating

(iii) Change due to radiation exposure

(iv) Change due to heating and radiation exposure

These are discussed in more detail below with reference to their effect on the additive dose method used. For the purposes of illustration, sensitivity models are based on a nominal 5Gy natural dose, with G1-3 doses as described above.

(i) No sensitivity change

The first of these is self-explanatory and needs no further description. Regression lines would be parallel, ED and I would give the correct result for a sample (fig 5.38a).

$C_{i,j} = S_0 B_{i,j}$ where C= counts , S_o= original sensitivity, B= dose, i=disc, j=glow

(ii) Change due to heating

Change in sensitivity due to past heating may be viewed in terms of S, the sensitivity and H, a sensitivity factor related to the heating event. As such, the sensitivity of a sample at each point in the readout cycle may be described in terms of

$$C_{i,j} = S_{i,j-1} B_{i,j}$$

$S_{i,j} = S_{i,j-1} H_j$ where H= sensitivity change due to past heating (H_o=1)

It is worth noting that H_2 need not equal H_1 (and in the majority of cases probably does not). The resulting effect on the regression is dependent on the values of H at any point in the readout but at any one point each disc in the run will have the same sensitivity. As such, whilst the gradient of each regression line will change with the value of H, ED and I values will still be valid (fig 5.38b).

(iii) Change due to past irradiation

Due to the varying doses given to discs at different points in the run it is necessary to consider the sensitivity change for individual discs.

A cumulative sensitivity change for a particular disc may be viewed in terms of

$$C_{i,j} = S_{i,j-1} B_{i,j}$$

$$S_{i,j} = S_{i,j-1} + k\, B_{i,j-1}$$

where k is a constant associated with sensitivity increase due to past irradiation.

Where k_i=k_2.etc the sensitivity can be seen as the original sensitivity multiplied by a factor proportional to past radiation doses. Expressed in these terms, giving a sample a 10Gy dose, followed by a second 10Gy dose will produce the same effect as if one 20 Gy irradiation (or a 5 and 15 Gy etc) were given.

It can therefore be seen that on G2, discs will exhibit differing sensitivity due to G1 dose, but by G3 all will have had the same predose (of 13.5Gy). The G2 response will be arced (as described above) due to the reversal of G2 doses. In this situation, ED regression will be valid, however intercept values (despite exhibiting the same gradient of slope as ED) will be larger/smaller than their true value depending on the value of β (fig 5.38c).

(iv) Change in sensitivity due to heating and past radiation exposure

When a change in sensitivity occurs both as a result of past heating and past radiation exposure the situation is more complex.

$$C_{i,j} = S_{i,j-1} B_{i,j}$$

$$S_{i,j} = H_{j-1}(S_{i,j-1} + kB_{i,j-1})$$

(In effect the previous equations are a simplified form of this, with k=0 for heating only and H=1 for dose only).

When $H_1 \neq H_2$ etc the effect is essentially the same as if k varied for each glow.

The result is a situation whereby G2 and G3 sensitivity varies from disc to disc.

When nominal values for H and k are entered into the above equation it becomes clear that the value of ED, I and the ratio of $2^{nd}/1^{st}$ slope are all governed by this unequal sensitisation on third glow.

By modelling different values for H_1 and H_2 it is possible to examine the relationship between ED+I and the slope change (fig 5.39). The relationship bears a strong resemblance to that observed within the dataset. The advantage of a multiple trap population in the feldspar system being that the various traps represented within different portions of the glow curve exhibit differing sensitivity changes, allowing the above effect to be seen. It is worth noting that in this situation, an apparent ED plateau will be observed when neighbouring 10°C integrals experience a similar sensitivity change.

For very small DDSC effects, when sensitivity change =1 (i.e. no change between first and second) the ED+I approximates the correct value – this is due to the fact that whilst a DDSC may have occurred and effected the value of the intercept regression, it will not effect gradient, thus when there is no measurable sensitivity change between first and second glow it indicates a situation where the contribution from previous heating is insignificant to the sensitivity change (i.e third glow is of equal sensitivity). If a decay curve is fitted to the dataset, the value at x=1 (no sensitivity change) approximates the correct value of ED+I. The value for both feldspar runs at x=1 is on average 4.5±0.2Gy, in good agreement with the expected result.

However, it is evident from figure 5.40 that the larger the DDSC, the greater the effect on both ED and I. For large DDSC, the value of I is no longer valid (as discussed above). The true value of ED will also drift from the sensitivity change =1 point on the graph. In samples where the intercept value is known to be zero, it would be possible to determine the likely magnitude of over/underestimation of ED based on the intercept value at 1.

However, such information is clearly not available for samples from Orkney and Shetland, thus some other means of determining the magnitude of the effect must be found. Fig 5.41 shows the likely effect on the curvature of the intercept line with varying sensitivity increase/decrease. As discussed with reference to DDSC above, for b values greater than

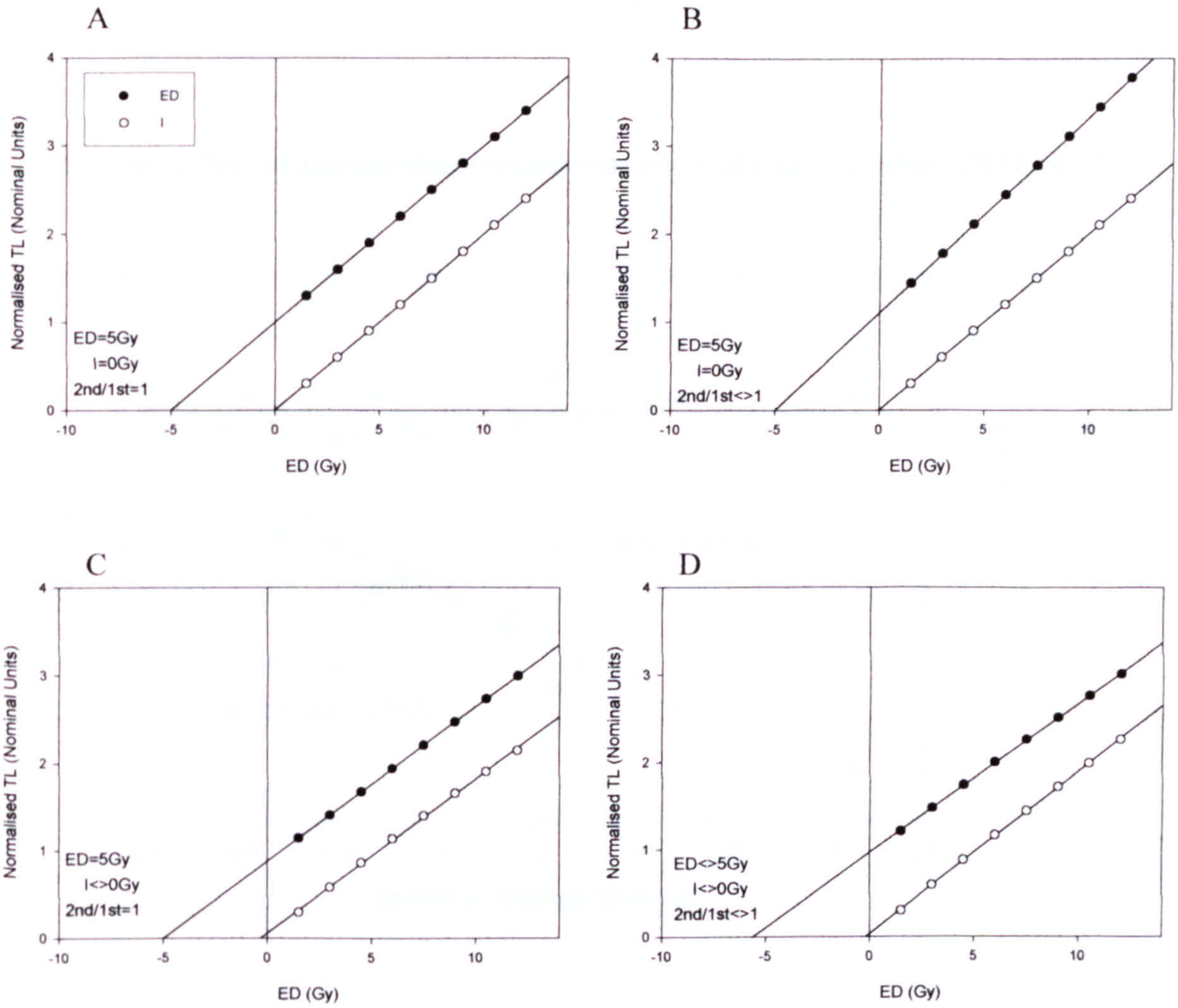

Fig 5.38 Effect of sensitivity change on regression results (a) No Sensitivity Change (b) Change due to heating (c) Change due to past irradiation (d) Change due to past heating and irradiation.

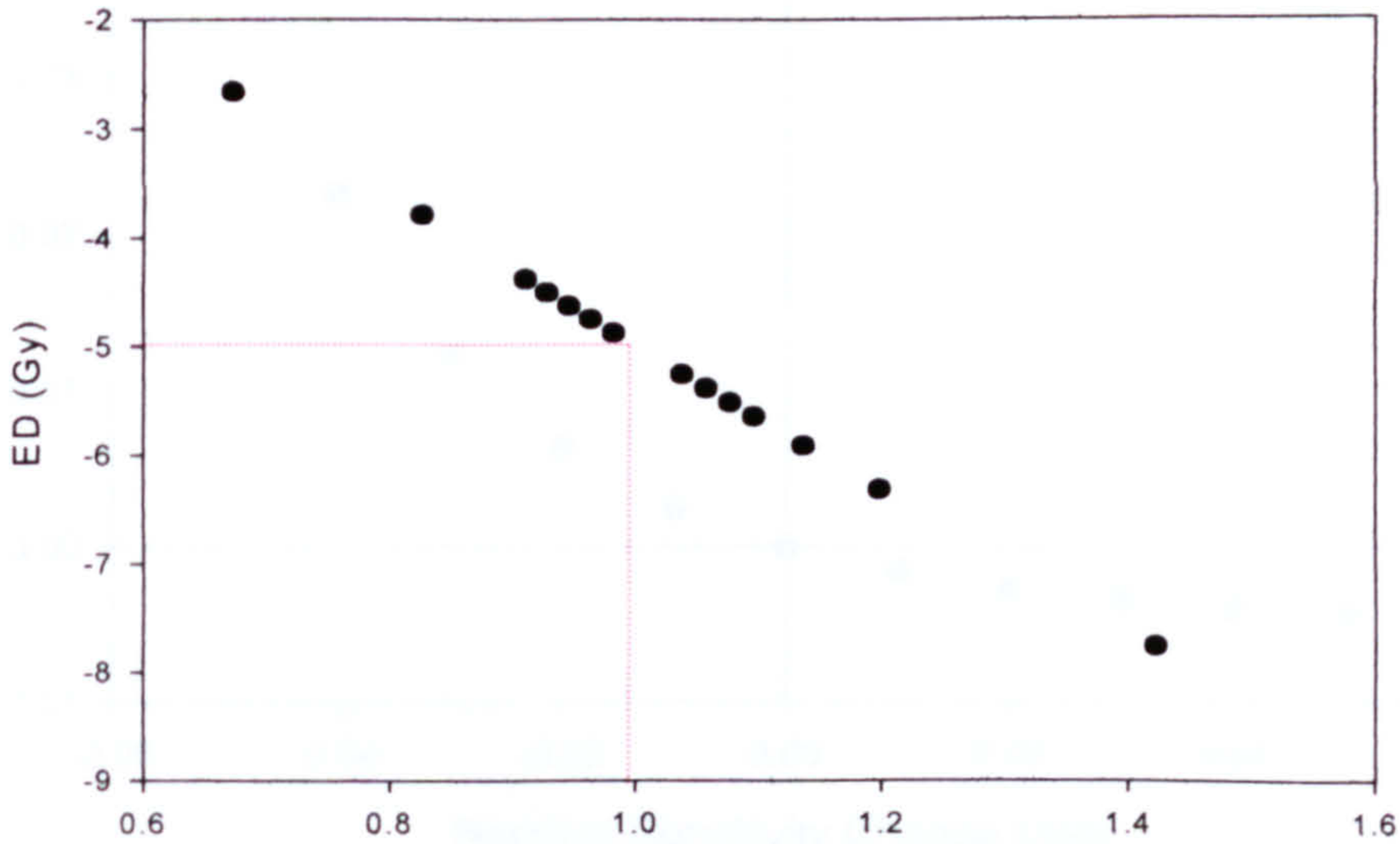

Fig 5.39 Predicted Relationship between ED and Sensitivity Change

Fig 5.40 Effect of increased/decreased sensitivity change on value of ED and I

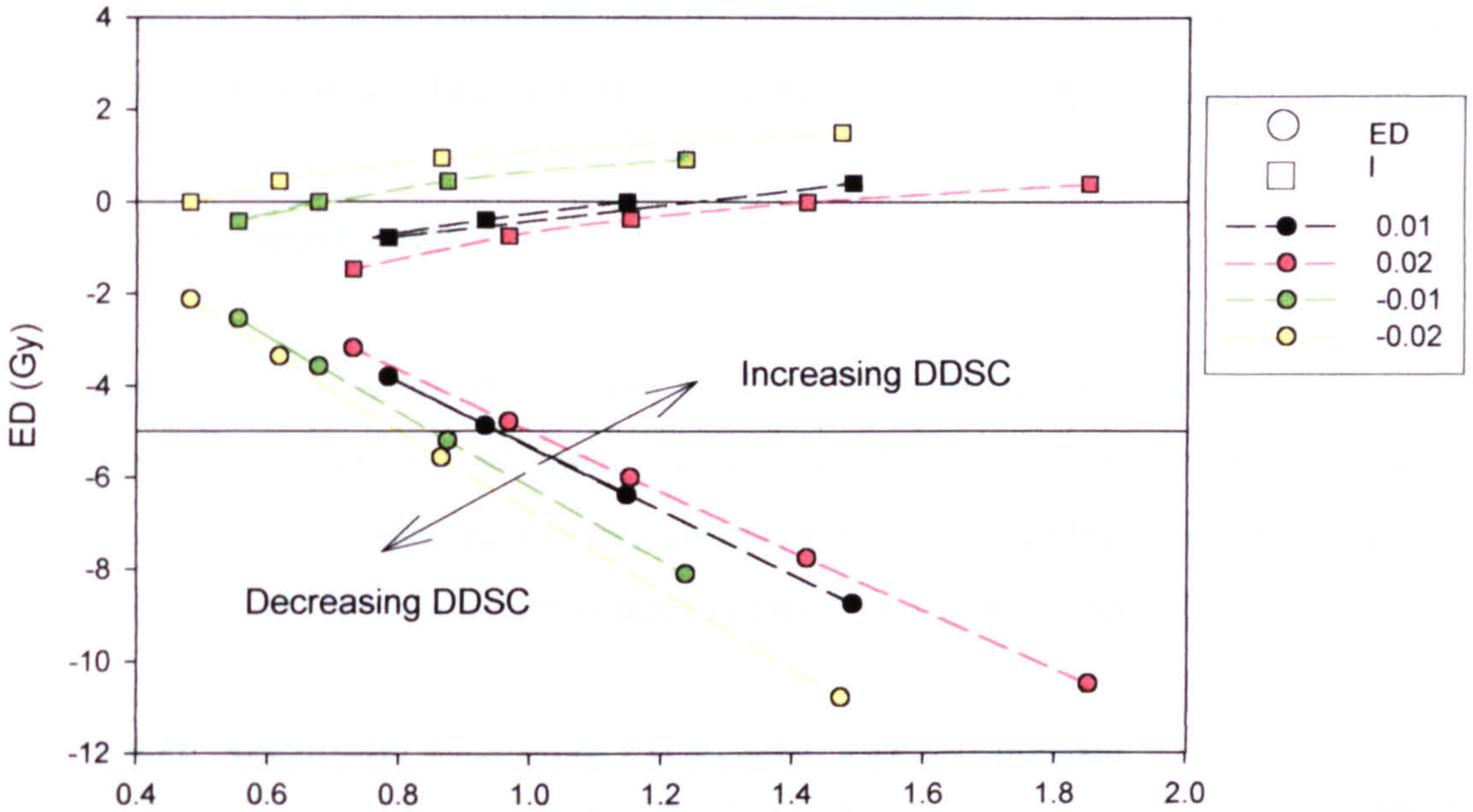

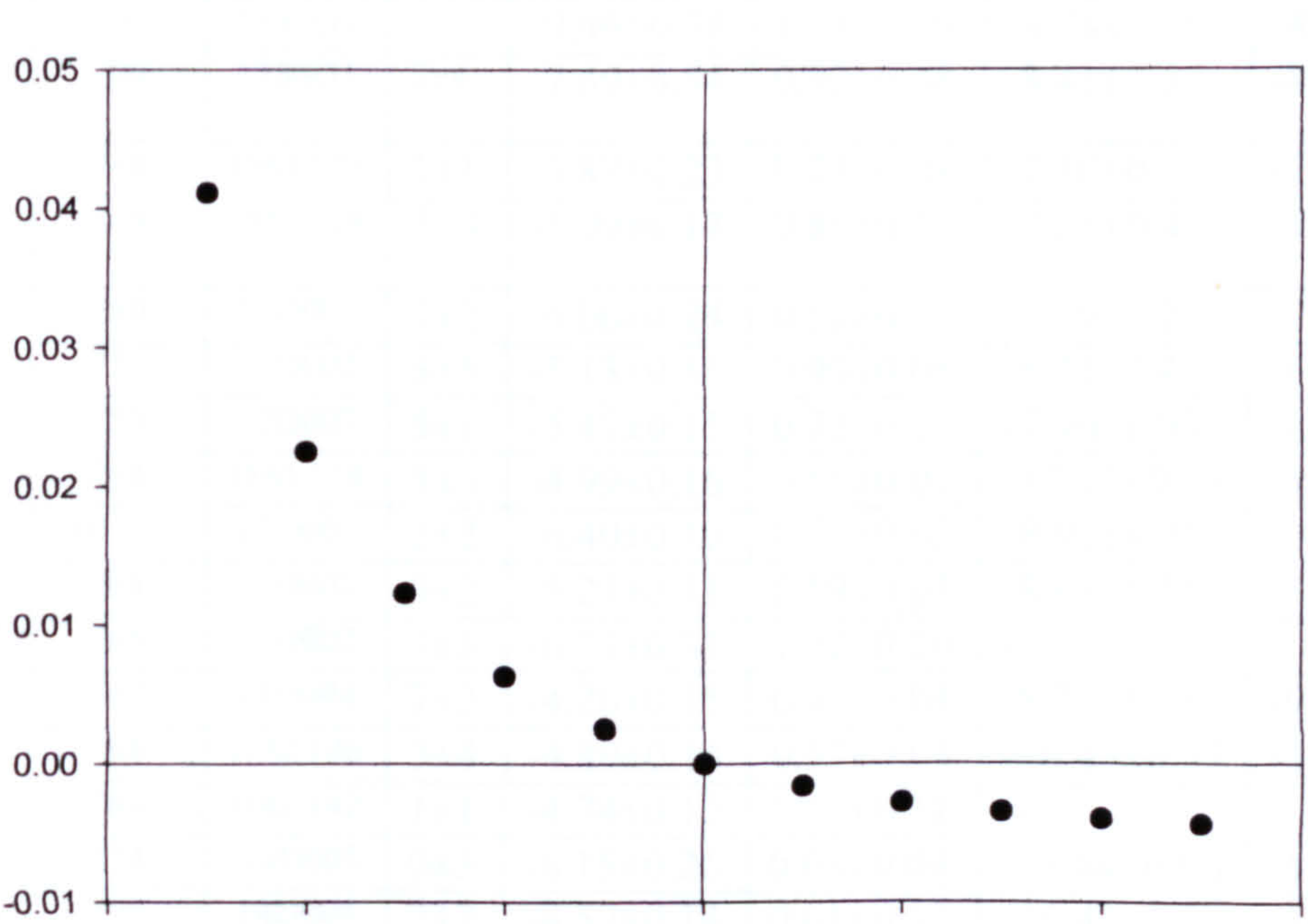

Fig 5.41 Predicted relationship between curvature of intercept line and sensitivity change

zero, a decrease in sensitivity is expected. B values may therefore be utilised to express the likelihood o over/underestimation at the sensitivity change =1 point.

Reference to fig 5.31 indicates that a larger degree of sensitivity change should be expected in the Orkney dataset, with only minimal change within the Shetland samples.

5.3.4.5 Corrected Dataset

The corrections outlined above were made to both Orkney and Shetland datasets where possible. The results are tabulated below. A direct correction between observed fading and the sensitivity corrected ED has also been made. In addition, an indication as to the likelihood of over/underestimation due to correction has also been tabulated.

Table 5.10 Sensitivity Corrected ED Results, Orkney Dataset

Site	SUTL	Run No.	% Fad	ED (Gy)	$2^{nd}/1^{st}$ Slope	Sensitivity Corrected ED (Gy)	Fading Corrected ED (Gy)	B ≈0
Liddle	1379	LID001	0±3	-8.78±0.20	0.82±0.14	-10.61±0.94	-10.61±0.94	Y
	1381	1381G1	1±2	-9.46±0.34	1.11±0.09	-8.74±0.96	-8.83±0.99	Y
	1386	1386G1	2±4	-7.69±0.54	0.92±0.08	-8.41±0.56	-8.58±0.66	Y
DALE TL12	748	DAL123	1±1	-3.87±0.23	0.72±0.04	-7.10±0.39	-7.17±0.40	N
	749	DAL128	5±3	-5.99±0.17	0.86±0.12	-7.21±0.47	-7.57±0.54	N
	750	12D001	1±2	-6.06±0.24	0.86±0.04	-6.99±1.25	-7.06±1.27	N
	751	12D002	5±5	-5.13±0.16	0.90±0.06	-6.21±2.47	-6.52±2.61	N
	753	12D007	5±1	-5.47±0.15	0.72±0.17	-7.90±0.93	-8.30±0.98	N
	754	DAL124	5±3	-4.99±0.16	0.65±0.02	-13.13±0.79	-13.78±0.92	Y
DALE TL13	760	13D005	2±2	-6.40±0.10	0.71±0.02	-8.92±1.01	-9.10±1.05	N
	764	13D001	0±2	-5.21±0.11	0.69±0.03	-8.48±1.18	-8.48±1.18	N
	765	13D002	0±3	-6.13±0.33	1.02±0.10	--		N
	767	13D004	7±2	-4.26±0.15	0.41±0.04	-8.27±1.35	-9.08±1.49	N
DALE TL14	768	DAL146	3±4	-4.89±0.14	0.57±0.04	-10.45±0.75	-10.76±0.87	Y
	769	DAL142	1±1	-4.74±0.12	1.12±0.11	--		N
	774	14D003	0±3	-6.15±0.26	0.63±0.04	-13.64±0.96	-13.64±0.96	Y
	775	14D004	2±2	-4.52±0.14	0.61±0.02	-10.42±1.07	-10.63±1.11	N
	777	DAL147	5±3	-4.51±0.13	0.67±0.02	-6.53±2.12	-6.86±2.24	N
	779	779	2±1	-6.06±0.13	0.55±0.11	-11.47±1.39	-11.70±1.42	N
TL 15	782	15D001	1±2	----	----	----	----	N
	785	15D004	1±1	-5.44±0.21	0.82±0.09	-6.57±1.09	-6.64±1.10	N

Site	SUTL	Run No.	% Fad	ED (Gy)	2nd/1st Slope	Sensitivity Corrected ED (Gy)	Fading Corrected ED (Gy)	B ≈0
Skaill	815	SKA002	5±2	-6.59±0.10	0.47±0.05	-10.00±1.20	-10.50±1.28	Y
	815	SKA008	1±1	-5.34±0.33	0.70±0.09	-8.23±1.35	-8.31±1.37	Y
	817	SKA010	14±6	-6.15±0.16	1.07±0.16	---		N
	1343	1343G1	0±1	-4.04±0.10	0.69±0.11	---		N
	1360	1360G1	1±2	-7.54±0.27	0.88±0.05	-8.65±1.03	-8.74±1.05	N
K. of Mer.	794	MER003	7±3	-5.62±0.15	0.71±0.04	-9.32±0.56	-9.97±0.66	Y
	795	MER004	6±1	-6.48±0.14	0.79±0.06	-14.36±0.85	-15.16±0.91	Y
	802	MER005	9±3	-7.77±0.14	0.71±0.14	-9.47±1.37	-10.32±1.52	N
	803	MER006	15±4	-8.22±0.19	0.80±0.15	-10.17±0.96	-10.20±1.05	N
War.	842	WAR01	-2±3	-9.42±0.13	0.86±0.06	-15.89±3.42	-15.89±3.38	N
	857	WAR04	6±2	-5.48±0.18	0.69±0.03	-14.40±1.16	-15.26±1.26	N
Fersness	823	FER001	1±2	-6.23±0.16	0.48±0.17	-12.76±2.10	-12.83±2.20	Y
	824	FER002	8±1	-6.04±0.15	0.67±0.05	-9.70±0.83	-10.48±0.90	N
	831	FER003	0±3	-8.52±0.37	0.77±0.06	-12.30±2.16	12.30±2.16	Y
	831	FER005	0±2	-5.00±0.50	0.86±0.04	-12.25±1.03	-12.25±1.03	N
Stenaquoy	836	STN005	-1±2	-8.64±0.41	0.94±0.14	-8.61±1.23	-8.61±1.23	N
	838	STN003	4±3	-6.15±0.25	1.04±0.16	-6.94±2.58	-7.22±2.69	N
	839	STN004	1±1	-4.01±0.13	0.86±0.11	-5.87±1.79	-5.93±1.81	N

Table 5.11 Sensitivity Corrected ED Results, Shetland Dataset

Site	SUTL	Run No.	% Fad	ED (Gy)	2nd/1st Slope	Sensitivity Corrected ED (Gy)	Fading Corrected ED (Gy)	B ≈0
Cruester	949	CRU021	1±2	-7.93±0.15	0.76±0.06	-12.65±1.64	-12.73±1.68	Y
	951	CRU022	0±2	-6.37±0.18	0.64±0.11	-12.17±0.54	-12.10±0.59	Y
	953	CRU023	6±3	-8.7±0.68	0.73±0.06	-12.29±0.23	-12.93±0.44	Y
	958	CRU024	3±1	-7.09±0.21	0.85±0.08	-10.88±1.15	-11.12±1.19	Y
	968	CRU025	6±3	-6.31±0.82	0.61±0.03	-10.24±0.63	-10.81±0.73	Y
	1051	CRU006	0±2	-8.55±0.23	0.92±0.47	-12.04±0.55	-12.00±0.60	Y
	1051	CRU044	0±1	-8.92±0.69	0.80±0.02	-14.28±0.31	-14.20±0.34	Y
	1054	CRU029	7±5	-5.27±0.29	0.65±0.05	-9.65±0.87	-10.33±1.05	Y
	1062	CRU031	6±2	-8.15±0.33	0.74±0.03	-13.58±0.43	-14.31±0.53	Y
	1068	CRU045	0±3	-12.67±1.20	0.99±0.08	-14.48±2.13	-14.40±2.17	Y
	1088	CRU034	1±4	-8.06±0.35	0.81±0.05	-11.36±1.63	-11.47±1.66	Y
	1100	CRU043	1±2	-7.55±0.54	0.32±0.13	-16.52±0.51	-16.69±0.61	Y
Houlls	970	HL001	0±3	-10.94±0.24	0.68±0.04	-23.67±2.54	-23.67±2.54	Y

5.4 Age Calculations

Dose rate information for each sample is given in Chapter 4, and tabulated in summary form below together with calculated ages for corrected datasets based on the sensitisation corrections outlined above.

With reference to table 5.10 and 5.11, it is predicted that many of the Orkney samples will experience underestimation in age estimate due to a larger degree of DDSC noted. Where indicated, these should be seen as minimum age estimates. Date ranges are represented graphically in figure 5.42.

Table 5.12 Age Calculation, Orkney Dataset

Site	SUTL	Pos	Run No.	Annual Dose ($mGya^{-1}$)	ED (Gy)	Sens Corr , ED (Gy)	Sens Corr Age (Ka)	Mean Unit Age (ka)	Mean Site Age (ka)
Liddle	1379	1	LID001	4.31±0.21	-8.78±0.20	-10.61±0.94	2.46±0.13*		
	1381	1	1381G1	3.55±0.28	-9.46±0.34	-8.83±0.99	2.49±0.34*		**2.44±0.11**
	1386	3	1386G1	3.68±0.28	-7.69±0.54	-8.58±0.66	2.33±0.25*		
DALE	748	12	DAL123 (16)	3.21±0.25	-3.87±0.23	-7.17±0.40	2.23±0.21*		**2.56±0.09**
	749		DAL128	3.03±0.26	-5.99±0.17	-7.57±0.54	2.50±0.28*		
	750		12D001	2.99±0.27	-6.06±0.24	-7.06±1.27	2.36±0.48*	**2.51±0.13**	
	751		12D002	2.91±0.25	-5.13±0.16	-6.52±2.61	2.24±0.92*		
	753		12D007	3.59±0.23	-5.47±0.15	-8.30±0.98	2.31±0.31*		
	754		DAL124	3.24±0.25	-4.99±0.16	-13.78±0.92	4.25±0.43		
	760	13	13D005	3.98±0.23	-6.40±0.10	-9.10±1.05	2.29±0.30*		
	764		13D001	3.26±0.21	-5.21±0.11	-8.48±1.18	2.60±0.40*		
	765		13D002	3.63±0.25	-6.13±0.33			**2.48±0.22**	
	767		13D004	3.22±0.23	-4.26±0.15	-9.08±1.49	2.82±0.50*		
	768	14	DAL146	3.48±0.27	-4.89±0.14	-10.76±0.87	3.07±0.35		
	769		DAL142	3.34±0.24	-4.74±0.12			**3.24±0.19**	
	774		14D003	3.64±0.24	-6.15±0.26	-13.64±0.96	3.74±0.36		
	775		14D004	3.50±0.24	-4.52±0.14	-10.63±1.11	3.04±0.38		
	777		DAL147	3.09±0.22	-4.51±0.13	-6.86±2.24	2.22±0.74*		

	779		779	3.39±0.26	-6.06±0.13	-11.70±1.42	3.45±0.50*	
	785	15	15D004	3.39±0.28	-5.44±0.21	-6.64±1.10	1.96±0.36*	**1.96±0.36**
Skaill	815	5	SKA002	3.82±0.25	-6.59±0.10	-10.50±1.28	2.75±0.38	
	815	5	SKA008	3.13±0.18	-5.34±0.33	-8.31±1.37	2.65±0.46	
	817	6	SKA010	3.04±0.23	-6.15±0.16			**2.32±0.19**
	1343	1	1343G1	3.49±0.21	-4.04±0.10			
	1360	3	1360G1	4.35±0.23	-7.54±0.27	-8.74±1.05	2.01±0.26*	
K. of Merr.	794	8	MER003	2.71±0.22	-5.62±0.15	-9.97±0.66	3.68±0.39	
	795	8	MER004	2.84±0.19	-6.48±0.14	-15.16±0.91	5.32±0.48	
	802	7	MER005	4.36±0.33	-7.77±0.14	-10.32±1.52	2.36±0.39*	**3.08±0.19**
	803	7	MER006	4.45±0.35	-8.22±0.19	-10.20±1.05	2.29±0.30*	
War.	842	9	WAR001	4.01±0.10	-9.42±0.13	-15.89±3.38	3.94±0.85*	**4.00±0.38**
	857	10	WAR004	3.79±0.25	-5.48±0.18	-15.26±1.26	4.01±0.42*	
Fersness	823	3	FER001	2.93±0.19	-6.23±0.16	-12.83±2.20	4.37±0.80	
	824	3	FER002	3.32±0.20	-6.04±0.15	-10.48±0.90	3.13±0.33*	
	831	4	FER003	2.96±0.24	-8.52±0.37	-12.30±2.16	4.16±0.80	**3.51±0.24**
	831	4	FER005	3.28±0.24	-5.00±0.50	-12.25±1.03	3.72±0.42*	
Stenaquoy	836	1	STN005	3.41±0.24	-8.64±0.41	-8.61±1.23	2.52±0.40*	
	838	2	STN003	3.51±0.24	-6.15±0.25	-7.22±2.69	2.06±0.78*	
	839	2	STN004	3.36±0.23	-4.01±0.13	-5.93±1.81	1.76±0.55*	**2.23±0.30**

*** Indicates Minimum Age**

Table 5.13 Age Calculation, Shetland Dataset

Site	SUTL	Pos	Run No.	Annual Dose ($mGya^{-1}$)	ED (Gy)	Sens Corr ED (Gy)	Sens Corr Age (ka)	Mean Site Age (ka)
Cruester	949	1	CRU021	3.44±0.21	-7.93±0.15	-12.73±1.68	3.69±0.54	
	951	1	CRU022	3.22±0.23	-6.37±0.18	-12.10±0.59	3.76±0.32	
	953	1	CRU023	3.74±0.27	-8.7±0.68	-12.93±0.44	3.45±0.28	
	958	2	CRU024	3.07±0.21	-7.09±0.21	-11.12±1.19	3.62±0.46	
	968	4	CRU025	3.32±0.25	-6.31±0.82	-10.81±0.73	3.25±0.33	
	1051	5	CRU006	4.03±0.25	-8.55±0.23	-12.00±0.60	2.98±0.24	
	1051	5	CRU044	3.64±0.25	-8.92±0.69	-14.20±0.34	3.90±0.28	**3.49±0.09**
	1054	6	CRU029	3.70±0.21	-5.27±0.29	-10.33±1.05	2.78±0.32	
	1062	8	CRU031	3.27±0.22	-8.15±0.33	-14.31±0.53	4.37±0.34	
	1068	9	CRU045	3.38±0.23	-12.67±1.20	-14.40±2.17	4.26±0.70	
	1088	15	CRU034	4.35±0.23	-8.06±0.35	-11.47±1.66	2.64±0.41	
	1100	19	CRU043	4.39±0.24	-7.55±0.54	-16.69±0.61	3.80±0.25	
Houlls	970	1	HL001	5.07±0.20	-10.94±0.24	-23.67±2.54	4.67±0.54	**4.67±0.54**

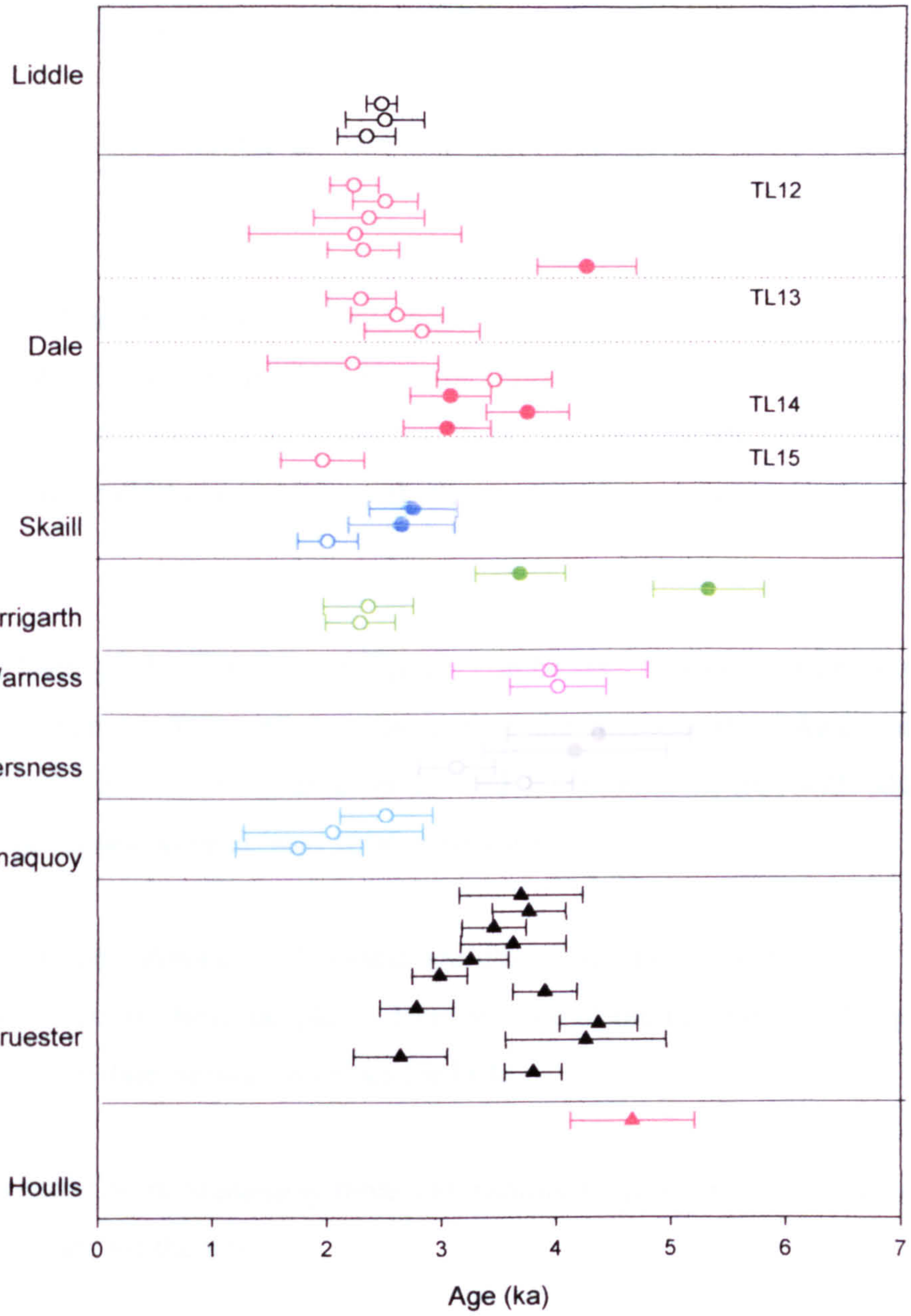

Fig 5.42 Summary of feldspar age estimates from Orkney and Shetland
Open circles represent minimum age estimates

Interpretation of the dates obtained for individual sites must clearly respect the nature of the minimum age estimates for samples. Dates obtained for samples in Orkney suggest an age of at least 2000 years for the majority of sites.

At Liddle, three samples dated give age estimates centering on the mid 1st millennium BC. Despite being minimum age estimates, these dates are coherent with the latest dates for Liddle reported by Huxtable et al (1976).

Dates from Skaill burnt mound are also consistent with the site being in use in the mid 1st millennium BC.

The majority of age estimates for Dale burnt mound are similarly centred on the mid 1st millennium BC. However, the four dates not represented by minimum values suggest the true age of the monument to be closer to 2nd –3rd millennium BC date. These four dates also appear in stratigraphic order, with the earlier dates located in the lower context (TL12).

At Knoll of Merrigarth, a similar discrepancy can be seen between minimum age estimates and dates thought to represent the true age of the monument. Again minimum age estimated for the mound are centred on the mid 1st millennium BC, with additional dates suggesting the mound to be at least 1000 years earlier in age.

The minimum age estimates at Fersness are closer in value to other dates, suggesting a lesser DDSC effect in these samples. Here the age of the mound would appear to be 3rd millennium BC in date, similar to values for Dale.

All samples dated from Stenaquoy represent minimum age estimates, indicating an age of at least 2000 years for the site.

Samples from Shetland proved more successful, with all thought to have been adequately corrected for sensitization effects. At Cruester a 2000 year spread in age is seen, ranging in date from 500-2500BC and centred on 1500BC. The single sample dated from Houlls appears to be contemporary with the earlier Cruester dates.

5.5 Summary

The feldspar additive dose TL method has been investigated using an IAEA feldspar irradiated to a known dose. Simulation of datasets has highlighted the benefits of increasing disc numbers to 16 or 24 where possible. Evidence for shifts in peak position due to poor thermal contact has been presented, and a correction method outlined. The correction method has been shown to significantly increase the ED plateau length in a number of samples.

A large number of samples from Orkney and Shetland were investigated using the modified procedure based on the above results. Not all produced regressable data. The lithology of the majority of samples that failed includes large phenocrysts of high internal activity minerals which may contribute significantly to the scatter seen by virtue of variable dose rate received at different positions within the sample. Spurious luminescence and low sensitivity may also contribute to these failures. Mixed mineralogy of discs was also identified as a possible cause of failure.

A rise in ED with temperature was observed in a number of samples. Samples affected are not confined to a specific site, neither are they unique in their lithology. This would suggest that individual samples within sites may have failed to reach the required temperature to adequately empty higher temperature traps. Whilst it is possible within feldspar TL runs to reject the part of the signal affected, this may be of interest to subsequent OSL investigations where signal differentiation is more complex.

Characteristics of successful runs have been documented and as a result, a hitherto unrecognized relationship between sensitivity change and ED recognized. This relationship has been identified in the majority of samples investigated, and also in samples from other burnt mounds previously dated in a similar manner. Modelling of possible sensitivity changes has suggested this relationship to be related to an unequal predose effect on glow three, rendering glow three normalization invalid. However, due to the structured nature of the additive dose method, the normalization process has failed in a structured and apparently predictable manner.

It is possible, with additional work, that such behaviour may be successfully circumvented in future. At present however an attempt has been made to correct existing data. By exploiting the different sensitivity changes within the multi-component feldspar glow curves, in combination with modeling, it has been possible to suggest a correction procedure for the dataset. The success of the correction is dependent on the degree of DDSC encountered by each sample. In a number of cases, the correction may underestimate the age, thus minimum age estimates have been quoted where appropriate. Corrections have been applied and appear to give coherent data that suggest the burnt mounds sampled to have been in use from the 1st to 4th millennium BC.

Chapter 6 Optically Stimulated Luminescence Investigations

6.1 Introduction

As outlined in chapter 2, there are many approaches to determining the stored dose in quartz and feldspar minerals. Over recent years the focus of many procedures has switched from TL to OSL techniques, due in part to advances in optical readout equipment.

The use of infrared stimulated luminescence (IRSL) techniques in feldspar dating has proved successful in a number of studies of unheated material (e.g Janotta et al, 1997, Lang and Wagner, 1997), however initial screening of samples showed poor sensitivity to infrared stimulation. As such, optical methods were confined to blue OSL investigations of quartz material, which showed more promising screening results.

In order to investigate possible age duration within mounds, both precision and accuracy are of importance. Past applications of SAR methods to unheated material have reported a high degree of precision – a result both interpolation of the ED and the removal of the need to normalize discs. However, comparative results of multiple and single aliquot OSL dating of heated material reported in Murray and Mejdahl (1999) suggest measurement error not to be the dominant issue with regard to precision. The dose distribution within minerals may be a key issue in the precision obtained. SAR methods are however ideally suited to investigating the heterogeneity of dose within a sample due to the large number of ED estimates obtained.

Other issues such as incomplete zeroing of the geological signal are also in need of further work. Whilst methods have been developed in sediment dating for identifying poorly bleached material (Bailey, 2003), the applicability of such techniques to heated material is yet to be investigated fully.

A validation of the SAR procedure was carried out using a sub-selection of samples from both Orkney and Shetland burnt mounds. Each sample was first heated to remove any luminescence signal, then given a known dose in order to assess the ability of the SAR method to recover a the dose accurately.

In addition, further validation procedures were carried out to investigate potential issues of uncorrected sensitivity changes occurring between readout of the natural signal and administration of a test dose signal.

As a result of the positive outcome of such investigations, ninety four samples from Orkney and Shetland were selected for further analysis and put through a standardised SAR procedure. Detailed analysis of the run characteristics of each sample is presented, and relationships between many attributes considered. A general discussion of incomplete zeroing of the geological signal and microdosimetric effects is also present in light of variation noted in the ED distribution of certain samples. Age estimates for each sample are calculated on the basis of ED results and annual dose rate calculations detailed in chapter 4.

6.2 Investigation of the SAR procedure

6.2.1 Dose Recovery Procedures

6.2.1.1 Methodology

Four samples were selected from different sites in Orkney and Shetland to reflect the differing geologies of the region. Sets of 4 quartz discs for each sample were dispensed onto stainless steel discs as described in chapter 5, with the exception of SUTL777 for which 16 discs were dispensed. The measurement procedure for each disc is outlined in fig 6.1.

The natural signal of each disc was bleached in a lightbox for 16hrs to remove the natural signal. After an 86 hr storage period discs were again bleached in order to minimize recuperation through the 110°C peak. Each disc was then irradiated to a dose of 5.1Gy using a ^{90}Sr elsec beta source and stored for a further 16hr period prior to commencement of measurement cycle. Samples were then placed on an automatic Riso TL/OSL reader and measured according to the procedure outlined in fig 6.1 Doses of 2,5,10,0 and 2Gy were given, with 0.5Gy test doses between. A fixed preheat of 10s at 240°C, with a cut heat of 10s at160°C for test doses was used for four disc samples. Sample SUTL777 was run using a variety of preheats ranging from 220-280°C, with four discs per preheat temperature The recycling ratio was assessed through the repeat 2Gy cycles.

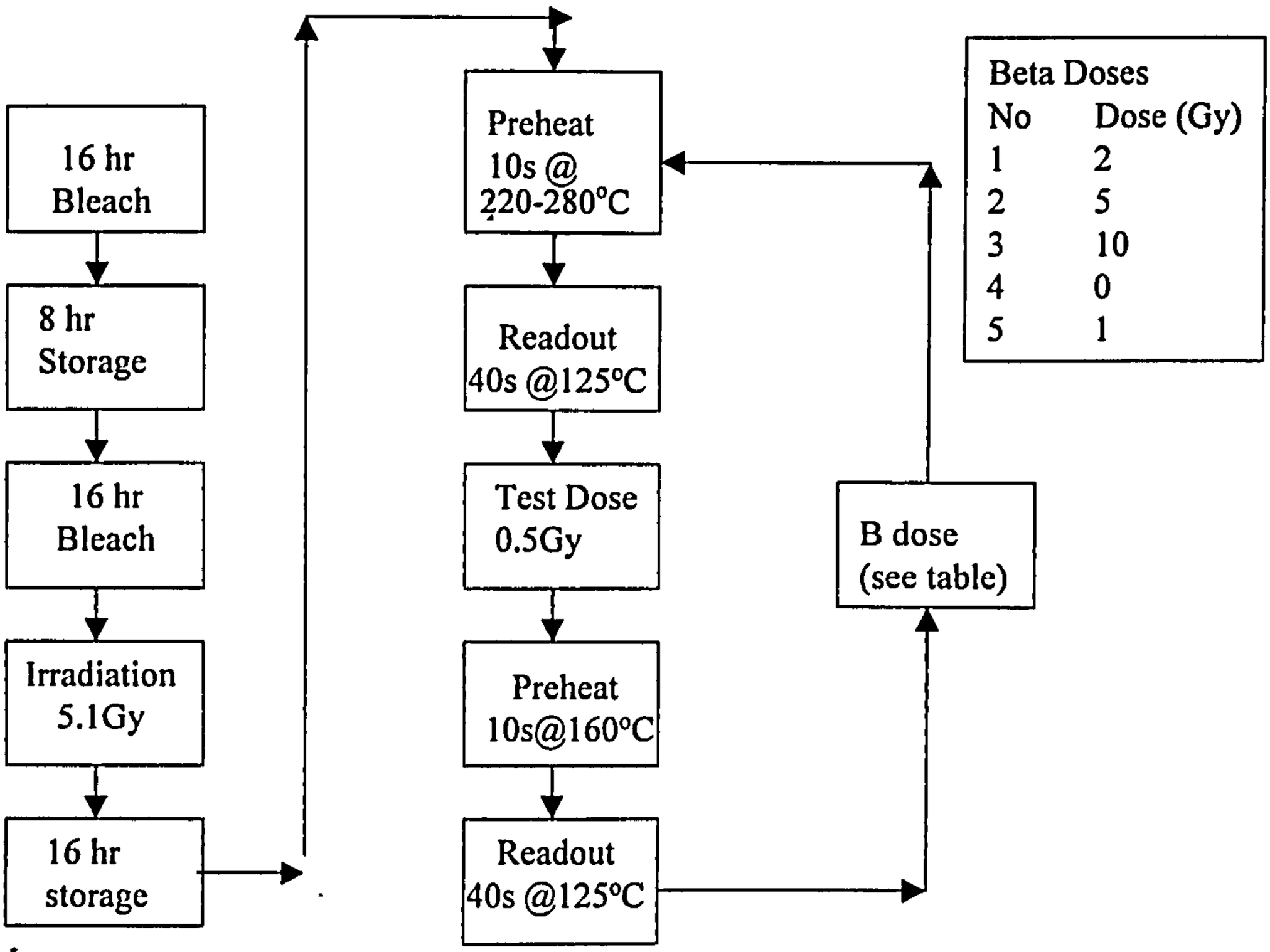

Fig 6.1 Flowchart of Dose Recovery Procedure

6.2.1.2 Equipment Details

All measurements were carried out using a TL/OSL Rison (TL-DA015) reader equipped with 470nm blue LEDs and a 1W 830nm IR laser diode (Botter-Jensen et al, 2000). The reader was fitted with Schott RG715 and green GG420 longpass filters on the IR and blue stimulation sources respectively and Hogn U340 filters on the detection side, together with ^{90}Sr beta sources, delivering approximately $0.1Gya^{-1}$.

6.2.1.3 Results

6.2.1.3.1 Intensity

Signal intensities varied from sample to sample, ranging from 10^4-10^6 counts in the first 1.6s of measurement (fig 6.2). Variation in signal intensity between discs is also evident. In the case of samples SUTL815 and 1051, this cannot be solely explained in terms of sample mass and suggests heterogeneity in sample response.

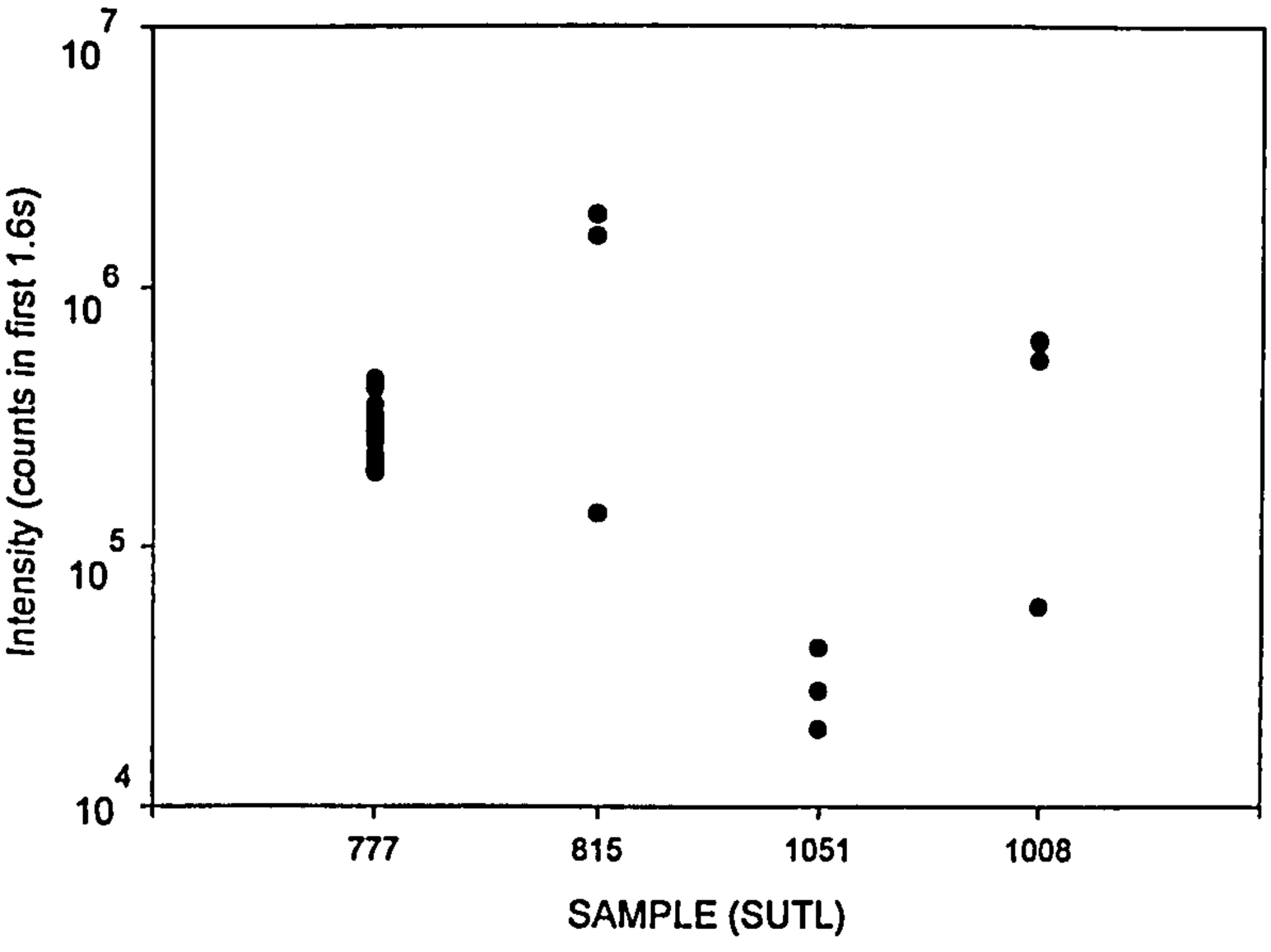

Figure 6.2 Signal Intensity of dose recovery samples (response to 5.1 Gy dose)

6.2.1.3.2 Sensitivity Change

The sensitivity change of each sample was monitored through comparison of test dose intensities. Figure 6.3 shows the sensitivity change at each cycle normalized to the first test dose. All samples show a non-linear increase in sensitivity. Variation in the rate of change can also be seen from disc to disc. Sample SUTL777 also shows a sensitivity change related to preheating, indicating a higher degree of sensitivity change with increased preheat temperature.

6.2.1.3.3 Recycling Ratio

Recycling ratios for all samples were within error of 1 suggesting adequate correction for the increase in sensitivity noted. No relationship between recycling ratio, intensity and sensitivity change were noted.

6.2.1.3.4 Dose Estimate

All EDs were within error of 5.1 Gy. The distribution in ED values was gaussian in nature (fig 6.4) and, in the case of SUTL777, showed no variation in value with preheat temperature. No relationship between ED, recycling ratio or sensitivity change was noted, though the intensity of the initial signal was seen to have an affect on the level of precision obtained. The increased number of discs for sample SUTL777 would appear to have decreased the associated error on this sample.

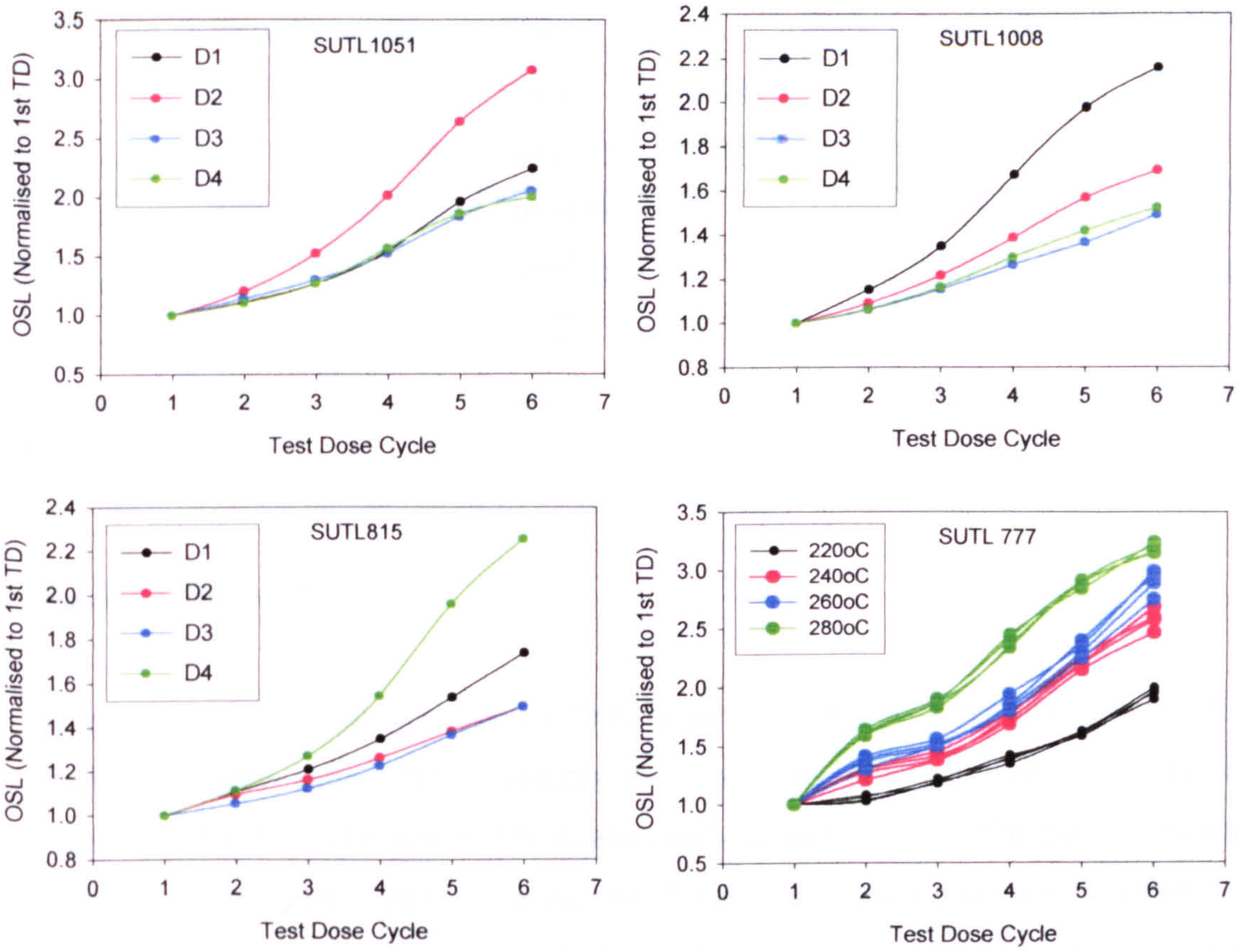

Fig 6.3 Sensitivity change at each test dose cycle

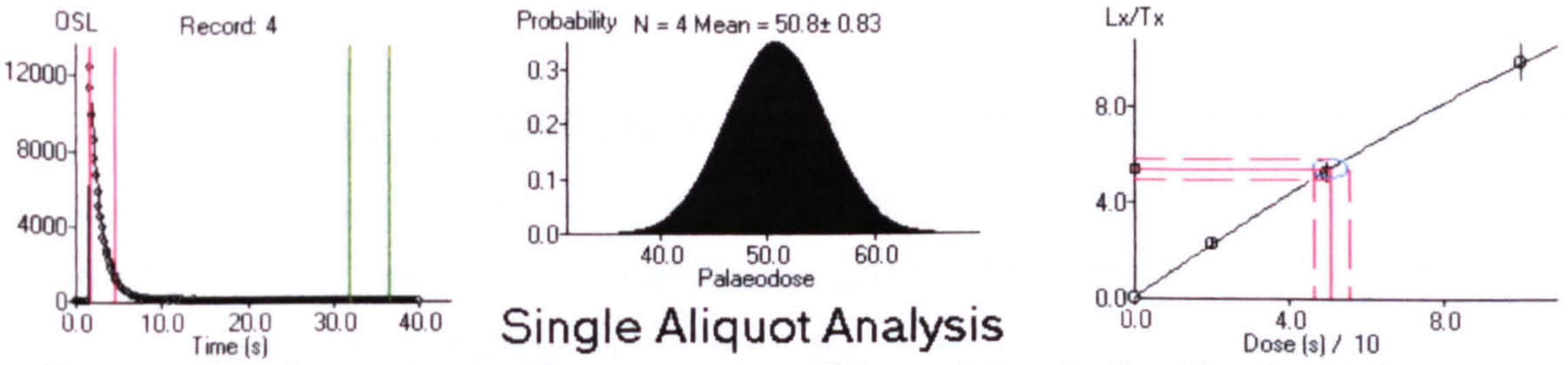

Fig 6.4 Example of Decay curve, ED weighted distribution histogram and regenerative curve for SUTL 1008.

Table 6.1 Results of dose recovery experiments

Site	Sample (SUTL)	No. of Discs	Avg. Initial Intensity	Avg. Sens. Change (TD6/TD1)	Avg. Recycling Ratio	ED (Gy)
Dale	777	16	200,000	2.3	1.01±0.02	5.14±0.04
Skaill	815	4	150,000	1.7	0.99±0.02	5.08±0.08
Cruester	1051	4	9,500	2.3	0.97±0.04	5.15±0.17
Loch of Garths	1008	4	16,000	1.7	1.03±0.03	5.08±0.08

6.2.1.3.5 Summary

Dose recovery experiments indicate that, in the case of laboratory administered doses, the SAR technique successfully corrects for sensitivity changes throughout the run and estimates the dose administered both accurately and precisely. The precision of the dose estimate can be seen to depend on the initial intensity of the signal and the number of discs per sample. An increase in sensitivity change with preheat temperature has also been noted, though in the case of the one sample investigated, no adverse affect on the ED obtained was noted.

6.2.2 Combined Regenerative Additive Procedure

6.2.2.1 Methodology

A new procedure was developed to further investigate the ability of the SAR protocol to accurately correct for sensitivity changes on first readout (for equipment details see section 6.2.1.2). The procedure combined SAR and SARA methods by adding increasing beta doses to aliquots containing their natural doses, and running each through a standard SAR protocol. Where sensitivity change has been adequately corrected for, a regression plot of SAR ED against N, $N+B_1$, $N+B_2$ etc should produce equivalent estimates of the natural ED (fig 6.5). The measurement procedure followed is similar to dose recovery experiments and outlined below in fig 6.6. Twelve samples were selected for analysis, with sets of 16 discs dispensed for each. Pairs of discs were irradiated from 0-10.5Gy to form the $N+\beta$ responses.

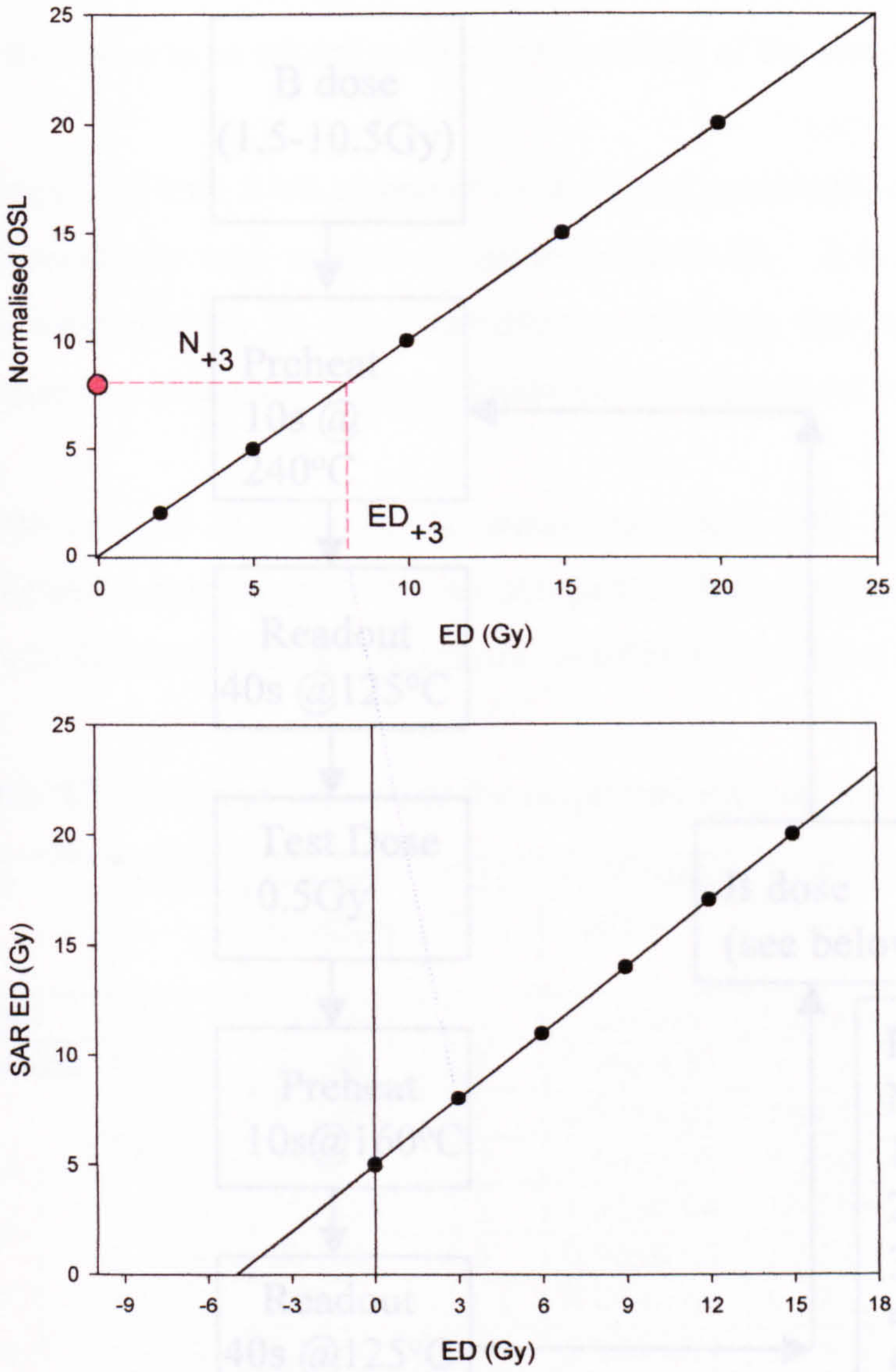

Fig 6.5 Diagramatic representation of regenerative/additive procedure. Portions of sample are given an added beta dose on top of their natural signal and SAR measurements conducted. The calculated ED's from each portion, representing the combined natural + beta dose, are then plotted against added beta dose and the natural signal calculated as the X-intercept of the regression.

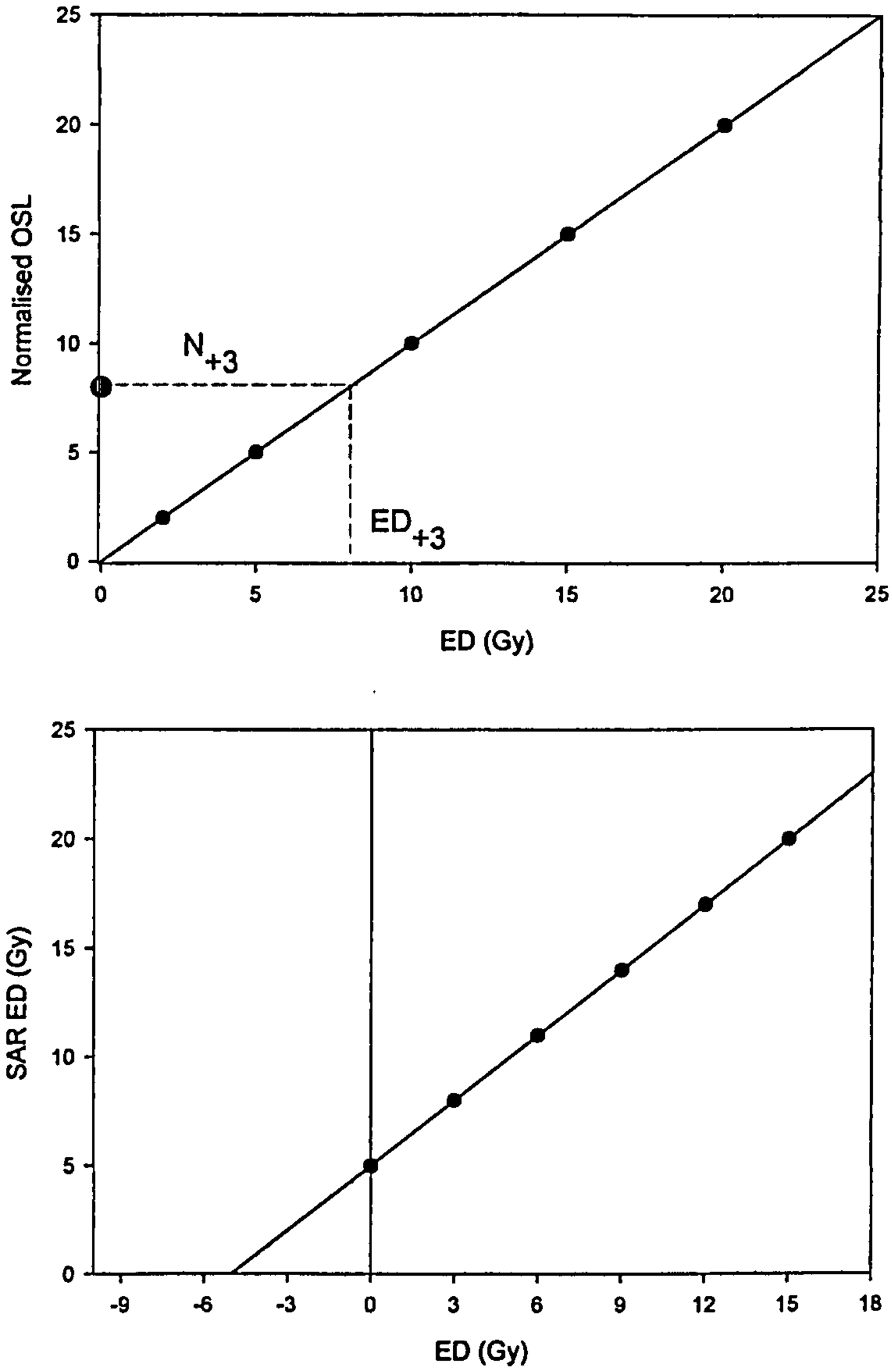

Fig 6.5 Diagramatic representation of regenerative/additive procedure. Portions of sample are given an added beta dose on top of their natural signal and SAR measurements conducted. The calculated ED's from each portion, representing the combined natural + beta dose, are then plotted against added beta dose and the natural signal calculated as the X-intercept of the regression.

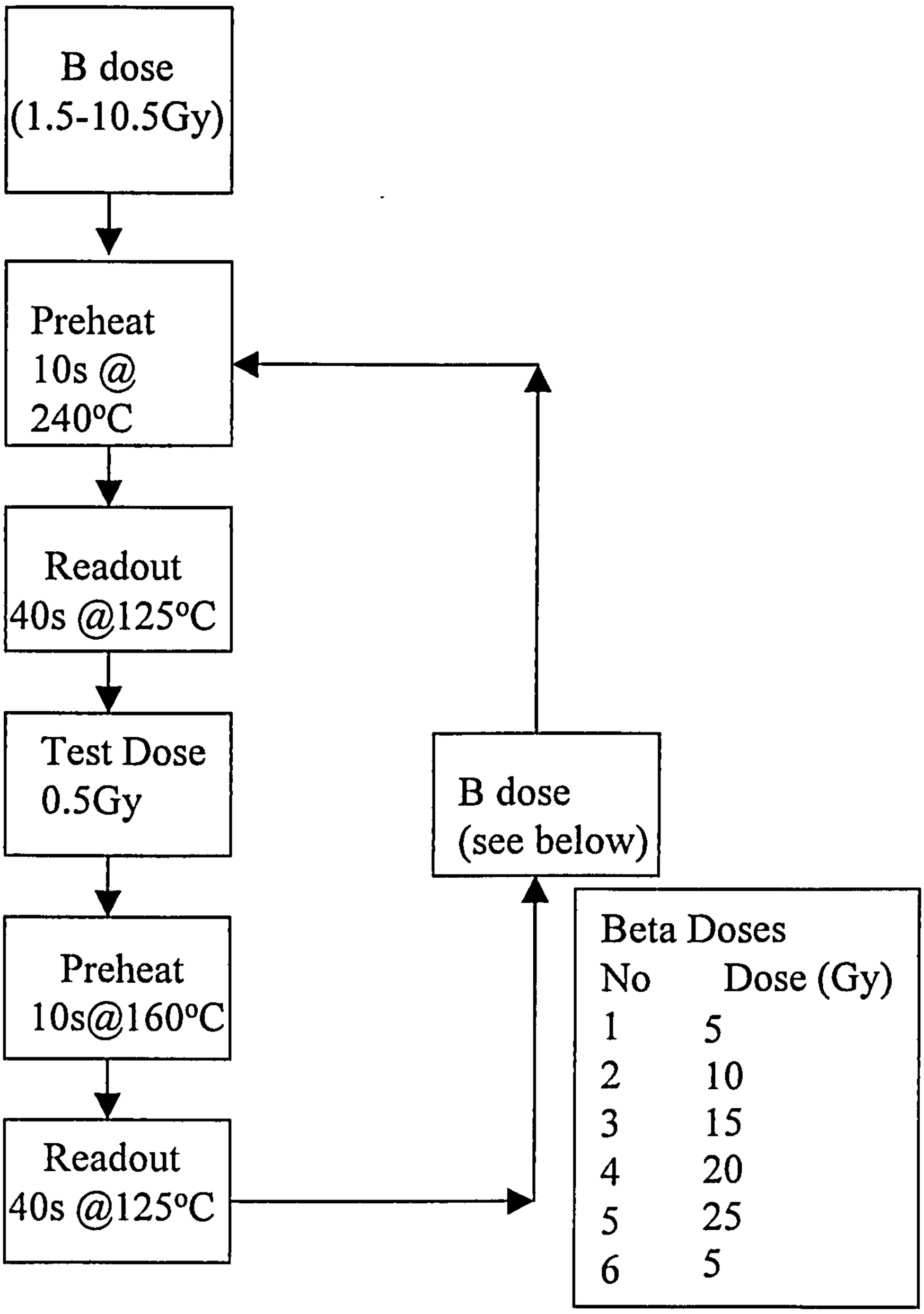

Fig 6.6 Flowchart of combined regenerative additive procedure

6.2.2.2 Results

Combined regenerative additive results are summarized below in table 6.2. The intensity of the natural signal on SAR measurements varied from sample to sample, ranging from 2,500-200,000 counts in the first 1.6s of measurement. All samples showed an increase in sensitivity throughout the run (fig6.7), with the exception of SUTL 1100-1A which showed a sensitivity decrease relative to the first TD response. All recycling ratios are within

error of 1. With the exception of samples SUTL1051 and 1100-1A, fractional errors on ED were seen to be related to the initial intensity of the sample (fig 6.8).

Examples of both SAR regenerative curve and combined regression are given in fig. 6.9, with results for each method compared in fig. 6.10. It is clear that in all but two cases, both estimates are in good agreement, indicating that the SAR run has successfully corrected for sensitivity changes within the natural readout cycle.

In the case of SUTL1068, the errors associated with the regression fit of combined SAR/SARA data are such that the comparison between the two is highly imprecise. Only sample SUTL1075 shows significant deviation from the 1:1 line.

Table 6.2 Summary of results for combined regenerative additive procedure

Site	SUTL	Natural Intensity	TD7/ TD1	Recycling Ratio	SAR ED (Gy)	SAR/SARA ED (Gy)	SAR: SAR/SARA ED Ratio
Skaill	815	110,000	3.5	1.02±0.04	9.50±0.11	8.43±0.10	1.13±0.02
Cruester	968	50,000	3.5	0.98±0.03	9.02±0.33	8.78±0.57	1.03±0.08
	969	100,000	4.2	0.97±0.05	10.45±0.23	9.48±0.91	1.10±0.11
	1051	2500	3.7	1.00±0.03	9.7±0.242	10.34±0.88	0.94±0.08
	1053	100,000	3.2	1.01±0.04	10.55±0.24	9.81±0.61	1.07±0.07
	1054	20,000	4.5	0.96±0.04	10.18±0.65	10.52±1.08	0.96±0.12
	1055	20,000	11.5	0.95±0.06	9.88±0.71	9.94±0.60	0.99±0.09
	1068	80,000	5.5	1.00±0.03	11.30±0.19	14.51±2.82	0.78±0.15
	1075	25,000	3	1.00±0.03	11.25±0.75	8.25±0.51	1.36±0.12
	1097	30,000	1.5	1.07±0.07	11.10±0.68	11.30±0.63	0.98±0.08
	1100-1A	200,000	0.6	1.02±0.03	11.57±0.59	11.43±0.50	1.01±0.07

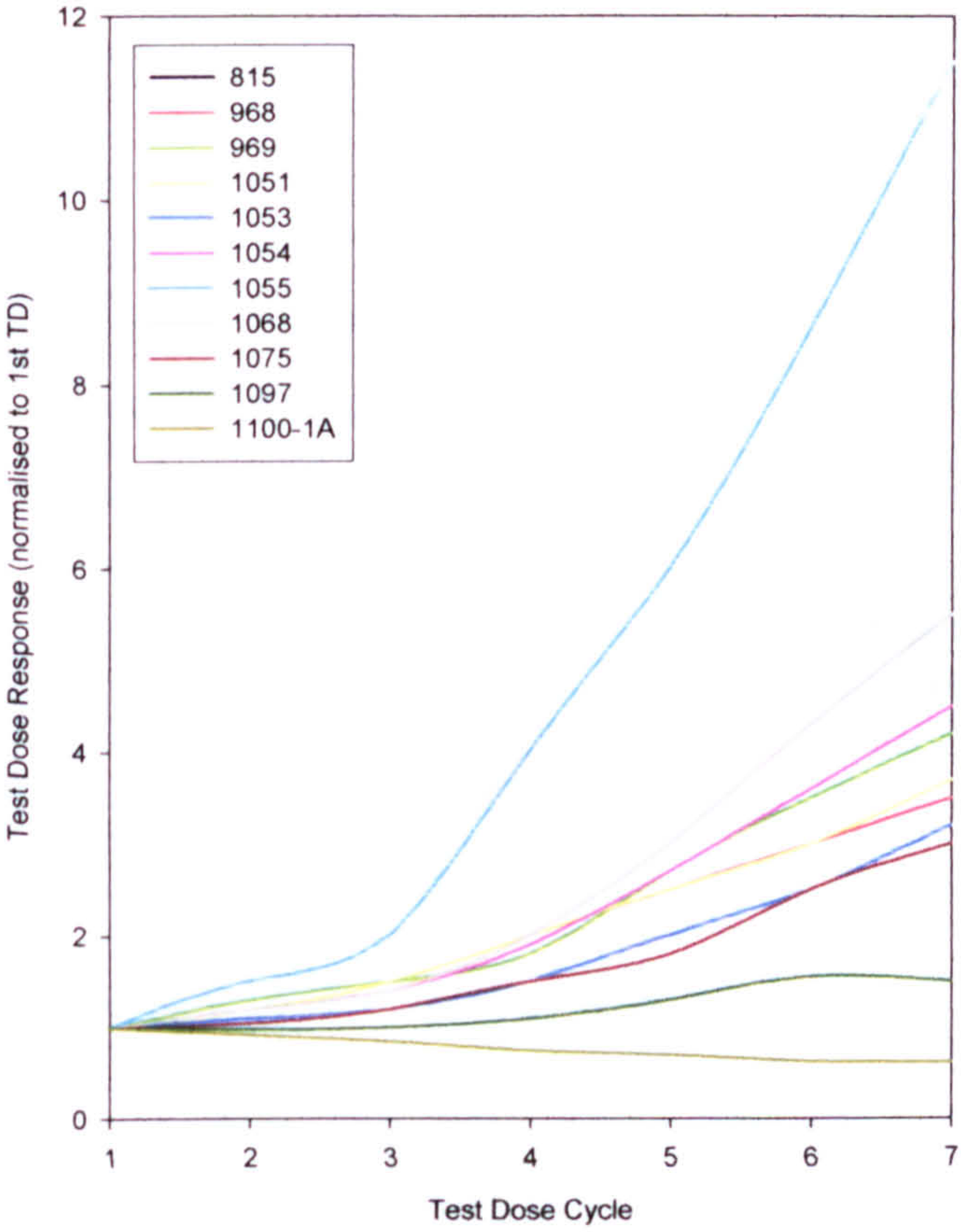

Fig 6.7 Change in test dose during SAR procedure for combined regenerative additive procedure

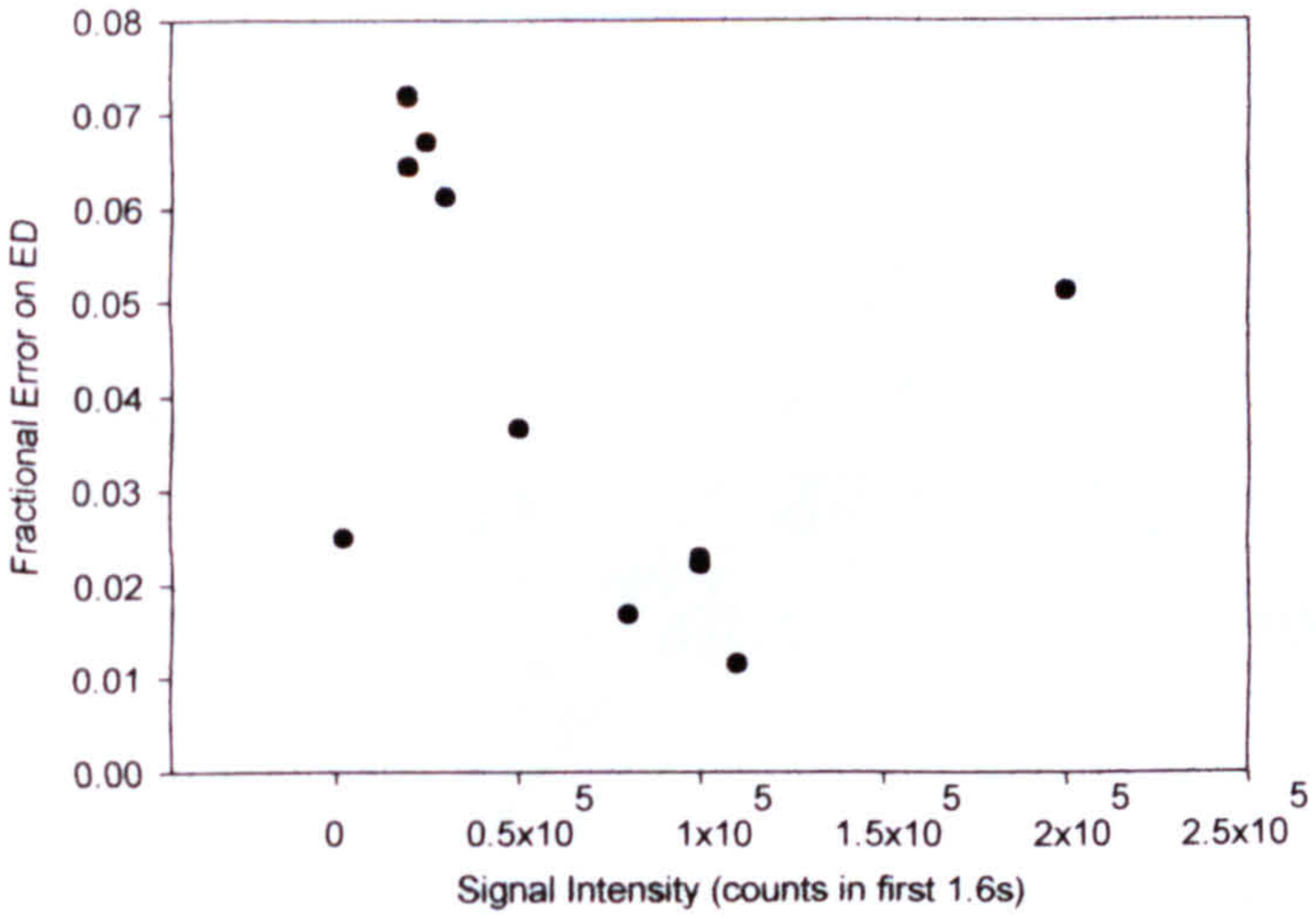

Fig 6.8 Relationship between fractional error on SAR ED and natural signal intensity for combined regenerative additive procedure

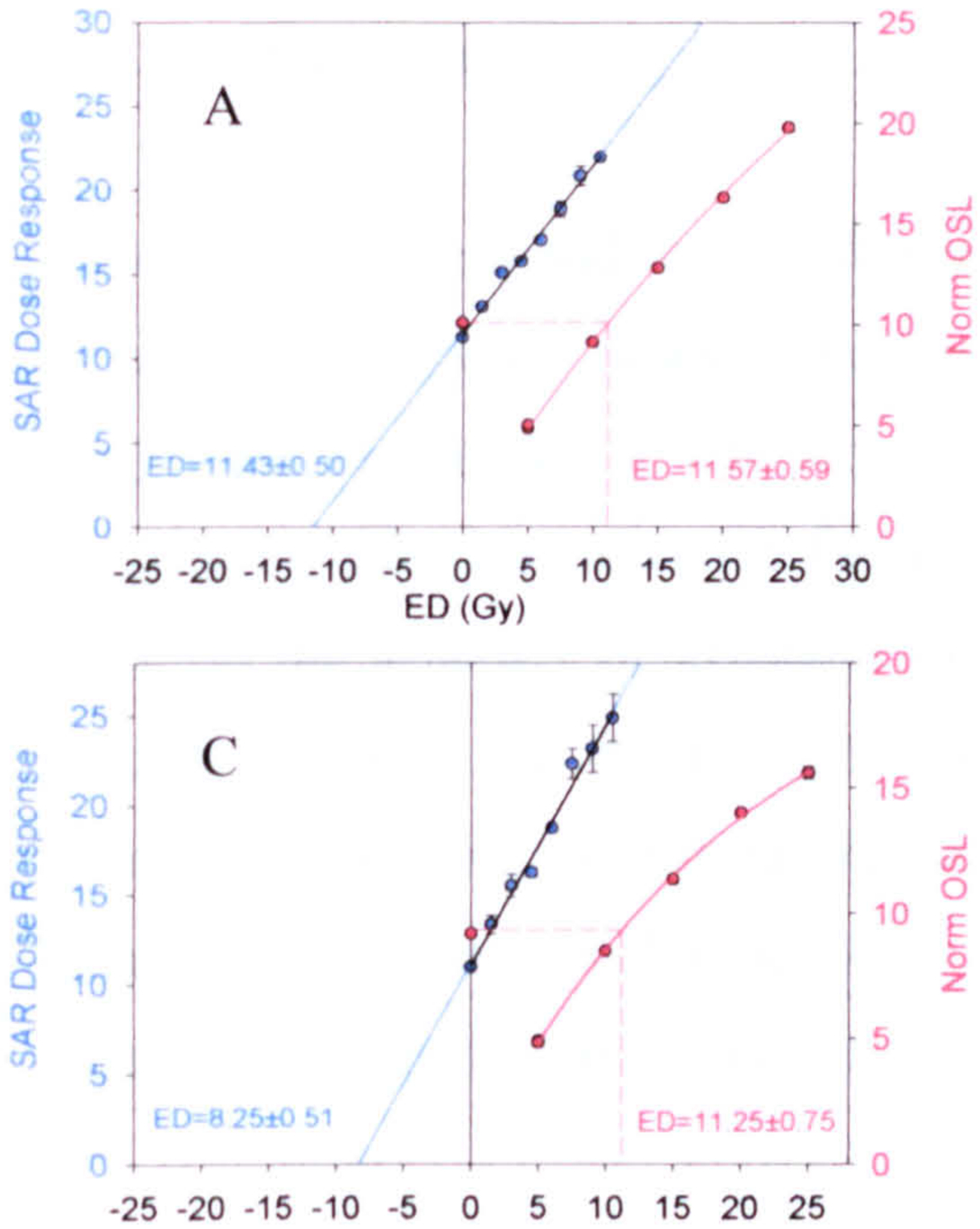

Fig 6.9 Examples of SAR and combined regenerative regression curves (a) SUTL1100 (b) SUTL1068 (c) SUTL 1075

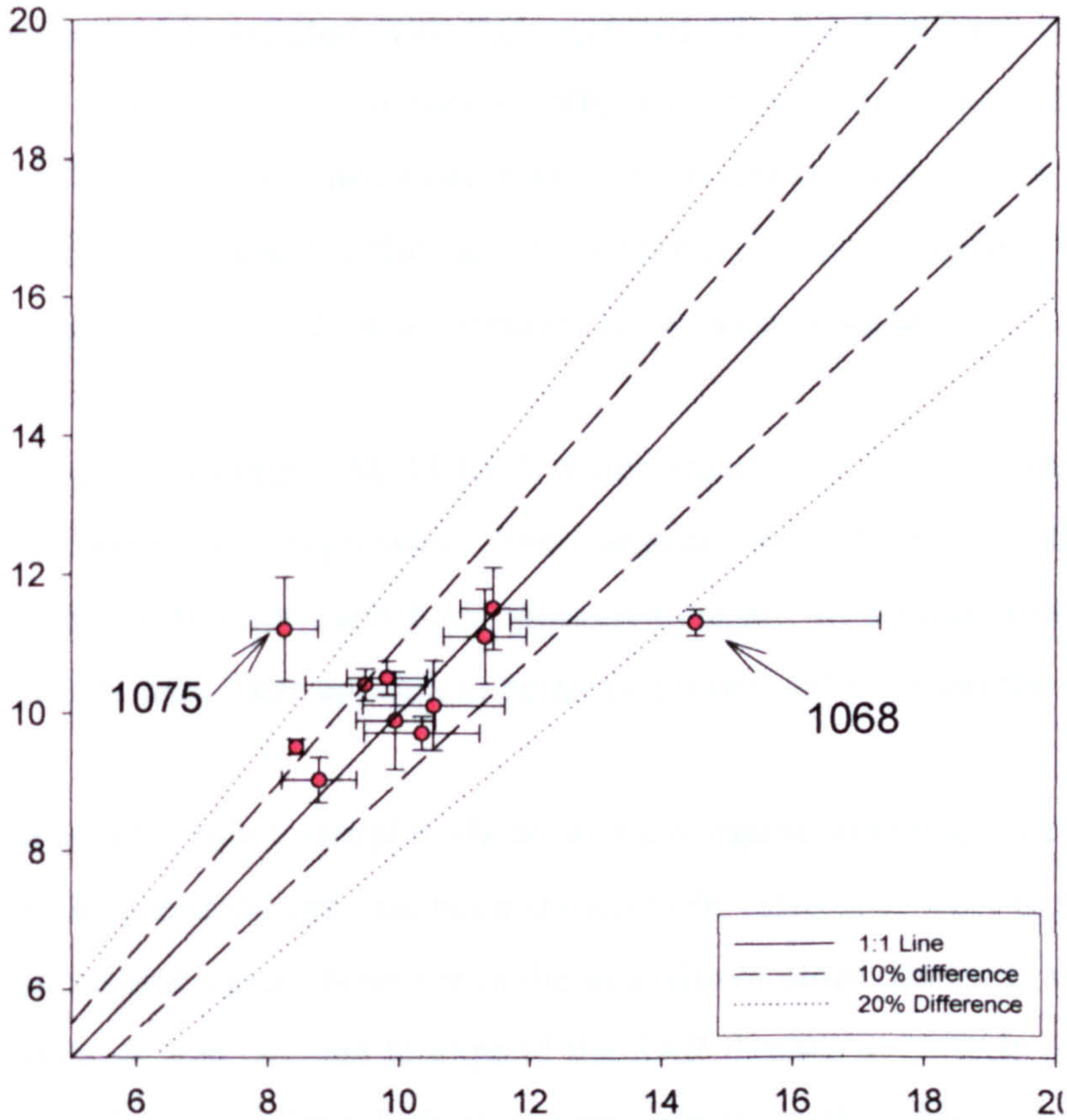

Fig 6.10 Comparison of SAR and SAR/SARA EDs

6.2.3 Summary

Both dose recovery and combined regenerative/additive procedures have shown promising results. Laboratory doses were successfully recovered for all four samples selected, regardless of geology or intensity. The recycling ratio of each was within error of 1 suggesting effective correction for sensitivity after the initial readout cycle. Results also confirm the accuracy of irradiator calibration. Whilst these results are encouraging, it should be noted that the ability to recover a known laboratory dose has necessitated the need to bleach out the natural signal prior to irradiation. The combined regenerative additive procedure has eliminated this step, allowing for investigation of the way in which the natural signal behaves within the SAR procedure.

Results suggest that in all but two samples, the SAR procedure corrects for sensitivity change on first readout. As discussed above, one of the outlying samples –SUTL1068 has a large error associated with the regressed ED due to scatter of points on the regression line. With reference to figure 6.9b, it is clear that the scatter in the regression line is related to more than one or two points and is unrepresentative of the precision seen in other samples. It is possible this scatter is related to contamination within the sample, or is a reflection of uneven dose distribution in the natural signal.

However it is sample SUTL1075 which stands out from the rest of the dataset. Both regenerative and regression lines appear well defined with little obvious scatter. Recycling ratios for each SAR measurement are all within error of 1, with an average of 1.00±0.03 thus there appears to be no systematic error within the readout cycle

Results from other samples show an encouraging agreement between datasets. Precision on SAR measurements has been shown to be related, at least in part, to the initial intensity of the natural signal, however in the majority of cases, intensity was high (>10,000 counts). As such, it was decided to expand the SAR dataset to include other samples from Orkney and Shetland. Whilst a lack of material precludes the addition of the additive procedure to standard measurements, it was hoped that full documentation of individual disc and sample characteristics may help to highlight samples which may behave in a similar manner to SUTL1075.

6.3 SAR dating of samples from Orkney and Shetland

6.3.1 Methodology

A number of different variations on the same protocol were employed in the measurement of ED, determined in part by the quartz yields within particular samples. The protocol used was based on that recommended by Murray and Wintle (2000) and is illustrated in fig 6.11, with test doses being used to monitor and correct for sensitivity changes throughout the run.

Where material permitted, varying preheat temperatures were investigated (from 200-280°C). Where insufficient material was present a single preheat of 240°C was used.

All measurements were made over a 100s period, with 250 data channels recorded per reading. The first and last 10 channels were measured prior and post stimulation source activation in order to monitor variation in reader background.
Analysis was carried out using the ANALYST v.3.0 Programme.

The first 4s of each decay curve were analysed. Each dose point was normalized to its test dose and a regeneration curve constructed. Where appropriate a linear or exponential curve was fitted to the dataset and ED calculated. The error on ED included a fitting error. Recycling ratios and IR response were recorded for further analysis (see below).

Tables 6.3 and 6.4 summarise samples run by site, listing grain size used, the number of discs run, filenames and the reader used.

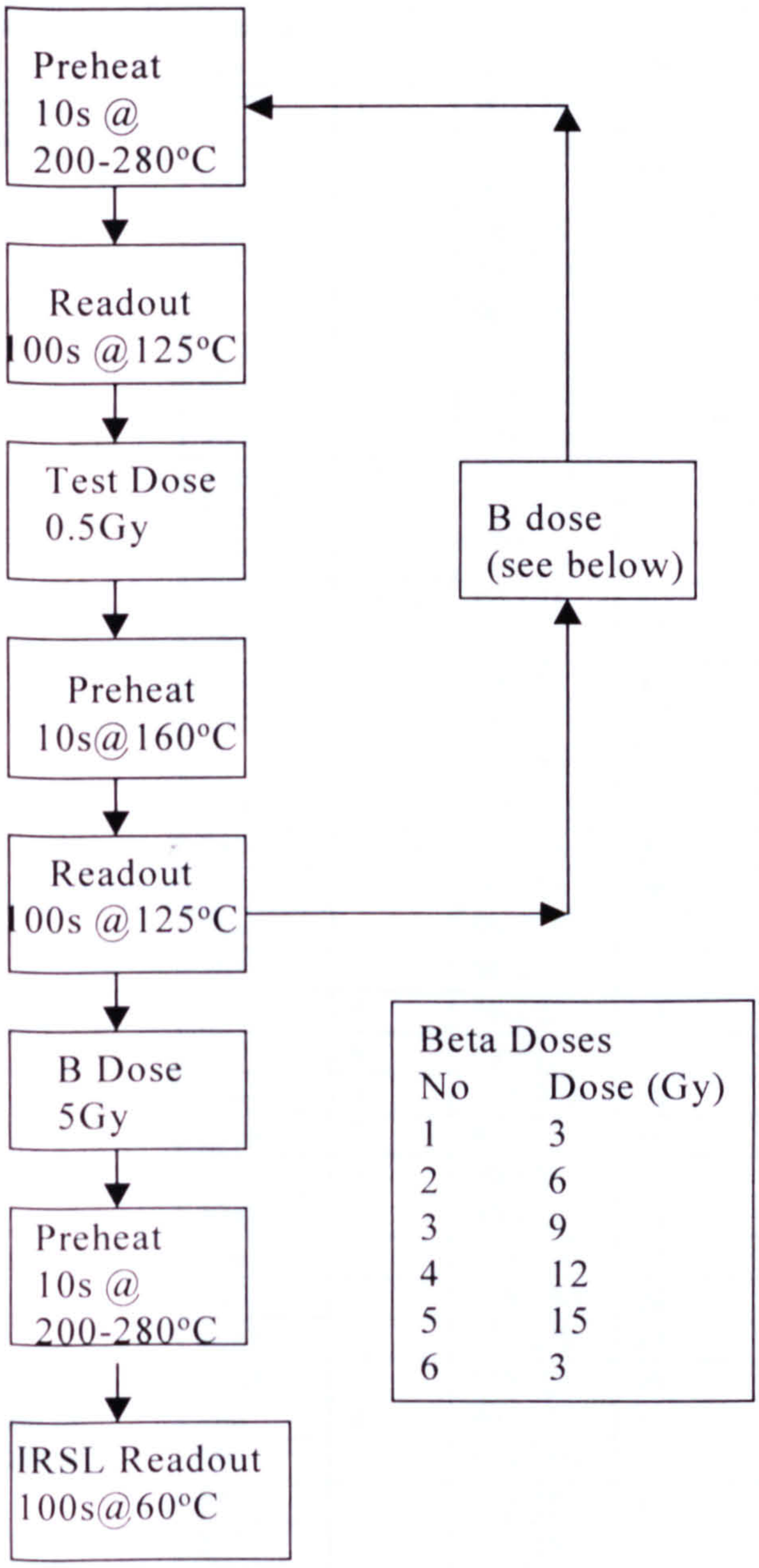

Fig 6.11 Flowchart of SAR Protocol utilized

Table 6.3 Summary of Run Information, Orkney Samples

Site	Sample No	Pos.	Frac (um)	No. of Discs	Reader	Run Name	Readout Temps (oC)
Liddle	1379	1	90-125	20	2	IA2SAR9	220-280
DALE	748	TL12	125-250	4	2	IA4DSAR5	240
	749		90-125	20	1	IA1SAR1	200-280
	750		90-125	4	1	EDAY01	240
	751		125-250	20	1	IA1SAR3	200-280
			90-125	4	1	EDAY01	240
	753		125-250	4	2	IA4SAR5	240
	754		125-250	10	2	IA2SAR5	200-280
	755		125-250	20	1	IA1SAR1	200-280
	760	TL13	125-250	4	2	IA4DSAR5	240
	765		125-250	10	2	IA2SAR5	200-280
	767		125-250	4	2	IA4DSAR5	240
	768	TL14	90-125	4	1	EDAY01	240
	769		90-125	4	1	EDAY01	240
	774		90-125	4	1	IA4DSAR5	240
	777		90-125	4	2	IA4DSAR4	240
			125-250	4	2	IA4DSAR5	240
	779		125-250	4	2	IA4DSAR5	240
	782	TL15	90-125	20	1	IA1SAR3	200-280
	783		90-125	20	1	IA1SAR2	200-280
	784		90-125	20	1	IA1SAR2	200-280
	785		90-125	16	2	IA48D1	260
Skaill	815	5	90-125	14	1	IMCA1	240
	817	6	90-125	20	2	IA2SAR6	200-280
	1343	1	125-250	16	2	IA48D2	240
	1354	2	90-125	16	2	IA48D3	240
	1358	3	90-125	16	2	IA48D1	240
	1360		90-125	16	2	IA48D2	240
	1361		125-250	20	1	IA1SAR9	220-280
	1362		125-250	20	1	IA1SAR9	220-280
	1363		125-250	20	2	IA2SAR8	220-280
	1364		125-250	20	2	IA2SAR8	220-280
Knoll of Merrigarth	794	8	90-125	4	1	EDAY01	240
	795		125-250	4	2	IA4DSAR5	240
	802	7	125-250	4	2	IA4DSAR5	240
	803		125-250	4	2	IA4DSAR5	240
Warness	849	11	125-250	16	2	IA48D2	240
	857	10	90-125	4	1	EDAY01	240
			125-250	4	1	IA4DSAR6	240
Stackelbrae	1374	2	125-250	8	2	IA48D1	240
Fersness	823	3	125-250	4	2	IA4DSAR5	240
	824		125-250	4	1	IA4DSAR6	240
Stenaquoy	836	1	125-250	4	1	IA4DSAR6	240
	838	2	90-125	20	2	IA2SAR4	200-280
	839		125-250	4	1	IA4DSAR6	240

Table 6.4 Summary of Run Information, Shetland Samples

Site	Sample No	Pos	Fraction (um)	No. of Discs	Reader	Run Name	Readout Temps (oC)
Cruester	951	1	125-250	4	2	IA4DSAR4	240
	953		125-250	20	1	IA1SAR7	200-280
	958	2	90-125	20	2	IA2SAR11	200-280
	968	4	125-250	16	2	IASARA2	240
	969		125-250	20	1	IA1SAR4	200-280
	1051	5	125-250	16	2	IASARA3	240
	1053		125-250	20	2	IA2SAR11	200-280
	1054	6	125-250	4	2	IA4DSAR1	240
	1055		90-125	4	2	IA4DSAR2	240
	1059	7	90-125	4	2	IA4DSAR6	240
	1062	8	90-125	4	2	IA4DSAR4	240
	1063		125-250	4	2	IA4DSAR2	240
	1064		90-125	20	2	IA2DSAR5	200-280
	1068	9	125-250	4	2	IA4DSAR4	240
	1075	11	90-125	4	2	IA4DSAR1	240
	1076		90-125	4	2	IA4DSAR2	240
	1077		90-125	4	2	IA4DSAR2	240
	1081	13	125-250	20	2	IA2SAR10	200-280
	1086	15	90-125	4	2	IA4DSAR2	240
	1087		90-125	4	2	IA4DSAR2	240
	1088		90-125	4	2	IA4DSAR1	240
	1094A	17	90-125	4	2	IA4DSAR2	240
	1095		90-125	4	2	IA4DSAR1	240
	1096		90-125	4	2	IA4DSAR1	240
	1097		125-250	4	2	IA4DSAR3	240
	1100-1A	19	90-125	4	2	IA4DSAR1	240
	1100-1B		90-125	4	2	IA4DSAR3	240
	1100-2A		90-125	10	2	IA2SAR9	200-280
	1100-2B		90-125	4	2	IA4DSAR3	240
Houlls	970	1	90-125	4	2	IA4DSAR3	240
	971		90-125	4	2	IA4DSAR3	240
				16	2	9718393	240
	976		90-125	4	2	IA4DSAR3	240
			125-250	4	2	IA4DSAR3	240
	978		90-125	4	2	IA4DSAR3	240
	983	2	125-250	16	2	9718393	240
	991	3	90-125	4	2	IA4DSAR3	240
	993	3	125-250	16	2	9718393	240
	1003	4	90-125	4	2	IA4DSAR4	240
	1004		90-125	8	2	IA4DSAR4	240
Loch of Garths	1006	1	90-125	20	1	IA1SAR6	200-280
	1007		90-125	20	1	IA1SAR6	200-280
	1008		125-250	20	1	IA1SAR5	200-280
	1017	2	125-250	20	1	IA1SAR5	200-280
				4	1	IA4DSAR6	240
	1018		125-250	20	2	IA2SAR4	200-280
				4	2	IA4SAR4	240
	1020		125-250	20	1	IA1SAR4	200-280
				4	2	IA2SAR4	240

6.3.2 Run Characteristics

6.3.2.1 Introduction

There are a number of important run characteristics, which help to categorize the behaviour of samples and aid in the interpretation of the results. The natural sensitivity of the sample may influence the error associated with each ED measurement. Individual ED measurements may be affected by a number of factors, including contamination, preheat treatment and the failure of sensitivity corrections. On a sample-to-sample basis, the distribution of EDs measured should be routinely examined for signs of excess variation associated with microdosimetric effects. Incomplete resetting of the geological signal (as discussed in chapter 2) may also be a source of variance from disc to disc and sample to sample. Run characteristics for each sample are summarized in tables 6.5 and 6.6.

Table 6.5 Summary of sample characteristics, Orkney Samples

Site	Sample No	Natural Intensity	Average TD7/TD1	TD Behaviour	Recycling Ratio	IR Resp	ED (Gy)
Liddle	1379	77,000	1.35	LI	0.99±0.05	10	14.2±2.06
DALE	748	4,800	1.45	LI	1.02±0.10	113	12.05±1.07
	749	4,300	1.55	LI	1.15±0.06	202	10.3±0.96
	750	15,000	3.58	N LI	0.96±0.02	106	10.48±0.58
	751	800,000	0.78	NLD	1.00±0.07	7	9.19±0.1
		300,000	2.36	LI	1.06±0.01	53	10.70±0.14
	753	15,400	0.80	NLD	1.04±0.06	328	9.6±0.45
	754	31,000	4.00	LI	0.99±0.02	-11	11.58±0.25
	755	4,100	1.90	N LI	1.15±0.06	918	3.11±0.16
	760	301,000	3.13	N LI	1.04±0.06	153	12.58±0.63
	765	2,000	1.98	LI	0.90±0.04	11	16.3±0.72
	767	17,500	3.81	LI	0.98±0.07	4	12.6±0.82
	768	250	1.98	LI	0.99±0.06	6	-----
	769	1,000	5.6	LI	1.39±0.13	15	8.04±1.39
	774	10,400	1.80	LI	1.14±0.10	215	11.4±0.85
	777	475,100	2.52	N LI	1.01±0.06	13	9.03±0.40
		2,403,500	1.70	N LI	1.05±0.05	41	9.08±0.40
	779	43,000	2.60	N LI	1.05±0.06	225	11.85±0.50
	782	70,000	1.29	LI	1.09±0.05	148	13.6±0.40
	783	302,000	1.32	N LI	0.98±0.02	167	10.81±0.20
	784	110,000	1.21	N LI	1.01±0.03	94	10.05±0.20
	785	2,000	1.23	LI	0.99±0.02	54	-------
Skaill	815	110,000	1.17	LI	1.02±0.03	16	9.50±0.11
	817	123,000	2.43	N LI	0.97±0.02	13	12.09±0.38
	1343	10,000	3.51	N LI	1.09±0.04	25	8.3±0.73
	1354	15,000	2.16	LI	1.19±0.06	53	9.2±0.69
	1358	7,500	1.93	LI	1.05±0.01	72	11.6±0.87
	1360	15,000	2.03	LI	1.00±0.01	1000	9.52±2.42
	1361	600	1.90	NLI	1.00±0.05	313	0.61±0.18
	1362	1000	1.52	LI	---	106	-----

Site	Sample No	Natural Intensity	Average TD7/TD1	TD Behaviour	Recycling Ratio	IR Resp	ED (Gy)
	1363	1,500	1.61	LI	1.09±0.04	1588	0.80±0.07
	1364	1,500	1.78		1.19±0.06	1026	1.03±0.10
Knoll of Merrigarth	794	150,000	2.16	LI	1.05±0.01	10	10.70±0.43
	795	50	2.41	LI	1.00±0.06	8	12.03±0.64
	802	43,000	2.28	LI	1.03±0.06	6	13.30±0.74
	803	12,000	1.07	NLI	1.00±0.09	-1	12.05±0.90
Warness	849	100,000	1.32	NLI	0.97±0.05	15	12.7±0.43
	857	25,000	3.05	LI	0.99±0.02	17	17.13±0.71
		17,000	2.16	LI	1.08±0.08	14	16.83±1.13
Stackelbrae	1374	15,000	1.02	NLI	1.02±0.10	96	5.9±1.69
Fersness	823	120,000	1.87	LI	1.04±0.06	98	12.4±0.59
	824	80,000	1.39	LI	1.00±0.06	73	11.43±0.53
Stenaquoy	836	14,000	1.65	NLI	0.91±0.07	1264	11.43±0.86
	838	140,000	2.98	LI	0.99±0.02	13	9.31±0.23
	839	83,000	2.14	LI	1.01±0.06	-12	9.83±0.48

Key to TD behaviour codes L=linear, NL= non-linear, I=increase, D=decrease, NC=no change

Table 6.6 Summary of sample characteristics, Shetland Samples

Site	Sample No	Natural Intensity	Average TD7/TD1	TD Resp	Recycling Ratio	IR Resp	ED (Gy)
Cruester	951	8500	4.21	NLI	1.01±0.04	8	12.55±0.60
	953	10000	1.19	NLI	0.98±0.06	30	9.93±0.20
	958	80000	1.36	LI	1.01±0.03	12	10.37±0.25
	968	15000	1.48	NLI	0.97±0.04	11	10.20±0.50
	969	116000	1.34	LI	1.02±0.03	297	10.45±0.23
	1051	2500	1.62	LI	1.07±0.06	486	3.53±0.26
	1053	103000	1.81	NLI	1.01±0.03	12	10.55±0.24
	1054	16000	2.98	NLI	1.03±0.07	-6	10.18±0.65
	1055	19000	16.30	LI	0.99±0.06	8	9.88±0.71
	1059	84000	0.79	LD	1.08±0.06	-9	36.1±12.84
	1062	9000	3.30	NLI	1.04±0.08	-7	13.08±0.67
	1063	15000	2.01	LI	1.15±0.03	2552	11.38±0.96
	1064	47000	1.86	NLI	1.02±0.06	12	4.46±0.12
	1068	80000	1.28	NLI	0.98±0.03	14	13.38±0.48
	1075	23000	2.40	LI	1.03±0.07	25	11.25±0.75
	1076	1800	1.33	LI	1.04±0.10	-41	9.7±1.79
	1077	650	0.93	NLD	---	60	---
	1081	700	1.26	NLI	1.07±0.03	3	13.2±0.27
	1086	800	1.19	NLI	1.05±0.12	3	13.4±1.73
	1087	500	0.93	LD	--	5	--
	1088	500	1.00	NC	--	23	--
	1094A	1000	1.54	LI	1.01±0.16	7	12.2±0.70
	1095	400	1.02	LI	---	42	---
	1096	5500	1.02	NLI	-----	108	-----
	1097	32000	1.39	LI	1.08±0.07	259	11.1±0.68
	1100-1A	200000	0.74	LD	1.02±0.06	45	11.58±0.59
	1100-1B	98000	0.87	LD	1.05±0.06	4	14.3±0.82
	1100-2A	120000	1.16	NLI	0.99±0.06	8	11.9±0.54

Site	Sample No	Natural Intensity	Average TD7/TD1	TD Resp	Recycling Ratio	IR Resp	ED (Gy)
	1100-2B	5400	1.45	LI	1.07±0.14	-6	15.65±2.57
Houlls	970	63000	2.28	NLI	1.00±0.06	4	16.03±1.05
	971	1600	1.21	LI	0.86±1.03	-7	10.8±3.83
	976	5200	3.29	LI	1.02±0.10	15	17.17±2.70
		12500	3.61	NLI	1.06±0.08	34	17.7±2.04
	978	22300	3.34	NLI	1.01±0.07	-11	15.93±1.79
	983	22000	3.06	LI	1.00±0.07	-9	23.33±1.47
	991	260000	3.13	NLI	1.06±0.06	13	17.15±1.42
	993	3100	1.59	NLI	0.9±0.22	2	15.7±6.96
	1003	97000	3.47	LI	1.00±0.06	-9	17.08±0.82
	1004	15400	2.85	LI	0.99±0.08	-10	19.4±1.49
Loch of Garths	1006	26000	1.59	LI	1.06±0.03	1102	6.17±0.16
	1007	96000	1.57	NLI	1.04±0.03	18241	5.06±0.11
	1008	43000	1.22	LI	1.10±0.06	-6	7.8±0.38
	1017	98000	1.16	LI	1.02±0.03	31	15.20±0.33
		91000	1.17	LI	1.03±0.06	39	18.43±1.22
	1018	30000	1.86	NLI	1.08±0.03	740	12.39±0.35
		30000	2.18	LI	1.00±0.07	735	14.5±1.1
	1020	330000	1.70	NLI	1.03±0.02	91742	3.92±0.08

Key to TD behaviour codes L=linear, NL= non-linear, I=increase, D=decrease, NC=no change

6.3.2.2 Intensity of Natural Signal

The intensity of the natural signal was analysed by means of comparing the first 4s of each decay curve. Machine background was subtracted from the signal prior to analysis (no late-light subtraction was performed).

The intensity of the natural signal varied from sample to sample and site to site. Examples are shown in fig 6.12. A wide range of intensities were seen ranging from a few hundred counts to several million (fig 6.13). Cruester, Houlls and Dale showed considerable variation between samples. All other sites showed intensities in the region of 10,000-100,000 with the exception of three samples from Skaill , which are in the region of several hundred counts – these samples correlate with OSL sand samples taken as part of a wider environmental study of the burnt mound. Average intensity of each sample is recorded in tables 6.5 and 6.6.

No indication of an increase in natural intensity with preheat temperature was noted on any run for which a variety of preheats used. Fig 6.15 shows the relationship between natural intensity and the fractional error of the ED. It is clear that in the majority of cases, the intensity of the sample affects the overall precision of the ED obtained.

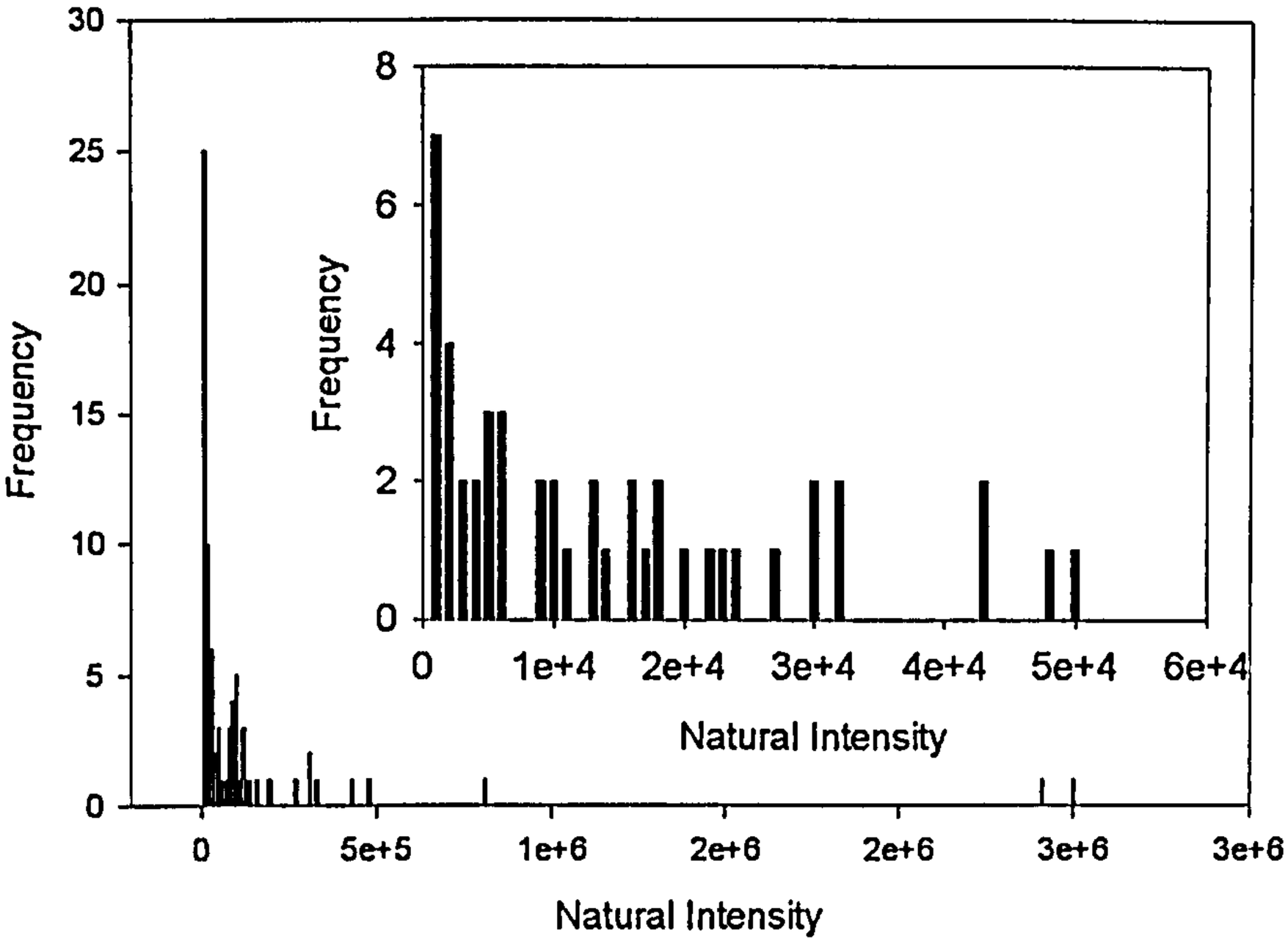

Fig 6.12 Histogram of natural intensity for each disc in Orkney and Shetland dataset

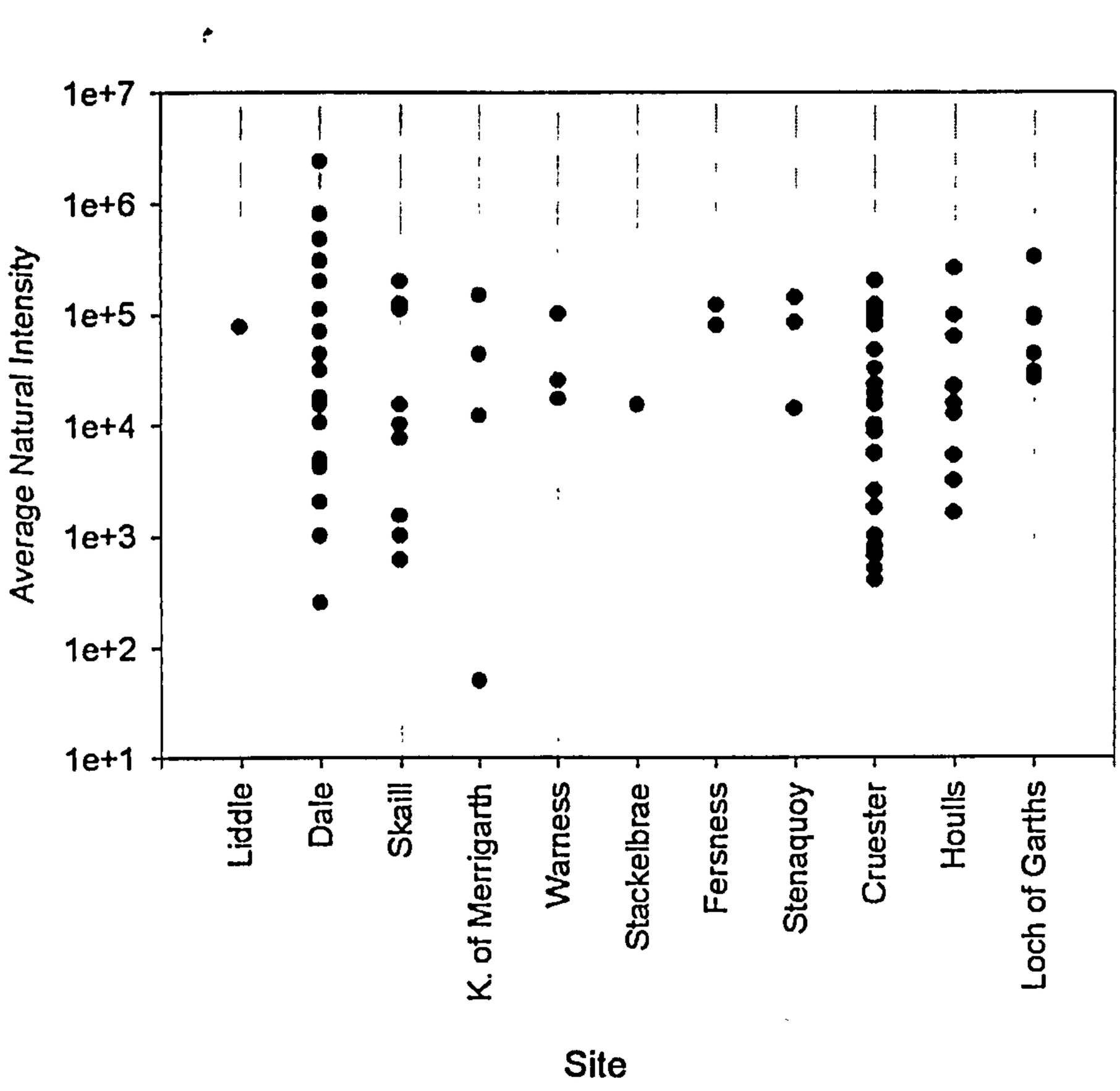

Fig 6.13 Vertical Point plot of average natural intensity for each sample in Orkney and Shetland dataset, grouped by site

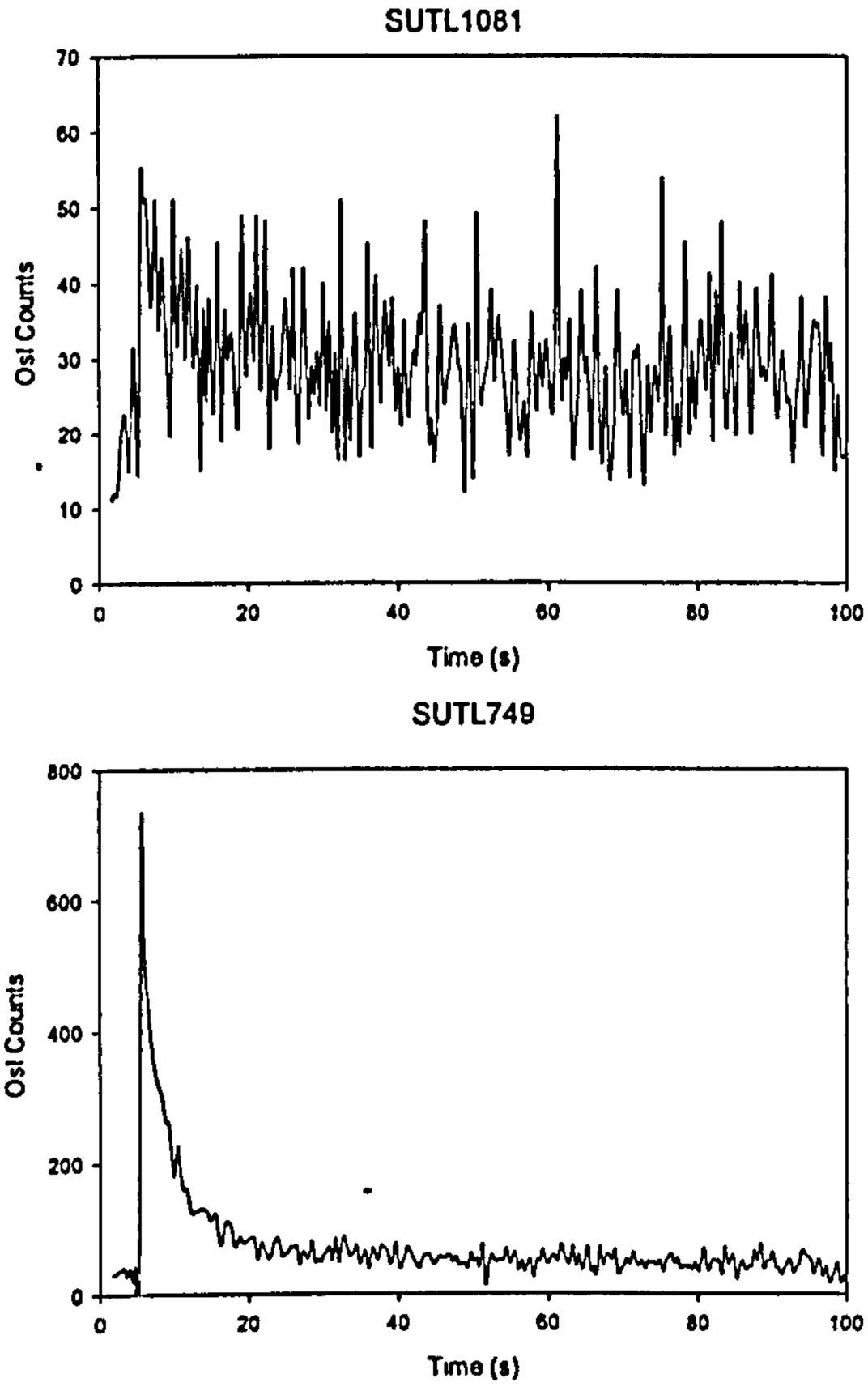

Fig 6.14 Examples of decay curves (a) SUTL1081 (b) SUTL749 (c) SUTL 1017

Fig 6.15 Relationship between Natural OSL sensitivity and fractional ED error.

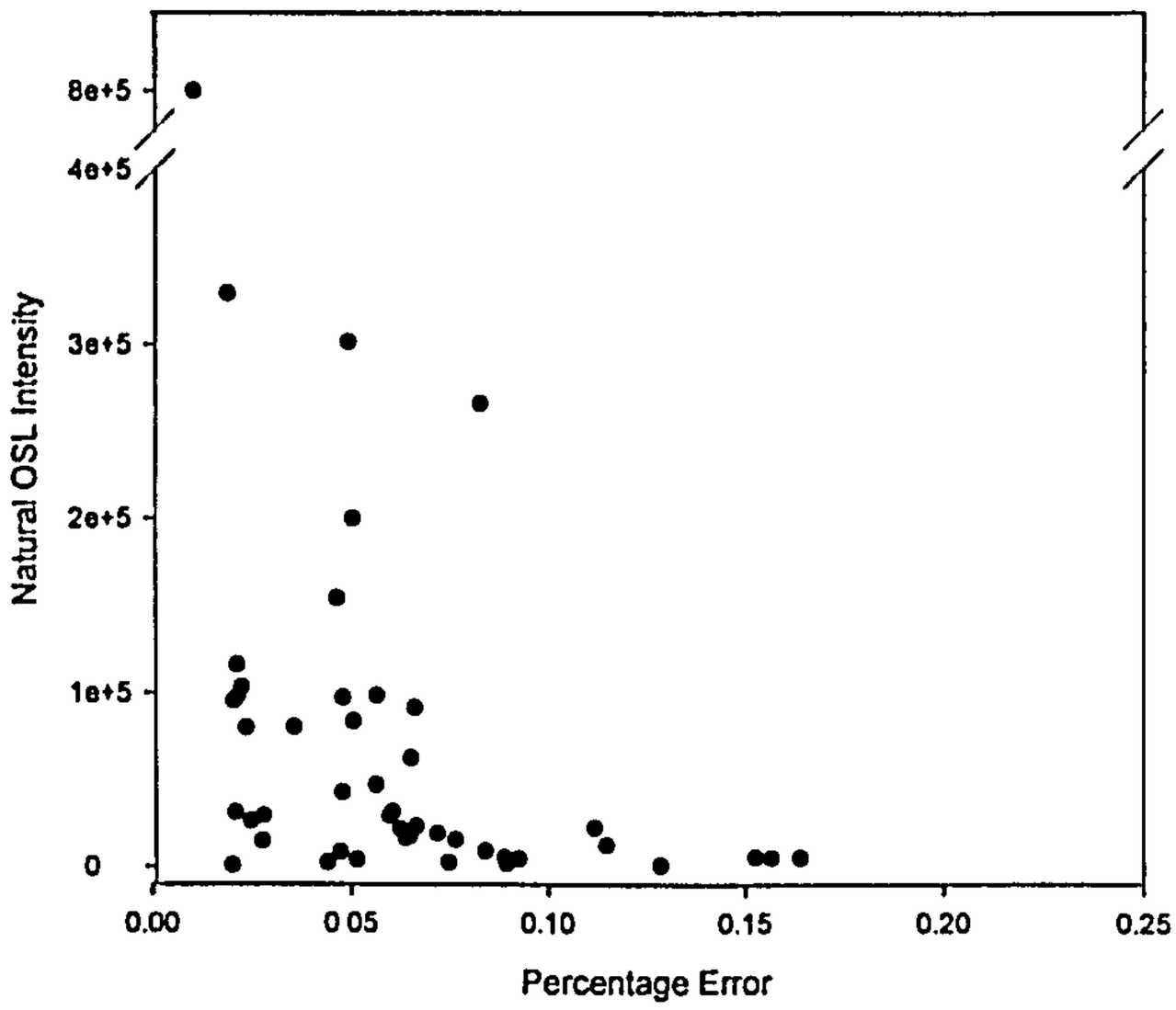

6.3.2.3 Preheat Temperature

Where material permitted, the dependence of ED on preheat temperature was investigated. Previous SAR OSL studies highlight the need for careful observation of the effect of preheat temperature, reporting both an increase and decrease in ED with temperature.

Temperature dependence of ED was investigated over five preheat temperature bands – 200, 220, 240, 260 and 280°C. The vast majority of samples showed no preheat dependence however on occasion both increase and decrease in ED was noted with temperature (fig 6.16 and 6.17). Trends were quantified by fitting a linear regression through points. The gradient of each regression was noted for future comparison with other attributes (see recycling and IR sections). Where evidence of increased/decreased ED existed discs in the effected temperature bands were rejected.

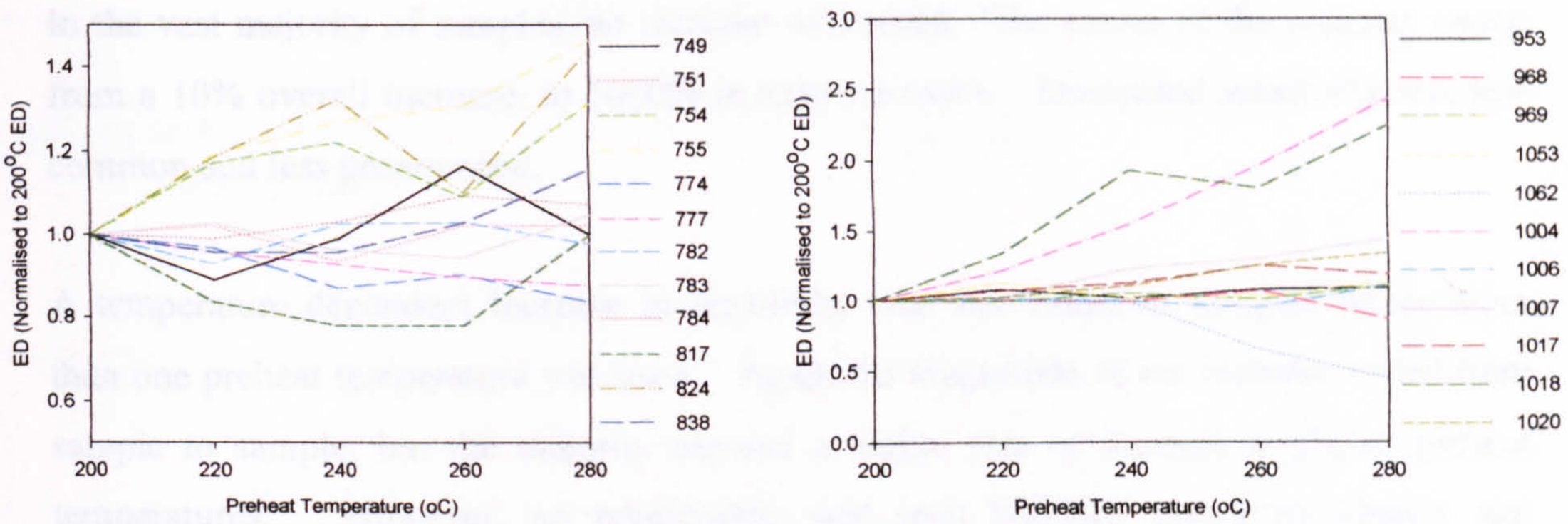

Fig 6.16 Normalised ED as a function of preheat temperature for (a) Orkney Samples and (b) Shetland Samples

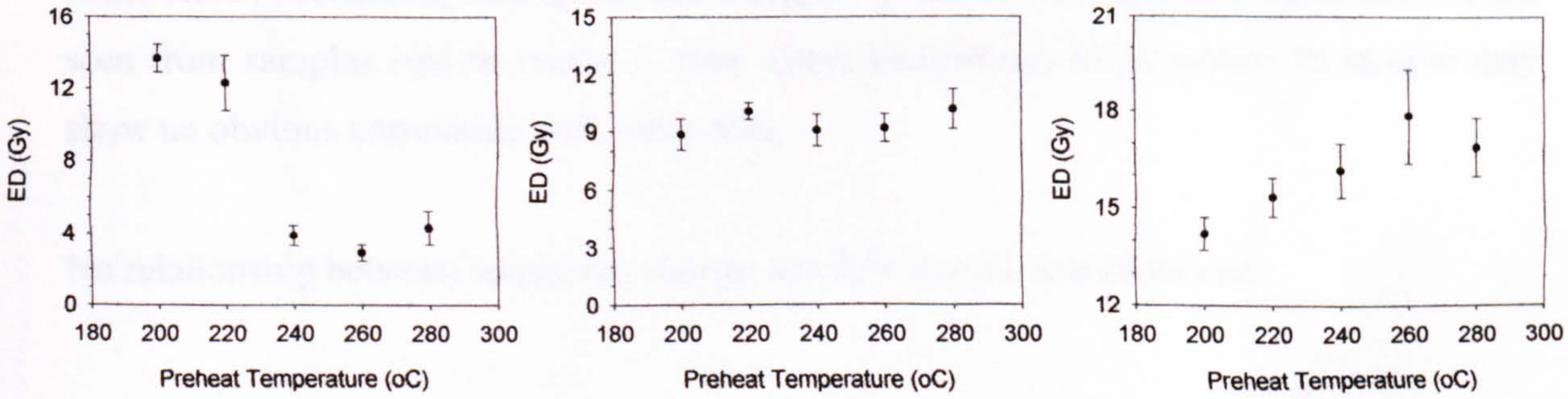

Fig 6.17 Variation in preheat plateau (a) SUTL 1055 Decrease in ED with Temperature (b) SUTL1053 Constant with Temperature (c) SUTL1017 Increase in ED with Temperature

6.3.2.4 Sensitivity Change

The sensitivity change of each sample was monitored throughout the run by comparing the test dose response at each cycle. For each disc, the first 4s of the test dose signal was normalized to the first test dose response and examined for signs of change.

Observed behavior could be categorized into one of the following:

(i) no change (1%)
(ii) linear increase (53%)
(iii) non-linear increase (38%)
(iv) linear decrease (5%)
(v) non-linear decrease (3%)

In the vast majority of samples, an increase was noted. The extent of the increase varied from a 10% overall increase, to 1000% in extreme cases. Decreased sensitivity was less common and less pronounced.

A temperature dependent increase in sensitivity was also noted in samples where more than one preheat temperature was used. Again the magnitude of the increase varied from sample to sample, but the majority showed a higher rate of increase at higher preheat temperatures. However, no relationship was seen between sensitivity change and observed changes in ED with preheat temperature.

The ratio of last to first test dose for each sample is shown in tables 6.5 and 6.6 as a gauge to the relative sensitivity change of each sample. It should be noted that higher ratios were seen from samples run on reader 2, thus direct comparison from sample to sample may show no obvious correlation with other data.

No relationship between sensitivity change and ED or error was observed.

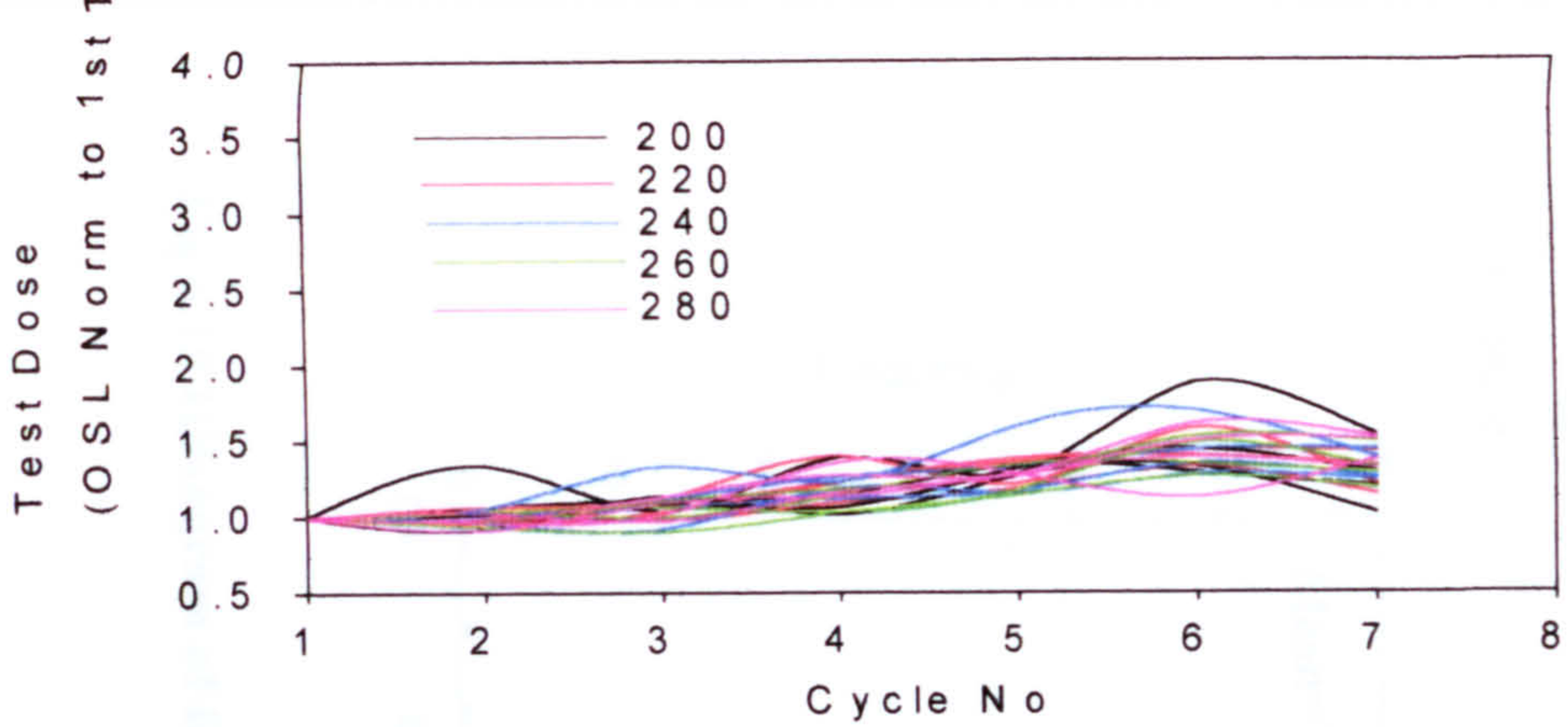

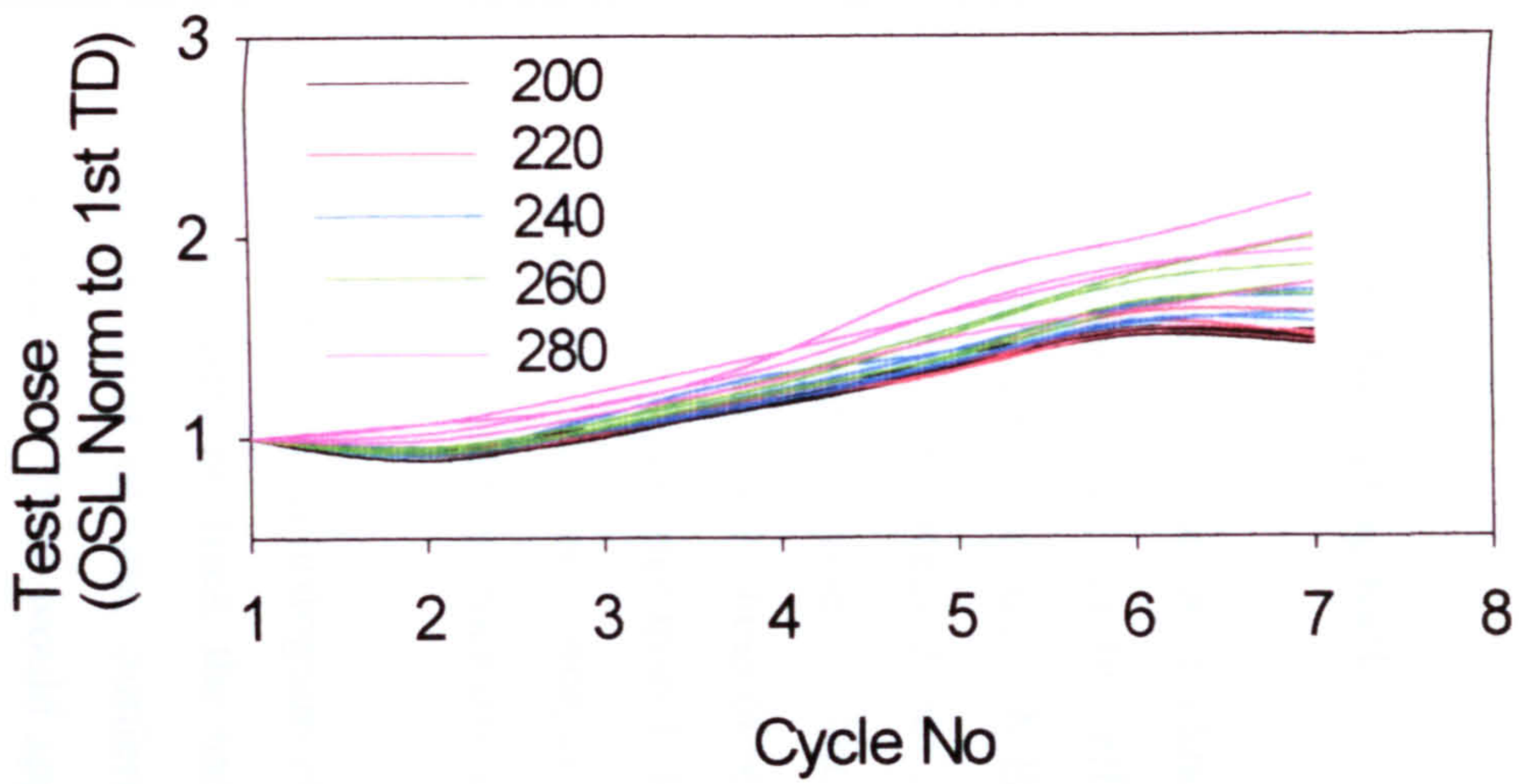

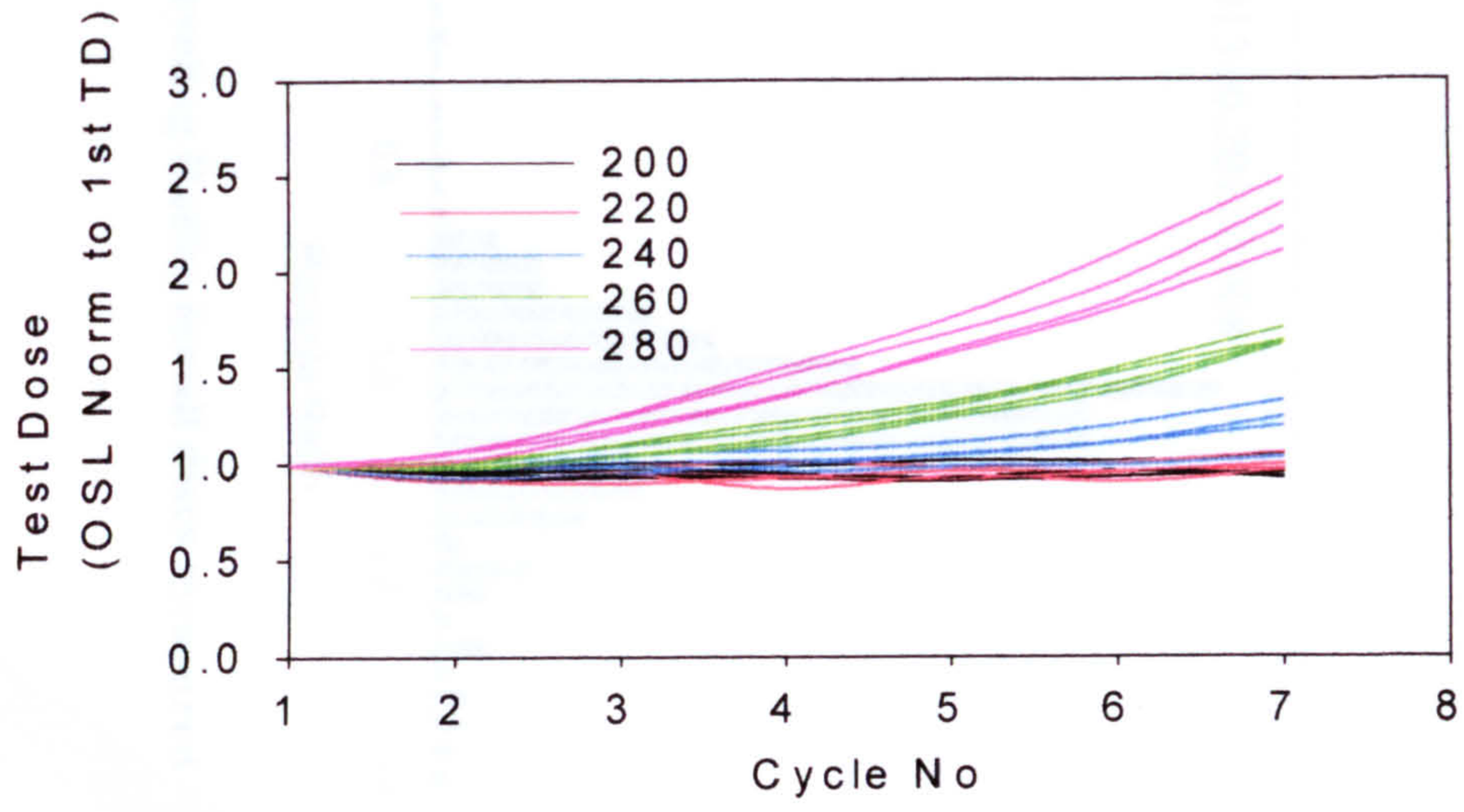

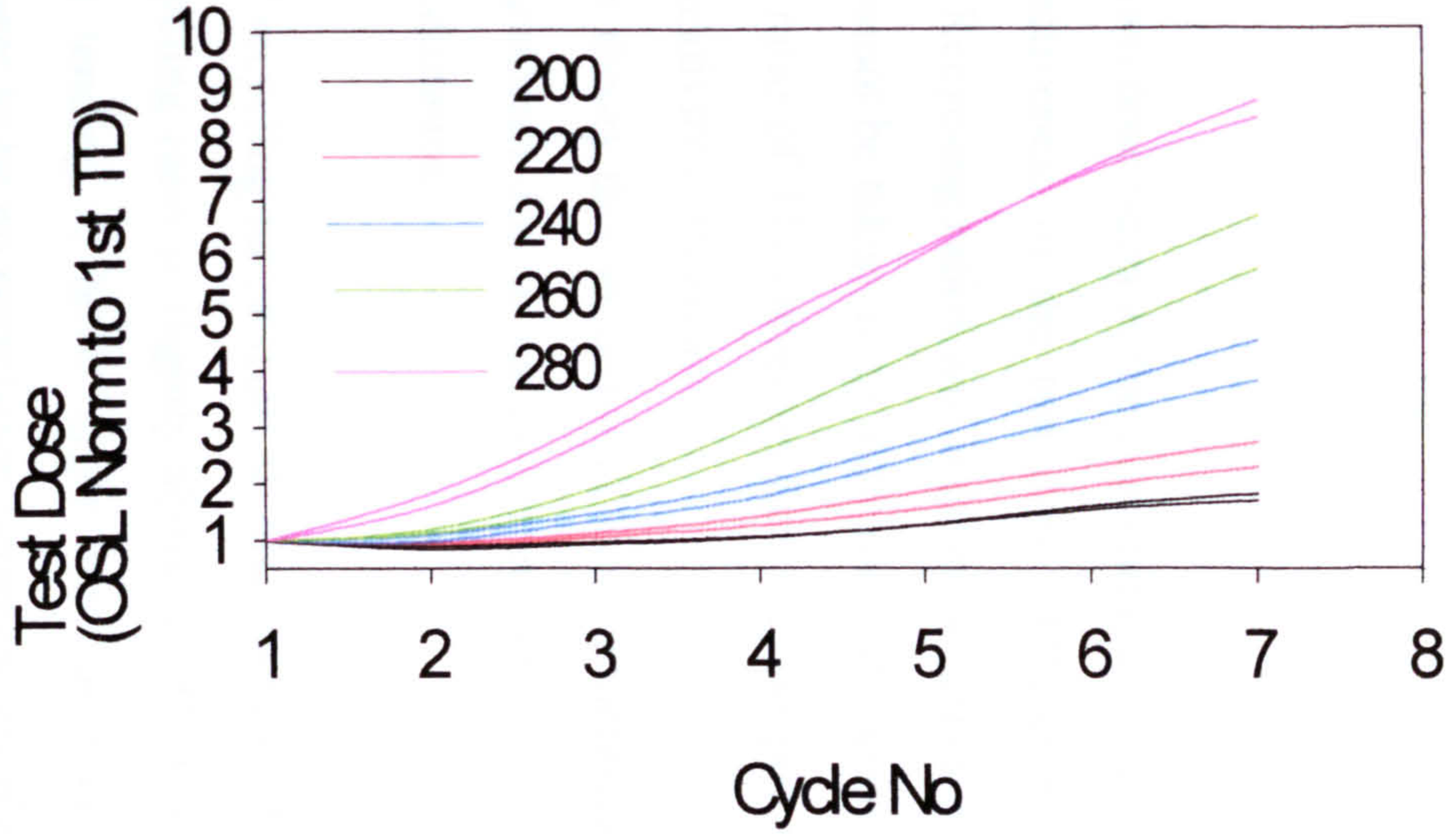

Fig 6.18 Variation in Sensitivity Change throughout runs (A) SUTL 755 very slight increase with cycle – very scattered no evidence of increase with temperature (B) SUTL 1064 Near linear increase with TD, slight seperation by temperature (C)SUTL 958 – No increase 200-220, exponential increase at 240-280°C (D) SUTL 754 Linear increase with TD, also marked increase with temperature 1000% increase by TD7.

6.3.2.5 Recycling Ratio

Repeat measurements of a known dose point at the beginning and end of each run are used as a cross check for the effectiveness of the test dose (TD) correction for sensitivity changes within the run. (N.B Recycling ratios will indicate whether laboratory doses have been correctly corrected, but cannot be taken as an indication of appropriate corrections for natural readout cycle). The ratio of TD corrected last recycle point to first is used to express the effectiveness of sensitivity corrections.

If the ratio is greater than 1, in theory this should lead to an underestimation of ED as the regression line has a steeper gradient due to under-correction. Likewise, a ratio of less than one should produce overestimation.

Fig 6.19 shows a histogram of recycling ratios from all discs measured. It is clear that for the majority of discs, the recycling ratio is slightly above 1. However, the majority are within error of one, outliers tending to have larger associated errors than the main population. There would appear to be no correlation between sensitization (expressed as the ratio of last to first TD response) and recycling ratio (fig 6.20). Neither was any relationship seen between sensitivity change and observed changes in ED with preheat temperature.

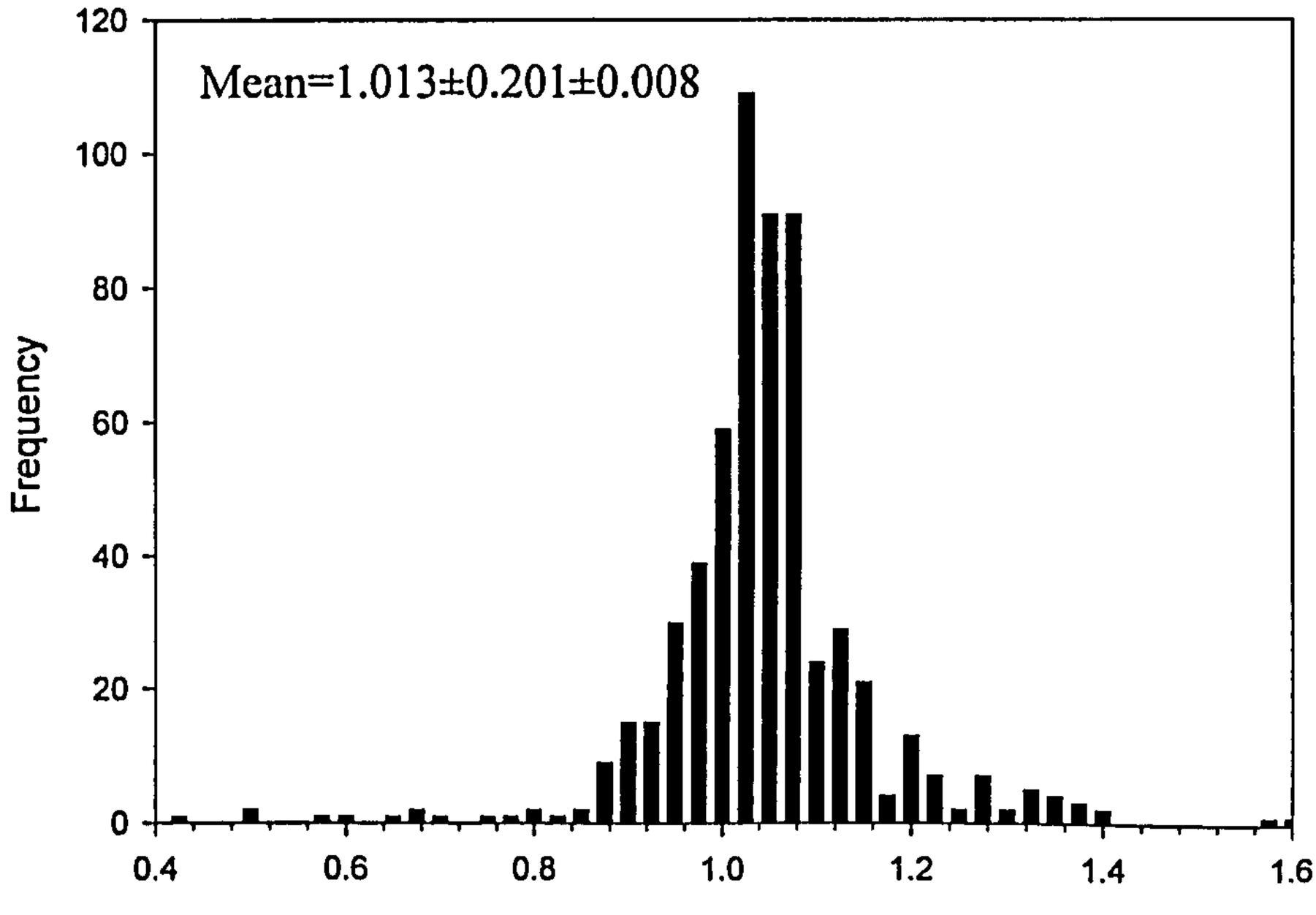

Fig 6.19 Histogram of Recycling Ratios for all discs measured

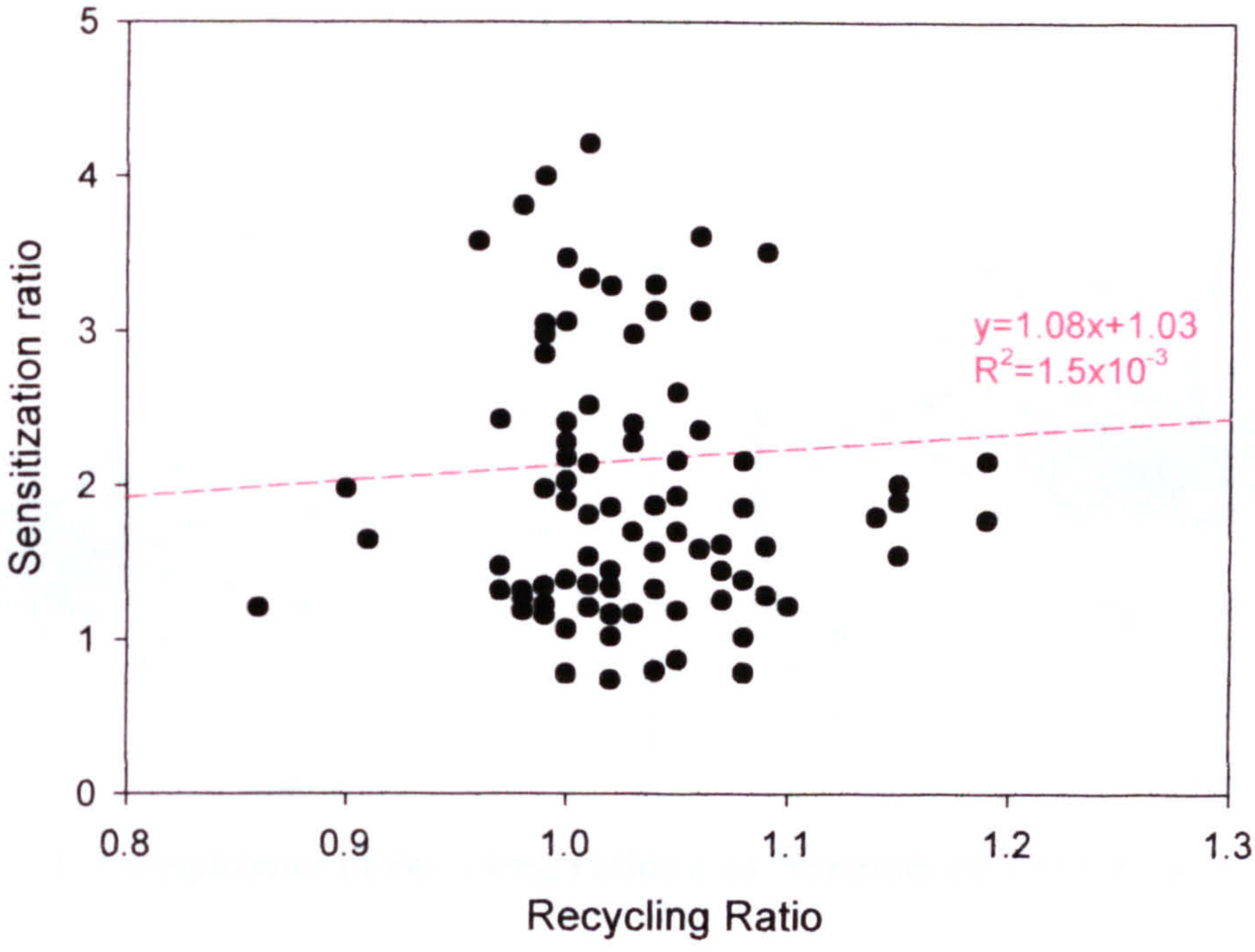

Fig 6.20 Relationship between sensitization and recycling ratio

As discussed above, the recycling ratio is generally taken as an indication of the success or otherwise of the test dose in correcting for sensitivity change. For samples not within error of 1 it is necessary to make the decision as to whether to exclude them from the dataset. Rather than taking an arbitrary cut off (e.g. 5-10%) the dataset as a whole was examined for signs of a relationship between the recycling ratio and the estimated ED.

The recycling ratio of each measured disc was plotted against the normalized ED[7] for that disc. It is evident from fig 6.21 that no clear trend was seen, however a number of samples with discs with sit outwith the main normalized ED distribution were identified, though no relationship between ED and recycling ratio was noted. As such, discs were not rejected on the grounds of their recycling ratios unless the ED also lay clearly outwith the mean distribution for that sample.

[7] The normalised ED for each disc was calculated as the ratio of disc ED to average ED for that sample

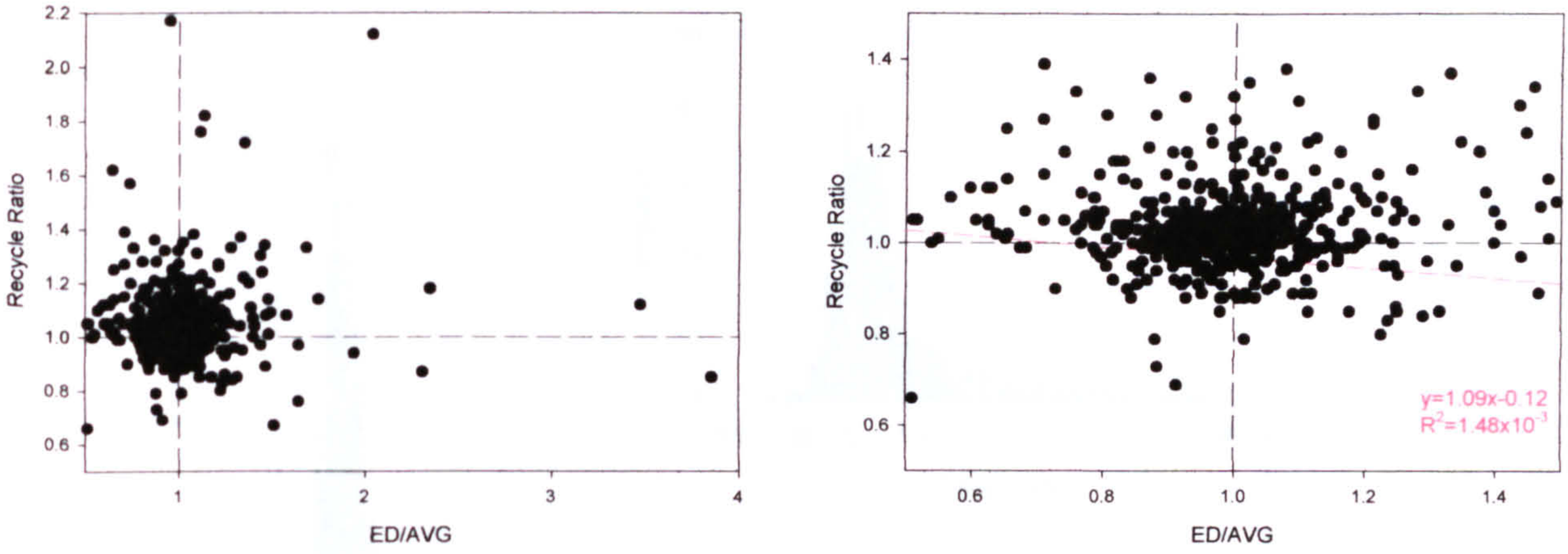

Fig 6.21 Comparison of recycling ratios and Normalized ED for each disc measured.

6.3.2.6 IR Response

The response of all samples to a 5Gy β dose was monitored at the end of each run. Where practicable, temperature dependence was also investigated by means of varying the preheat temperature prior to readout. The first 4s of each decay curve was monitored for elevated IR signals above background.

A histogram of IR response for all discs run shows that the majority of discs have no discernable IR signal (fig 6.22). A small proportion show signals in excess of several hundred (the largest being ~100,000 counts in first five channels). There was no particular site dependency in samples with higher IR responses, though both the Loch of Garths and Skaill had a higher proportion of samples with significant IR response than the rest. In samples which did exhibit IR greater than a few hundred counts, variation was seen from disc to disc, with some discs showing almost no signal, others a magnitude of two difference.

There was no evidence of a variation in IR response with increased preheat temperatures. However, samples with high IR values appeared in some cases to exhibit poor ED preheat plateaus (see above for details).

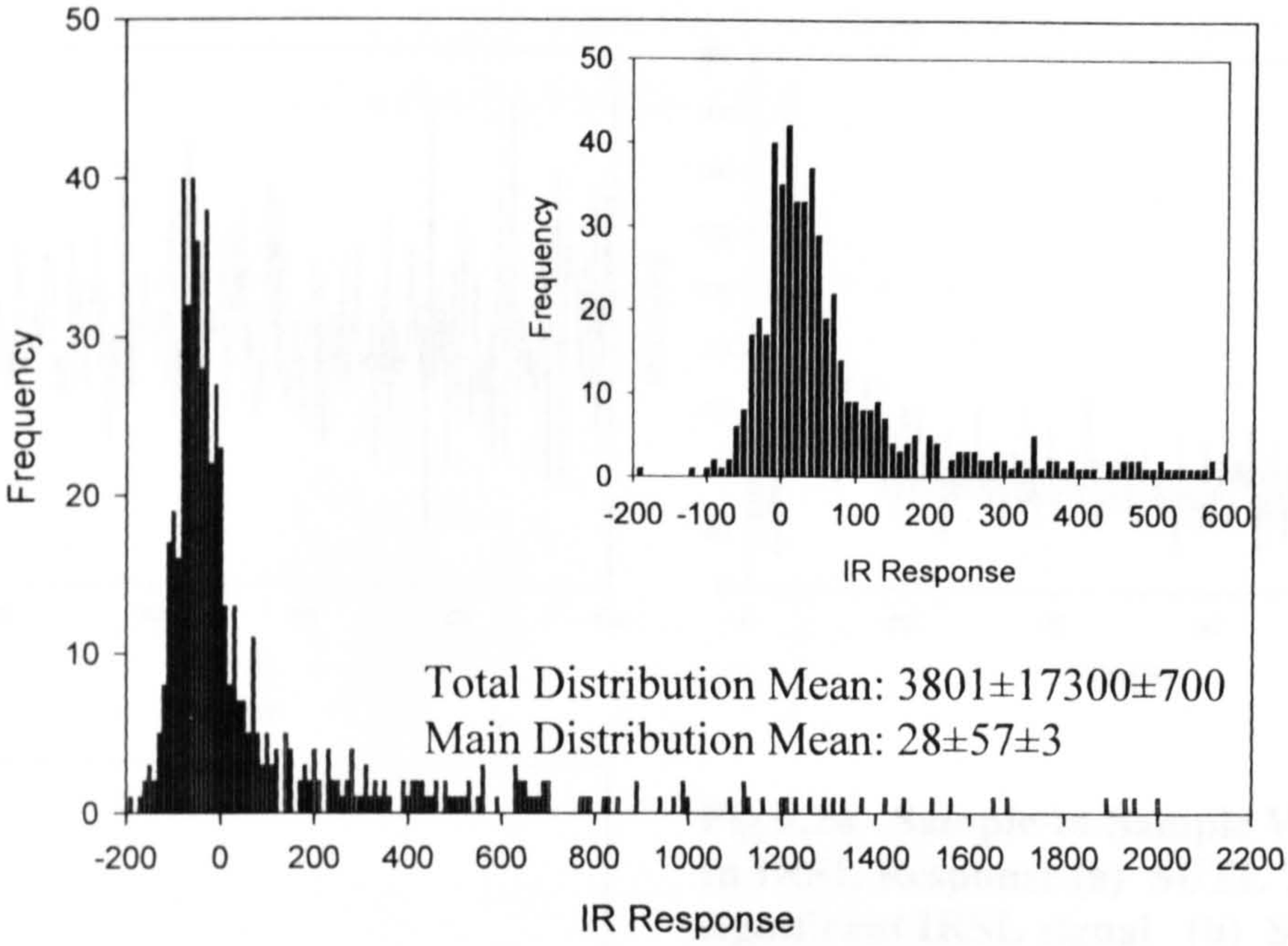

Fig 6.22 Histogram of IR response for each disc measured

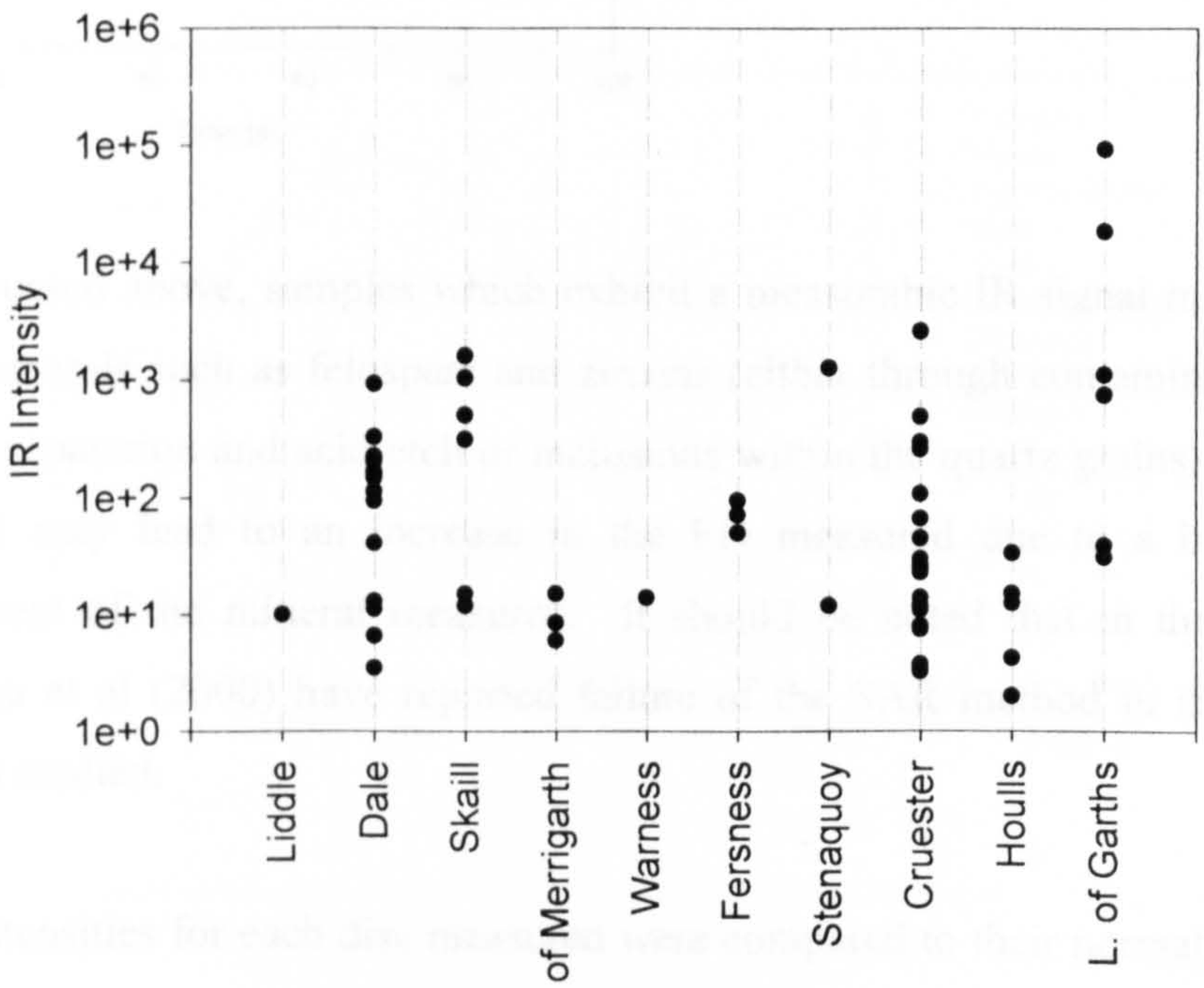

Fig 6.23 Vertical dot plot of average IR response per sample, grouped by site

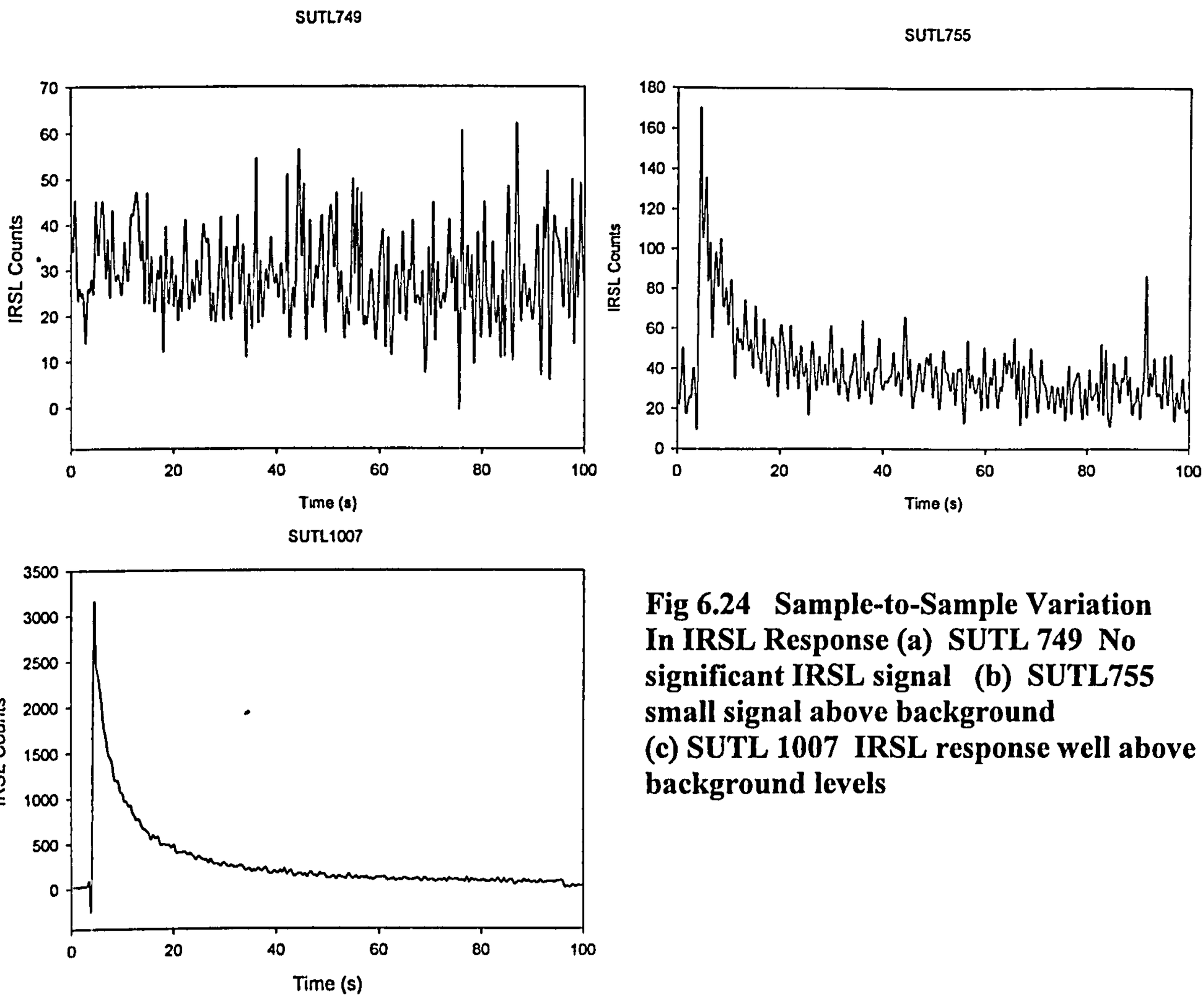

Fig 6.24 Sample-to-Sample Variation In IRSL Response (a) SUTL 749 No significant IRSL signal (b) SUTL755 small signal above background (c) SUTL 1007 IRSL response well above background levels

As discussed above, samples which exhibit a measurable IR signal may contain traces of other minerals such as feldspars and zircons (either through contamination, failure of the density separation and acid etch or inclusions within the quartz grains). Theoretically such material may lead to an increase in the ED measured due to a higher internal dose component of the mineral measured. It should be noted that in the case of feldspars, Wallinga et al (2000) have reported failure of the SAR method in the small number of samples studied.

IRSL intensities for each disc measured were compared to their normalized ED in order to identify any underlying relationship between the two. Variation in the IRSL intensity of discs were noted within samples and it was expected that this variation may affect the ED measured. Fig 6.25 shows there to be no clear relationship between IRSL intensity and normalized ED. Again, no relationship between IR and the discs which lie outwith the

main normalized ED distribution was evident. However, when the relationship is examined on a sample-by-sample basis, there would appear to be a small number of discs that sit outwith the normal distribution (fig 6.26).

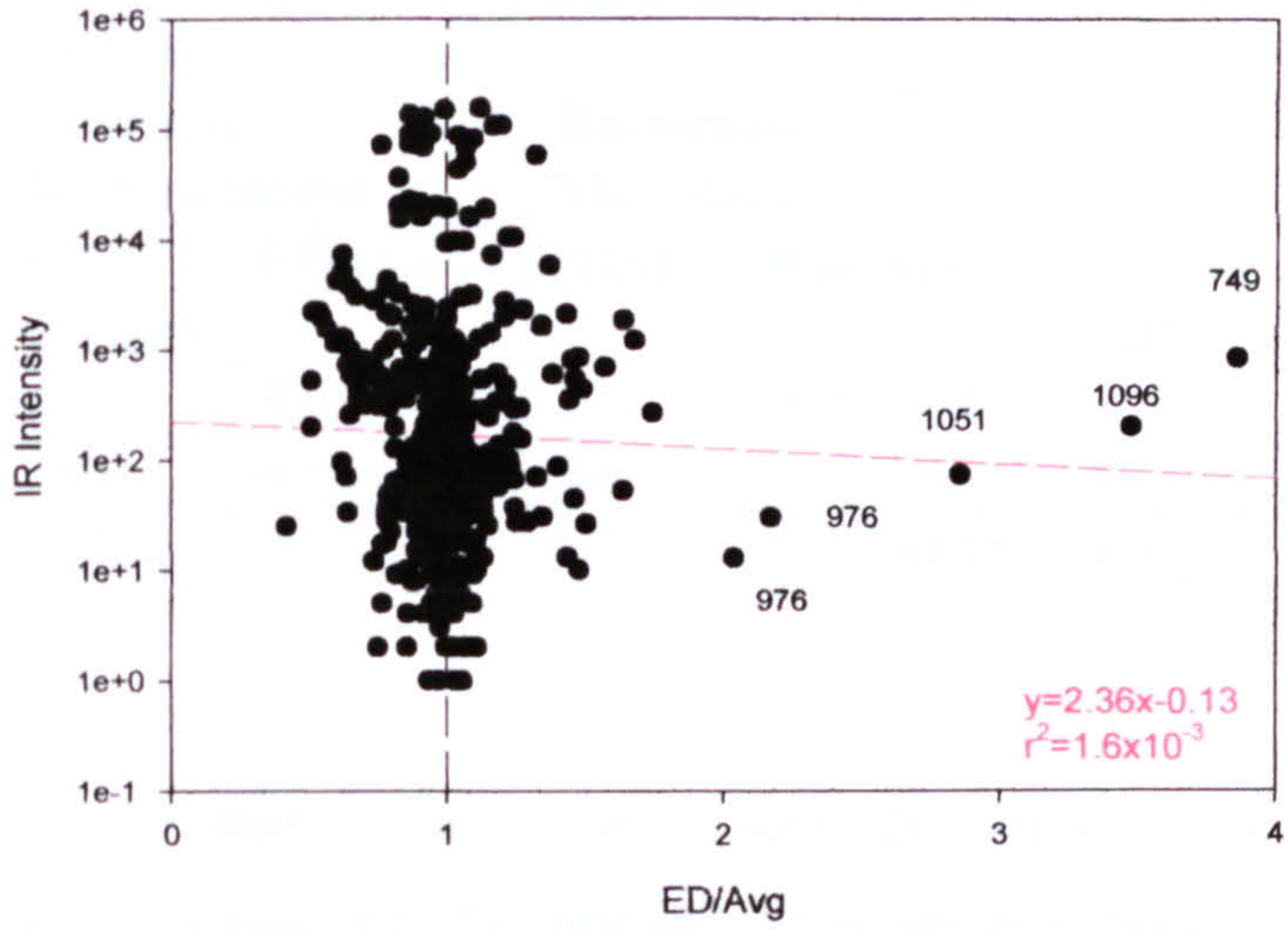

Fig 6.25 Relationship between IRSL intensity and normalized ED for each disc

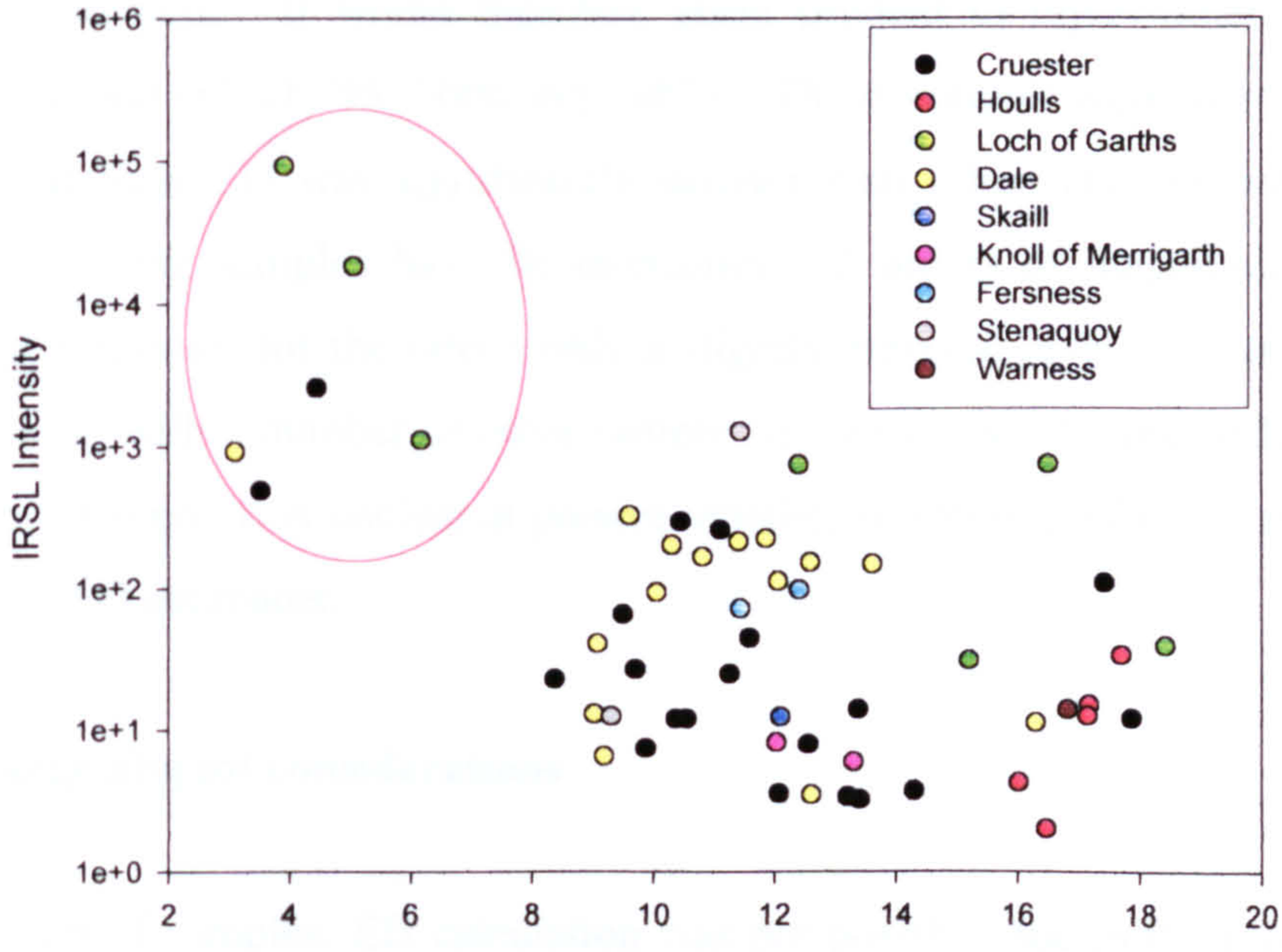

Fig 6.26 Relationship between IRSL intensity and ED on a sample-to-sample basis. Red circle identifies samples that sit outwith the general distribution.

Where material permitted, the samples identified were re-etched in 40% HF acid for a further 40 minutes and re-run. The resulting EDs were 3-5 times higher than previously, with minimal IRSL signals (see table 6.7).

Table 6.7 Comparison of re-etched and original measurements for samples with high IRSL intensities

Sample (SUTL)	Original Measurement		Re-etched Measurement			
	IRSL Counts	ED (Gy)	IRSL	ED (Gy)	% of orig. IRSL Signal	% Increase in ED
1051	486	3.53±0.26	27	9.7±0.24	5.5	275
1064	2552	4.45±0.12	3.6	12.07±0.50	0.1	271
1020	91742	3.92±0.08	97	13.7±0.45	0.1	349

It would appear that in these three cases the presence of IR sensitive material has significantly decreased the ED obtained. Further investigation of these samples would be required to provide an explanation as to the suppressed EDs seen within this group. Both fading and uncorrected sensitivity changes on the natural readout cycle (note that the test dose adequately corrects subsequent doses thus the recycling ratio is at or near to one) are potential candidates. It would therefore seem prudent to reject other samples that lie within this group (SUTL755, 1006 and 1007). These samples were identified by virtue of the fact that their ED was significantly smaller than other samples within the dataset. Whilst two of the samples have IR intensities 1-2 orders of magnitude larger than the average IR response, for the others only a slightly elevated level is seen. Such IR levels are in keeping with a number of other samples for which no obvious difference in the ED distribution is seen. It is unclear at present whether re-etching of this material would also yield higher ED estimates.

6.3.2.7 Large aliquot considerations

For a number of samples, ED calculation was not possible due to the low intensity of the signal producing a high degree of scatter on individual disc measurements. A revised large aliquot protocol was implemented to explore other approaches to data analysis. By summing the intensities of signals from each disc, creating one 'large' disc as opposed to many small discs, it was possible to construct less scattered regeneration curves and

produce ED estimates for a proportion of the affected samples. Results for affected samples are detailed in table 6.8 below.

Table 6.8 Large aliquot analysis of low intensity samples

Site	Sample (SUTL)	ED (Gy)
Dale	768	----
	785	----
Skaill	1362	0.38±0.13
Cruester	1077	14.83±2.51
	1087	---
	1088	8.02±2.44

6.3.2.8 Distribution of EDs

The distribution of EDs for all 20-sample discs was examined in order to identify possible evidence for contamination and other effects that may influence the average ED result.

Each distribution fell into one of the following categories:

(a) single distribution

(b) singe dominant distribution with smaller secondary distribution

(c) Double distribution

(d) Multiple component scattered distribution

Examples of each are illustrated in fig 6.27. Histograms of all sample distributions can be found in appendix G.

The majority of EDs are not normally distributed. The distribution is not related to IR contamination or failure of the recycling ratio (see above).

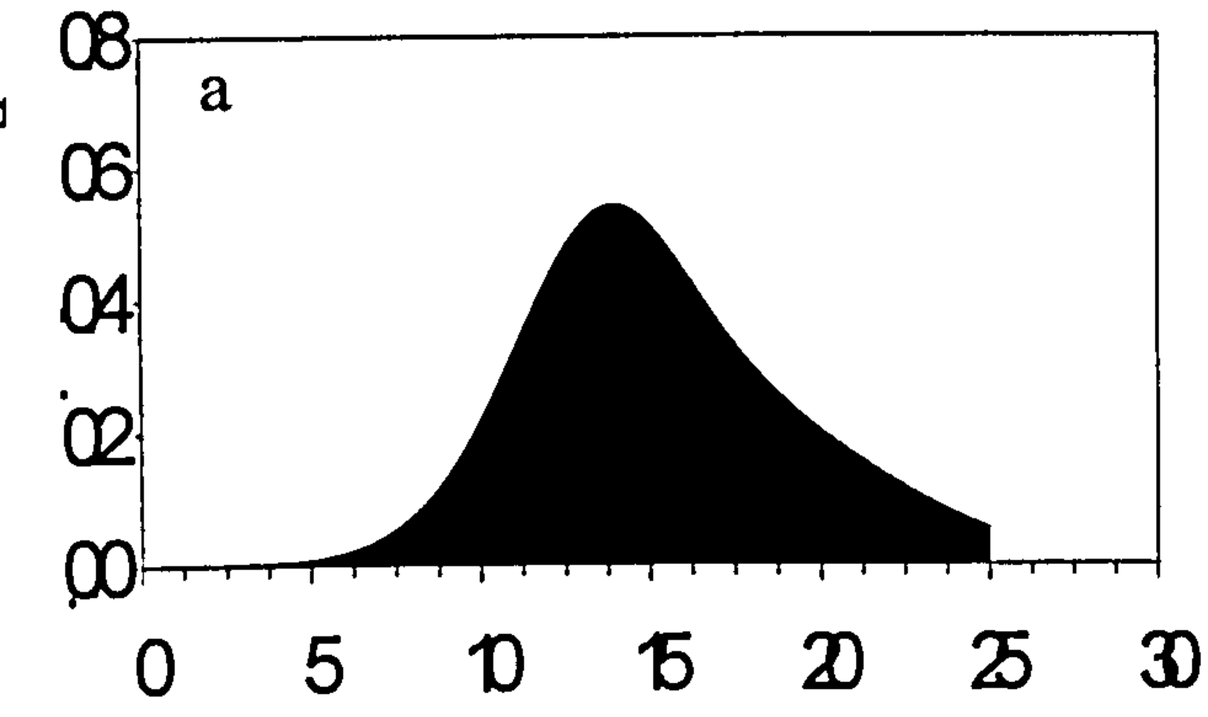

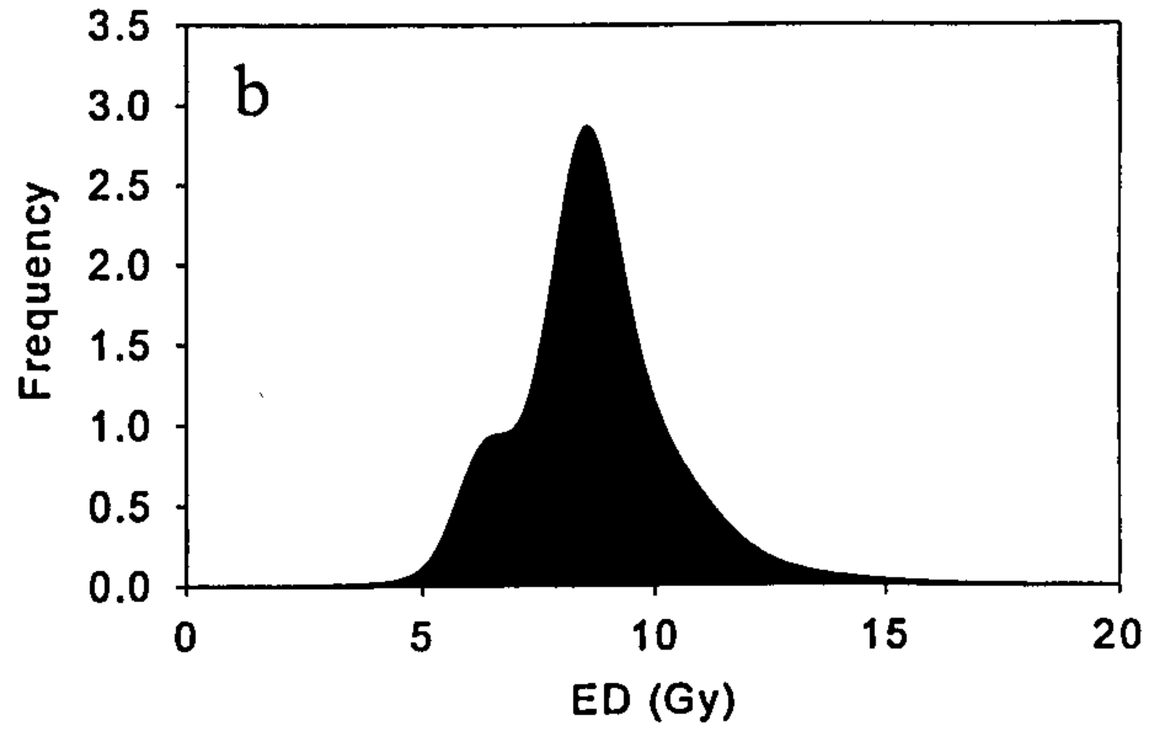

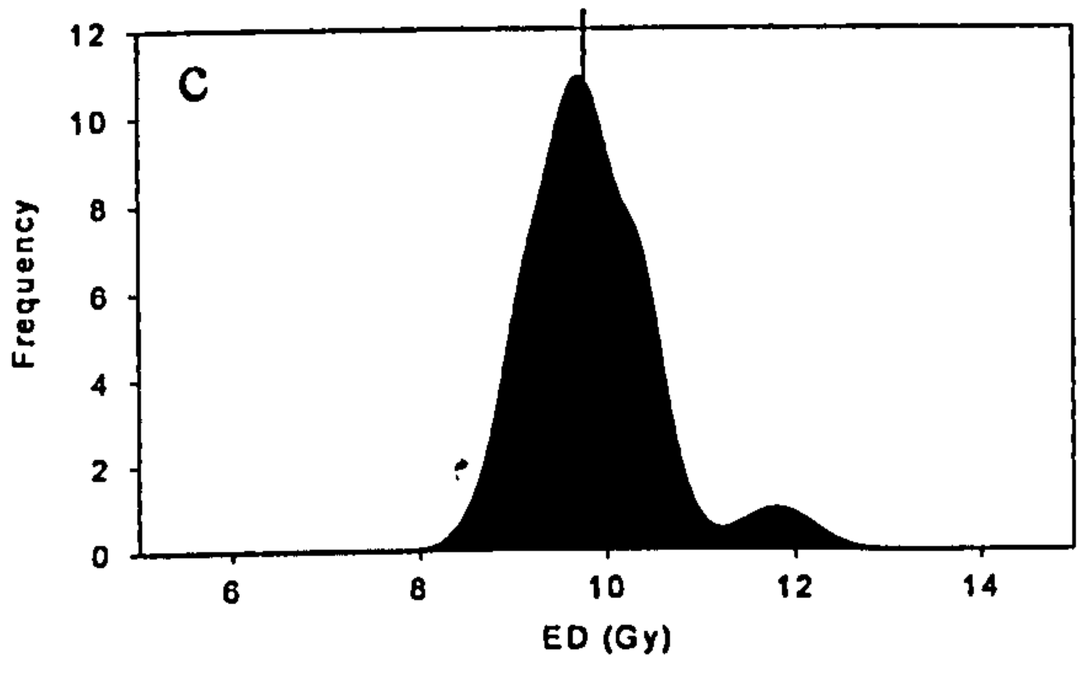

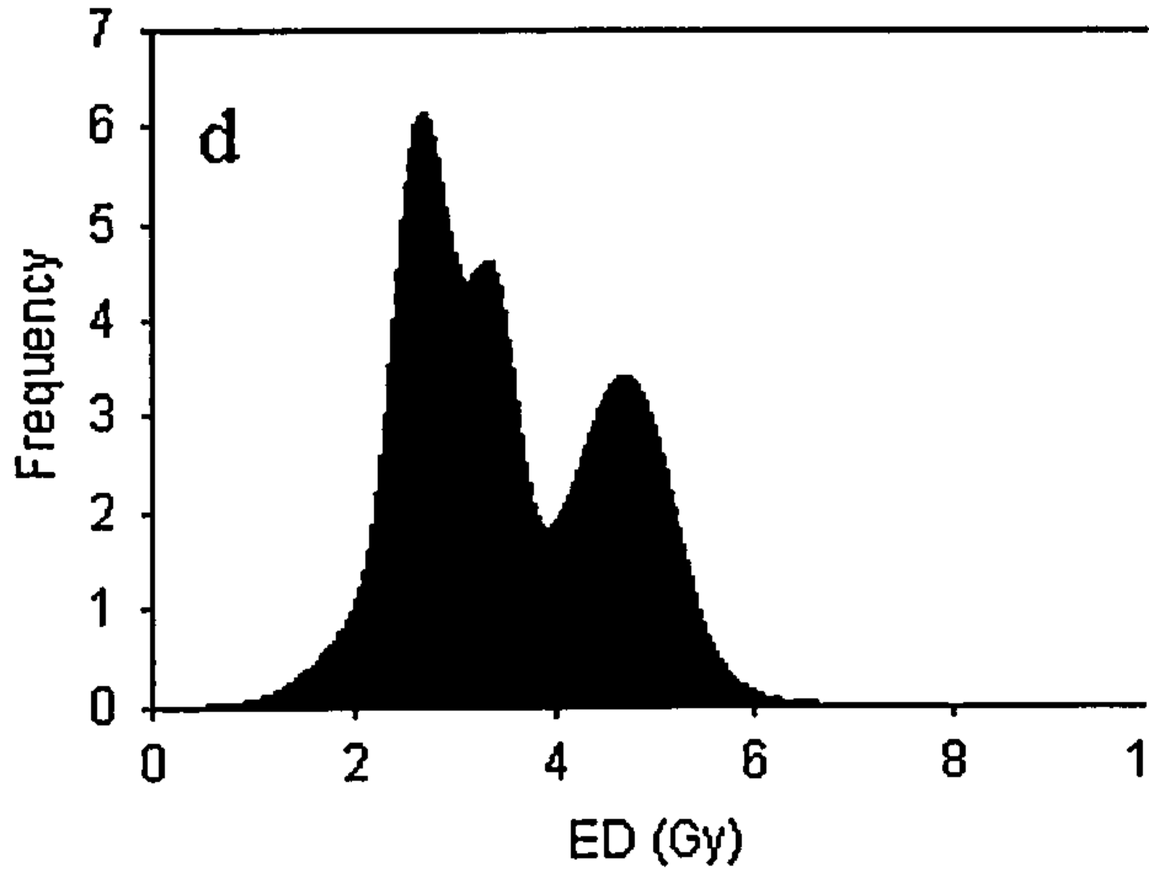

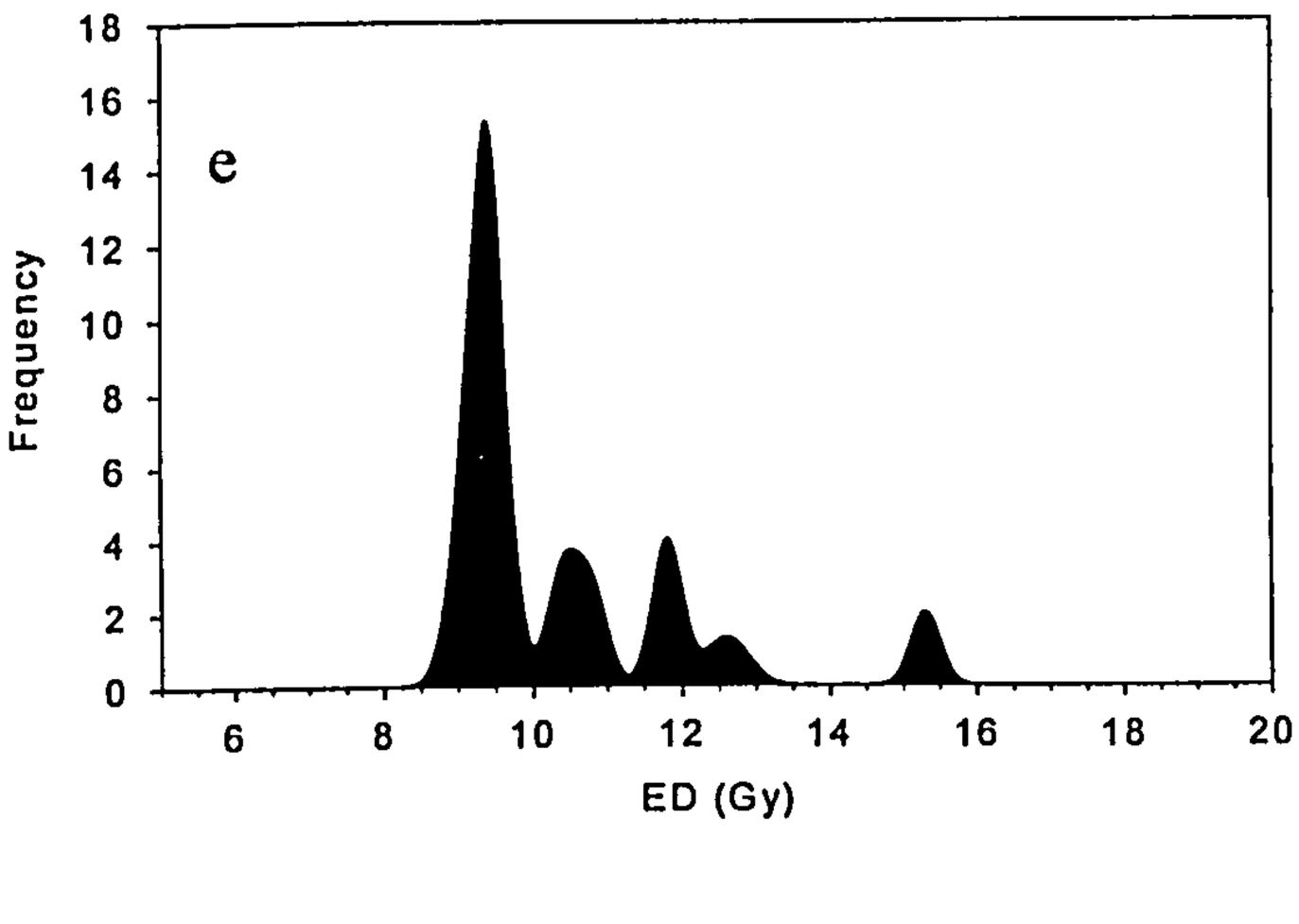

Fig 6.27 Examples of ED distributions (a) SUTL765 Single distribution (b) SUTL749 and (c) SUTL958 Main distribution with minor peak (d) SUTL755 Double peaked distribution (e) SUTL 968 Multiple component peaks.

6.3.2.9 Summary

Samples from Orkney and Shetland show great variation in the natural intensity of the OSL signal observed. This variation is seen both within and between sites. Whilst site to site variations may in part be attributed to differences in geology, variation within sites would appear, at least in part, to be attributed to the past heating of the material. In the Cruester dataset, several orders of magnitude lower intensities are noted in the majority of hearth stones compared to the burnt stones.

On occasion, the poor sensitivity of samples prevented ED calculation due to the near 1:1 ratio of signal to background. Large aliquot analysis of such samples has allowed a number of additional ED measurements to be calculated.

Differing sensitivity changes were also noted in samples. A few showed a decrease over the run cycles, though the majority show an increase of the order of 50-100% by the end of the run. The evidence for increased sensitivity change with preheat temperature also indicates a temperature dependent relationship.

Recycling ratios are, on average, slightly greater than one, though many are within error of it. The predicted effect of such ratios - an overestimation of ED was not observed within the dataset, thus the recycling ratio was seen as a poor indicator of the success or otherwise of the run protocol.

IRSL response to a 5Gy dose showed that the vast majority of samples had little or no signal. There were however a few notable exceptions which, on further investigation showed a strong relationship between ED and IRSL intensity, with the ED value being suppressed. Re-etched material provided higher EDs and confirmed the presence or IRSL material in earlier runs.

For the samples studied here, there would appear to be no direct link between sensitivity change and OSL/IRSL intensities, nor to the ED calculated. However, larger sensitivity changes were seen in the majority of samples with higher preheat temperatures and, on occasion, evidence for a preheat dependence on the ED obtained was identified.

Perhaps the most worrying observation on sample behaviour was in the distribution of EDs seen for each sample. The majority were not normally distributed and, as discussed above, the distribution appears unrelated to either IR contamination or failure of the recycling ratio. Similar distributions have been noted in burnt stones from Scandinavia (A. Murray, pers. comm.). This distributional variation may also help to explain the variation in ED noted in the different methods for SUTL1075 (section 6.2).

Clearly it would be unwise to either discount or accept such data without further investigation into the likely cause of the variation seen. A number of possible causes for the distributions seen are outlined in the proceeding sections prior to recommendations for the treatment of the dataset.

6.4 Further Analysis

6.4.1 Introduction

As outlined above, the distribution in EDs from individual samples is more than would be expected in a normally distributed sample. There are a number of possible explanations for the distribution seen. In cases of samples with a dominant peak and a smaller peak that is outwith the main distributional area and can be attributed to only a few discs, contamination is the most probable cause. However, in samples where a wider and more continuous range of EDs are seen this is unlikely to be the case and other alternatives need to be examined. The two main candidates for such effects are incomplete zeroing of the geological signal, and microdosimetric effects within the matrix of the stone. Each is outlined in more detail below.

6.4.2 Incomplete zeroing of geological signal

Incomplete zeroing of the geological signal of OSL samples has been the subject of numerous studies in recent years. These studies have been concerned with the solar resetting of sediments and have suggested a number of methods for identification of

partially reset material. With regard to burnt stone, the resetting mechanism is clearly related to past heating of the material and therefore requires further attention.

It is likely that the samples in this study were heated on an open fire before being immersed in water. This process may have been repeated on numerous occasions for individual stones over a period of time. Reconstruction of the thermal history of such samples is problematic. No clear data exist as to the likely duration and temperature of heating of the stones. It is however possible to set limits on the likely time and temperature. The time each stone spent at a given temperature will depend on a number of factors:

(i) The average firing time per batch of stones heated
(ii) The position within the fire of the stone
(iii) The thermal conductivity of the stone
(iv) The number of firings each stone has experienced.

Experimental reconstructions of burnt mounds (e.g O'Kelly, 1954) suggest the likely firing time of any one stone to be between 15 minutes and a couple of hours. Buckley (1990) suggests that sandstones similar to the samples studied in Orkney and at the site of Cruester in Shetland, can withstand 5-12 reheats before fracturing to such an extent that their size is deemed unusable. As such an upper and lower limit may be placed on the likely total firing time of 15mins and 24 hrs respectively. (In the case of Houlls and the Loch of Garths, the maximum number of times an individual stone may have been reheated may be significantly higher.) The temperature that the core of the stone reaches will depend on the size and thermal characteristics of the stone, its position within the fire, and on the fuel type used. Spencer (1996) conducted luminescence based high temperature measurements on burnt stones from mounds on Mainland Scotland and determined, on the basis of residual geological signals, that stones may have been subjected to temperatures in excess of 500°C. However, given the limited fuel resources in the Northern Isles, it is perhaps prudent to consider a lower range of temperatures in the region of 100-400°C.

Given a set temperature and time, the mean lifetime of the 325°C peak can be described in terms of:

$\tau = s^{-1} \exp^{\frac{E}{kT}}$ Where τ is the mean lifetime (s);

E is the activation energy or trap depth (eV)

s is a frequency factor related to the probability of escape (s^{-1})

T is the storage temperature (K)

and k is Boltzmann's constant (eV K^{-1})

A survey of the literature indicates values for E in the region of 1.6-1.7eV and s in the region of 1-4x$10^{13}s^{-1}$. (Spooner and Questiaux, 2000, Wintle, 1975, Franklin et al, 2000, Murray and Wintle, 1999, Huntley et al, 1996). Taking average values of 1.65eV and 2.5x$10^{13}s^{-1}$, the depletion of geological signal can be calculated for a fixed time and temperature. The number of mean life decays a sample must go through before the remnant geological signal is reduced to an acceptable level is dependent on the magnitude of the geological and archaeological signals. Saturation of the quartz signal is likely to occur in the region of several 100 Gy. In comparison, for samples studied, the archaeological signal is in the region of ~10Gys. For age to be estimated accurately, in this case the geological signal would need to ~1 order of magnitude smaller than the archaeological signal i.e. ~0.1Gy. This would take c.7 mean life times to occur.

As can be seen from fig 6.28, for firing durations at the lower end of the range, temperatures in the region of 270°C are required to reduce the geological signal to an acceptable level. When time is increased to a hypothetical maximum of 24 hours, this temperature decreases to ~200°C. Clearly, therefore, there is a significant possibility that some stones may not have reached either the required time or temperature during anthropogenic heating. Where either temperature or time is close to the 'critical' value, a gradient of zeroed and partially zeroed material may form within the stone. Subsequent laboratory preparation and mixing of minerals from the central core of the stone may therefore lead to mixed distributions of EDs depending on the proportion of poorly zeroed material contained on each disc.

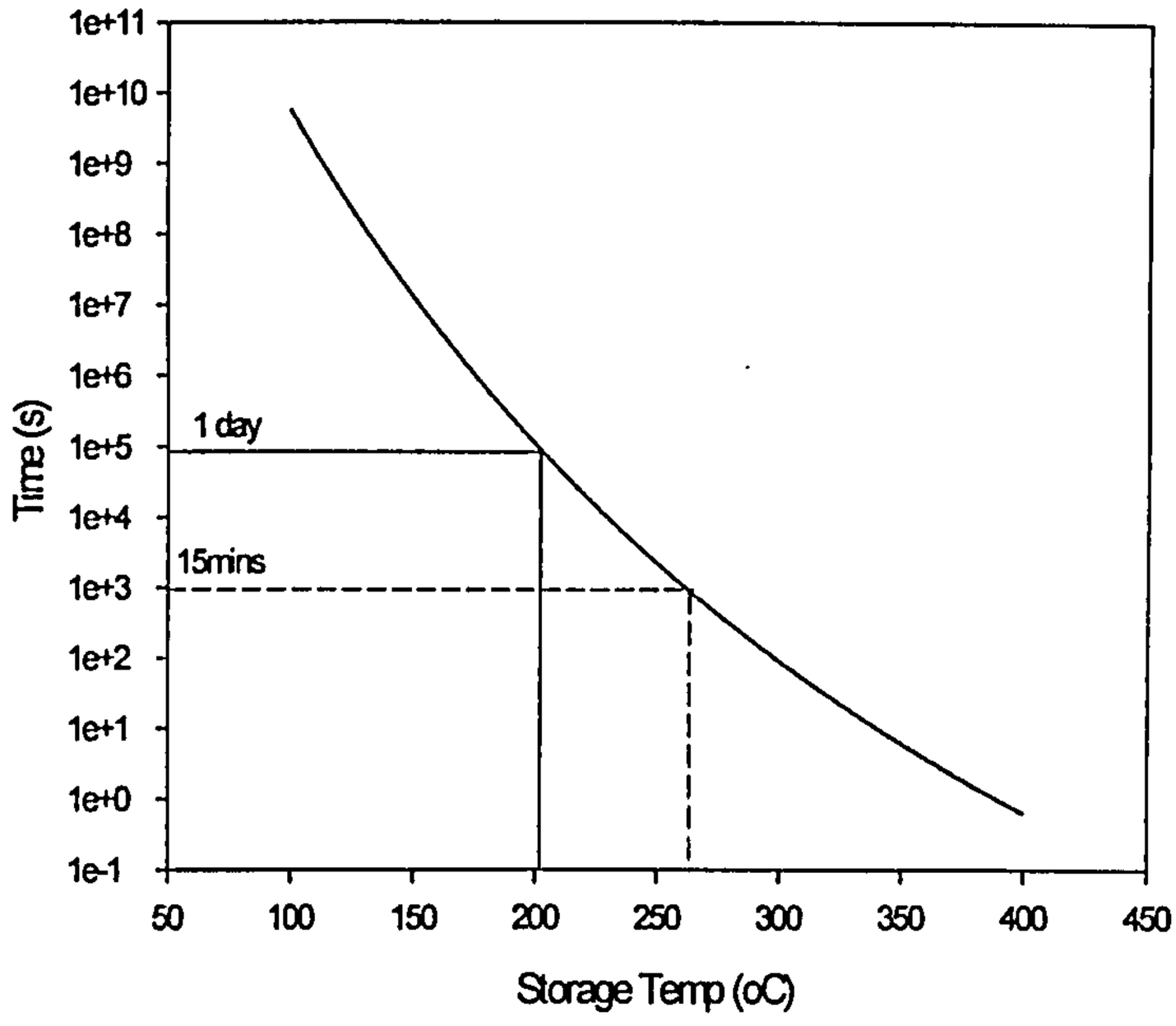

Fig 6.28: Time for 7τ to be reached at varying temperatures (for E=1.65eV, s=2.5x10^{13}s^{-1})

Incomplete zeroing is likely to take place in large samples where a significant difference exists between the maximum temperature reached at outside and core. Incomplete zeroing may also occur as a result of uneven heating – stones at the extremities of a fire may show a gradient which reflects the direction of heat. In this situation, the hypothetical ED slice would be higher at the 'cooler' edge of the sample, and lowest at the edge in closest proximity to the heat source. Such a situation is also likely to occur in relation to the heating of hearthstone, as discussed in Chapter 4. It is possible to investigate both such situations within the dataset obtained from Orkney and Shetland.

Chapter 4 details sample weight, which may be used as a crude estimate of mass. When plotted against the standard deviation on ED measurements for each sample (which is a reflection of the scatter in ED) no obvious trends are seen, with both small and large samples showing higher amounts of scatter (fig 6.29). This may be expected due to variations in heating temperatures at different sites, and at different firing events, though there is no obvious correlation between scatter and site/geology.

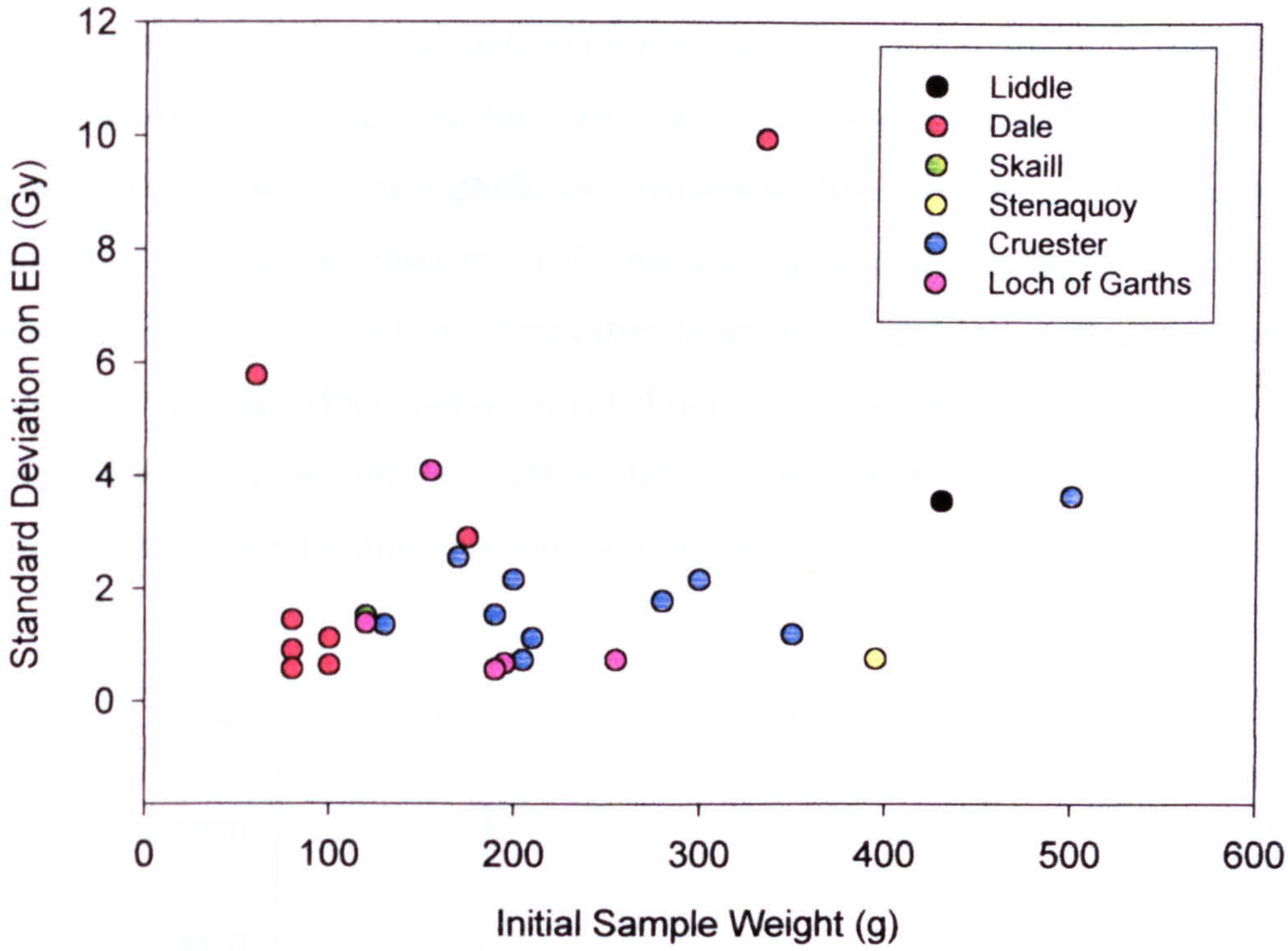

Fig 6.29 Relationship between scatter on ED measurement and initial sample weight for 20 disc runs, grouped by site.

In terms of thermal gradients within individual samples, information exists within the results presented in section 6.3 to investigate this effect further. As discussed in chapter 4, it was anticipated that a thermal gradient may exist within the Cruester hearthstones prepared. One sample, SUTL1100 was quarter sectioned to allow investigation of the ED distribution within various sections of the stone (see fig 6.30).

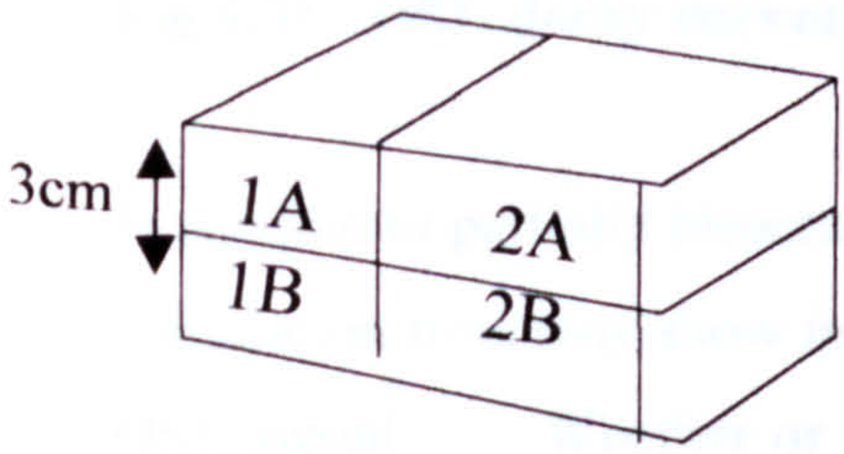

Pos	Ed (Gy)	Pos	ED (Gy)
1A	11.58±0.59	2A	11.90±0.54
1B	14.30±0.82	2B	15.65±2.57

Fig 6.30 Diagramatic representation of sectioning of SUTL1100 (not to scale) and ED results for each portion

It is clear from the results that a 20-30% increase in ED value is seen from top to bottom of a hearthstone which was only 3cm in thickness. It is interesting to note that, if the above interpretation is correct, and the variation in ED seen is related to heating temperature (as duration is unlikely to be significantly different) then the heating would also appear to have an effect on both the intensity of the natural signal, and the shape of the OSL decay curve (fig 6.31). The possibility that other hearthstone and burnt stone samples may also be prone to such an effect cannot be ruled out. Without an effective means of identification of such an effect within the existing dataset, the date obtained for each sample can at best only represent a maximum age for the sample.

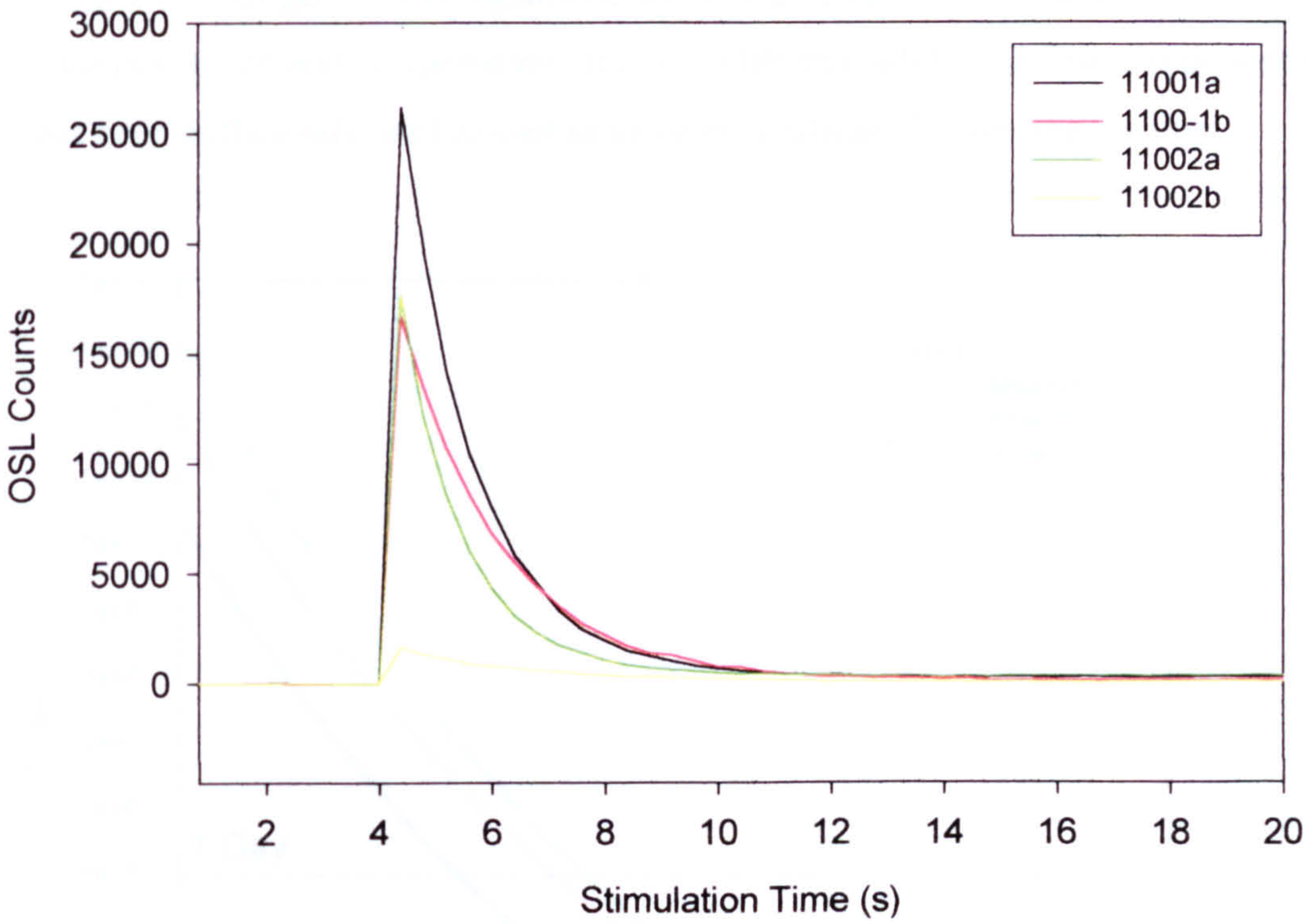

Fig 6.31 OSL decay curves for different portions of sample SUTL1100

In relation to partially bleached sediments, Bailey (2003) suggests that a plot of ED against stimulation time may show incomplete zeroing of the medium and slow components of the OSL signal. Whether or not such a plot is also sensitive to poorly fired material will depend on the trap parameters of the fast, medium and slow components of the OSL signal and the temperature which the stone has attained. Whilst the parameters of the traps which contribute to the OSL signal of quartz are poorly defined, recent linearly modulated

OSL (LM-OSL) work by Singarayer and Bailey (2003) has reported both activation energies and frequency factors for fast, medium and two of the slow components of the signal from a variety of sedimentary deposits. Whilst it is unclear whether such values may be representative of the material within this study, the results are worthy of further consideration. Singarayer and Bailey report activation energies of 1.74, 1.8, 2.02 and 1.23 eV for fast, medium, slow-1 and slow-2 components respectively, with frequency factors of $8.9x10^{13}$, $1.5x10^{13}$, $6.9x10^{14}$ and $4.7x10^{10}s^{-1}$. (The slow-2 component by virtue of its component parameters is thermally unstable and not suited to luminescence dating.) A similar analysis to the broad estimates of parameters for the 325°C peak may be carried out for each of these components and shows there to be a distinct possibility of differences in the residual levels of geological signals between traps (fig 6.32). It can therefore be seen that for varying times and temperatures, it is possible that whilst the fast component of the signal has been sufficiently well zeroed as to be insignificant in size, the medium

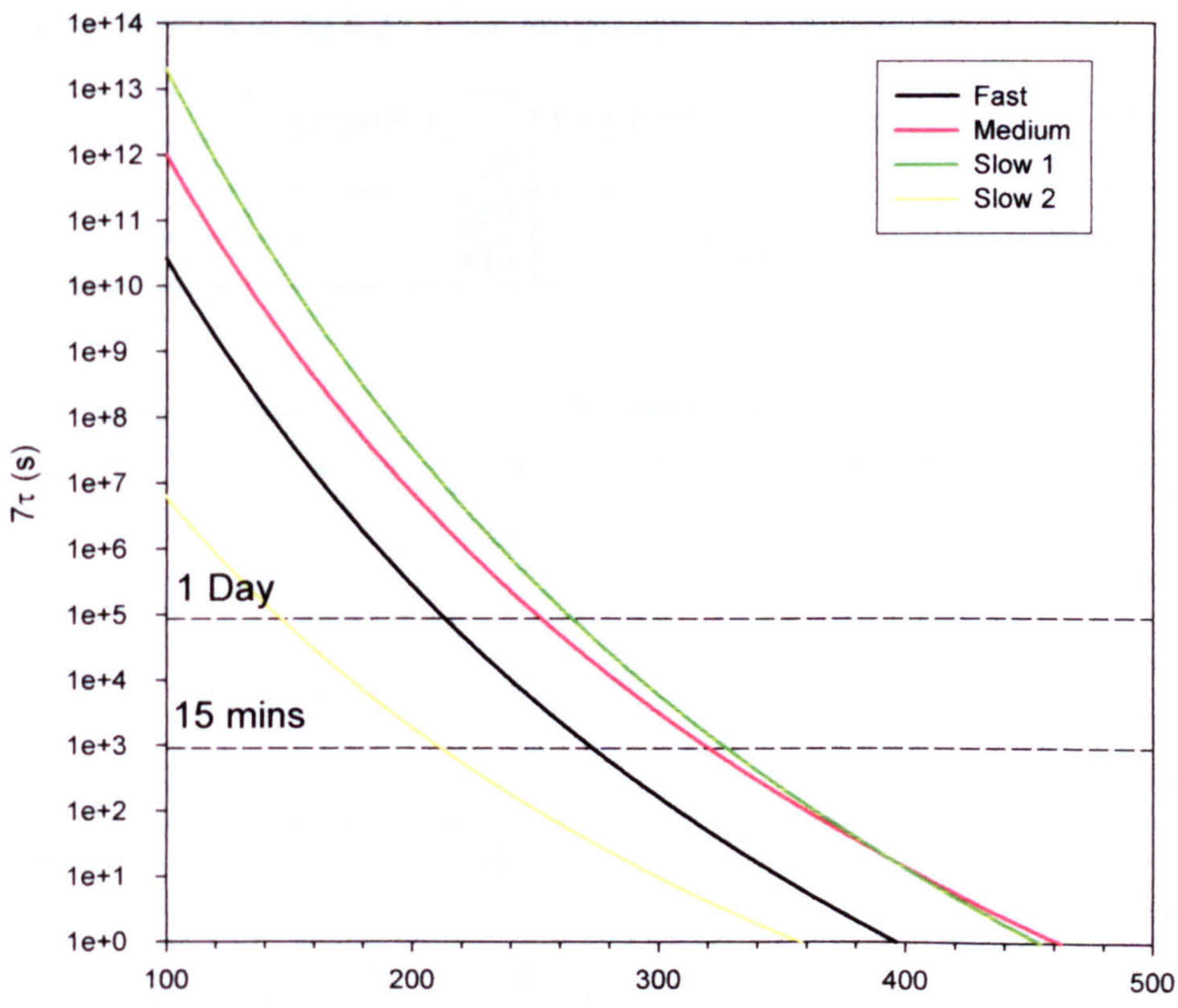

Fig 6.32 Time for 7τ to be reached at varying temperatures for fast, medium, slow-1 and slow-2 components (E=1.74, 1.8, 2.02 and 1.23 eV, s=$8.9x10^{13}$, $1.5x10^{13}$, $6.9x10^{14}$ and $4.7x10^{10}s^{-1}$ values from Singarayer and Bailey, 2003).

and slow may contain a considerable residual dose (table 6.9). For short duration heats, a critical value of approximately 340°C for such trap parameters would be required to effectively zero all components of the signal. It should however be noted that without further detailed LM-OSL work on specific samples studied within this chapter, it is impossible to determine whether decay characteristics would be similar.

However, the change in shape in the decay curve of sample SUTL1100 noted above may be a strong indication of an increased contribution to the signal from the medium and slow components in poorly fired material. Comparison of De(t) plots for the different portions of sample SUTL1100 show both top portions to show only a minor rise in ED which is within error of the mean value, whilst bottom portions show a more pronounced increase in varying proportions (fig 6.33).

Table 6.9 . Comparisons of residual geological dose left after heating to varying temperatures for varying times (based on geological dose of 100Gy, using trap parameters defined in fig 6.32 after Singarayer and Bailey, 2003)

Time	Temp(oC)	Fast (Gy)	Medium (Gy)	Slow-1 (Gy)
1 day	220	0.00	20.83	62.75
6 hr	260	0.00	0.02	2.32
15 mins	340	0.00	0.00	0.00

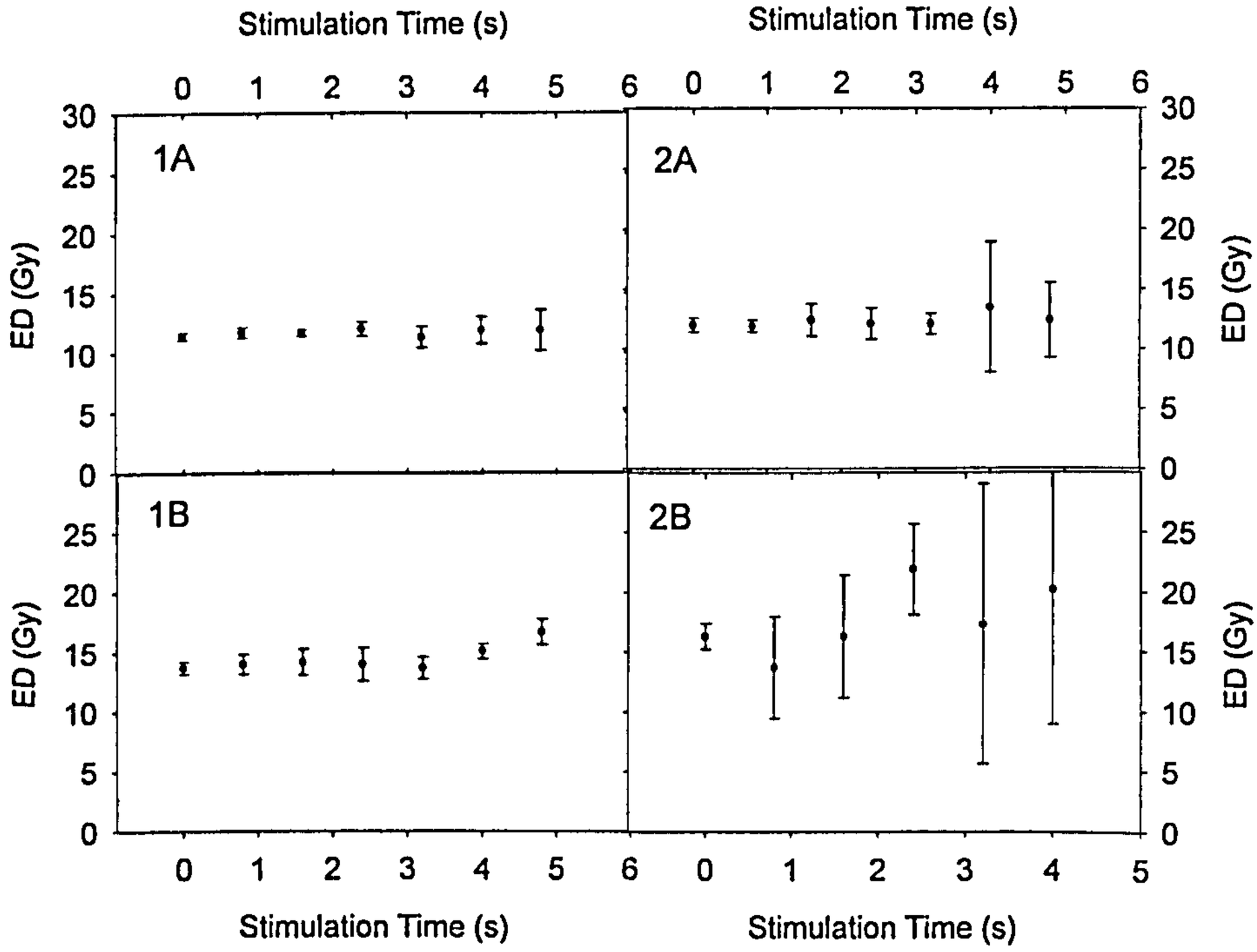

Fig 6.33 De(t) plots for different portions of sample SUTL1100

The degree of rise within the De(t) plot may be quantified for comparison by fitting a linear regression through each dataset, with the gradient describing the deviation of the plot from a constant value, with samples showing a positive value indicating a rise in the De(t) plot. When the gradient of each De(t) plot for sample SUTL1100 is compared to the ED for the corresponding portion a near linear relationship can be seen (fig 6.30).

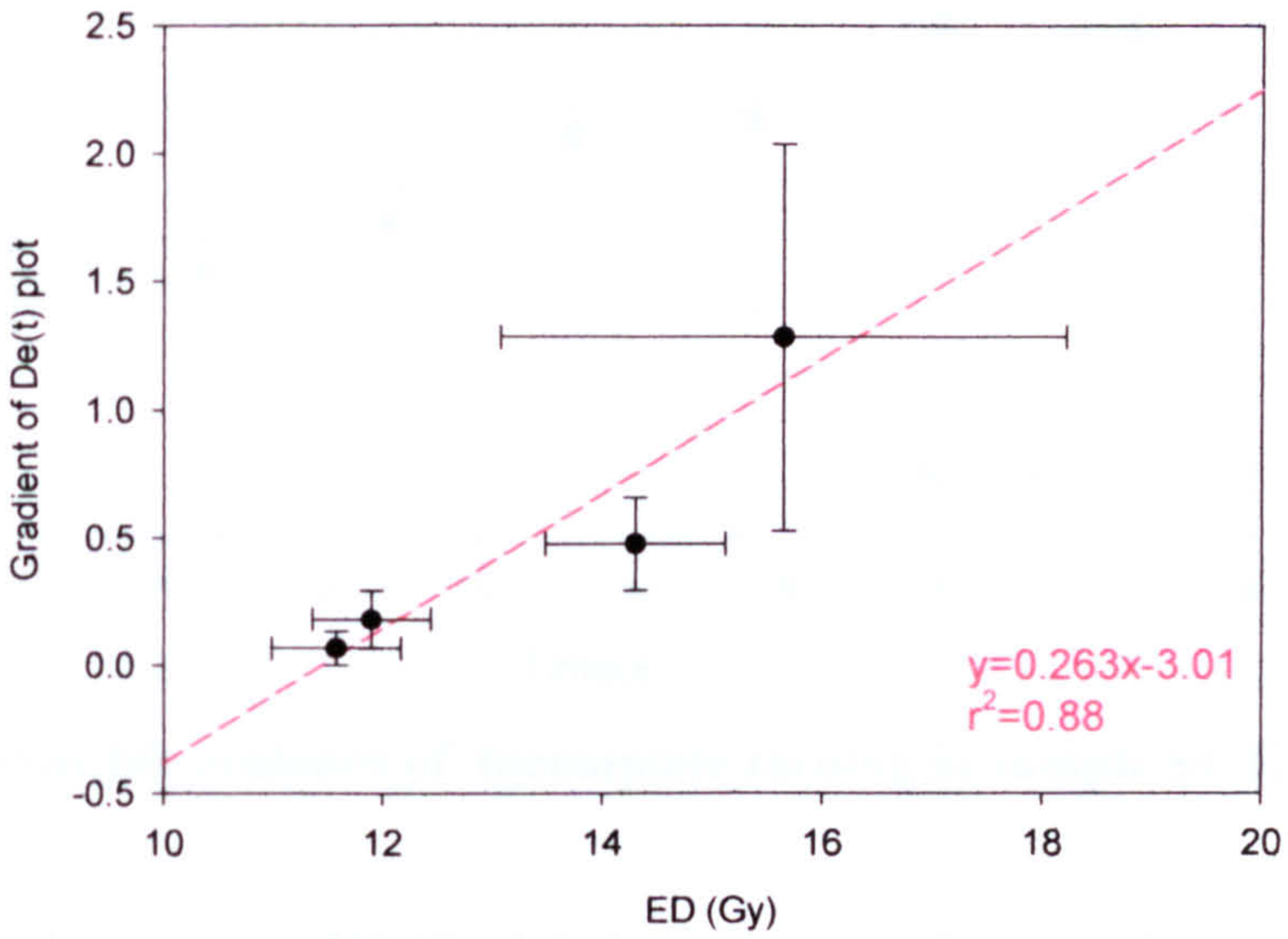

Fig 6.34 Comparison of gradient of De(t) plot and ED for different portions of sample SUTL1100.

This would appear to confirm that, in the case of this sample, the De(t) plot is a useful method of determining incomplete zeroing of the sample, with portions of the sample predicted to have been heated to a lesser extent showing a greater degree of change. In this situation, it would seem appropriate to quote the age determined from SUTL1100-1A as a maximum age for the sample. The near linear relationship observed between gradient and ED may also prove significant where samples with large ED distributions show similar behaviour.

As other samples were not sectioned in the above manner, such analysis is not a viable path of further investigation. Whilst measured OSL signals from the vast majority of samples will contain a mixture of grains from varying parts of the stone, with some discs by random chance containing more material from the core of a sample, others more from the outside, the above relationship was not identified in any of the other datasets.

However, when the average ED of the sample was compared at different stimulation times, a number of samples showed an increase in ED with time, potentially indicating poor zeroing (fig 6.35, table 6.10).

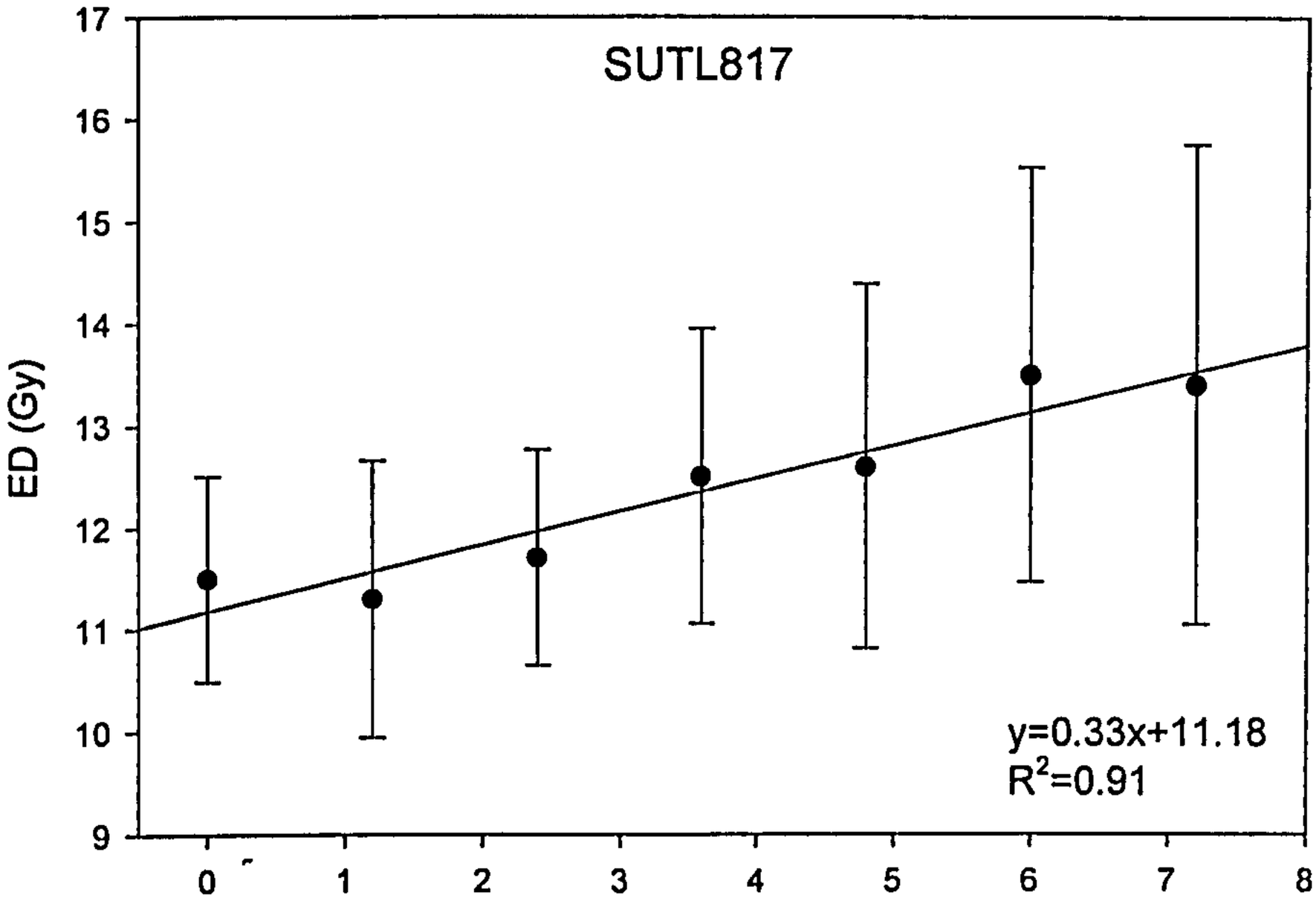

Fig 6.35 Possible evidence of incomplete zeroing in sample SUTL817

Table 6.10 Summary of De(t) plot characteristics for samples with rising plateau

Site	Sample	Original ED (Gy)	Yo*	A*	R^2
Dale	751	10.70±0.14	10.23±0.17	0.375±0.072	0.96
	765	16.3±0.72	12.78±0.15	2.63±0.072	0.99
	767	12.6±0.82	12.12±0.20	0.417±0.096	0.95
	779	11.85±0.50	11.78±0.22	0.065±0.005	0.98
	782	13.6±0.40	13.46±0.14	0.126±0.033	0.79
Skaill	817	12.09±0.38	10.98±0.22	0.327±0.046	0.91
Knoll of Merrigarth	794	10.70±0.43	9.96±0.86	0.652±0.436	0.86
	795	12.03±0.64	10.90±0.94	0.758±0.342	0.71
Fersness	824	11.43±0.53	11.40±0.18	0.233±0.063	0.87
Houlls	976-90	17.17±2.70	13.90±1.26	3.33±1.16	0.95
	976-125	17.70±2.04	15.00±2.46	5.01±2.47	0.86

* Yo and a describe the linear fit of the De(t) plot, where Y=Yo +aX, thus Yo describes the Y-intercept and a the gradient of the line.

It is clear from table 6.10 that variation in the slope of the De(t) plot is seen within the samples identified. Whilst some have only minor rises with time, others show indications of a steep gradient, potentially indicating a greater degree of variation between fast and medium components. It is possible that the intercept values of such plots represent a better estimate of ED than the measured value. Certainly where the fast component has been effectively zeroed, this would seem a valid assumption. However, further systematic work would be required to establish firmly the relationship between the two. As such, original ED values have been carried forward for age calculation on the premise that they represent the maximum age of the sample.

6.4.3 Microdosimetric Effects

It is possible that the distribution of EDs observed in samples from Orkney and Shetland relate to microdosimetric inhomogeneity between grains. As outlined in chapter 2, it is assumed that grains of a similar size and mineralogy have been exposed to a similar radiation field throughout their burial period.

However, a number of scenarios may cause inhomogeniety in the dose rate distribution. There are a number of ways in which inhomogeneity can occur, but small scale inhomogeneities of the kind postulated are confined to differences in α and β radiation fields. Such differences may occur when the distribution of radionuclides within the particular rock is uneven, either through clustering of material with low radionuclide concentrations such as quartz, or through proximity to minerals with a higher than average beta dose rate, such as zircons and some feldspar.

Clustering of quartz minerals will result in a suppressed dose rate due to the relative inactivity of the quartz grains. In effect, clustering would act as one large quartz grain that had fractured during pretreatment. The surrounding beta dose rate would be lower than the measured average, due to beta attenuation.

For example, clustering of approximately forty 90-125μm grains would cause the same effect on the group as for one 250-500μm grain, with dose rate decreasing towards the center of the group. In a situation similar to the majority of samples studied, where beta

dose rate is in the region of 2mGya^{-1}, gamma 1 mGya^{-1} and water content typically in the region of 5%, clustering on such a small scale would cause an overall decrease in dose rate of 5%. Similarly, a quartz grain in the centre of a cluster of larger feldspar grains will be subjected to a higher than average beta dose rate.

In the case of medium grained sandstone samples from Cruester where a high proportion of minerals are in the 250-500 size bracket, smaller quartz grains in proximity to these larger minerals may be adversely affected. Likewise, in the case of gneiss samples from Loch of Garths, large phenocrysts of feldspar were noted in preparation, with the majority of minerals greater than 500μm in size. Plachy and Sutton (1982) have highlighted similar problems in relation to quartz derived from granite.

The finer grained sandstones from Orkney, and mica schists and metamorphosed mudstones from Houlls may be less susceptible to such effects. Whilst SEM analysis of samples from Orkney has identified a high density of zircons within thick sections, such materials would predominantly increase the alpha dose, having relatively little effect on nearby samples. However, microdosimetric variations have been reported from burnt stone samples from Beaquoy, on Mainland Orkney (Huxtable et al, 1976), identified through variation in thick source alpha counting of different portions of the same sample.

There are a number of possible avenues of investigation which would give additional information on both the distribution of EDs and the distribution of radionuclides within samples.

The distribution of EDs could be further examined in samples with additional material by means of small aliquot SAR procedures (Spencer, 2003) or through single grain measurements (Duller et al, 2000). By reducing the number of grains associated with each measurement it would be possible to better characterize both the range of EDs observed and the average ED for the sample.

The distribution of radionuclides may be investigated in a number of ways. U distribution may be studied through fission track mapping, K through SEM elemental mapping.

Concentrations of U and Th may be studied by laser ablation ICPMS, or indirectly through α autoradiography.

Whilst both avenues of investigation would provide data of interest to the discussion, neither provides a solution to the problem. Dosimetry is based on the average β dose rate of the material. To do better than this requires not only knowledge of the position within the stone of each grain on a particular disc, but also the β dose rate each grain has experienced. Luminescence scanners are being developed in a number of laboratories, however at present they lack the sensitivity to be able to accurately measure small doses. Nevertheless, if combined with detailed radiometric modeling, in the future this may prove one possible solution to the problem.

At present, within the confines of this study, the average dose rate is the only information available for each set of samples. As such, it would seem appropriate to take the average ED from the distribution of EDs seen, rather than singling out the lowest ED peak or 'initial rise', a technique employed in sediment dating. Whilst it is hoped that on balance, the majority of grains will have received an average dose rate, it is acknowledged that in certain circumstances, this assumption may be invalid for some or indeed all grains within a particular sample.

6.5 Age Calculations

Dose rate information for each sample is given in Chapter 4, and tabulated in summary form below together with calculated ages for each sample. The mean age for each unit, together with a mean age for each site is also calculated.

Age calculations for each sample are represented graphically in fig 6.36. It can be seen that on the whole there is consistency between the age obtained for samples on a site by site basis. Samples identified as having a rising De(t) plateau, appear to be distributed at the lower age range of samples for each site, giving weight to the argument that they represent partially zeroed material.

Table 6.11 Age Calculation, Orkney Dataset

Site	Pos	SUTL No	Annual Dose ($mGya^{-1}$)	ED (Gy)	Age (ka)	Mean Unit Age (ka)	Mean Site Age (ka)
Liddle	1	1379	3.62±0.13	14.2±2.06	3.92±0.59		3.92±0.59
DALE	12	748	2.83±0.18	12.05±1.07	4.26±0.47		3.88±0.07
		749	2.65±0.20	10.3±0.96	3.89±0.47		
		750	2.61±0.21	10.48±0.58	4.02±0.39		
		751	2.48±0.17	9.19±0.1	3.71±0.26		
			2.53±0.18	10.70±0.14	4.23±0.31*		
		753	2.89±0.15	9.6±0.45	3.32±0.23		
		754	2.80±0.15	13.24±0.78	4.73±0.38	3.81±0.13	
	13	760	3.28±0.16	12.58±0.63	3.84±0.27		
		765	3.25±0.18	16.3±0.72	5.02±0.36*		
		767	2.52±0.15	12.6±0.82	5.00±0.44*	4.10±0.15	
	14	768	3.10±0.21	8.85±1.12	2.85±0.41		
		769	2.89±0.17	8.04±1.39	2.78±0.51		
		774	2.94±0.16	11.4±0.85	3.88±0.36		
		777	2.39±0.13	9.03±0.40	3.78±0.27		
			2.39±0.13	9.08±0.40	3.80±0.27		
		779	2.70±0.20	11.85±0.50	4.39±0.37*	3.72±0.13	
	15	782	3.12±0.16	13.6±0.40	4.36±0.26*		
		783	2.84±0.16	10.81±0.20	3.81±0.23		
		784	2.77±0.18	10.05±0.20	3.63±0.25	3.92±0.13	
Skaill	5	815	3.13±0.18	9.50±0.11	3.04±0.18		3.03±0.08
	6	817	2.67±0.16	12.09±0.38	4.53±0.31*		
	1	1343	2.79±0.12	8.30±0.73	2.97±0.29		
	2	1354	2.78±0.13	9.20±0.69	3.31±0.29		
	3	1358	2.98±0.13	11.60±0.87	3.89±0.34		
		1360	3.65±0.15	9.52±0.24	2.61±0.13		
	O1	1361	1.43±0.08	0.61±0.18	0.43±0.13		1.03±0.06
	O2	1362	1.41±0.08	0.38±0.13	0.27±0.09		
	O3	1363	1.29±0.09	0.80±0.07	0.62±0.07		
	O4	1364	1.10±0.06	1.03±0.10	0.94±0.10		
Knoll of Merrigarth	8	794	2.34±0.14	10.70±0.43	4.57±0.33*		3.86±0.20
		795	2.42±0.09	12.03±0.64	4.97±0.32*	4.39±0.31	
	7	802	3.58±0.28	13.30±0.74	3.72±0.36		
		803	3.68±0.30	12.05±0.90	3.27±0.36	3.50±0.25	
Warness	11	849	2.47±0.19	12.7±0.43	5.14±0.43		5.41±0.25
	10	857	3.09±0.18	17.13±0.71	5.54±0.40		
			3.03±0.19	16.83±1.13	5.55±0.51		
Stackelbrae		1374	2.38±0.14	5.9±1.69	2.48±0.72		2.48±0.72
Fersness	3	823	2.49±0.09	12.4±0.59	4.98±0.30		4.68±0.20
		824	2.58±0.10	11.43±0.53	4.43±0.27		
Stenquoy	1	836	2.96±0.1	11.43±0.86	3.86±0.32		3.54±0.15
	2	838	2.82±0.17	9.31±0.23	3.30±0.22		
		839	2.66±0.16	9.83±0.48	3.70±0.29		

*** indicates maximum age estimate**

Table 6.12 Age Calculation, Shetland Dataset

Site	Pos	SUTL No	Annual Dose ($mGya^{-1}$)	ED (Gy)	Age (ka)	Mean Unit Age (ka)	Mean Site Age (ka)
Cruester	1	951	2.79±0.11	12.55±0.60	4.50±0.28	3.80±0.17	3.64±0.05
		953	2.92±0.17	9.93±0.20	3.40±0.21		
	2	958	2.70±0.12	10.37±0.25	3.84±0.19	3.84±0.19	
	4	968	2.89±0.14	10.20±0.50	3.53±0.24	3.51±0.16	
		969	2.99±0.18	10.45±0.23	3.49±0.22		
	5	1051	3.21±0.15	10.34±0.88	3.22±0.31	3.43±0.16	
		1053	3.01±0.15	10.55±0.24	3.50±0.19		
	6	1054	2.95±0.13	10.18±0.65	3.45±0.27	3.39±0.20	
		1055	2.98±0.14	9.88±0.71	3.32±0.28		
	8	1062	2.70±0.14	13.08±0.67	4.84±0.35	4.21±0.23	
		1063	3.02±0.18	11.38±0.96	3.77±0.39		
		1064	3.27±0.16	12.31±1.38	3.76±0.46		
	9	1068	2.95±0.15	13.38±0.48	4.54±0.28	4.54±0.28	
	11	1075	2.99±0.19	11.25±0.75	3.76±0.35	3.78±0.29	
		1076	2.94±0.21	9.7±1.79	3.30±0.65		
		1077	3.09±0.25	14.83±2.51	4.80±0.90		
	13	1081	3.28±0.13	13.20±0.27	4.02±0.18	4.02±0.18	
	15	1086	3.71±0.14	13.40±1.73	3.61±0.49	3.28±0.24	
		1088	3.66±0.16	11.90±0.15	3.25±0.15		
	17	1094A	3.14±0.14	12.20±0.70	3.89±0.28	3.71±0.19	
		1097	3.12±0.12	11.1±0.68	3.56±0.26		
	19	1100-1A	3.70±0.15	11.58±0.59	3.13±0.20*	3.13±0.20	
Houlls	1	970	4.37±0.11	16.03±1.05	3.67±0.26	3.98±0.19	3.95±0.12
		971	3.85±0.17	14.8±3.83	3.84±1.01		
		976	2.99±0.08	17.17±2.70	5.74±0.92*		
			2.94±0.08	17.70±2.04	6.02±0.71*		
		978	4.03±0.10	15.93±1.79	3.95±0.45		
	2	983	4.77±0.15	23.33±1.47	4.89±0.34	4.89±0.34	
	3	991	5.04±0.29	17.15±1.42	3.40±0.34	3.38±0.33	
		993	5.15±0.16	15.7±6.98	3.05±1.36		
	4	1003	4.76±0.19	17.08±0.82	3.59±0.22	3.82±0.19	
		1004	4.28±0.17	19.4±1.49	4.53±0.39		
Loch of Garths	1	1006	2.56±0.17	6.17±0.16	2.41±0.17	2.41±0.17	2.85±0.07
	2	1017	4.49±0.19	15.20±0.33	3.39±0.16	2.92±0.07	
			4.49±0.19	18.43±1.22	4.10±0.32		
		1018	5.05±0.18	12.39±0.35	2.45±0.11		
			5.05±0.18	14.5±1.1	2.87±0.24		
		1020	4.38±0.16	13.49±0.32	3.08±0.13		

*** indicates maximum age estimate**

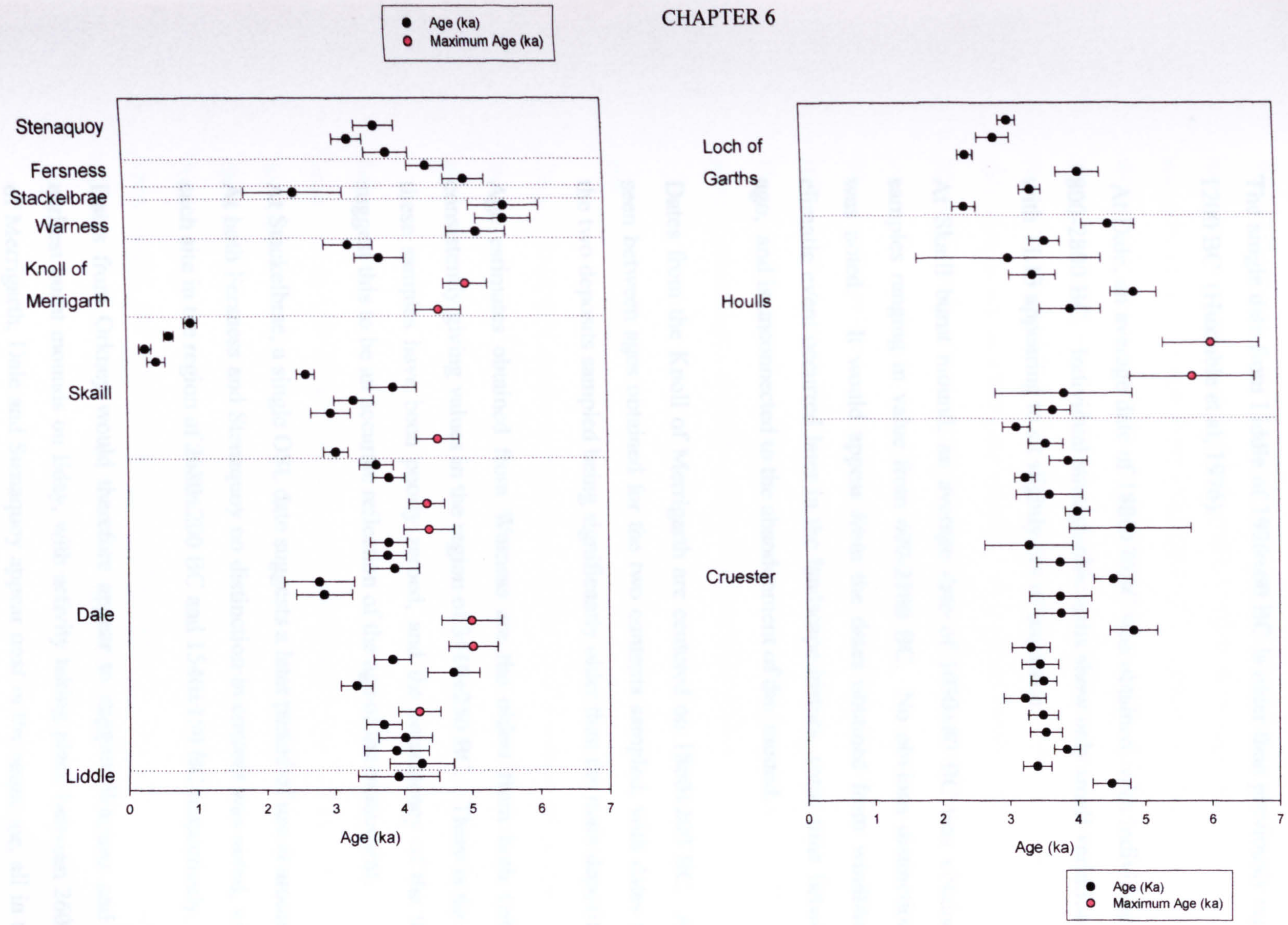

Fig 6.36 Calculated Quartz Ages from (a) Orkney and (b) Shetland Sites

Dates obtained for samples from Orkney range in value from 500-3500 BC, with noticeable differences both between and, on occasion within individual sites.

The single date from Liddle of 1920±60 BC is older than previously reported dates of 300-1200 BC (Huxtable et al, 1976).

At Dale, an average date of 1880±70BC was obtained, with individual dates ranging from 800-2800 BC. Individual stratigraphic units show only small variation in their mean ages, with TL13 appearing to sit slightly out of sequence.

At Skaill burnt mound, an average date of 1030±80 BC was obtained, with individual samples ranging in value from 600-2100 BC. No obvious distinction between contexts was noted. It would appear from the dates obtained from windblown sands that this climatic event occurred later in the landscape history, some time between 300-1000 years ago, and is unconnected to the abandonment of the mound.

Dates from the Knoll of Merrigarth are centered on 1860±200 BC. A distinction can be seen between ages obtained for the two contexts sampled, with dates from the smaller of the two deposits sampled being significantly older than the main deposit.

Age estimates obtained from Warness are the oldest from both Orkney and Shetland, consistently giving values in the region of 3410±250 BC. There is no evidence to suggest these samples have been poorly zeroed, and the consistency of the three dates obtained suggest this to be an accurate reflection of the age of the monument.

At Stackelbrae, a single OSL date suggests a later period of use at around 480±720 BC.
At both Fersness and Stenaquoy no distinction in context was noted, with average ages for each site in the region of 2680±200 BC and 1540±150 BC respectively.

Dates from Orkney would therefore appear to suggest Warness and Fersness to be the earliest burnt mounds on Eday, with activity taking place between 2600-3400 BC. Knoll of Merrigarth, Dale and Stenaquoy appear next in the sequence, all in use at around 1600-1800 BC. Liddle, on Mainland also appears to be in use at this time. Skaill and

Stackelbrae appear to have come into use much later in the sequence, possibly at around 500-1000 BC, although the age resolution is not good for either site.

Within Shetland, ages of individual samples range from 400-3100 BC. At Cruester the majority of samples are tightly confined within the period 1640±50 BC, though individual samples range in value from 1100-2800 BC. There would also appear to be evidence of slight differences in dates for contexts which relate spacially to different areas of the mound. At Houlls, a mean age for the site of 1950±120 BC was obtained, though samples ranged considerably in date from 1000-4000 BC. Again variation in age is seen from different locations within the mound. At Loch of Garths, samples range in date from 400-2100 BC, with a mean age for the site of around 850±70 BC.

The overall pattern seen in Shetland would therefore appear comparable to that observed within Orkney, with Houlls and Cruester apparently in use around the same time as Dale, Knoll of Merrigarth and Liddle. Loch of Garths appears slightly later in the sequence, giving similar age estimates to both Skaill and Stackelbrae.

6.6 Summary

Quartz SAR OSL methods have been outlined and a number of problematic issues relating to the procedure investigated. On the whole, such investigations were encouraging and on the basis of this a large number of samples were therefore selected for further analysis.

Many aspects of sample behaviour were investigated in detail. Intensity of samples was seen to vary both within and on a site to site basis. One sample presented strong evidence to suggest that the intensity of the OSL signal was related to past heating. Sensitisation of the sample during the run was noted to be greater with increased preheat temperatures, but had little effect on the measured ED. Variation in the recycling ratios from disc to disc were noted, but no obvious relationship between this and the ED obtained was seen. Sensitivity corrections would therefore appear not to be the major source of variation in the EDs observed.

IR was measured for each disc and in three cases, high IRSL values correlated to samples with a supressed ED value. Possible causes of this suppression are discussed in more

detail in chapter 7. In a number of cases where low sensitivity prevented accurate measurement of ED, a 'large aliquot' approach which combined the luminescence signal from all discs proved successful.

Differences in the ED distributions of individual samples were noted and further investigated with incomplete zeroing of the geological signal and microdosimetric effects considered.

Incomplete zeroing was discussed in terms of likely trap parameters and heating scenarios, and strong evidence for the existence of such an effect presented from one sectioned hearthstone sample. This also highlighted the effectiveness of a De(t) plot in identifying potential unzeroed material in a number of cases. Age estimates from these samples were therefore quoted as maximum ages.

Despite concerns over likely microdosimetric effects, average EDs gave coherent age estimates for individual sites, suggesting a period of use for the sites sampled in the region of 500-3500 BC in the case of Orkney, and 400-2800 BC for Shetland. Variation in age was noted both between and within individual sites.

CHAPTER 7 DISCUSSION OF RESULTS

7.1 Introduction

This chapter summarizes the results presented in the previous two chapters, and compares the age estimates obtained by two different luminescence methods. Observations are made on the concordance or otherwise of results, and suggestions put forward as to possible causes of discontinuity between the two datasets. Other chronological information, in the form of a series of radiocarbon dates, is summarized before conclusions are drawn as to the reliability of the quartz and feldspar methods.

Each study area is discussed on a site-by-site basis and fundamental questions are addressed with regard to the ability of luminescence dating to accurately assess the likely duration of use of individual sites are addressed. A local and regional picture of burnt mound use within the two areas is constructed, with observations on likely patterns of use made. These observations are set within the archaeological landscape of the two regions and against the larger chronological picture of burnt mounds in Scotland.

7.2 Luminescence Results

Luminescence results from feldspar multiple aliquot additive TL and quartz single aliquot OSL methods are outlined in detail in the previous two chapters. A number of methodological problems have been highlighted with regards to the measurement of ED which brings into question the accuracy of one or the other dataset. In addition, sample specific problems relating to the effective zeroing of material and the homogeneity of the annual dose rate within samples have also been raised. A comparison of results from both methods is detailed below, and consideration is given to possible reasons for the observed discrepancies.

Luminescence dates from both feldspar and quartz methods are summarized in table 7.1 and 7.2 below, together with an age ratio comparison for samples for which both methods were employed. Samples from Shetland are in reasonable agreement with an average ratio of feldspar:quartz ages of 0.98±0.05. In Orkney however the majority of feldspar derived dates represent minimum age estimates which, when compared to dates derived from quartz SAR, appear in the region of 20-40% lower, with an average ratio value of 0.73±0.03.

A number of potential samples were highlighted in Chapter 5 and 6 as being poorly zeroed. Where both feldspar and quartz datasets were available for samples, a correlation between those identified through their feldspar ED plateau plot as potentially poorly zeroed, and samples which exhibit an increasing De(t) plot on quartz runs. Samples common to both are SUTL 751, 754, 765, 794, 795, 824, 1100. Two samples, SUTL 767 and 817 do however show discrepancies with quartz De(t) plots indicating poor zeroing, but no evidence within the feldspar data. However, on both occasions the feldspar regression at higher temperatures is dominated by large errors due to low signal intensities in this area. The concordance of these results are of significance to the development of procedures for identifying poorly zeroed material in OSL studies as they suggest the De(t) plot to be a good indicator of problematic samples.

Potential problems relating to the correction method applied to the feldspar dataset were outlined in chapter 5, with the Orkney samples highlighted as potentially being subject to error as a result of the larger DDSC indicated by way of curvature in the intercept regression line. A plot of the degree of curvature against age ratio for paired samples indicates a strong correlation between the two (fig 7.2). Nevertheless, there are a number of samples for which agreement between both methods are seen. When age ratios are plotted in relation to the geology of individual samples from Orkney (fig 7.3) it becomes clear that these samples are derived almost exclusively from Rousay flagstones, with samples of a lower ratio corresponding to those derived from Eday beds. The larger dose dependent effects would therefore seem related to the parent rock source of the sample.

Whilst all samples suffer a small dose dependent effect which is enough to dramatically alter the measured value of ED in the majority of cases, the correlation between quartz and feldspar ages for samples from Cruester, Houlls and Rousay Flag samples from Orkney offer strong validation of the appropriateness of the correction method outlined in chapter 5 for samples with minimal DDSC. It would therefore seem appropriate to conclude that the quartz dataset, together with samples from Orkney that originate from Rousay Flagstone, offer the best estimate of age of the samples.

Table 7.1 Feldspar and Quartz age estimates for samples from Orkney

Site	SUTL	Pos	Feldspar Age (ka)	Quartz Age (ka)	Ratio Feldspar: Quartz Ages	Date
Lid.	1379	1	2.46±0.13	3.92±0.59	0.63±0.10	1920±590 BC
	1381	1	2.49±0.34			
	1386	3	2.33±0.25			
Dale	748	12	2.23±0.21	4.26±0.47	0.52±0.08	2260±470 BC
	749		2.50±0.28	3.89±0.47	0.64±0.11	1890±470 BC
	750		2.36±0.48	4.02±0.39	0.59±0.13	2020±390 BC
	751		2.24±0.92	3.71±0.26 4.23±0.31	0.60±0.25 0.53±0.22	1880±280 BC
	753		2.31±0.31	3.32±0.23	0.70±0.11	1320±230 BC
	754		4.25±0.43	4.73±0.38	0.90±0.12	2490±400 BC
	760	13	2.29±0.30	3.84±0.27	0.60±0.09	1840±270 BC
	764	13	2.60±0.40			
	765	13		5.02±0.36		3020±360 BC
	767	13	2.82±0.50	5.00±0.44	0.56±0.11 0.59±0.11	3000±360 BC
	768	14	3.07±0.35	2.85±0.41	1.08±0.20	960±400 BC
	769	14		2.78±0.50		780±500 BC
	774	14	3.74±0.36	3.88±0.36	0.96±0.13	1800±360 BC
	775	14	3.04±0.38			1040±380 BC
	777	14	2.22±0.74	3.78±0.27 3.80±0.27	0.59±0.20 0.58±0.20	1790±270 BC
	779	14	3.45±0.50	4.39±0.37	0.79±0.13	1910±330 BC
	782	15		4.36±0.26		2360±260 BC
	783			3.81±0.23		1810±230 BC
	784			3.63±0.25		1630±250 BC
	785		1.96±0.36			
Skaill	815	5	2.75±0.38 2.65±0.46	3.04±0.18	0.90±0.14 0.87±0.16	930±150 BC
	817	6		4.53±0.31		2530±310 BC
	1343	1		2.97±0.29		970±290 BC
	1354	2		3.31±0.29		1310±290 BC
	1358	3		3.89±0.34		1890±340 BC
	1360		2.01±0.26	2.61±0.13	0.77±0.11	610±130 BC
	1361	O1		0.43±0.13		AD 1570±130
	1362	O2		0.27±0.09		AD 1730±90
	1363	O3		0.62±0.07		AD 1380±70
	1364	O4		0.94±0.10		AD 1060±100
K. of Merr.	794	8	3.68±0.39	4.57±0.33	0.81±0.10	3150±280 BC
	795	8	5.32±0.48	4.97±0.32	1.07±0.12	2130±250 BC
	802	7	2.36±0.39	3.72±0.36	0.63±0.12	1720±360 BC
	803	7	2.29±0.30	3.27±0.36	0.70±0.12	1270±360 BC
War.	842	9	3.94±0.85			
	849	11		5.14±0.43		3140±430 BC
	857	10	4.01±0.42	5.54±0.40 5.55±0.51	0.72±0.10	3550±510 BC
Stac	1374			2.48±0.72		480±720 BC

Fersness	823	3	4.37±0.80	4.98.±0.30	0.88±0.17	2900±300 BC
	824	3	3.13±0.33	4.43±0.27	0.71±0.09	2430±270 BC
	831	4	4.16±0.80 3.72±0.42			1820±370 BC
Sten	836	1	2.52±0.40	3.86±0.32	0.65±0.12	1860±320 BC
	838	2	2.06±0.78	3.30±0.22	0.62±0.24	1330±220 BC
	839	2	1.76±0.55	3.70±0.29	0.48±0.15	1700±290 BC

Red indicates minimum age estimate, blue maximum age estimate

Table 7.2 Feldspar and Quartz age estimates for samples from Shetland

Site	Pos	Sample No	Feldspar Age (ka)	Quartz Age (ka)	Feldspar: Quartz Age Ratio	Date
Cruester	1	949	3.69±0.54			1690±540 BC
		951	3.76±0.32	4.50±0.28	0.84±0.09	2180±210 BC
		953	3.45±0.28	3.40±0.21	1.01±0.10	1420±170 BC
	2	958	3.62±0.46	3.84±0.19	0.94±0.13	1810±180 BC
	4	968	3.25±0.33	3.53±0.24	0.92±0.11	1430±190 BC
		969		3.49±0.22		1490±220 BC
	5	1051	2.98±0.24 3.90±0.28	3.22±0.31	0.93±0.12 1.21±0.15	1070±190 BC
		1053		3.50±0.19		1500±190 BC
	6	1054	2.78±0.32	3.45±0.27	0.81±0.11	1150±205 BC
		1055		3.32±0.28		1320±280 BC
	8	1062	4.37±0.34	4.84±0.35	0.90±0.10	2600±240 BC
		1063		3.77±0.39		1770±390 BC
		1064		3.76±0.46		1760±460 BC
	9	1068	4.26±0.70	4.54±0.28	0.94±0.16	2500±260 BC
	11	1075		3.76±0.35		1760±350 BC
		1076		3.30±0.65		1300±650 BC
		1077		4.80±0.90		2800±900 BC
	13	1081		4.02±0.18		2020±180 BC
	15	1086		3.61±0.49		1610±490 BC
		1088	2.64±0.41	3.25±0.15	0.81±0.13	1180±140 BC
	17	1094A		3.89±0.28		1890±280 BC
		1097		3.56±0.26		1560±260 BC
	19	1100-1A	3.80±0.25	3.13±0.20	1.21±0.11	1390±160 BC
Houlls	1	970	4.67±0.54	3.67±0.26	1.27±0.17	1670±260 BC
		971		3.84±1.01		1840±1010 BC
		976		5.74±0.92 6.02±0.71		2880±580 BC
		978		3.95±0.45		1950±450 BC
	2	983		4.89±0.34		2890±340 BC
	3	991		3.40±0.34		1400±340 BC
		993		3.05±1.36		1050±1360 BC
	4	1003		3.59±0.22		1590±220 BC
		1004		4.53±0.39		2530±390 BC
Loch of Garths	1	1006		2.41±0.17		410±170 BC
	2	1017		3.39±0.16		1390±160 BC
				4.10±0.32		2100±320 BC
		1018		2.45±0.11		450±110 BC
				2.87±0.24		870±240 BC
		1020		3.08±0.13		1080±130 BC

Red indicates minimum age estimate, blue maximum age estimate

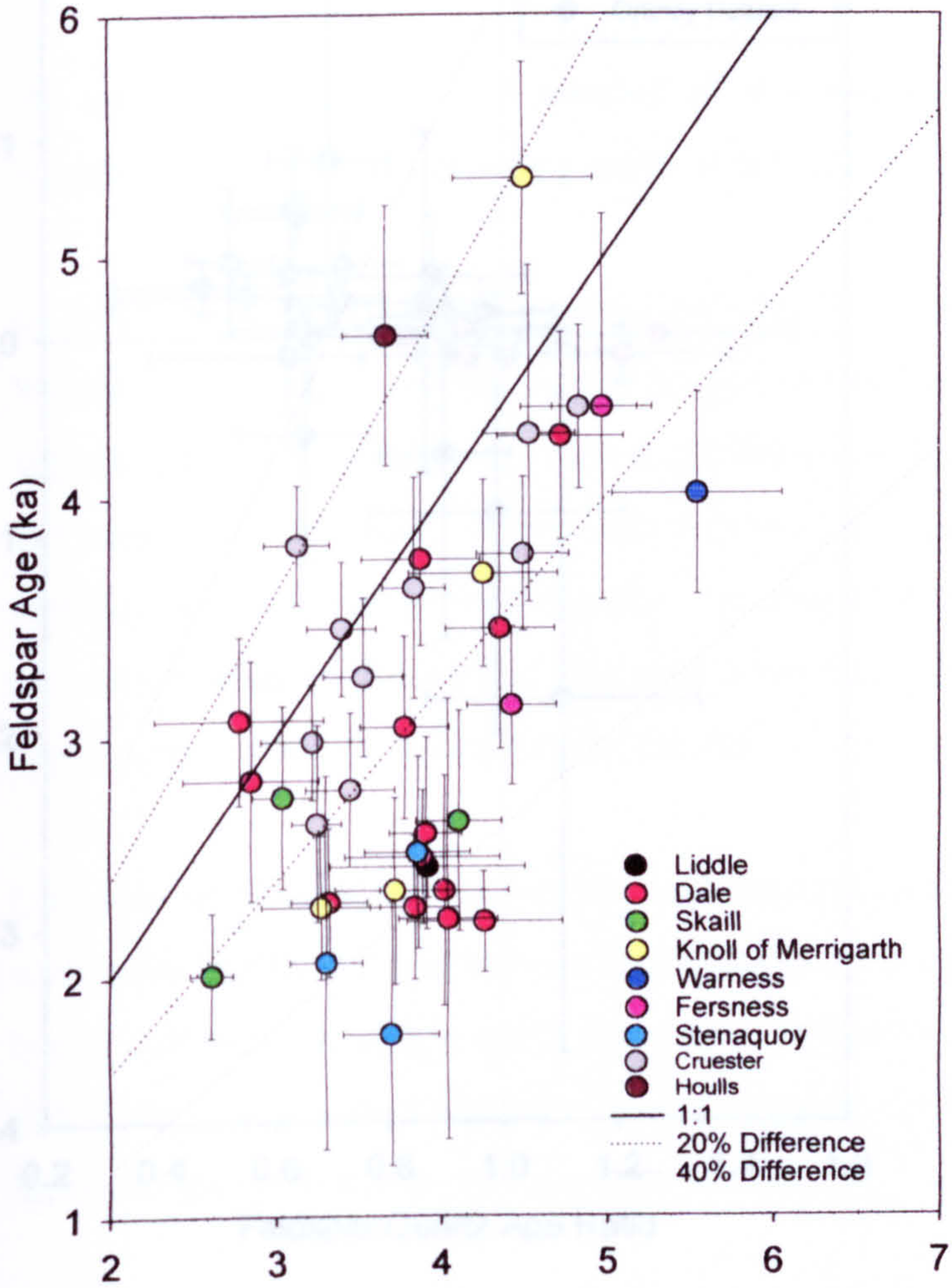

Fig 7.1 Comparison of Feldspar and Quartz age estimates for samples from Orkney and Shetland

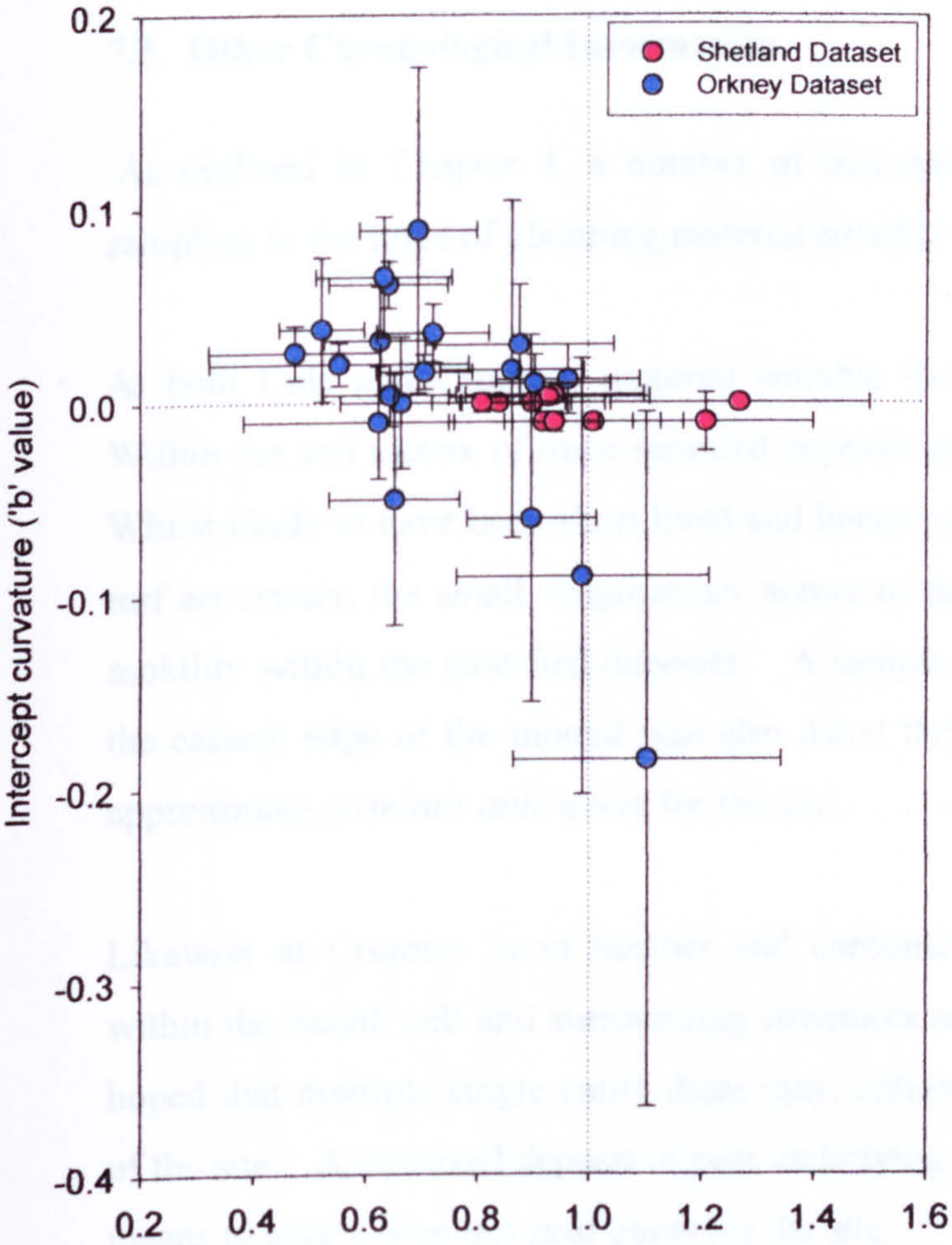

Fig 7.2 Relationship between degree of DDSC in feldspar dataset (measured through curvature of intercept line) and Feldspar:Quartz age ratio in samples from Orkney and Shetland

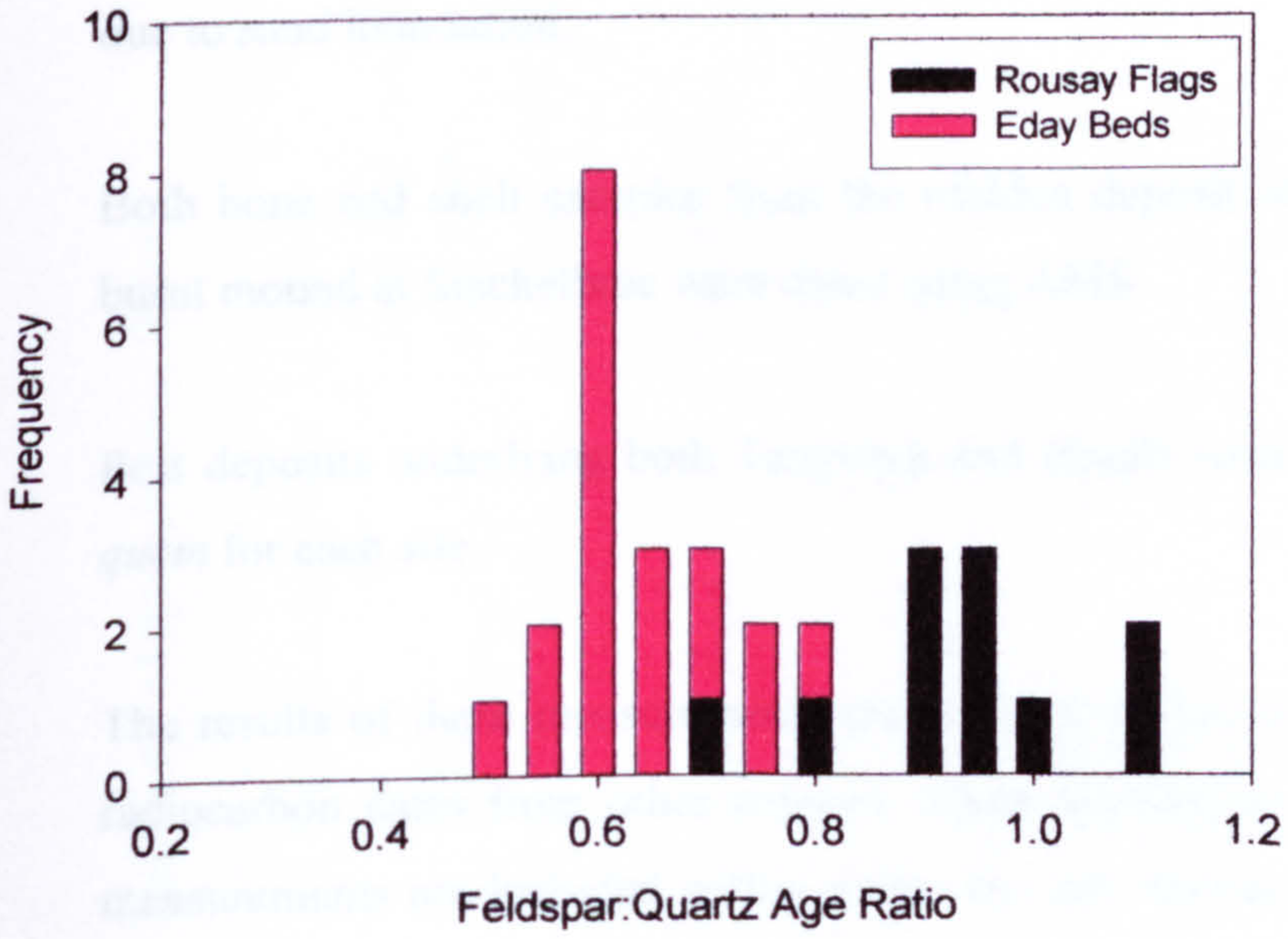

Fig 7.3 Histogram of Feldspar:Quartz Age ratios for different geologies, Orkney Dataset.

7.3 Other Chronological Information

As outlined in Chapter 4, a number of soil and peat samples were collected at time of sampling in the hope of obtaining material suitable for radiocarbon dating.

- At both Dale and Cruester, material suitable for AMS radiocarbon dating was identified. Within the soil matrix of three sampled deposits at Dale, pieces of burnt turf were identified. Whilst likely to have been short lived and hence reflect the time of cutting and burning of the turf accurately, the small, fragmentary nature of the material raises questions as to its likely mobility within the stratified deposits. A sample of the peat layer which partially overrides the eastern edge of the mound was also dated through radiometric carbon dating to give an approximate *terminus ante quem* for the site.

Likewise at Cruester burnt heather and carbonized cereal grains recovered from deposits within the hearth cell and surrounding structures are also likely to be mobile, however it was hoped that multiple single entity dates may, collectively shed further light on the chronology of the site. A localized deposit of peat underlying the site was also dated through radiometric means to give a *terminus post quem* for the site.

At Skaill, a series of dates on the two peat layers found associated with the site were conducted to determine both the onset of peat accumulation and the interruption in growth due to sand inundation.

Both bone and shell samples from the midden deposit which partially underlies part of the burnt mound at Stackelbrae were dated using AMS.

Peat deposits underlying both Tangwick and Houlls were also dated to give a *terminus post quem* for each site.

The results of these measurements are outlined below in table 7.3, together with additional radiocarbon dates from other sources, where appropriate to the site. The results of these measurements are included within a site- by- site discussion in the subsequent section, after comparison with both quartz and feldspar datasets below.

Table 7.3 Summary of Radiocarbon Dates

Site	Sample Description	Context	Relationship	Lab Code	Radiocarbon Age (BP)	Calibrated Date (1 sigma)
Liddle	Peat	First Peat formed in flag lined gulley	Should post-date occupation of site	SRR-525*[A]	2908±45	1210-1010 cal BC
	Heather roots	Bottom of Trough	Should post-date occupation of site	SRR-701*[A]	2826±75	1130-890 cal BC
Dale	Burnt Turf	TL12(112)	Should be contemporary with material from TL12 position	AA 48054	3505±45	1890-1740 cal BC
				AA 48055	3155±50	1500-1380 cal BC
				AA 48053	3760±55	2290-2040 cal BC
	Burnt Turf	TL13(110)	Should be contemporary with material from TL13 position	AA 48057	3510±45	1890-1740 cal BC
				AA 48056	3580±45	1980-1870 cal BC
	Burnt Turf	TL14 (107)	Should be contemporary with material from TL14 position	AA 48058	3440±50	1880-1680 cal BC
	Peat	Peat Deposit (102) formed above main mound	Should Post Date mound activity	GU 9796	1230±50	cal AD 720-890
Skaill	Peat	Lower Peat Deposit (011), North Facing Section	Should Post Date Mound Activity	GU 9793	1280±60	cal AD 660-810
		Lower Peat Deposit (011), South Facing Section		GU 9794	1670±50	cal AD 260-430
		Upper Peat Deposit (003), North Facing Section		GU 9795	620±50	cal AD 1300-1400
Stackelbrae	Cow Bone	Midden context which mound partially overlaps	Should Predate mound activity	AA 84053	830±40	cal AD 1185-1265
	Shell			GU 9789	1200±50	cal AD 1160-1280
Cruester	Peat	Below Mound	Predate mound activity	GU 9791	4040±50	2630-2470 cal BC

Site	Sample Description	Context	Relationship	Lab Code	Radiocarbon Age (BP)	Calibrated Date (1 sigma)
	Ericaceae	(072) From deposit accumulated between floors #6 and #7 in hearth cell	Should post date floor #6	AA 49614	3220±35	1520-1440 cal BC
		(076) From deposit accumulated between floors #4 and #5 in hearth cell	Should post date floor #4	AA 49616	3055±35	1390-1260 cal BC
				AA 49615	3040±35	1380-1220 cal BC
	Ericaceae	(074) From deposit accumulated between floors #5 and #6 in hearth cell	Should post date floor #5	AA 69617	3145±35	1490-1320 cal BC
	Carbonised Cereal Grain: Hordeum vulgare			AA 52539*[B]	2810±40	1005-900 cal BC
	Carbonised Cereal Grain: Hordeum vulgare	Sandy silt deposit (052) in Cell F	Contemporary or post date activity in Cell F	AA 52537*[B]	2960±35	1260-1120 cal BC
				AA 52536*[B]	3055±40	1390-1260 cal BC
	Carbonised Cereal Grain: Hordeum	Compact dark brown sandy silt layer in Cell B	Contemp. or post date activity Cell B	AA 52538*[B]	2980±35	1290-1120 cal BC
Tangwick	Peat	Below Mound Deposit	Predate mound activity	GU 9790	4860±60	3710-3530 cal BC
	Charred Barley Grain	Silty Deposit on top of peat layer below mound	Predate or beginning of mound activity	OxA 8195[8C]	3390±55	1750-1600 cal BC
	Charred Iris Rhizome	Thick Silty layer containing much pottery between early and late mound deposit	Post Date Early mound use, predate later mound use	OxA 8196[8C]	2815±40	1005-905 cal BC
Houlls	Peat	Below Mound Deposit	Should Predate mound activity	GU 9792	6740±60	5720-5560 cal BC

Notes **(i)** Radiocarbon dates denoted * are from the following sources: (A) Huxtable et al (1976) (B) Hazel Moore, pers. comm. (C) Moore and Wilson (2000). **(ii)** AMS dates are coded AA and OxA, all other dates refer to radiometric measurements

7.4 Summary of chronological Information

At two sites, Dale and Cruester, radiocarbon dates exist for contexts which also have associated luminescence dates. At Dale, contexts 107, 110 and 112 show excellent agreement between radiocarbon and quartz luminescence ages, despite the less than ideal nature of the radiocarbon material. At Cruester, a series of dates from within the hearth cell again show close correlation with quartz OSL dates. Neither shows any consistency with either uncorrected feldspar ages, or those corrected which exhibit a higher degree of sensitivity change. The overall agreement between all three methods is encouraging, suggesting that feldspar correction in suitable samples was effective and that the dose rates calculated for both quartz and feldspar mineral fractions are appropriate.

7.5 Synthesis of Chronological Information on a site by site basis

7.5.1 Introduction

Chronological information for each site is summarized below in relation to the archaeological context from which each sample derived. Where successful correction of the feldspar dataset has occurred, a weighted mean of feldspar and quartz ages has been quoted. All luminescence dates have been converted to calendar years BC/AD with radiocarbon dates quoted in calibrated years BC/AD. Both sets of results are quoted with their 1 sigma errors.

7.5.2 Orkney Samples

7.5.2.1 Liddle Burnt Mound

A single date from Liddle burnt mound was obtained by Quartz OSL SAR methods. The date of 1920±590 BC is earlier than previously reported luminescence dates of 300-1300 BC (Huxtable et al, 1976). It is not possible, given the limitations of the sampling strategy, to make any firm inferences over the discrepancy between the two dates. Whether the discontinuity represents an earlier phase of activity on the site, or systematic errors in one or more of the procedures is uncertain. It is however worth noting that the feldspar ages which were discarded due to the degree of sensitivity change exhibited by samples, are more in keeping with earlier estimates, ranging from 300-500 BC. These dates, together with those published by Huxtable et al are notably younger than two radiocarbon dates relating to the

post mound period (1210-1010 cal BC and 1130-890±110 cal BC). It would be of interest to resample varying parts of the mound in the future in order to better test this hypothesis.

7.5.2.2 Dale Burnt Mound

A total of 20 samples were selected for further analysis from Dale burnt mound, representing contexts 112, 110, 107 and 117 (TL12, 13, 14 and 15 respectively). As discussed above, the feldspar dataset proved problematic, such that thirteen of the samples gave only minimum age estimates. As these appear significantly later that their quartz pairs, only the four samples not included within this group have been discussed below. Seventeen dates were also obtained by quartz methods. In addition, six AMS dates were obtained from burnt turf within deposits 112, 110 and 107, and one radiometric date was obtained for a peat layer overlying the eastern edge of the mound. This information is summarized below in table 7.4. Where both quartz and feldspar dates have been obtained, the weighted mean of the two has been used in age estimates quoted.

Table 7.4 Summary of Chronological Information from Dale Burnt Mound

Context (in Stratigraphic Order)	Luminescence Dates	Radiocarbon Dates	Mean Age of Unit[a]
102		cal AD 720-890	805±85AD
TL14 - 107	780±500 BC 960±400 BC 1040±380 BC 1790±270 BC 1800±360 BC 1910±330BC	1880-1680 cal BC	1635±100 BC
TL13 -110	1840±270 BC 3000±360 BC 3020±360 BC	1890-1740 cal BC 1980-1870 cal BC	1855±95 BC
TL12- 112	1320±230 BC 1880±280 BC 1890±470 BC 2020±390 BC 2260±470 BC 2490±400BC	1500-1380 cal BC 1890-1740 cal BC 2290-2040 cal BC	1800±60 BC
Unstratified			
TL15-117	1630±250 BC 1810±230 BC 2360±260 BC		1720±170 BC

[a] Maximum age estimates (indicated in blue) have been excluded from mean age estimates

There are a number of observations which can be made about the above dataset. It is clear that the date for peat formation over the mound is significantly later than the main period of use of the mound, centred around 1750±60 BC. Radiocarbon dates for each of the three stratified units are in good agreement with the luminescence results. Both show a mixture of dates within individual contexts suggesting mobilization of carbonaceous material, and movement or reuse of stones post deposition. Dates from contexts 107 and 112 are in stratigraphic order, and appear to show variation in age in the region of a few centuries. The mid context, 110 is statistically similar to the basal deposit (112), suggesting contemporaity in use. Dates from the western side of the mound are also similar in age, showing good agreement with the mean age for the site.

7.5.2.3 Skaill Burnt Mound

The chronological information available for Skaill burnt mound and its surrounding deposits is threefold – a combination of radiocarbon dates of peat, OSL dates of wind blown sand and OSL dates of burnt stone from various positions within the mound (figs 7.4 &7.5). The mean age for burnt stones from the mound is 1145±105 BC, though samples range in age from 610-2110 BC. There is no obvious correlation between earlier and later dates spatially within the mound.

The post-mound deposits sampled tell an interesting story of the environmental history of the site post abandonment. The lower peat layer, which partially covers the base of the mound on both sides of the excavated section, was forming throughout the mid-late first millennium AD, with dates from the bottom and top of the deposit of cal AD 260-430 and cal AD 660-810 respectively. A large deposit of windblown sand at the turn of the millennium (AD 1060±100) is then seen to interrupt growth. Sommerville (2003) has traced deposits of sand across the hill behind the mound to Fersness Bay and suggests, on the basis of calcium content and OSL sensitivity that this sand is derived from the deposits at Fersness Bay, transported by a large storm event. Whilst later dates are obtained from other OSL sampling positions, ranging from late 14th to early 18th century AD, it is possible that these derive from more localized events where the sand, emplaced in the earlier period, has been re-exposed and re-zeroed. Peat growth was seen to re-start some time around the mid 14th

Fig 7.4 Summary of Chronological information from Burnt Stone Deposits, Skaill Burnt Mound

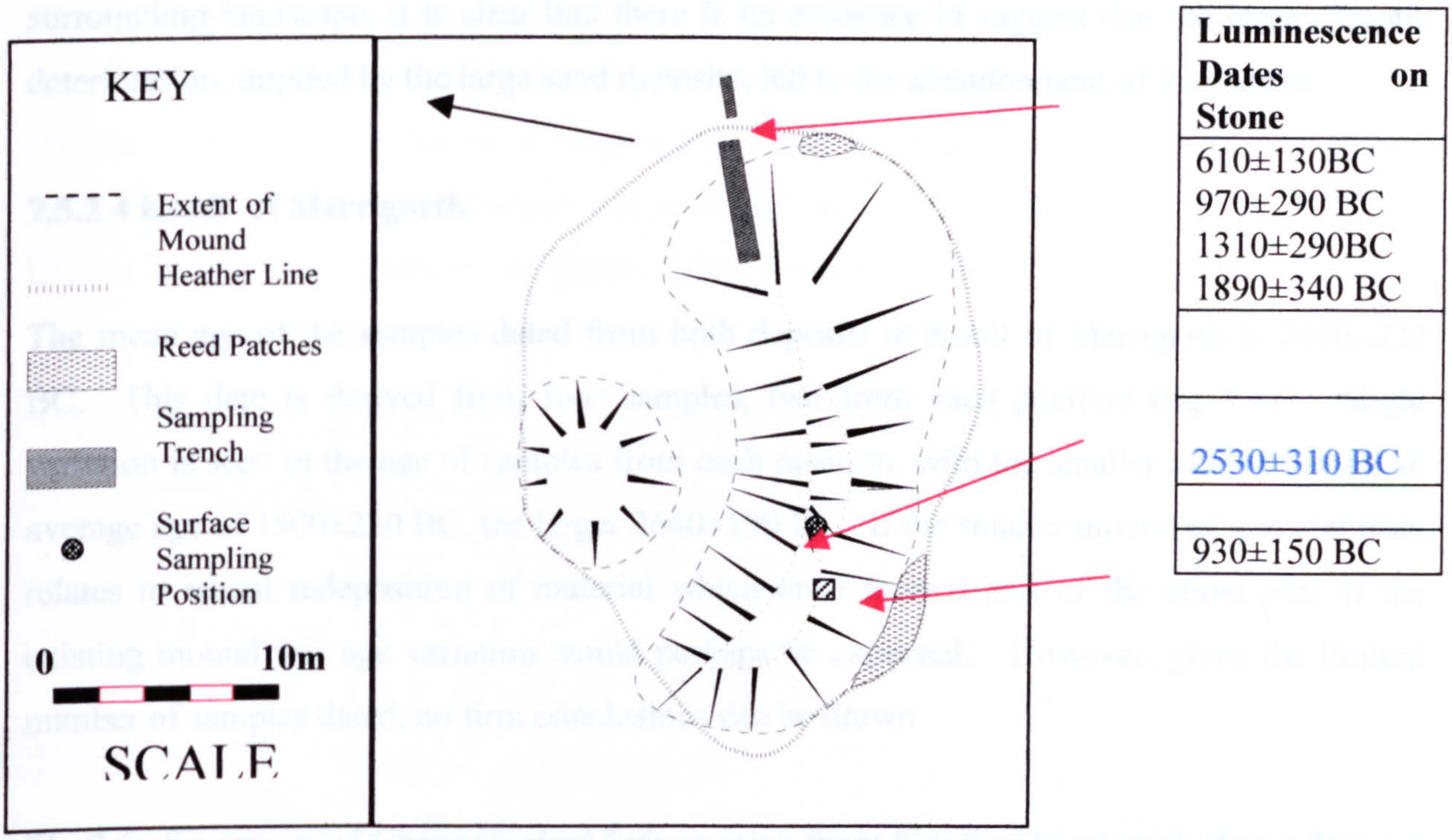

Luminescence Dates on Stone
610±130BC
970±290 BC
1310±290BC
1890±340 BC
2530±310 BC
930±150 BC

Fig 7.5 Summary of Chronological information from deposits overlying Eastern edge of Skaill Burnt Mound
(blue=radiocarbon date from peat, yellow= OSL date from sand, pink=avg TL/OSL date from heated stone

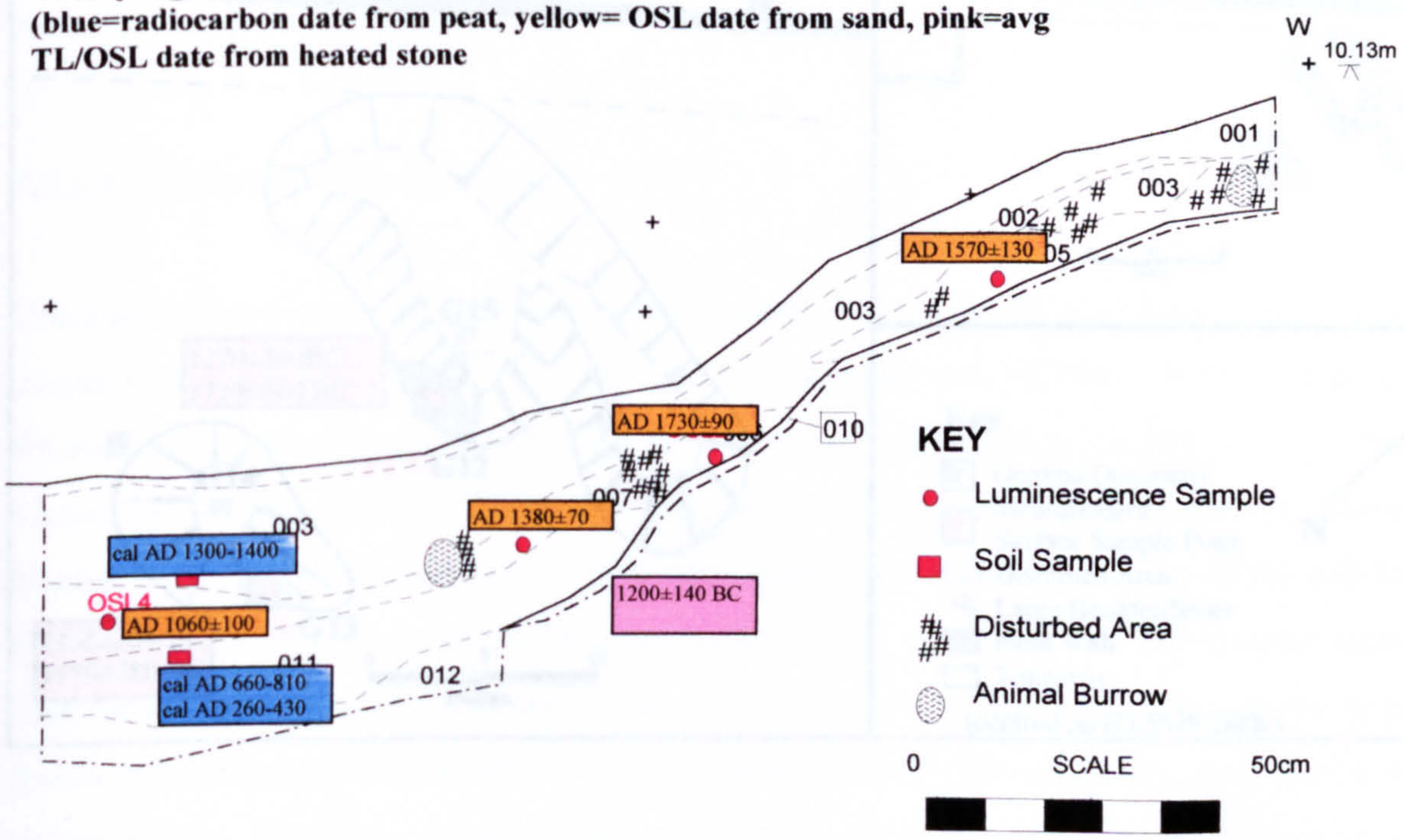

century AD, most probably gradually encroaching on the mound once again, covering the later sand deposits. Whilst this information is of great interest to the development of the surrounding landscape, it is clear that there is no evidence to suggest that the large climatic deterioration, implied by the large sand deposits, led to the abandonment of the mound.

7.5.2.4 Knoll of Merrigarth

The mean age of the samples dated from both deposits at Knoll of Merrigarth is 2070±220 BC. This date is derived from four samples, two from each position (fig 7.6). Slight variation is seen in the age of samples from each position, with the smaller mound having an average age of 1500±250 BC, the larger 2640±190 BC. If the smaller mound of material truly relates to recent redeposition of material which once formed part of the upper part of the existing mound this age variation would perhaps be expected. However, given the limited number of samples dated, no firm conclusions can be drawn.

Fig 7.6 Summary of Chronological Information from Knoll of Merigarth Burnt Mound

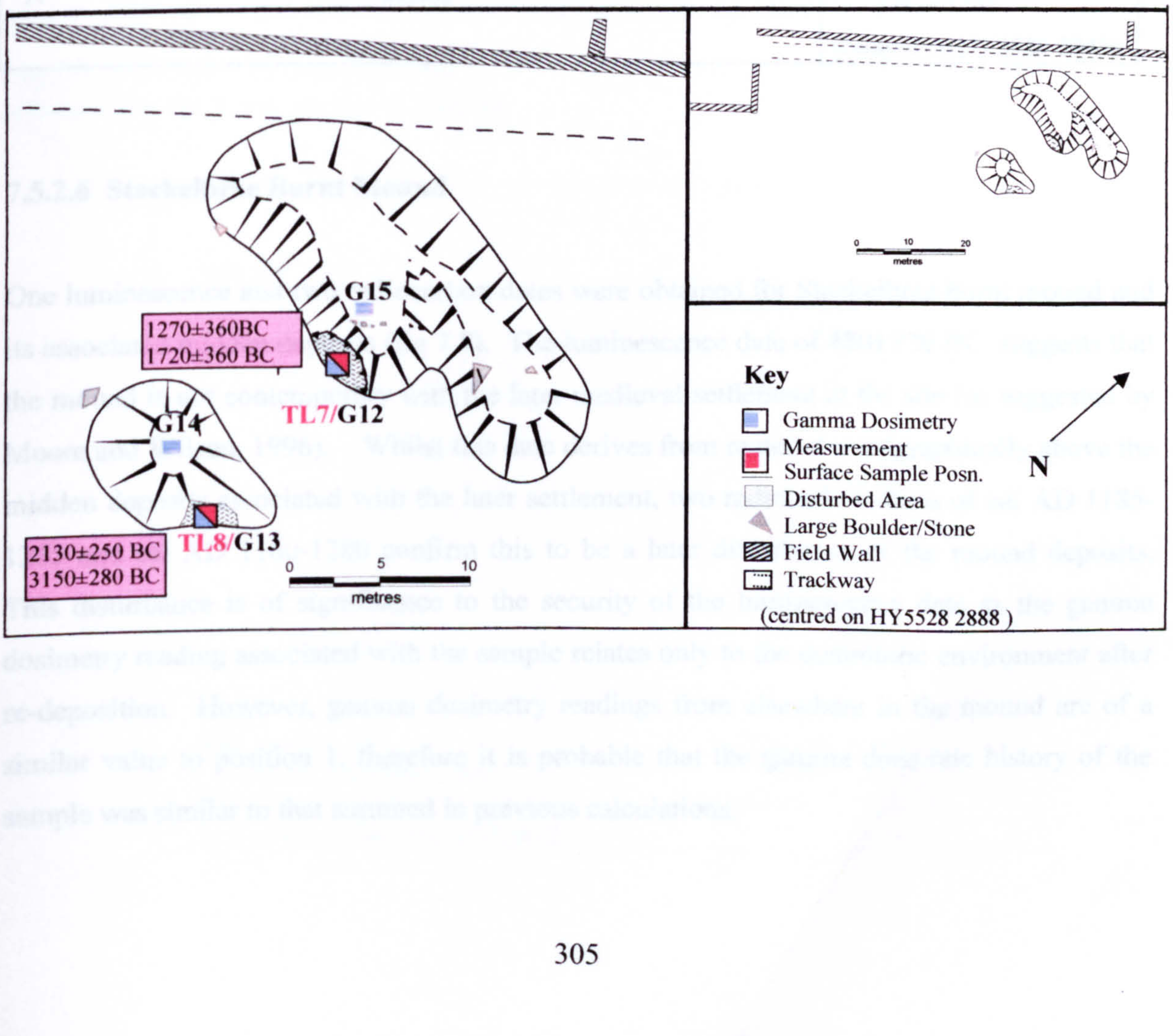

7.5.2.5 Warness Burnt Mound

Whilst a number of samples from Warness were prepared, only two produced reliable results. These two samples, from positions TL10 and TL11 are significantly older than the expected age of the mound, at 3550±450 BC and 3140±430 BC respectively (fig 7.7). As discussed in chapter 7, there is no evidence to suggest that either of these samples is poorly zeroed and, thus without evidence to the contrary the mean age for the site would appear to be 3340±310 BC, an intriguing age given the evidence of structures associated with the mound.

Fig 7.7 Summary of chronological information from Warness burnt mound

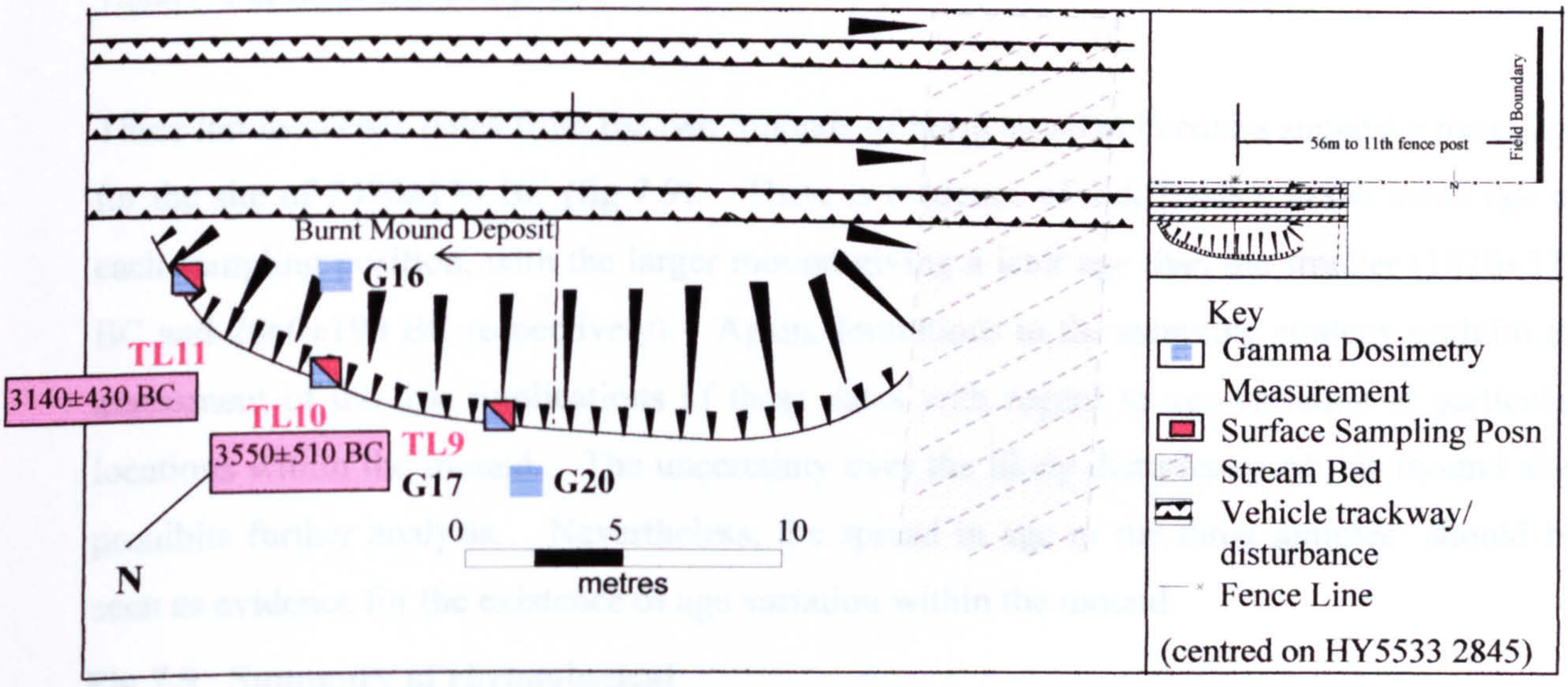

7.5.2.6 Stackelbrae Burnt Mound

One luminescence and two radiocarbon dates were obtained for Stackelbrae burnt mound and its associated midden deposits (fig 7.8). The luminescence date of 480±720 BC suggests that the mound is not contemporary with the later medieval settlement at the site (as suggested by Moore and Wilson, 1996). Whilst this date derives from material stratigraphically above the midden deposits associated with the later settlement, two radiocarbon dates of cal AD 1185-1265 and cal AD 1160-1280 confirm this to be a later disturbance of the mound deposits. This disturbance is of significance to the security of the luminescence date as the gamma dosimetry reading associated with the sample relates only to the dosimetric environment after re-deposition. However, gamma dosimetry readings from elsewhere in the mound are of a similar value to position 1, therefore it is probable that the gamma dose rate history of the sample was similar to that assumed in previous calculations.

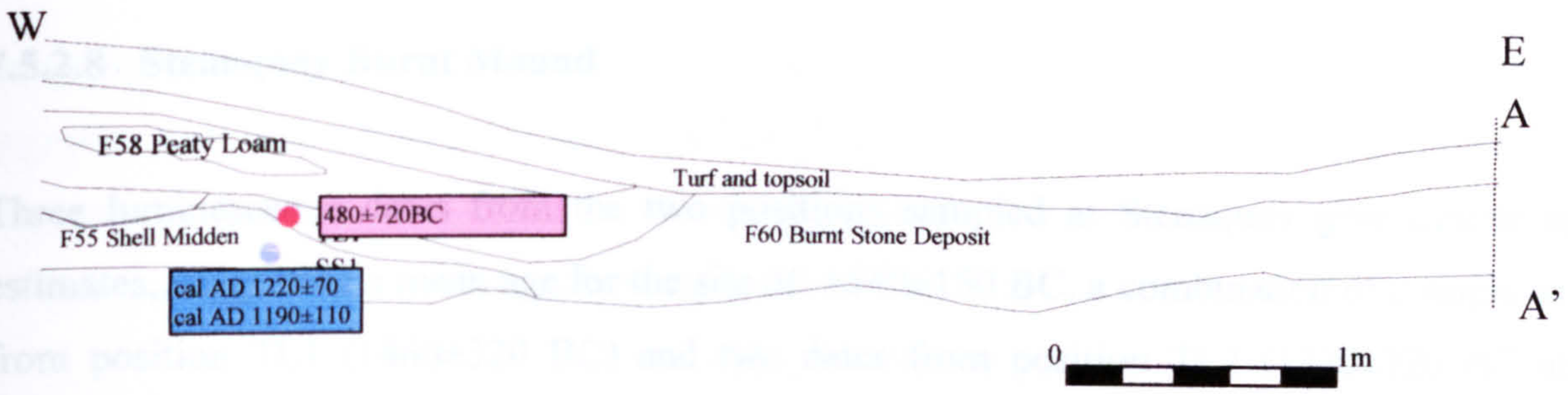

Fig 7.8 Summary of chronological information from Stackelbrae burnt mound

7.5.2.7 Fersness Burnt Mound

Three luminescence dates from the two mounds of burnt stone at Fersness suggest a mean age for the site of 2470±170 BC (fig 7.9). There is evidence of a difference in the mean age of each sampling position, with the larger mound giving a later age than the smaller (1820±370 BC and 2660±190 BC respectively). Again, limitations in the sampling strategy prohibit an assessment of the true implications of these dates with regard to age variation at particular locations within the mound. The uncertainty over the likely disturbance of this mound also prohibits further analysis. Nevertheless, the spread in age of the three samples should be seen as evidence for the existence of age variation within the mound.

Fig 7.9 Summary of chronological information for Fersness burnt mound

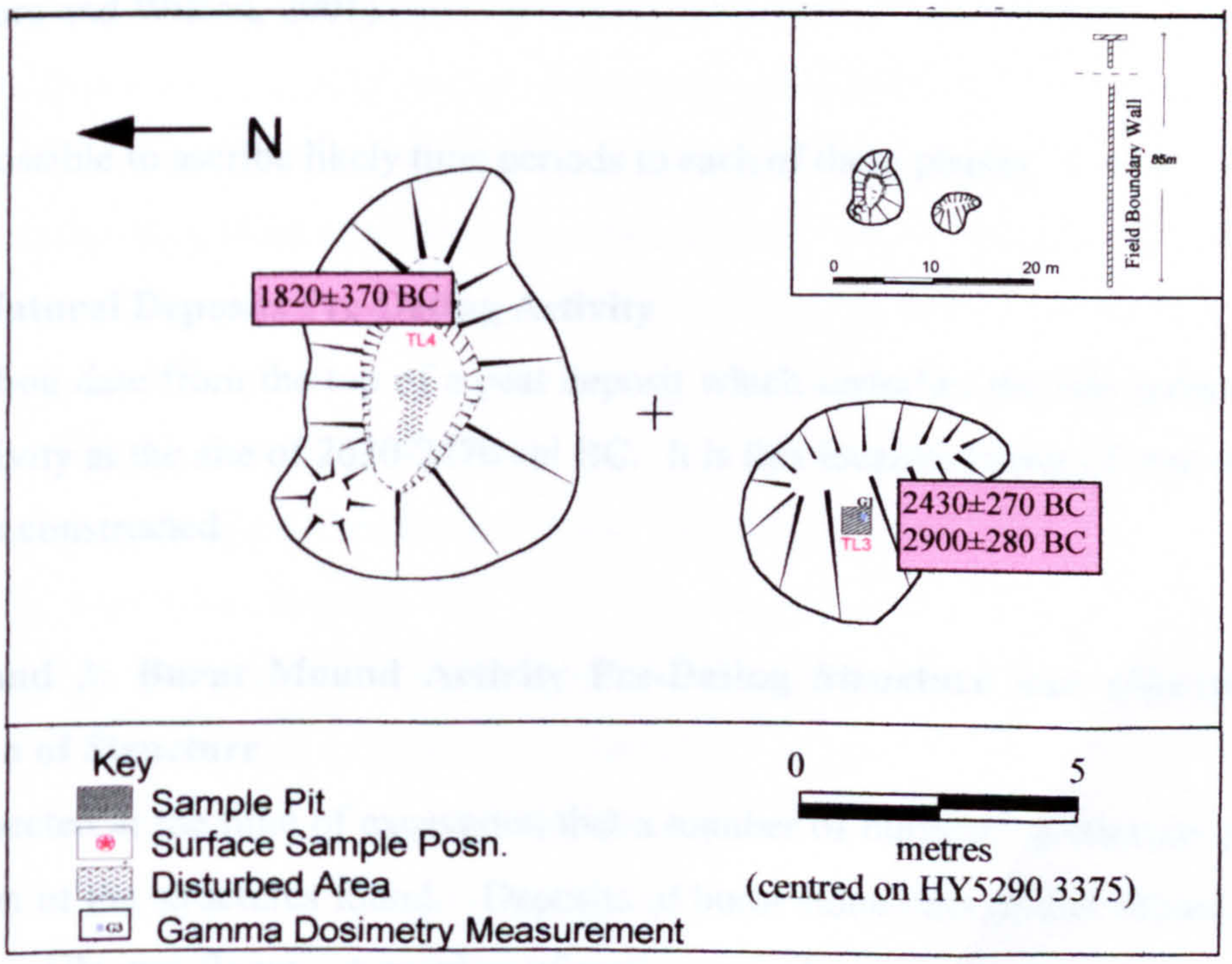

7.5.2.8 Stenaquoy Burnt Mound

Three luminescence dates from the two positions sampled at Stenaquoy give similar age estimates, suggesting a mean age for the site of 1540±150 BC, a combination of a single date from position TL1 (1860±320 BC) and two dates from position TL2 (1330±220 BC and 1700±290 BC). Given the disturbed nature of the mound, having been ploughed, it is expected that these samples originally came from a variety of different locations within the mound, suggesting it to be in use in the period 1300-1900 BC.

7.5.3 Shetland Samples

7.5.3.1 Cruester Burnt Mound

A detailed chronological picture has been built up of the formation and continued use of Cruester burnt mound by combining evidence from excavation with both radiocarbon and luminescence dates. At time of excavation, four phases of site activity were identified:

Phase 1: Natural Deposits Pre-Dating Activity

Phase 2: Burnt Mound Activity Pre-Dating Structure

Phase 3: Construction and Occupation of Structure

Phase 4: Collapse and Abandonment of Structure

(From Moore and Wilson, 2001).

It is now possible to ascribe likely time periods to each of these phases.

Phase 1: Natural Deposits Pre-Dating Activity

A radiocarbon date from the top of a peat deposit which underlies the site gives a maximum age for activity at the site of 2630-2470 cal BC. It is this localized layer of peat on which the mound was constructed.

Phase 2 and 3: Burnt Mound Activity Pre-Dating Structure and Construction and Occupation of Structure

It was suspected at the time of excavation that a number of burnt stone deposits predated the construction of the structures found. Deposits of burnt stone were found behind, underlying and within walls and floors. A number of walls were also noted to have been revetted into

stone deposits (Moore and Wilson, 2001). Remodelling of the mound during construction, together with later additions to the mound are likely to produce a mixed distribution of ages from the material sampled from the mound, however when looked at alongside material from within the structures, certain trends become clearer (fig 7.10).

Six distinct locations within the mound were dated with between 1-3 samples per position. The average age of all 13 samples which represent the mound deposit is 1810±70 BC, however certain areas appear to be associated with earlier and later material. Two of the oldest dates in the sequence are located north of the structure, within the TL sample trench and in material found directly above the wall head of the hearth cell. In addition, older material is also present to the west of the structures in deposits exposed in the coastal section. Again, one of these dates relates to a context directly above the 'cistern' which appears embedded within the mound. All samples which predate 2000BC are located within these two areas. Evidence of later activity also exists within these areas, and in a small isolated deposit of stones at the eastern end of the section where both samples dated gave indistinguishable ages centred on 1455±145 BC. It is probable that this isolated deposit relates to a single firing event, where material has been dumped outwith the main mound deposit.

A series of radiocarbon and luminescence dates for the various floor levels found within the hearth cell give detailed information on the likely period of use of this particular structure (table 7.5). There is a degree of scatter within both radiocarbon and luminescence results and evidence for the presence of older material, not unsurprisingly within the stratified sequences. The oldest material, a burnt stone from between floors 6 and 7, appears well out of sequence with the surrounding dates, and is probably derived from an earlier period of activity on the mound, possibly infiltration from the surrounding overburden. Likewise a date of 1500±190 BC for material found over the 8th floor is also out of sequence. Several of the hearth stones appear to give older age estimates than those stratigraphically lower in the sequence. No evidence for incomplete zeroing was seen in the luminescence data and it may be that an underestimation of the dose rate of these samples is responsible for the excess age. When outlying dates are excluded, a sequence of events beginning at the start of the 14th Century BC and continuing into the 11th Century BC is indicated, giving an approximate interval of hearth replacement in the region of 40 years. Additional radiocarbon dates from elsewhere with the structures associated with the mound are also confined to this period (fig 7.10).

Fig 7.10 Summary of Chronological Information for Cruester Burnt Mound

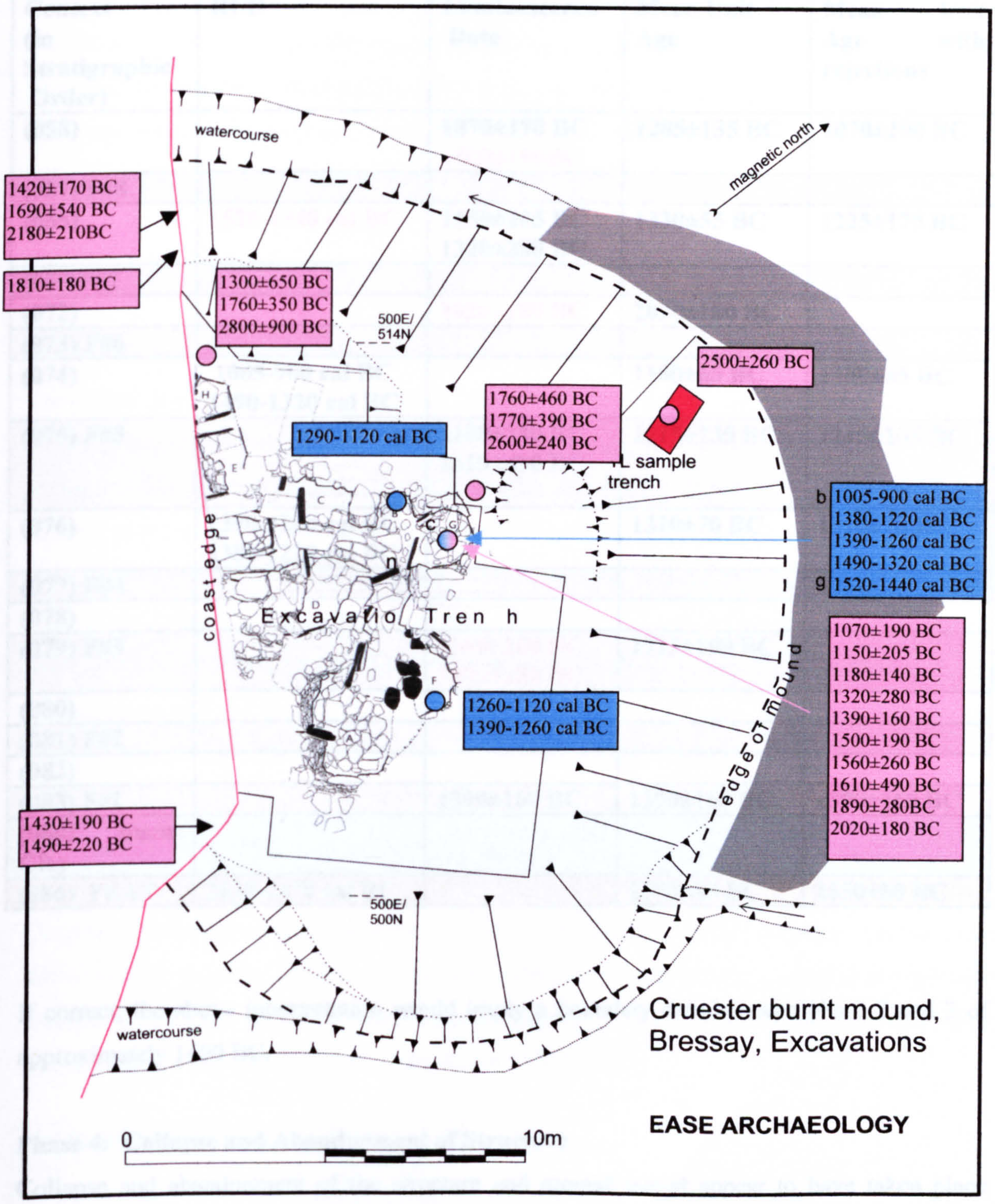

Table 7.5 Summary of chronological information from hearth cell, Cruester burnt mound

Context (in Stratigraphic Order)	RCD	Luminescence Date	Mean Unit Age	Mean Unit Age with rejections
(058)		1070±190 BC 1500±190BC	1285±135 BC	1070±190 BC
(057) F#8				
(055)	1520-1440 cal BC	1150±205 BC 1320±280 BC	1330±55 BC	1225±170 BC
(059)F#7				
(072)		2020±180 BC	2020±180 BC	
(073) F#6				
(074)	1005-900 cal BC 1490-1320 cal BC		1180±65 BC	1180±65 BC
(075) F#5		1180±140 BC 1610±490 BC	1215±135 BC	1215±135 BC
(076)	1390-1260 cal BC 1380-1220 cal BC		1310±70 BC	1310±70 BC
(077) F#4				
(078)				
(079) F#3		1560±260 BC 1890±280 BC	1715±190 BC	
(080)				
(081) F#2				
(082)				
(083) F#1		1390±160 BC	1390±160 BC	1390±160 BC
(084) Burnt Clay				
(086) PEAT	2630-2470 cal BC		2550±80 BC	2550±80 BC

If correct, the above interpretation would imply a boundary date between phase 2 and 3 of approximately 1400 BC.

Phase 4: Collapse and Abandonment of Structure

Collapse and abandonment of the structure and mound would appear to have taken place some time after 1000 BC.

7.5.3.2 Tangwick Burnt Mound

As discussed in preceding chapters, it was not possible to obtain luminescence dates for the samples collected from Tangwick due to a lack of quartz minerals within the sample, and probable microdosimetric inhomogeneity leading to excess scatter in feldspar runs. Whilst this is disappointing from the point of view of site interpretation, one additional radiocarbon date was obtained for the peat underlying the site (3710-3530 cal BC) which gives additional information on the environmental landscape prior to activity at the site.

7.5.3.3 Houlls Burnt Mound

A total of nine luminescence and 1 radiocarbon dates were obtained from the mound and associated deposits at Houlls (fig 7.11). A *terminus post quem* for the mound activity was given by the single radiocarbon date of the uppermost part of the peat deposit underlying the mound. The peat is surprisingly early in date at 5720-5560 cal BC. The mean age for activity at the site is considerably later at 1950±120 BC. However, a wide scatter in age is seen spanning the 2nd-4th millennium BC. Mean ages for each of the four sampling positions, TL1-4 are 1985±190 BC, 2890±340 BC, 1380±330 BC and 1820±190 BC respectively. With the exception of position TL3, all positions contain evidence of early activity on site beginning around 2500-3000BC. The latest date in the sequence, from TL3 puts the last phase of activity identified through these samples as around 1000 BC.

7.5.3.4 Loch of Garths

Despite the large number of samples collected at the loch of Garths, only four luminescence dates were obtained for the mound due to a combination of insufficient material and probable feldspar contamination in the quartz mineral fraction. The four dates range in value from 400-1700BC, with a mean value for the site of 910±85 BC.

Unit (in stratigraphic Order)	Dates
TL2	660±200 BC 1080±130 BC 1740±250 BC
TL1	410±170 BC

Fig 7.11 Summary of chronological information from Houlls burnt mound (a) in plan and (b) in section

A

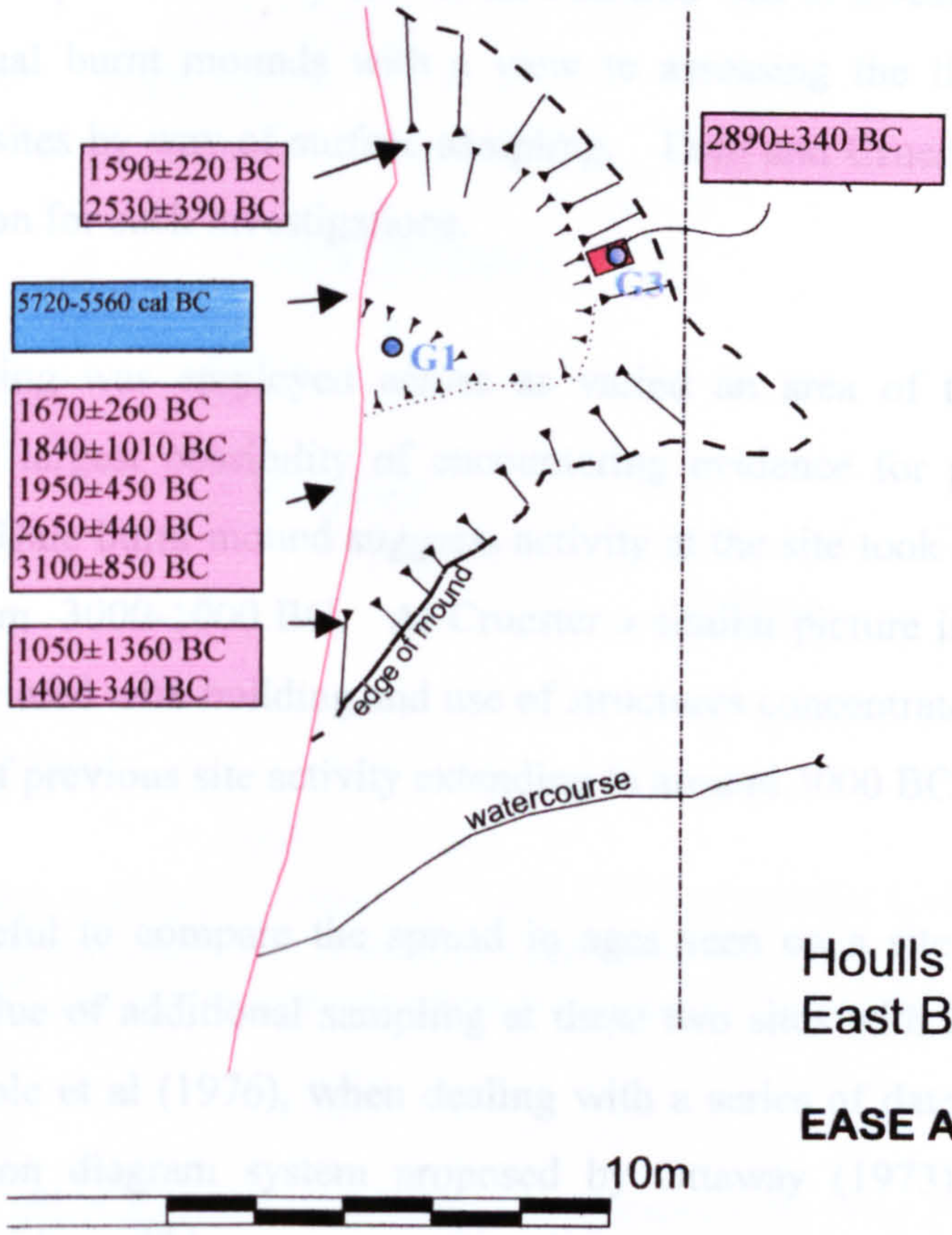

B

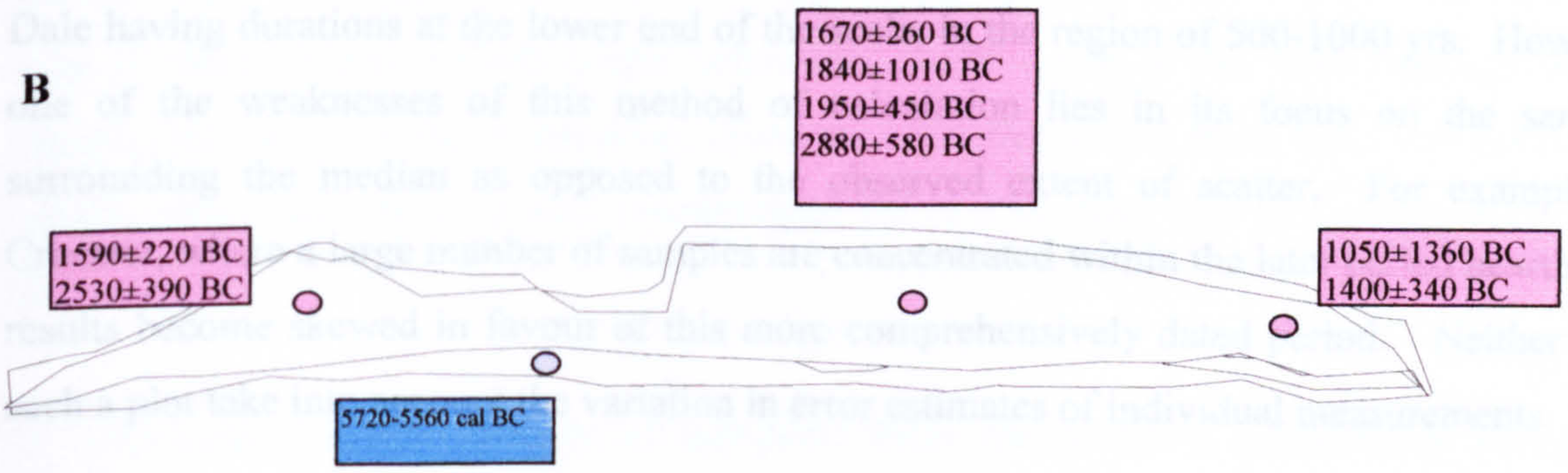

7.6 Evidence for duration of use of burnt mound sites

As outlined in chapter 3, one key aim of the research was to investigate the likely duration of use of individual burnt mounds with a view to assessing the likely significance of dates obtained from sites by way of surface sampling. Dale and Cruester burnt mounds were the focus of attention for such investigations.

Detailed sampling was employed across as varied an area of the mound as possible to encapsulate the largest possibility of encountering evidence for prolonged use of the site. Evidence from Dale burnt mound suggests activity at the site took place over a two thousand year period, from 3000-1000 BC. At Cruester a similar picture is seen, with the main bulk of activity associated with building and use of structures concentrated between 1000-1400BC, with evidence of previous site activity extending to around 3000 BC.

It would be useful to compare the spread in ages seen on a site by site basis in order to compare the value of additional sampling at these two sites with sites represented by fewer dates. Huxtable et al (1976), when dealing with a series of dates from mainland Orkney, used a dispersion diagram system proposed by Ottaway (1973) to determine the likely duration of each site. This system arranges dates in chronological order, and the duration is taken as the interquartile range. This can be represented as a box plot and is shown for all sites in figure 7.12 with values tabulated in table 7.6. It can be seen from this plot that there is considerable variation in the calculated duration of use for each site, with both Cruester and Dale having durations at the lower end of the scale, in the region of 500-1000 yrs. However, one of the weaknesses of this method of calculation lies in its focus on the samples surrounding the median as opposed to the observed extent of scatter. For example, at Cruester, where a large number of samples are concentrated within the later period hearth cell, results become skewed in favour of this more comprehensively dated period. Neither does such a plot take into account the variation in error estimates of individual measurements.

Nevertheless, the plot produces an informative comparison on a site to site basis, showing clearly the variation seen across Eday and Shetland. It is of interest to note that combined plots of all Eday and Shetland samples show similar distributions. However, the large number of outlying samples in both single and combined site plots suggests this method may significantly underestimate the duration of use of the mound.

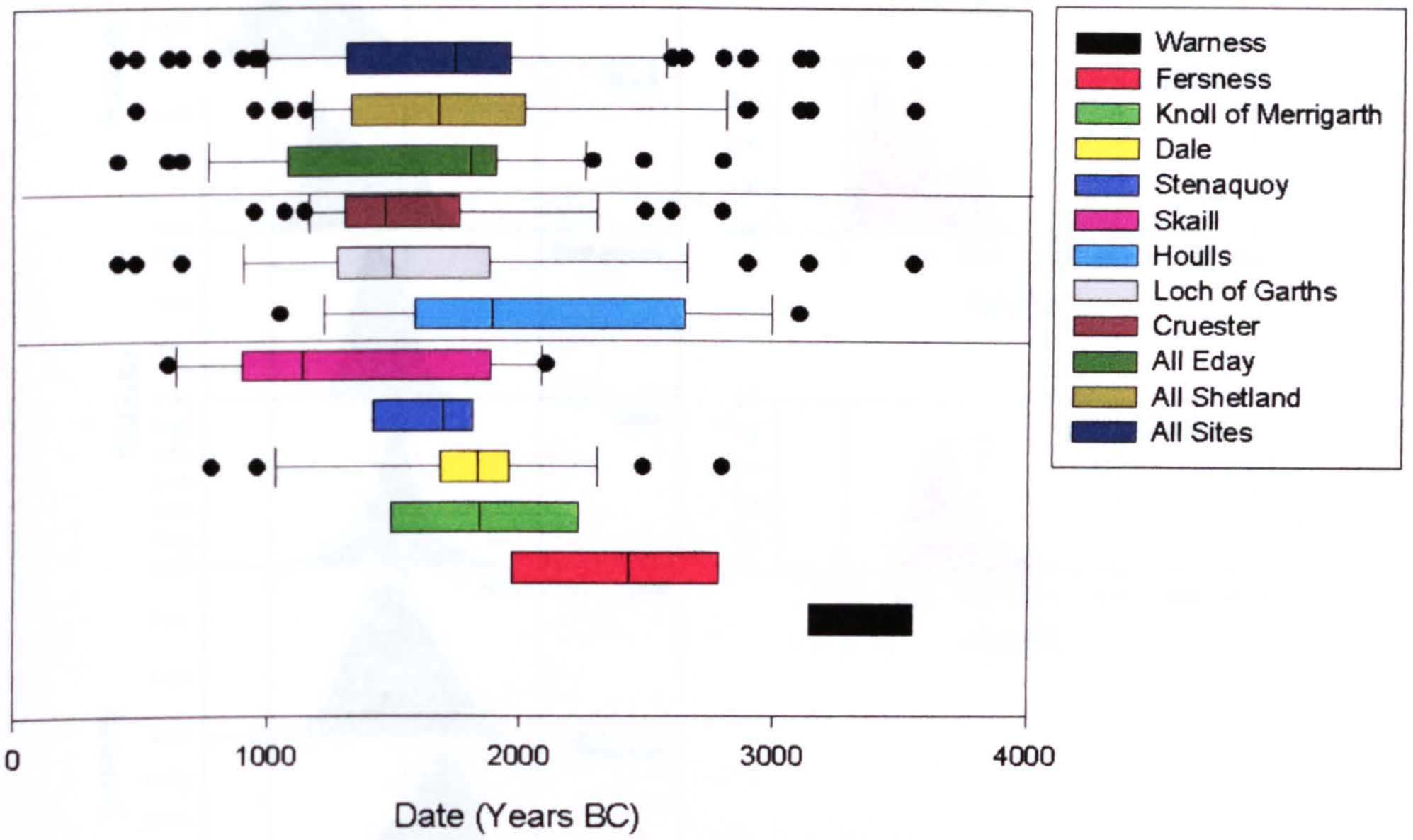

Fig 7.12 Box plot showing median, 25th and 75th percentiles (coloured) and 10th and 90th percentiles (whiskers) together with outlying data (At least 3 datapoints are required to calculate the 25th and 75th percentile, and 5 for the 10th and 90th).

A second approach to duration which takes into account the error on individual samples, is to construct a probability density function (PDF) of the combined gaussian distributions of each sample. This produces a probability distribution for each site showing both the range in ages seen, together with an indication of the likelihood of a sample belonging to a particular time period. Fig 7.13 illustrates the PDFs for each of the sampled sites[8]. Whilst such plots are easy to interpret and provide useful information with regard to the most common date of samples for each site, the distribution, or duration implied within them takes into account all sample errors and, as such, may overestimate the true duration due to the long tails of the distribution.

A third method combines PDFs of individual dates and produces a probability plot of the minimum spread between earliest and latest dates. This method is not subject to the

[8] Radiocarbon data have been included within the plot, though a gaussian distribution has been assumed.

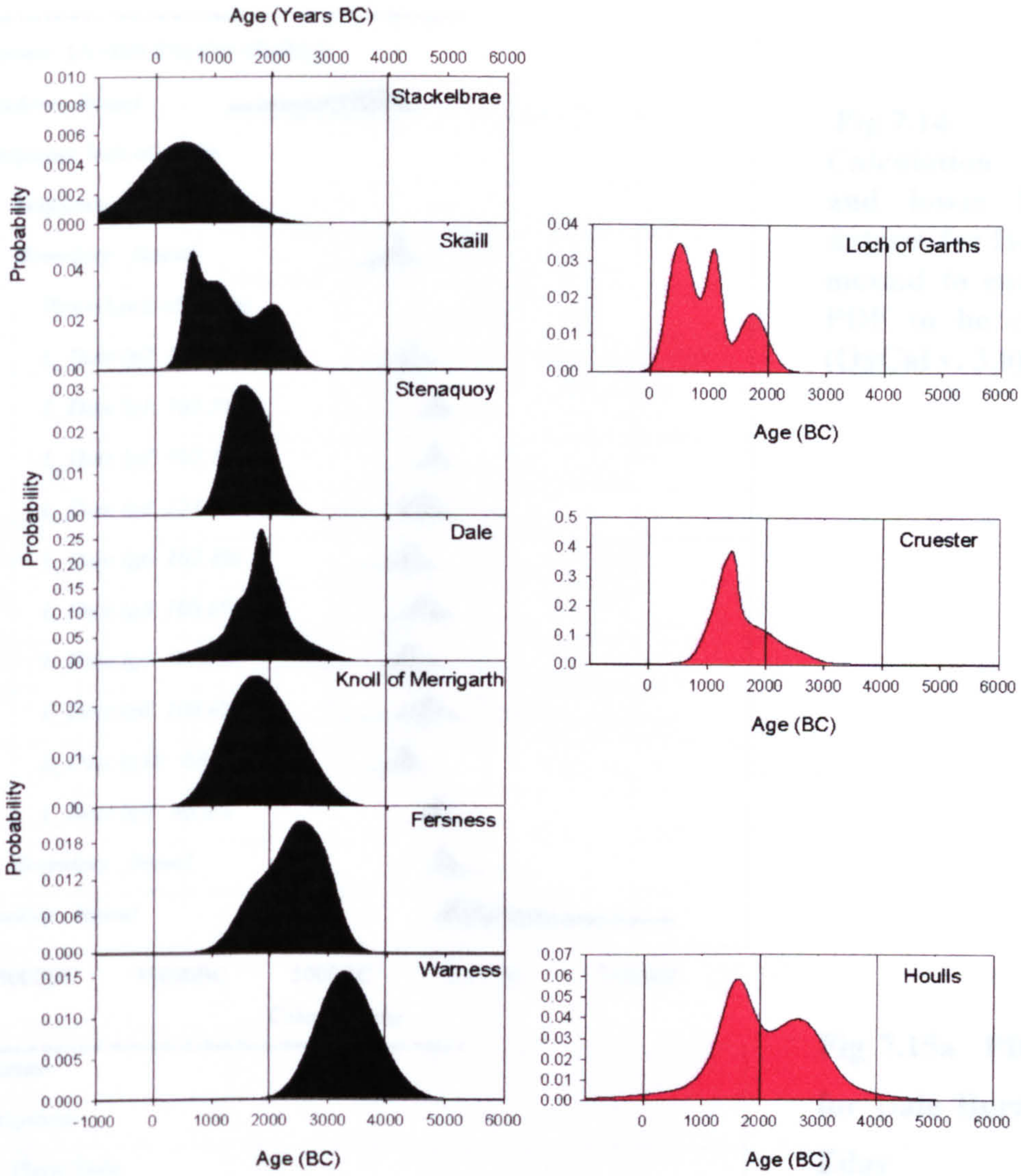

Fig 7.13 PDFs for Eday and Shetland sites

same degree of error, as data on the tails of distribution are given less weighting in the calculation. Such a function is inbuilt into the OxCAL v.3.0 programme for the calibration and analysis of radiocarbon and other dates (Bronk Ramsey, 1998). An illustration of the method of calculation is shown in figure 7.14, where the upper and lower bounds of the dataset are calculated to enable a PDF of the span between them to be constructed. The resulting PDF's for a selection of sites are illustrated in figure 7.15 with full site span widths tabulated in table 7.6.

It can be seen that considerable variation exists in the implied duration of use of the various burnt mounds. At Warness, Fersness, Knoll of Merrigarth and Stenaquoy the zero lower limit of the span distribution indicates all dates to be within error of one another. Clearly, given the confines of the sampling strategy at these sites, this should not be taken as an

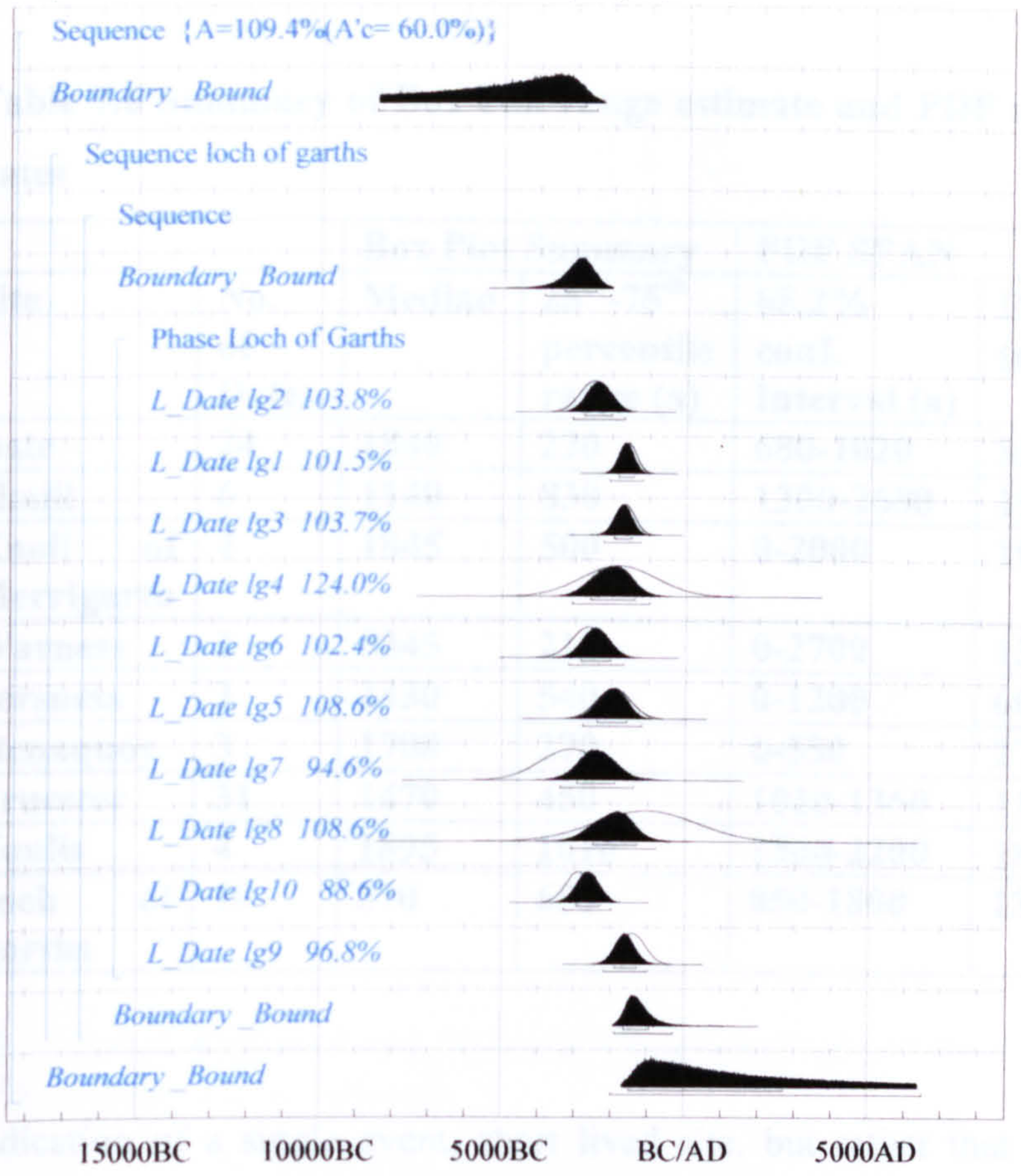

Fig 7.14 Calculation of upper and lower bounds of dataset for Houlls burnt mound to enable SPAN PDF to be constructed (OxCal v. 3.0).

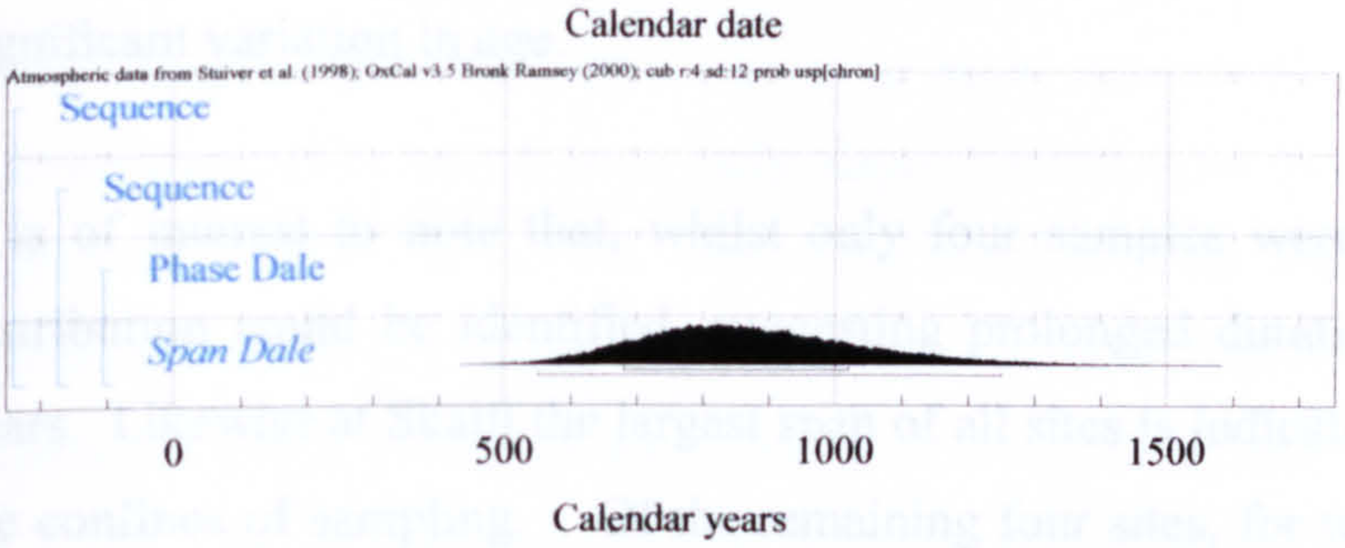

Fig 7.15a PDF of span for Dale Burnt Mound, Eday (OxCal v.3.0)

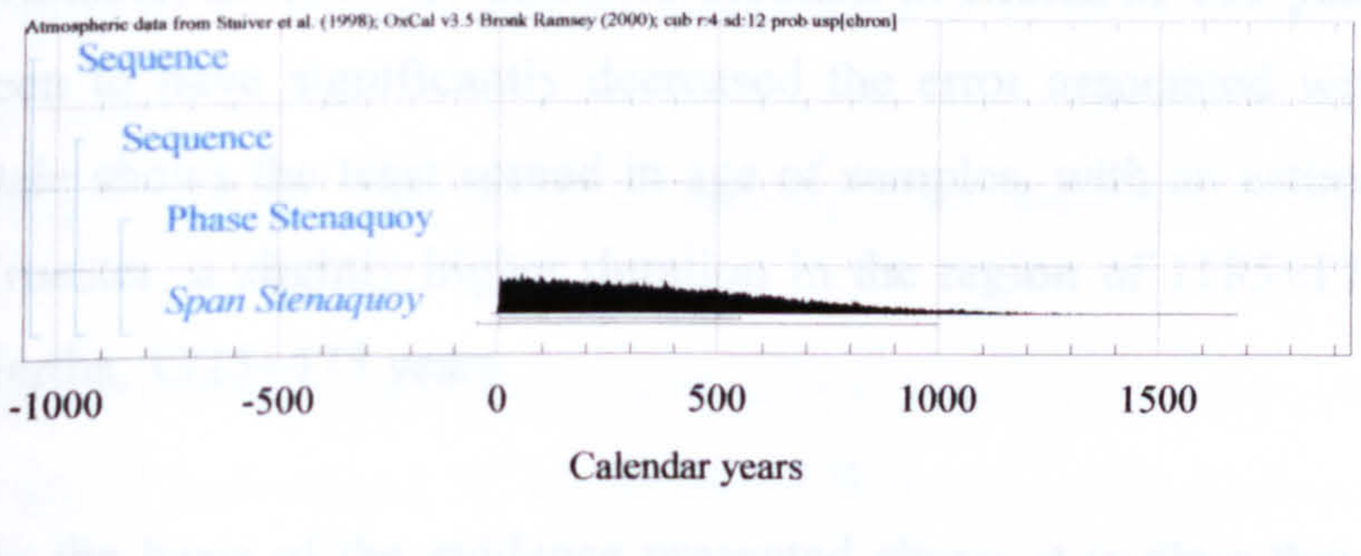

Fig 7.15b PDF of span for Stenaquoy Burnt Mound, Eday (OxCal v.3.0)

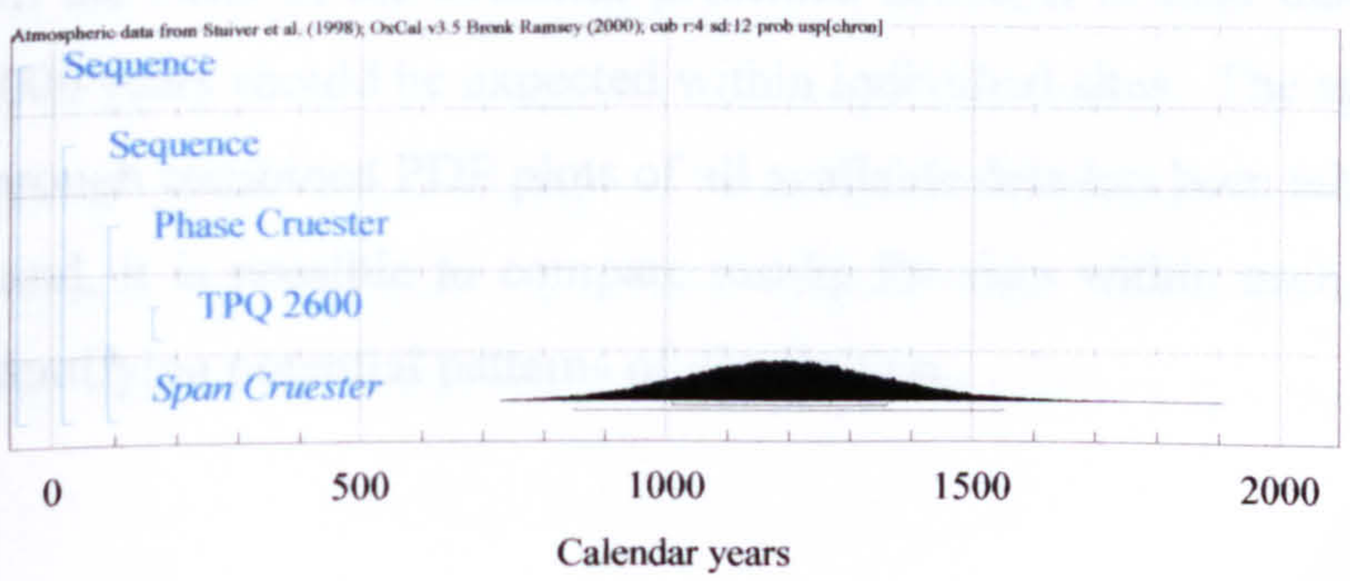

Fig 7.15c PDF of span for Cruester Burnt Mound, Bressay, Shetland. (OxCal v.3.0)

Table 7.6 Summary of Box Plot range estimate and PDF span for all sites with multiple dates

		Box Plot Summary		PDF SPAN		
Site	No. of Dates	Median	25^{th}-75^{th} percentile range (a)	68.2% conf. Interval (a)	Duration (a)	Age range (years AD/ BC)
Dale	24	1840	220	680-1020	850±170	2500-1200 BC
Skaill	6	1140	830	1300-2600	1950±650	2300-400 BC
Knoll of Merrigarth	4	1845	500	0-2000	1000±1000	2700-900 BC
Warness	2	3345	210	0-2700	1350±1350	4100-2600 BC
Fersness	3	2430	540	0-1200	600±600	3200-1500 BC
Stenaquoy	3	1700	270	0-550	275±275	2100-1150 BC
Cruester	31	1470	450	1010-1360	1185±175	2400-900 BC
Houlls	4	1895	1010	1500-2200	1850±350	1900-200 BC
Loch of Garths	10	870	650	850-1800	1325±475	3200-1100 BC

indication of a single event, short lived site, but rather that the samples dated showed no significant variation in age.

It is of interest to note that, whilst only four samples were dated from Houlls, a distinct distribution could be identified, suggesting prolonged duration in the region of 1500-2200 years. Likewise at Skaill the largest span of all sites is indicated at 1950±650 years in spite of the confines of sampling. Of the remaining four sites, for which a larger amount of data is available, all show evidence of duration in excess of 700 years. The additional data can be seen to have significantly decreased the error associated with the span estimate (fig 7.16). Dale shows the least spread in age of samples, with an estimated span of 850±170 years. At Cruester, a slightly higher duration in the region of 1185±175 years is seen and, at Loch of Garths, 1325±475 years.

On the basis of the evidence presented above, it is clear that duration of use of the order of 1000 years should be expected within individual sites. The age range of each site, determined through combined PDF plots of all available data has been tabulated in table 7.6. With this in mind, it is possible to compare results for sites within each sampling region in the hope of identifying potential patterns of distribution.

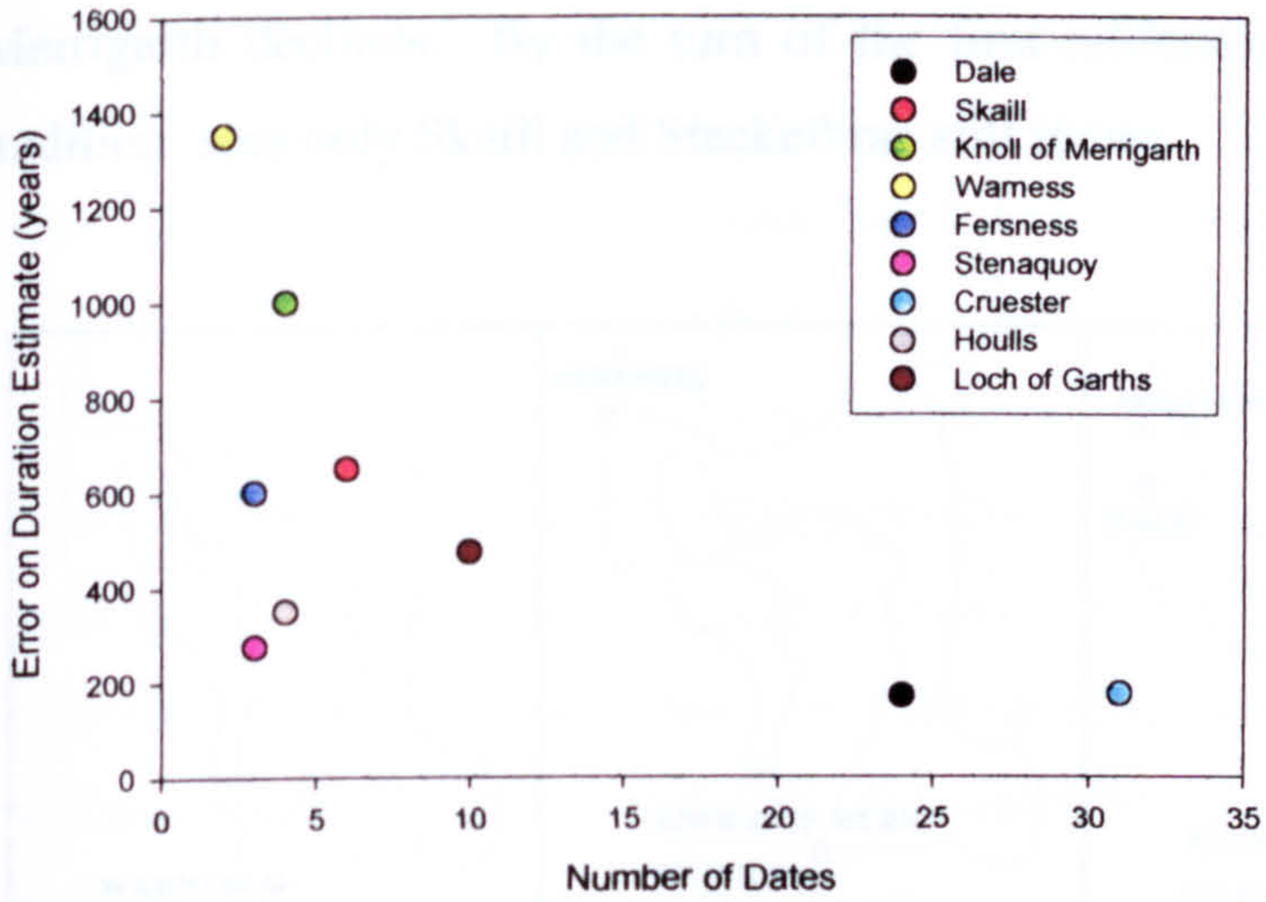

Fig 7.16 Relationship between number of dates measured and error of duration estimate

7.7 Local, Regional and National Chronological Summary

7.7.1 Eday Burnt Mounds

Dating evidence from the seven surviving burnt mounds on Eday indicates a burnt mound tradition that can be traced from early stages through a mean period of use to its diminishing stages over a 5000 year period. By taking account of the likely duration of use of each site, calculated from evidence above to be in the region of 1000 years, a distribution map can be constructed which traces the locational shift of burnt mounds through 1000 year time slices (fig 7.17). Again limitations on the evidence should be re-iterated. The duration calculated in section 7.5 for each mound should be seen as the minimum duration of the site implied by the dated samples. Any mound may expand either way along the timescale with further dating evidence. Nevertheless, patterns in the distribution can be seen.

Early evidence suggests the burnt mound tradition on Eday began some time around the end of the 5th millennium BC at the site of Warness on the southern coast. In the following 1000 year time period activity is seen at the nearby site of Knoll of Merrigarth, and at Fersness on the west side of the island. These two sites continue in use through the time of greatest activity on the island during the 3000-1000 BC period. Only Warness shows little evidence of activity at this time. Additional sites of Dale, Skaill and Stenaquoy are also in use at this time, with Stackelbrae coming into use at the end of the period, as evidence from Knoll of

Merrigarth declines. By the turn of the first millennium BC, decline in the burnt mound tradition sees only Skaill and Stackelbrae still in use.

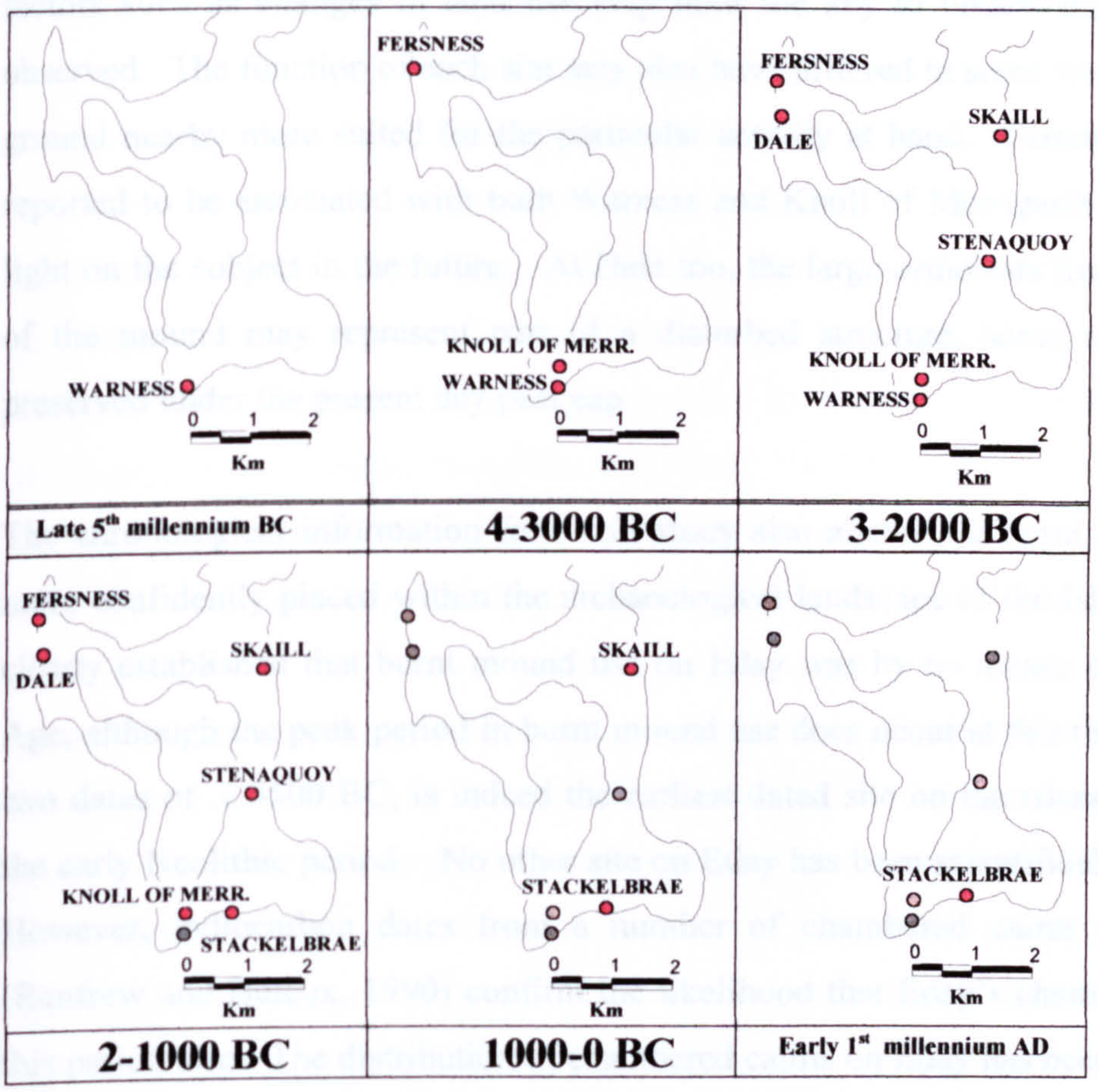

Fig 7.17 Chronology of Burnt Mound use on the Island of Eday, Orkney.

On the two areas of Eday for which two or more mounds are located within short walking distance of one another (less than ½ km) to the south, and at Westside, a sequence of mound use can be seen. In the south, burnt mound use begins at Warness, moving eastward towards Knoll of Merrigarth and finally to Stackelbrae. On the Westside early evidence from Fersness predates the site of Dale to the south and it would be of interest to postulate whether the destroyed mound at Warrenhall to the south of Dale belongs to this group also, and if so when in the sequence usage occurs. Whilst each of these sites overlaps in its chronological distribution with its predecessor, the main period of activity implied within the confines of the data suggests sequential use of each site.

The implied shift in focus of activity along and down the coastline is intriguing. Such marginal shifts in location are unlikely to be a result of settlement relocation due to their close proximity. Perhaps local environmental factors such as changes in drainage systems, or social factors such as changes in land use may hold the key to understanding the apparent shift observed. The function of each site may also have differed in some way as to make an area of ground nearby more suited for the particular activity at hand. Certainly there are structures reported to be associated with both Warness and Knoll of Merrigarth which may shed more light on the subject in the future. At Dale too, the large orthostats found atop the main body of the mound may represent part of a disturbed structure, some of which may well be preserved under the present day peat cap.

The chronological information from this study also allows the burnt mounds of Eday to be more confidently placed within the archaeological landscape of the Island. It has now been clearly established that burnt mound use on Eday was by no means confined to the Bronze Age, although the peak period in burnt mound use does occur at this time. Warness, with its two dates of c.3500 BC, is indeed the earliest dated site on the island, sitting firmly within the early Neolithic period. No other site on Eday has been scientifically dated to this period. However, radiocarbon dates from a number of chambered cairns elsewhere on Orkney (Renfrew and Buteux, 1990) confirm the likelihood that Eday's chambered cairns belong to this period also. The distribution of chambered cairns on Eday has been illustrated in Chapter 4 and it is interesting to note that the two site types appear in mutually exclusive areas, with the chambered cairns distributed from the centre of Eday northwards, and on the Calf of Eday, and the burnt mounds from the central area southwards. Whether the absence of chambered cairns to the south and burnt mounds to the north is indicative of some sociological or environmental aspect of past land use, or is merely an apparent gap in the archaeological record, is at this point unclear.

A number of key excavations of settlement sites elsewhere on Orkney give an informative insight into society at this time. Excavations at the Knap of Howar, Papa Westray revealed a remarkably well preserved multicellular house set within a midden deposit. Nine radiocarbon dates from various parts of the site indicate its occupation to have been centred around the period 3700-2800 BC (Ritchie, 1984). Analysis of the midden deposits suggests fish and shellfish to have played a role in the economy of the site, however it is thought that the economy was mainly based on the rearing of cattle and sheep (Ritchie, 1993). There is a

marked contrast between the 'farmstead' of the Knap of Howar and later Neolithic 'villages' at Barnhouse, Skara Brae and the Links of Noltland leading Clarke and Sharples to conclude that "There can be no doubt that life was both communal and organized" (Clarke and Sharples, 1985, 69).

An increase in the number of burnt mounds on Eday in the third millennium BC comes at a time when many have argued for a move from egalitarian society to one of communal organization based on chiefdoms, reflected in the monumentality of funeral and 'ritual' monuments of Maes Howe, the Stones of Stenness and the Ring of Brodgar (Renfrew, 1979, Ritchie, 1993). With the possible exception of the Stones of Stenness, Eday is home to one of the largest freestanding monoliths on Orkney, the Stone of Setter, located on the north of the island and standing to a height of 4.5m. However it is impossible on present evidence to tell whether this and other standing stones on Eday relate definitively to this period.

Bronze Age Eday sees a peak in burnt mound activity, with all dated sites in use at some point thoughout the period. The Bronze Age on Orkney is typically seen as the ending of the communal organization implied by earlier monuments. A large number of barrows and cairns are attributed to this period and settlement is generally thought to have become more dispersed. A number of sub-peat dykes on Eday may indicate settlement and demarcation of land at this time. Whilst Øvrevik (1993), in her discussion of the Bronze Age sites on Orkney, portrays Eday as possessing numerous habitation, funerary and ceremonial sites, it is worth noting that many, if not all, sites depicted have no formal evidence for occupation in the Bronze Age period. Traces of settlement at Doomy, Fersness, Greentoft, Linkataing and Warness have never been fully investigated. However, the proximity of a number of these sites to the burnt mounds dated to this period is perhaps worthy of future research.

That burnt mound use on Eday continues into the Iron Age period is of great importance to the archaeological interpretation of the Eday landscape. The island is unique in possessing no identifiable brochs and, with the exception of a cache of Iron Age pottery in a peat bank at North Park, possesses little definite evidence of Iron Age activity (Lamb, 1984).

7.7.2 Shetland Burnt Mounds

The dating evidence collected from the four burnt mounds sampled in Shetland is of a different nature to that of Eday. Whereas sampling at Eday intentionally focused on a geographically linked group of related mounds, Shetland sampling was more disperse. As discussed above, dating of samples from Tangwick proved unsuccessful for reasons which will be discussed in more detail in later sections. Of the three mounds for which data were obtained, differing degrees of clarity is seen. At Cruester, the combination of excavation and sampling has allowed a detailed and relatively precise picture of mound formation, structural construction and subsequent abandonment of the site to be assembled. It is unfortunate in this respect that sampling at Tangwick was unsuccessful as excavation there indicated a similar scenario of earlier use, building of structures and later burnt stone deposits (Moore and Wilson 1999). It would have been interesting to compare both duration and site remodelling at these two sites. Information from Houlls and the Loch of Garths is clearly less detailed being, as it is, unsupported by excavation. Nevertheless, the apparent chronologies of the three sites can be compared.

Evidence from Houlls suggests the mound to have been active from the Neolithic/Bronze Age boundary onwards. An extended duration in the region of 2000 years is indicated, with no evidence from the site suggesting a date later than the beginning of the 1st millennium BC.

Dates from both the Loch of Garths and Cruester indicate activity at the site to have begun later, at the turn of the 2nd millennium BC. Both sites show evidence for continued use throughout the Bronze Age period, with termination of use at, or before, the beginning of the Iron Age. A similar picture is implied by existing radiocarbon dates for Tangwick.

With the exception of a few early dates at Houlls, the previously established chronology of a Bronze Age span for burnt mound use on Shetland would therefore seem to be adhered to. The marginal positioning of these sites, together with observations during excavation suggest them to be specialized sites rather than settlement. Hunter's observations (1996) of the positioning of burnt mounds within the landscape of Fair Isle would seem a good comparison upon which to draw, with settlements being potentially located nearby. Certainly, survey of West Burra has highlighted a number of burnt mounds in close proximity to possible settlements (Hedges, 1984) and Canter's GIS survey of mainland Shetland (1998) has shown

the distributional link between settlement and mound, though clearly without further work the chronological link between such sites is at best speculative.

7.7.3 Contribution to the National Burnt Mound Chronology

Existing chronological patterns from across Scotland is summarized in Chapter 3, with main periods of use identified. The new chronological information from Orkney and Shetland gained in this study may now be added to this evidence to provide a more detailed picture of burnt mound use throughout Scotland. Figure 7.18 summarizes present and past evidence of burnt mound use in Scotland over 500 year time intervals.

The contribution of Warness and Houlls, and later Knoll of Merrigarth and Fersness, to the group of early burnt mounds from the period 3500-2500 BC is an important addition. The previous handful of early sites have been confined to the borders and western coast of Scotland, but it is now clear that this does not reflect the true distribution of Neolithic burnt mounds and there is now no foundation upon which to argue a spread in 'burnt mound culture' northwards across Scotland. It is likely that many more Neolithic burnt mounds are present within the existing distribution.

The predominant Bronze Age peak in burnt mound activity is mirrored in the new data obtained, with both Orkney and Shetland sites added to the distribution. It is important to note however that various Orcadian sites have now been added to the list of early Bronze Age burnt mounds. New sites have also been added to the small Iron Age distribution. The absence of burnt mounds in Orkney and Shetland from the 1st millennium AD onwards is also confirmed.

The single luminescence date from Liddle is not, in itself, sufficient to resolve differences between radiocarbon and existing luminescence data, however it does suggest a longer period of use for the site.

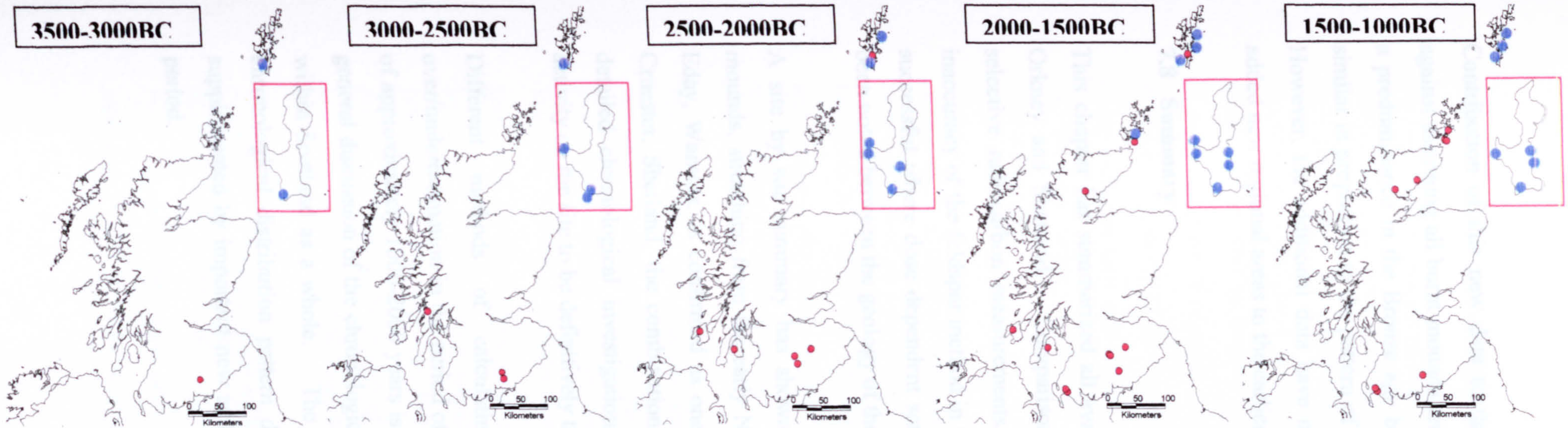

Fig 7.18 Revised Chronological Summary of Burnt Mounds in Scotland (New data in Blue; Inset Eday)

Contribution of this new data to the Scottish chronology has strengthened the argument against assuming all burnt mounds are Bronze Age. The distribution of new dates, showing a predominance in the Bronze age but with earlier Neolithic and later Iron Age activity is similar in proportion to the pattern of dates observed prior to commencement of this research. However, the additional data have not only enhanced these patterns, but have importantly added new regional areas to the earlier prehistoric period.

7.8 Summary

This chapter has summarized all available dating evidence for the eleven sites sampled on Orkney and Shetland. Comparison of feldspar and quartz age estimates, together with selective radiocarbon measurements, has confirmed earlier suspicions with regard to the inaccuracy of the feldspar method in this case. Corrections suggested in chapter 6 have been successful where dose dependent sensitivity change is at a minimum and a correlation has been noted between the geology of the sample and degree of sensitivity change.

A site by site summary has shown large variations in the dates obtained for individual mounds, stretching from the early Neolithic period through to the Iron Age. One site on Eday, Warness, is confirmed as one of the oldest sites on Eday and indeed Orkney. At Cruester, Shetland, the combination of excavation and sampling has led one of the most detailed chronological investigations of a burnt mound undertaken, allowing phases of activity on the site to be definitively tied down.

Different methods of calculating duration are discussed in terms of likely over/underestimation in the period of site activity. Where sufficient samples exist, a period of approximately 1000-2000 years is indicated by available data. This is reflected in a more general discussion of the chronological development of burnt mounds in the two regions, and within Scotland as a whole. The additional dates from these sites are seen to mirror the chronological distribution pattern discussed in chapter 2, however this pattern has been supplemented by important new additions of regions in the early Neolithic and Bronze Age period.

CHAPTER 8 CONCLUSIONS

Through an examination of available evidence for Scottish burnt mounds, a number of key problematic areas have been identified in relation to our understanding of these sites and their place within the archaeological record. Consideration of the distribution of known mounds has highlighted previously identified areas of dense distribution. Detailed analysis of the various degrees of information available for such sites has shown a number of potential areas of regional variation, including mound volume and features associated with sites. A survey of the literature regarding excavated mounds has enhanced knowledge of the variation seen, and together with chronological evidence points to the burnt mounds of Scotland being a diverse group of sites, distributionally, functionally, and chronologically.

A lack of an appropriate research framework for the selection of sites for excavation has been highlighted as a potential problem in the search for a greater understanding of these monuments. Chronology has been identified as one issue which may aid in site selection and luminescence dating outlined as the method most suited to determining the age of both excavated and unexcavated sites.

The potential of luminescence dating to provide chronological information through surface sampling of unexcavated sites has been outlined and a number of key concerns with regard to the value of such data and likely duration of any individual mound has been raised. With this in mind, a sampling strategy which combined detailed sampling at a number of sites, with surface sampling at other geographically linked sites was formulated. It was hoped that such sampling would provide an opportunity to compare the variation seen between sites with that seen from within an individual site. In addition, a larger scale project combining chronological information from burnt mounds dispersed over a wider area was undertaken in the hope of identifying and relating local and regional patterns.

A summary of luminescence methodology has highlighted a number of possible avenues of research with regard to the particular technique that may be employed to date burnt mound sites. A combination of multiple aliquot feldspar additive dose TL, and single aliquot regenerative OSL procedures were selected in light of past luminescence work in the field.

Feldspar additive dose methods was investigated by means of a standard material irradiated to a known dose. Observation of temperature shifts within individual glow curves, combined with simulated data indicated measurement problems relating to the reproducibility of thermal contact and correction methods were developed to compensate.

A large number of samples from Orkney and Shetland were investigated using the modified procedure, with characteristics of each run detailed for further analysis. Through such detailed analysis a unique relationship between the degree of sensitivity change from first to second glow measurement, and the ED obtained at various integrals along the glow curve was noted. Further investigation indicated that one possible explanation for the relationship lay in unequal sensitization of samples prior to third glow normalization, implying a sensitization process for samples which is not solely proportional to past irradiation dose. Modelling of possible sensitization processes outlined a potential cause of such unequal sensitization, showing the dramatic effect even a small degree of unequal sensitization may have on the observed ED. A correction method for samples minimally affected was outlined.

Quantification of the degree of such effect proved problematic however correlation between the degree of curvature of the second glow intercept regression gave encouraging results, allowing an independent assessment to be made as to the reliability of each corrected dataset.

Quartz SAR OSL methods were also investigated in detail. After investigation of the effectiveness of the technique at recovering a known dose, and of adequately correcting for sensitivity changes within the natural readout cycle, a large number of samples were put through routine analysis. The vast majority produced successful ED estimates. Samples which failed to produce usable data were attributed to either OSL low sensitivity or a high degree of contamination from IR sensitive material. Consideration of various aspects of run information showed no correlation between recycling ratios and ED obtained, suggesting sensitivity corrections played only a minor role in variation of ED on a disc to disc basis. Preheat was sent to have little effect on the outcome of ED calculations, though increased sensitivity was noted with increasing preheat temperatures. The observation of a large degree of scatter in ED on a disc to disc basis could not be explained by any of the

above characteristics and consideration was therefore given to the possibility of incomplete zeroing of the geological signal and to microdosimetric inhomogeneity.

Zeroing was investigated through the modelling of trap parameters within likely heating scenarios and the case established for the likelihood of unzeroed material being present. Sectioning of a hearthstone from Cruester provided evidence of such an effect and also validated the use of De(t) plots in identifying other samples with remnant geological signals. A number of other samples were highlighted in this way and were found to be identical to samples identified as poorly zeroed during feldspar additive dose runs.

With regard to microdosimetric inhomogeneity, it was concluded that such effects were likely to cause the distribution in EDs observed. Assumptions that the average ED from all discs would provide a better age estimate than individual disc measurements were based on the natûre of the annual dose rate information available. By definition, the annual dose rate includes 'average' elements such as beta dose rate and water content which within the confines of this work are a limiting factor.

Comparison of quartz and feldspar age estimates has strengthened the case set out for unequal sensitization of the feldspar dataset. A high correlation between both age estimates is seen in samples with minimal dose dependent effects, and a corresponding lower correlation with those showing higher degrees of change. Additional chronological information from a series of radiocarbon dates adds weight to this interpretation and also gives increased confidence in dose rate calculations for which errors between feldspar and quartz may have in common.

The success of this work has allowed a detailed picture of burnt mound use on the island of Eday to be built up. This has not only extended the presumed chronology for these sites within the Eday landscape, but has important implications for other mounds on Orkney. The site of Warness can now be confidently dated to the Early Neolithic Period, joining only a handful of sites elsewhere on Orkney which date to this period.

Sampling at Shetland has likewise provided impressive results with regard to the level of detail obtained from the site of Cruester, and given improved chronological information for other threatened sites along the coast. Unfortunately no additional information was

obtained from Tangwick due to the unsuitability of the material, both in terms of a lack of available quartz and high internal and external dose rates combined with large phenocrysts leading to presumed widespread microdosimetric inhomogeneity on a large scale.

At Cruester the combination of full scale excavation and sampling has highlighted the potential luminescence dating has to offer with regard to the understanding of site evolution in this diverse group of sites.

Positive aspects of the research include the following observations:

- An extensive literature review of the available evidence for burnt mounds in Scotland has identified hitherto unrecognized patterns of regional variation, most notably in the size of mounds distributed across Scotland.
- Detailed landscape considerations with regard to the two chosen study areas have shown, in the case of Eday that a preference in location can be closely tied to a number of physical landscape characteristics.
- Observations made whilst recording sites during sampling has added to the archaeological information held within the SMR for these sites. Plans of the sites provide reference for future work and, in the case of mounds threatened through coastal erosion and other processes, provide a means by which future disturbance may be quantified.
- The research has highlighted the need for careful observations of luminescence behaviour during routine dating runs. It is clear that it would be unwise to blindly apply any technique without due consideration to both sensitization and dosimetric issues.
- Feldspar investigations have highlighted a hitherto unidentified sample behaviour within a wide variety of geologically distinct samples. Observations from data collected previously from other burnt mounds suggest the sensitivity changes observed are not confined to samples from the Northern Isles.
- Modelling of various sensitization processes has given a better understanding of possible mechanisms for such discrepancies to occur and correction methods have been applied on the basis of these observations. These have proved successful in a percentage of cases.

- The sensitization process identified has important implications for luminescence work outwith the studies of burnt mounds. Often age shortfall in feldspar samples is automatically attributed to fading of the feldspar signal. It has been shown that fading is not the only mechanism by which underestimation may occur. In addition, the sensitization models imply deficiencies in the effectiveness of the plateau test in identifying fully zeroed samples. Observed ED plateaus in this case can be shown to be a byproduct of neighbouring traps undergoing similar sensitization during the readout cycle.
- Quartz OSL techniques have proved useful in identifying poorly zeroed material, important in the consideration of age overestimation. Correlation between samples identified through De(t) plots and those identified through feldspar ED plateau plots has strengthened the case for the use of De(t) plots as an aid to the identification of poorly zeroed material. The single aliquot nature of these measurements has also enabled ED distribution to be investigated and issues surrounding microdosimetric inhomogeneity highlighted for future research.
- The combination of results from feldspar, quartz and radiocarbon age estimates has allowed, in some cases, for a detailed site by site chronology to be built up.
- Detailed sampling at a number of sites has shown successfully that age variation within mounds can be detected and quantified through the use of luminescence dating. The precision of durational calculations will however depend on both the number of samples measured, and the nature of the sampling context. Excess variation in the age obtained from samples between sites indicates variation in the periods of use of some sites.
- The island of Eday now represents one of the most comprehensively dated areas of burnt mound activity in Scotland, allowing unique insight into the spread and decline of monument use throughout the prehistoric period.
- The early dates associated with the burnt mound at Warness on Eday is of tremendous importance to the understanding of the archaeological landscape of early Neolithic Orkney. It implies the use of hot stone technology, and potentially of a specialization of sites at a time contemporary with the settlement at Knap of Howar, Papa Westray. This tradition appears unbroken on Eday through the late Neolithic, Bronze Age and Early Iron Age period. Information obtained from the

site of Houlls, East Burra has likewise added to the catalogue of confirmed Neolithic activity on Shetland.

- An unintended byproduct of the research has been to produce a number of dates relating to environmental change on Orkney and Shetland. Within Eday, the combination of OSL dates of windblown sands at the site of Skaill, and radiocarbon dates from both Skaill and Dale has complemented work by Sommerville (2003) confirming the late development of some areas of peat on Eday and subsequent massive storm blow events indicated by the thick sand deposits seen across the island. Within Shetland, radiocarbon dates from peats at three of the four sites may be of interest to the further development of the environmental history of the region.

Limitations on the interpretation of results presented can be attributed to both methodological decisions and the sampling strategy employed. These include:

- The reliance upon assumed dose rates for the internal component of annual dose rate. Whilst agreement between both luminescence techniques and radiocarbon methods tend to indicate such assumptions are within error of correct values on a number of occasions, the potential for over/underestimation of dose rate due to such assumptions should not be overlooked.
- The limited size of bulk material available for gamma spectrometry measurements has led to decreased precision in the information obtained from this method. In retrospect bulk samples may easily have been supplemented by excess material cut from the stone to remove the outer 3mm beta irradiated layer. Alternatively, samples may have been sealed and gamma counted prior to preparation of minerals, allowing all material to be used. This second observation does however present logistical problems due to the need for storage and readout time associated with each sample.
- Investigation of fading in the feldspar dataset. Only minimal investigations were carried out with regards to fading. It is clear from recent work (Balsecue et al, 2003, Lamothe et al, 2003) that improved measurement procedures may better characterize and define the degree of fading expected within samples. Variation in

storage time and temperature, and also in the length, temperature and timing of preheats may shed further light on the issue. Whilst the agreement between quartz, feldspar and radiocarbon dates suggest fading to be minimal in corresponding samples, the potential for significant underestimation in age exists.

- Other aspects of both quartz and feldspar run characteristics may have been investigated – the effect of variation in the time and temperature of preheat, storage prior to readout, irradiation at elevated temperature, variation in the size and source of laboratory doses given may all have an effect on the ED obtained.
- With regard to sampling strategy, the information obtained via surface sampling is, by definition, more difficult to interpret than information from other sites. Whilst the intention was clearly to assess the value of this limited information, in retrospect varying the location of surface sampling position to more diverse areas of the mound, and increasing the number of positions and samples may have produced more useful information.

ASSESSMENT OF THE NEED AND DIRECTION OF FUTURE RESEARCH

With regard to future luminescence work on heated material, a number of key areas require further research.

- Microdosimetric inhomogeneity has been highlighted throught the thesis as a problem area. The magnitude of this effect requires quantification. Modelling of radionuclide distributions and implied dose rates within samples may prove informative in this respect. Likewise developments in luminescence equipment may in future allow measurements of both dose rate and luminescence signal to be made with reference to the position of grains within the matrix of the sample.
- There is clearly a need for better characterization of the behavioural effects seen within the feldspar dataset. It would be of interest to determine how widespread such effects are in terms of sampling material, and to gain a better understanding of the mechanisms involved in producing such an affect. This may in turn lead to the development of correction methods that can be applied to all samples regardless of the degree of sensitivity change experienced.
- Incomplete zeroing of the geological signal in samples from burnt mounds is another area worthy of future research. Increasing the number of individual

measurement obtained for each sample and decreasing the aliquot size may better distinguish between zeroed and partially zeroed material. In addition, investigation of the shape of the decay curve may also lead to identification characteristics.

- From an archaeological point of view, the positive outcome of this research highlights the unique information which luminescence sampling can produce. With regard to burnt mound archaeology, the ability to distinguish chronologically between groups of mounds may be vital to decisions with regard to excavations in key areas.
- Many burnt mounds have been identified as under threat from coastal erosion. Whilst a programme of excavations on Shetland has gathered information from a number of these mounds it is clear that the shear number threatened prohibit widescale excavation. Luminescence dating offers the potential to gather unique information with regard to the chronology of these mounds prior to their complete destruction. At the very least, samples should be collected from such mounds and stored for future analysis. The cost of sampling is relatively minor and a catalogue of material from these mounds, and others under threat of destruction may provide invaluable information for future archaeological research.
- The information obtained from detailed sampling across Eday would benefit from comparisons with other areas of Orkney. It would be of interest to compare distributional patterns from Eday with those from the other Nothern Isles in order to determine whether such patterns are the norm.
- With regard to the wider view of burnt mounds across Scotland, the smaller mounds noted in the south of Scotland, by virtue of their size may suggest significantly reduced duration. It would be informative to concentrate future work in this area.

REFERENCES

Abernethy, D, 1998, "Kilmartin Glen, cist/cup marks, burnt mound", Discovery and Excavation, Scotland, 20.

Aitken, M.J, 1969, "Thermoluminescent dosimetry of environmental radiation on archaeological sites", *Archaeometry,* 11, 109-114.

Aitken, M.J, 1985, *Thermoluminescence Dating,* Academic Press, London.

Aitken, M.J, 1990, *Science Based Dating in Archaeology*, Routledge, London

Aitken, M.J, Tite, M.S and Reid, J, 1964, "Thermoluminescence Dating of Ancient Ceramics", *Nature*, 202, 1032-1033.

Aitken, M.J and Bowman, S.G.E, 1975, "Thermoluminescent dating: Assessment of alpha particle contribution", *Archaeometry*, 17, 132-138.

Aitken, M.J, Huxtable, J, Wintle, A.G and Bowman, S.G.E, 1975, "Age determination by TL: review of progress at Oxford", *Proceedings of the 4th International Conference on Luminescent Dosimetry*, 1045-1055.

Anderson, J, 1873, "Notice of the Excavation of Kenny's Cairn", *Proceedings of the Society of Antiquaries of Scotland,* 9, 292-296.

Anthony, I.M.C, Sanderson, D, Housley, R, Downes, J and Robertson, J, 2000a, "Eday Burnt Mounds, Orkney (Eday Parish), archaeological works", *Discovery and Excavation, Scotland, 63.*

Anthony, I.M.C, Sanderson, D.C.W, Moore, H, Wilson, G, Turner, V, 2000b, *Characterisation and Dating of Burnt Mounds from Orkney and Shetland: Shetland Burnt Mounds,* SURRC.

Anthony, I.M.C, Sanderson, D.C.W, Cook, G.T, Abernethy, D and Housley, R.A, 2001, "Dating a burnt mound from Kilmartin, Argyll, Scotland", *Quaternary Science Reviews,* , 20, 921-926.

Anthony, I.M.C, Sanderson, D.C.W and Housley, R A, 2002, *Characterisation and Dating of Burnt Mounds from Orkney and Shetland: Orkney Burnt Mounds, Supplementary Report,* SURRC.

Armit, I and Braby, A, 1995, "Ceann nan Clachan: Burnt Mound and prehistoric structures", Discovery and Excavation, Scotland, 107.

Armit, I and Braby, A, 1996, "Ceann nan Clachan: Burnt Mound and prehistoric structures", Discovery and Excavation, Scotland, 106.

Armit, I and Braby, A, 1997, "Ceann nan Clachan: Burnt Mound and prehistoric structures", Discovery and Excavation, Scotland, 84.

Ashmore, P, 1999, "Dating the ring of stones and chambered cairn at Calanais" *Antiquity*, 73, 128-130.

Auclair, M, Lamothe, M, Hout, S, 2003, "The measurement of anomalous fading for feldspar IRSL using SAR", *Radiation Measurements,* in press.

Balescu, S, Lamothe, M, Mercier, N, Hout, S, Balteanu, D, Billard, A, and Hus, J, 2003, "Luminescence chronology of Pleistocene loess deposits from Romania: testing methods of age correction for anomalous fading in alkali feldspars", *Quaternary Science Reviews*, 22, 967-973.

Bailey, R.M, 1997, *The form of the optically stimulated luminescence signal of quartz: implications for dating,* Unpublished PhD Thesis, University of London.

Bailey, R.M, 2003, "Paper 1: The use of measurement-time dependent single aliquot equivalent dose estimates from quartz in the identification of incomplete signal resetting", *Radiation Measurements*, in press.

Bailey, R.M, 2001, "Towards a general kinetic model for optical and thermally stimulated luminescence of quartz", *Radiation Measurements*, 33, 17-45.

Banks, I, 1999, "Investigating Burnt Mounds in Clydesdale during Motorway Construction", *Glasgow Archaeological Journal,* 21, 1-28.

Barber, J, 1990, "Scottish burnt mounds: variations on a theme", in Buckley, V (ed), *Burnt Offerings: International Contributions to Burnt Mound Archaeology,* Wordwell, Dublin, 98-104.

Barber, J and Lehane, D, 1990, "Arran: Machrie Moor and Glaister in Buckley, V (ed), *Burnt Offerings: International Contributions to Burnt Mound Archaeology,* Wordwell, Dublin, 78.

Barber, J and Russell-White, C.J, 1990, "Preface", in Buckley, V (ed), *Burnt Offerings: International Contributions to Burnt Mound Archaeology,* Wordwell, Dublin, 59.

Barfield, L and Hodder, I, 1987, "Burnt mounds as saunas, and the prehistory of bathing", *Antiquity*, 61, 370-379.

Bateman, M.D and Herrero, A.D, 2001, "The timing and relation of aeolian sand deposition in central Spain to the aeolian sand record of NW Europe", *Quaternary Science Reviews,* 20, 779-782.

Bell,W.T, 1976, "The assessment of the radiation dose-rate for thermoluminescence dating", *Archaeometry,* 18, 107-111.

Bell, W.T, 1977, "Thermoluminescence dating: revised dose-rate data", *Archaeometry*, 19, 99-100.

Bell, W.T, 1979, "Thermoluminescence Dating: radiation dose-rate data", *Archaeometry*, 21, 243-245.

Bell, W.T, 1980, "Alpha dose attenuation in quartz grains for thermoluminescence dating", *Ancient TL,* 12, 4-8.

Berger, M.J, 1971, "Distribution of absorbed dose around point sources of electrons and beta particles in water and other media", *Journal of Nuclear Medicine*, 5, 5-23.

Bøtter-Jensen, L, Bulur, E, Duller, G.A.T and Murray, A.S, 2000, "Advances in luminescence instrument systems", *Radiation Measurements,* 32, 523-528.

Bowman, S.G.E, 1978, "Dose-rate dependence of natural calcium fluoride", *PACT*, 6, 292-294.

Bowman, S.G.E, 1979, "Phototransferred thermoluminescence in quartz and its potential use in dating", *PACT*, 3, 381-400.

Bowman, S.G.E and Huntley, D.J, 1984, "A new proposal for the expression of alpha efficiency in TL dating", *Ancient TL*, 2, 6-11.

Boyle, R, 1664, "Experiments and Considerations upon Colours with Observations on a Diamond that Shines in the Dark", Henry Herringham, London.

British Geological Survey, 1971b, *Western Shetland: Drift Edition*

British Geological Survey, 1978a, *Southern Shetland: Solid Edition*

British Geological Survey, 1978b, *Southern Shetland: Drift Edition*

British Geological Survey, 1982a, Central *Shetland: Solid Edition*

British Geological Survey, 1982b, Central *Shetland: Drift Edition*

Bronk Ramsey, C, 1998," Probability and Dating", *Radiocarbon*, 40, 461-474

Buckley, V (ed), 1990, *Burnt Offerings: International Contributions to Burnt Mound*

Archaeology, Wordwell, Dublin.

Butler, S, 1996, "Climate, ecology and land-use since the last ice age", in Turner, V (ed), *The Shaping of Shetland*, The Shetland Times Ltd, Lerwick, 3-11.

Canter, M, 1998, "Prehistoric Sites in the Shetland Landscape", in Turner, V (ed), *The Shaping of Shetland*, The Shetland Times Ltd, Lerwick, 47-60.

Clarke, D.V, and Sharples, N, 1985, "Settlements and subsistence in the Third Millennium BC", in Renfrew, C (ed) *The Prehistory of Orkney*, Edinburgh University Press, 54-82.

Clark, R.J and Sanderson, D.C.W, 1994, "Photostimulated luminescence excitation spectroscopy of feldspars and micas", *Radiation Measurements*, 23, 641-646.

Clarke, M.L, and Kayhko, J.A, 1997, "Evidence of Holocene Aeolian Activity in Sand Dunes from Lapland", *Quaternary Geochronology*, 16, 341-348.

Davidson D.A, and Jones, R.L, 1985, "The Environment of Orkney", in Renfrew, C (ed), *The Prehistory of Orkney*, Edinburgh University Press, Edinburgh, 10-35.

Debenham, N.C and Aitken, M.J, 1984, "Thermoluminescence dating of stalagmitic calcite", *Archaeometry*, 26, 155-170.

Deer, W.A, Howie, R.A and Zussman,J, 1966, *An Introduction to the Rock Forming Minerals*, Longmans, London.

Dockrill, S.J, Bond, J.M and O'Connor, T.P.O, 1998, "Beyond the Burnt Mound: The South Nesting Palaeolandscape Project", in Turner, V (ed), *The Shaping of Shetland*, The Shetland Times Ltd, Lerwick, p61-82.

Duller, G.A.T, 1991, "ED determinations using single aliquots", *Nuclear Tracks and Radiation Measurements*, 18, 371-378.

Duller, G.A.T, Botter-Jensen, L and Mejdahl, V, 1999, "An automated iterative procedure for determining palaeodoses using the SARA method", *Quaternary Geochronology*, 18, 293-301.

Duncan, J.S and Halliday, S, 1997, "Paddies Rickle Bridge to Johnstonebridge, Watching Brief", Discovery and Excavation, Scotland, 25.

Engelmenn, A, Neber, A, Frechen, M, Boenigk, W and Ronen, A, 2001, "Luminescence chronology of Upper Pleistocene and Holocene aeolianites from Netanya South - Sharon Coastal Plain, Israel", *Quaternary Science Reviews,* 20, 799-804.

Eskola, K Okkonen, J and Junger, H, 2003, "Luminescence dating of a coastal Stone Age dwelling place in Northern Finland", *Quaternary Science Reviews*, 22, 1287-1290.

Fehrentz, M and Radtke, U, 2001, "Luminescence Dating of Pleistocene outwash sediments of the Senne area", *Quaternary Science Reviews*, 20, 725-730.

Fleming, S.J, 1970, "Thermoluminescent dating: refinement of the quartz inclusion method", *Archaeometry*, 12, 133-145.

Fleming, S.J, 1973, "The pre-dose technique: a new thermoluminescence dating method", *Archaeometry*, 15, 13-30.

Fleming, S.J, 1979, *Thermoluminescence Techniques in Archaeology*, Clarendon Press, Oxford.

Fojut, N, 1986, *A guide to prehistoric Shetland*, Lerwick

Franklin, A.D, Prescott, J.R and Scholefield, R.B, 1995, "The mechanism of thermoluminescence in an Australian sedimentary quartz", *J. Luminescence*, 63, 317-326.

Fraser, D, 1983, *Land and Society in Neolithic Orkney*, BAR, British Series, 117, Oxford.

Frechen, M, Derman, B, Boenigk, W and Ronen, A, 2001, "Luminescence chronology of aeolianites from the section at Givat Olga - Coastal Plain of Israel", *Quaternary Science Reviews*, 20, 805-810.

Galloway, R.B, 1996, "ED determinations using only one sample: alternative analysis of data obtained from IR stimulation of feldspars", *Radiation Measurements*, 26, 103-106.

Garlic, G.F.J and Robinson, I, 1972, "The thermoluminescence of lunar samples", in *The Moon*, ed by Runcorn, S. and Urey, H, Int. Astronomers Union, Dordrecht, 324-329.

Göksu, H.Y, Fremlin, J.H, Irwin, H.T and Fryxell, R, 1974, "Age Determination of burned flint by a thermoluminescent method", *Science*, 183, 651-654.

Halliday, S.P, 1990, "Patterns of Fieldwork and the Distribution of Burnt Mounds in Scotland", in Buckley, V (ed), *Burnt Offerings: International Contributions to Burnt Mound Archaeology*, Wordwell, Dublin, p60-61.

Hedges, J,W, 1977, "Excavation of two Orcadian burnt mounds at Liddle and Beaquoy", *Proceedings of the Society of Antiquaries of Scotland,* 106, 39-98.

Hedges, J,W 1984, "Gordon Parry's West Burra Survey", *Glasgow Archaeological Journal,* 11, 41-59.

Hedges, J.W, 1986, "Bronze Age Structures at Tougs, Burra Isle, Shetland", *Glasgow Archaeological Journal*, 13, p1-43.

Hedges, J and Gowlett, J, 1986, " Radiocarbon dating by accelerator mass spectrometry", Scientific American, 254, 106.

Hilgers, A, Murray, A.S, Schlaak, N and Radtke, U, 2001, "Comparison of quartz OSL protocols using Lateglacial and holocene dune sands from Brandenburg, Germany", *Quaternary Science Reviews*, 20, 731-736.

Hore-Lacy, I, 2003, *Nuclear Electricity*, Uranium Information Centre and World Nuclear Association

Hunt, J, 1866, "Report of the Zetland Anthropological Expedition", *Memoirs of the Anthropological Society of London*, 2, 300-302

Hunter, J.R, 1996, *Fair Isle: The archaeology of an island community*, HMSO.

Hunter, J.R & Dockrill, S, 1990, "Recent research into burnt mounds on Fair Isle, Shetland and Sanday, Orkney", in Buckley, V (ed), *Burnt Offerings, International Contributions to Burnt Mound Archaeology*, Wordwell, Dublin, p62-68.

Huntley, D.J, Godfrey-Smith, D.I and Thewalt, M.L.W, 1985, "Optical Dating of Sediments", *Nature*, 313, 105-107.

Huntley, D.J and Lamothe, M, 2001, "Ubiquity of anomalous fading in K-feldspars and the measurement and correction for it in optical dating", *Canadian Journal of Earth Science*, 38, 1093-1106.

Huntley, D.J, and Prescott, J.R, 2001, "Improved methodology and new thermoluminescence ages for the dune sequence in south-east South Australia", *Quaternary Science Reviews,* 20, 687-700.

Huntley, D.J, Short, M.A, and Dunphy, K, 1996, "Deep traps in quartz and their use for optical dating", *Canadian Journal of Physics*, 74, 81-91.

Hurl, D,1990, "An anthropologists tale", in Buckley, V (ed), *Burnt Offerings: International Contributions to Burnt Mound Archaeology*, Wordwell, Dublin, p154-156.

Hutt, G and Smirnov, A, 1983, "Thermoluminescence dating of sediments by means of the quartz and feldspar inclusion methods", *PACT*, 9, 463-472.

Huxtable, J, Hedges, J.W, Renfrew, A.C and Aitken, M.J, 1976, "Dating a

settlement pattern by thermoluminescence: The burnt mounds of Orkney", *Archaeometry*, 18, 5-17.

Isaksson, S, 1996, "A protocol for the analysis of lipid residues in connection with prehistoric food habits", *Journal of Nordic Archaeological Science*, 9, 27-30.

Janotta, A, Radtke, U, Czwielung, K and Heidger, M, 1997, "Luminescence Dating (IRSL/TL) of lateglacial and holocene dune sands and sandy loesses near Bonn, Gifhorn and Diephloz (Germany)", *Quaternary Science Reviews*, 16, 349-355.

Jeffery, S, 1991, "Burnt Mounds, fulling and early textiles", *Burnt mounds and hot stone technology*, Sandwell, England.

Kennedy,G.C and Knopff, L, 1960, "Dating by Thermoluminescence", *Archaeology*, 13, 147-148

Krbetschek , M.R, Gotze, J, Dietrich, A and Trautmann, T, 1997, "Spectral Information From Minerals Relevant for Luminescence Dating", *Radiation Measurements*, 27, 695-748.

Lamb, R.G, 1984, *Eday and Stronsay, Orkney Islands area: an archaeological survey*, RCAHMS, Edinburgh

Lamothe, M, Auclair, M, Hamzaoui, C and Hout, S, 2003, "Towards a prediction of long term anomalous fading of feldspar IRSL", *Radiation Measurements*, in press

Lang, A and Wagner, G.A, 1997, "Infrared stimulated luminescence dating of holocene colluvial sediments using the 410nm emission", *Quaternary Science Reviews*, 16, 393-396.

Larsson, L, 1989, "Socioeconomic complexity and change in southern Sweden 500 BC-500 AD" in Larsson and Lundmark, L (eds), *Approaches to Swedish Prehistory*, BAR Int Ser 500, 355-362.

Lehane, D, 1990, "Arran: Machrie North and Glaister", in Buckley, V (ed), *Burnt Offerings: International Contributions to Burnt Mound Archaeology*, Wordwell,

Dublin, p77-79.

Lowe, C.E, 1990, "Kebister: burnt mounds and burnt mound material", in Buckley (ed), *Burnt Offerings: International Contributions to Burnt Mound Archaeology*, Wordwell, Dublin, p84-6.

Máté, I.D, 1990, "Soil analysis of the burnt mounds of the East Rhins", in Buckley, V (ed), *Burnt Offerings: International Contributions to Burnt Mound Archaeology*, Wordwell, Dublin, p175-178.

Maynard, D.J, 1993, "33.1 Birkhall burnt mound", Discovery and Excavation, Scotland, 19.

McCullagh, R and Tipping, R, 1998, *The Lairg Project 1988-1996: The evolution af an archaeological landscape in Northern Scotland*, Scottish Trust for archaeological research, Edinburgh

McIntyre, A, 1998, "Survey and Excavation at Kilearnan Hill, Sutherland, 1982-3", *PSAS*, 128, 189-194.

McKeever, S, 1985, *Thermoluminescence of Solids*, Cambridge University Press, London.

Mejdahl, V, 1979, "Thermoluminescence Dating: beta dose attenuation in quartz grains", *Archaeometry,* 21, 61-73.

Mejdahl, V, 1983, "Feldspar inclusion dating of ceramics and burnt stones", *PACT*, 9, 351-364.

Mejdahl, V, 1985, "TL dating based on feldspars", *Nuclear Tracks and Radiation Measurements*, 10, 133-136.

Mejdahl V, and Bøtter-Jensen, L, 1994, "Luminescence Dating of archaeological materials using a new technique based on single aliquot measurements", Quaternary Geochronology 13, 551-554.

Mejdahl V, and Bøtter-Jensen, L, 1997, *"Experience with the SARA OSL method", Radiation Measurements, 27, 291-294.*

Moore, H and Wilson, G, 1996, *Castle of Stackelbrae*, Historic Scotland Report

Moore, H and Wilson, G, 1996b, *Shetland Burnt Mounds Survey and Excavation at Tangwick*, EASE

Moore, H and Wilson, G, 1999, "Food for thought: a survey of burnt mounds of Shetland and excavations at Tangwick", *Proceedings of the Society of Antiquaries of Scotland*, 129, 203-237.

Moore, H; and Wilson, G, 2000, *Burnt Mounds Dating Project: Shetland Burnt Mounds*, EASE.

Moore, H and Wilson, G, 2001, *Report on Excavations at Cruester Burnt Mound, Bressay, Shetland,* Historic Scotland Report.

Murray, A.S, 1996, "Incomplete stimulation of luminescence in young quartz sediments and its effect on the regenerated signal", *Radiation Measurements*, 26, 221-231.

Murray, A.S and Mejdahl, V, 1999, "Comparison of regenerative-dose single-aliquot and multiple aliquot (SARA) protocols using heated quartz from archaeological sites", *Quaternary Geochronology*, 18, 223-229.

Murray, A.S and Roberts, R.G, 1998, "Measurement of the equivalent dose in quartz using a regenerative-dose single-aliquot protocol", *Radiation Measurements*, 29, 503-515.

Murray, A.S. and Wintle, A.G., 1999, " Isothermal decay of optically stimulated luminescence in quartz", *Radiation Measurements*, 30, 119-125.

Murray, A.S and Wintle, A.G, 2000, "Luminescence dating of quartz using an improved single-aliquot regenerative-dose protocol", *Radiation Measurements,* 32, 57-73.

Mykura, 1976, *British Regional Geology: Orkney and Shetland*, HMSO, Edinburgh

Nambi, K.S.V. and Aitken, M.J. , 1986, "Annual dose conversion factors for TL and ESR dating", Archaeometry, 28, 202-205

Nuttall, R.D.H and Weil, J.A, 1980, "Two hydrogenic trapped-hole species in a-quartz", *Solid State Comm.*, 33, 99-102.

O'Drisceóil, D, 1988, "Burnt Mounds: cooking or bathing?", *Antiquity*, 62, 671-80.

Ó Drisceóil, D, 1990, "Irish Literature", in Buckley, V (ed), *Burnt Offerings: International Contributions to Burnt Mound Study*, Wordwell, Dublin, p157-163.

O'Kelly, M.J, 1954, "Excavations and experiments in ancient Irish cooking-places", *Journal of the Royal Society of Antiquaries of Ireland*, 84, 105-55.

Ottoway, B, 1973, "Dispersion diagrams: a new approach to the display of carbon-14 dates", *Archaeometry*, 15, 5-12.

Øvrevik, S, 1993, "The Second Millennium and After", in Renfrew, C, ed, *The Prehistory of Orkney*, Edinburgh University Press, 131-149.

Owen, O, 1998, "From Past to Present at Kebister: Unfolding the story of one Shetland Farm", in Turner, V (ed), *The Shaping of Shetland*, Shetland Times Ltd, 31-46.

Plachy, A.L and Sutton, S.R, 1982, "Determination of the dose-rate to quartz in granite", *PACT 6*, 188-194.

Pollard, T, 1993, "Kirkhill Farm", *GUARD Report No. 130.*

Porat, N, Armit, N, Zilberman, E and Enzel, Y, 1997, "Luminescence Dating of Fault-Related Alluvial Fan Sediments in the Southern Arava Valley, Israel", *Quaternary Geochronology,* 16, 397-402.

Prescott, J.R and Fox, P.J, 1993, "Three-dimensional thermoluminescence spectra of feldspars", *J. Phys. D*, 26, 2245-2254.

Prescott, J.R, and Stephan, L.G, 1982, "Contribution of cosmic radiation to environmental dose", *PACT*, 6, 17-25.

Radke, U, Janotta, A, Hilgers, A and Murray, A.S, 2001, "The potential of OSL and TL for dating Lateglacial and Holocene dune sands tested with independent age control of the Lacher See tephra (12880 a) at the Section 'Mainz-Gonsenheim'", *Quaternary Science Reviews,* 20, 719-724.

RCAHMS, 1946, Royal Commission on the Ancient and Historical Monuments of Scotland, *Inventory of the Ancient Monuments of Orkney and Shetland*, Edinburgh

RCAHMS, 1980, Royal Commission on the Ancient and Historical Monuments of Scotland, *Inventory of the Ancient Monuments of Orkney and Shetland*, Edinburgh

RCAHMS, 1995, Royal Commission on the Ancient and Historical Monuments of Scotland, CANMORE Database, NC71SE22.

Renfrew, C, 1979, *Investigations in Orkney*, Rep. Research Comm. Soc. Antiq. London, No. 38, London.

Renfrew,C (ed), 1985, *The prehistory of Orkney*, Edinburgh University Press, Edinburgh.

Renfrew, C and Buteux S, 1990, "Radiocarbon Dates from Orkney", in Renfrew, C, ed, *The Prehistory of Orkney*, Edinburgh University Press, 263-274.

Ritchie, A, 1984, "Excavation of a Neolithic farmstead at Knap of Howar, Papa Westray, Orkney", *Proceedings of the Society of Antiquaries of Scotland,* 113, 40-121.

Ritchie, A, 1993, "The First Settlers", in Renfrew, C, ed, *The Prehistory of Orkney*, Edinburgh University Press, 36-53.

Robertson, J, Anthony, I, Sanderson, D, Downes, J and Housley, R, 2000, *Characterisation and Dating of Burnt Mounds from Orkney and Shetland: Eday Burnt Mounds*, Historic Scotland Report.

Robins, M P, 1993, "Annandale and Eskdale District (Moffat parish, Kirkpatrick Juxta parish) : M74 survey" *Discovery and Excavation, Scotland,* 17.

Russell-White, C.J, 1990, "The East Rhins of Galloway", in Buckley, V (ed), *Burnt Offerings: International Contributions to Burnt Mound Archaeology*, Wordwell, Dublin, p70-76.

Sanderson, D.C.W, 1979, "A modified alpha counting system", *Ancient TL*, 9, 3-5.

Sanderson, D.C.W, 1987, *Thermoluminescence Dating of Scottish Vitrified Forts*, Unpublished PhD Thesis, Dept of Physics, Paisley College of Technology.

Sanderson, D.C.W, 1988a, "Fading of Thermoluminescence in Feldspars: Characteristics and Corrections", *Nuclear Tracks and Radiation Measurements,* 14, 155-161.

Sanderson, D.C.W, 1988b, "Thick Source Beta Counting (TSBC): A rapid method for measuring beta dose-rates", *Nuclear Tracks and Radiation Measurements*, 14, 203-208

Sanderson, D. C. W., Placido, F. and Tate, J. O., 1988, "Scottish vitrified forts: TL results for six study sites", *Nuclear Tracks and Radiation Measurements,* 14, 307-316.

Scott EM and **Sanderson DCW, 1988,** "Statistics and the additive dose method in TL dating", *Nuclear Tracks and Radiation Measurements,* 14, 345-354.

Singarayer, J.S and Bailey, R.M, 2003, "Further investigations of the quartz optically stimulated luminescence components using linear modulation", *Radiation Measurements*, in press.

Smith, D.J, 1998, *Fading and Tunnelling in Luminescence Dating of Volcanic Feldspars*, Unpublished BSc Dissertation, University of Strathclyde/ Scottish Universities Research and Reactor Centre.

Smith, J.A, 1883, "otes on some stone implements, etc, from Shetland, now presented to the Museum" *Proceedings of the Society of Antiquaries of Scotland*, 17, 293.

Sommerville, A.A, 2003, *Luminescence Dating of Wind Blown Sands from Archaeological Sites in Nothern Scotland*, Unpublished PhD Thesis, University of Glasgow.

Speller, K, Banks, I, Duffy, P and MacGregor, G, 1997, "Ladywell farm, Girvan, burnt mound, prehistoric and medieval features", Discovery and Excavation, Scotland, 73-74.

Spencer, J.Q, 1996, "The Development of Luminescence methods to measure thermal exposure in lithic and ceramic materials" Unpublished PhD Thesis, University of Glasgow.

Spencer, J.Q, Sanderson, D.C.W, Deckers, K, and Sommerville, A.A, 2003, "Assessing mixed dose distributions in young sediments identified using small aliquot and a simple two-step SAR procedure: the F-statistic as a diagnostic tool", *Radiation Measurements*, in press.

Spooner, N.A and Questiaux, D.G, 2000, "Kinetics of red, blue and UV thermoluminescence (TL) and optically-stimulated luminescence (OSL) from quartz", *Radiation Measurements*, 32, 659-666.

Stamp, L.D, 1944, *The Land of Britian, Vol 1: Scotland*, Geographical Publications Ltd, London

Strachan, Ralston and Finlayson, R, I and B, 1998, "Neolithic and later prehistoric structures, and early medieval metal-working at Blairhall Burn, Amisfield, Dumfriesshire", *Proceedings of the Society of Antiquaries of Scotland*, 128, 55-94.

Strickertsson, K, 1985, "The thermoluminescence of potassium feldspars - glow curve characteristics and initial rise measurements", *Nuclear Tracks and Radiation Measurements*, 10, 613-617.

Strickertsson, K, Murray, A.S, Lykke-Andersen, H, 2001, "Optically stimulated luminescence dates for late Pleistocene sediments from Stensnæs, Northern Jutland, Denmark", *Quaternary Science Reviews,* 20, 755-759.

Stuiver M., P.J. Reimer and T.F.Braziunas, 1998, "High-precision radiocarbon age calibration for terrestrial and marine samples", *Radiocarbon,* 40(3) 1127-1151

Suhr, N.H and Ingamells, C.O, 1966, "Solution technique for analysis of silicates", *Analytical Chemistry,* 38, 730-734.

Sutton, S.R and Zimmerman, D.W, 1976, "Thermoluminescent dating using zircon grains from archaeological ceramics", *Archaeometry*, 18, 125-134.

Tate, R, 1866, "Report of the Zetland Anthropological Expedition", Memoirs of the Anthropological Society of London, 2, 202-207..

Templer, R.H, 1985, "The Removal of Anomalous Fading in Zircon", *Nucl. Tracks*, 10, 531-537.

Templer, R.H, 1986, "The Localised Transition Model of Anomalous Fading", *Radiat. Prot. Dosim., 17, 493-497.*

Valladas, H, 1978, "Thermoluminescence dating of burnt stones from a prehistoric site", *PACT*, 2, 180-183.

Visockas, R, 1985, "Tunnelling Radiative Recombination Associated with Anomalous

Fading of Thermoluminescence of Labrodite", *Nucl. Tracks*, 10, 521-530.

Visocekas, R, Ceva, T, Marti, C, Lefaucheux, F and Robert, M.C, 1976, Tunnelling Processes in Afterglow of Calcite, *Phys. Stat. Sol (a)*, 35, 315-327.

Wallinga, J and Duller, G.A.T, 2000, "The effect of optical absorption on the infrared stimulated luminescence age obtained on coarse-grain feldspar", *Quaternary Science Reviews*, 20, 1035-1042.

Wallinga, J, Murray, A and Wintle, A, 2000, "The single-aliquot regenerative-dose (SAR) protocol applied to coarse-grain feldspar", *Radiation Measurements*, 32, 529-533.

Ward, T, 1992, "Survey of A74 and M74 road development routes", *Discovery and Excavation*, Scotland, 65.

Ward, T , 1994 , "Sites found when fieldwalking in Clydesdale", *Discovery and Excavation*, Scotland, 74.

Ward, T, 1998, "Manor Valley (Manor parish), survey and excavation", *Discovery and Excavation*, Scotland, 81.

Ward, T, 1999, "Manor Valley (Manor parish), survey", *Discovery and Excavation, Scotland*, 77.

Warren, S.E, 1978, "Thermoluminescence dating of pottery", *Archaeometry*, 20, 69-70.

Wintle, A.G, 1973, "Anomalous Fading of Thermoluminescence of Mineral Samples", *Nature*, 245, 143-4.

Wintle, A.G, 1975, "Thermal quenching of thermoluminescence in quartz", *Geophysical Journal of the Royal Astronomical Society*, 41, 107-113.

Wintle, A.G, 1977, Detailed Study of a Thermoluminescent Mineral Exhibiting Anomalous Fading", *J Luminescence*, 15, 385-393.

Wintle, A.G and Huntley, D.J, 1982, "Thermoluminescence Dating of Sediments", *Quaternary Science Reviews*, 1, 31-53.

Zimmerman, D.W, 1971, "Thermoluminescent dating using fine grains from pottery", *Archaeometry*, 13, 29-52.

Zimmerman, D.W, Yuhas, M.P and Meyers, P, 1974, "Thermoluminescence authenticity measurements on core material from the Bronze Horse of the New York Metropolitan Museum of Art", *Archaeometry*, *16, 19-30.*

APPENDIX A

DISTRIBUTION OF BURNT MOUNDS IN SCOTLAND

A.1a Distribution of Burnt Mounds on Shetland (Data from RCAHMS Canmore database)

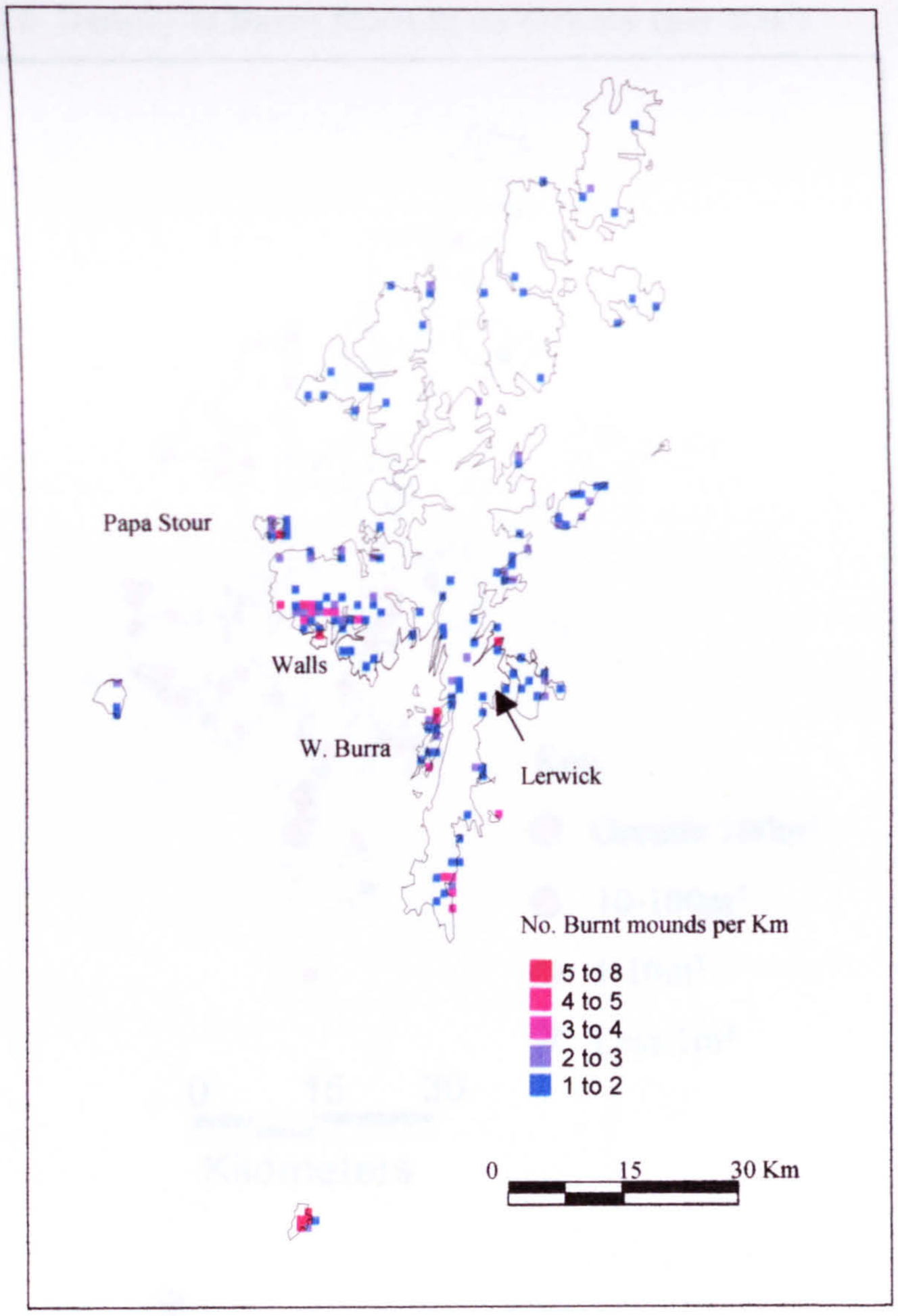

A.1b Density of Burnt Mounds on Shetland (per Km^2)

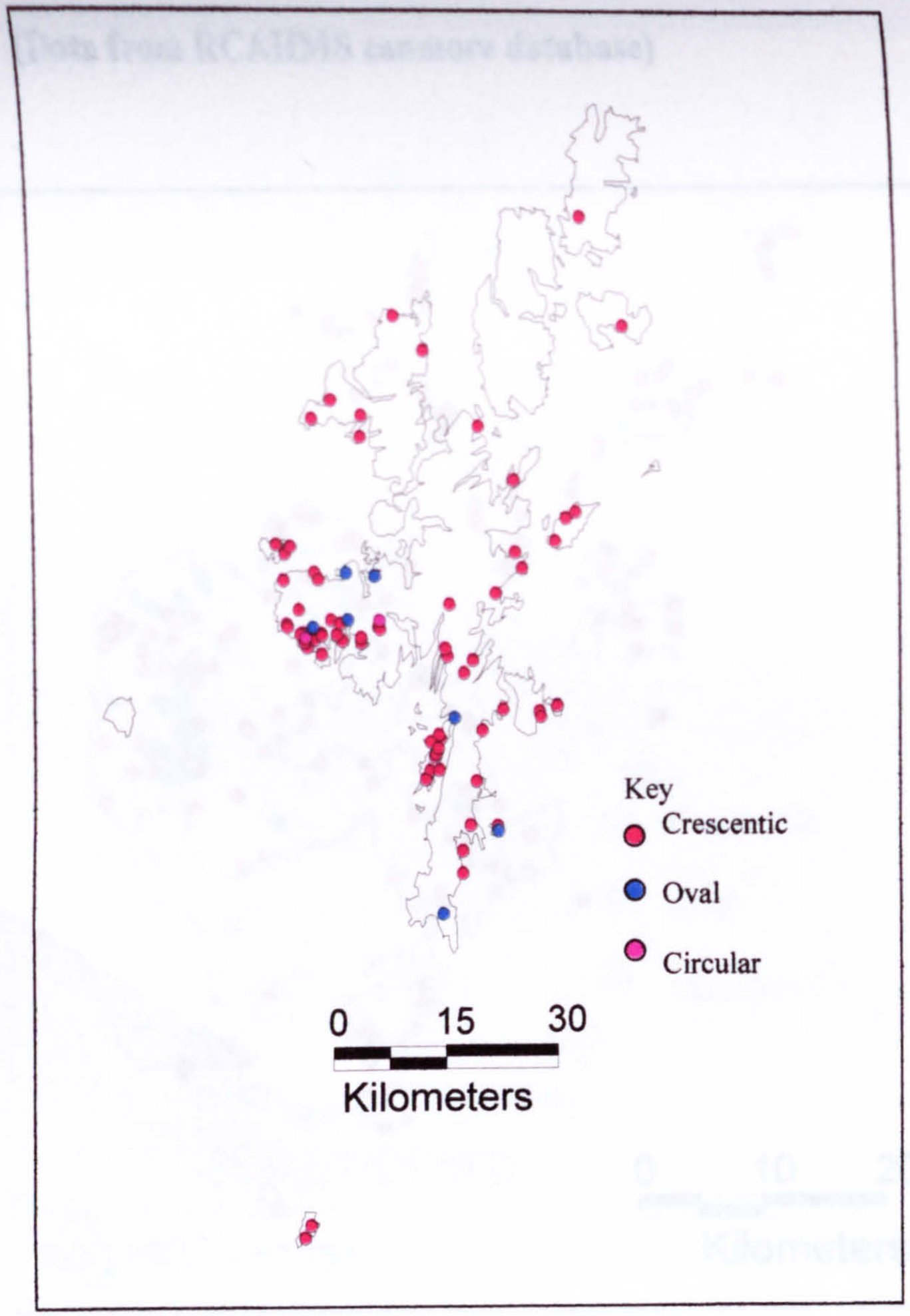

A.1c Shape Distribution, Shetland

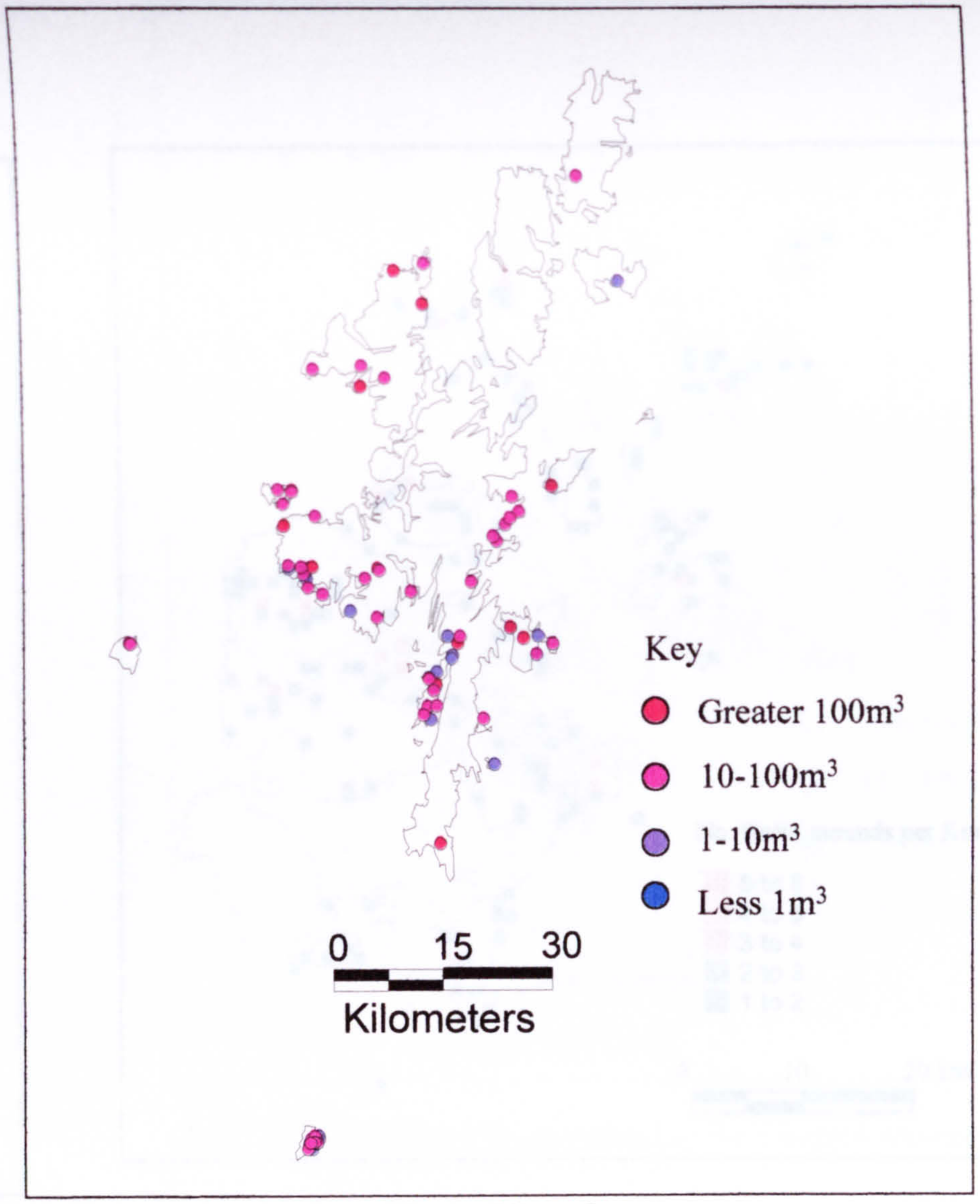

A.1d Distribution of Burnt Mounds by Volume, Shetland

A.2a Distribution of Burnt Mounds on Orkney

(Data from RCAHMS canmore database)

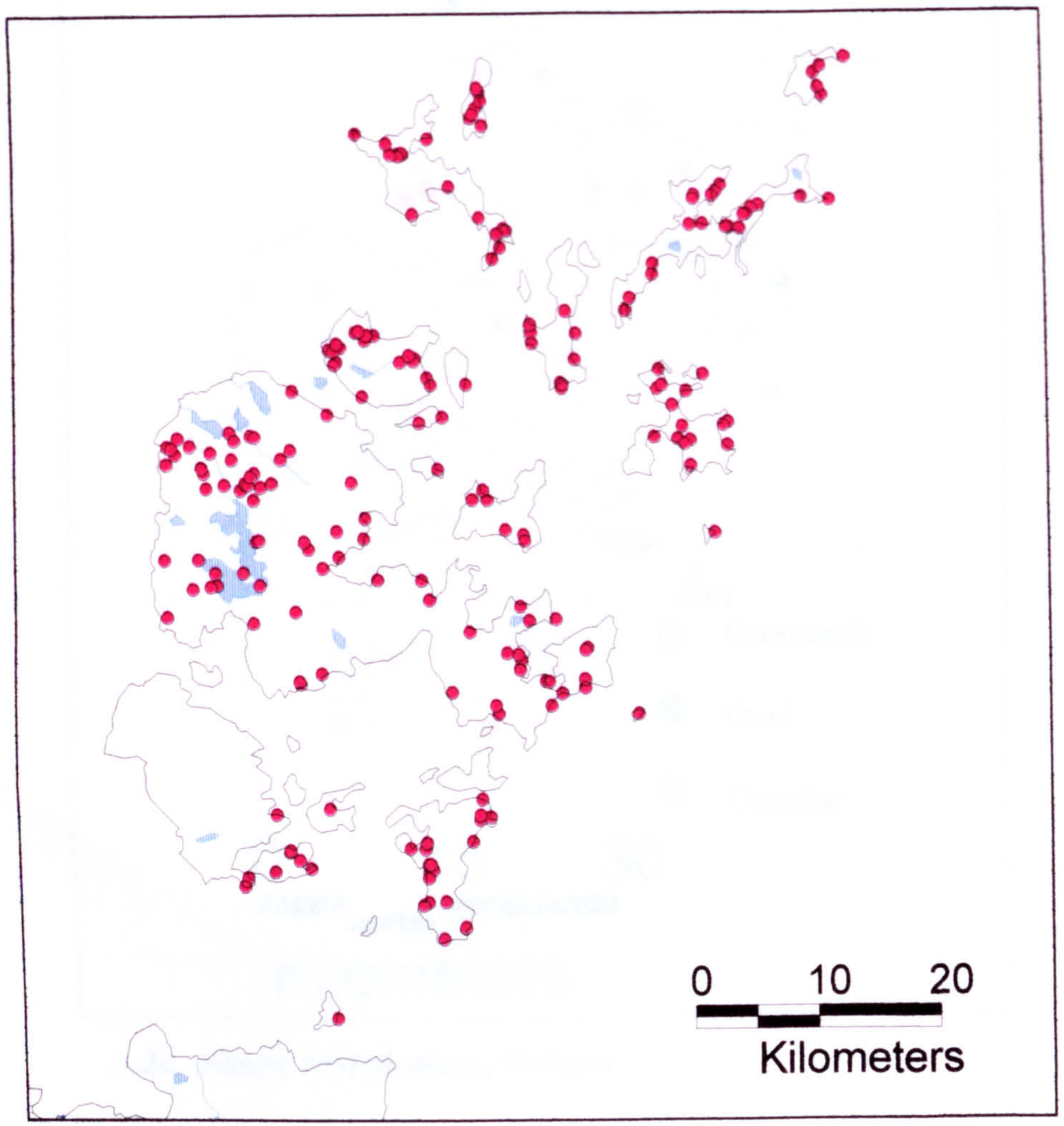

A.2b Density of Burnt Mounds on Orkney (per Km^2)

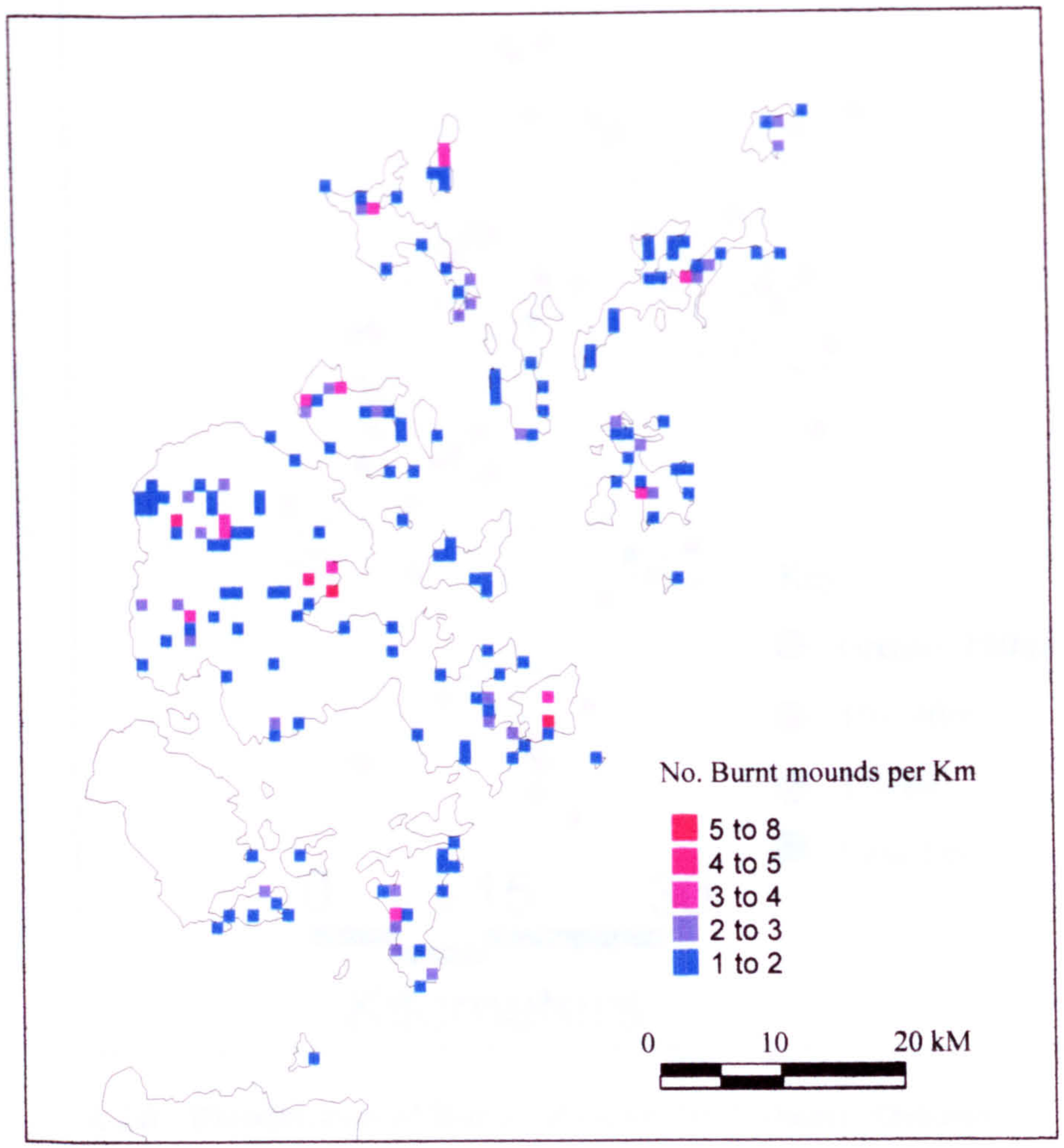

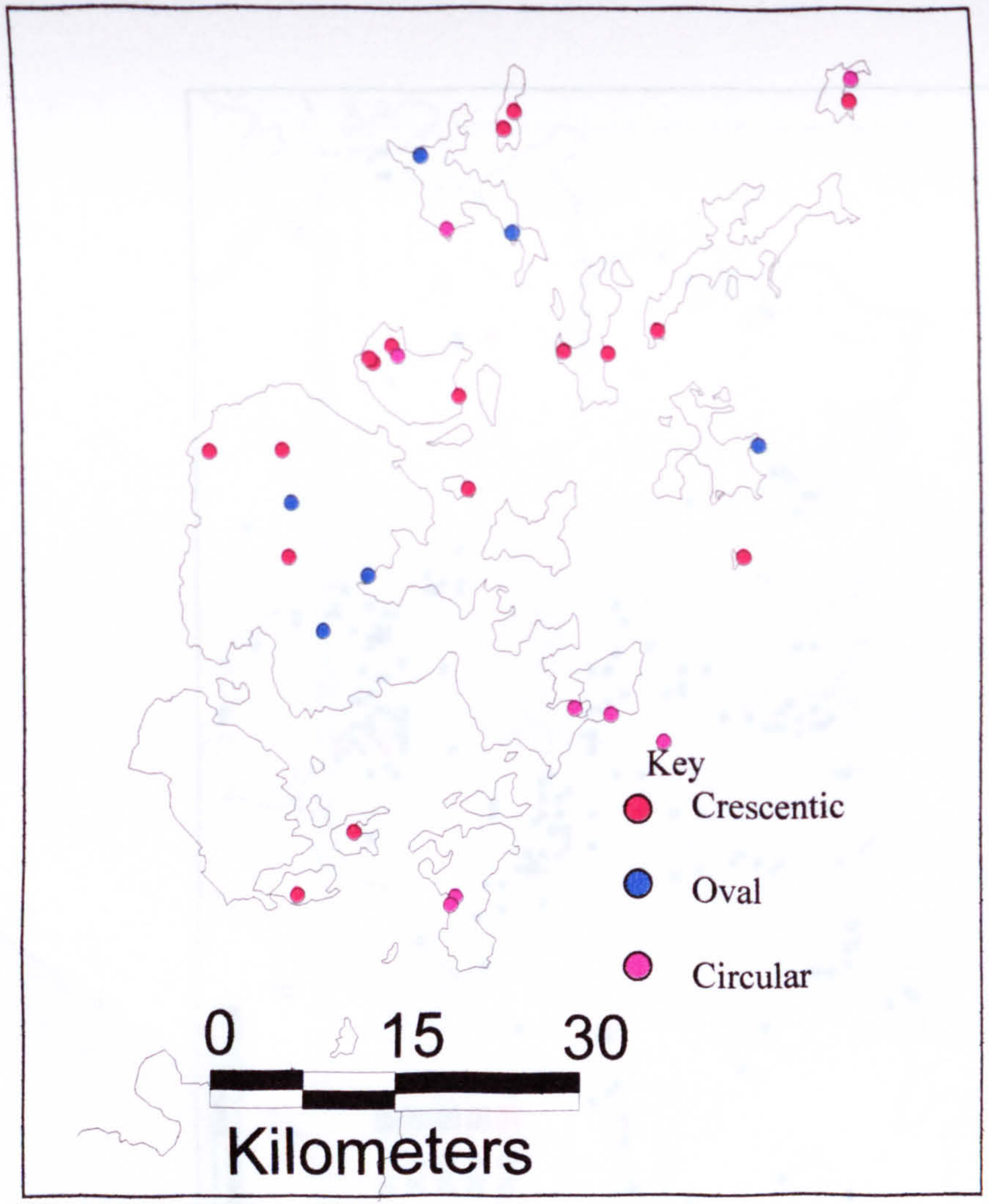

A.2c Shape Distribution, Orkney

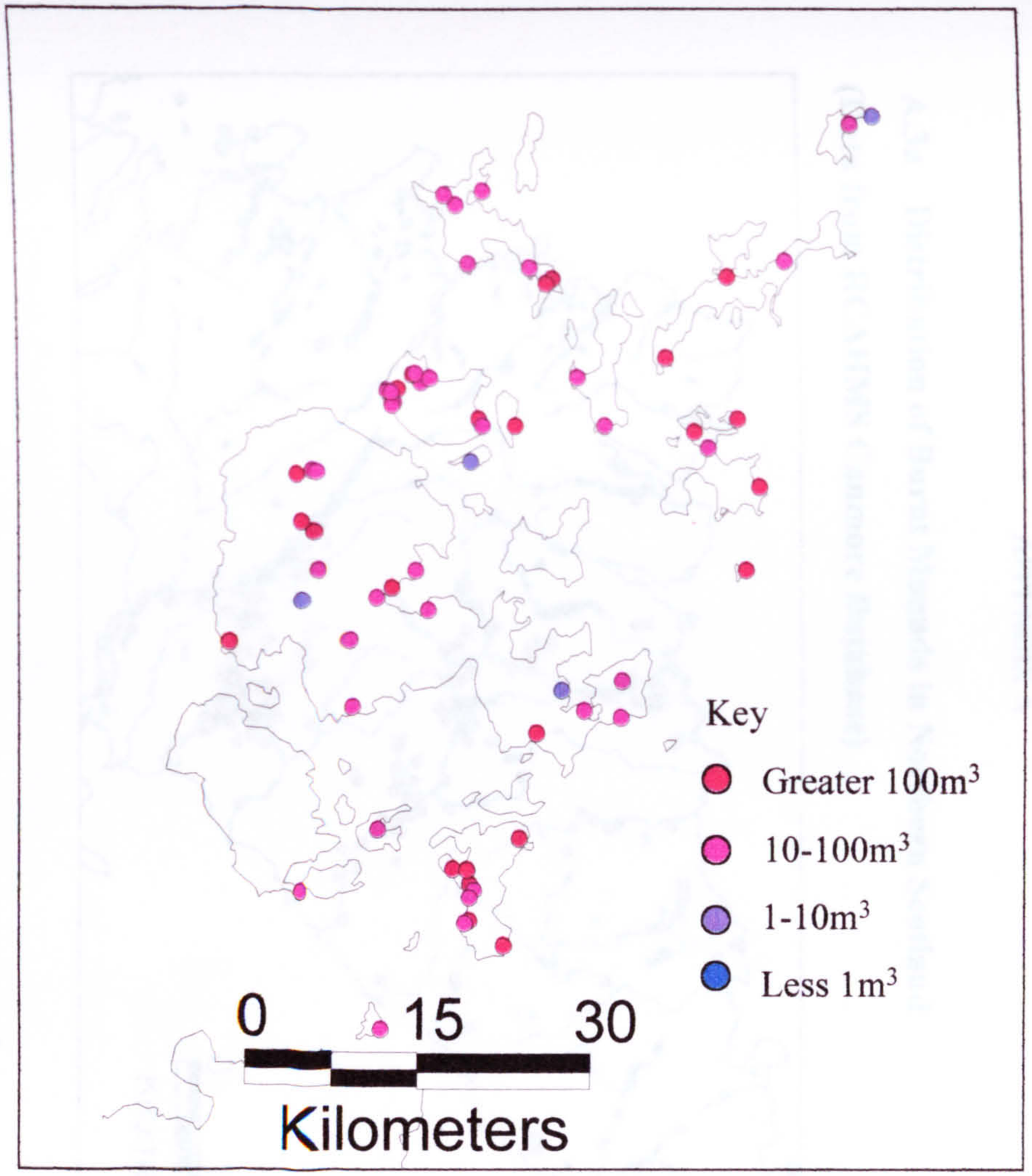

A.2d Distribution of Burnt Mounds By Volume, Orkney

A.3a Distribution of Burnt Mounds in Northern Scotland (Data from RCAHMS Canmore Database)

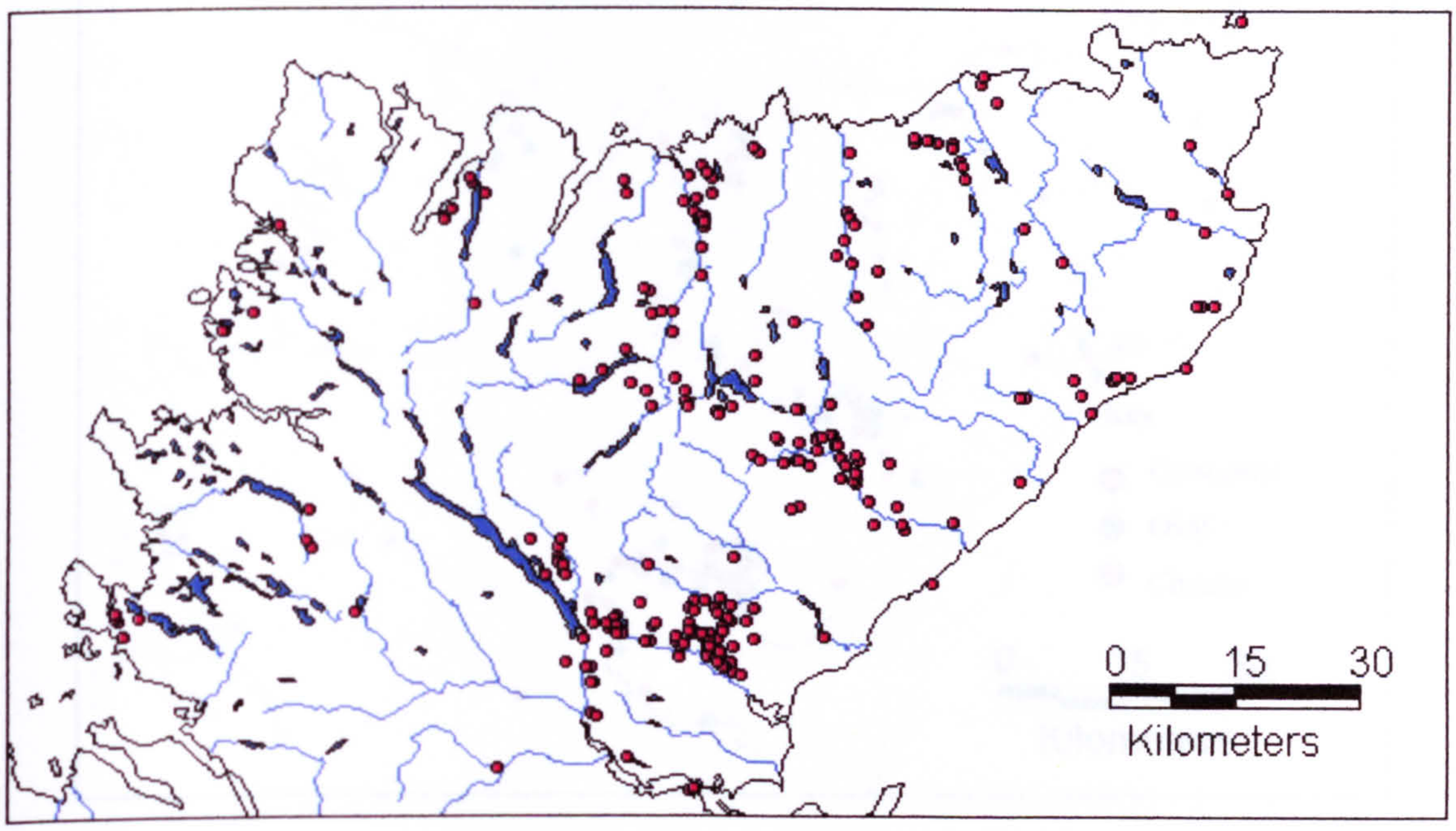

A.3b Density of Burnt Mounds in Northern Scotland (per km^2)

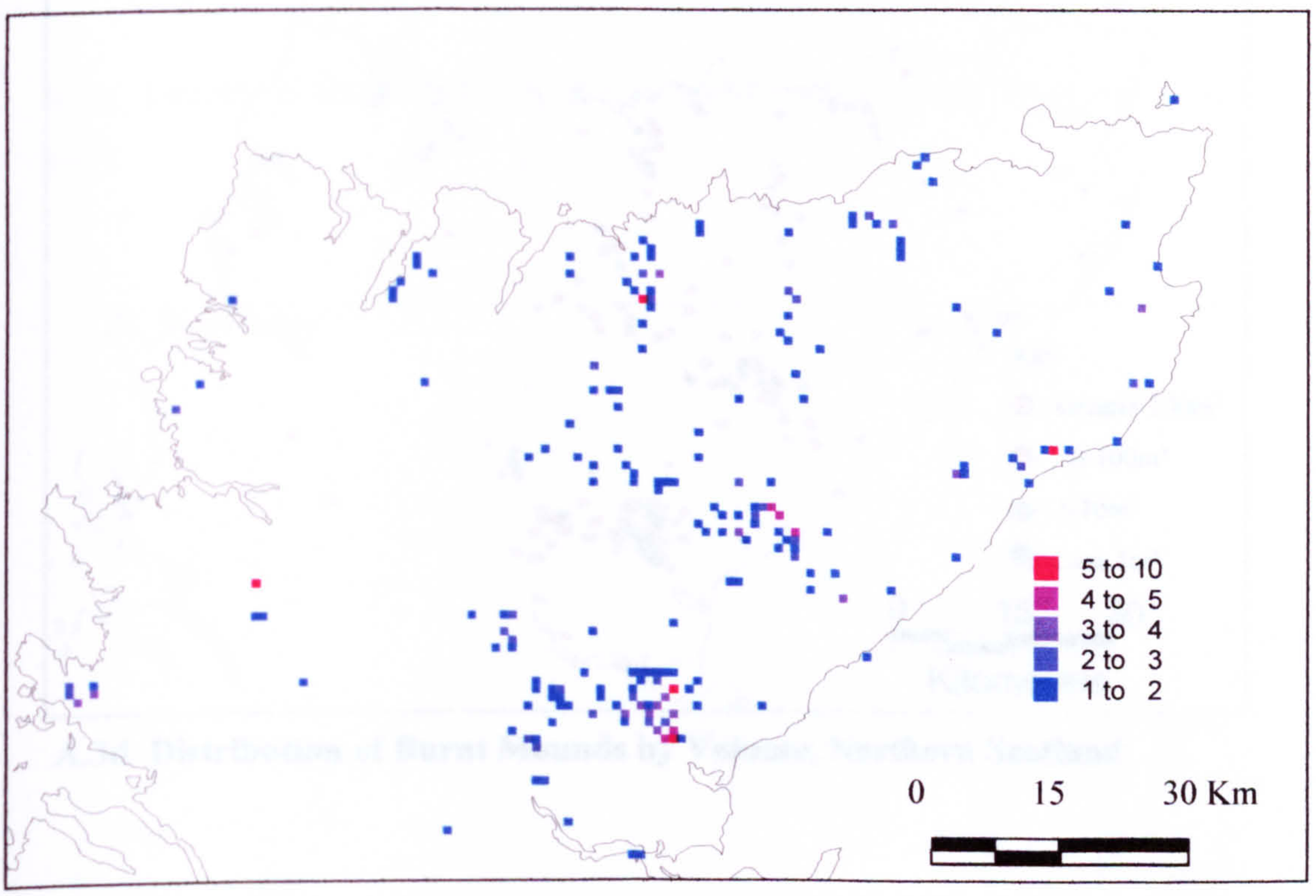

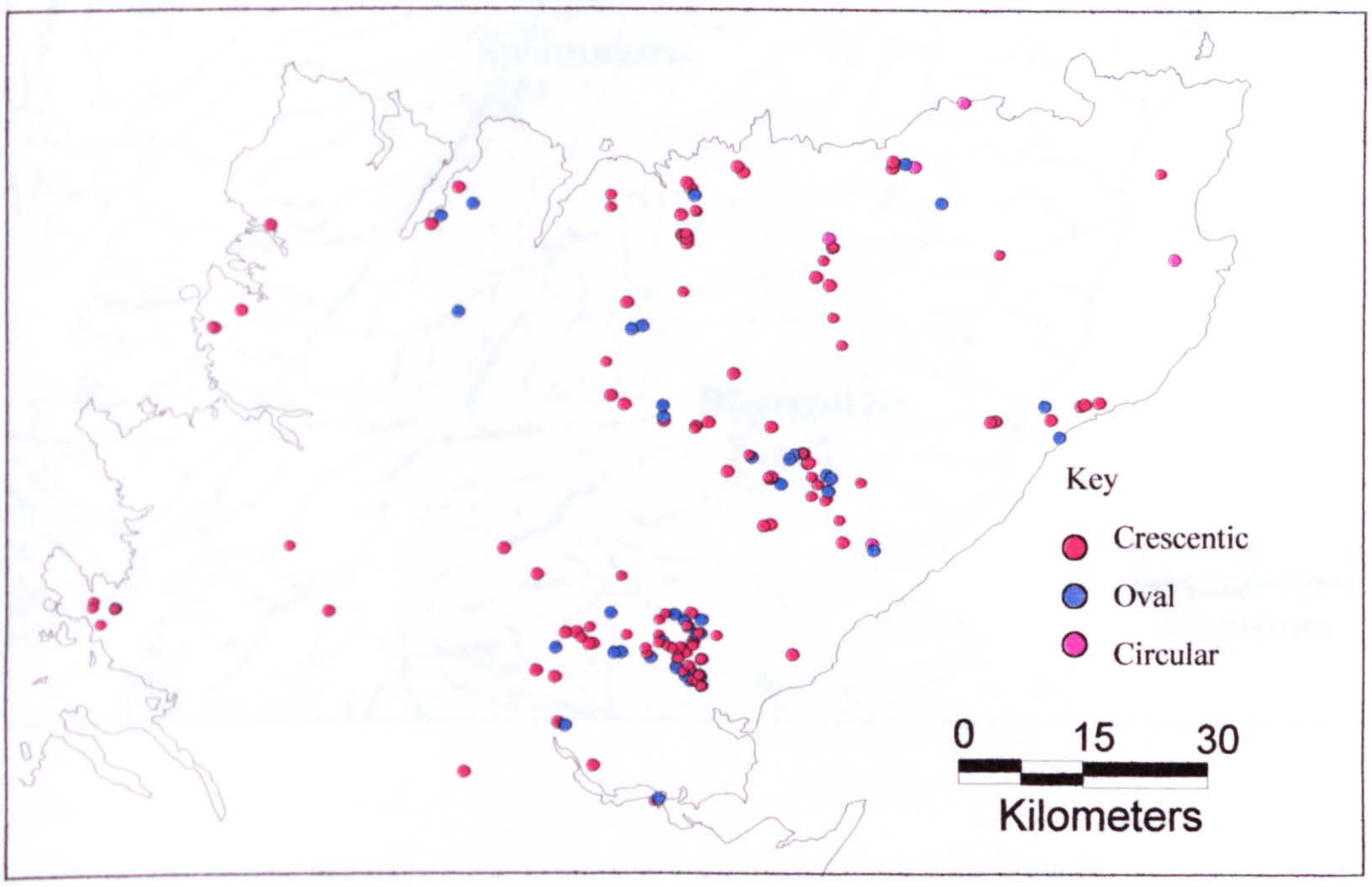

A.3c Shape Distribution, Northern Scotland

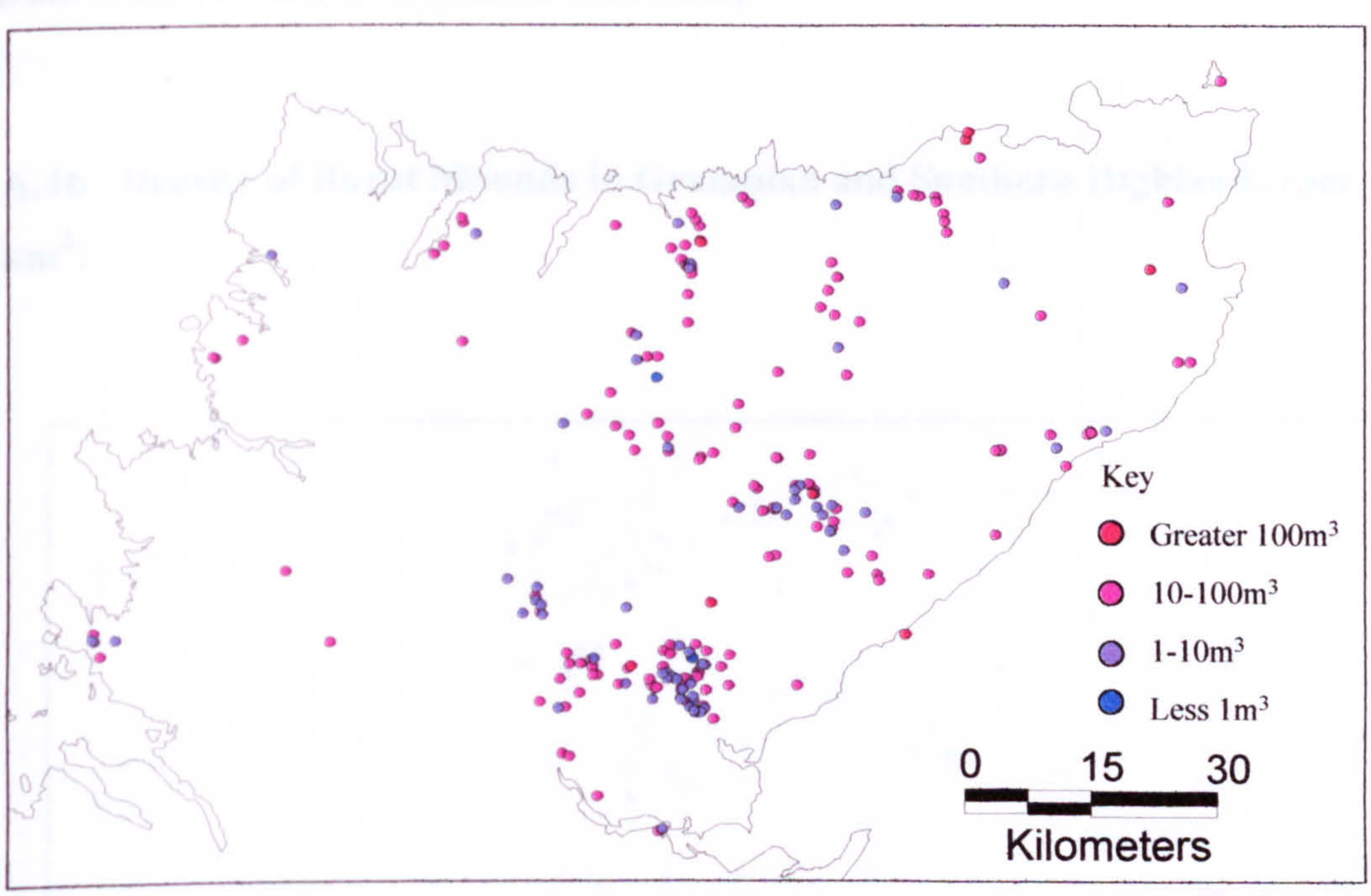

A.3d Distribution of Burnt Mounds by Volume, Northern Scotland

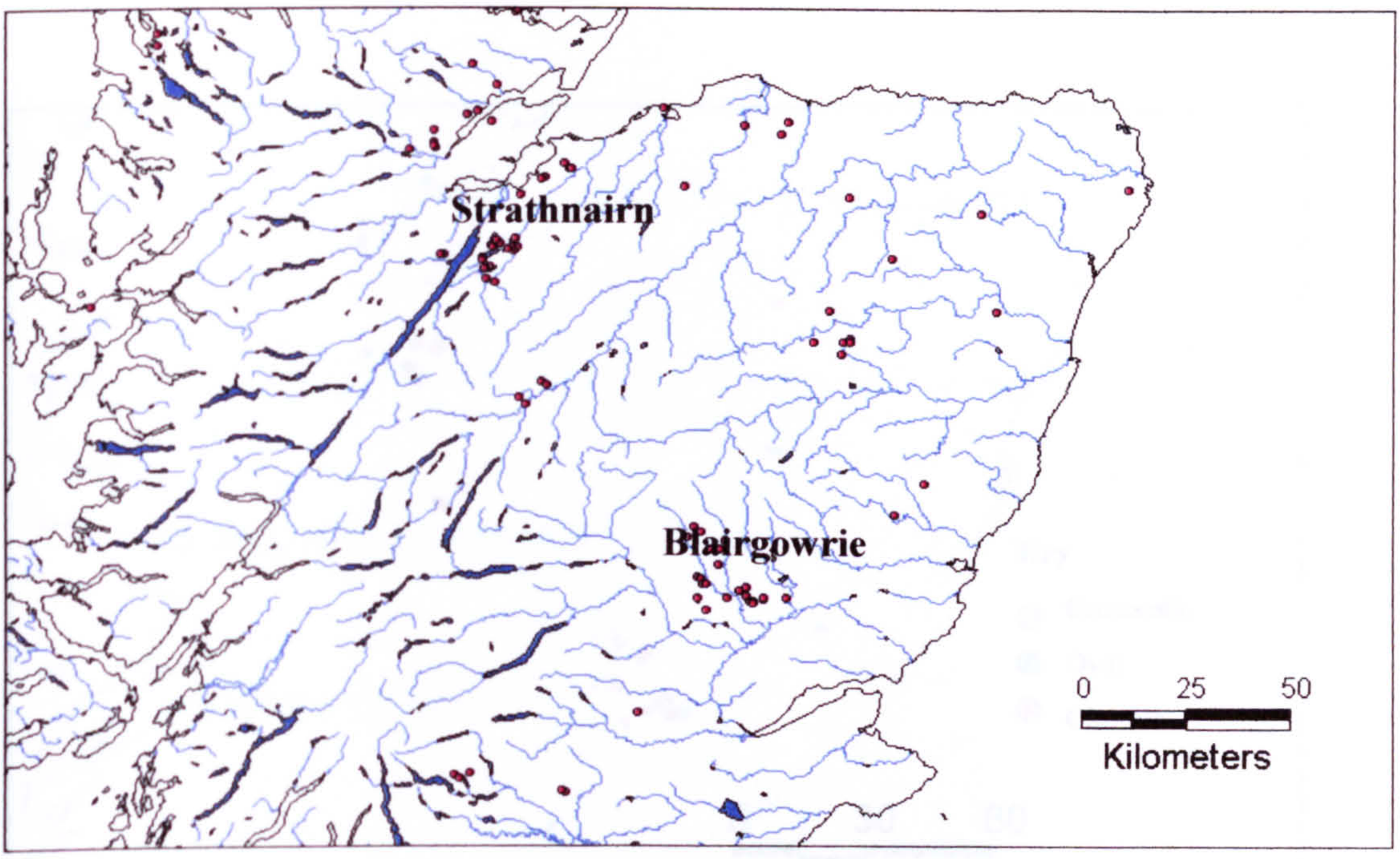

A.4a Distribution of Burnt Mounds in Grampian and Southern Highlands (Data from RCAHMS Canmore Database)

A.4b Density of Burnt Mounds in Grampian and Southern Highlands (per km^2)

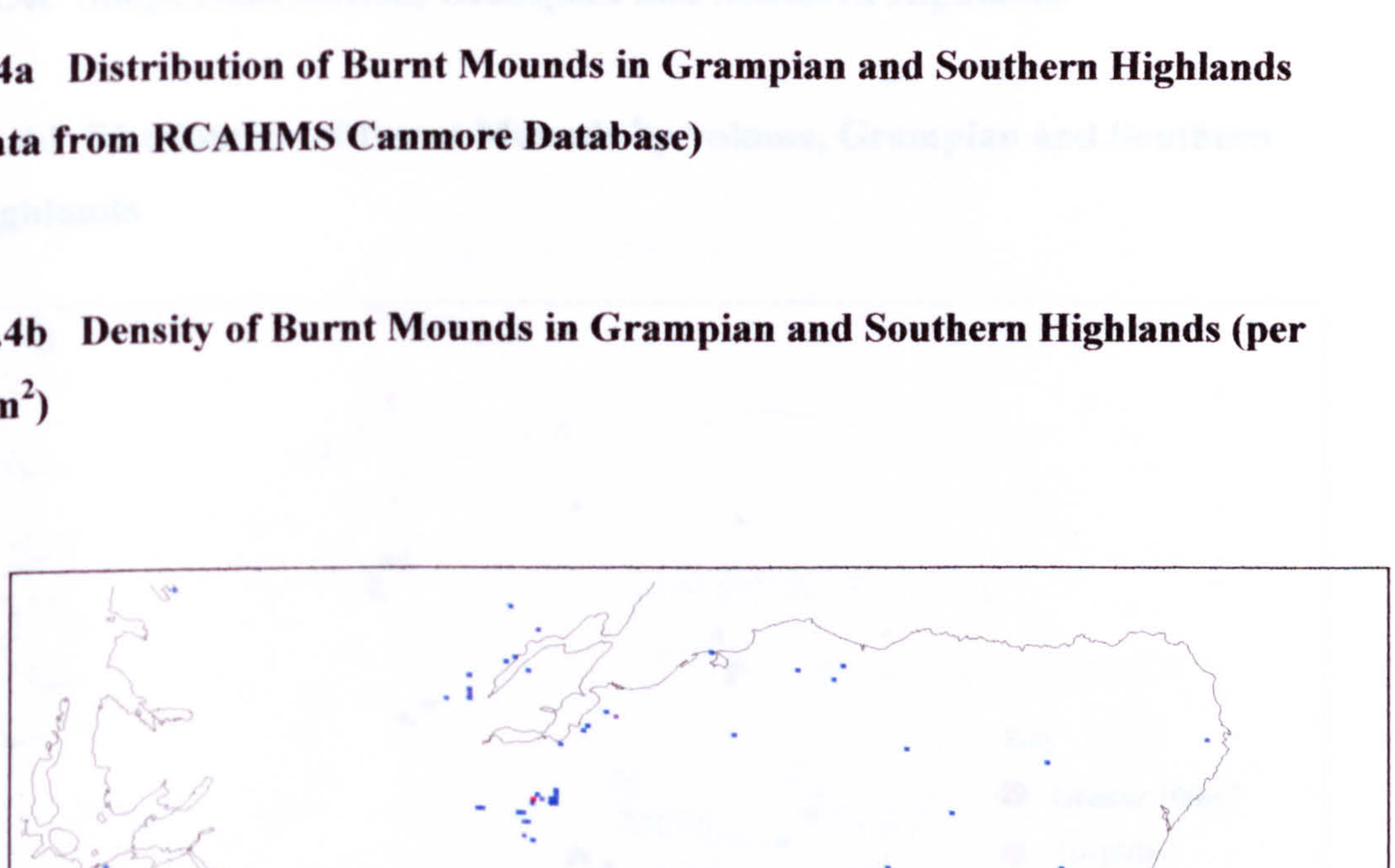

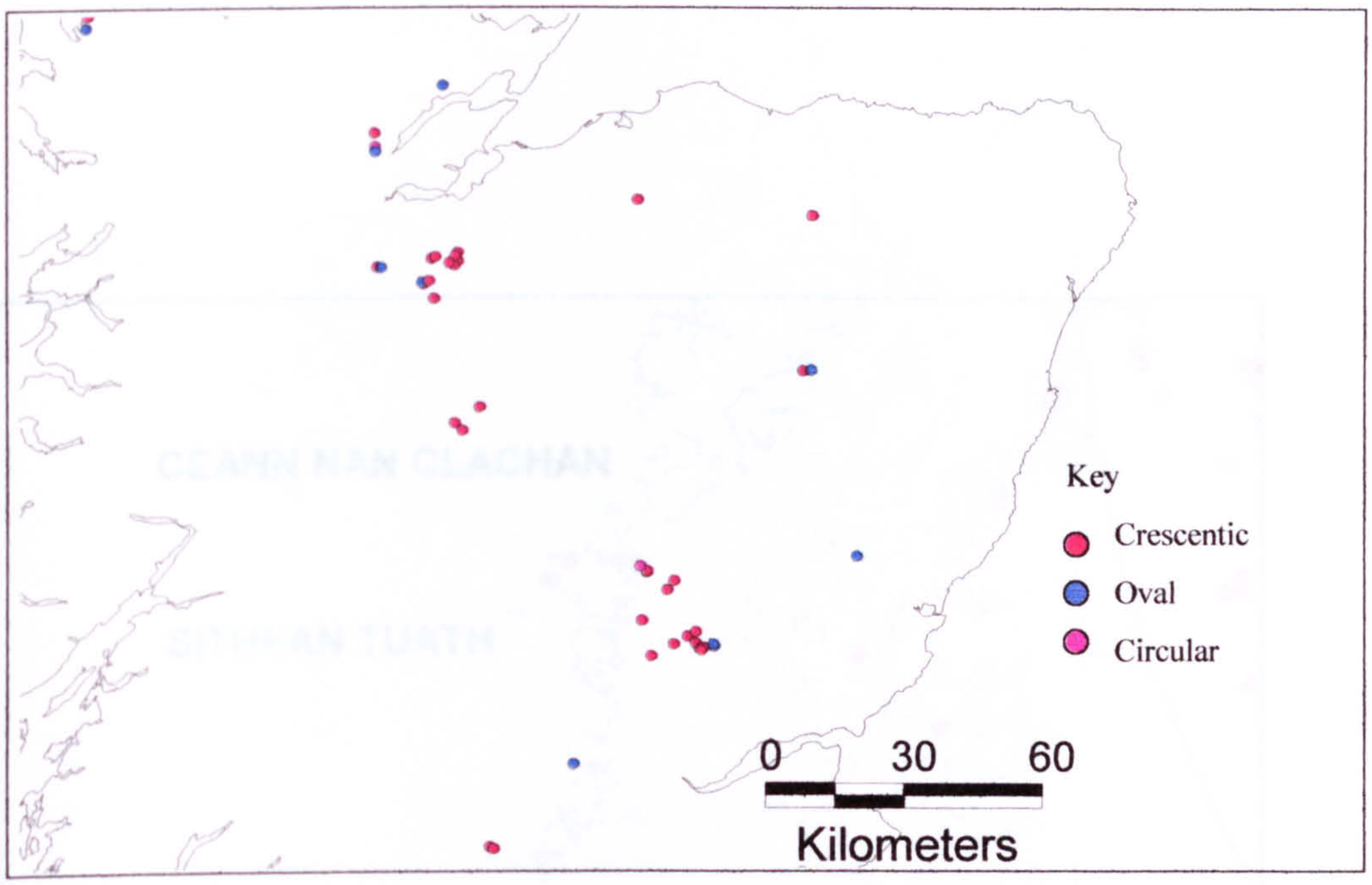

A.4c Shape Distribution, Grampian and Southern Highlands

A.4d Distribution of Burnt Mounds by volume, Grampian and Southern Highlands

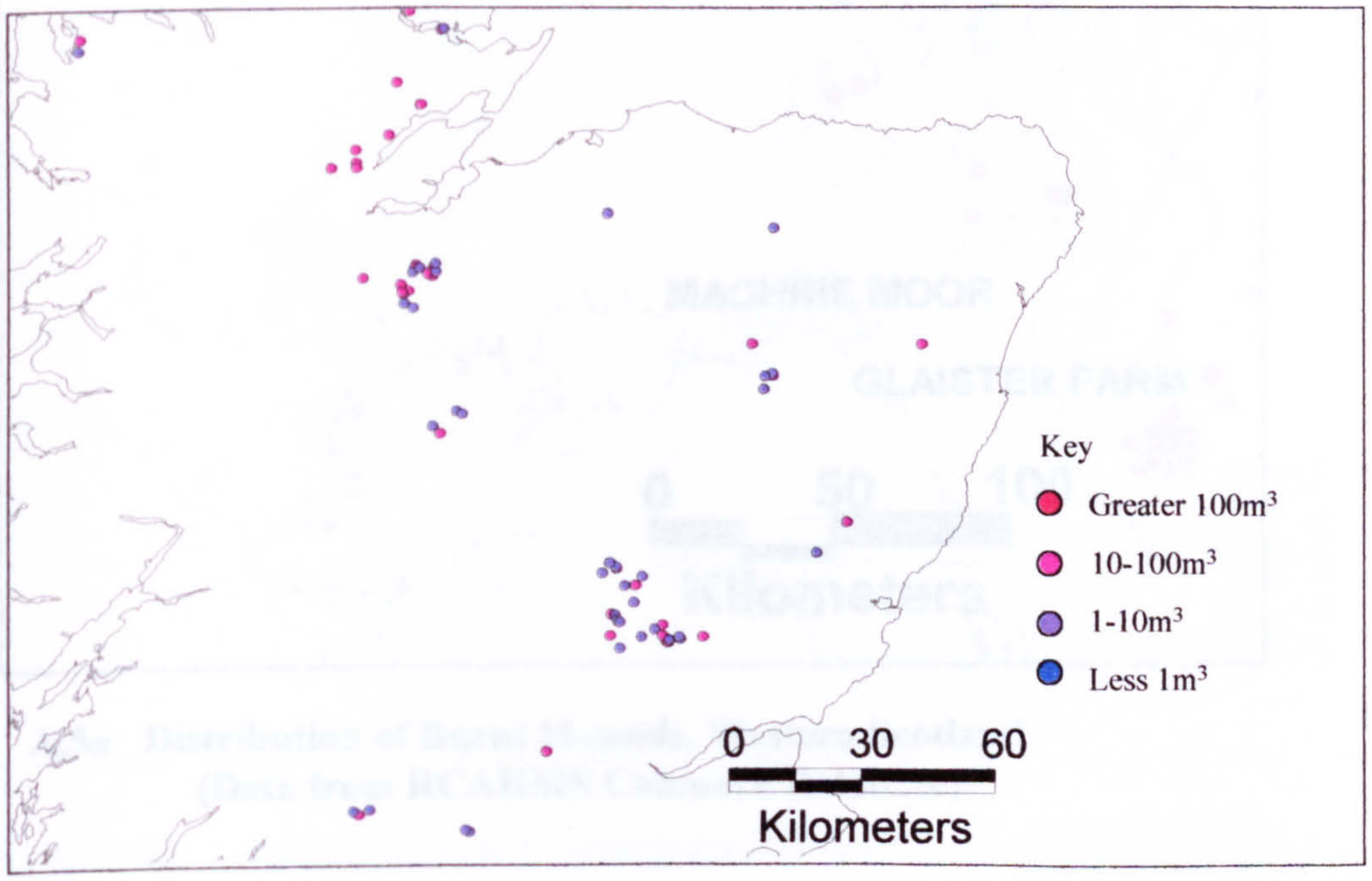

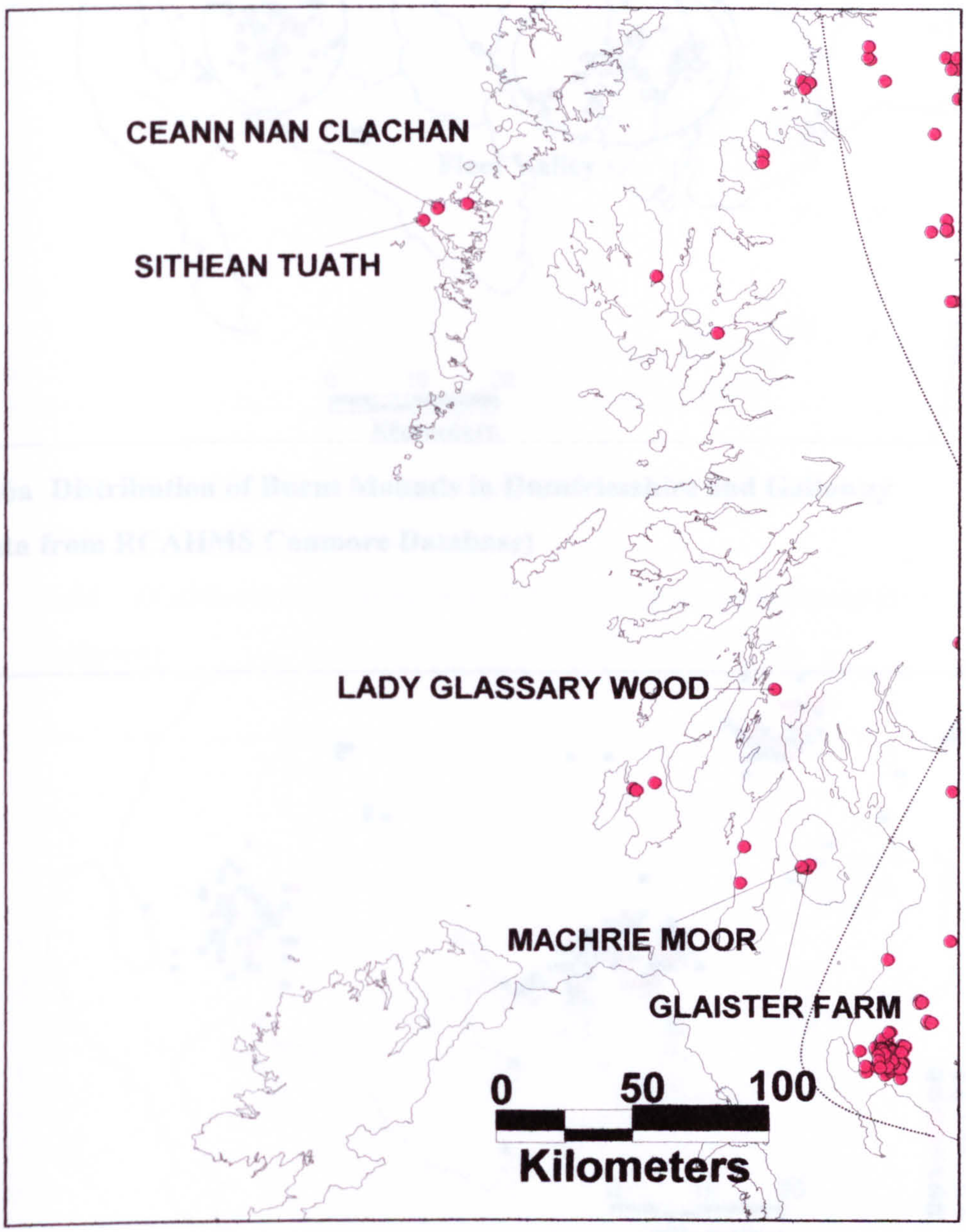

A.5a Distribution of Burnt Mounds, Western Scotland
(Data from RCAHMS Canmore Database)

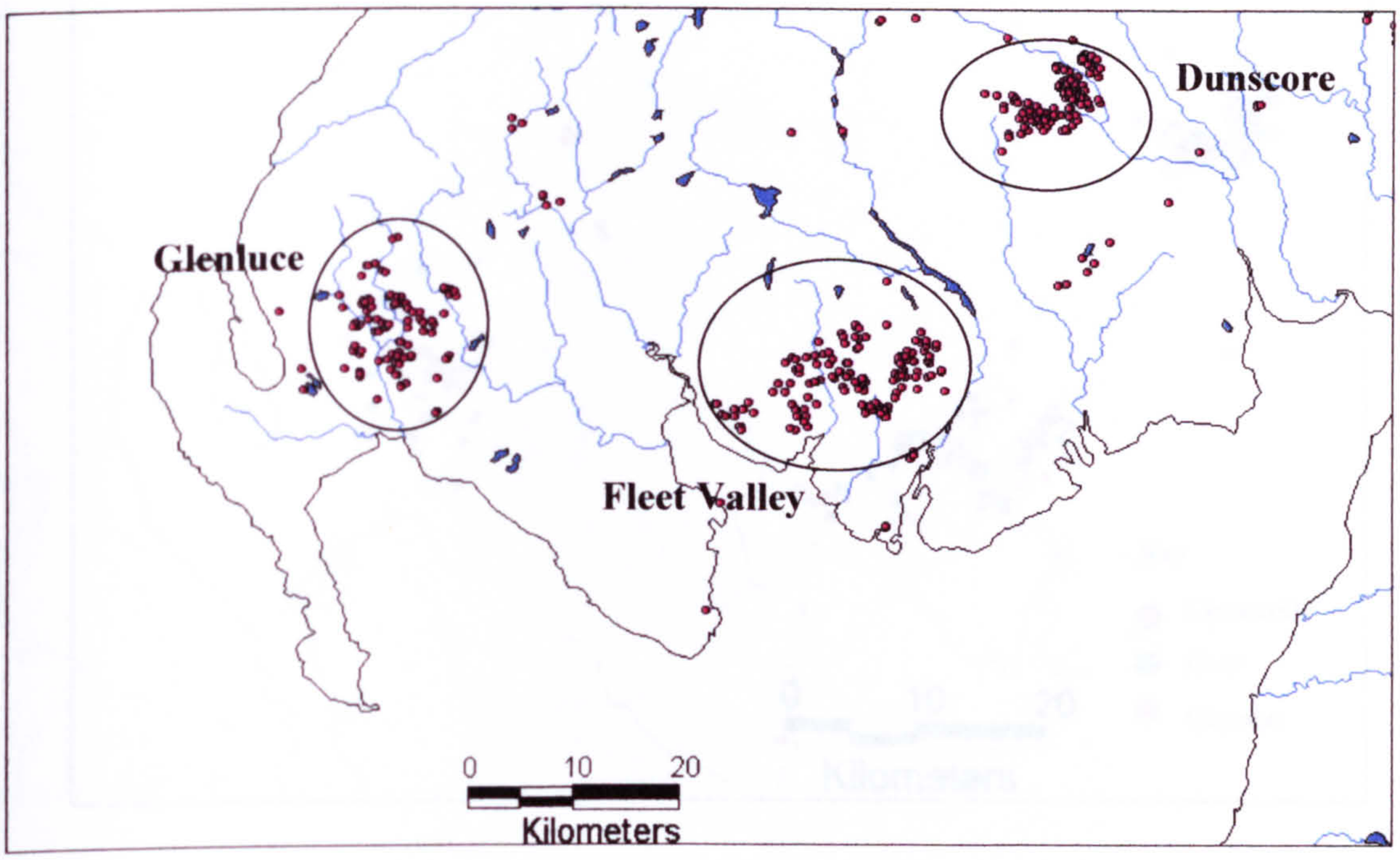

A.6a Distribution of Burnt Mounds in Dumfriesshire and Galloway (Data from RCAHMS Canmore Database)

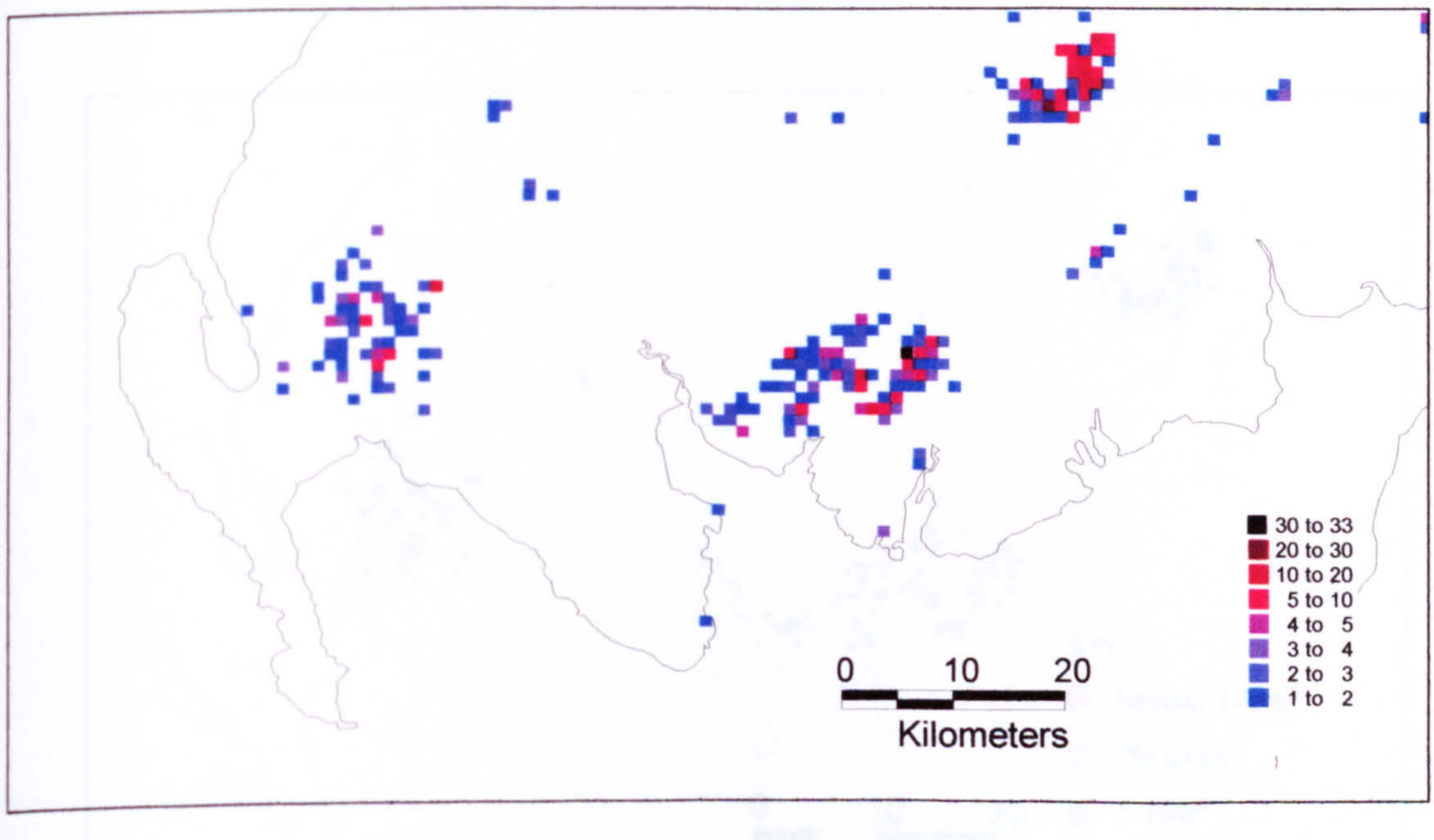

A.6b Density of Burnt Mounds in Dumfriesshire and Galloway (per Km^2)

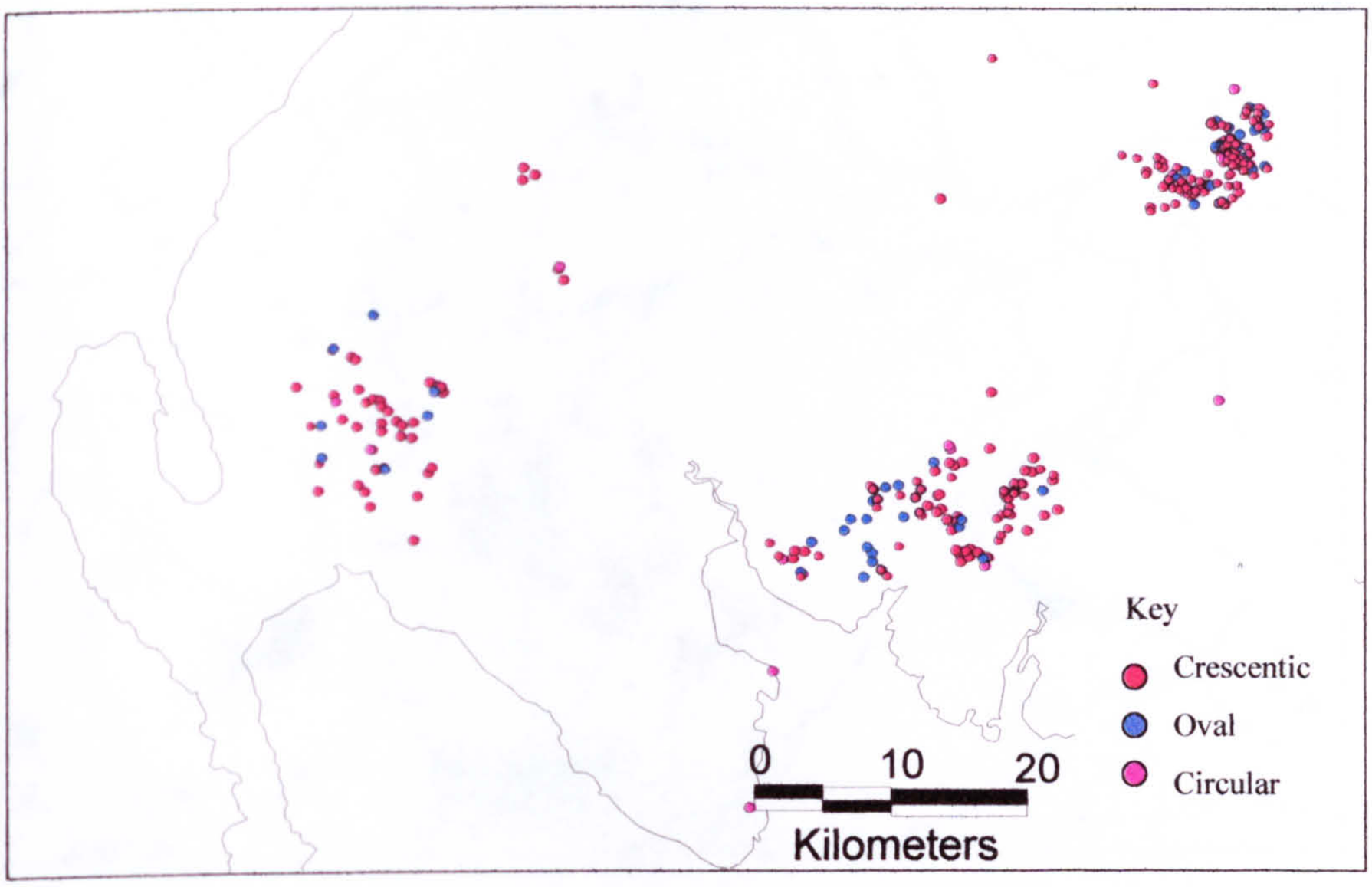

A.6c Shape Distribution, Dumfriesshire and Galloway

A.6d Distribution of Burnt Mounds by Volume, Dumfriesshire and Galloway

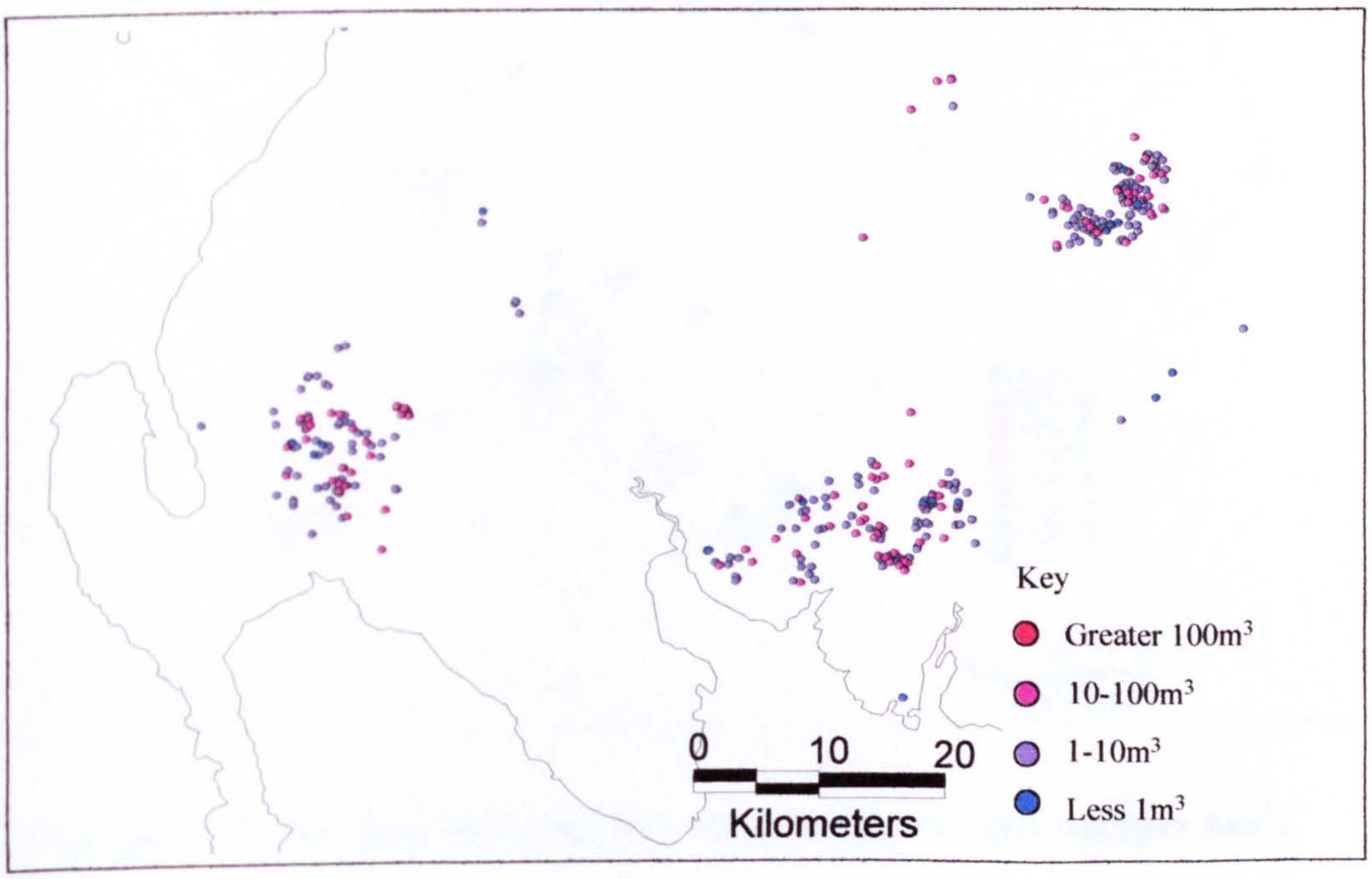

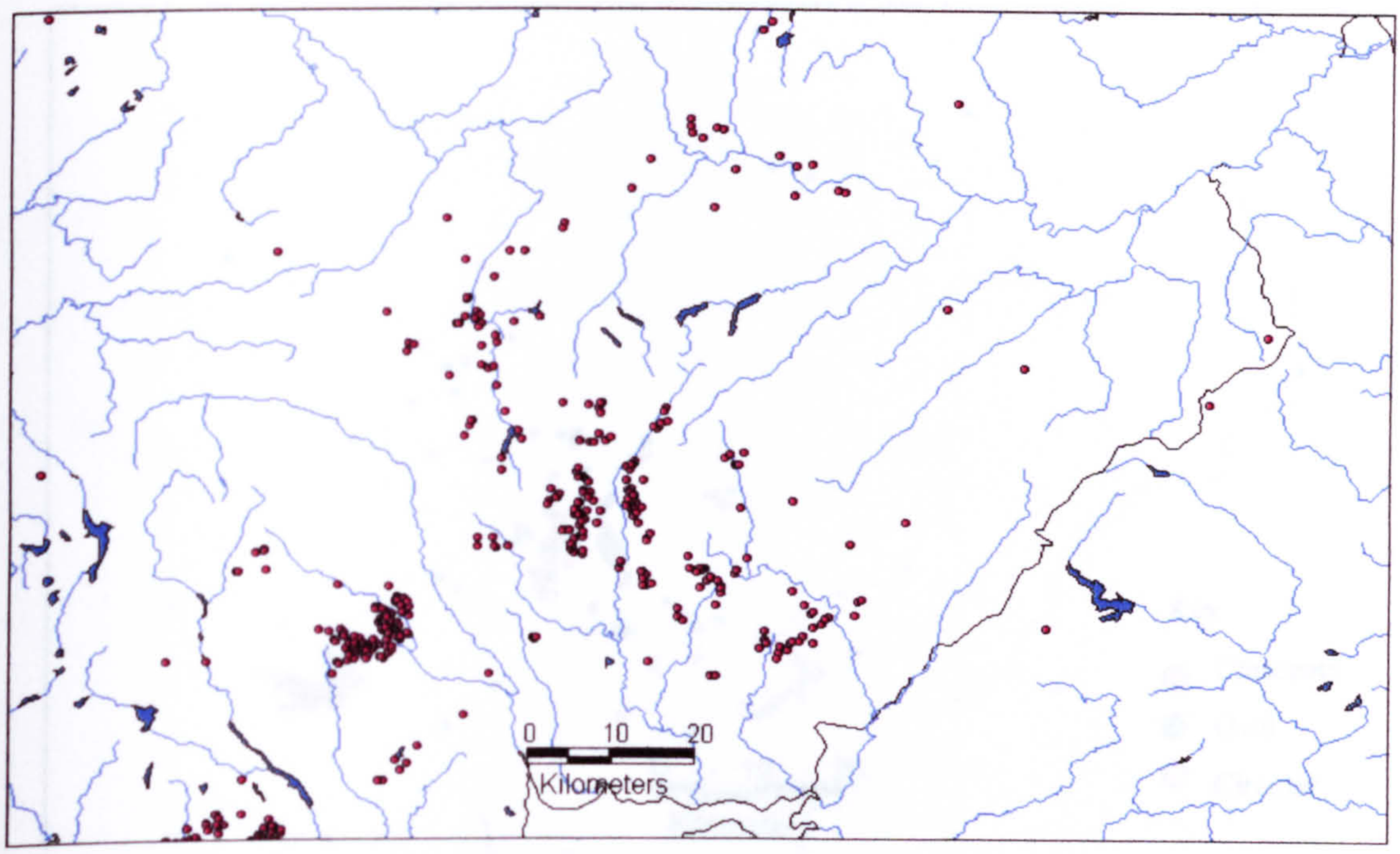

A.7a Distribution of Burnt Mounds in Borders and Southern Uplands (Data from RCAHMS Canmore Database)

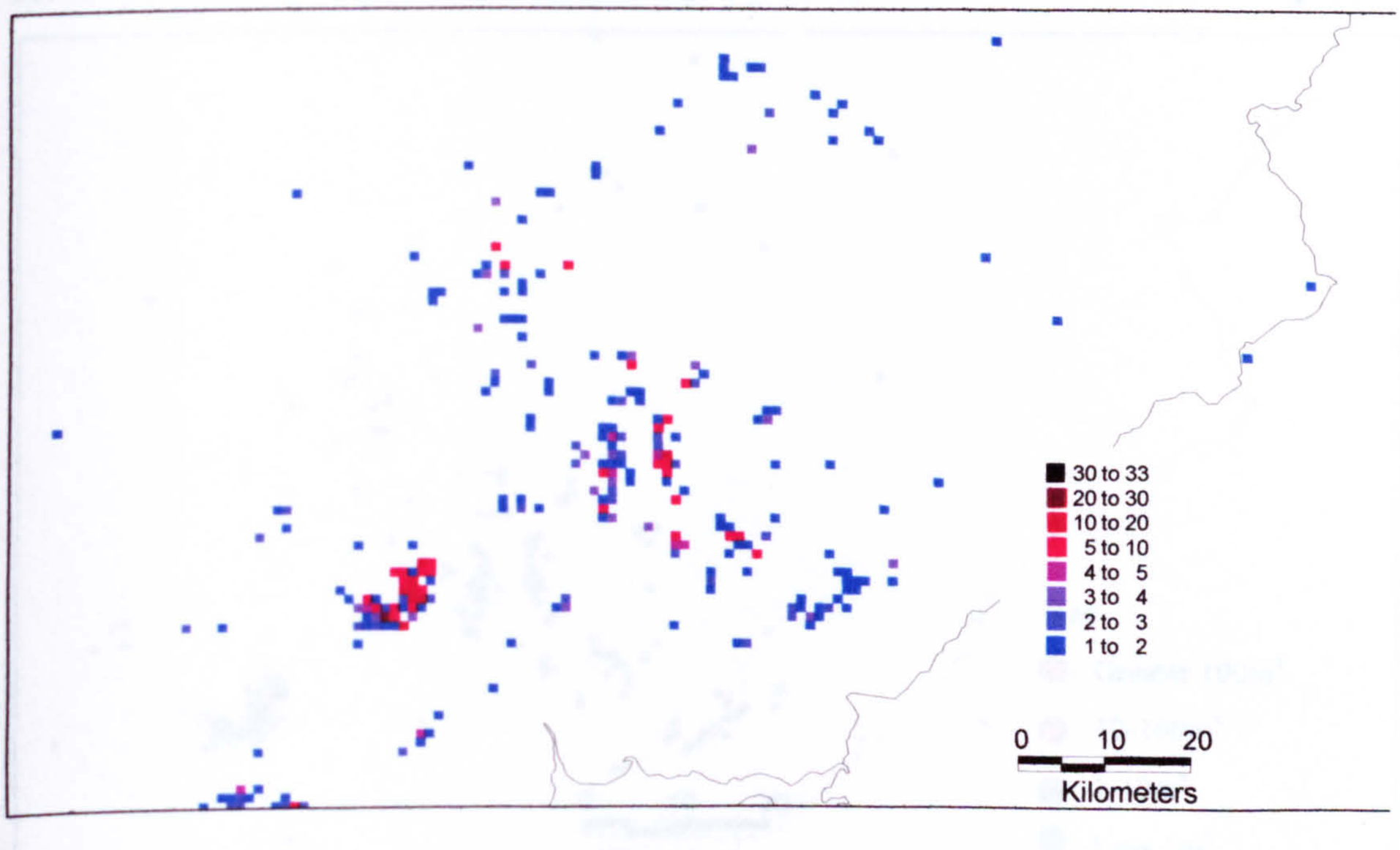

A.7b Density of Burnt Mounds in Borders and Southern Uplands (per km^2)

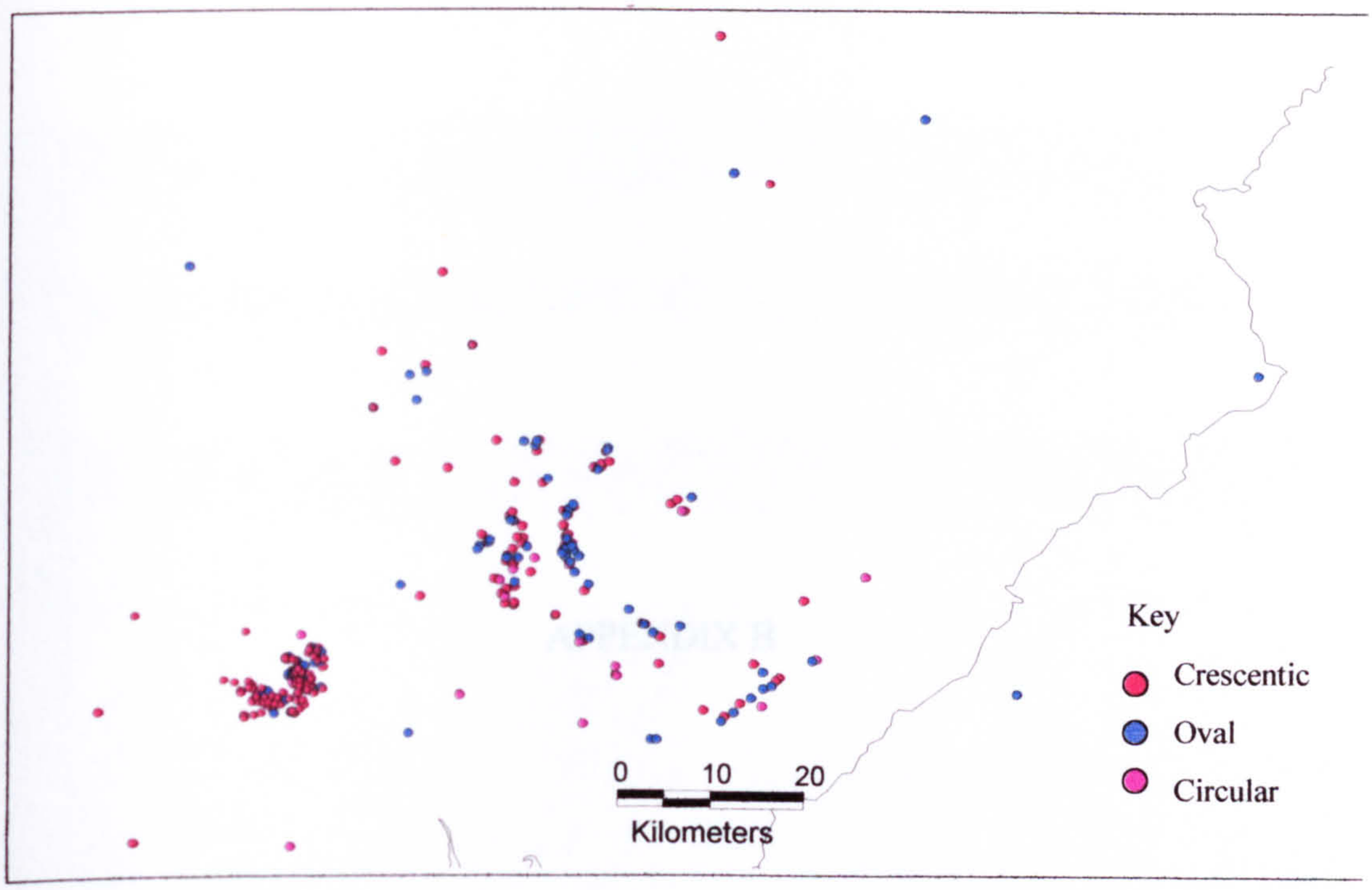

A.7c Distribution of Burnt Mounds by Shape, Borders and Southern Uplands

A.7d Distribution of Burnt Mounds by Volume, Borders and Southern Uplands

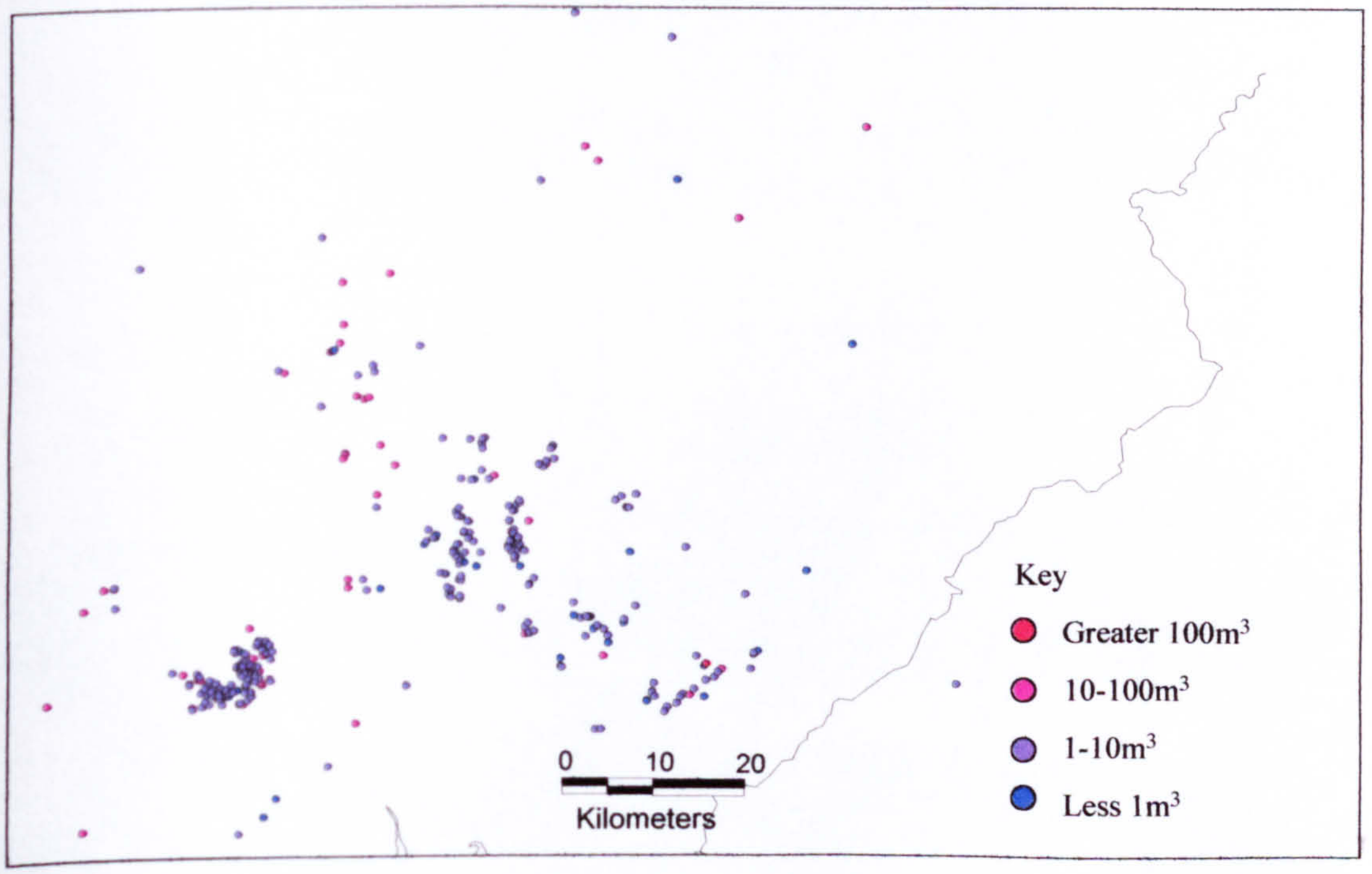

APPENDIX B

APPENDIX B

RADIOCARBON DATES FOR BURNT MOUNDS IN SCOTLAND

Site	NGR	Reference	Material	Lab Code	Cal Date	Lab Age	Error	d13c
Auld Taggart 2, Luce Bay	NX15166700	Russell-White 1990	charcoal	GU-2416	AD1020 to 1250	890	50	-24.9
Auld Taggart, Luce Bay	NX15136696	Russell-White 1990	charcoal	GU-2413	AD1000-1210	950	50	-26.8
Auld Taggart, Luce Bay	NX15136696	Russell-White 1990	charcoal	GU-2414	AD1060 to 1300	800	50	-29.1
Auld Taggart, Luce Bay	NX15136696	Russell-White 1990	charcoal	GU-2417	AD1020 to 1250	890	50	-26.7
Blairhall Burn	NX999846	Strachan et al 1998	charcoal	B-73548	1320 to 1130 cal BC	3000	80	
Borichill Mhor, Islay	NR307652	Russell-White 1990	charcoal	GU-1465	2500 to 1750 cal BC	3695	60	-25.5
Castle Hill	NS950200	Ward 1984	charcoal	AA-12589	2340 to 1920 cal BC	3725	65	-26.7
Castle Hill	NS950200	Ward 1998	charcoal	AA-12590	1690 to 1390 cal BC	3240	70	-26.3
Castle Hill	NS950200	Ward 1984	charcoal	AA-12591	2150 to 1770 cal BC	3615	65	-26.2
Cleuchbrae	NY10359330	Duncan 1999	wood	OxA-8832	1430 cal BC to 1130 cal BC	3055	45	-26.9
Cleuchbrae	NY10359330	Duncan 1999	charcoal	OxA-8833	1770 cal BC to 1520 cal BC	3380	40	-25.4
Cleuchbrae	NY10359330	Duncan 1999	wood	OxA-8800	1260 cal BC to 920 cal BC	2885	45	-28.5
Cleuchbrae	NY10359330	Duncan 1999	charcoal	OxA-8801	1500 cal BC to 1260 cal BC	3115	40	-26.5
Craggie Basin, Kildonan	NC915184	Russell-White 1990	charcoal	GU-2483	890 to 1160 AD	1030	50	-26.1
Cruise 1	NX188631	Russell-White 1990	charcoal	GU-2411	2030 to 1740 cal BC	3540	50	-26.4
Daer Reservoir, Crawford	NS986083	Ward 1998	charcoal	AA-30356	2570 cal BC to 2200 cal BC	3915	55	-26.9
Dervaird	NX224582	Russell-White 1990	wood	GU-2330	1620 to 1400 cal BC	3230	50	-27
Dervaird	NX224582	Russell-White 1990	charcoal	GU-2331	1530 to 1300 cal BC	3160	50	-27.7
Gabsnout 1	NX196610	Russell-White 1990	charcoal	GU-2415	1450 to 900 cal BC	2950	100	-26.2
Hopeterrick	NT210350	Ward 1999	charcoal	AA-30358	2200 cal BC to 1880 cal BC	3650	55	-23.8
Hopeterrick	NT210350	Ward 1999	charcoal	AA-30360	2470 cal BC to 2140 cal BC	3850	55	-25.8
Kilearnan Hill	NC953174	McIntyre 1998	charcoal	GU-1913	1130 to 790 cal BC	2750	80	-25.8
Kilearnan Hill	NC95201730	McIntyre 1998	charcoal	GU-1915	1300 to 1490 AD	510	60	-26.8
Kilearnan Hill	NC953174	McIntyre 1998	charcoal	GU-1912	1050 to 400 cal BC	2660	95	-26.4
Kilearnan Hill	NC953174	McIntyre 1998	charcoal	GU-1914	1150 to 830 cal BC	2815	60	-26.9
Kilearnan Hill	NC953174	McIntyre 1998	charcoal	GU-1921	1260 to 810 cal BC	2820	85	-27
Kirkhill Farm	NY10419258	Pollard 1993	charcoal	GU-3859	3100 to 2500 cal BC	4240	90	-26.7

Site	NGR	Reference	Material	Lab Code	Cal Date	Lab Age	Error	d13c
Kirkhill Farm	NY10419258	Pollard 1993	charcoal	GU-4189	3030 to 2690 cal BC	4280	50	-26.5
Kirkhill Farm	NY10419258	Pollard 1993	charcoal	GU-4191	2900 to 2600 cal BC	4200	50	-25.9
Kirkhill Farm	NY10419258	Pollard 1993	charcoal	GU-4192	3090 to 2700 cal BC	4300	60	-26
Kirkhill Farm	NY10419258	Pollard 1993	charcoal	GU-4193	2880 to 2580 cal BC	4150	50	-25.2
Lady Glassary Wood		Anthony et al 1999	charcoal	GU7865	2700-2460 cal BC	4030	60	
Lairg	NC5803	McCullagh and Tipping 1998	charcoal	GU-2822	1050 to 820 cal BC	2780	50	-26.7
Lairg	NC5803	McCullagh and Tipping 1998	charcoal	GU-3133	2020 to 1680 cal BC	3520	60	-26.2
Lairg	NC5803	McCullagh and Tipping 1998	charcoal	GU-3134	1600 to 1310 cal BC	3180	50	-26.2
Lairg	NC5803	McCullagh and Tipping 1998	charcoal	GU-2820	1390 to 1050 cal BC	2990	50	-26.1
Lairg	NC5803	McCullagh and Tipping 1998	charcoal	GU-2819	1600 to 1260 cal BC	3160	60	-25.8
Lairg	NC5803	McCullagh and Tipping 1998	charcoal	GU-2821	1150 to 830 cal BC	2830	50	-26.2
Lairg	NC5803	McCullagh and Tipping 1998	charcoal	GU-3135	1610 to 1120 cal BC	3120	90	-27.1
Lairg	NC5803	McCullagh and Tipping 1998	charcoal	GU-3136	1410 to 1110 cal BC	3020	50	-26.4
Liddle, Orkney	ND841465	Huxtable et al 1976	charcoal	SRR-701	1257 to 830 cal BC	2826	75	
Liddle, Orkney	ND841465	Huxtable et al 1976	peat	SRR-525	802 to 413 cal BC	2508	45	
Machrie North, Arran	NR899343	Barber and Lehane 1990	charcoal	GU-1566	2470 to 2040 cal BC	3825	65	-22.5
Machrie North, Arran	NR899343	Barber and Lehane 1990	charcoal	GU-1567	2490 to 2130 cal BC	3860	65	-25
Machrie North, Arran	NR899343	Barber and Lehane 1990	charcoal	GU-1568	2050 to 1400 cal BC	3405	115	-25
Machrie North, Arran	NR899343	Barber and Lehane 1990	charcoal	GU-1569	2460 to 2030 cal BC	3800	65	-25
Muirhead,	NY13148159	Robins 1993	charcoal	GU-3853	1390 to 940 cal BC	2960	70	-26.5
Muirhead,	NY13148159	Robins 1993	charcoal	GU-3854	1370 to 920 cal BC	2920	70	-26.3
Stair Lodge	NX17716686	Barber, 1990	charcoal	GU-2412	2200 to 1930 cal BC	3680	50	
Tangwick	HU23357751	Wilson & Moore 1999	charred grain	OxA-8195	1880 cal BC to 1520 cal BC	3390	55	-24.6
Tangwick	HU23357751	Wilson & Moore 1999	charred root	OxA-8196	1130 cal BC to 830 cal BC	2815	40	-24
Tougs,	HU378338	Hedges 1986	wood	GU-1110	2200 to 1500 cal BC	3525	75	-26.2
Tougs,	HU378338	Hedges 1986	wood	GU-1111	2300 to 1650 cal BC	3610	60	-29.3

APPENDIX C

TOPOGRAPHIC AND GEOLOGICAL DISTRIBUTION MAPS FOR AREAS SAMPLED IN SHETLAND

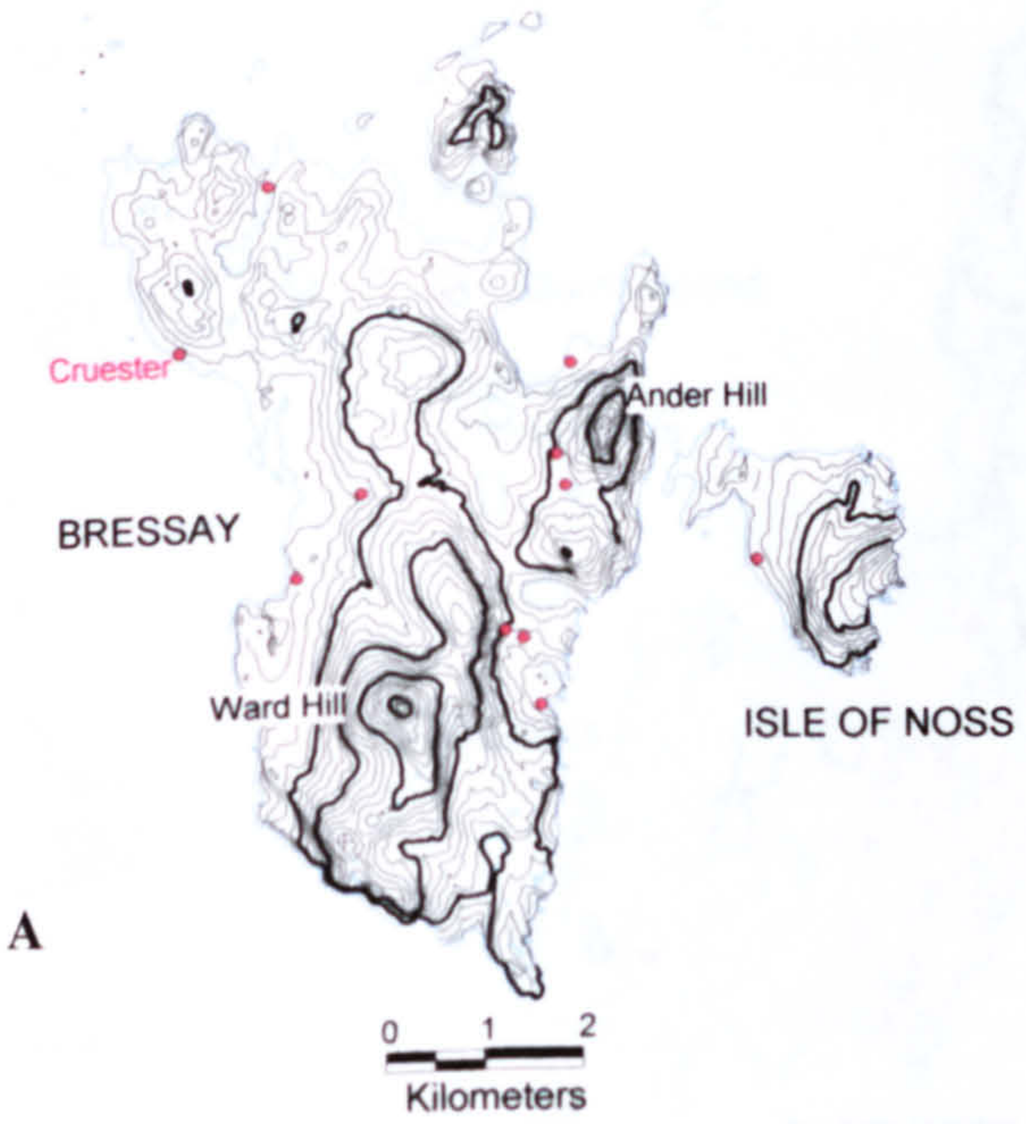

A

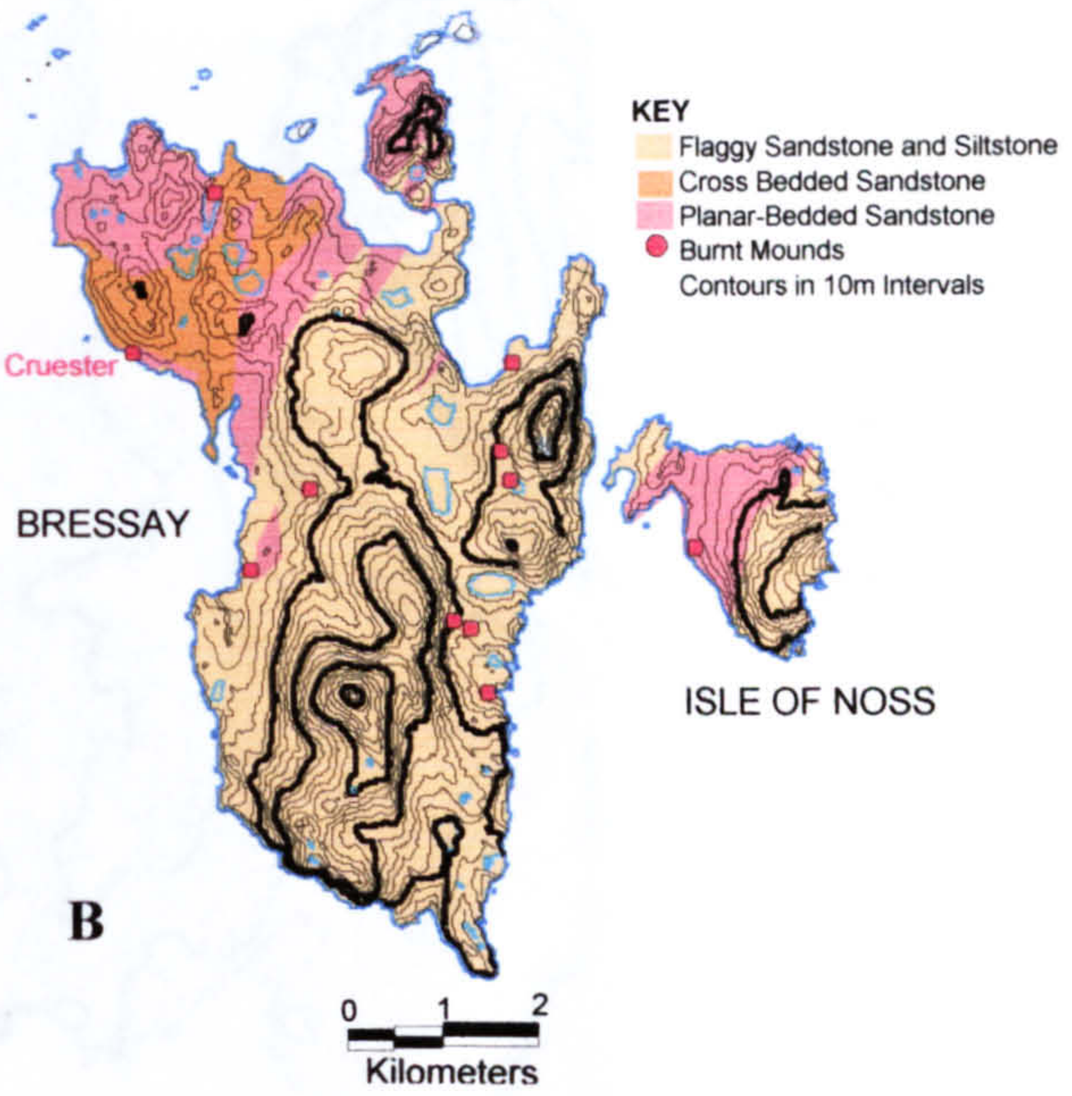

B

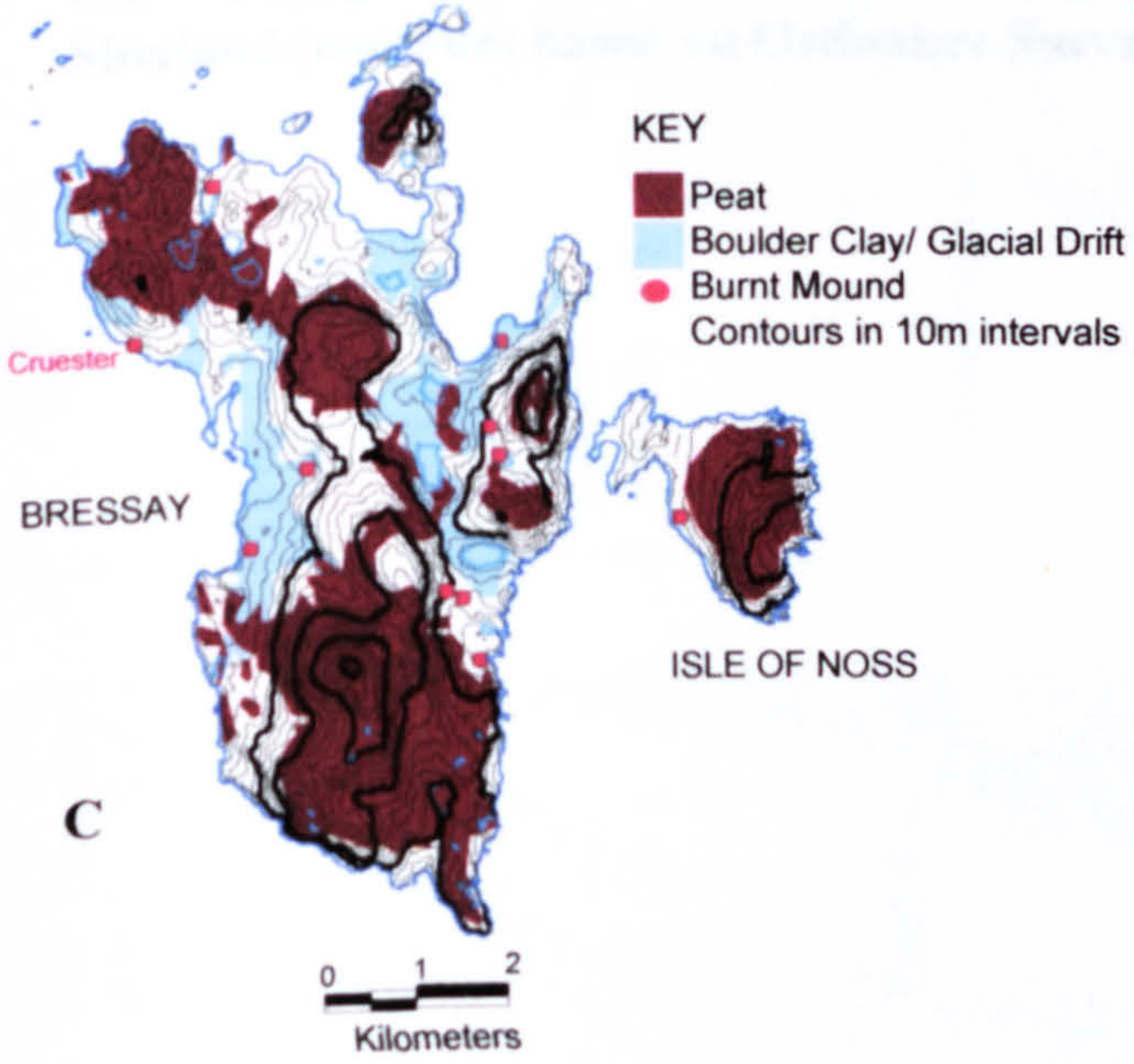

C

C.1 a. Distribution of Burnt Mounds on Bressay in Relation to Topography (contours based on Ordnance Survey Digimap Panorama data)

b. Distribution of Burnt Mounds on Bressay in Relation to Solid Geology (BGS, 1982a)

c. Distribution of Burnt Mounds on Bressay in Relation to Drift Geology (BGS, 1982b)

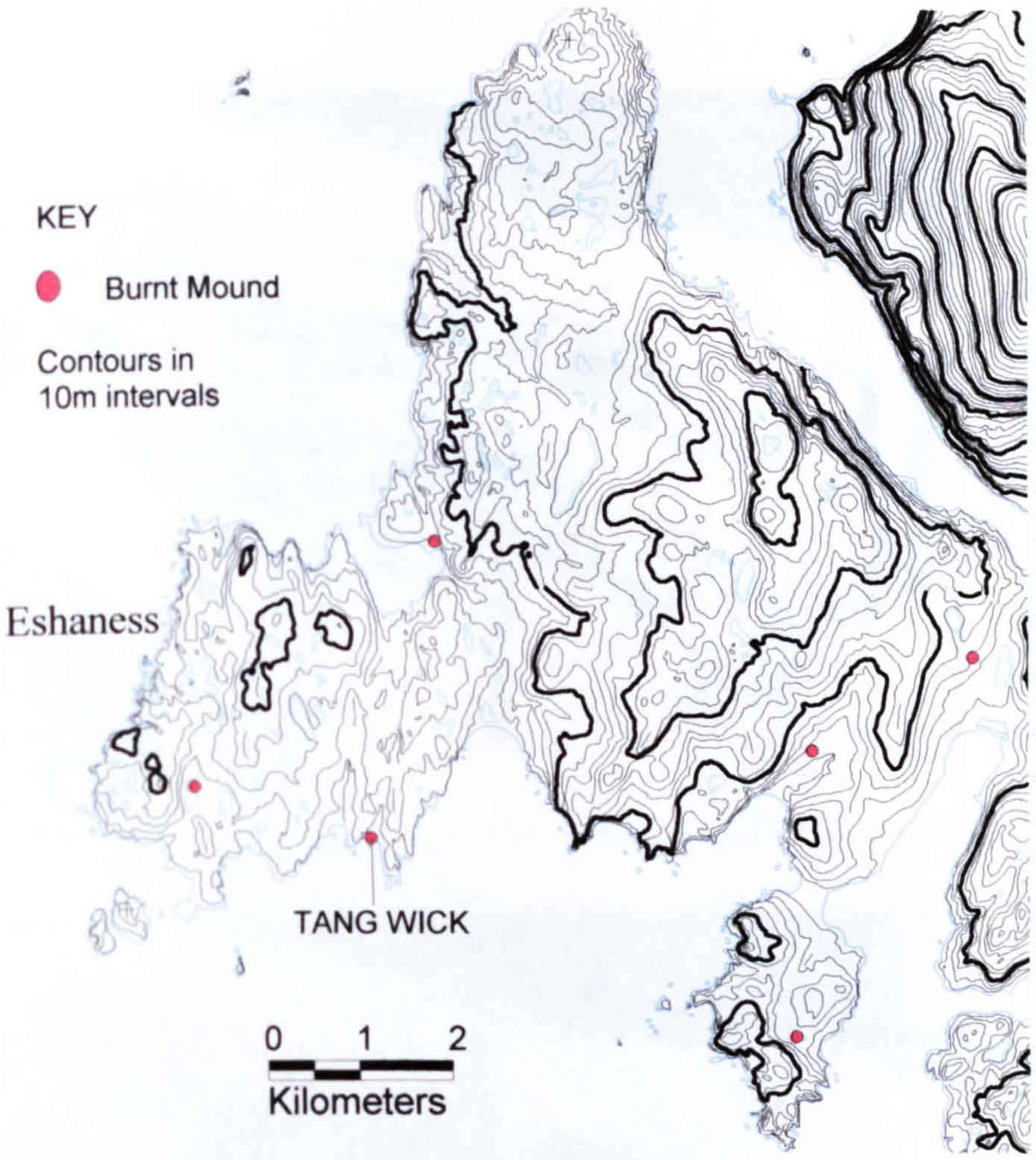

C.2 Topography and distribution of Burnt Mounds on Eshaness Peninsula, Shetland (contours based on Ordnance Survey Digimap Panorama data)

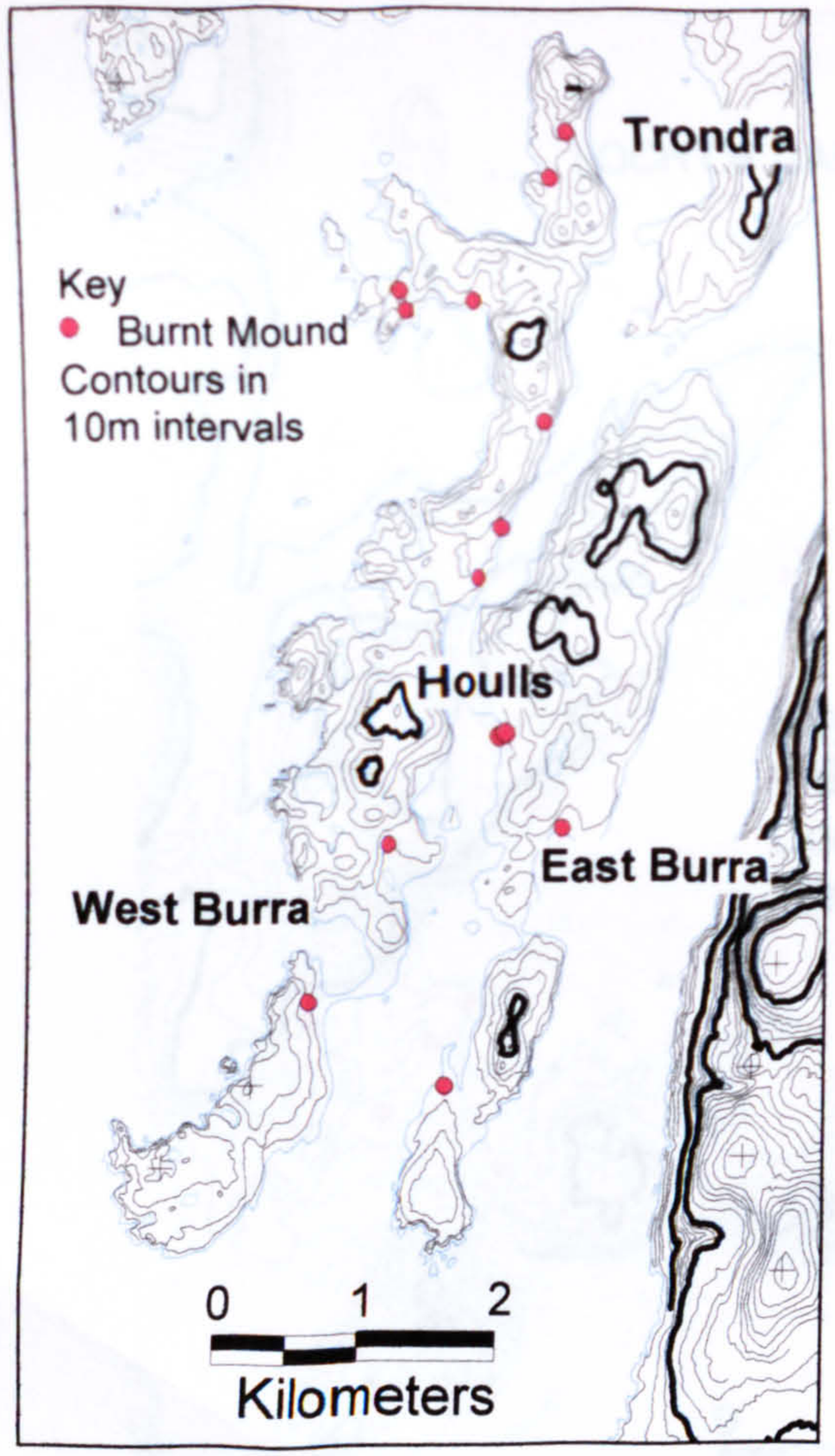

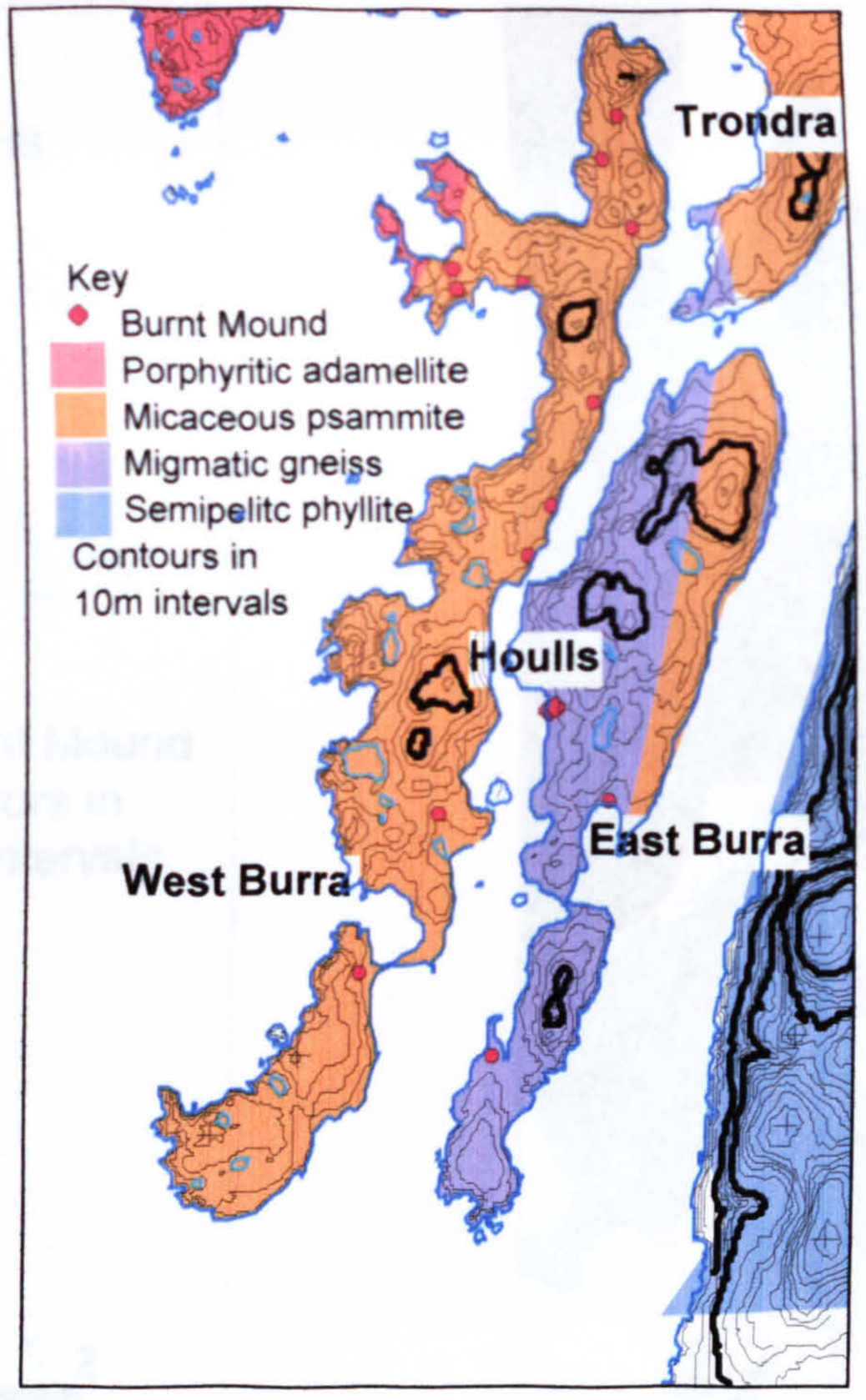

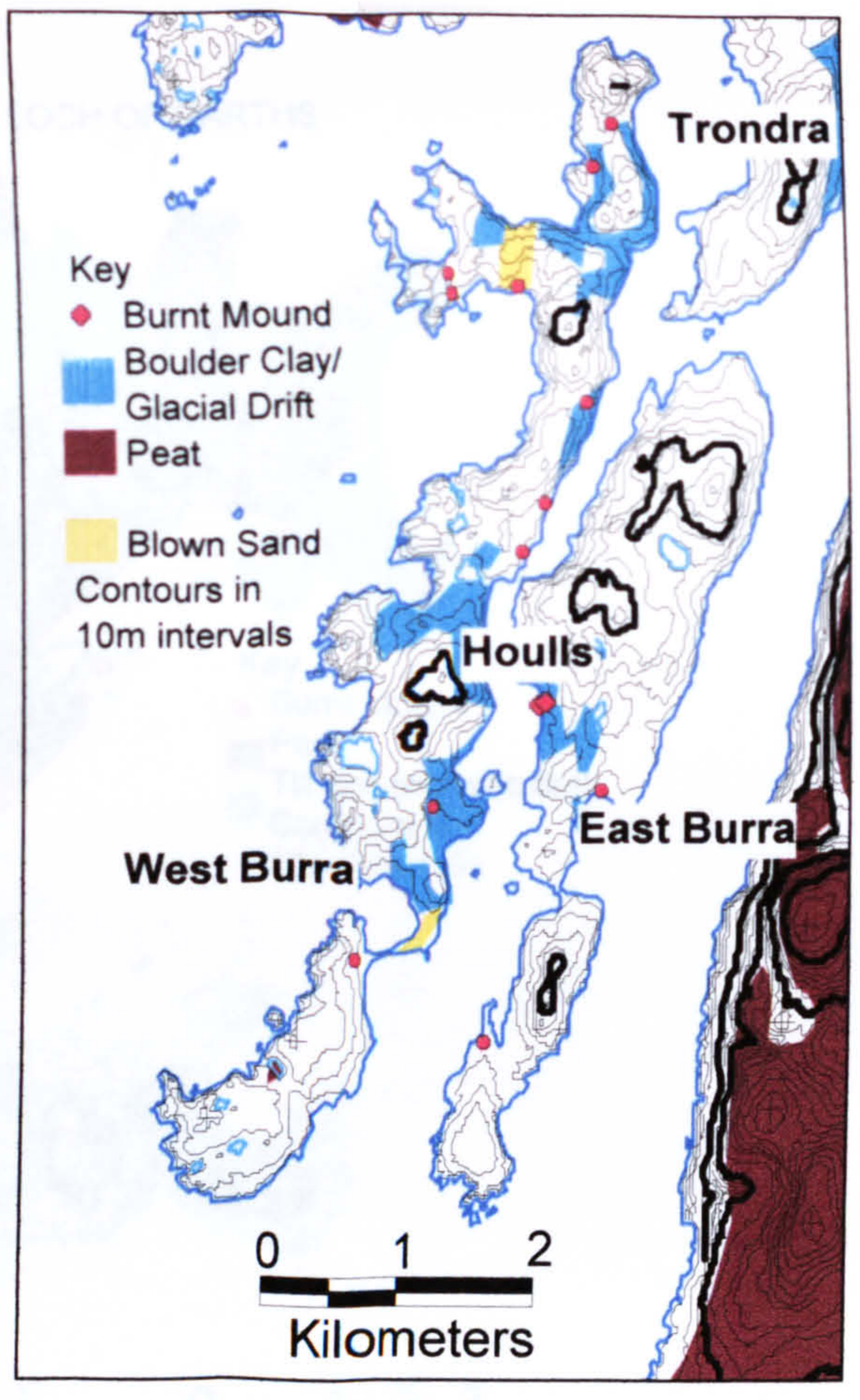

C.3 a. Distribution of Burnt Mounds on Burra in Relation to Topography (contours based on Ordnance Survey Digimap Panorama data) b. Distribution of Burnt Mounds on Burra in Relation to Solid Geology (BGS 1978a) c. Distribution of Burnt Mounds on Burra in Relation to Drift Geology (BGS 1978b)

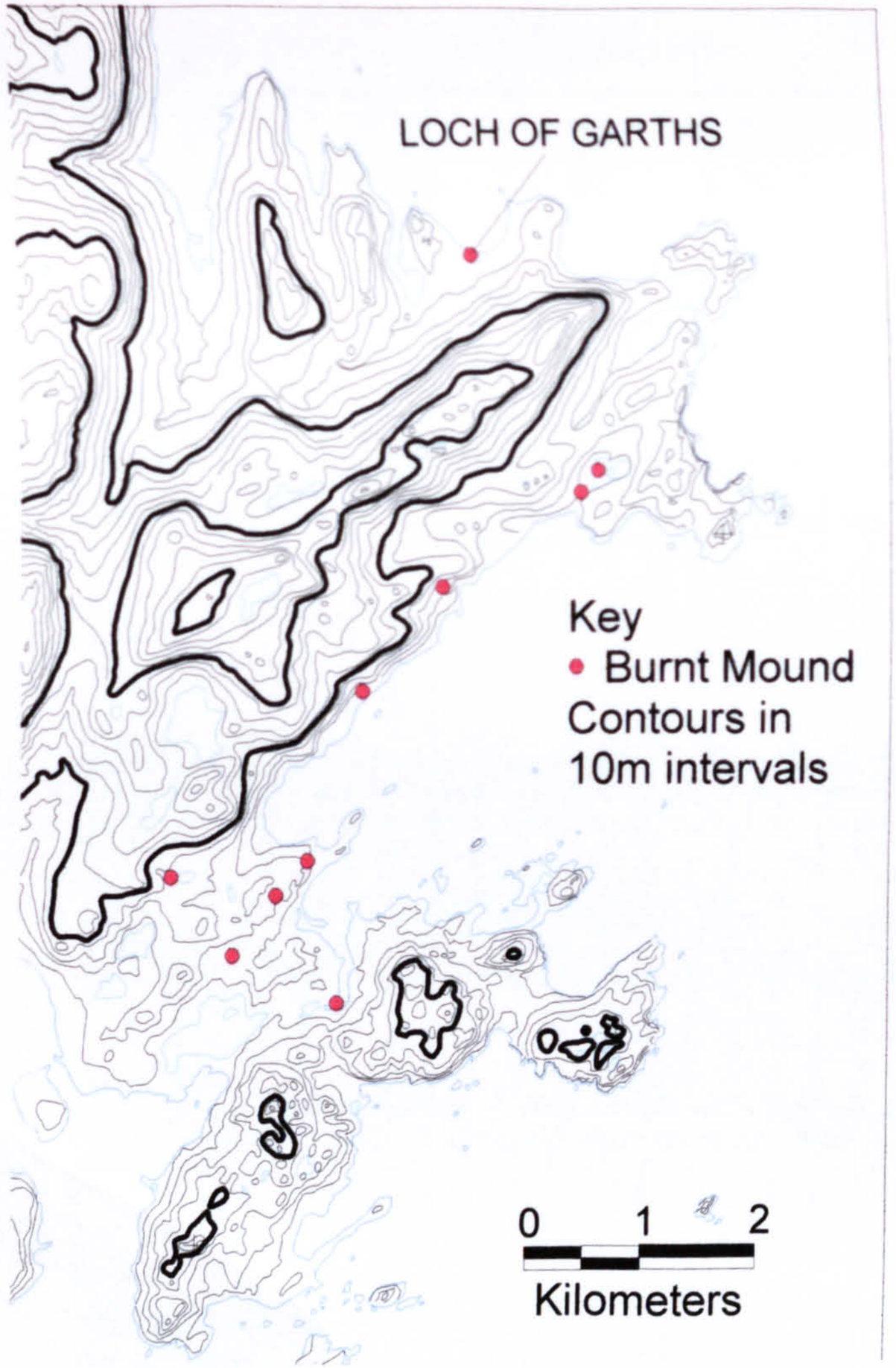

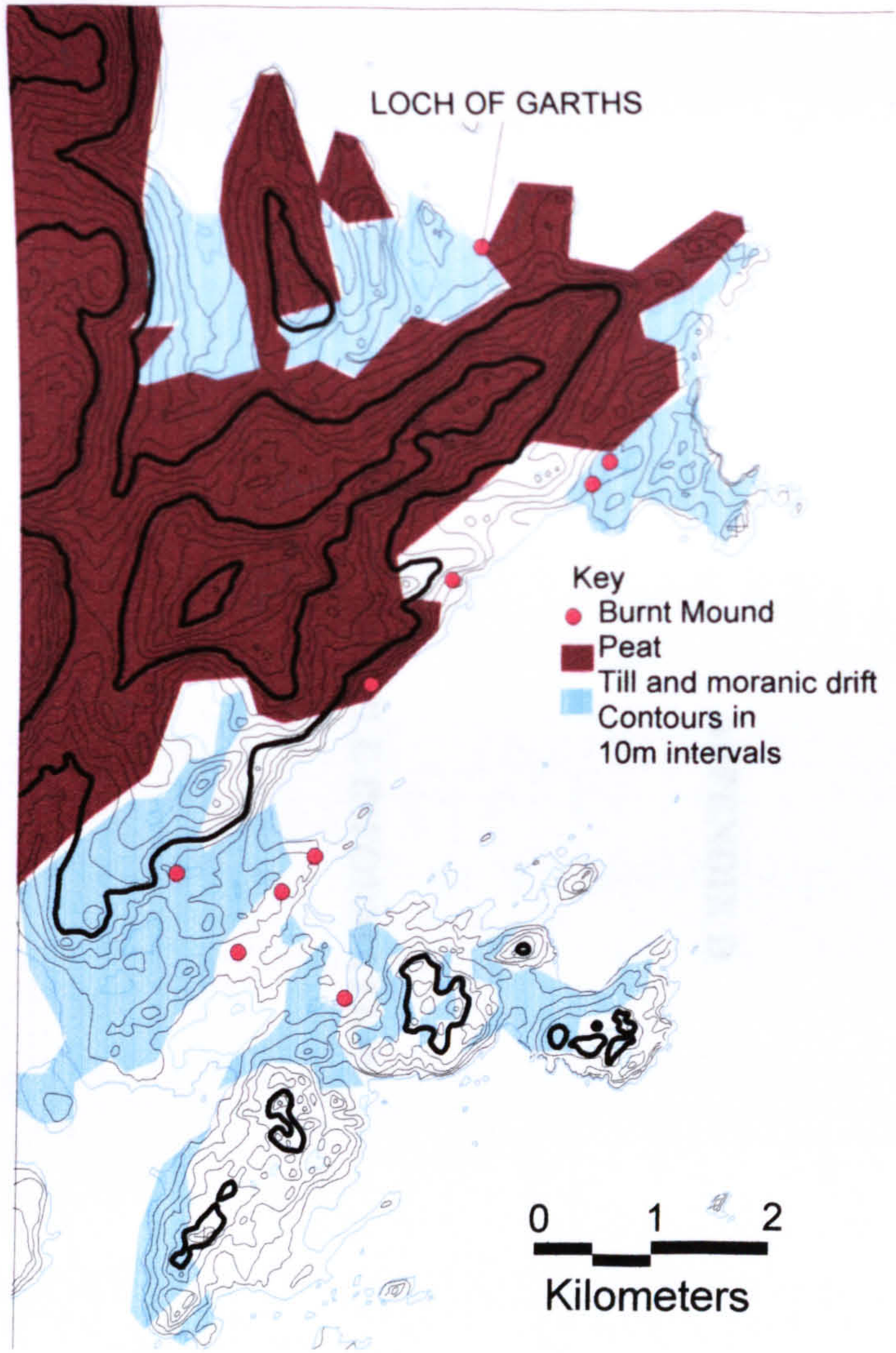

C.4 a. Distribution of Burnt mounds in Relation to Topography, Nesting, Shetland (contours based on Ordnance Survey Digimap Panorama data) b. Distribution of Burnt mounds in Relation to Drift Geology, Nesting, Shetland (BGS, 1971b)

APPENDIX D

SAMPLE INFORMATION

Table D1 Percentage yields for sieved fractions, Orkney Samples

Site	Pos	SUTL No.	Trimmed sample Weight (g)	<90µm (%)	90-125µm (%)	125-250µm (%)	250-500µm (%)
Liddle	1	1379	29.5	0.7	23.4	45.1	30.8
		1381	5.8	5.2	10.3	36.2	48.3
	2	1386	10.8	38.0	4.6	23.1	34.3
Dale	12	748	14.8	48.0	9.5	16.9	25.7
		749	23.0	45.7	17.0	25.7	11.7
		750	18.2	63.2	10.4	18.7	7.7
		751	26.8	60.1	9.3	17.2	13.4
		753	18.6	53.8	4.8	18.8	22.6
		754	16.2	53.7	11.1	19.8	15.4
		755	15.7	65.6	8.9	12.7	12.7
	13	760	24.6	52.4	8.9	18.3	20.3
		764	20.5	60.5	6.3	16.1	17.1
		765	23.6	55.5	8.9	14.8	20.8
		767	22.2	54.5	9.0	18.0	18.5
	14	768	18.3	47.0	9.3	17.5	26.2
		769	18.6	60.8	8.1	15.1	16.1
		774	18.8	54.3	8.5	16.0	21.3
		775	18.1	52.5	7.7	9.9	29.8
		777	28.3	44.2	16.6	16.3	23.0
		779	19.8	57.6	6.1	23.2	13.1
	15	782	25.7	56.8	14.4	21.4	7.4
		783	20.0	48.4	24.7	21.5	5.5
		784	14.5	40.7	22.8	27.6	9.0
		785	10.2	32.5	19.2	34.5	13.8
Skaill	1	1343	30.8	37.7	18.2	29.2	14.9
	2	1354	32.4	56.5	8.6	19.4	15.4
	3	1358	15.2	49.3	10.5	24.3	15.8
		1360	36.4	47.3	13.5	19.2	20.1
	5	815	134.9	5.6	9.6	71.9	12.9
	6	817	33.5	18.5	24.7	44.3	12.5
	O-1	1361	99.8	0.7	0.8	70.9	27.6
	O-2	1362	169.8	0.4	0.4	83.3	15.9
	O-3	1363	225.5	0.9	2.3	92.2	4.5
	O-4	1364	241.3	1.1	0.7	77.9	20.3
Knoll of Merrigarth	8	794	19.6	48.8	7.8	17.7	25.7
		795	28.9	66.7	3.3	15.7	14.3
	7	802	15.3	10.7	32.6	29.6	27.2
		803	26.5	32.2	12.5	36.4	19.0
Warness	9	842	17.5	60.7	12.1	13.6	13.6
	10	853	9.9	43.6	8.9	17.4	30.1
		857	45.1	26.4	11.7	42.5	19.3
	11	849	18.4	38.4	7.3	39.4	14.9
Stackelbrae	2	1374	6.0	41.7	6.7	23.3	28.3
Fersness	3	823	19.0	51.5	9.0	19.5	20.0
		824	18.8	49.4	14.3	18.3	18.0
	4	831	13.2	53.0	10.0	18.9	18.1
		833	16.2	41.4	6.9	21.6	30.1
Stenaquoy	1	836	25.7	55.4	20.4	17.3	6.9
	2	838	92.3	12.9	7.6	60.8	18.6
		839	15.5	38.9	24.3	22.6	14.2

Table D2 Percentage yields for sieved fractions, Shetland Samples

Site	Pos	SUTL No.	Trimmed sample Weight (g)	<90µm (%)	90-125µm (%)	125-250µm (%)	250-500µm (%)
Cruester	1	949	45.75	36.5	42.4	8.4	12.7
		951	16.7	55.1	28.1	6.0	10.8
		953	29.6	53.7	29.7	13.5	3.0
	2	958	37.6	68.6	21.3	3.5	6.6
	4	968	11.8	69.5	20.3	3.4	6.8
		969	20.2	56.9	27.7	5.4	9.9
	5	1051	23.2	60.3	23.3	4.7	11.6
		1053	18.8	54.8	26.6	6.9	11.7
	6	1054	27	68.1	25.9	4.1	1.9
		1055	37.3	62.2	24.4	4.8	8.6
	7	1059	33.1	32.6	38.1	10.9	18.4
	8	1062	50.1	69.7	18.8	4.2	7.4
		1063	31.1	72.0	19.6	3.2	5.1
		1064	52.1	65.3	25.5	3.6	5.6
	9	1068	23.3	64.8	24.9	3.9	6.4
	11	1075	23.2	34.5	47.8	8.6	9.1
		1076	74.2	21.2	46.8	8.9	23.2
		1077	47.87	53.2	26.9	6.9	13.0
	13	1081	13.7	65.0	23.8	26.5	24.4
	15	1086	36.2	24.1	27.9	24.0	24.0
		1087	22.3	34.0	29.6	25.6	10.8
		1088	32	33.5	31.1	25.3	10.1
	17	1094A	5.7	36.8	33.3	21.1	8.8
		1094B	13.2	39.4	34.1	20.5	6.1
		1095	50.1	37.3	35.1	10.8	16.8
		1096	41.9	39.4	35.1	11.2	14.3
		1097	38.5	78.4	16.1	2.1	3.4
	19	1100-1A	31.6	32.6	29.4	12.0	25.9
		1100-1B	12.9	27.9	32.6	13.2	26.4
		1100-2A	28.6	29.7	32.9	10.1	27.3
		1100-2B	13.5	25.2	28.1	12.6	34.1
Tangwick	1	1033	76.6	85.9	7.3	2.1	4.7
		1034	41.1	88.8	6.1	2.2	2.9
	2	1040	91.4	84.1	7.9	2.1	5.9
		1041	27.4	83.2	6.9	3.3	6.6
		1043	8.5	49.4	29.4	2.4	18.8
Houlls	1	970	36	46.9	28.9	8.9	15.3
		971	38	42.1	30.8	8.4	18.7
		976	21	53.3	35.7	11.0	0.0
		978	30.1	38.9	30.9	9.6	20.6
	2	983	16.9	47.9	27.8	7.7	16.6
	3	991	26.2	38.2	27.9	10.7	23.3
		993	15	44.0	29.3	8.0	18.7
	4	1003	27.8	28.8	28.1	11.2	32.0
		1004	31.6	42.7	25.9	8.9	22.5
Loch of Garths	1	1006	21	45.7	32.9	8.6	12.9
		1007	29.6	42.9	30.4	8.4	18.2
		1008	9.6	59.4	26.0	6.3	8.3
	2	1017	9.1	61.5	23.1	4.4	11.0
		1018	12.9	58.9	26.4	4.7	10.1
		1020	17.5	49.7	32.6	7.4	10.3

Table D3 Mineral yields, Orkney Samples

Site	Pos	SUTL No.	Size Frac (μm)	2.51-2.58 gcc^{-1} (mg)	2.58-2.62 gcc^{-1} (mg)	2.62-2.74 gcc^{-1} (mg)	>2.74gcc^{-1} (mg)	Quartz Yield (mg)
Liddle	1	1379	90-125	215	744	412	272	213
		1381	125-250	160	40	0	0	0
	2	1386	125-250	60	80	200	0	0
Dale	12	748	90-125	11.7	20.8	103.7	5.6	0
		749	90-125	110	131	1526	40	42
		750	90-125	14	442	258	41	5
			125-250	33	125	800	91	0.3
		751	90-125	20	465	355	426	52
			125-250	60	700	700	140	172
		753	90-125	27.5		330.5	10	10
		754	125-250	0.8	32.9	524.5	57.9	21
		755	90-125	0	0	28.9	0	0
			125-250	0	0	73.1	277.2	17
	13	760	90-125	71	567	5	0	16
		764	90-125	0	182	121	0	10
			125-250	0	287	500	40	1.6
		765	90-125	36	162	867	40	123
			125-250	102	206	550	135	40
		767	90-125	26.3	53.7	216	44.7	19
	14	768	90-125	122	374	192	20	56
		769	90-125	0	125	233	0	18
			125-250	342	370	312	30	2.8
		774	90-125	115	99	913	0	12
		775	90-125	33.7	58.8	207.6	72.2	43
		777	90-125	125	452	2041	175	126
		779	90-125	20.7	106	40.8	32.6	3
	15	782	90-125	91.8	108.1	1198	0	96
		783	90-125	149	112	1853	0	152
		784	90-125	142	100	1416	100	265
		785	90-125	0	40	0	60	0
Skaill	1	1343	90-125	100	100	600	40	121
	2	1354	90-125	50	0	300	40	90
	3	1358	90-125	40	0	200	40	76
		1360	90-125	300	200	300	100	106
	5	815	90-125	315	1145	1214	188	210
	6	817	90-125	171.7	716	494	100.7	240
	O-1	1361	125-250	27	67	500	26	325
	O-2	1362	125-250	49	11	917	39	716
	O-3	1363	125-250	63	19	1246	46	906
	O-4	1364	125-250	32	43	1211	21	814
Knoll of Merrigarth	8	794	90-125	72.4	270.8	136	36.8	
		795	90-125	36.8	238.3	60	19.9	0
			125-250	79	463	169	56	25
	7	802	90-125	103.3	395.8	66.1	24.8	0
			125-250	--	--	--	--	20
		803	90-125	180	228.7	67.6	33	0
			125-250	---	---	--	---	67
Warness	9	842	90-125	109	578.3	54.6	30.9	0
	10	853	90-125	34	12	0	0	0
		857	90-125	169.3	1285	85.3	44.3	2

Site	Pos	SUTL No.	Size Frac (μm)	2.51-2.58 gcc^{-1} (mg)	2.58-2.62 gcc^{-1} (mg)	2.62-2.74 gcc^{-1}(mg)	>2.74gcc^{-1} (mg)	Quartz Yield (mg)
			125-250	---	---	---	---	76
	11	849	90-125	217.6	304	22.2	9	12
			125-250	---	---	---	----	65
Stackelbrae	2	1374	125-250	10	0	400	20	6
Fersness	3	823	90-125	30	566	128	14	0
			125-250	---	---	---	---	12
		824	90-125	108	760	205	75	45
			125-250	---	---	---	---	39
	4	831	90-125	49	333	103	25.7	46
		833	90-125	15.8	43	0	12	0
Stenaquoy	1	836	90-125	216	1151	101	30	3
			125-250	---	---	---	---	29
	2	838	90-125	277	1434	191.7	61.5	59
		839	90-125	150.8	799.5	1424	211.6	470

Table D4 Mineral Yields, Shetland Samples

Site	Pos	SUTL No.	Size Frac (μm)	2.51-2.58 gcc^{-1} (mg)	2.58-2.62 gcc^{-1} (mg)	2.62-2.74 gcc^{-1}(mg)	>2.74 gcc^{-1} (mg)	Quartz Yield (mg)
Cruester	1	949	90-125	152	165	970	495	11
		951	125-250	96.4	336	1148	132.8	29
		953	125-250	180	706	817	117.3	126
	2	958	90-125	42.5	88	203	0	60
	4	968	125-250	138	286	310	72	267
		969	125-250	125	335	2687.4	201	1016
	5	1051	125-250	139.3	272	438	182	219
		1053	125-250	153	493	931	280	516
	6	1054	90-125	48.5	151.4	9.6	199.5	0
			125-250	195	593	2713	362	350
		1055	90-125	65	322.9	287.9	102	60
	7	1059	90-125	18	95	224	35	76
	8	1062	90-125	119	406	433	107	33
		1063	90-125	29.3	52	87.9	102.2	0
			90-125	90	223	1260	705.7	26
		1064	90-125	32.2	174.3	176.7	103.9	90
	9	1068	90-125	25.2	187	41.3	34.3	7
			125-250	143.2	737.7	730.9	129.4	96
	11	1075	90-125	27	143	108	0	60
		1076	90-125	263	340	1736	225	1071
		1077	90-125	8	0	450	140	100
	13	1081	90-125	0	67	163.3	59.4	11
			125-250	48.5	155.4	1714.7	506.7	46
	15	1086	90-125	0	33.4	791	250	17
		1087	90-125	25	30	907	257	336
		1088	90-125	52	61	1114	393	401
	17	1094A	125-250	17	34	412	57	36
		1094B	125-250	15	0	758	244	41
		1095	90-125	96	252	1134	213	31
		1096	90-125	110	196	1444	204	11
		1097	125-250	36	129	2005	535	939
	19	1100-1A	90-125	109	99	1000	250	470
		1100-1B	90-125	29	0	213	152.8	49

Site	Pos	SUTL No.	Size Frac (μm)	2.51-2.58 gcc^{-1} (mg)	2.58-2.62 gcc^{-1} (mg)	2.62-2.74 gcc^{-1}(mg)	>2.74 gcc^{-1} (mg)	Quartz Yield (mg)
		1100-2A	90-125	85	62	150	660	36
		1100-2B	90-125	40	0	60	65	41
Tangwick	1	1033	90-125	77	90	0	0	0
		1034	125-250	36	165	380	106	0
	2	1040	125-250	11	110	101	61	0
		1041	125-250	0	302	218	20	0
		1043	125-250	20	20	400	350	0
Houlls	1	970	90-125	60	118	663	219	29
		971	90-125	13	77	361	49	62
		976	90-125	10	23	100	0	19
			125-250	80	112	3900	720	36
		978	90-125	0	0	700	165	11
	2	983	90-125	0	93	60	0	1
			125-250	234	658	1986	385	914
	3	991	90-125	42	90	295	110	27
		993	90-125	0	30	0	0	0
			125-250	416	822	1005	250	828
	4	1003	90-125	42	877	50	0	20
		1004	90-125	23	206	338	131	107
Loch of Garths	1	1006	90-125	0	0	762.4	138.5	139
		1007	90-125	0	0	324	155	46
		1008	90-125	21.9	50.6	10	52	0
			125-250	58.4	706.9	707.3	308.7	127
	2	1017	125-250	286.2	437.1	674.6	172.7	326
		1018	125-250	19.7	33.6	1590	544	802
		1020	90-125	0	22.6	321	121	0
			125-250	0	38	1893	811	197

Table D5 Results of Water Content Measurements, Orkney Samples

Site	Pos	SUTL No.	FW	SW	Water Content (%)
Liddle	1	1379	6.3	6.6	4±3
		1381	17.1	17.3	9±8
	2	1386	11.5	12.0	6±6
Dale	12	748	7.3	10.1	5±5
		749	13.4	13.6	7±7
		750	18.0	18.4	9±9
		751	13.5	13.7	7±7
		753	5.6	6.2	3±3
		754	9.1	9.3	5±4
		755	14.7	15.5	8±7
	13	760	5.4	6.5	4±3
		764	2.6	4.7	3±2
		765	6.9	7.1	4±3
		767	6.4	9.1	5±4
	14	768	11.3	12.5	7±6
		769	8.3	8.5	5±4
		774	7.1	7.6	4±4
		775	11.1	12.5	6±6
		777	5.7	7.1	4±3
		779	9.2	12.0	6±6
	15	782	11.2	11.4	6±5
		783	7.4	8.7	5±4
		784	14.1	14.4	7±7
		785	17.7	18.2	9±9
Skaill	1	1343	1.2	4.6	3±2
	2	1354	2.2	5.7	3±3
	3	1358	1.0	4.6	3±2
		1360	2.6	6.3	32)3
	5	815	0.7	5.3	3±2
	6	817	0.7	7.3	4±3
	O-1	1361	15.6	32.7	20±5
	O-2	1362	16.4	49.3	20±5
	O-3	1363	13.2	22.4	20±5
	O-4	1364	19.6	21.1	20±5
Knoll of Merrigarth	8	794	1.8	2.4	2±2
		795	2.4	6.8	4±3
	7	802	10.2	15.9	8±8
		803	7.2	14.9	8±7
Warness	9	842	4.9	8.8	5±4
	10	853	9.7	11.2	6±6
		857	3.3	10.7	6±5
	11	849	10.5	10.6	6±5
Stackelbrae	2	1374	7.1	9.2	5±4
Fersness	3	823	1.7	7.7	4±3
		824	1.7	8.7	5±4
	4	831	2.4	5.6	3±2
		833	7.5	8.9	5±4
Stenaquoy	1	836	7.3	9.7	5±5
	2	838	1.1	6.7	4±3
		839	0.9	11.6	6±6

Table D6 Results of Water Content Measurements, Shetland Samples

Site	Pos	SUTL No.	FW	SW	Water Content (%)
Cruester	1	949	5.9	6.8	4±3
		951	0.1	5.0	3±2
		953	5.0	5.4	3±2
	2	958	4.1	6.0	3±3
	4	968	1.8	7.0	4±3
		969	1.3	2.0	1±1
	5	1051	3.1	3.2	2±1
		1053	2.9	3.6	2±2
	6	1054	4.9	5.1	3±2
		1055	6.5	6.9	4±3
	7	1059	5.5	6.5	4±3
	8	1062	5.0	6.0	3±3
		1063	7.7	7.8	4±4
		1064	3.0	4.0	2±2
	9	1068	2.0	3.0	2±1
	11	1075	4.0	4.1	2±2
		1076	11.9	11.9	6±6
		1077	4.5	4.6	3±2
	13	1081	3.2	3.2	2±1
	15	1086	2.6	2.6	2±1
		1087	1.9	2.5	2±1
		1088	2.7	3.6	2±2
	17	1094	1.8	1.9	1±1
		1095	2.1	2.5	2±1
		1096	1.7	1.9	1±1
		1097	2.9	3.5	2±2
	19	1100	3.2	5.0	3±2
Tangwick	1	1033	4.2	4.3	2±2
		1034	1.5	2.3	1±1
	2	1040	3.3	4.6	3±2
		1041	1.4	1.9	1±1
		1043	2.4	3.4	2±1
Houlls	1	970	4.1	4.4	2±2
		971	2.3	2.4	2±1
		976	3.1	3.4	2±1
		978	2.5	2.6	2±1
	2	983	1.6	2.4	2±1
	3	991	1.4	1.7	1±1
		993	3.3	3.9	2±2
	4	1003	2.0	2.1	1±1
		1004	2.1	2.3	1±1
Loch of Garths	1	1006	1.6	1.7	1±1
		1007	1.9	2.1	1±1
		1008	3.2	3.2	2±1
	2	1017	1.5	2.4	2±1
		1018	1.4	3.0	2±1
		1020	2.3	2.3	1±1

APPENDIX E

STRETCH AND SHIFT CORRECTION PROCEDURE

E1 STRETCH

The stretch (st) was calculated as the ratio of $t½P_{avg}$:$T½P_d$

Where $t½\ P_d$ is the disc T ½ - Peak temperature integral and $t½\ P_{avg}$ is the average temperature integral. The original spectrum was read into D(1,i), where i=1 to 500 (each temperature channel); then copied to D(2,i).

Where the value of st was less than 1 - implying the need to shrink the glow curve, the following corrections were made:

```
For i=1 to 500
        ll=st*i
        ul=st*(i+1) ' lower and upper limits of destination channels
        N=INT(LL)
        M=int(ul)
        IF N>500 THEN RETURN
        f=(1+N-ll)/st 'fraction of original counts going into channel int(ll)
      P=1-f

        d(1,N)=d(1,N)+f*d(2,i)
        d(1,M)=d(1,M)+P*d(2,i)
```

Where st was greater than 1, implying the need to stretch the glow curve:

```
      ll=st*i
        ul=st*(i+1) ' lower and upper limits of destination channels
        N=1+INT(LL)
        M=1+int(ul)
      IF N>500 THEN RETURN
        f=(N-ll)/st 'fraction of original counts going into channel int(ll)
      P=1-F


IF N+1=M THEN

        d(1,N)=d(1,N)+f*d(2,i)
        d(1,N+1)=d(1,N+1)+P*d(2,i)


IF N+1<> m THEN

                P=1/ST
```

```
H=1-P-F

d(1,N)=d(1,N)+f*d(2,i)
d(1,N+1)=d(1,N+1)+P*d(2,i)
d(1,n+2)=d(1,N+2)+H*d(2,I)
```

E2: SHIFT

For a positive shift – i.e shifting the glow curve up the temperature scale,

```
for i=1 to 500-sh
d(1,i)=d(2,i+sh)
```

For a negative shift,

```
for i=sh to 500
d(1,i)=d(2,i-sh)
```

APPENDIX F

FELDSPAR ADDITIVE DOSE PLATEAU PLOTS

F.1 LIDDLE

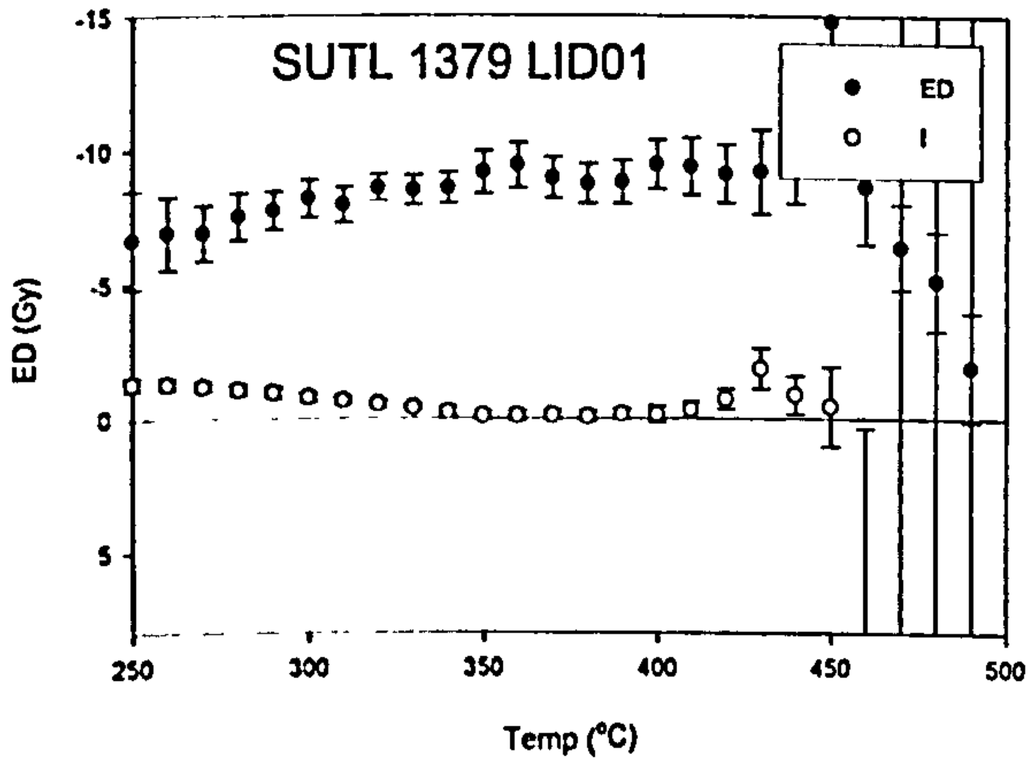

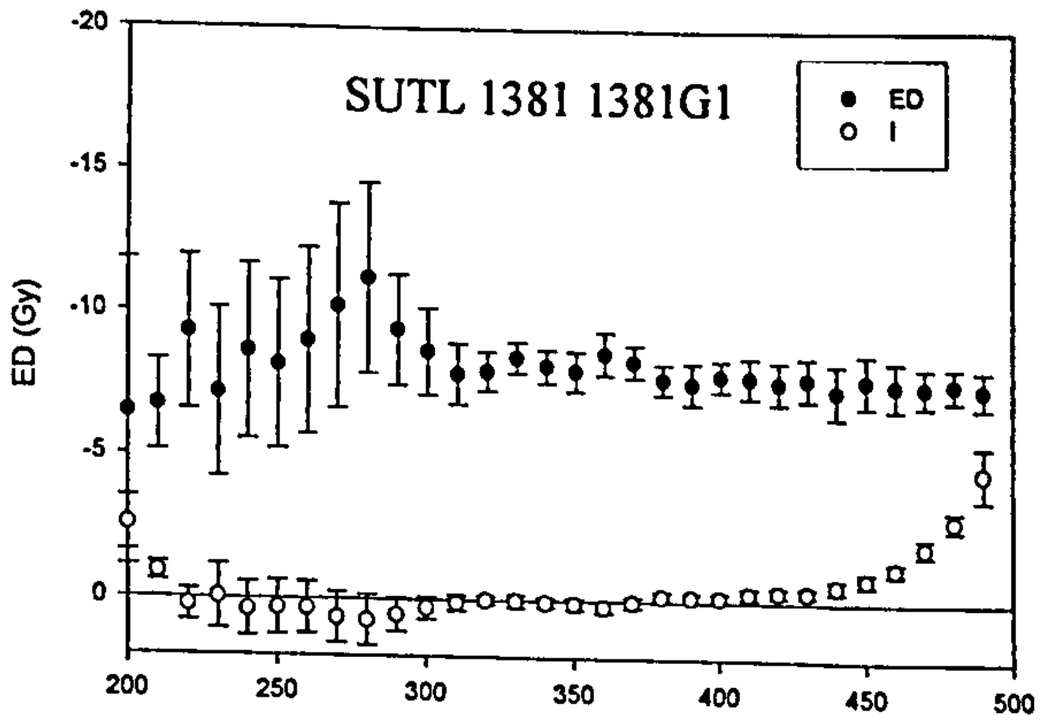

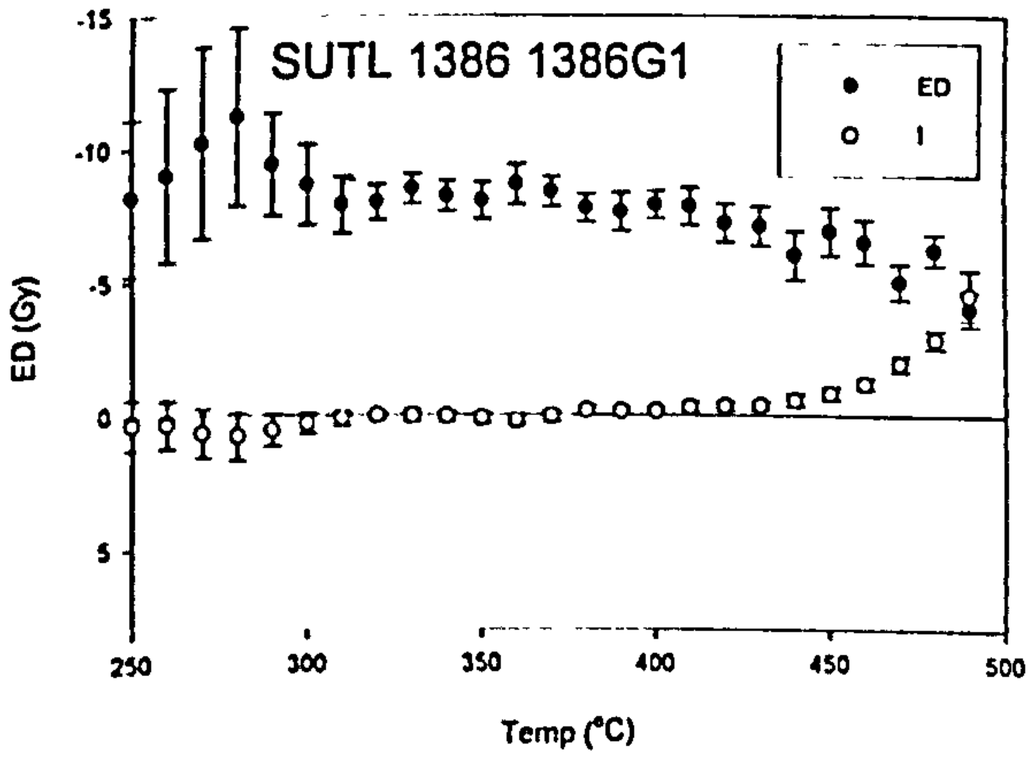

F.2 DALE

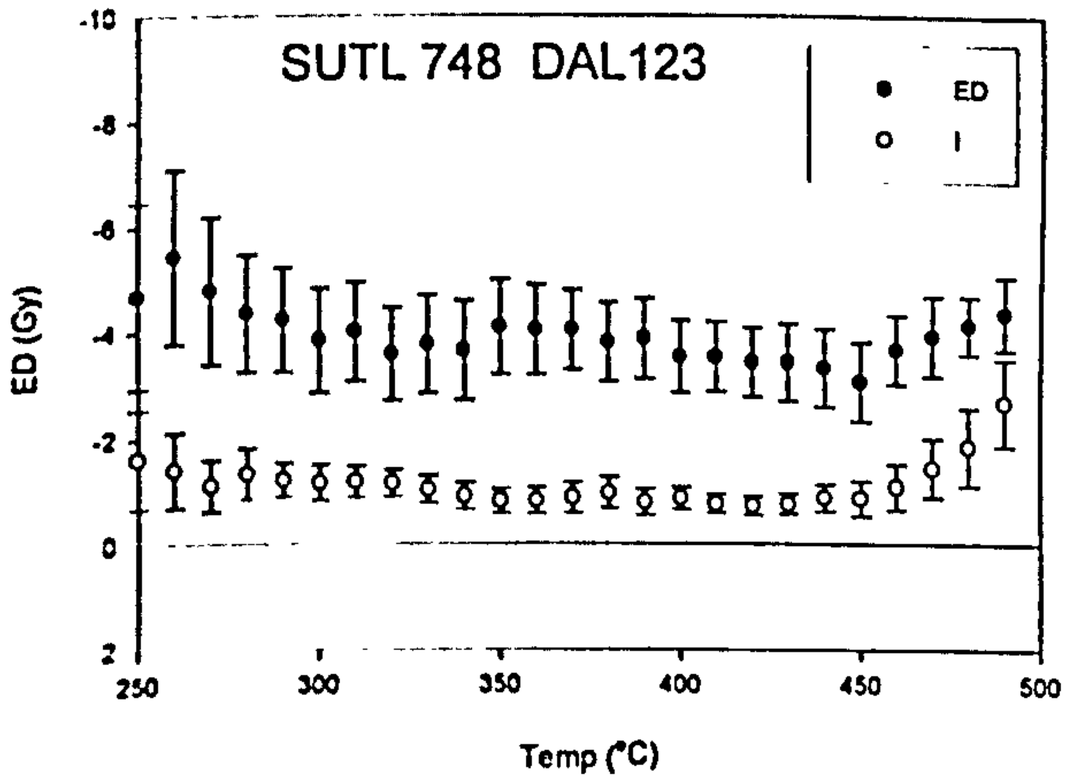

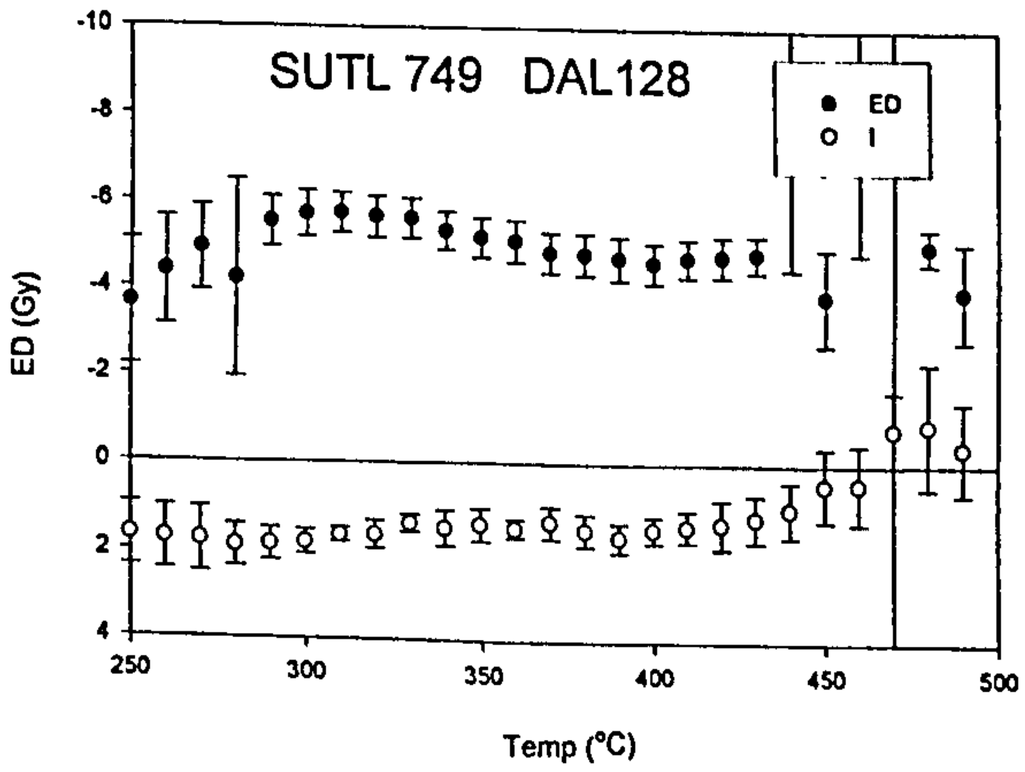

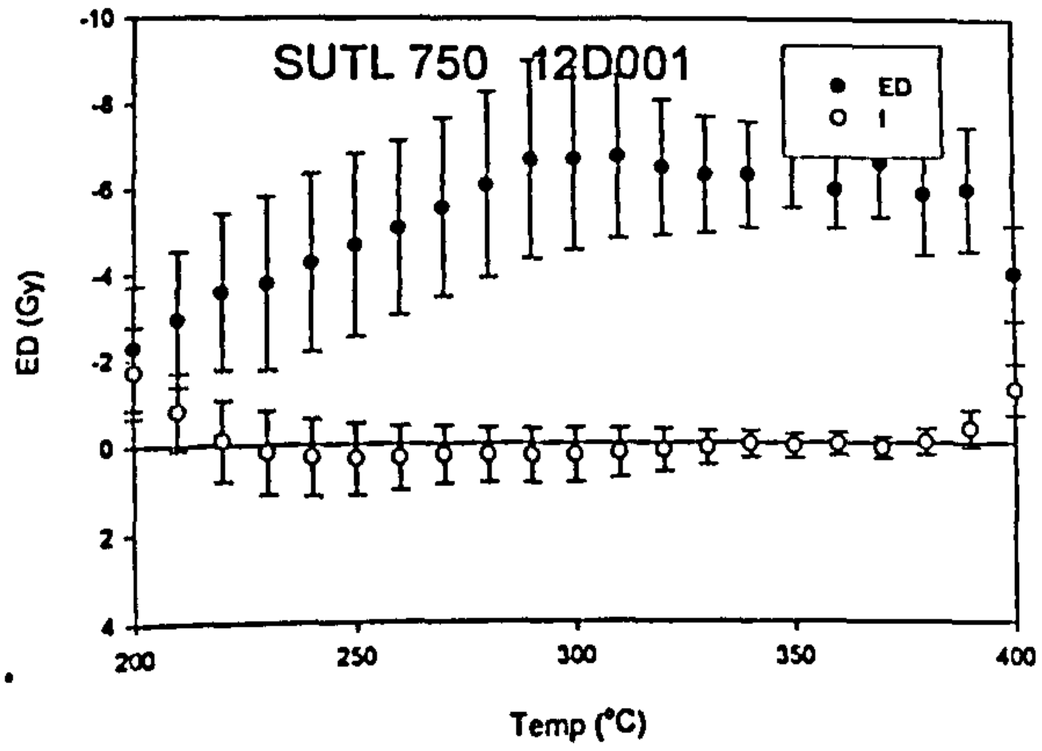
SUTL 750 12D001
ED
I
ED (Gy)
Temp (°C)

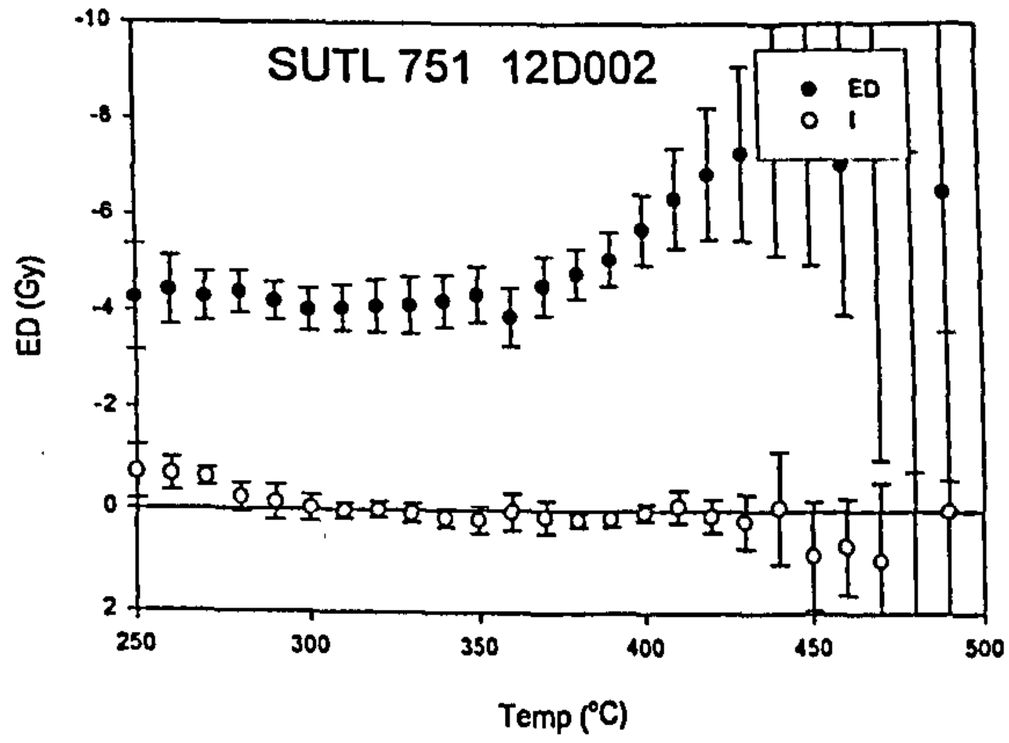
SUTL 751 12D002
ED
I
ED (Gy)
Temp (°C)

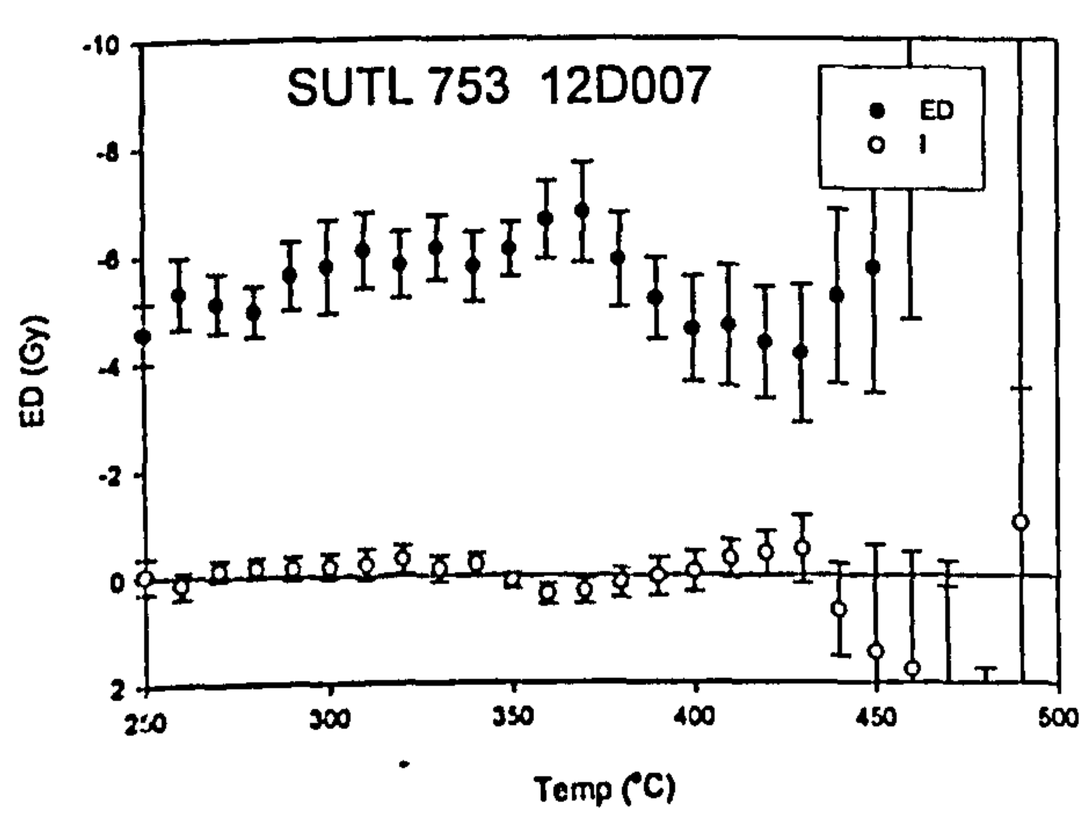
SUTL 753 12D007
ED
I
ED (Gy)
Temp (°C)

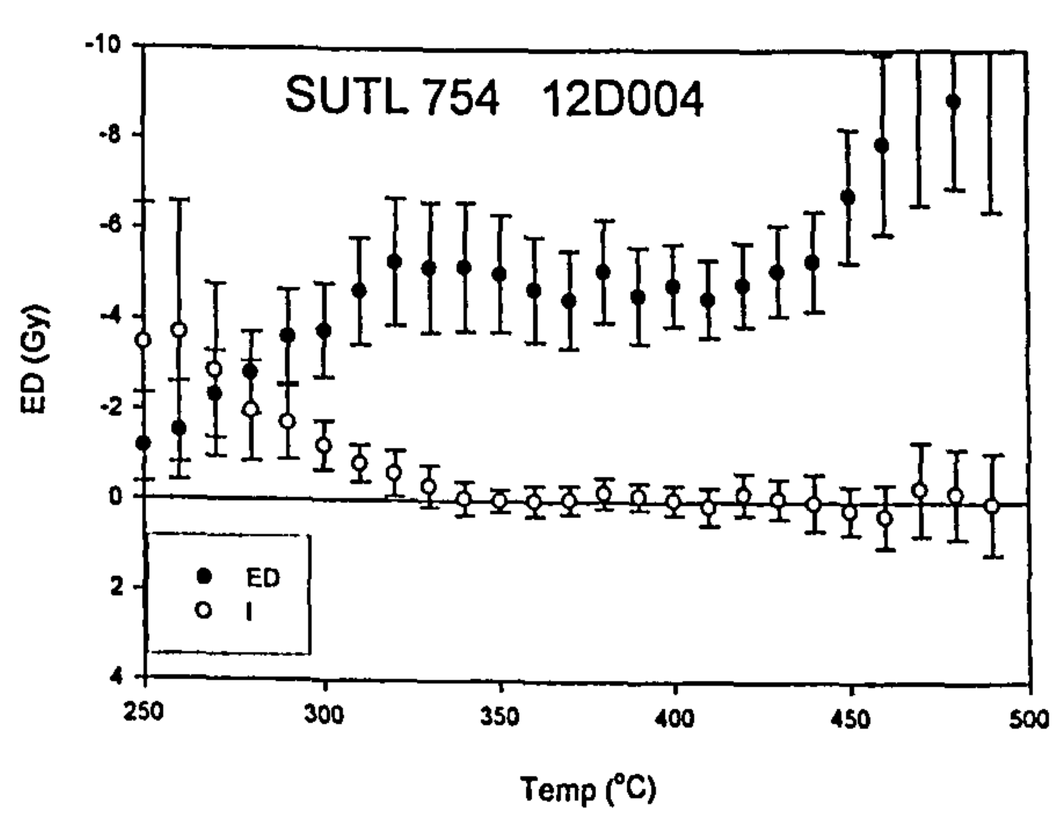
SUTL 754 12D004
ED
I
ED (Gy)
Temp (°C)

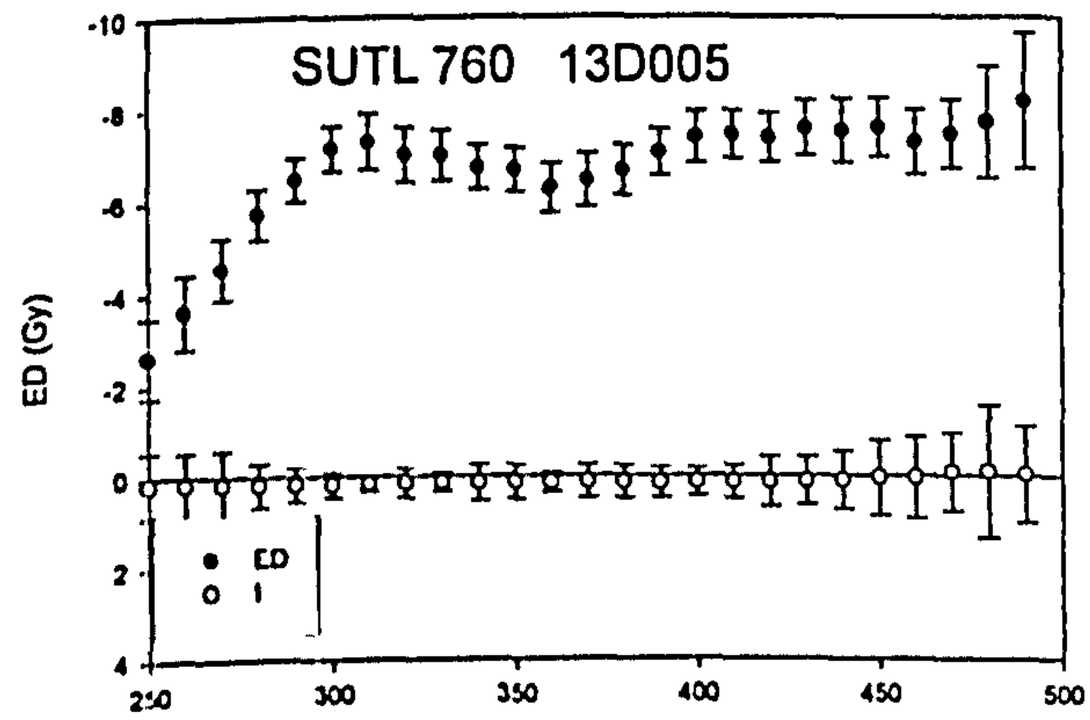
SUTL 760 13D005
ED
I
ED (Gy)
Temp (°C)

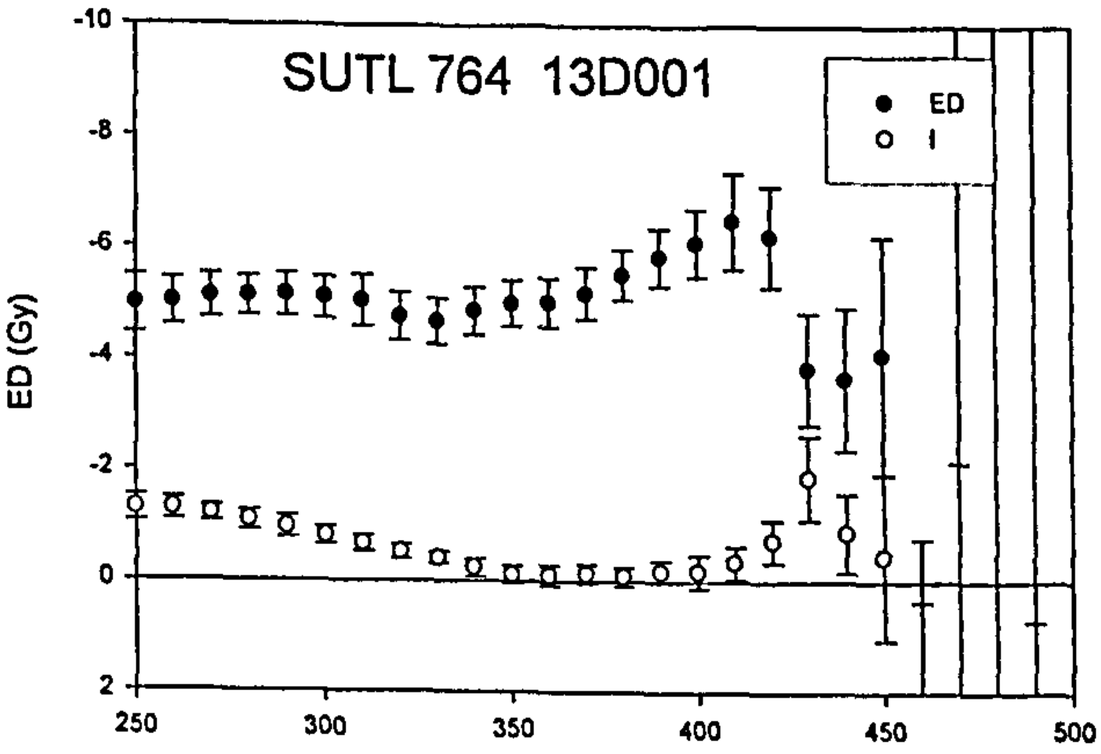
SUTL 764 13D001
ED
I
ED (Gy)
Temp (°C)

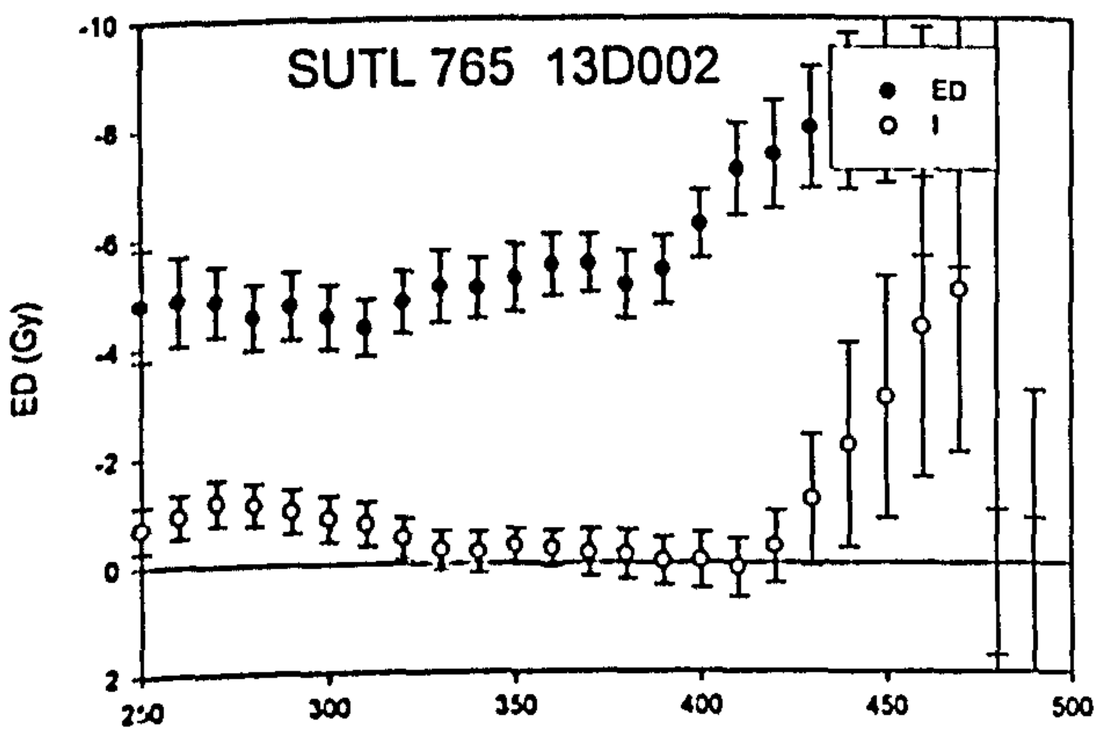
SUTL 765 13D002
ED
I
ED (Gy)
Temp (°C)

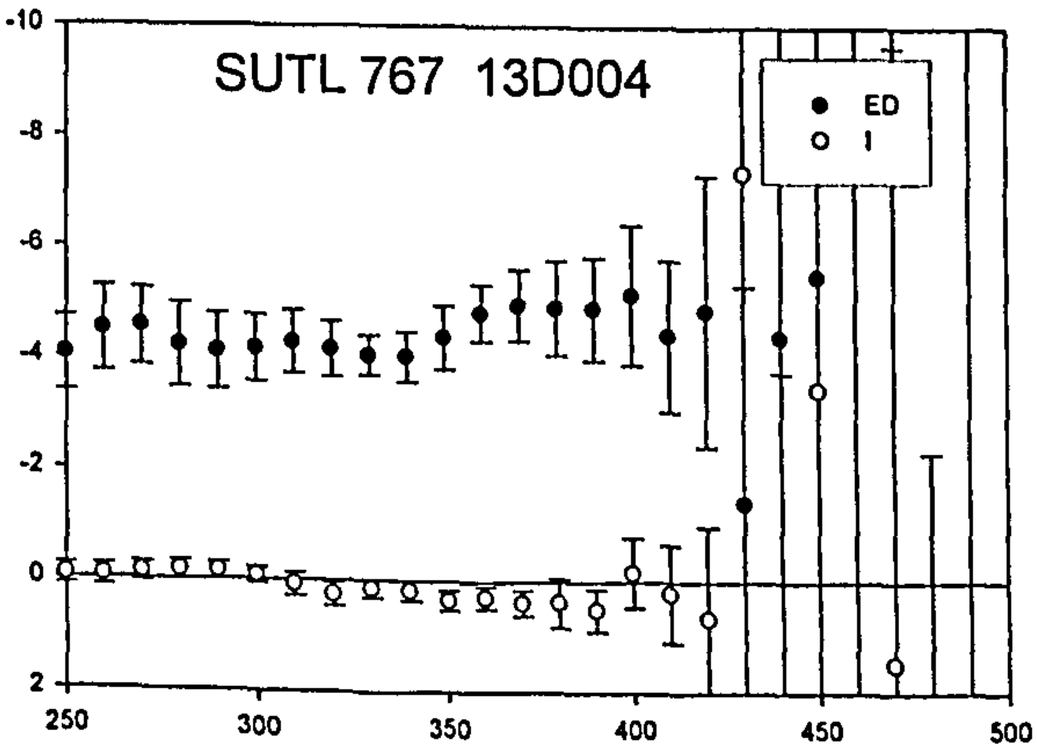
SUTL 767 13D004
ED
I
ED (Gy)
Temp (°C)

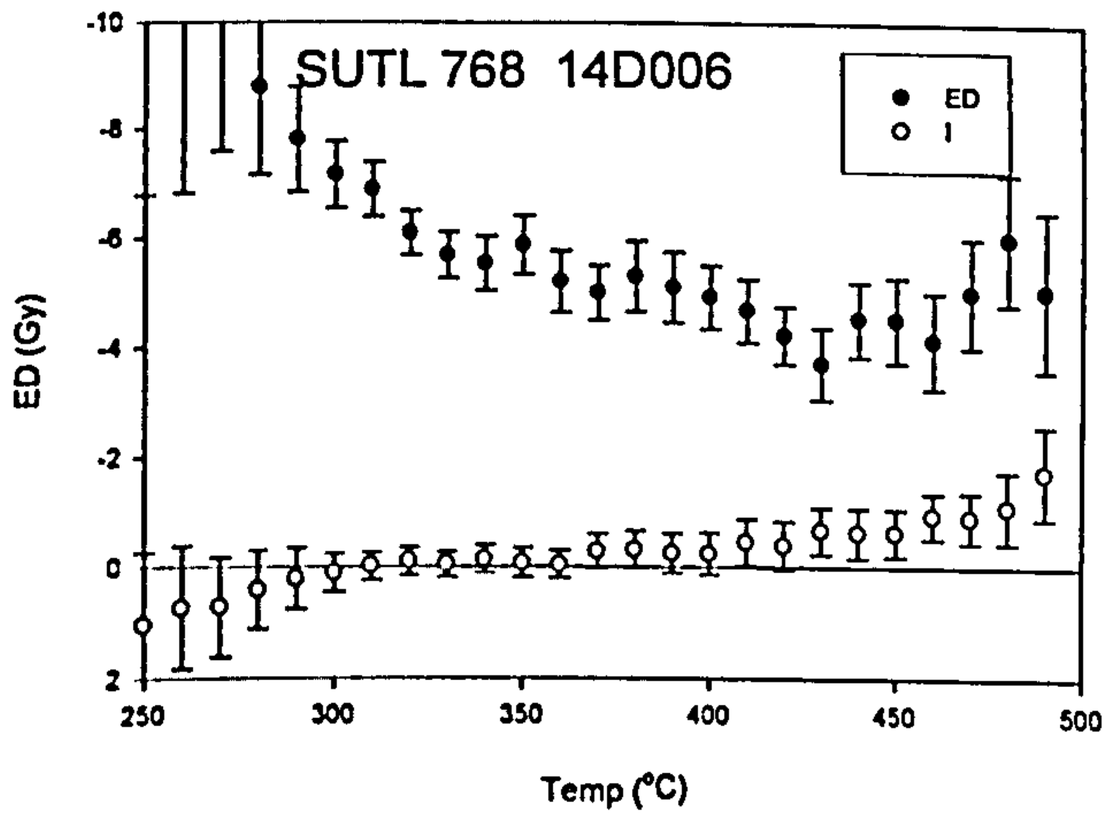
SUTL 768 14D006
ED
I
ED (Gy)
Temp (°C)

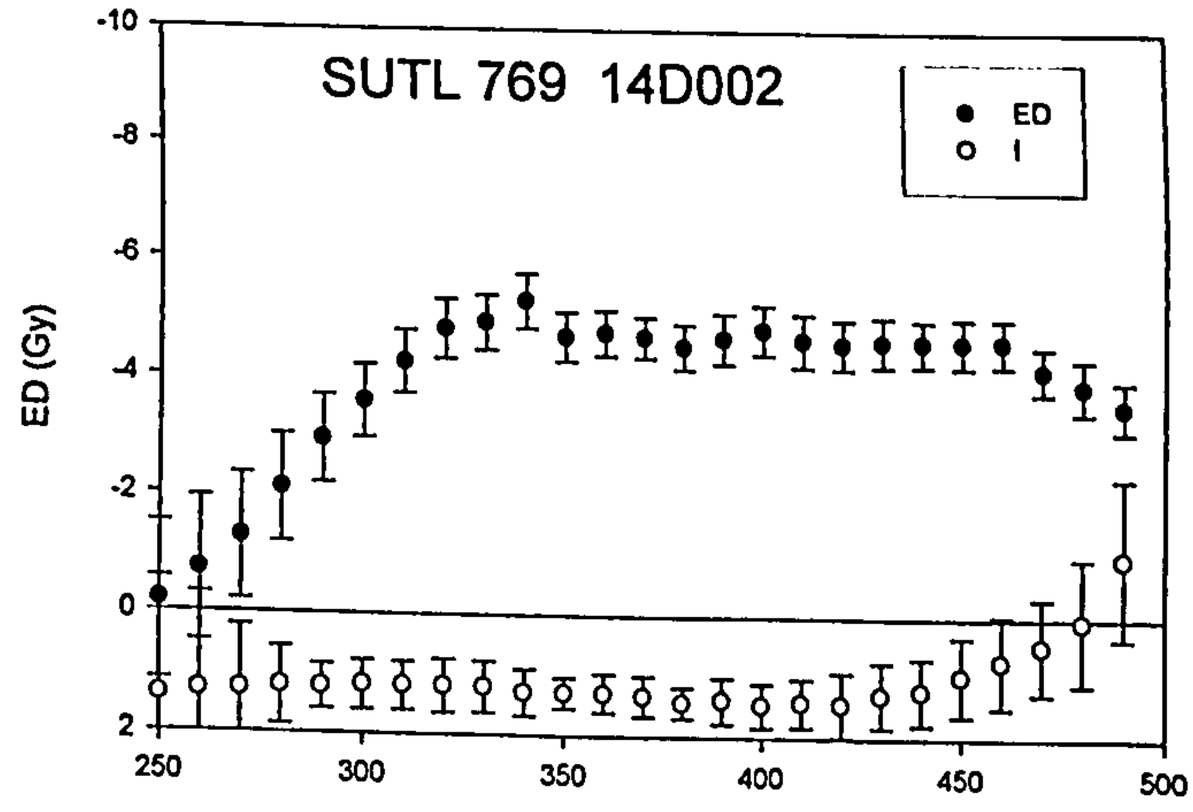
SUTL 769 14D002
ED
I
ED (Gy)
Temp (°C)

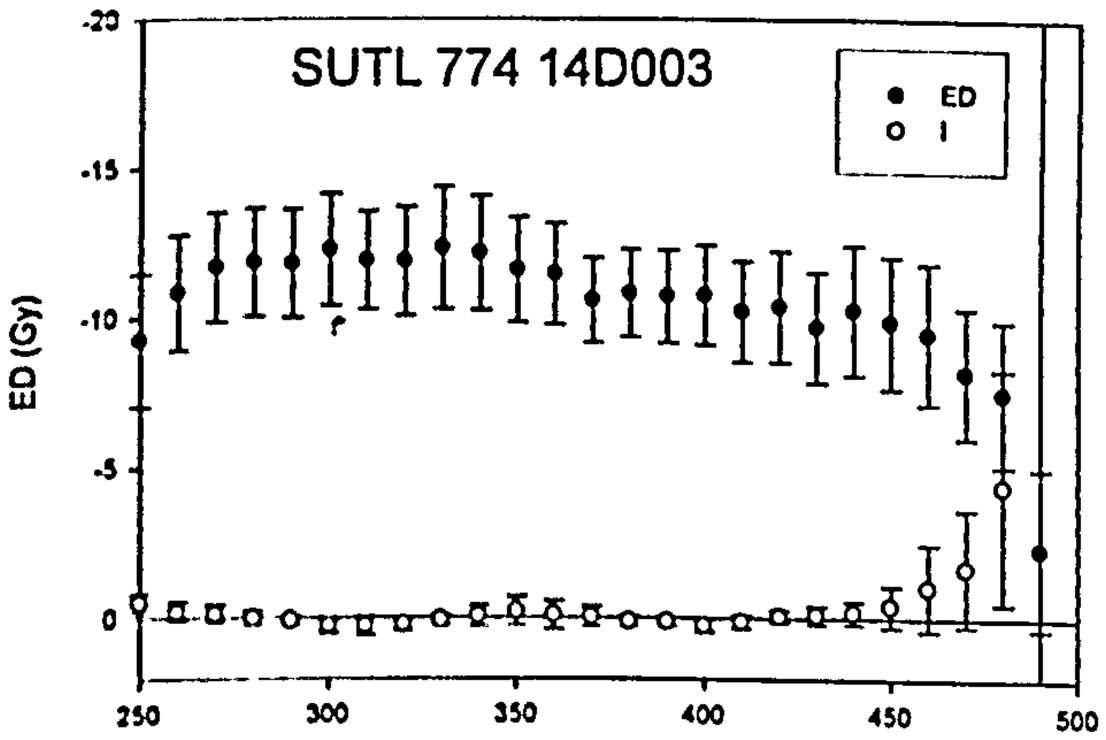
SUTL 774 14D003
ED
I
ED (Gy)
Temp (°C)

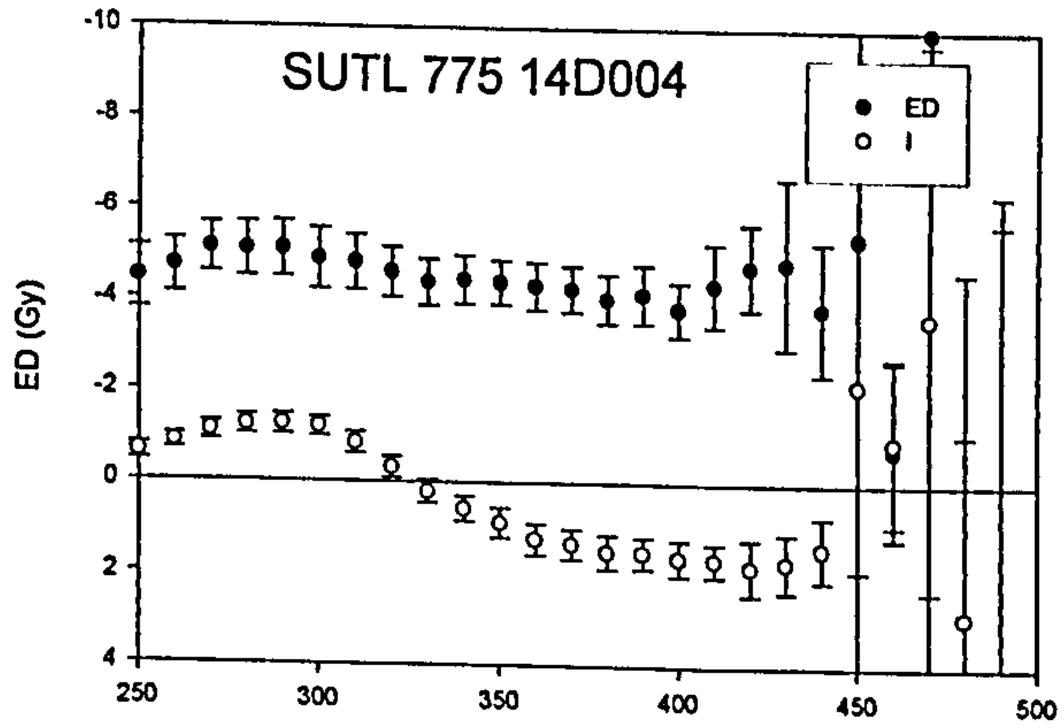
SUTL 775 14D004
ED
I
ED (Gy)
Temp (°C)

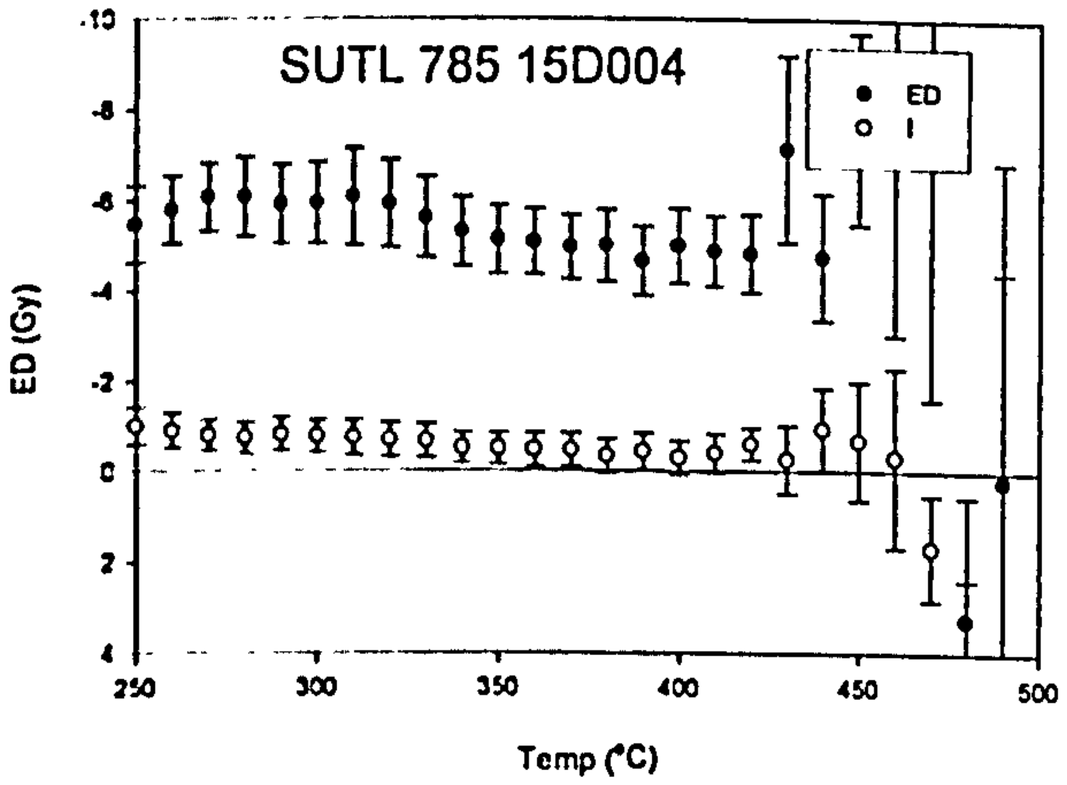
SUTL 785 15D004
ED
I
ED (Gy)
Temp (°C)

F.3 SKAILL

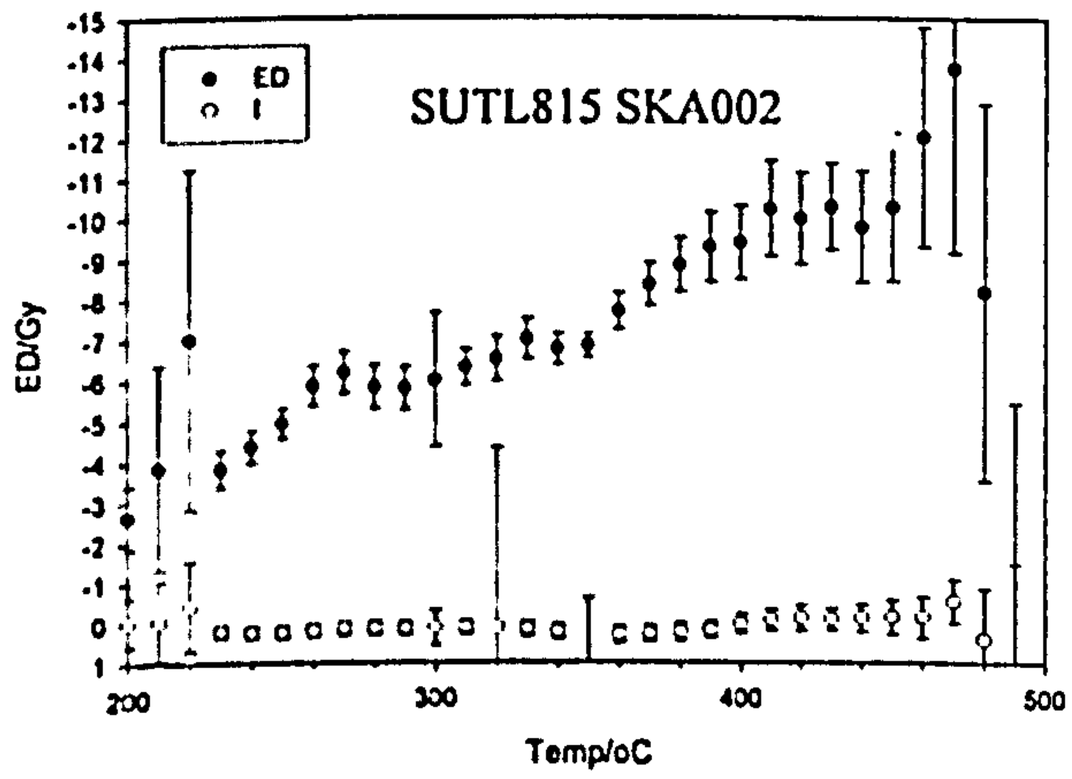

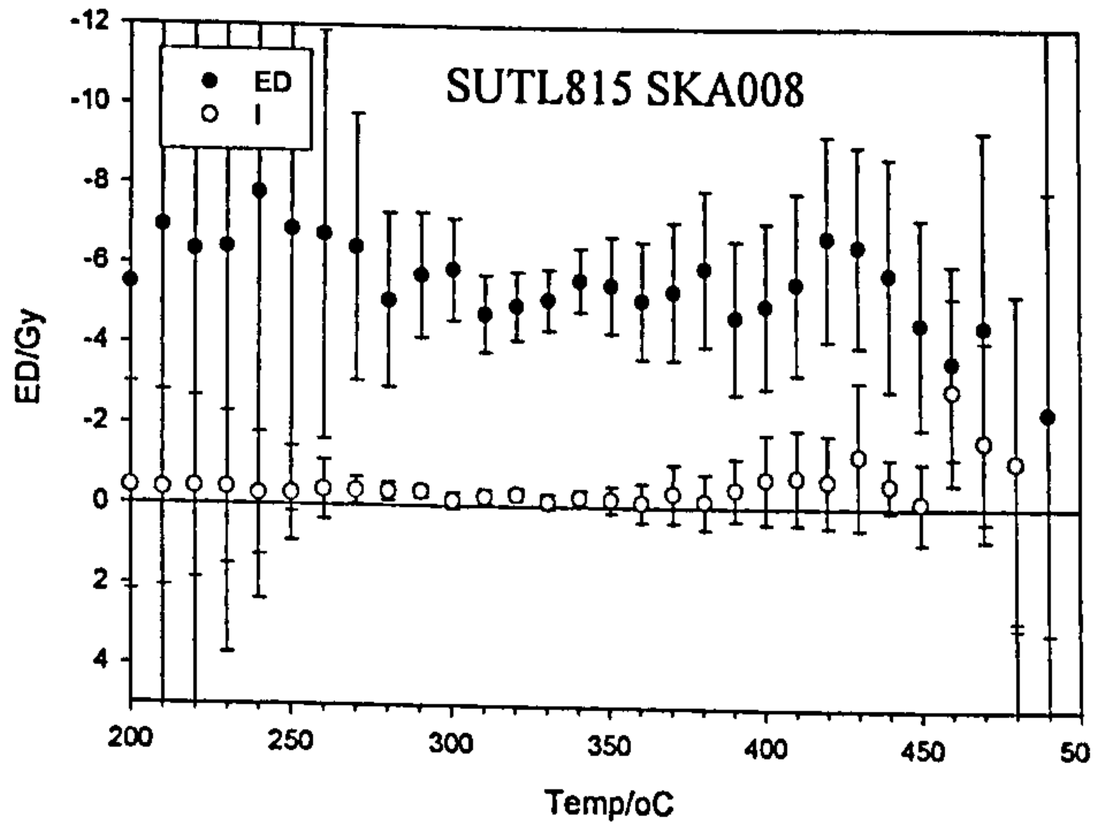

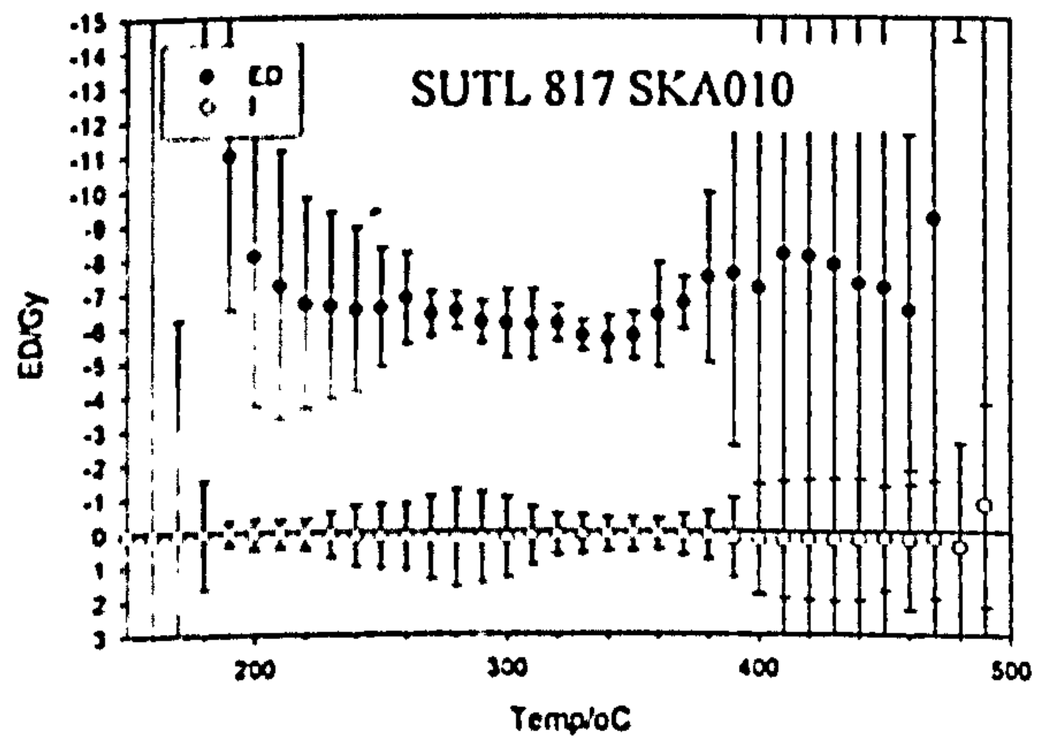

F.4 KNOLL OF MERRIGARTH

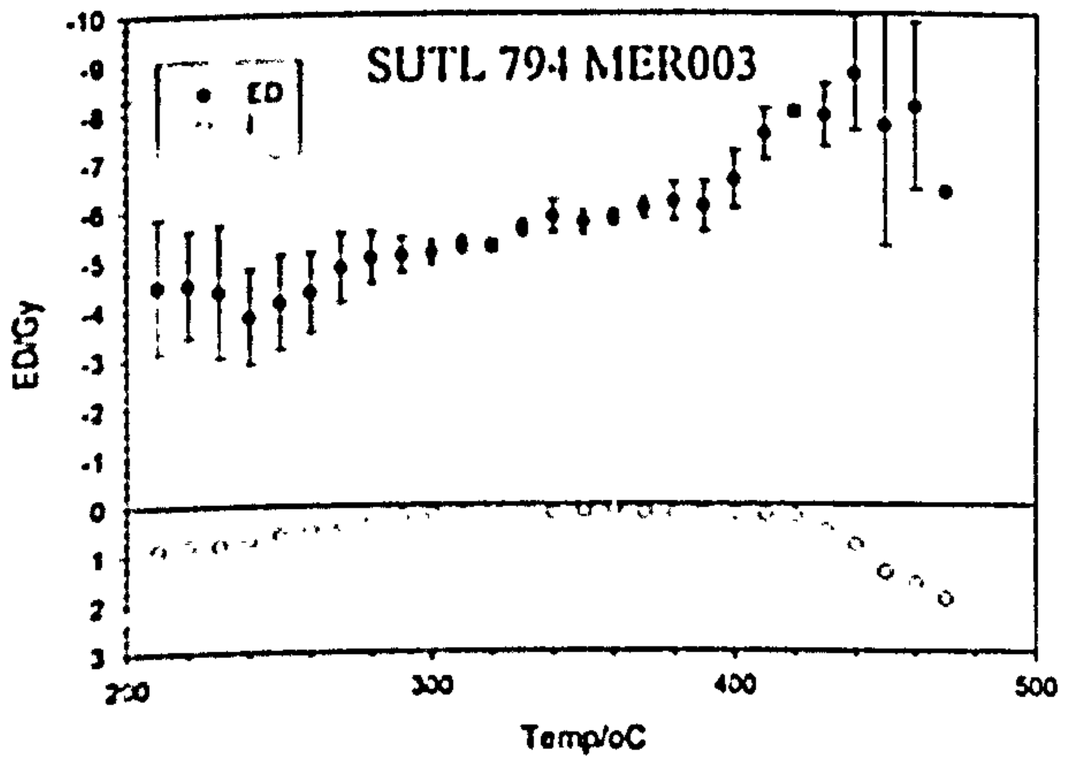

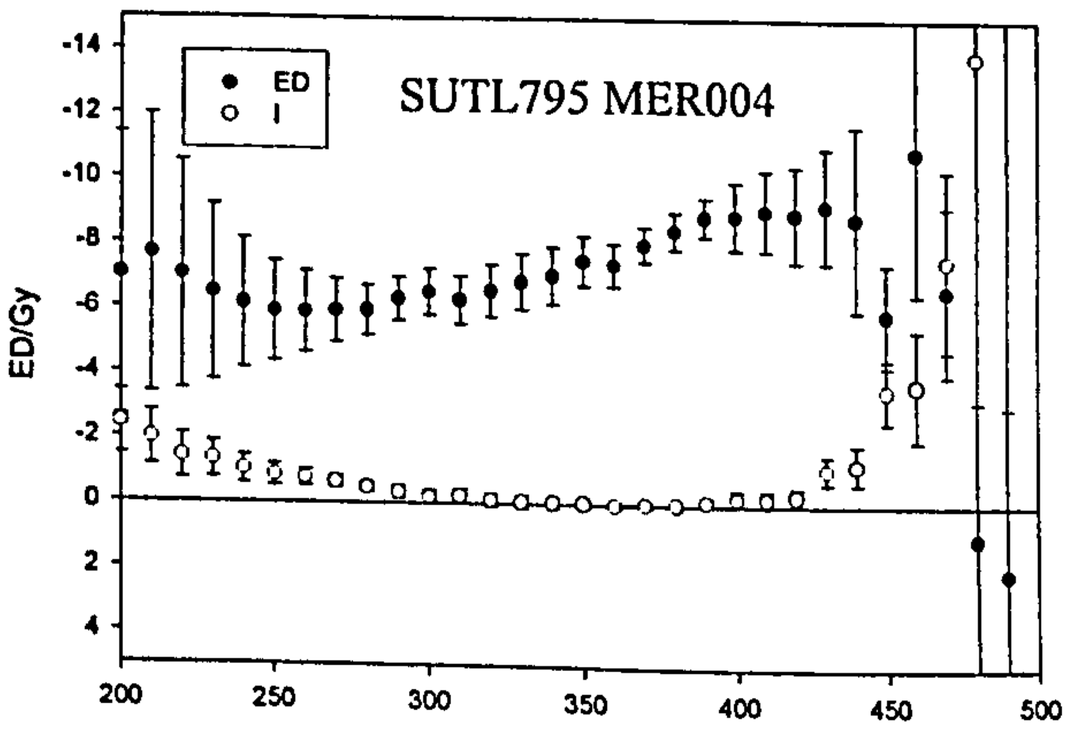

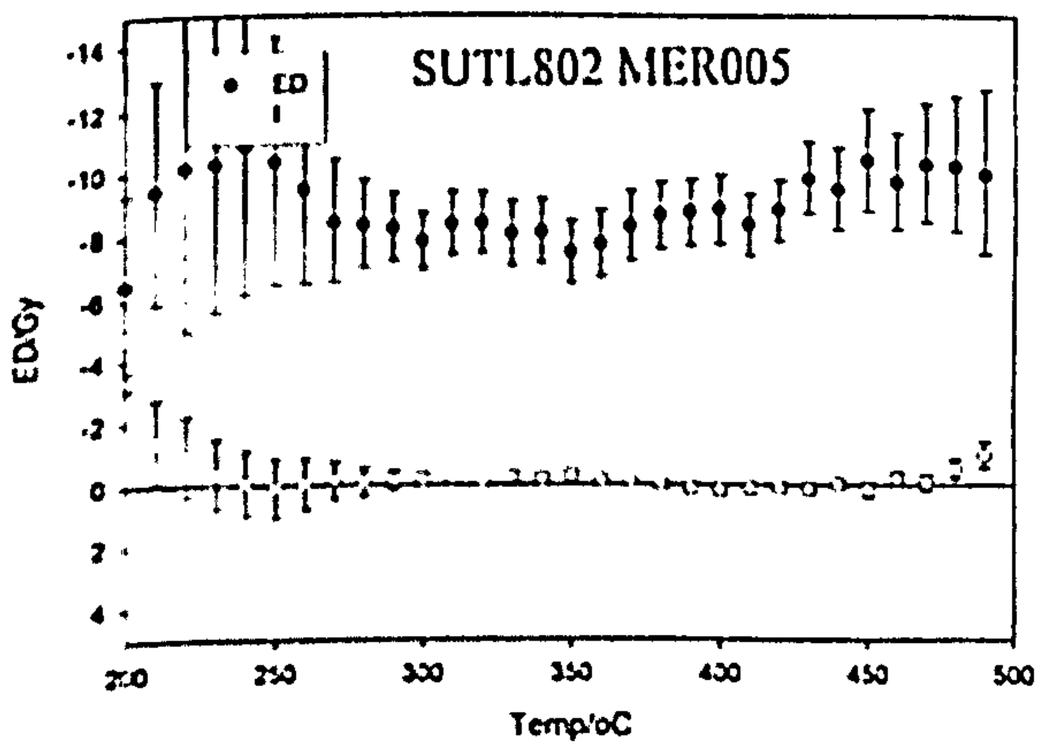

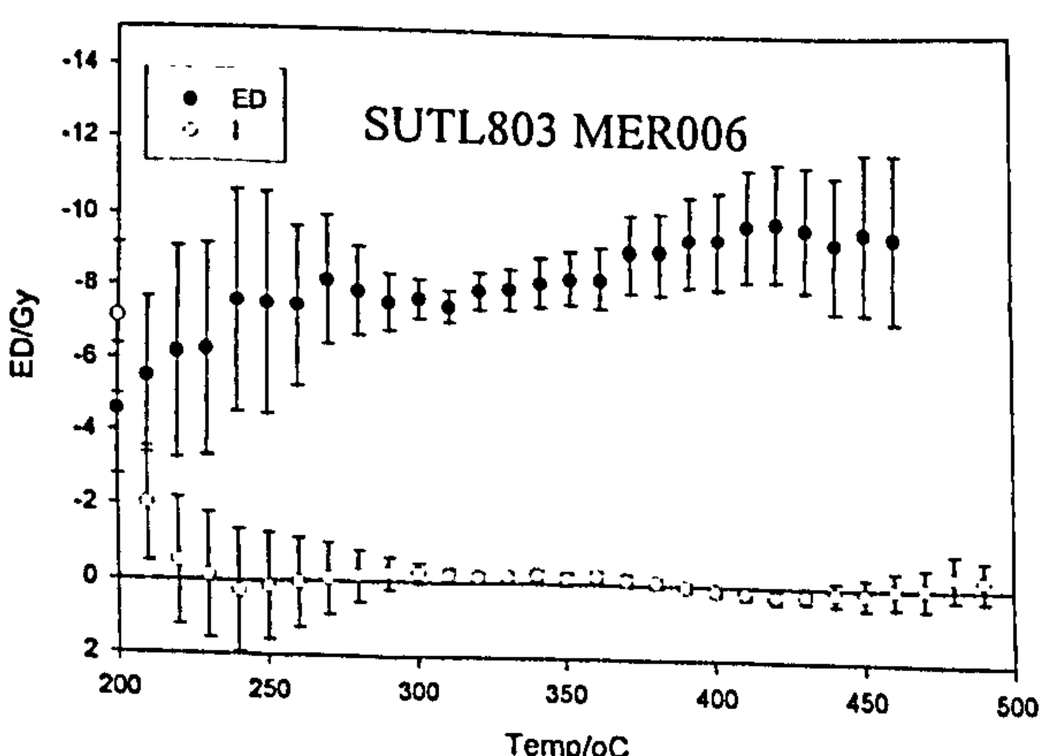

F.5 WARNESS

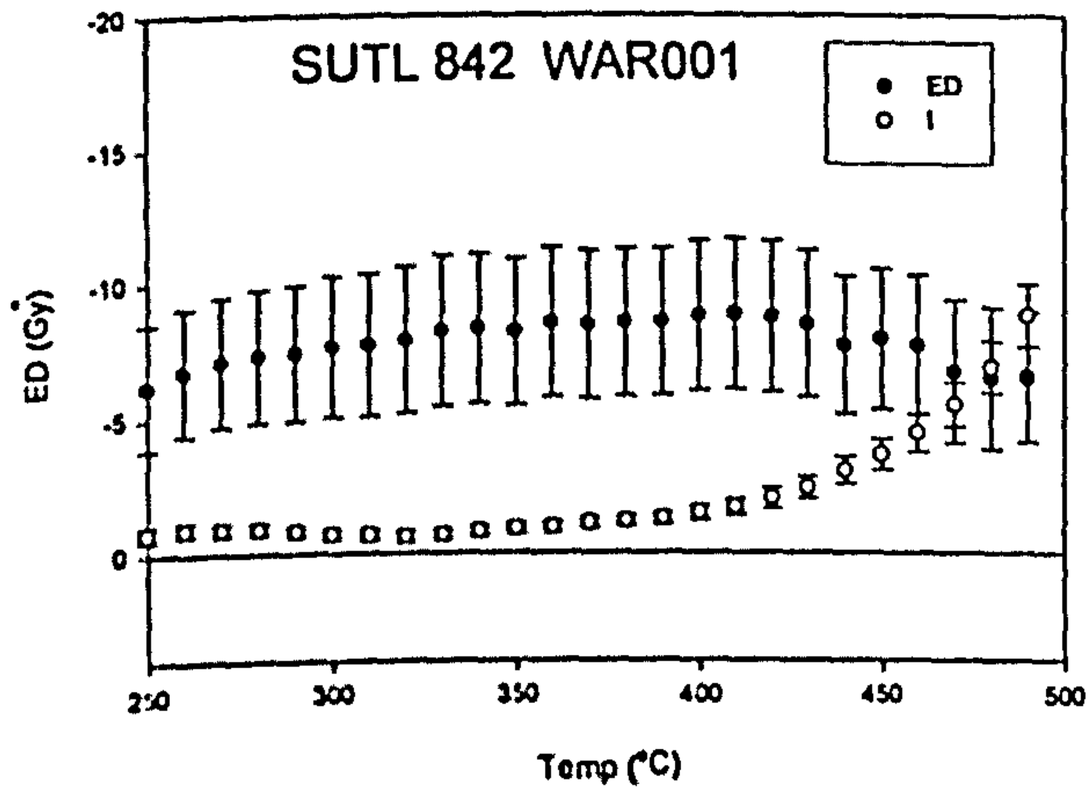

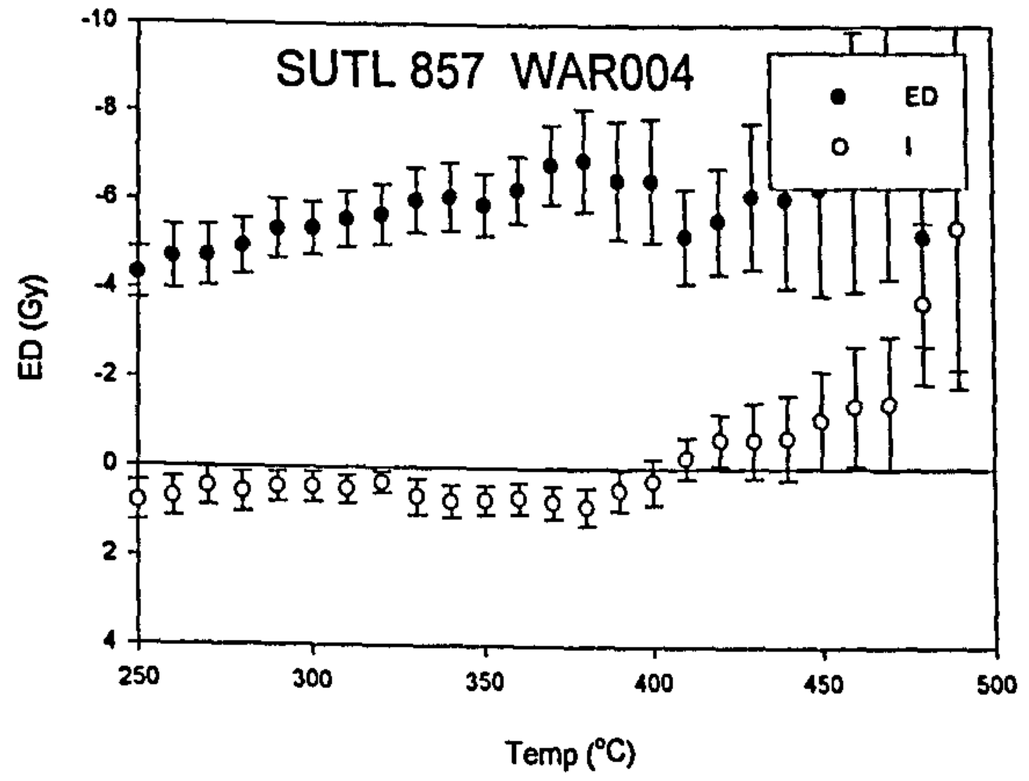

F.6 FERSNESS

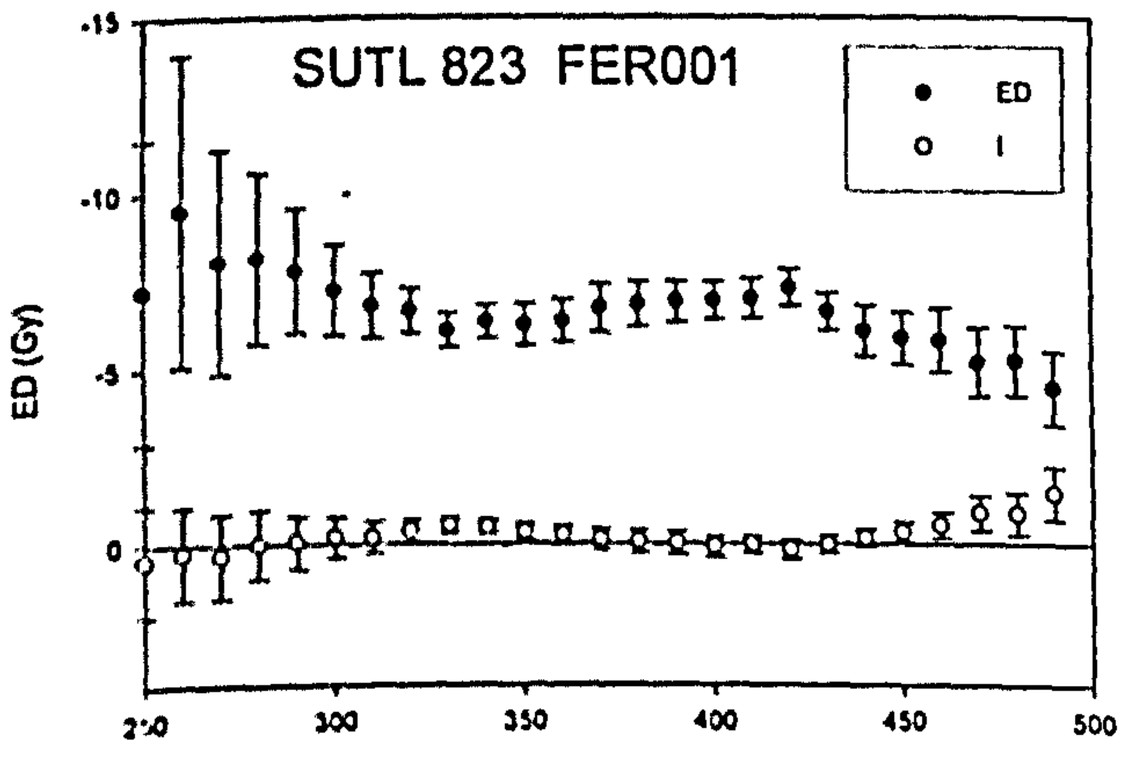

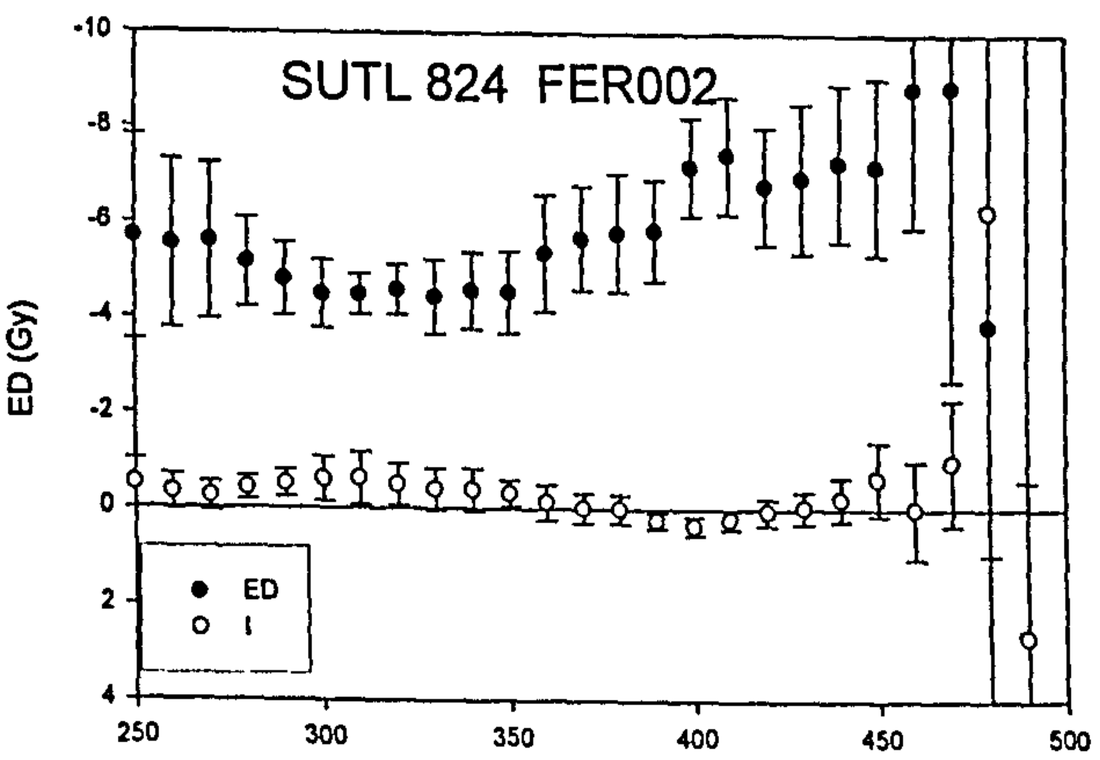

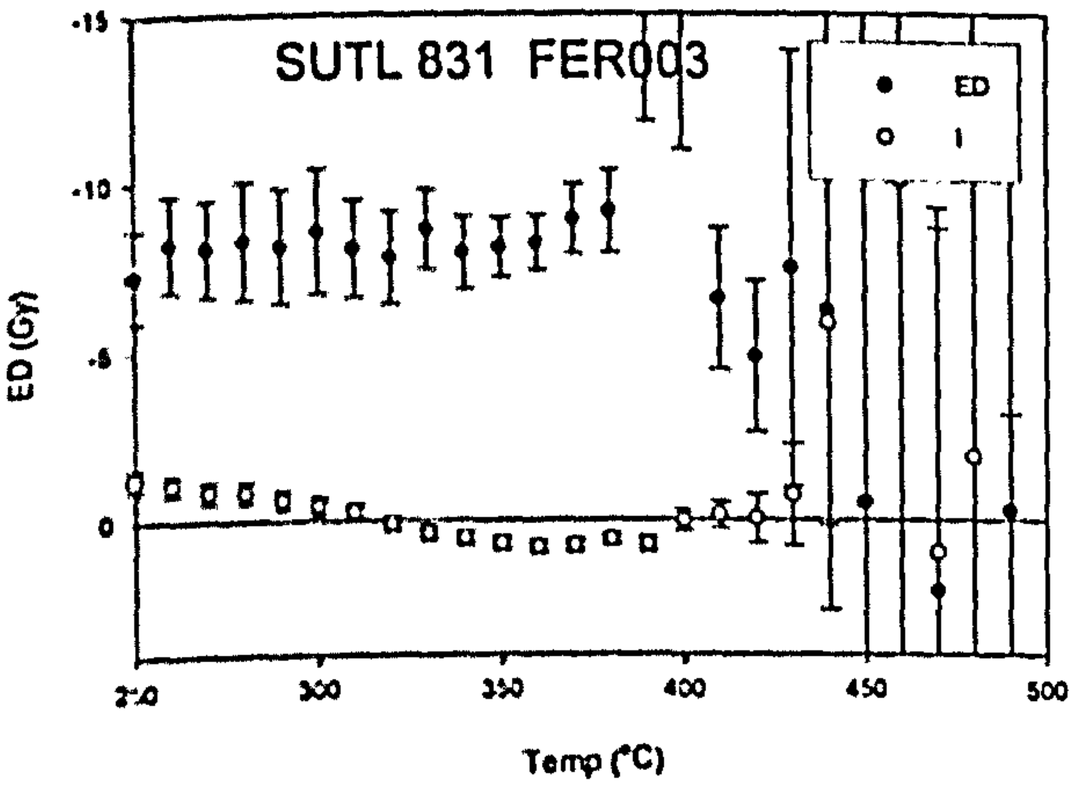

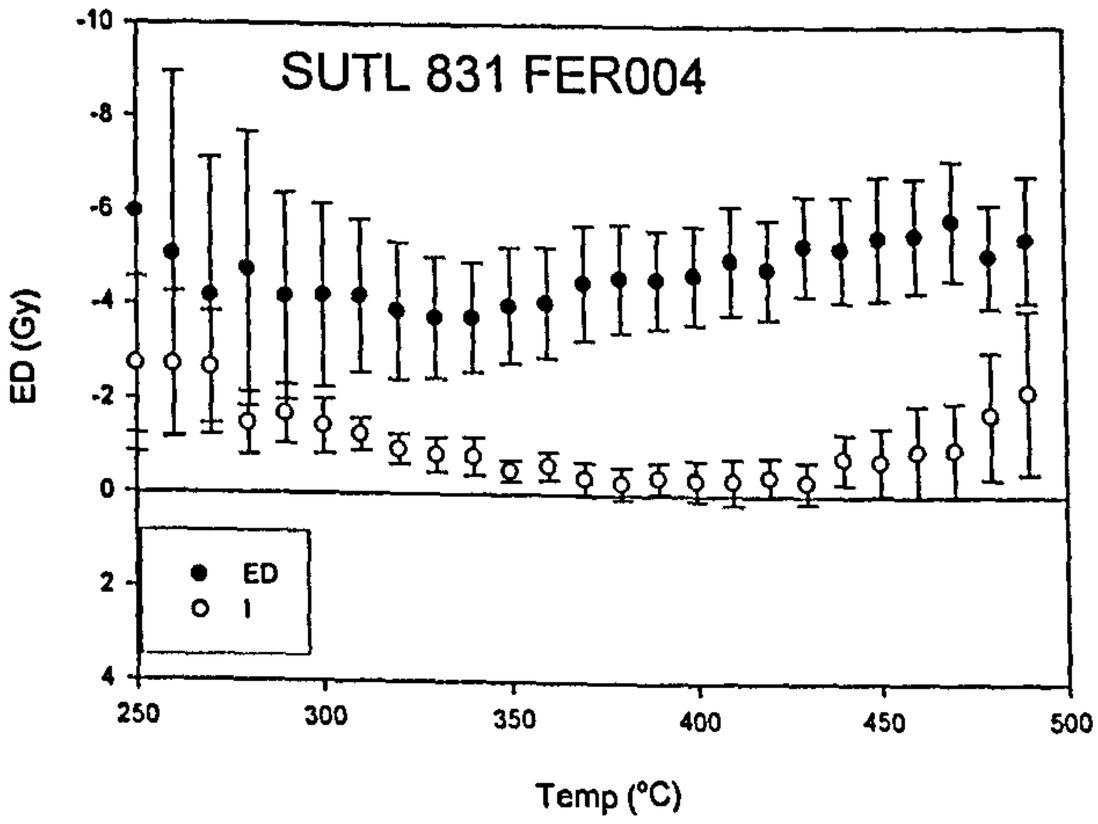

F.7 STENAQUOY

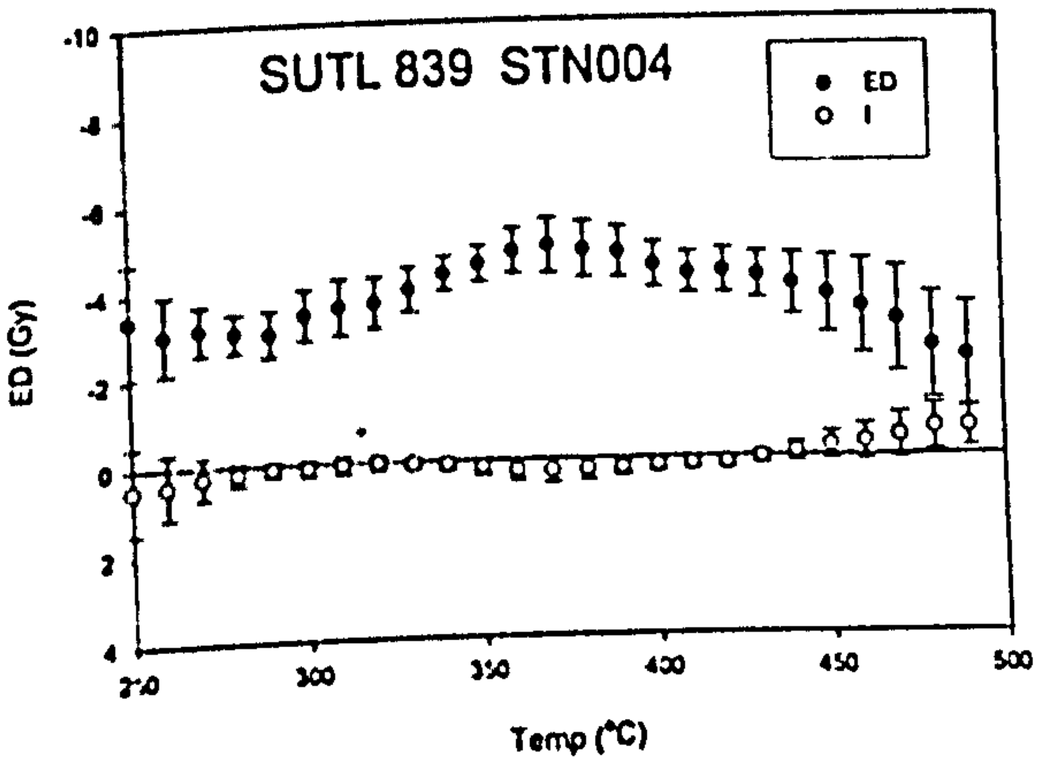

F.8 CRUESTER

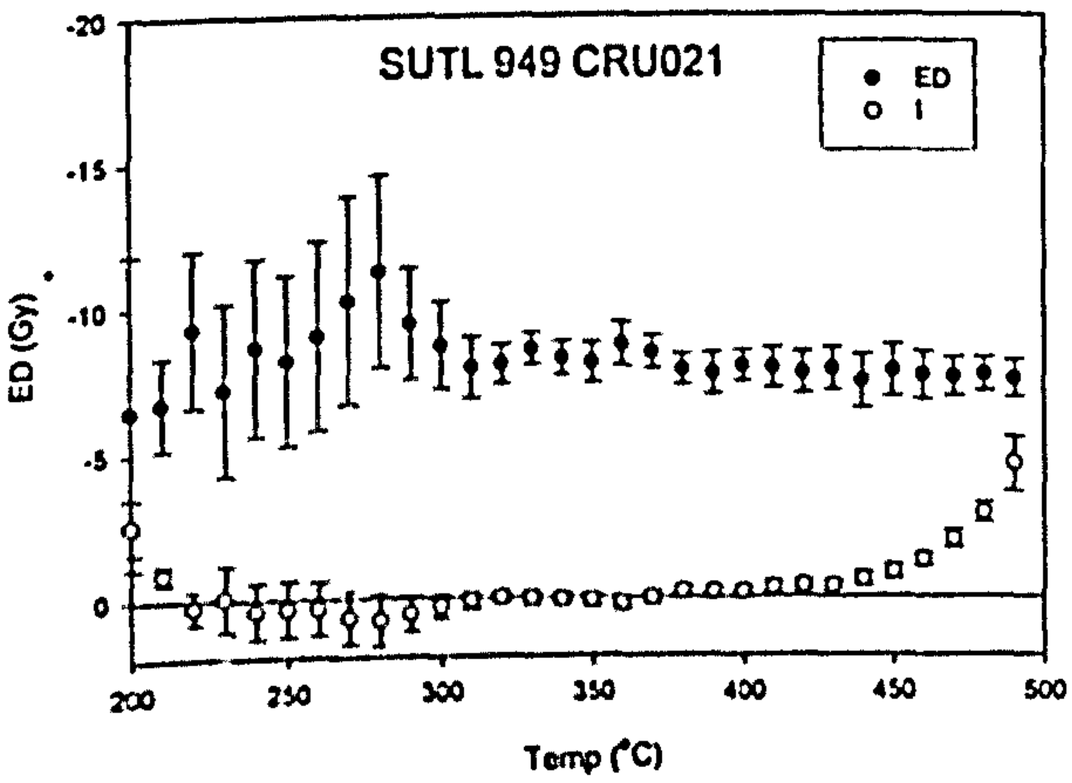
SUTL 949 CRU021
ED
I
ED (Gy)
Temp (°C)

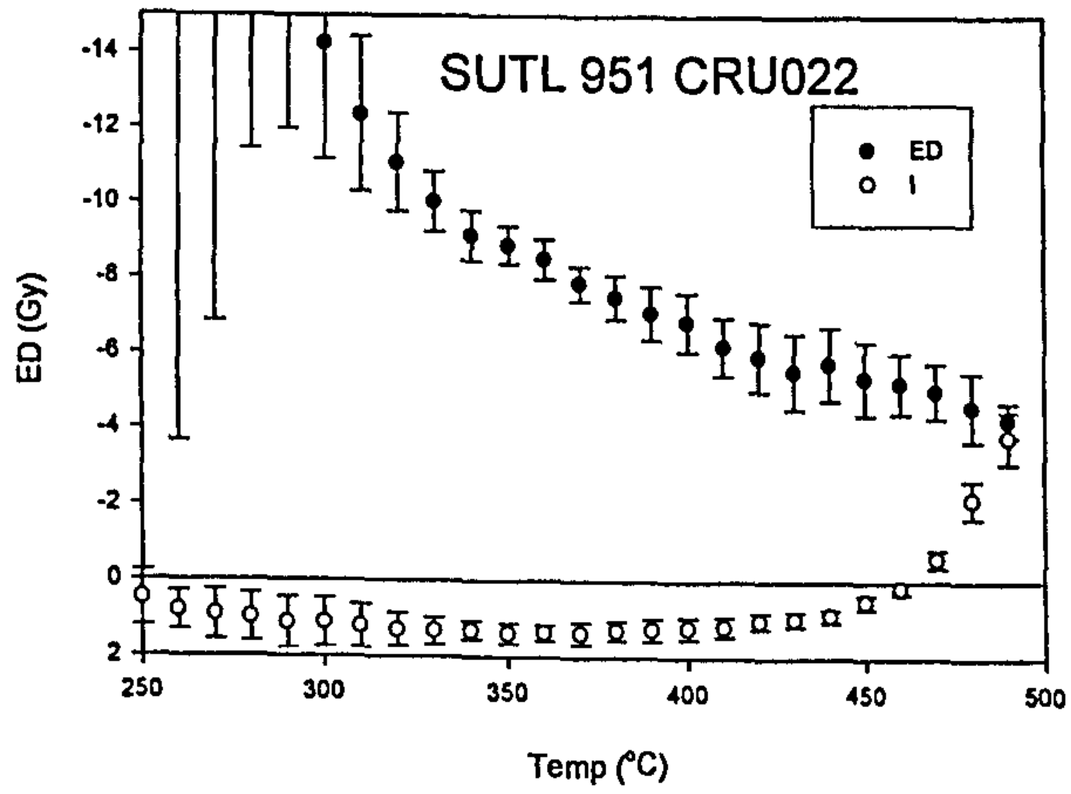
SUTL 951 CRU022
ED
I
ED (Gy)
Temp (°C)

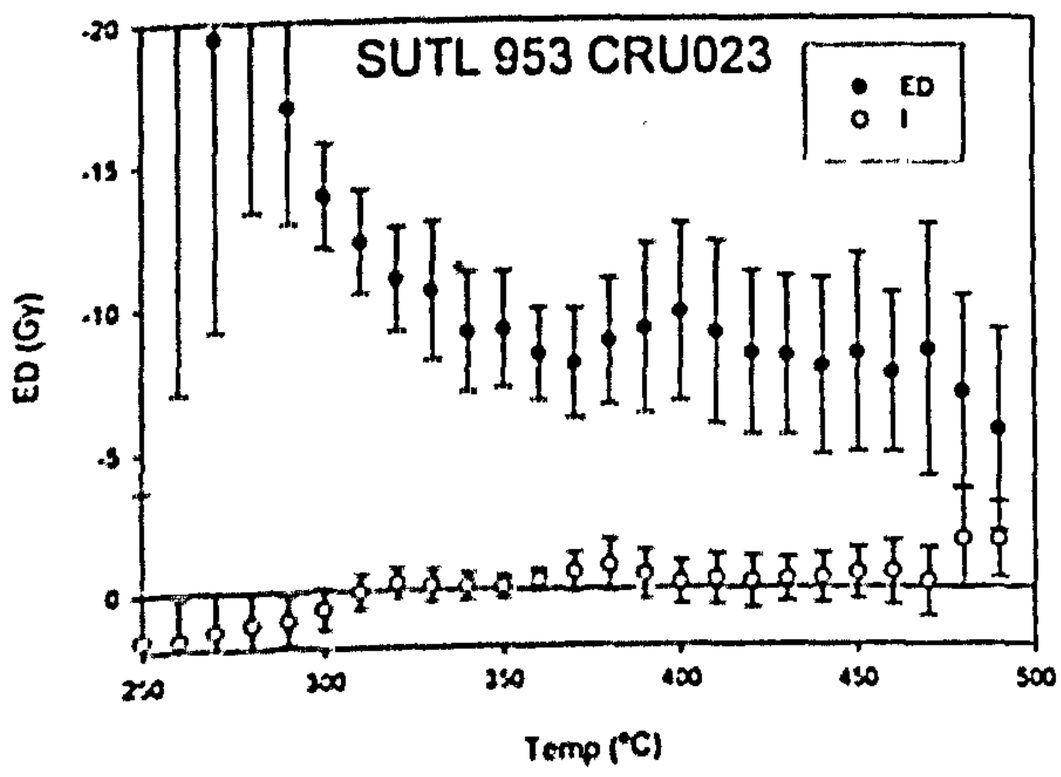
SUTL 953 CRU023
ED
I
ED (Gy)
Temp (°C)

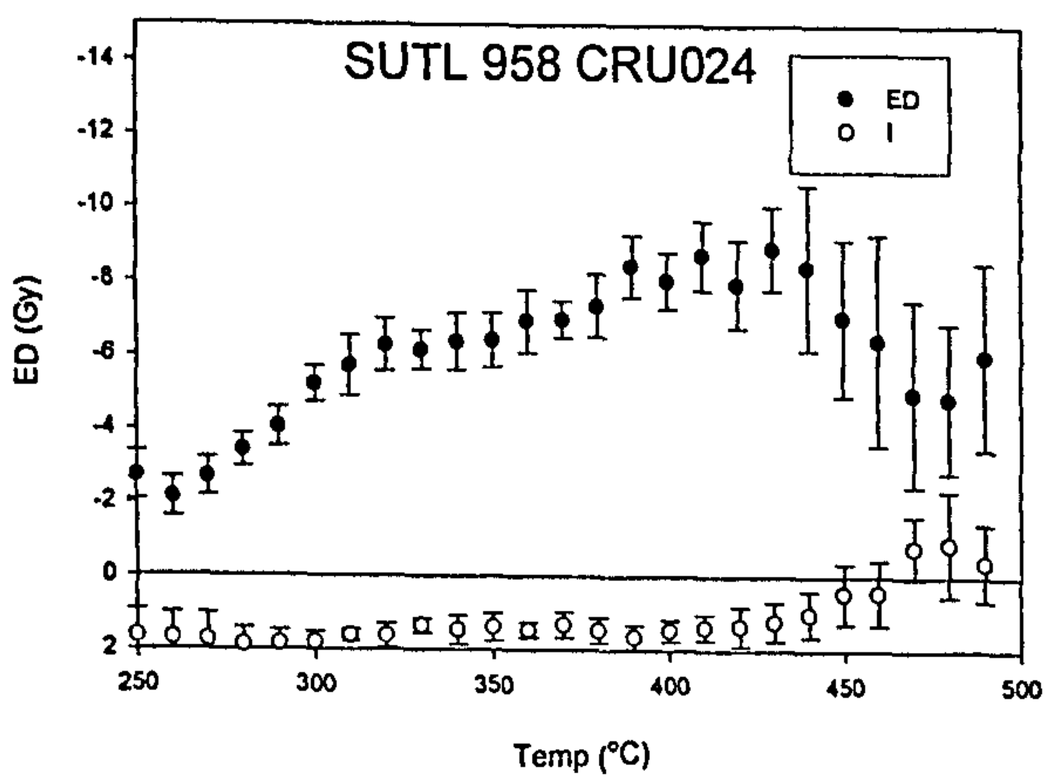
SUTL 958 CRU024
ED
I
ED (Gy)
Temp (°C)

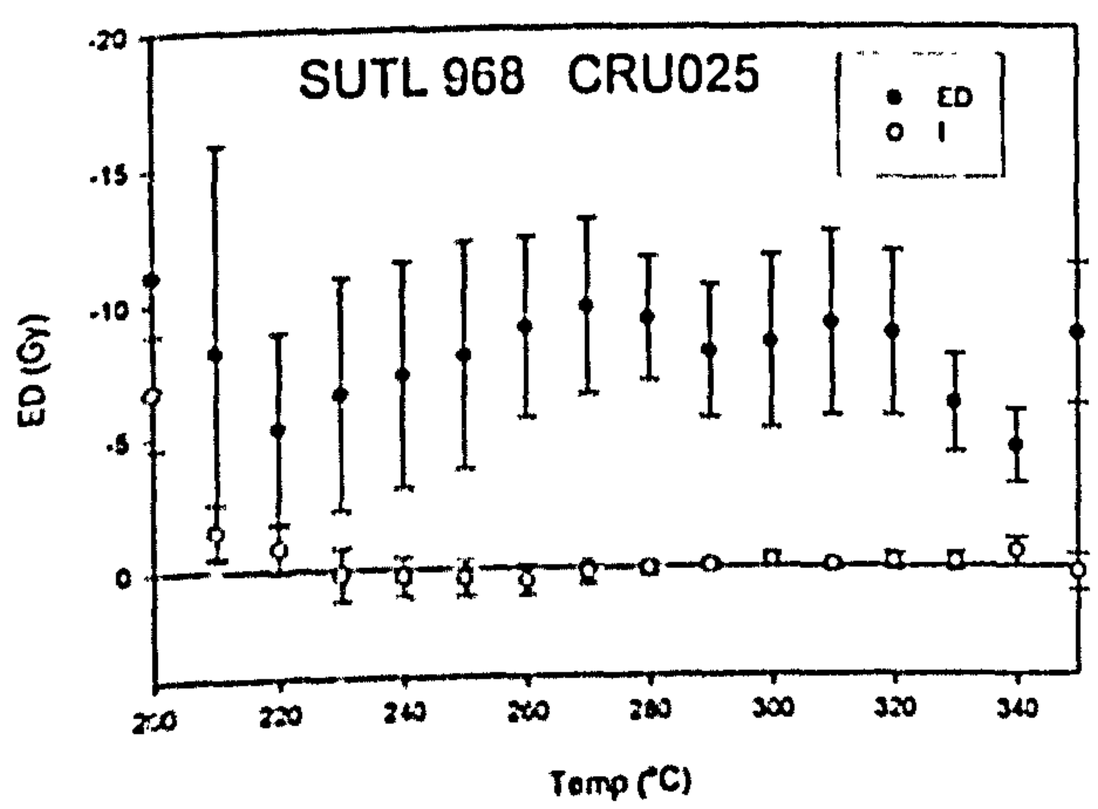
SUTL 968 CRU025
ED
I
ED (Gy)
Temp (°C)

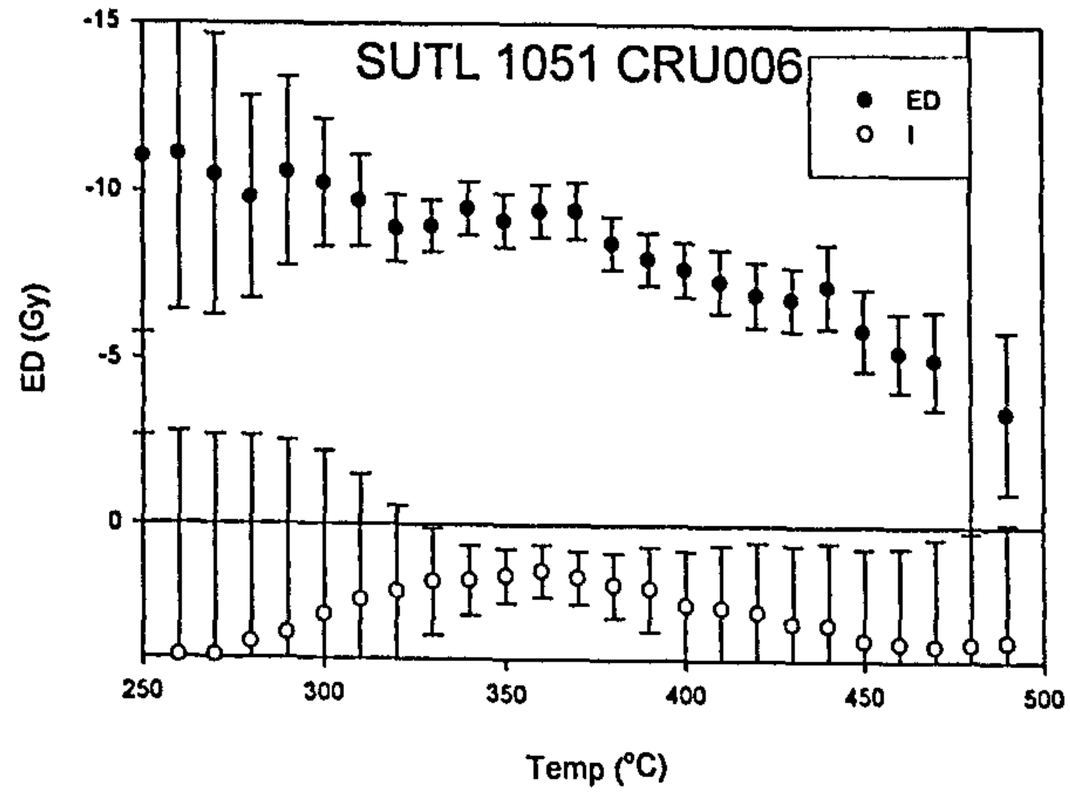
SUTL 1051 CRU006
ED
I
ED (Gy)
Temp (°C)

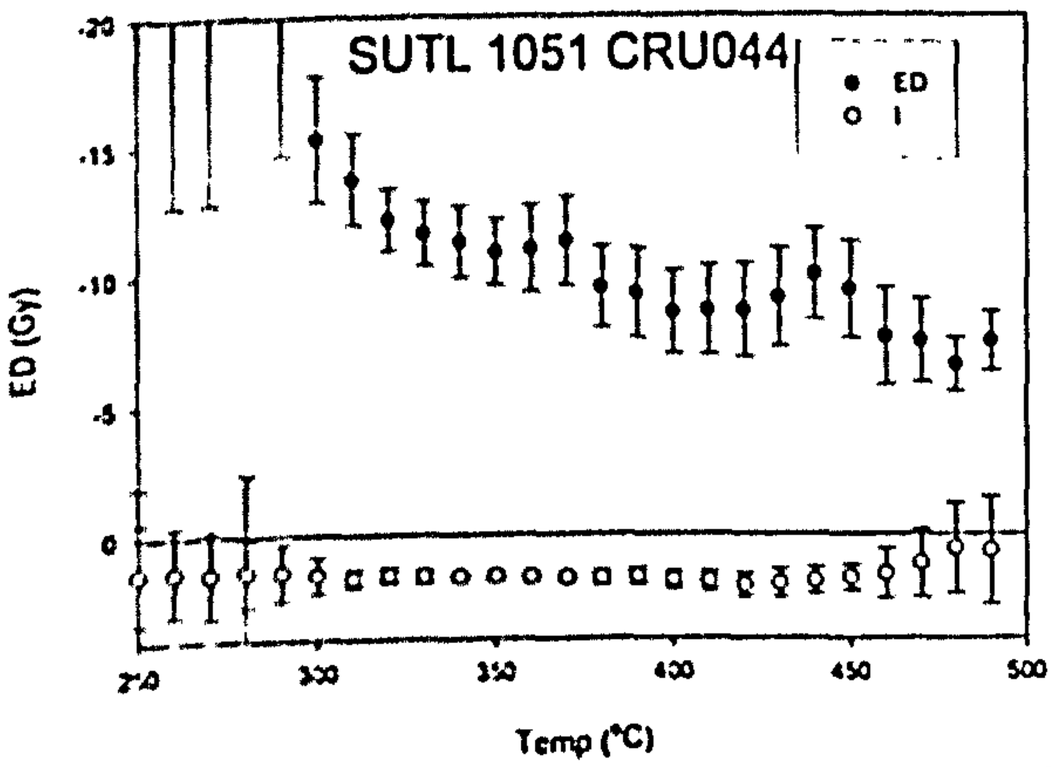
SUTL 1051 CRU044
ED
I
ED (Gy)
Temp (°C)

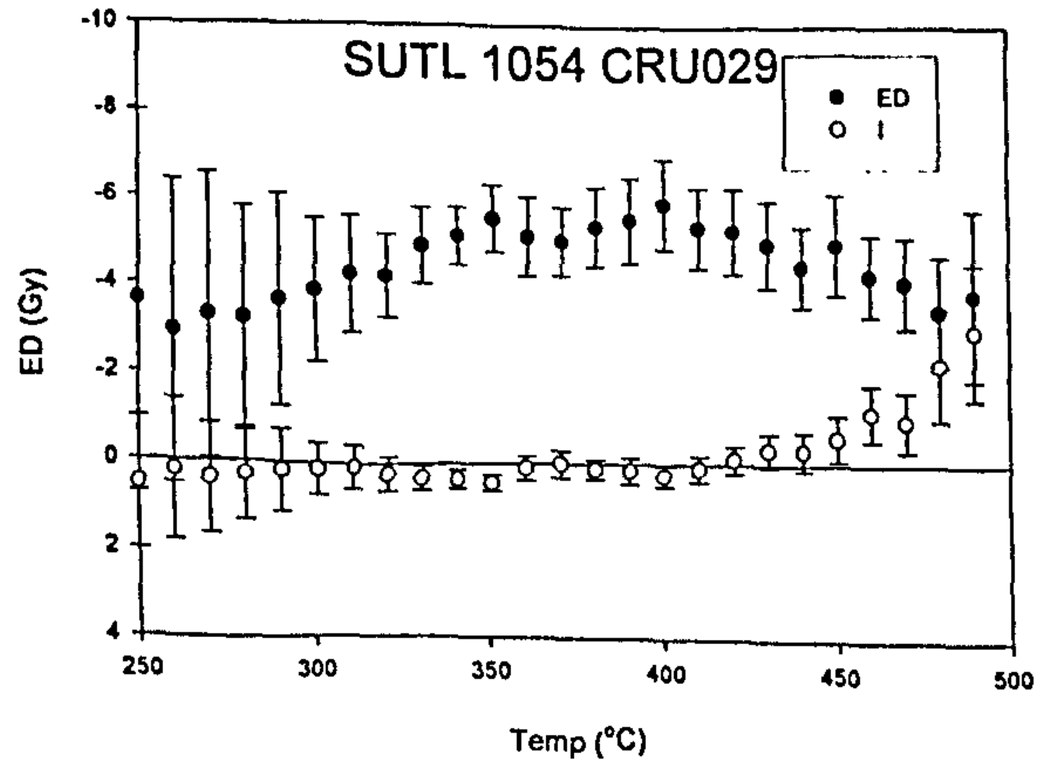
SUTL 1054 CRU029
ED
I
ED (Gy)
Temp (°C)

APPENDIX F

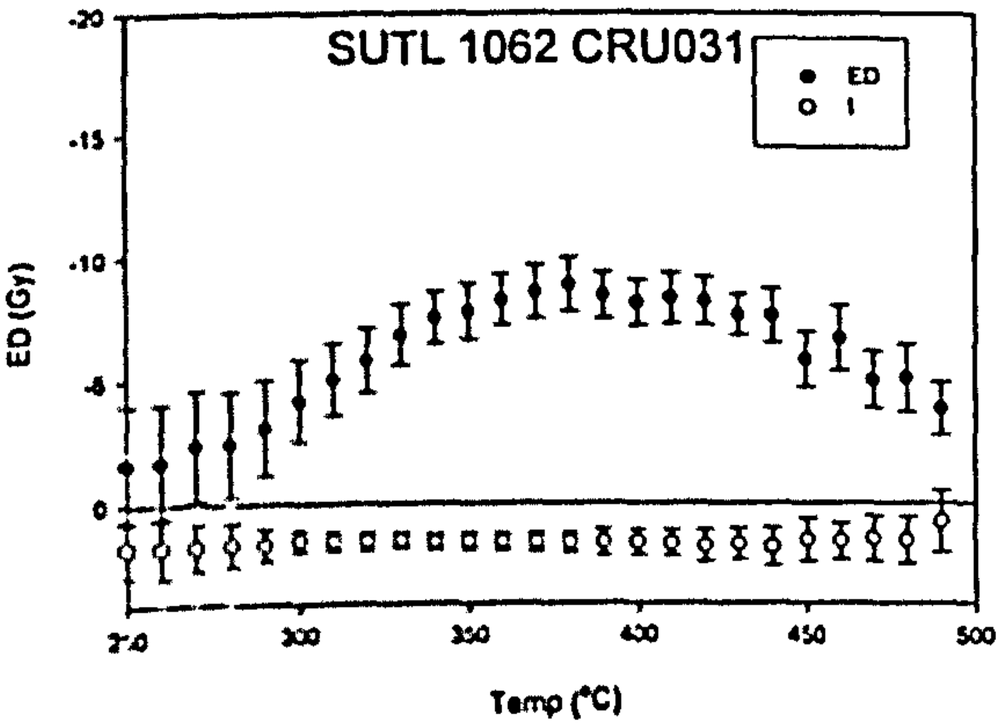

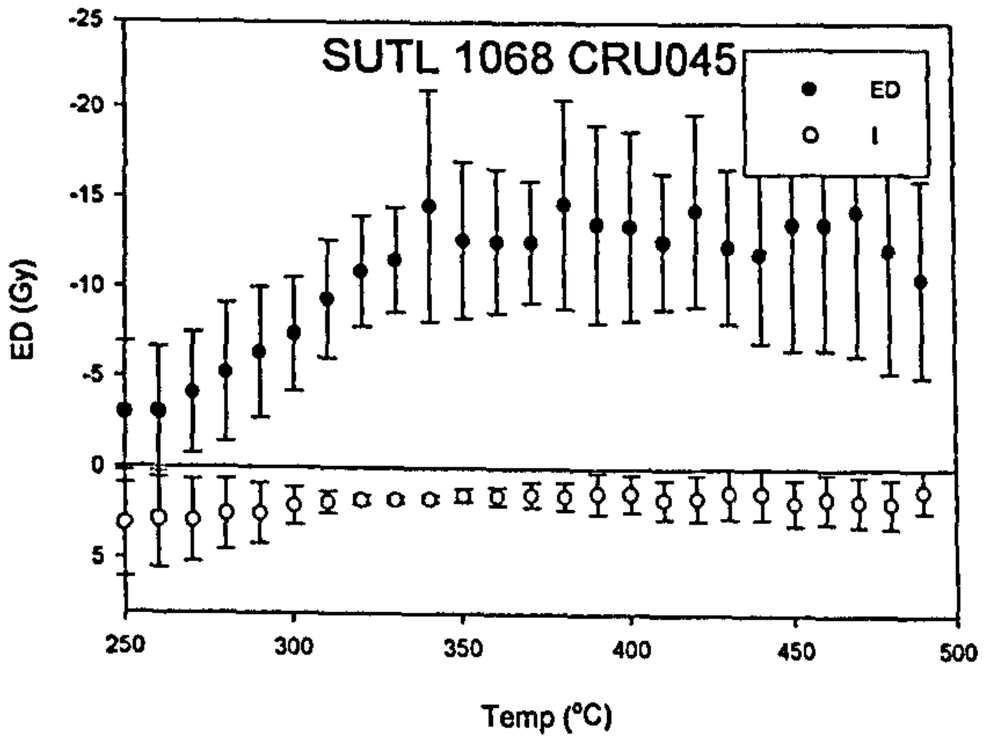

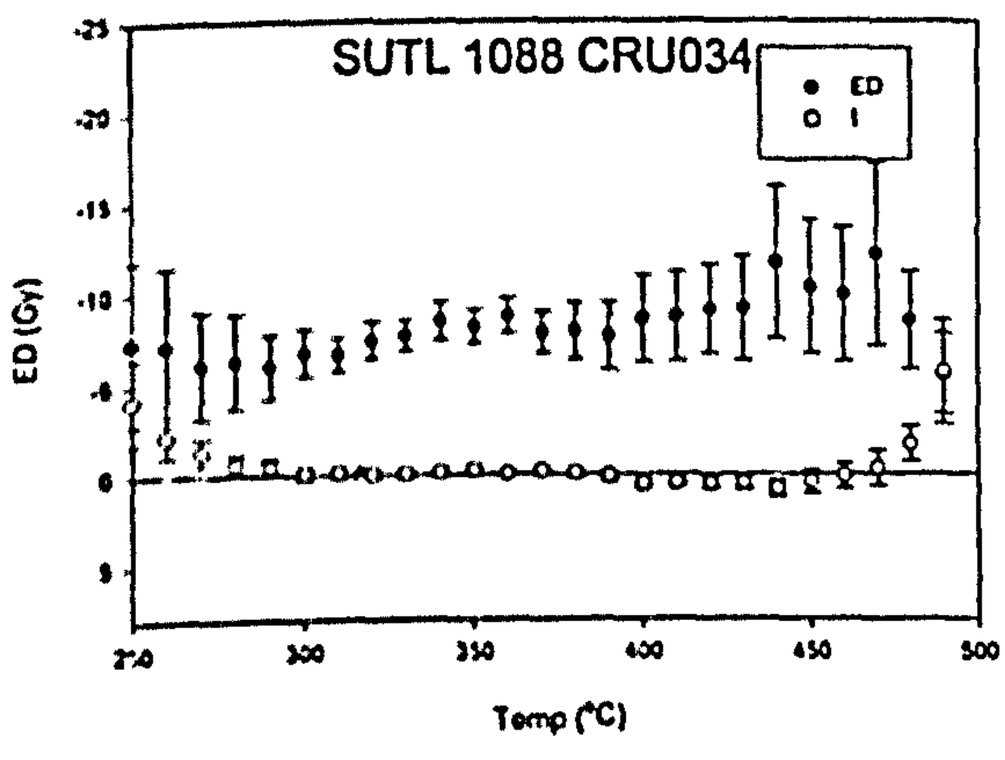

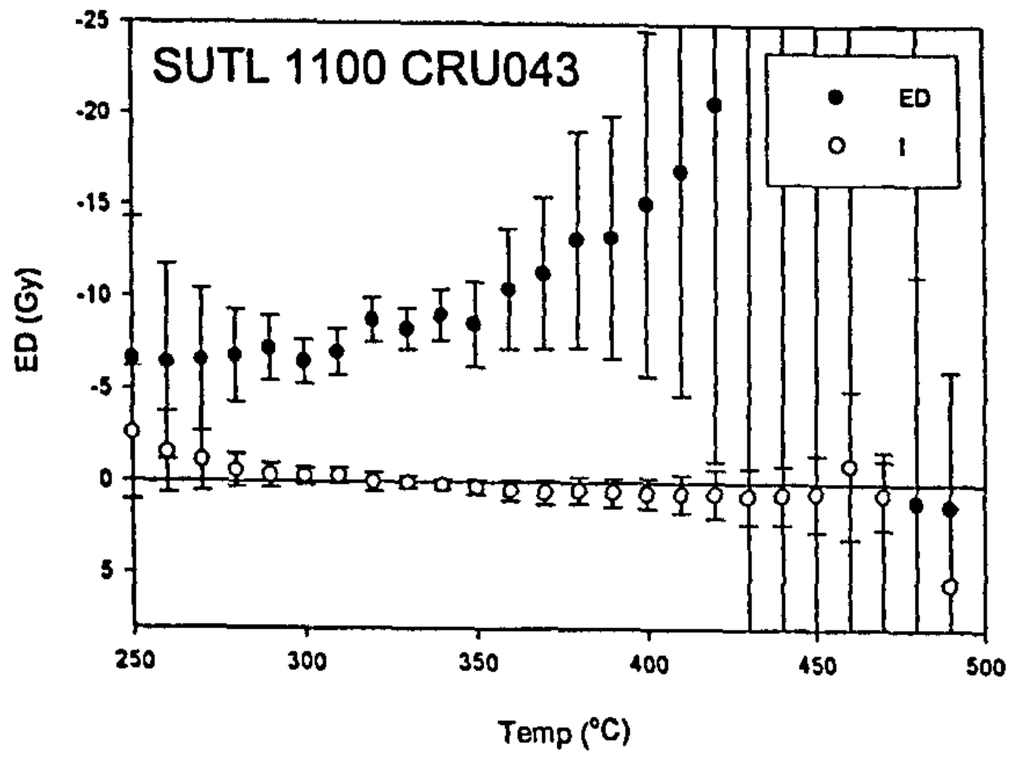

F.9 HOULLS

APPENDIX G

QUARTZ SAR RUN SUMMARY

G.1 LIDDLE

SUTL 1379

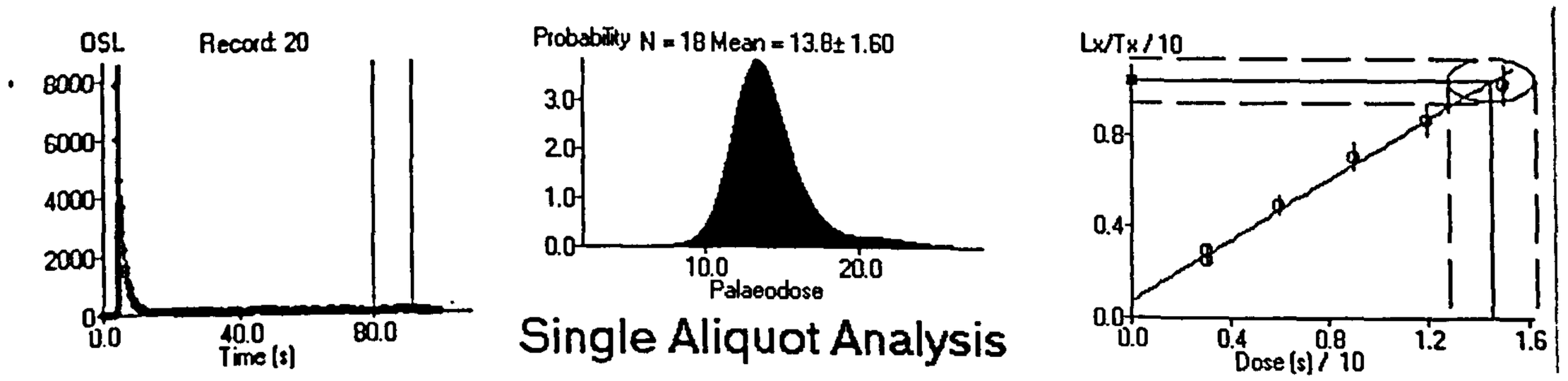

G.2 DALE

SUTL 748

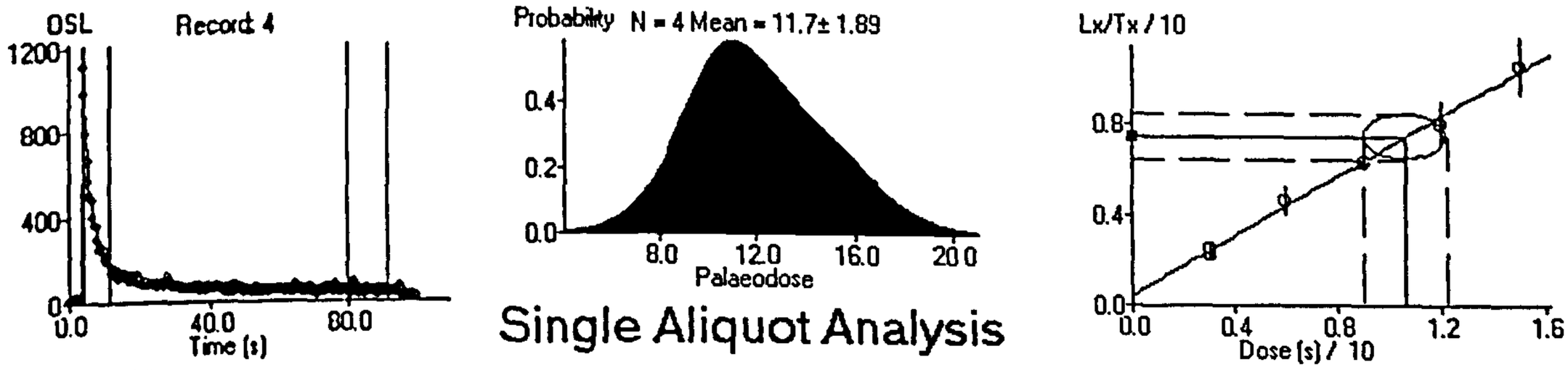

SUTL 749

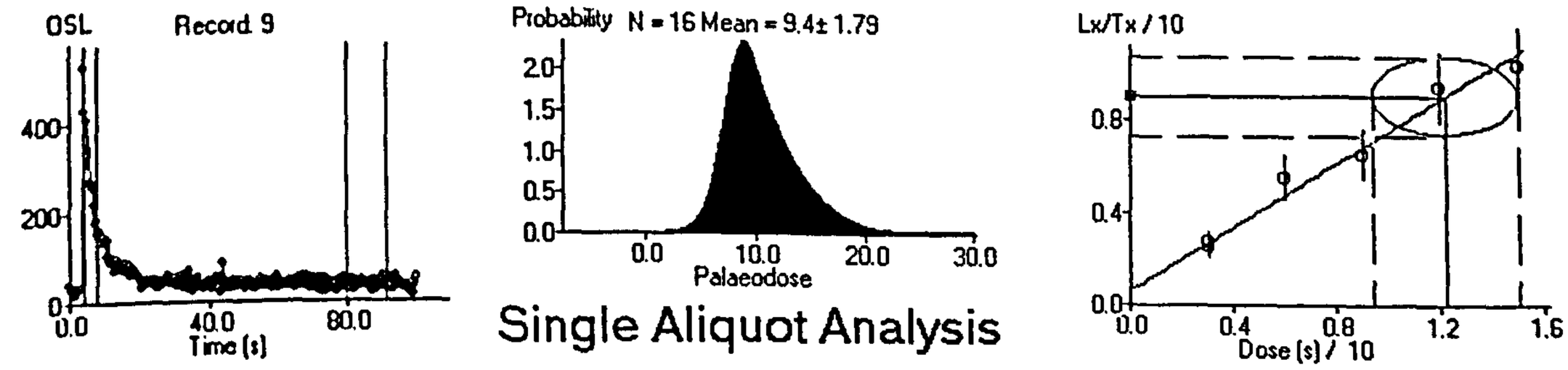

SUTL 751

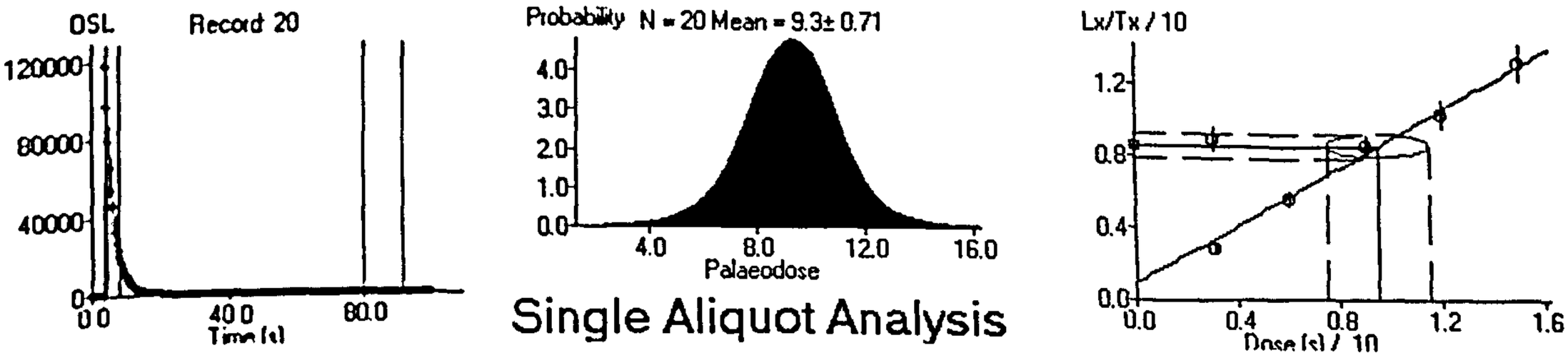

SUTL 753

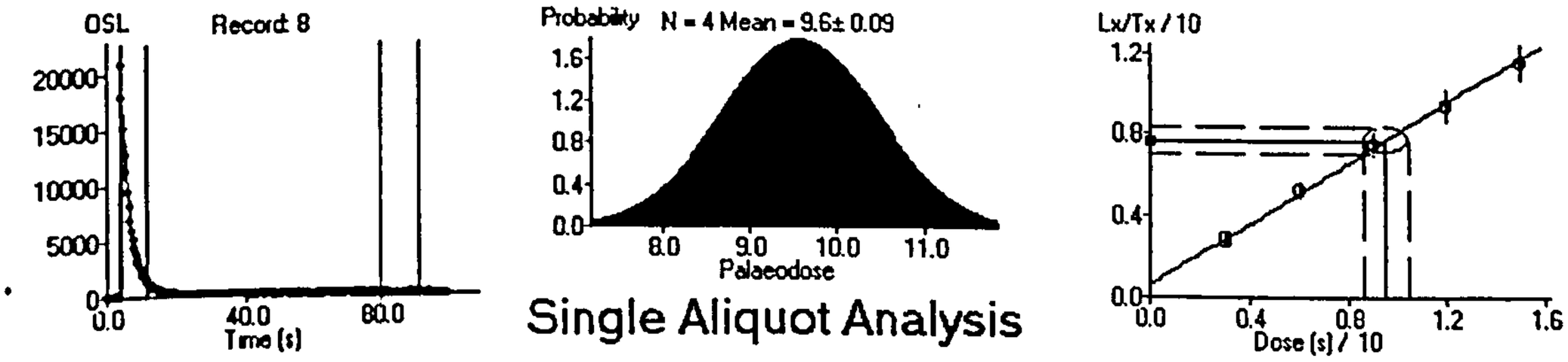

SUTL 760

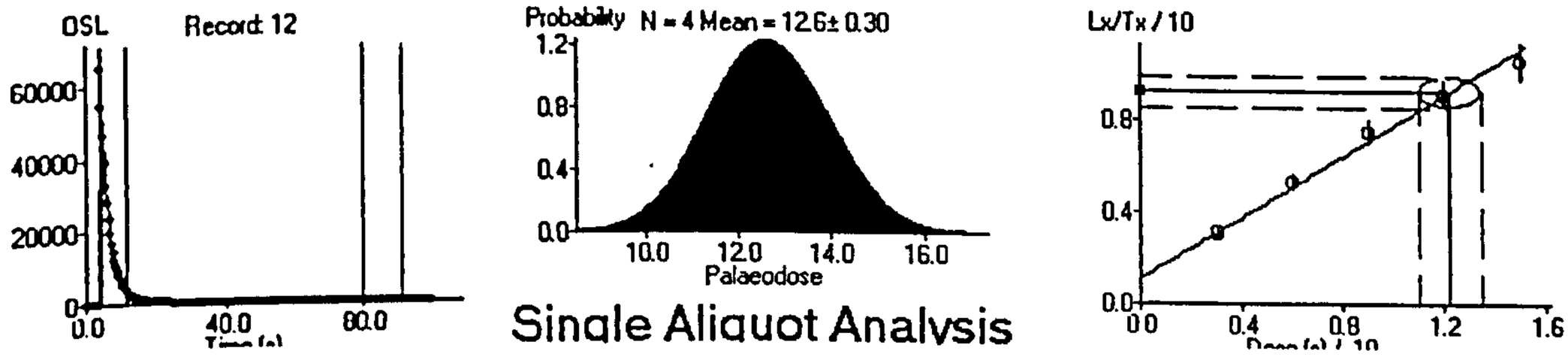

SUTL 767

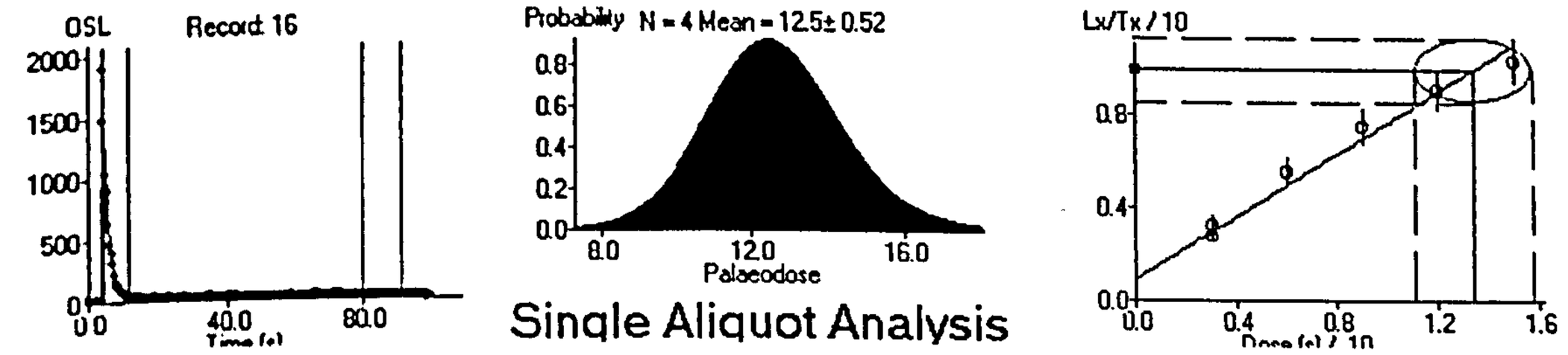

SUTL 774

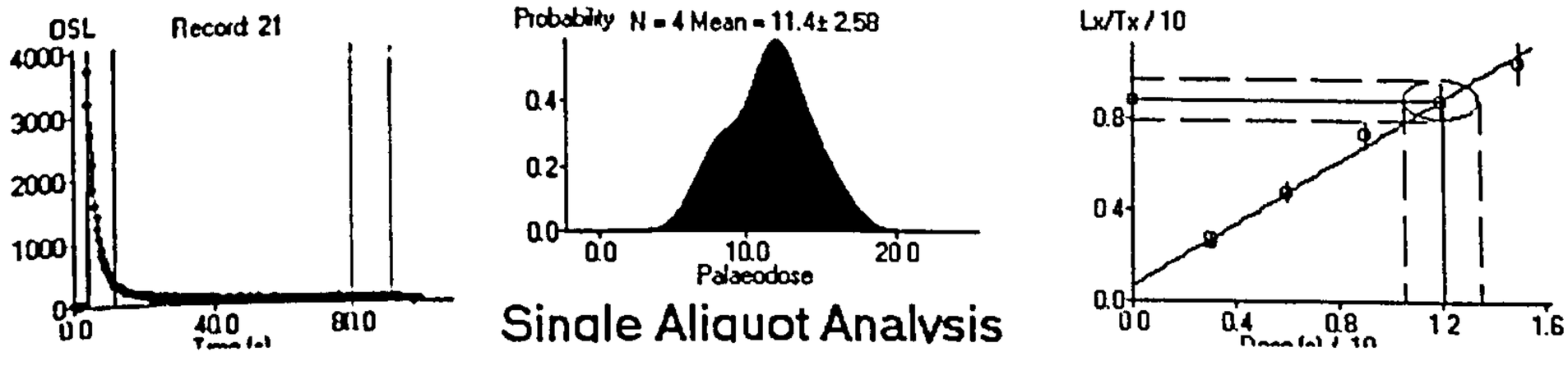

SUTL 777

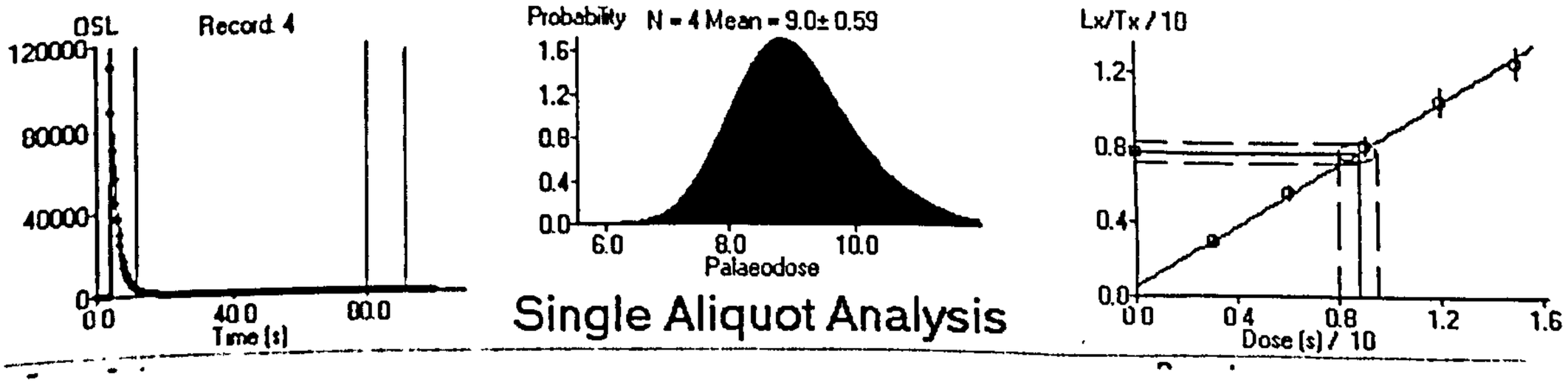

SUTL 779

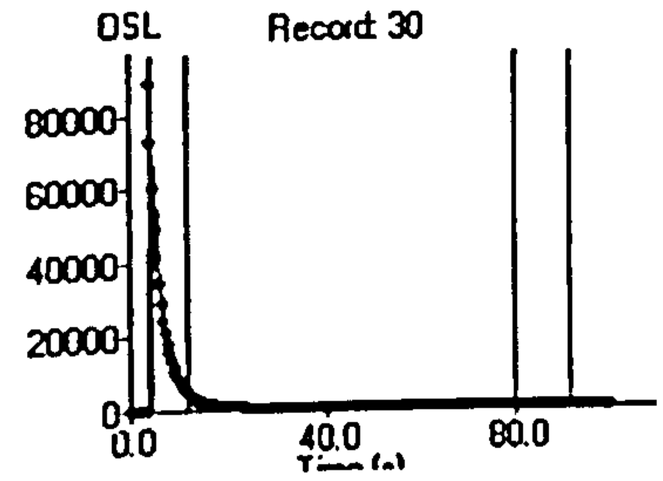

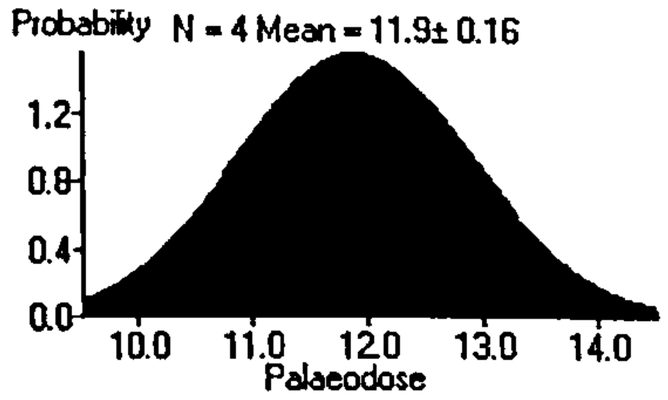

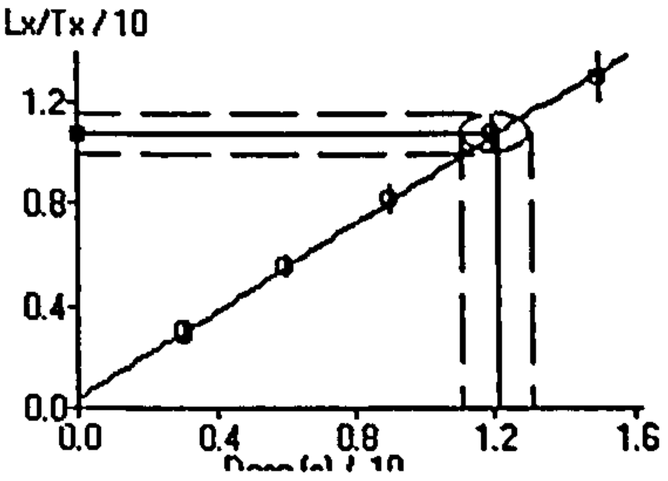

Sinale Aliquot Analysis

SUTL 782

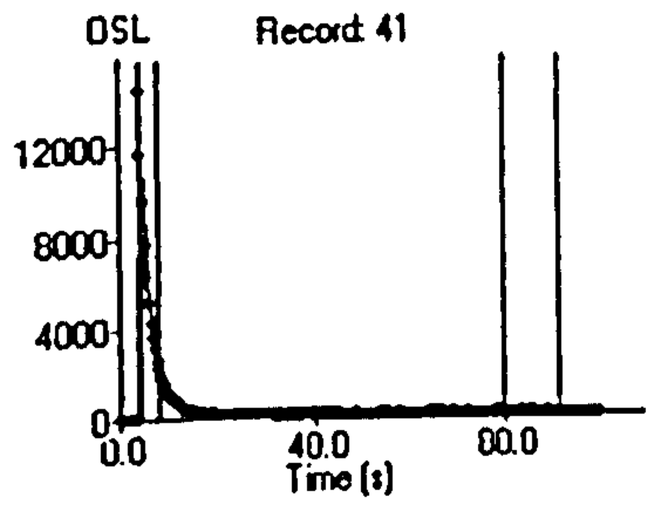

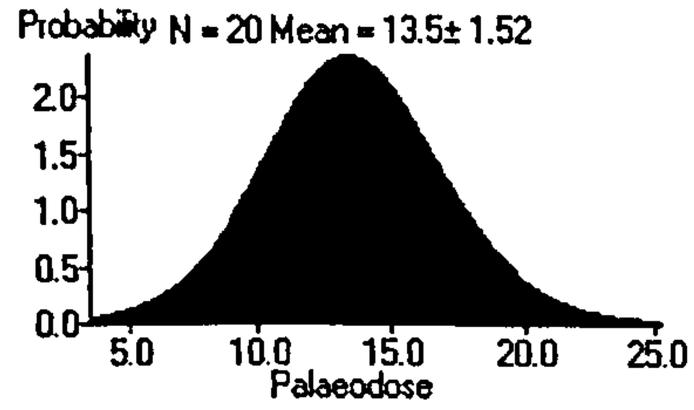

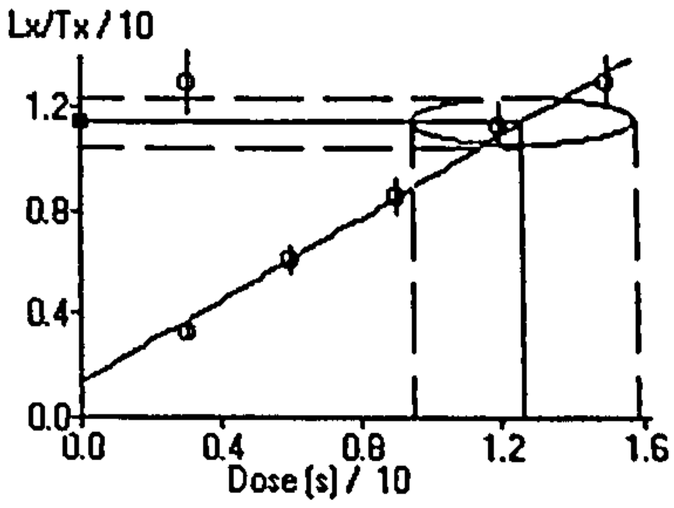

Single Aliquot Analysis

SUTL 783

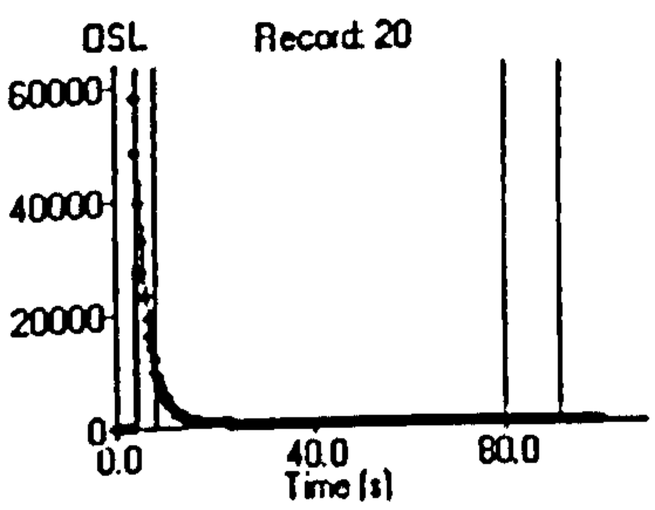

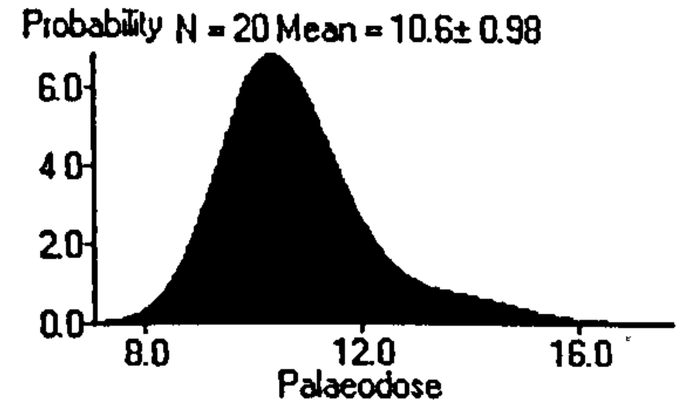

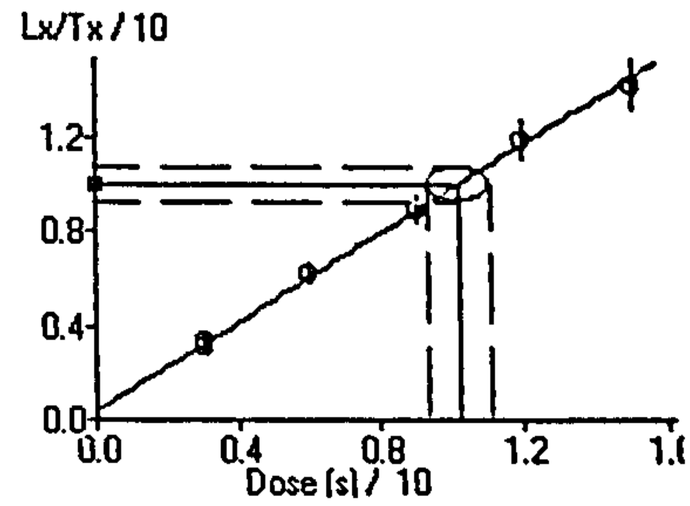

Single Aliquot Analysis

SUTL 784

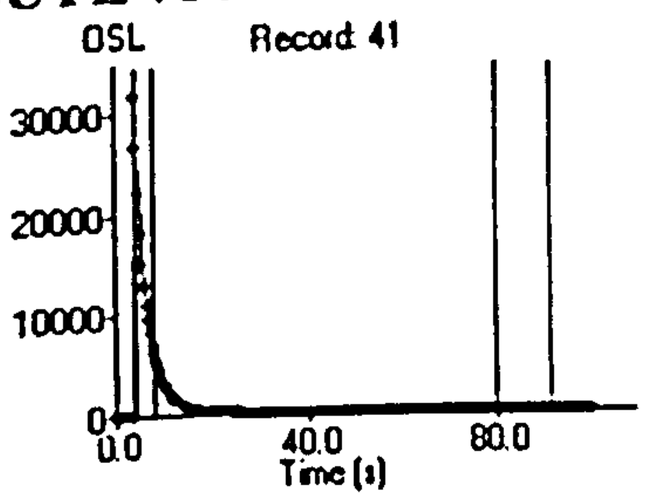

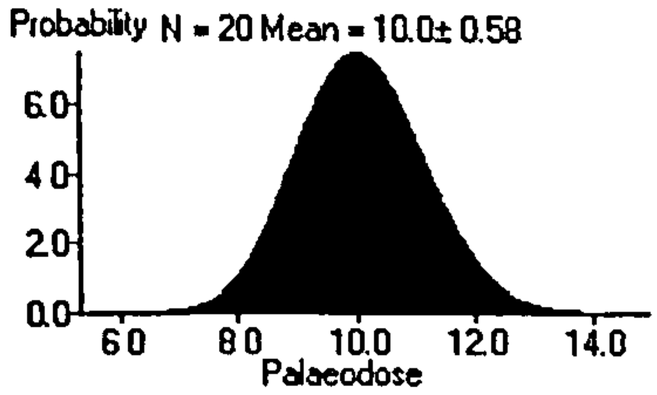

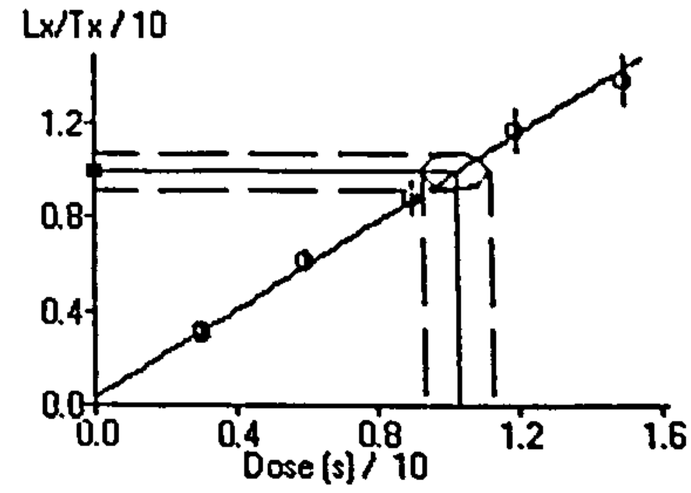

Single Aliquot Analysis

G.3 SKAILL

SUTL1361

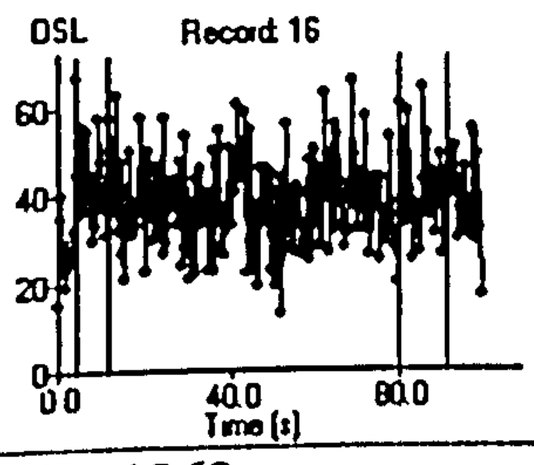

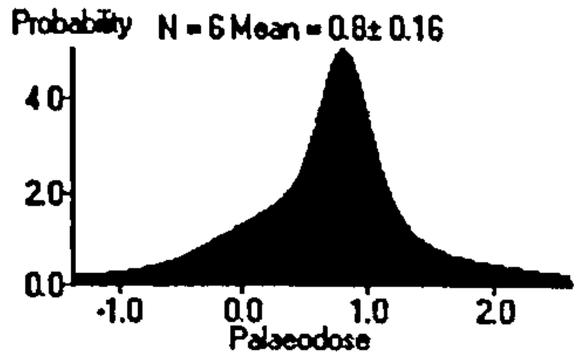

Single Aliquot Analysis

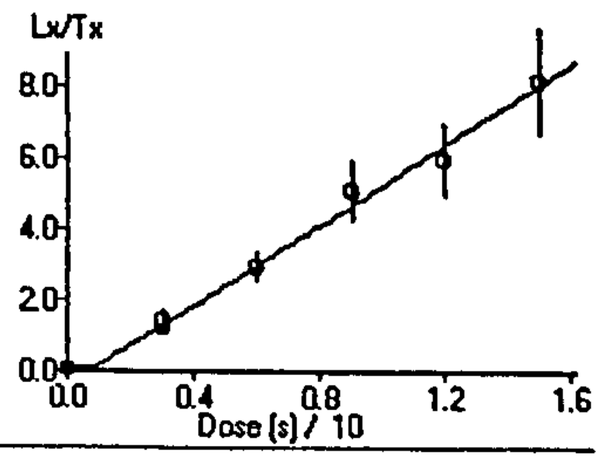

SUTL 1362

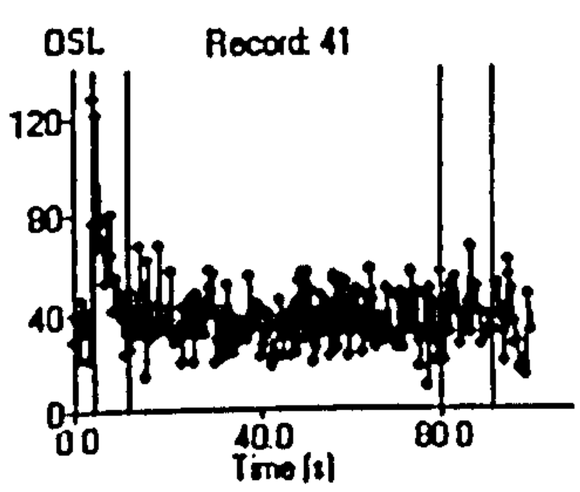

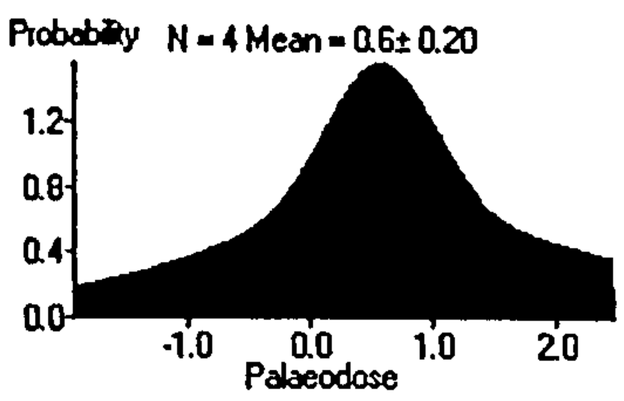

Single Aliquot Analysis

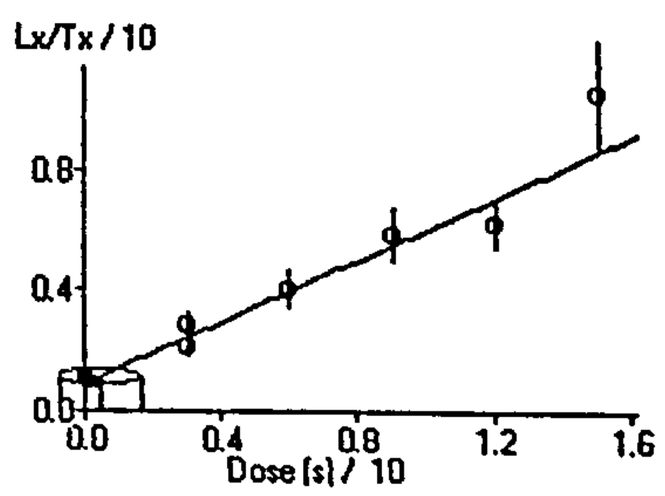

SUTL 1363

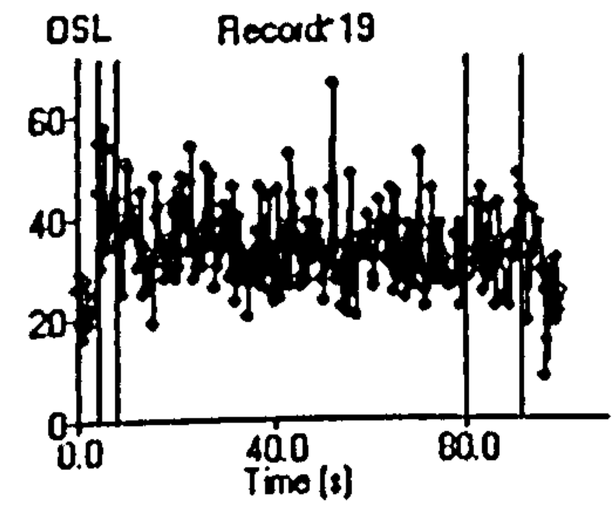

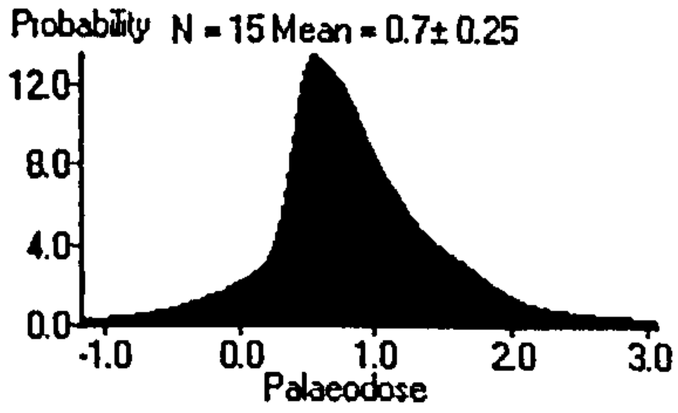

Single Aliquot Analysis

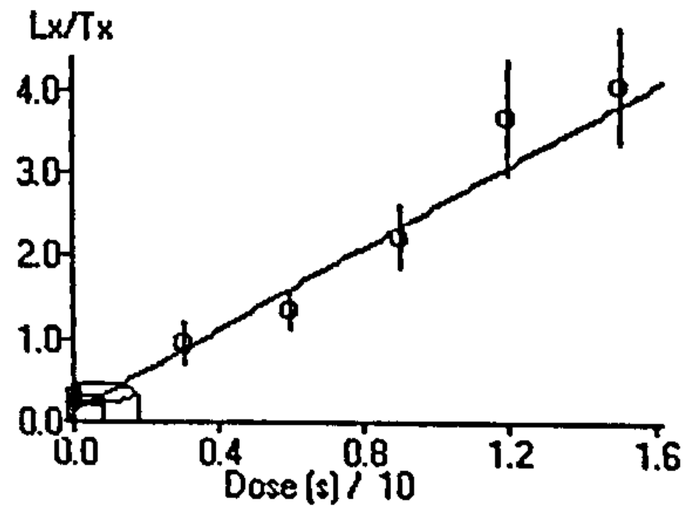

SUTL 1364

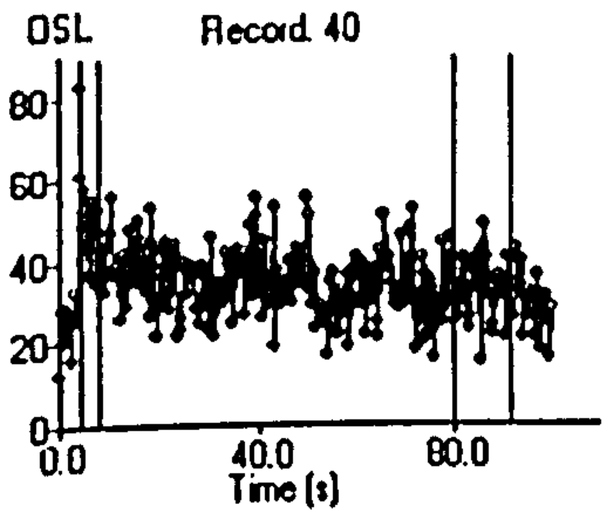

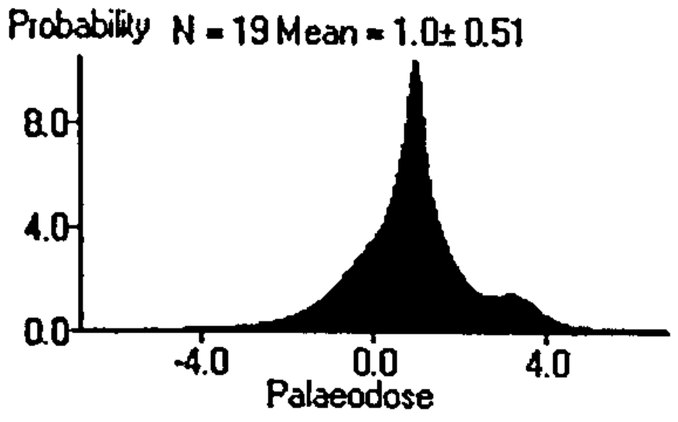

Single Aliquot Analysis

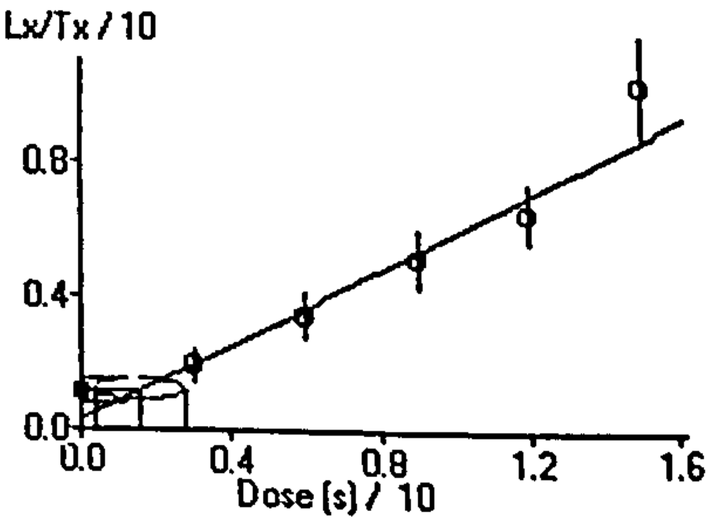

G.4 Knoll of Merrigarth

SUTL 795

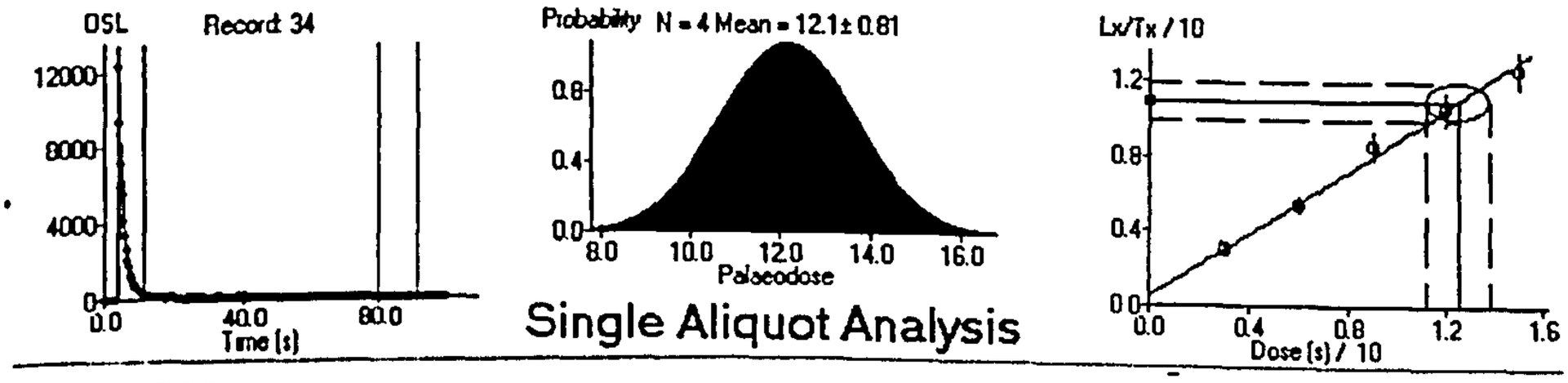

SUTL 802

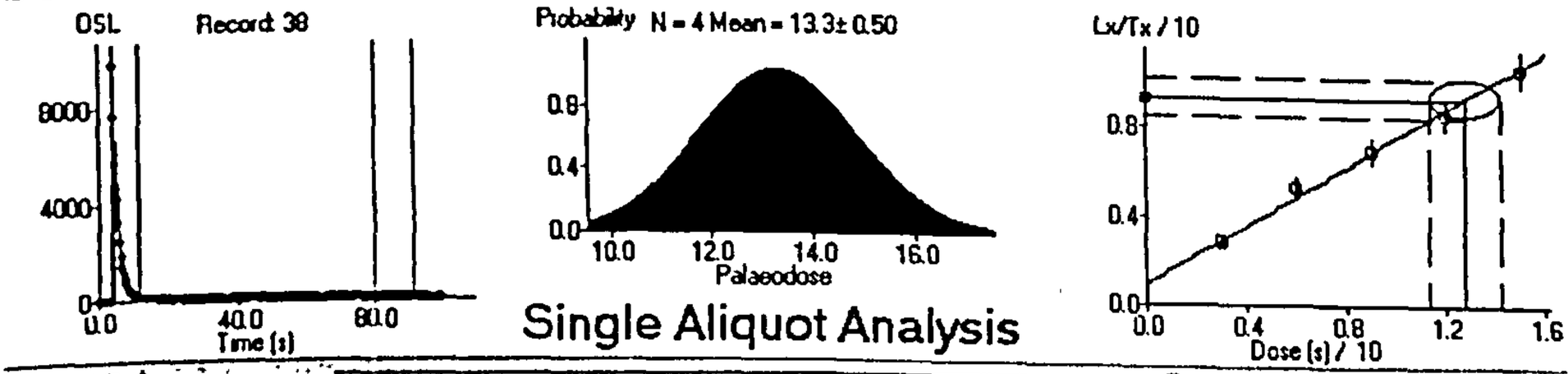

SUTL 803

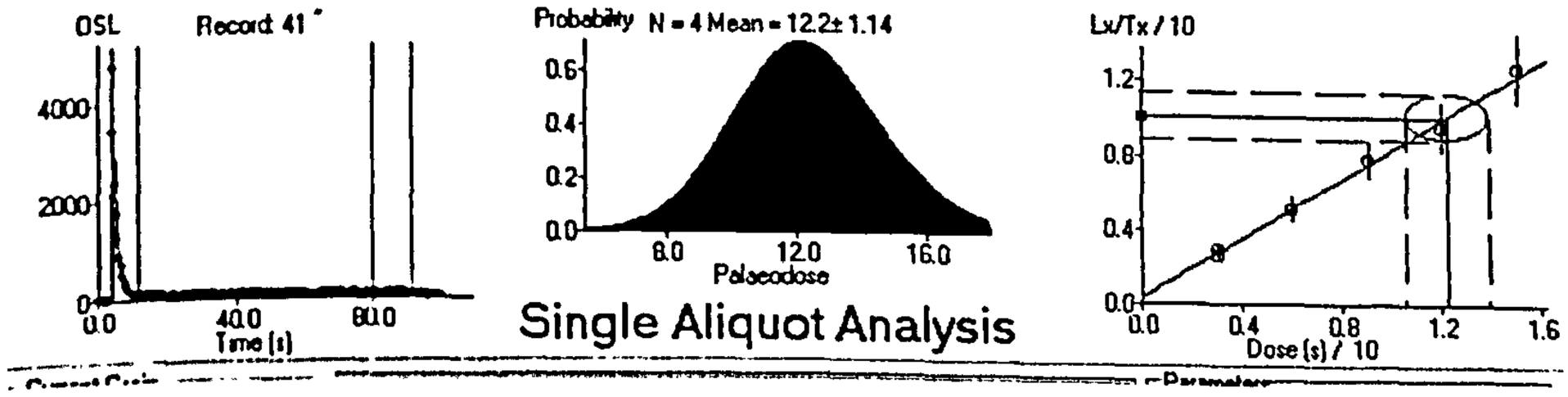

G.5 Fersness

SUTL 823

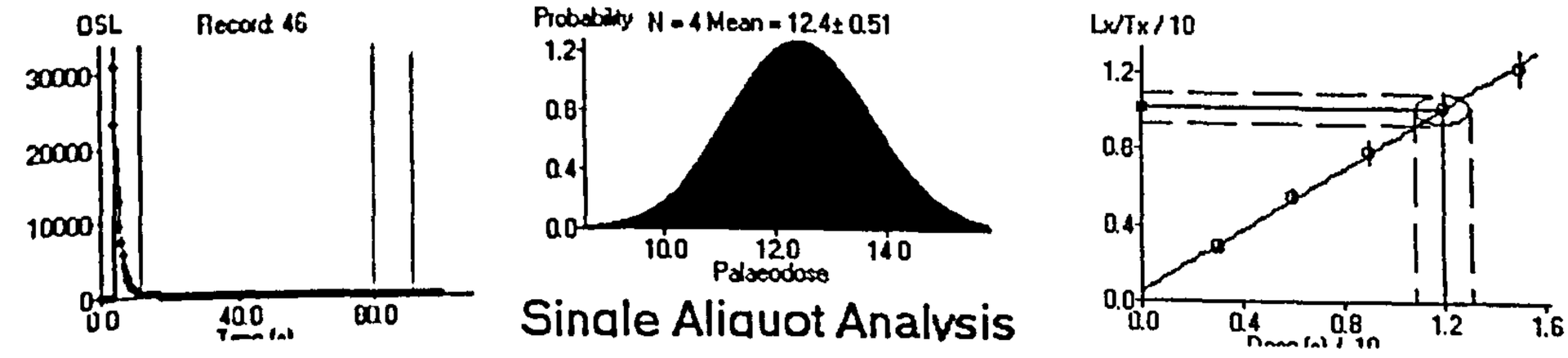

G.6 Cruester

SUTL 951

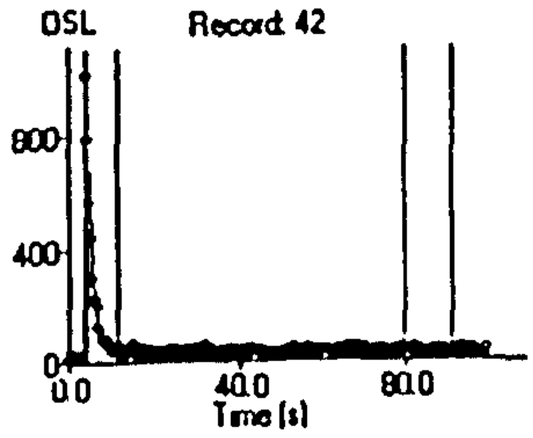

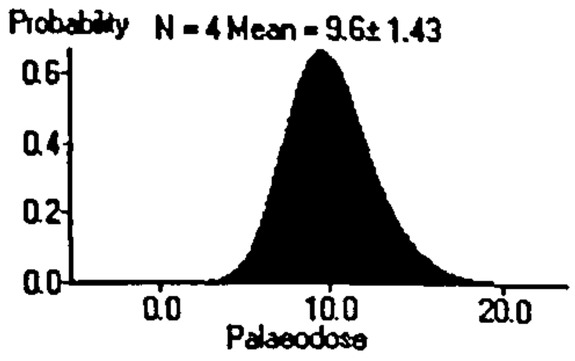

Single Aliquot Analysis

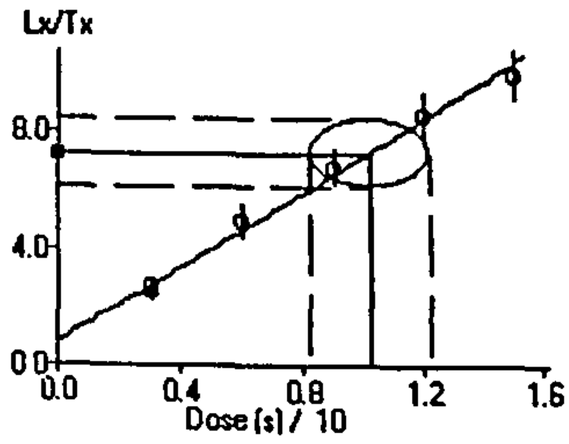

SUTL 953

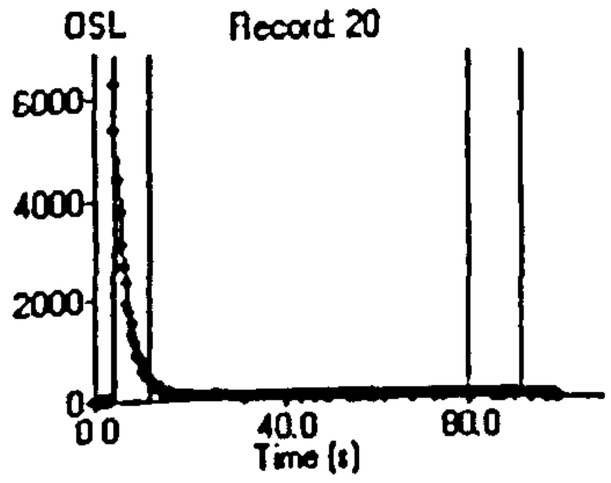

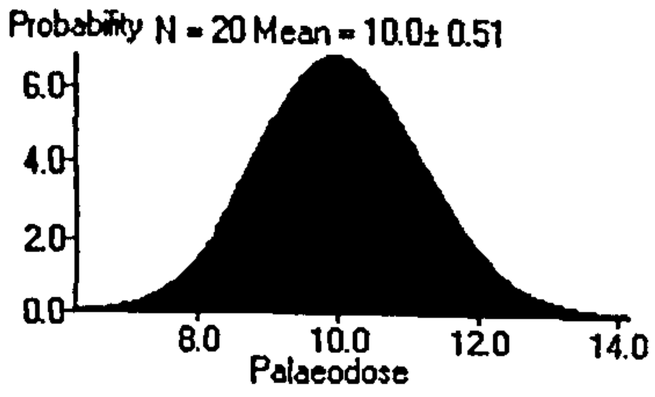

Single Aliquot Analysis

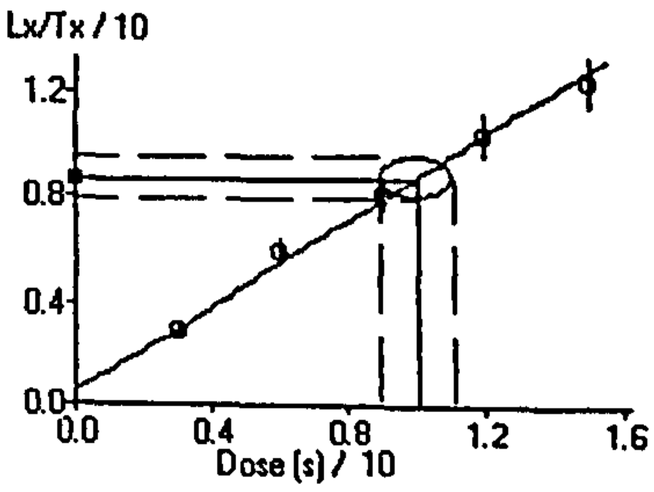

SUTL 958

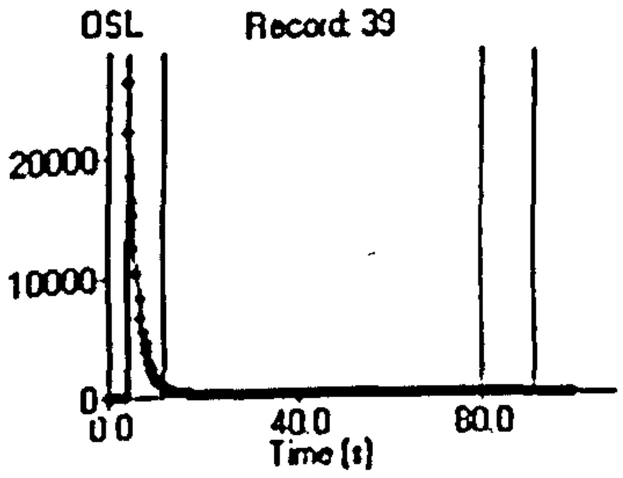

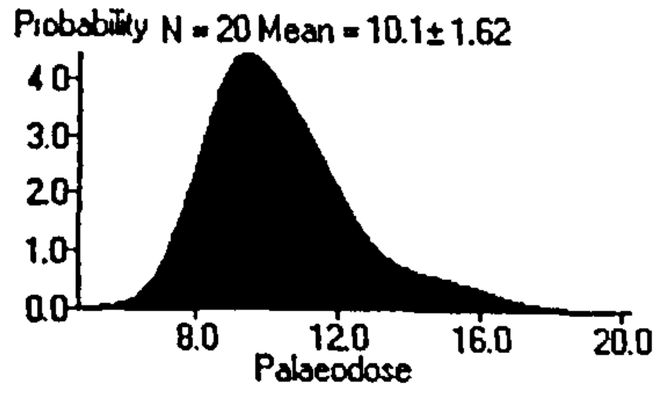

Single Aliquot Analysis

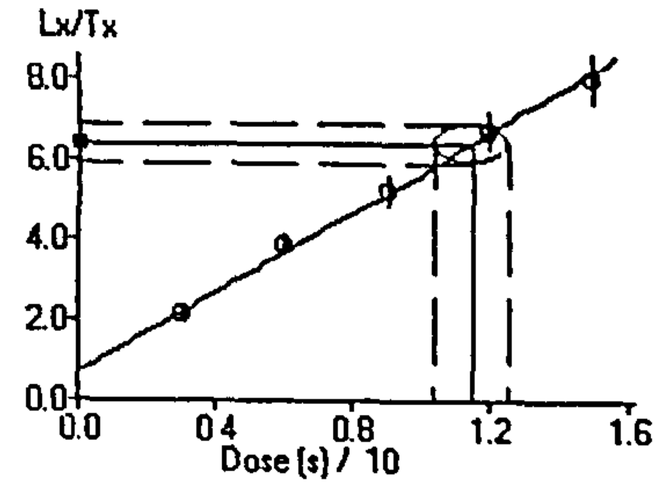

SUTL 968

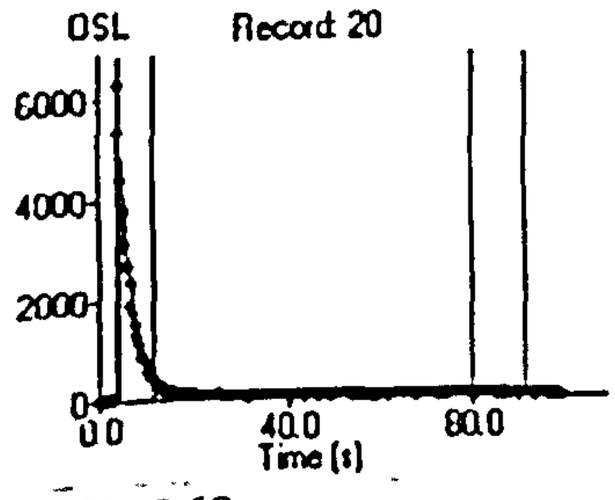

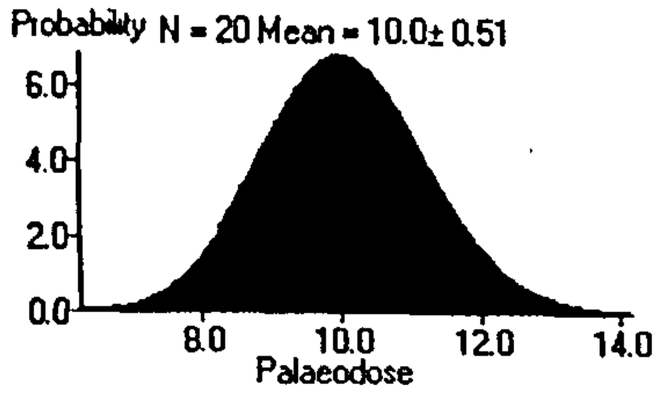

Single Aliquot Analysis

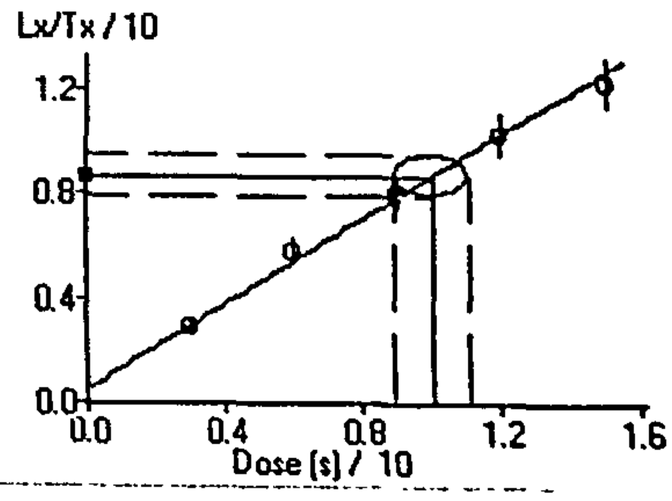

SUTL 969

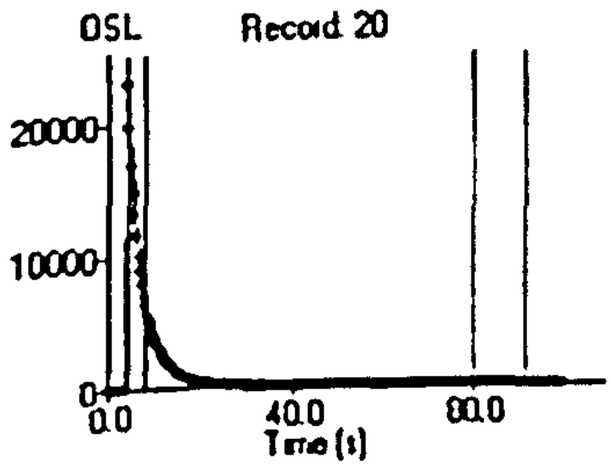

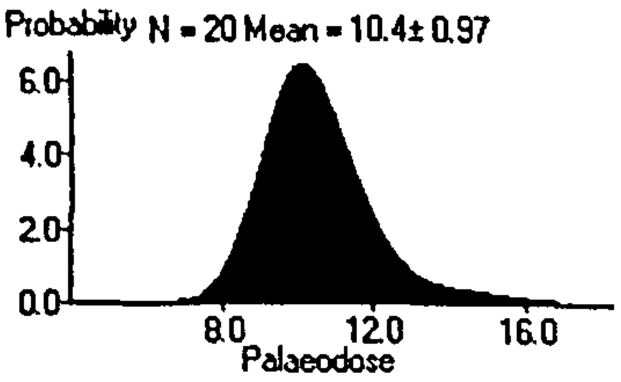

Single Aliquot Analysis

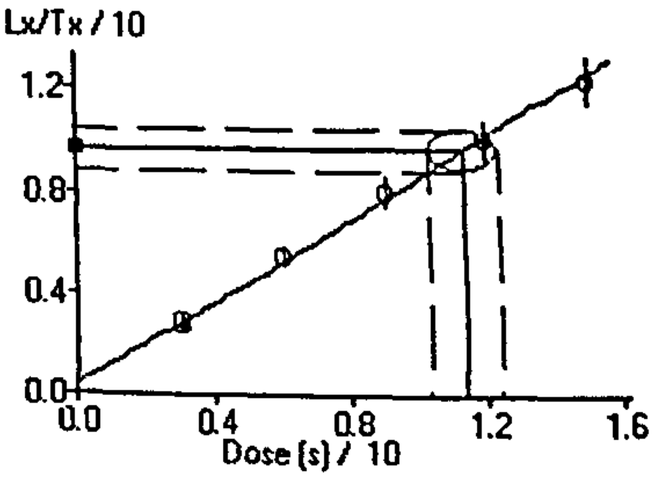

SUTL 1051

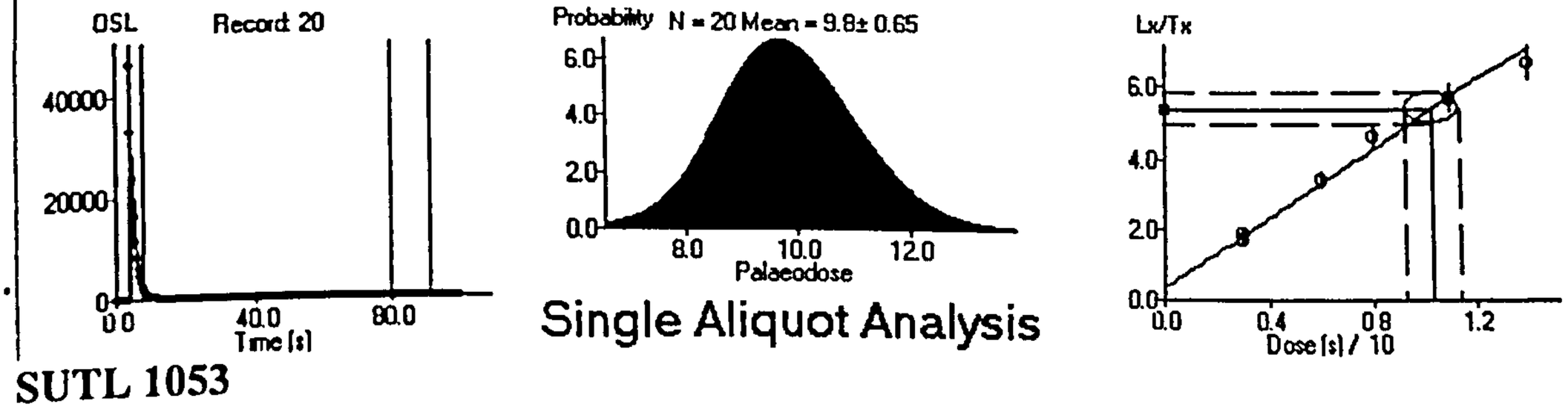

SUTL 1053

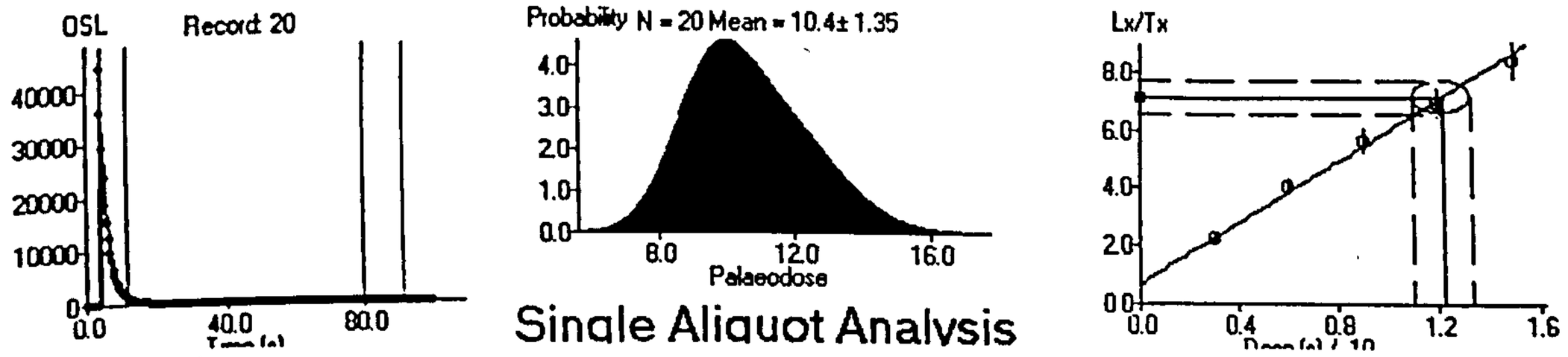

SUTL 1054

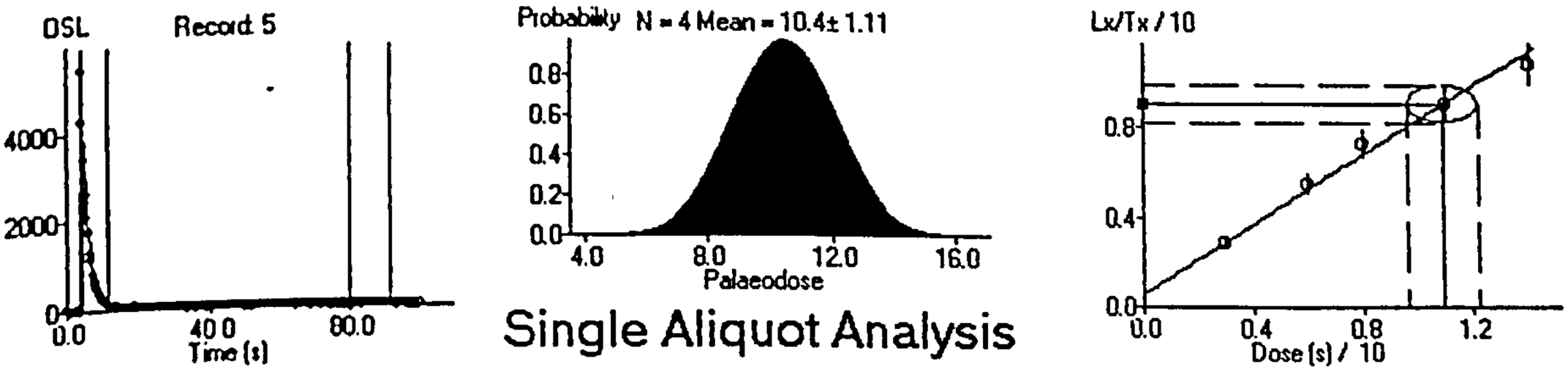

SUTL 1055

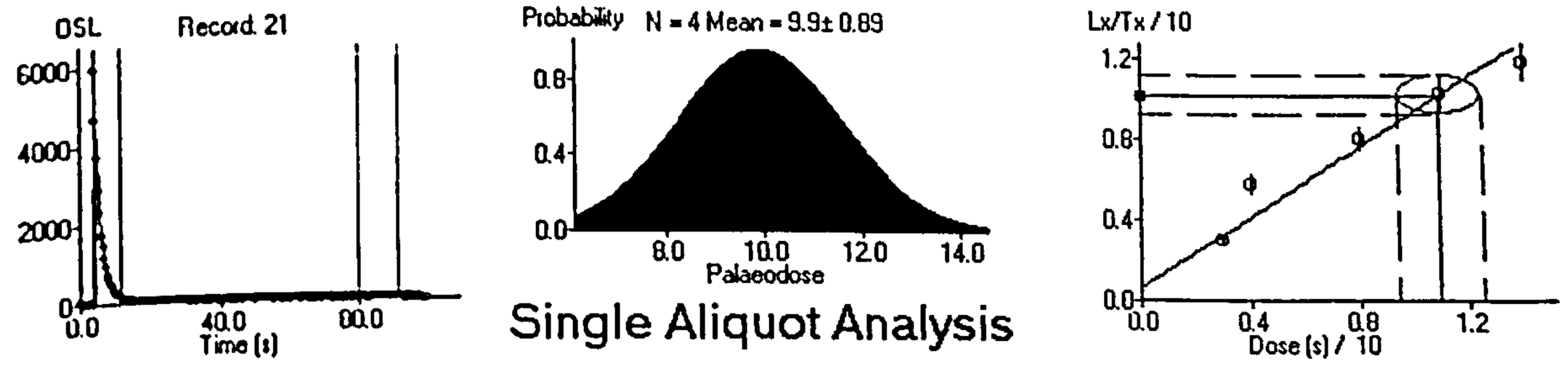

SUTL 1059

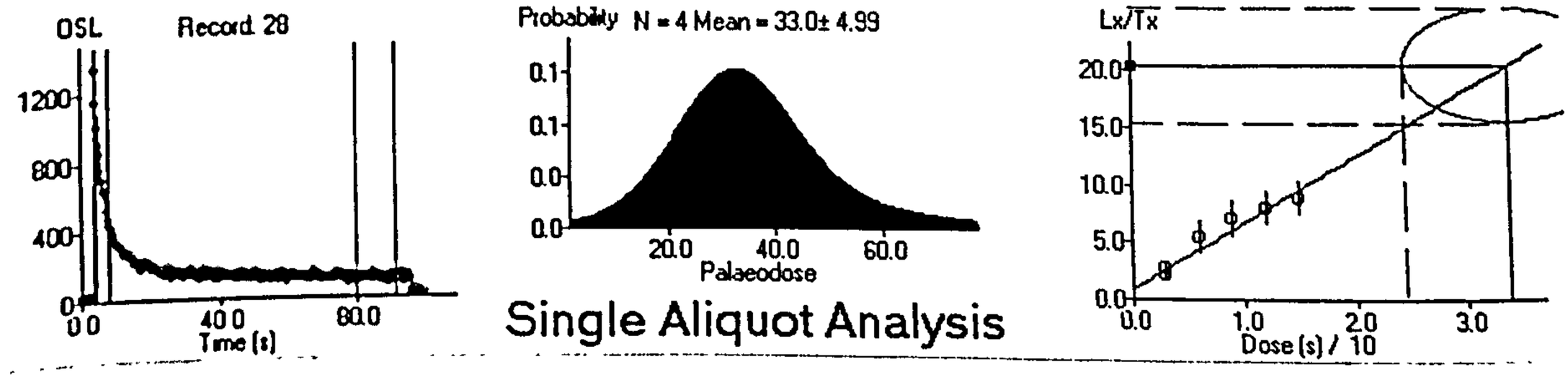

SUTL 1062

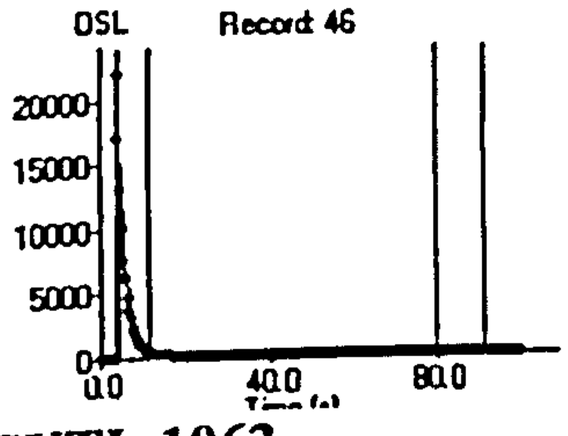

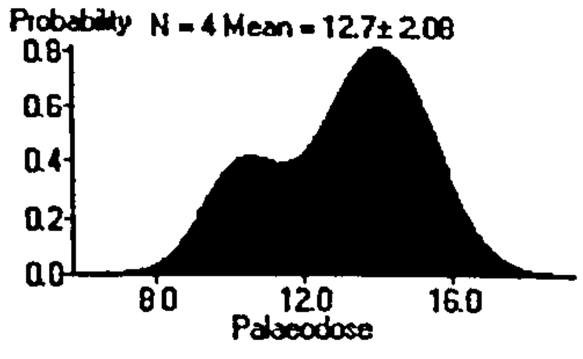

Single Aliquot Analysis

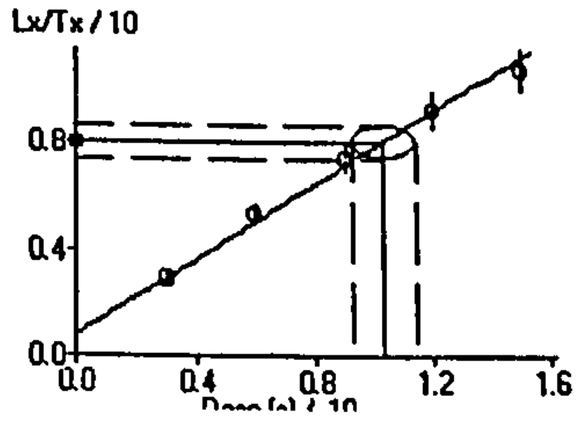

SUTL 1063

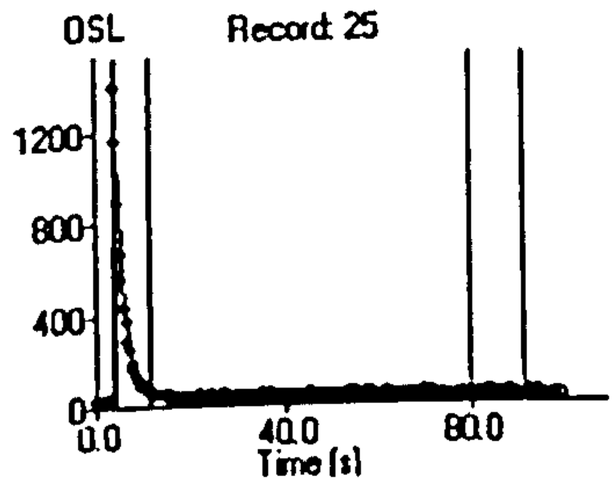

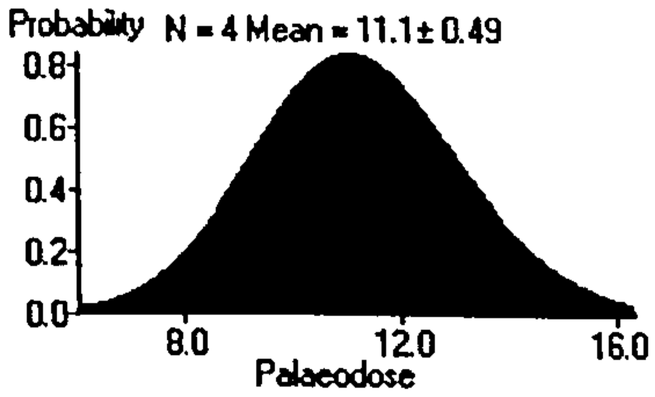

Single Aliquot Analysis

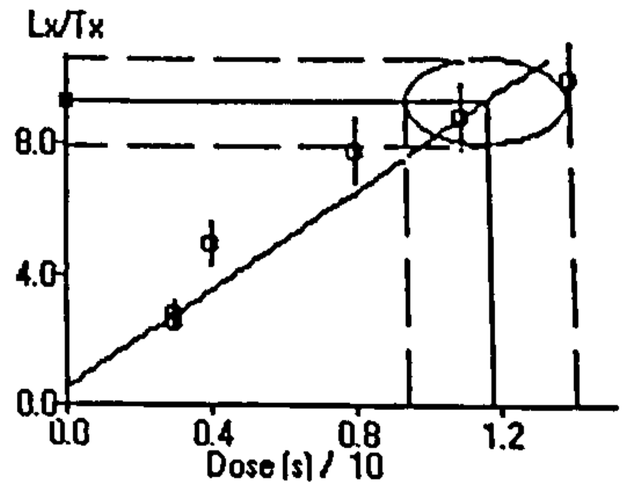

SUTL 1064

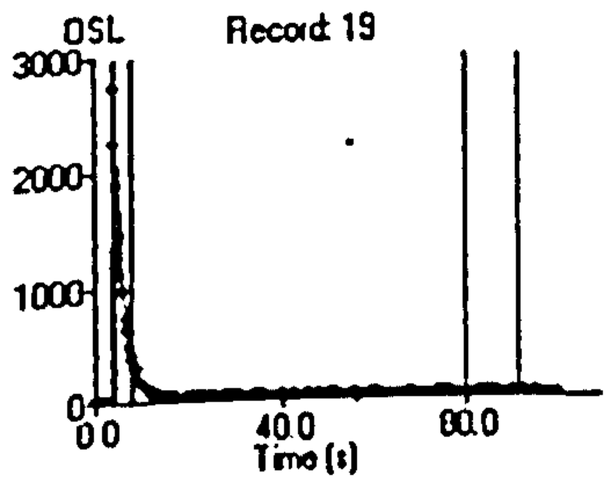

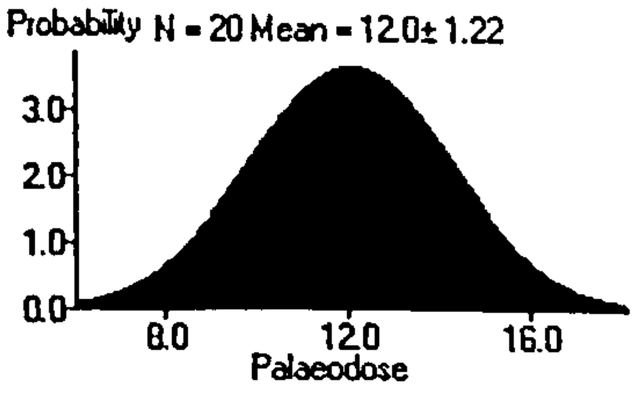

Single Aliquot Analysis

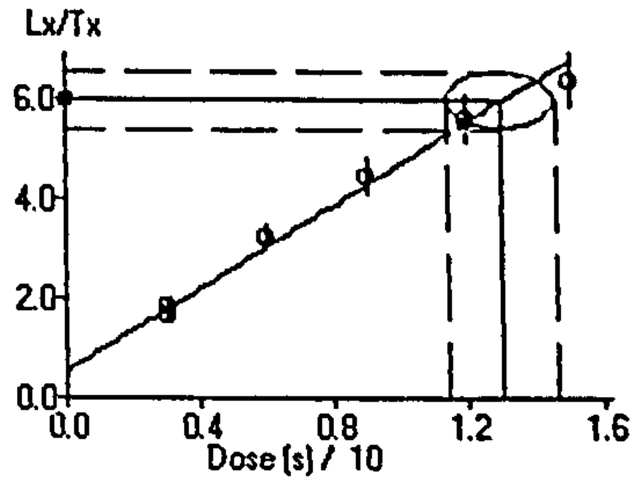

SUTL 1068

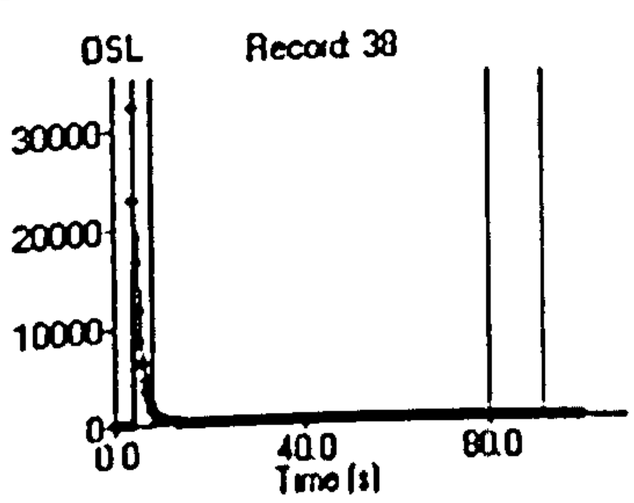

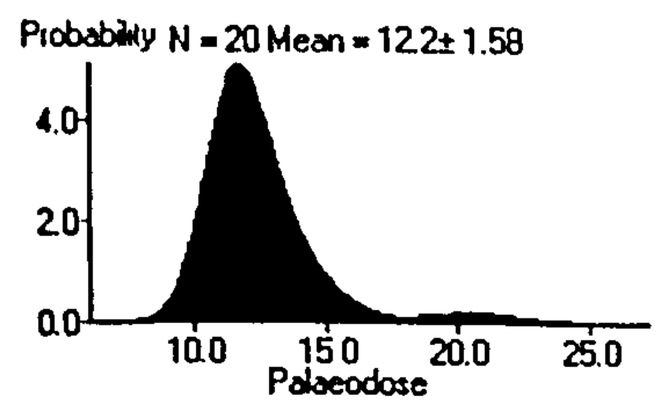

Single Aliquot Analysis

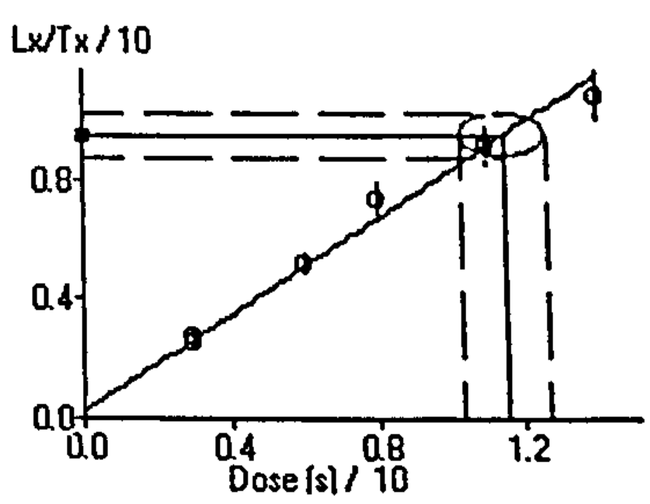

SUTL 1075

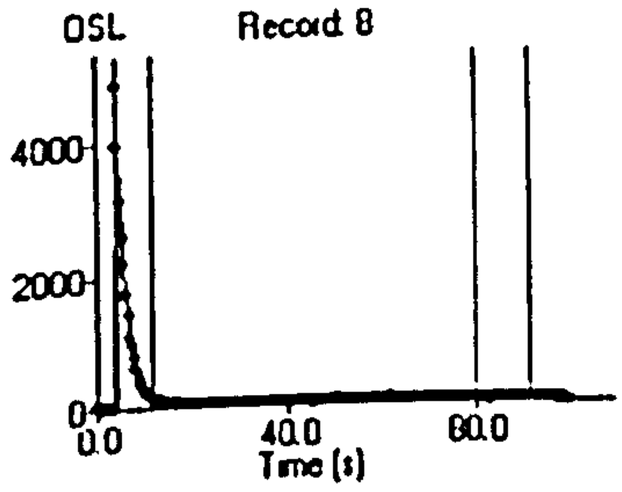

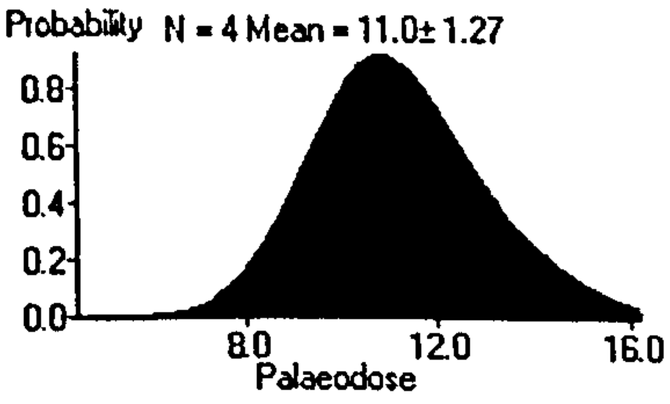

Single Aliquot Analysis

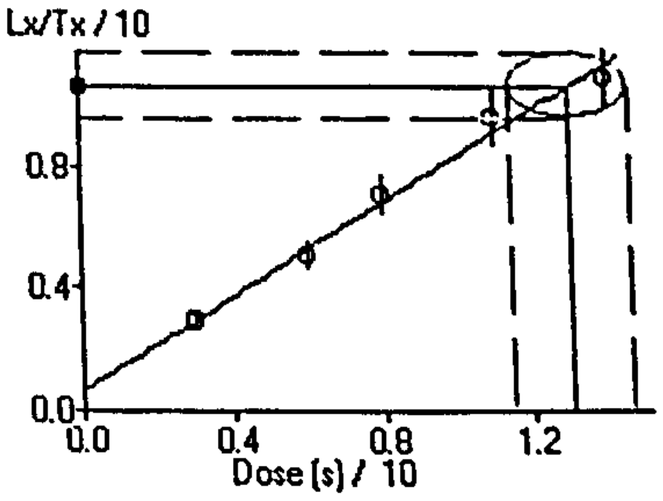

SUTL 1076

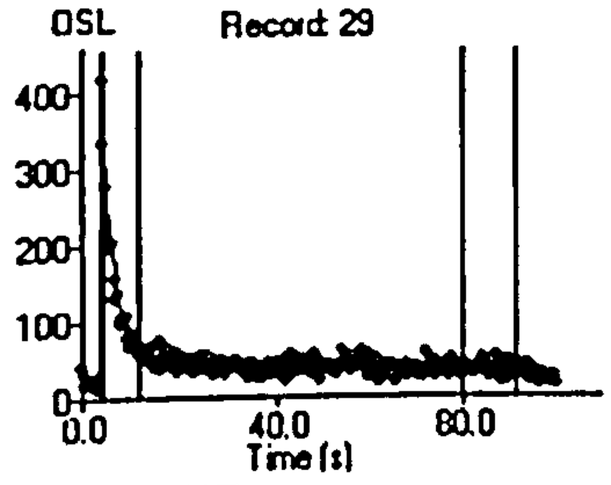

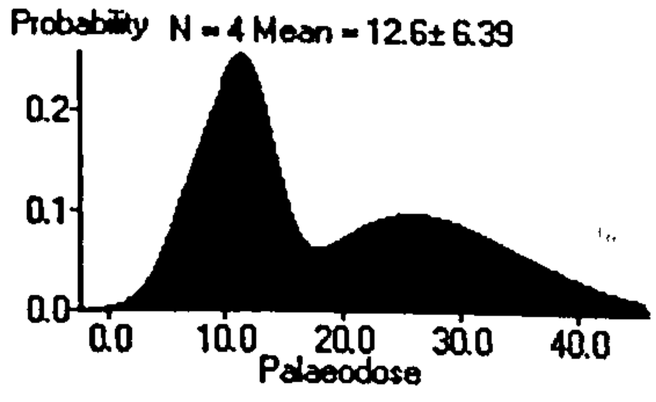

Single Aliquot Analysis

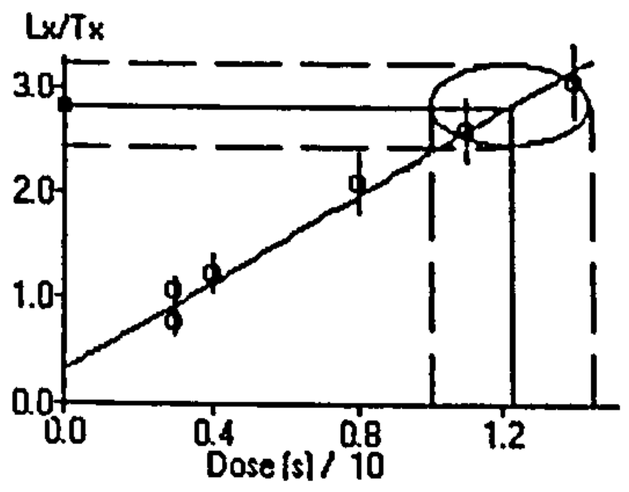

SUTL 1077

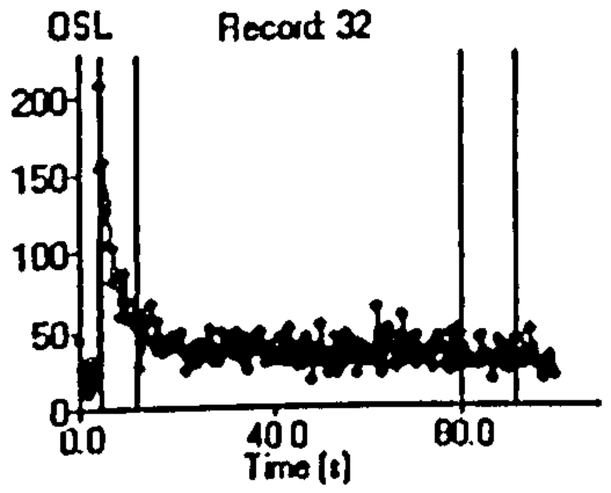

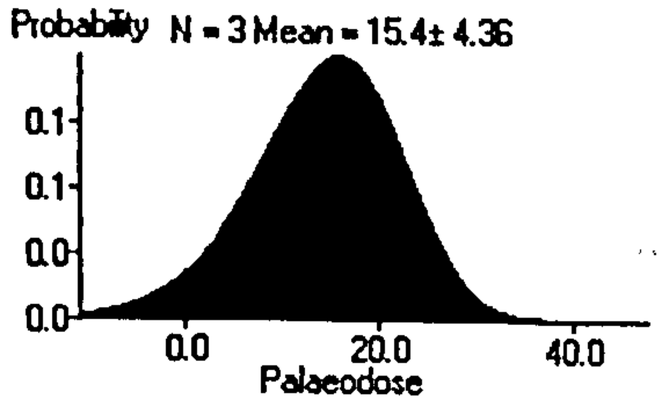

Single Aliquot Analysis

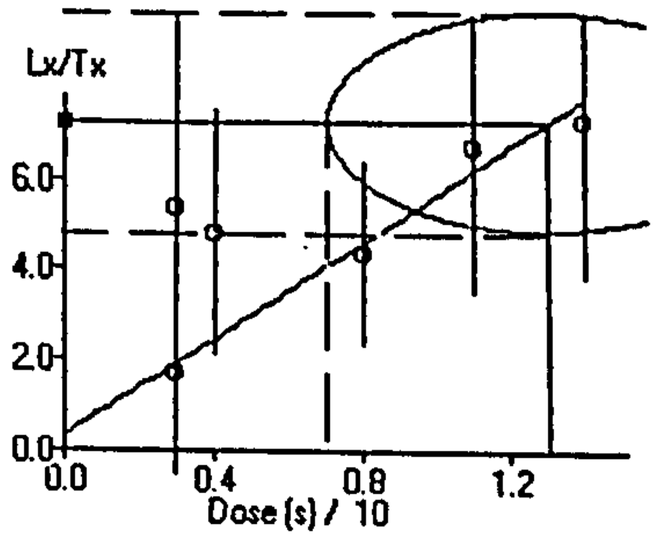

SUTL 1081

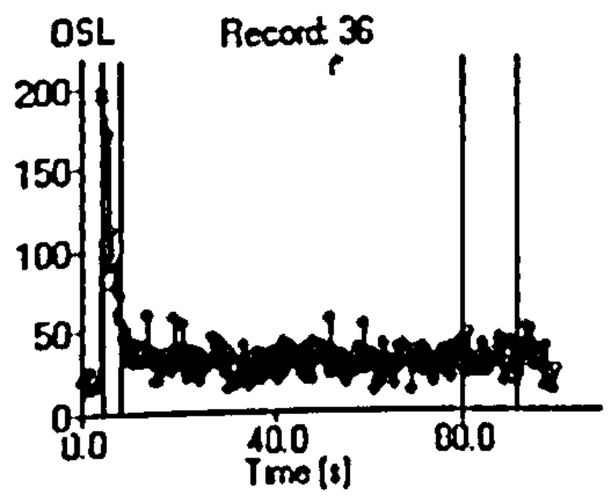

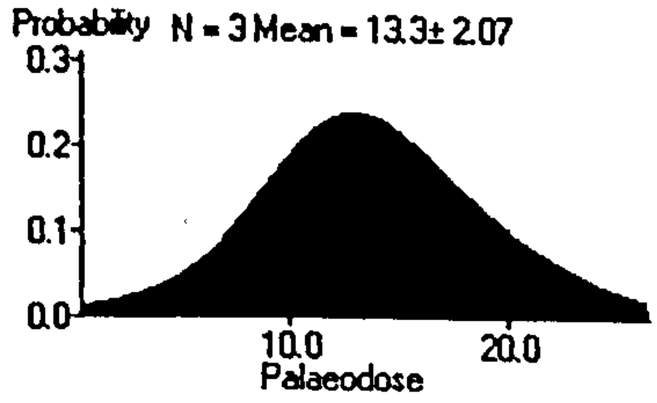

Single Aliquot Analysis

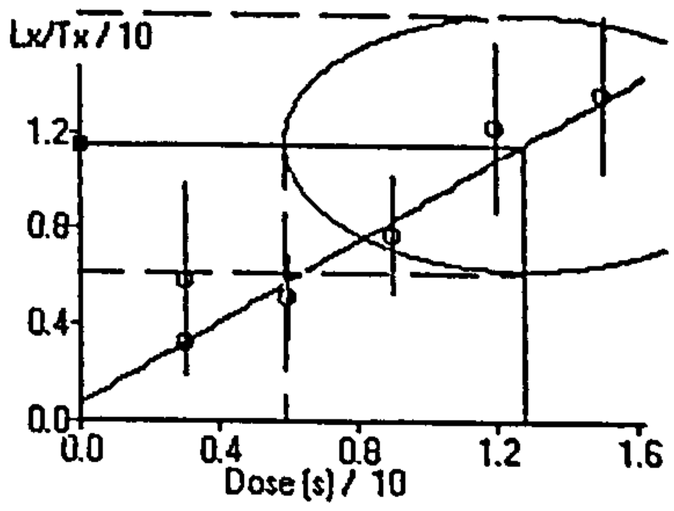

SUTL 1086

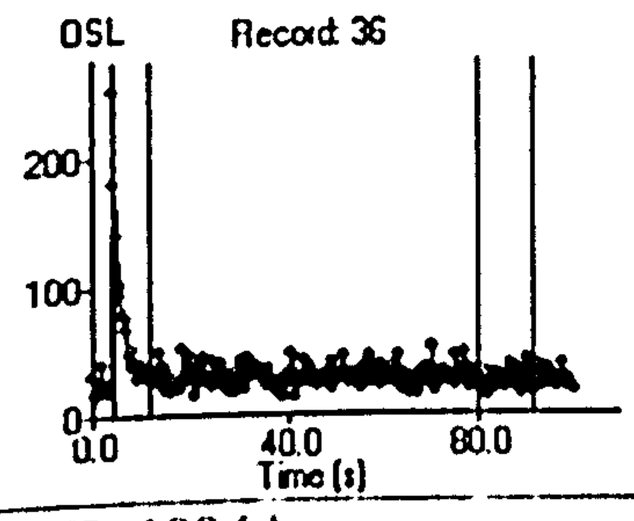

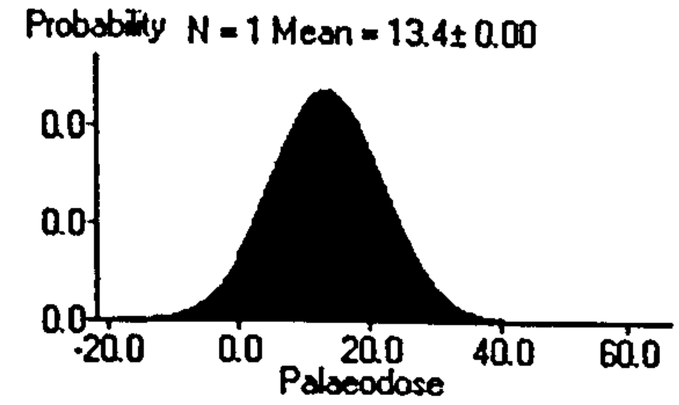

Single Aliquot Analysis

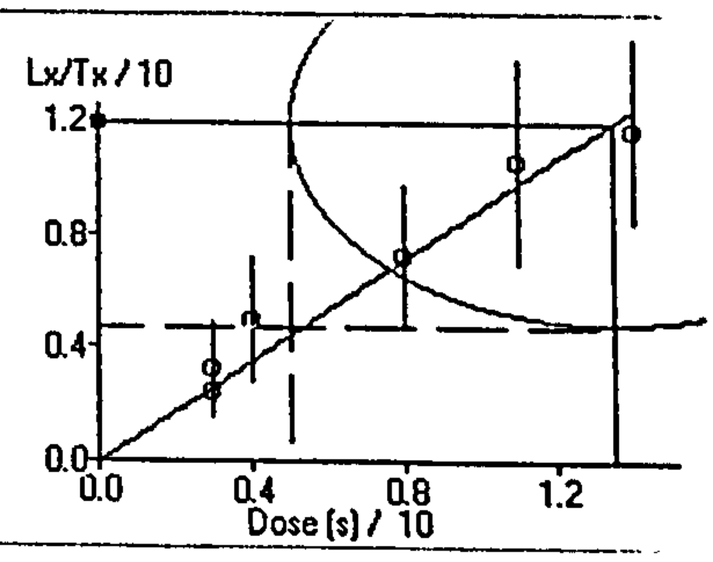

SUTL 1094A

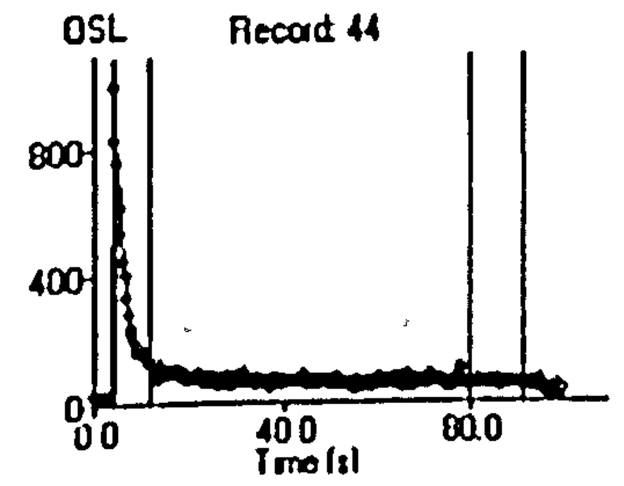

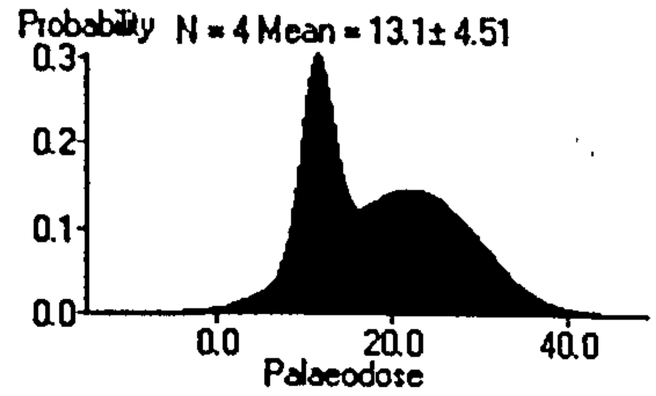

Single Aliquot Analysis

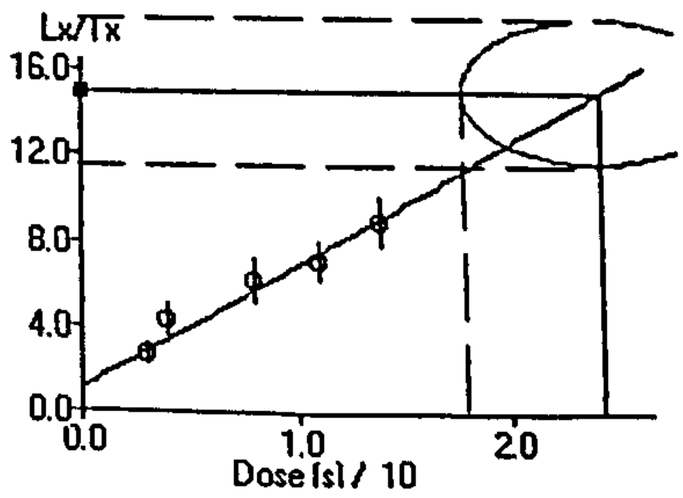

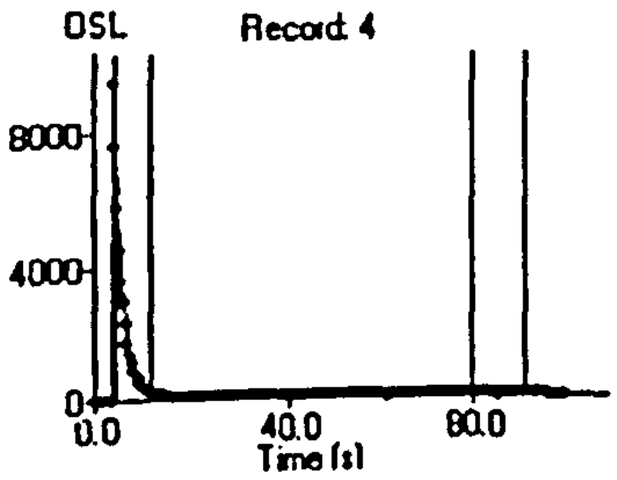

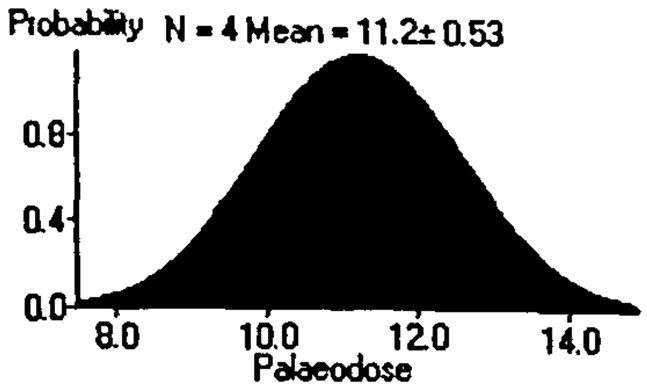

Single Aliquot Analysis

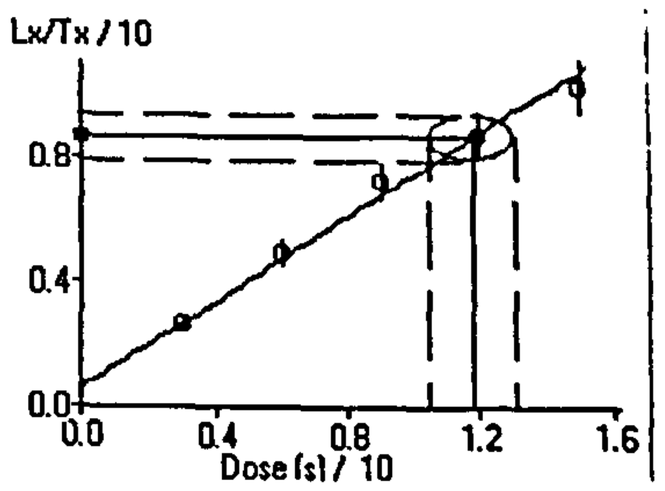

SUTL 1100-1A

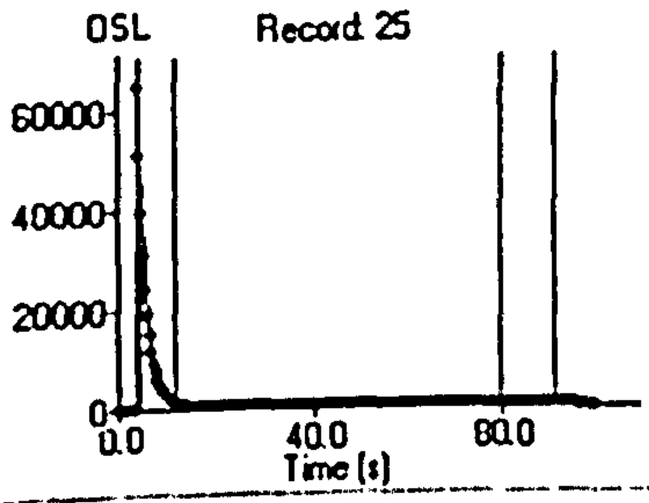

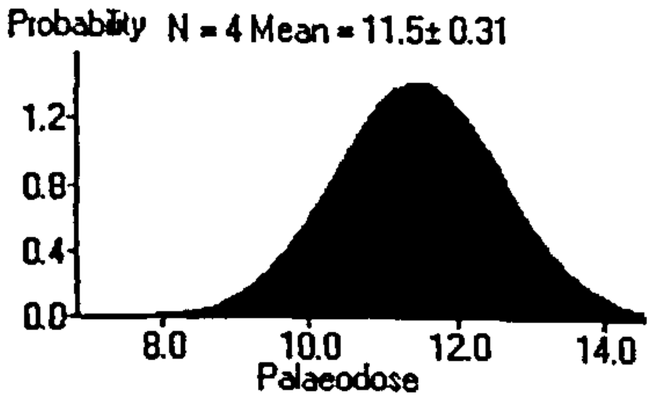

Single Aliquot Analysis

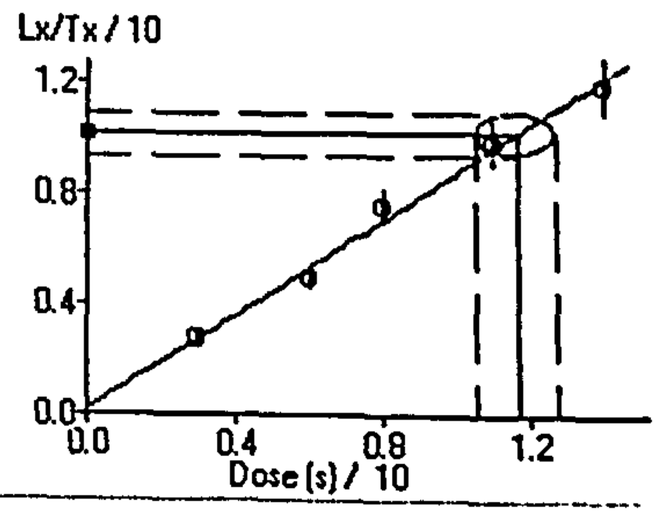

SUTL1100-1B

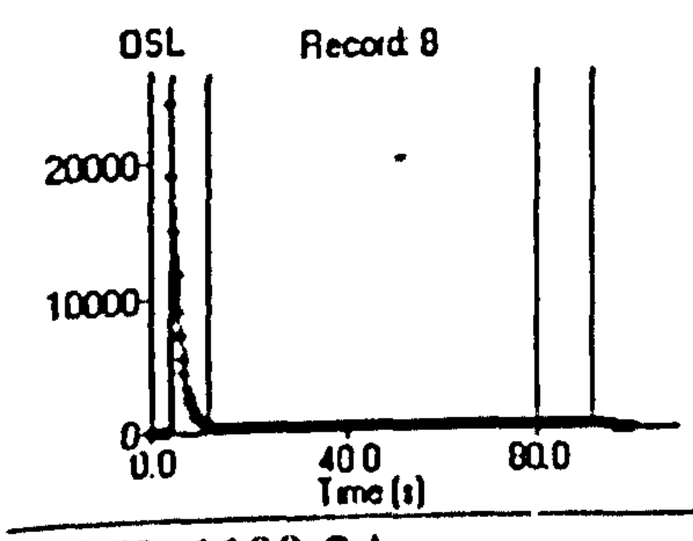

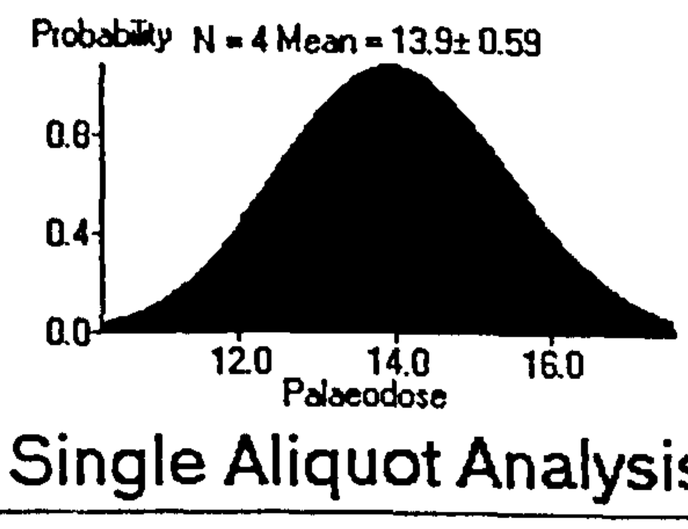

Single Aliquot Analysis

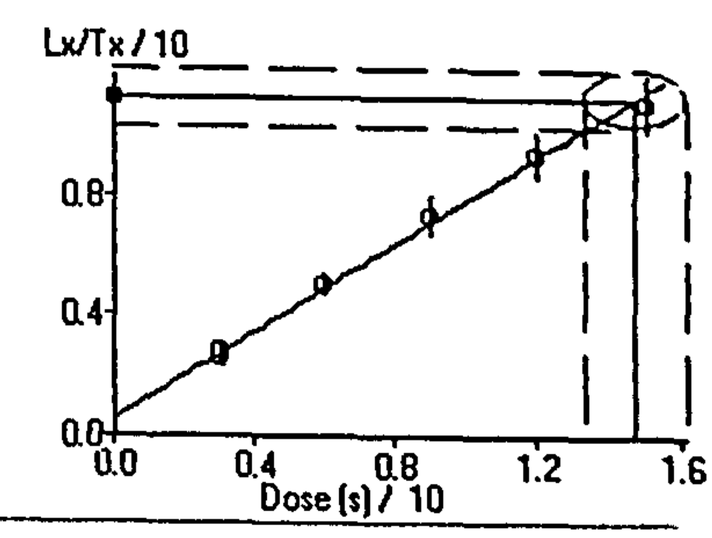

SUTL 1100-2A

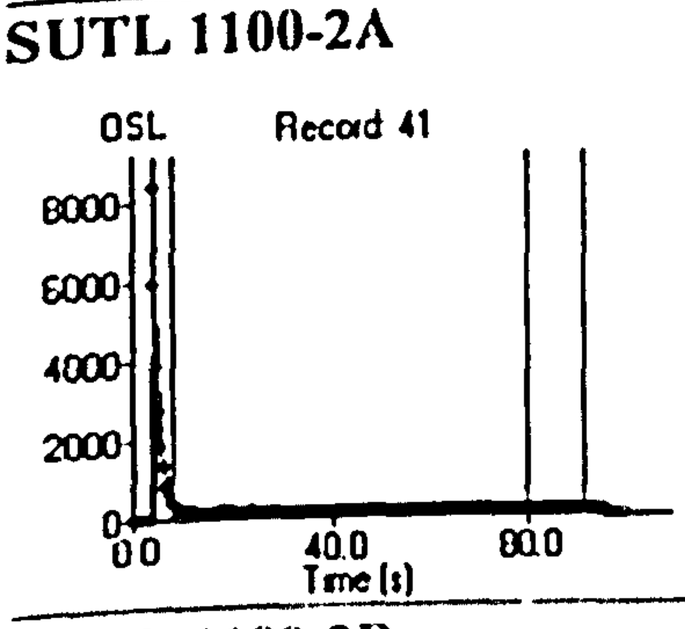

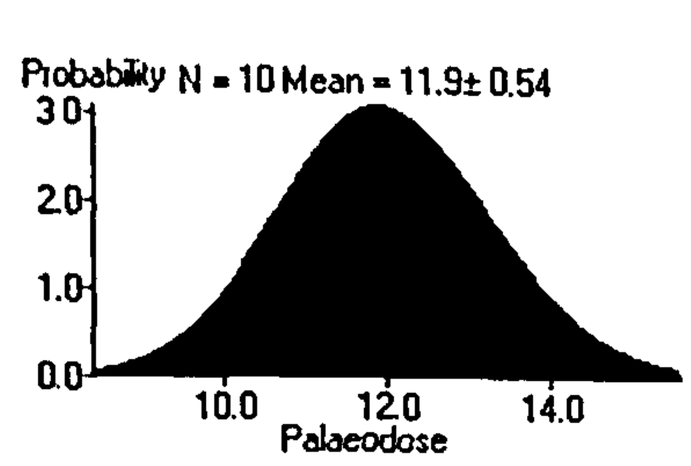

Single Aliquot Analysis

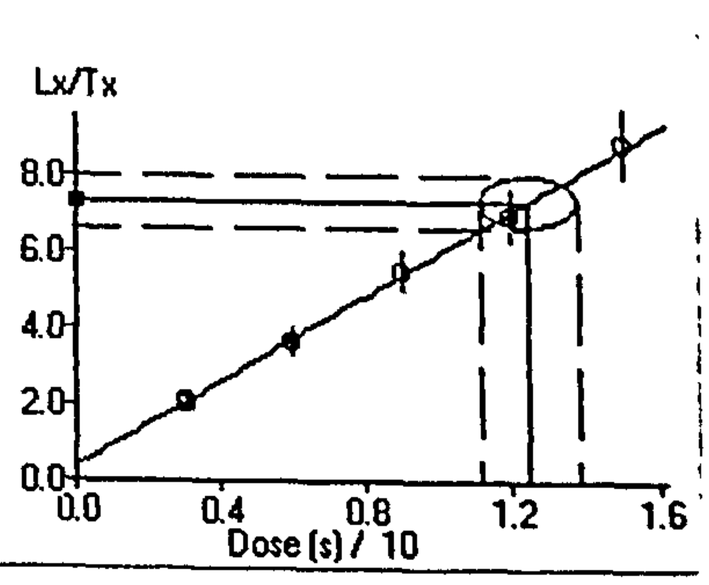

SUTL 1100-2B

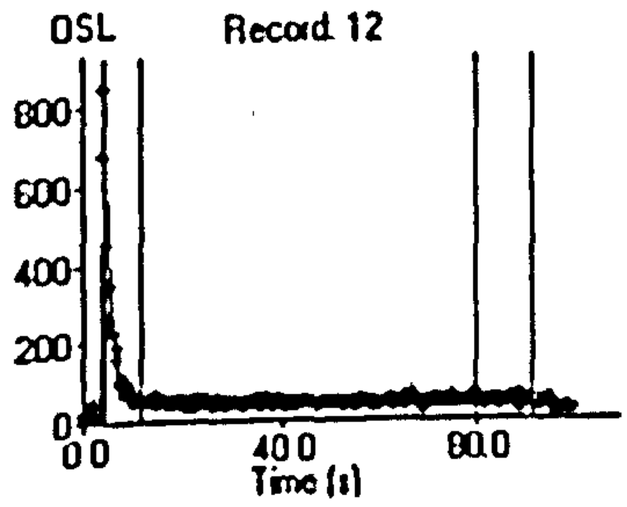

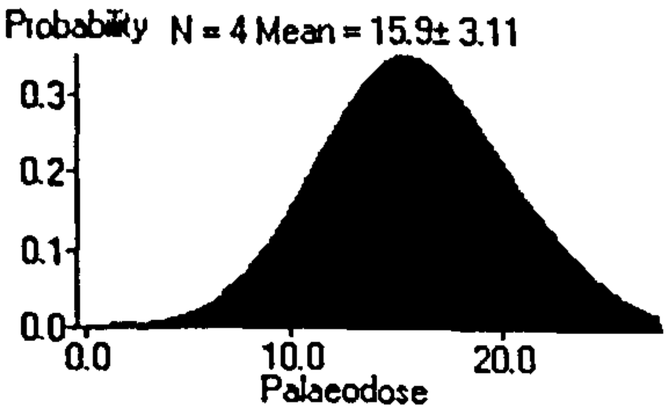

Single Aliquot Analysis

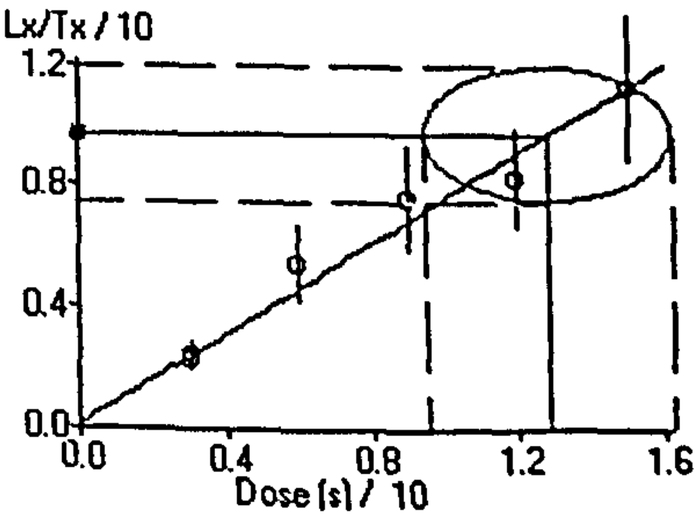

G.7 Houlls

SUTL 970

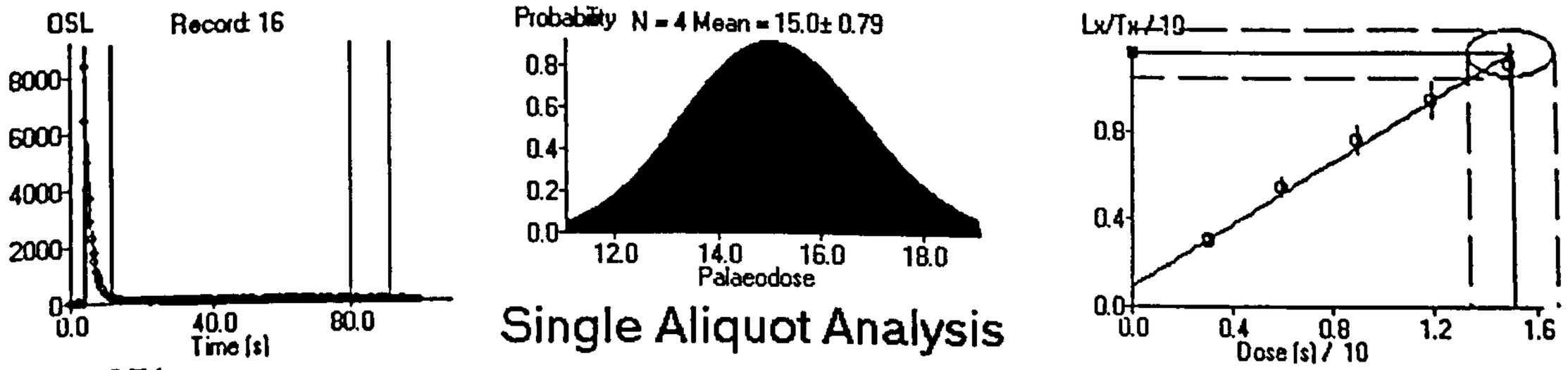

SUTL 971

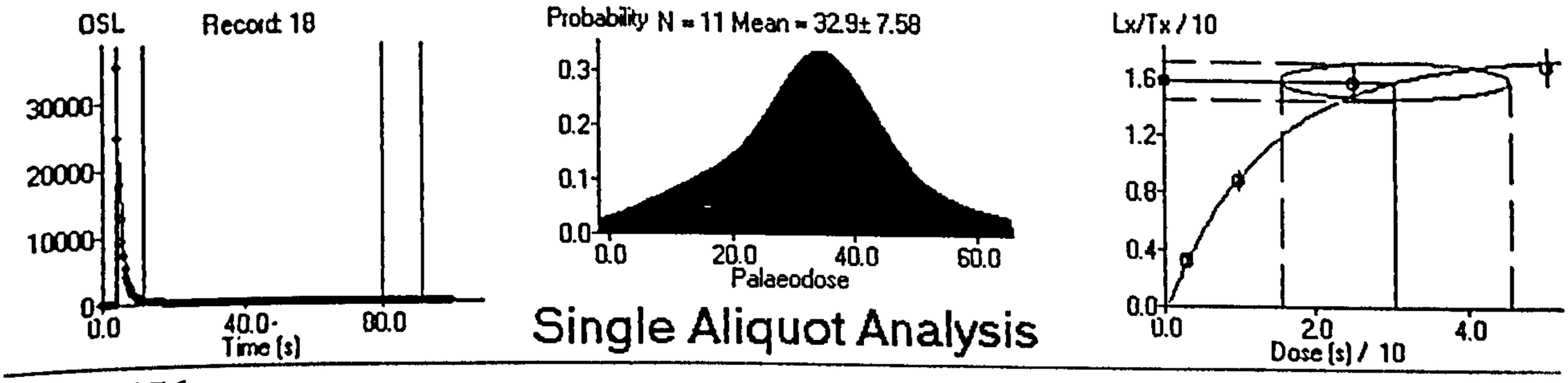

SUTL 976

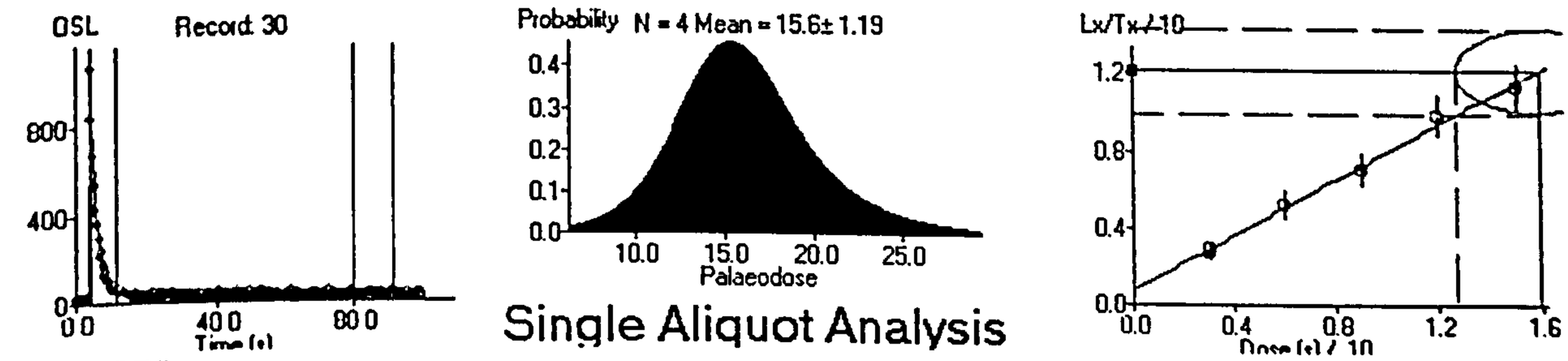

SUTL 978

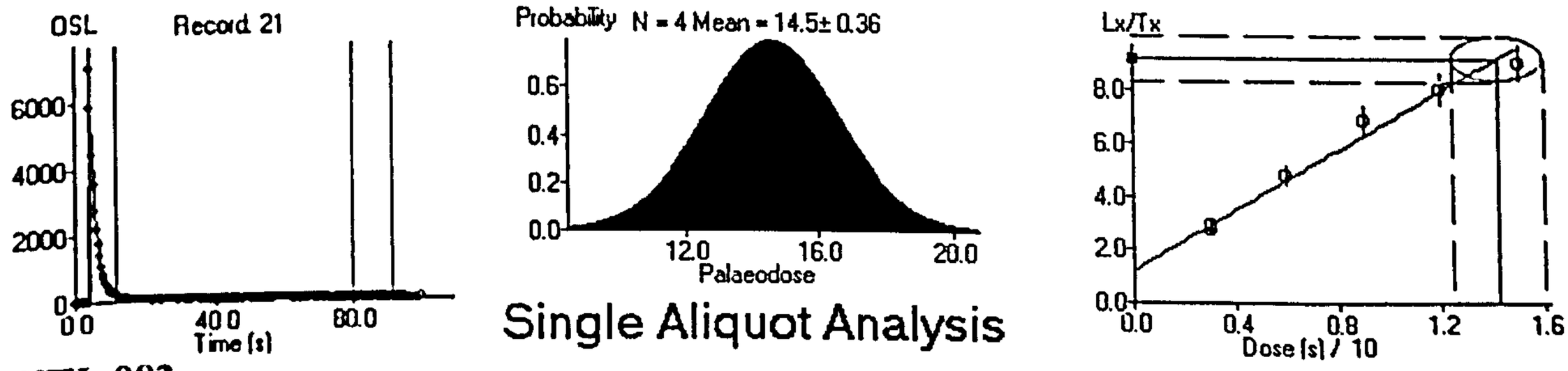

SUTL 983

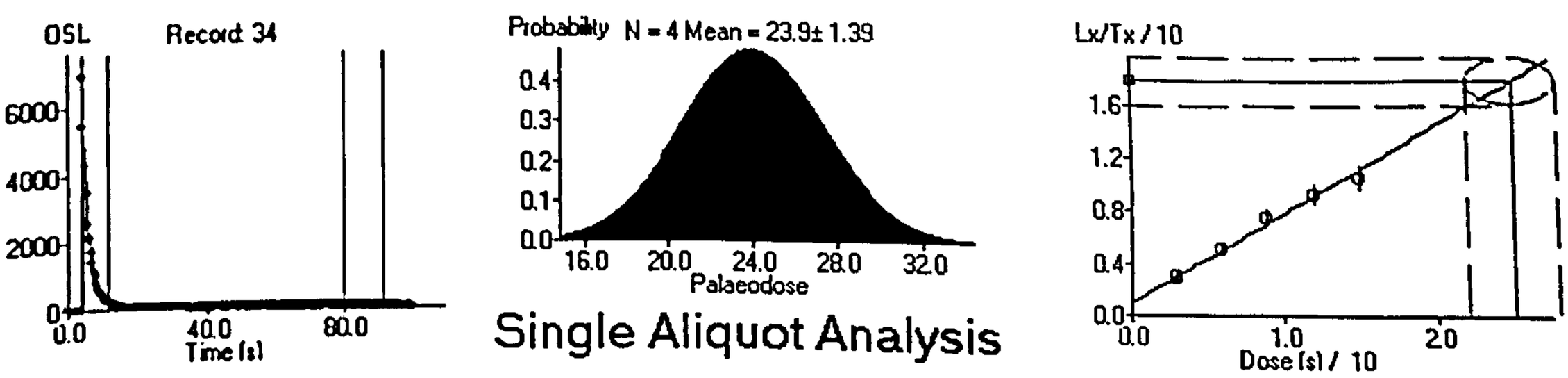

SUTL 991

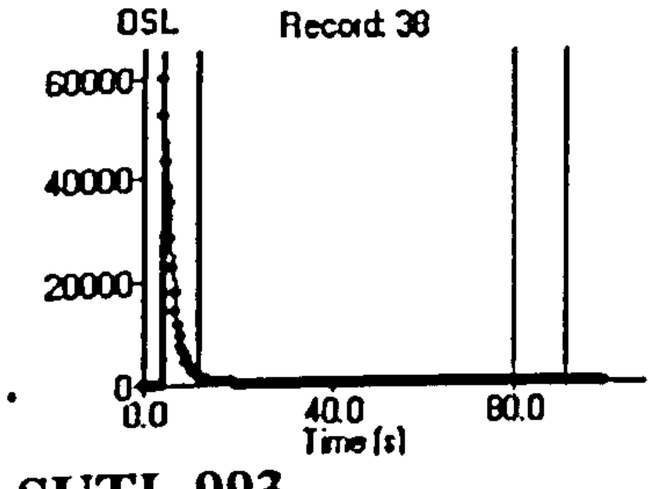

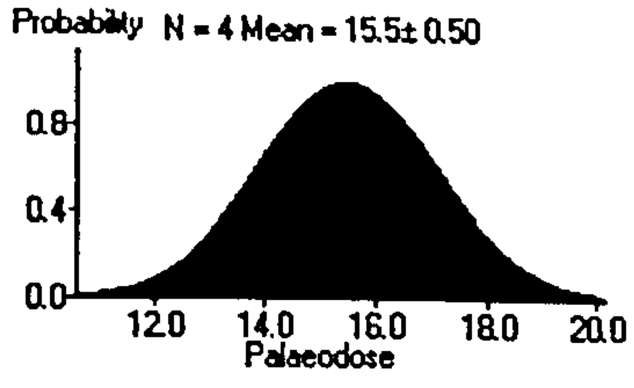

Single Aliquot Analysis

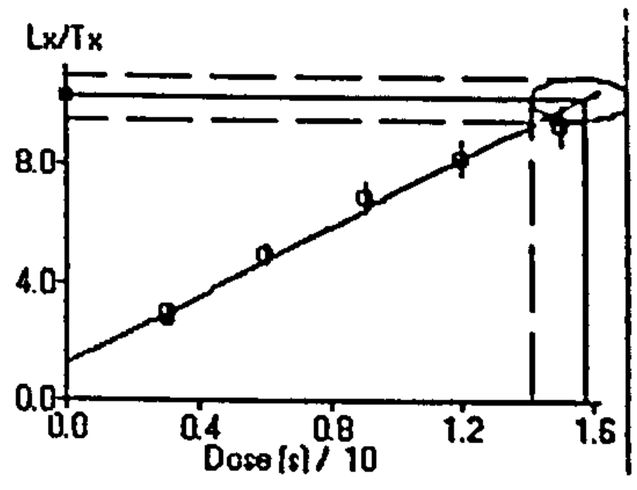

SUTL 993

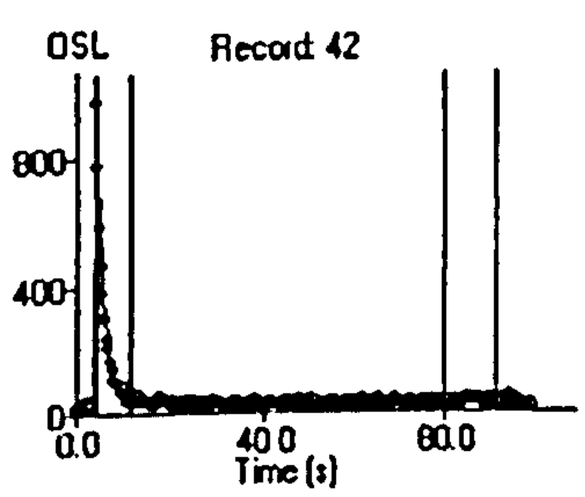

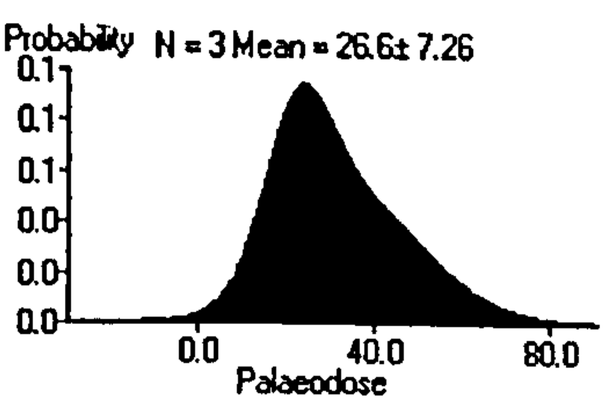

Single Aliquot Analysis

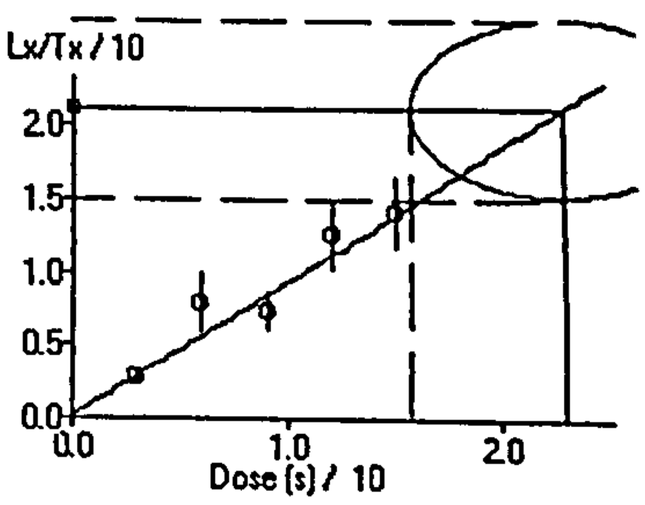

SUTL 1003

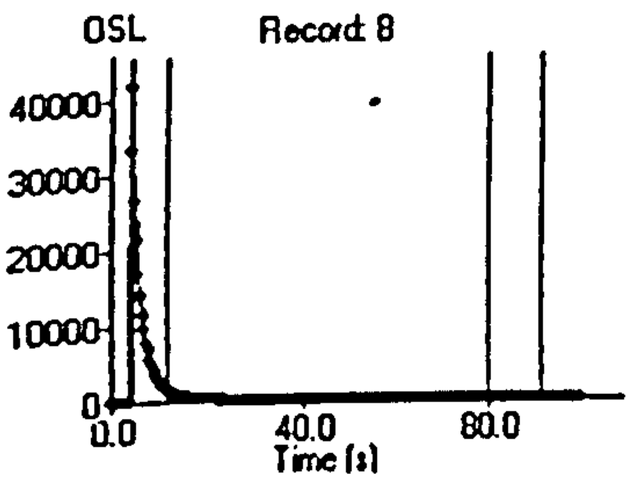

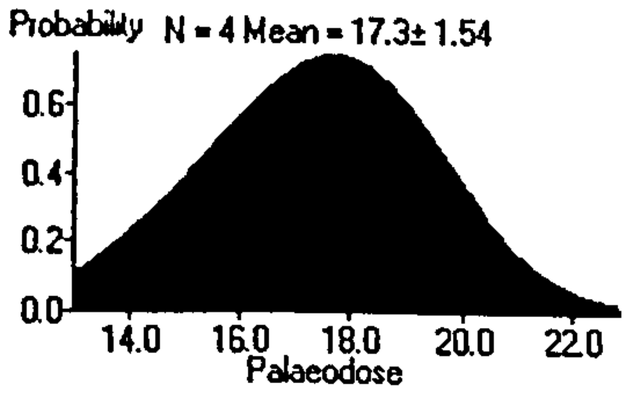

Single Aliquot Analysis

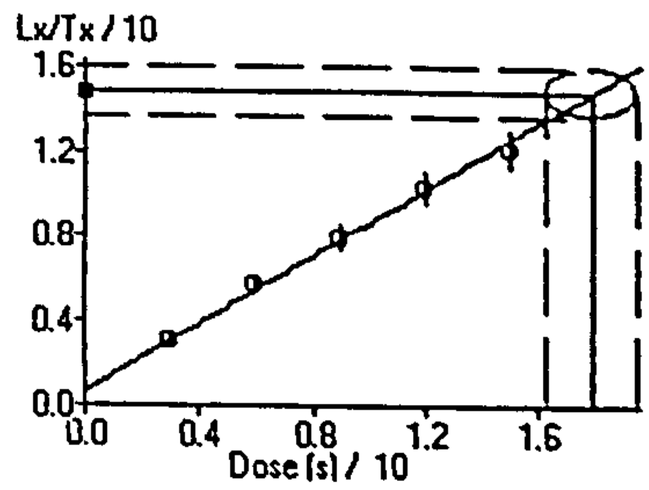

SUTL 1004

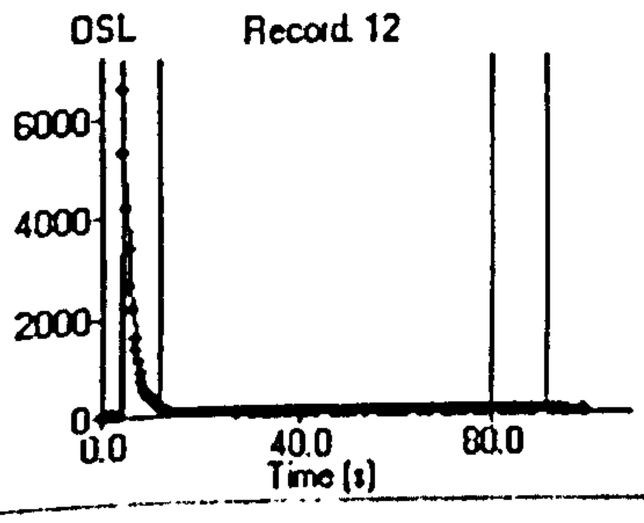

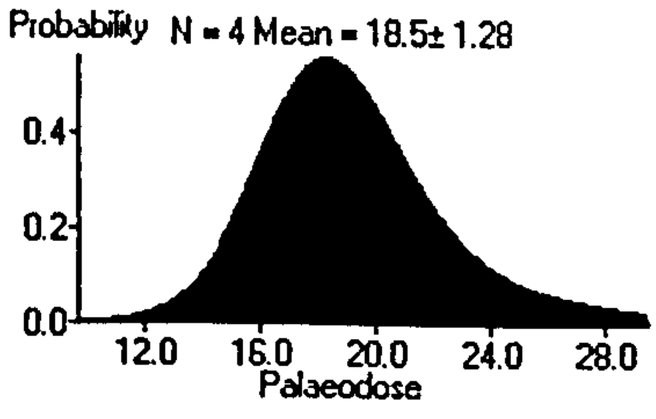

Single Aliquot Analysis

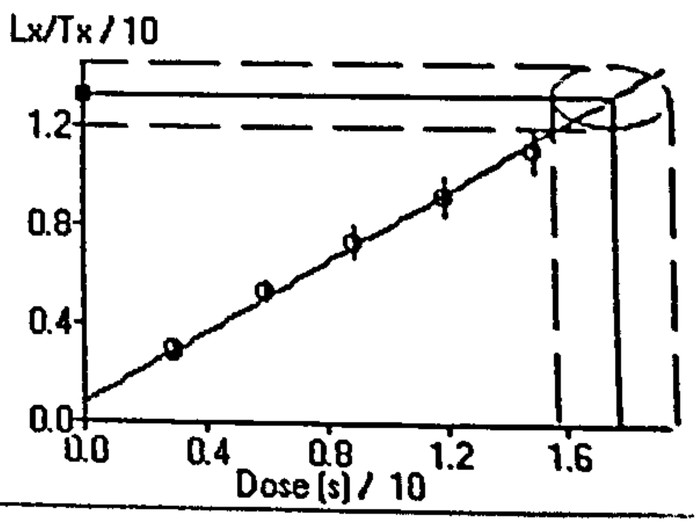

G.8 Loch of Garths

SUTL 1008

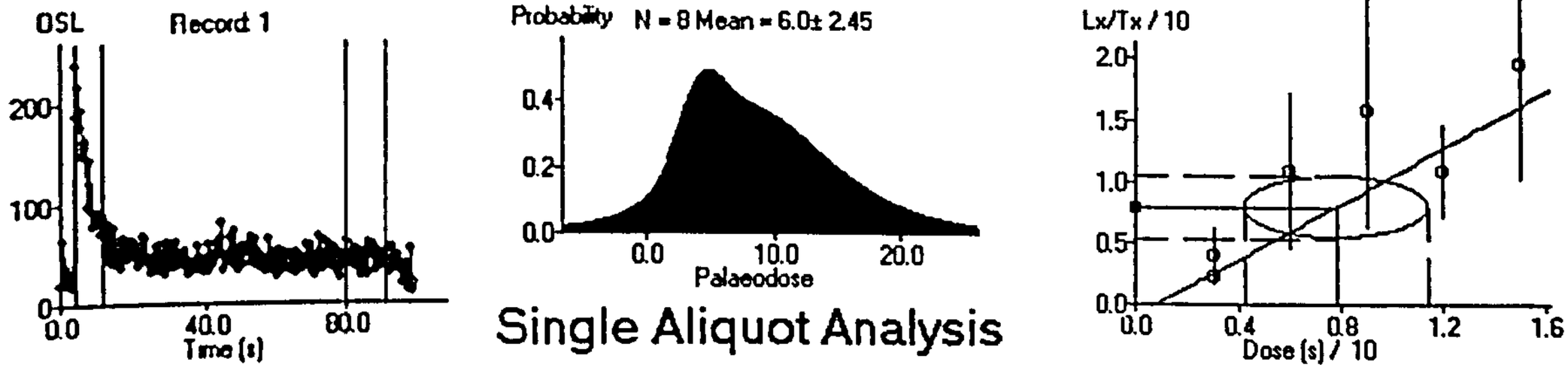

SUTL 1017

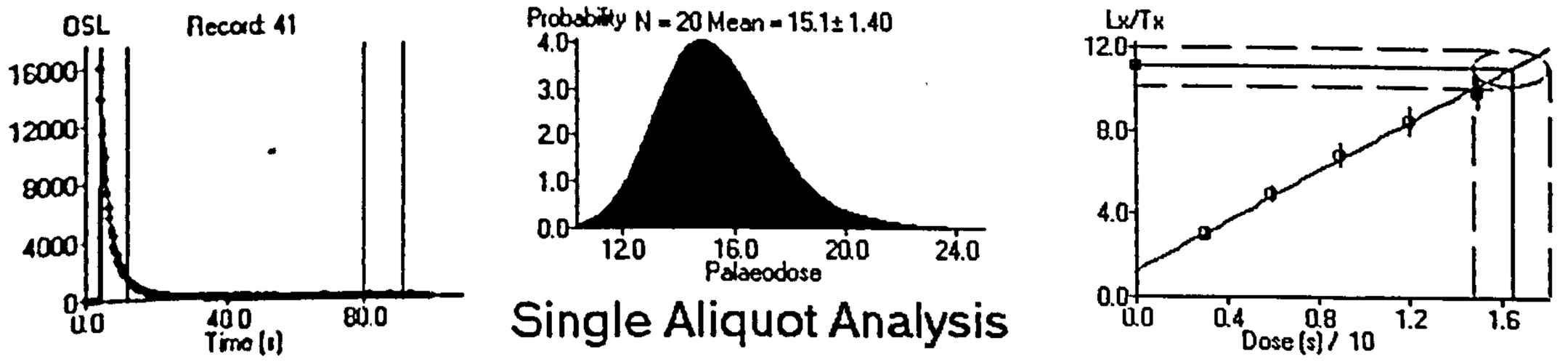

SUTL 1018

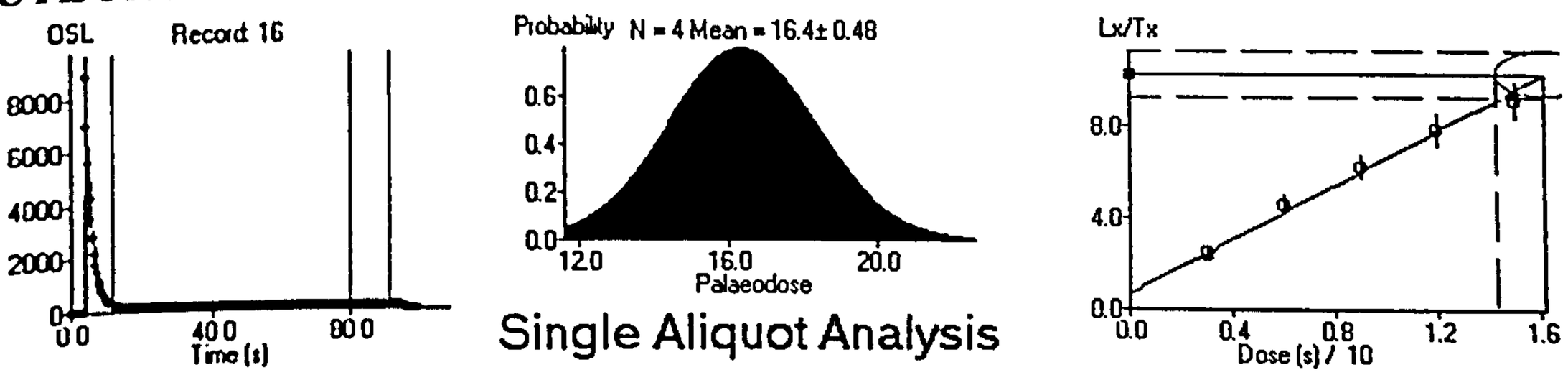

SUTL 1020

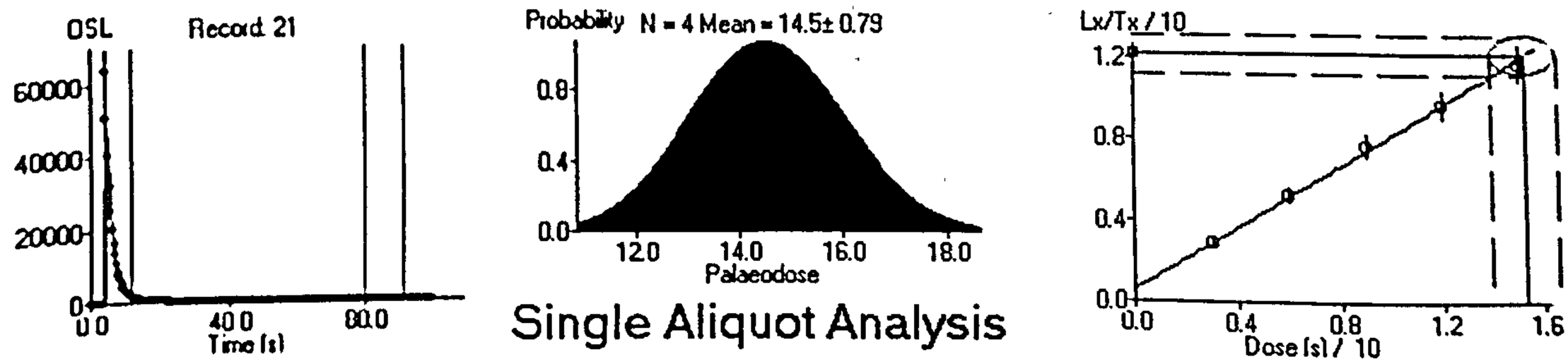

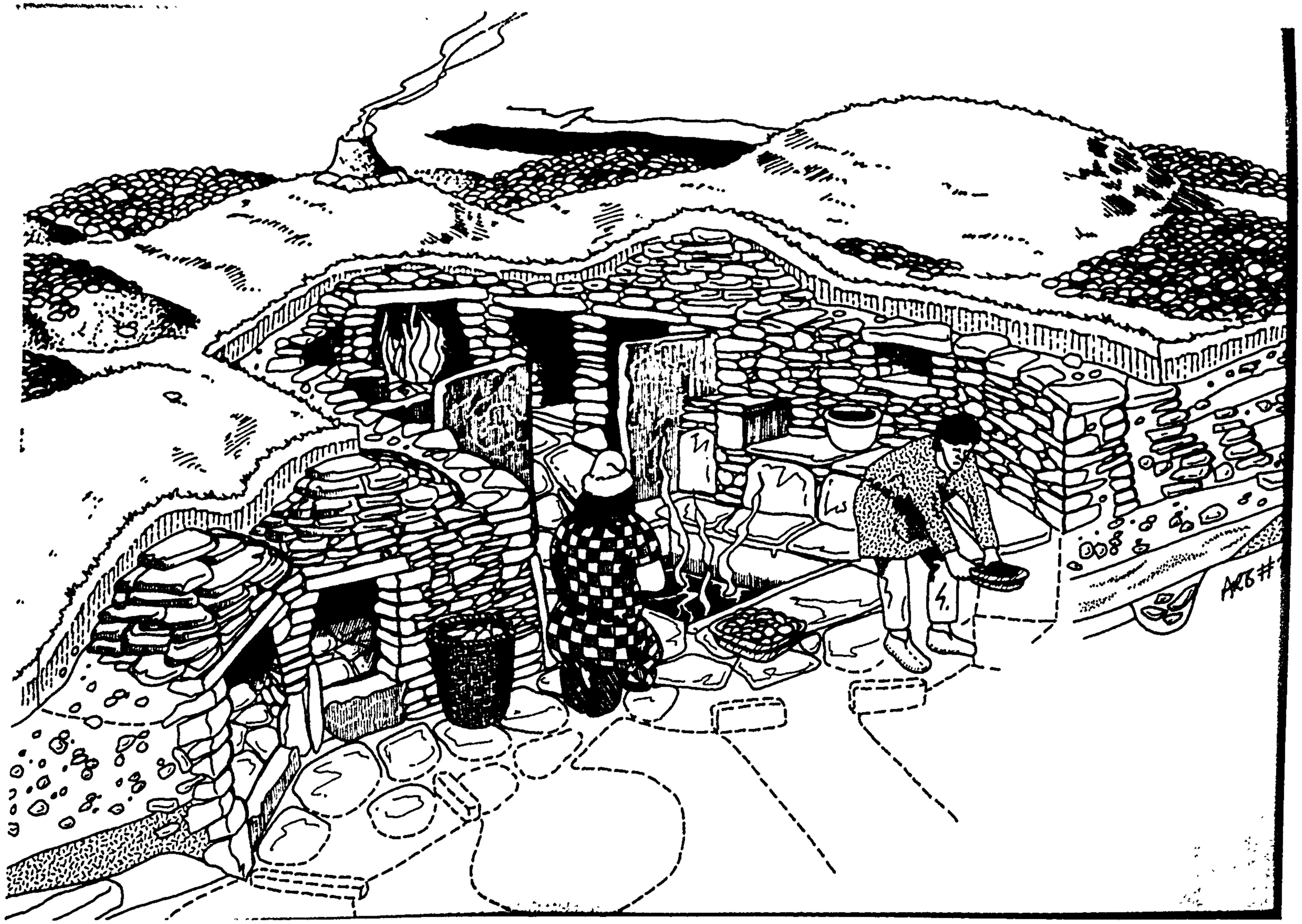

Appendix H: Artists Impression of Cruester Burnt Mound, Bressay
(Reproduced with Kind Permission of Alan Braby, supplied by EASE Archaeology)

APPENDIX I

PHOTOGRAPHIC SITE RECORD

I.1 Dale Burnt Mound
(From Robertson et al, 2000)

COLOUR PHOTOGRAPHS

PHOTOGRAPH No 1: Dale Burnt Mound general view of site facing East

PHOTOGRAPH No 2:
Detail of East half of mound facing South.
Shows mound prior to cleaning back. Note the rabbit damage just right of centre of the exposed section.

PHOTOGRAPH No 3:
Detail of West half of mound facing South.
Shows mound prior to cleaning back. Note the jumble of flags and the stepped edge indicating the level of disturbance.

APPENDIX I

COLOUR PHOTOGRAPHS

PHOTOGRAPH No 4: Dale Burnt Mound East Section, facing South.

PHOTOGRAPH No 5: Detail of East Section, showing peat and nature of stones, facing South.

COLOUR PHOTOGRAPHS

PHOTOGRAPH No 6: Dale Burnt Mound West Sondage, facing South.

PHOTOGRAPH No 7: East facing section of West Sondage, shows slope of sondage due to loose nature of rubble.

I.2 Skaill Burnt Mound

Photograph No. 1: View of Skaill Burnt Mound from East pre-excavation

Photograph No. 2: Skaill Burnt Mound - Main trench after De-turfing, from East

Photograph No. 3: Skaill Burnt Mound - Main trench after removal of upper sand layers →

Photograph No. 4 Skaill Burnt Mound - Composite of North Facing Section

Photograph No. 5 Skaill Burnt Mound - Composite of South Facing Section

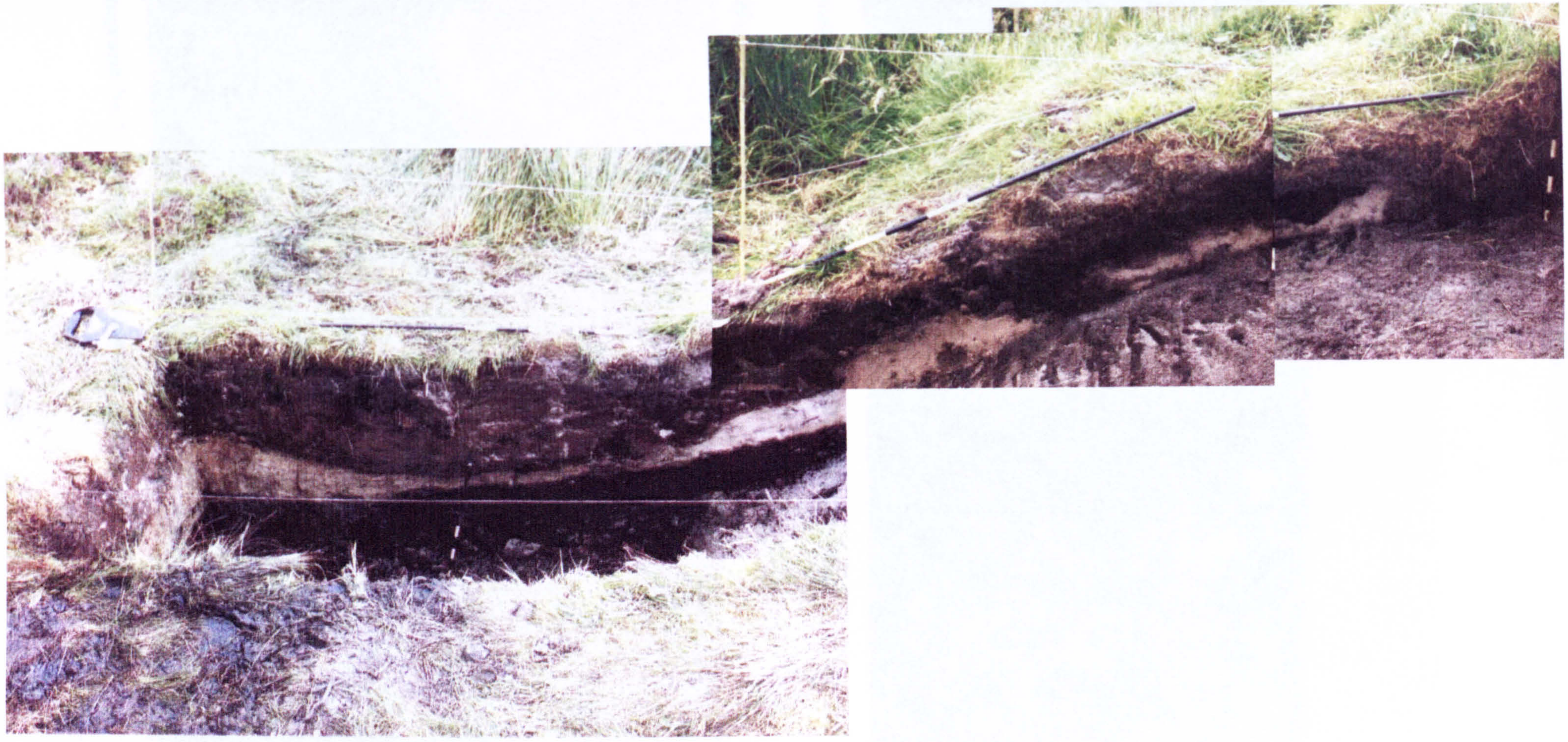

I.3 Knoll of Merrigarth Burnt Mound

Photograph No. 1: Knoll of Merrigarth position 1, from SSE

I.4 Warness Burnt Mound

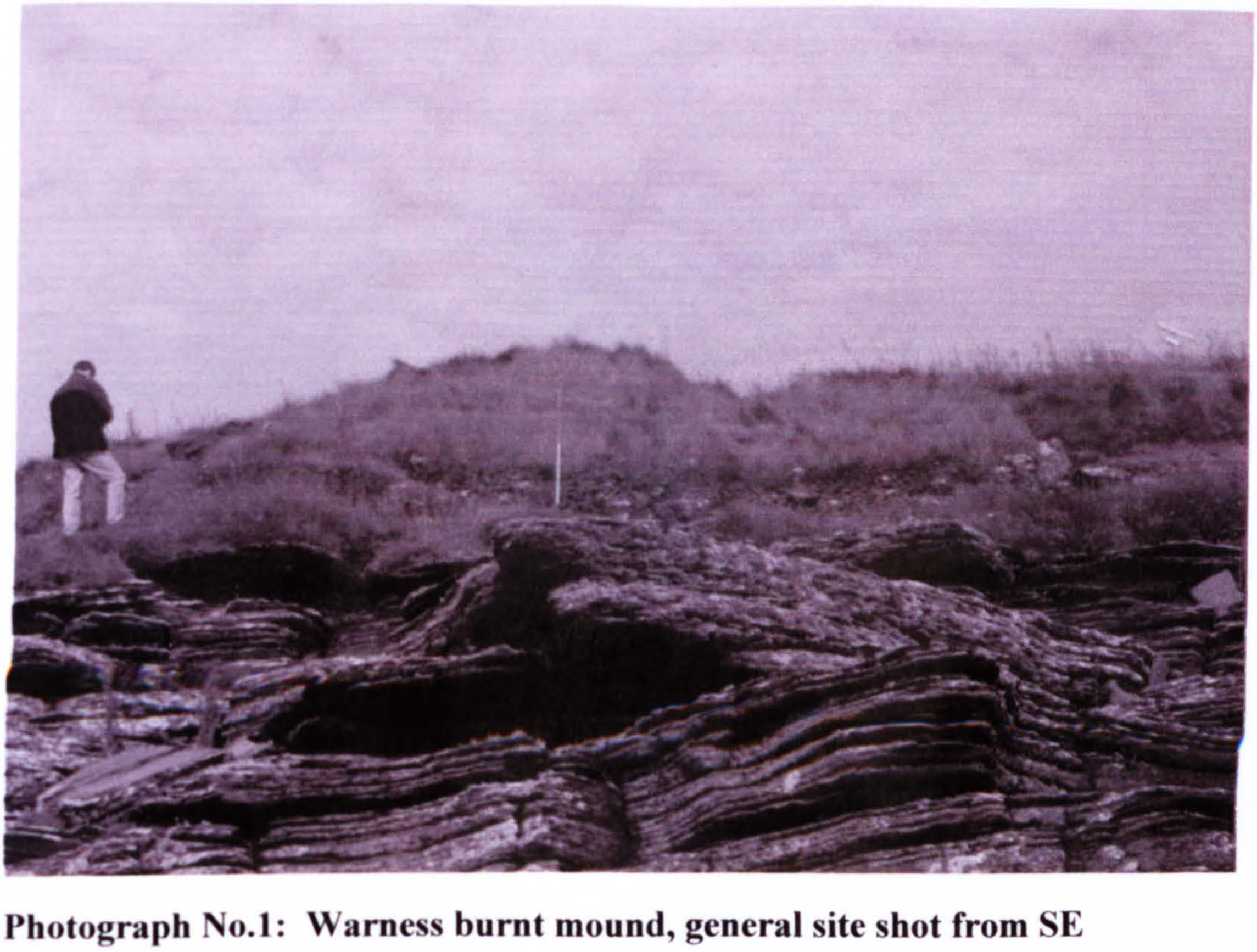

Photograph No.1: Warness burnt mound, general site shot from SE

I.5 Fersness Burnt Mound

Photograph No. 1: Fersness Burnt Mound, Sampling area on small mound, from W

I.6 Stenaquoy Burnt Mound

Photograph No. 1: Stenaquoy burnt mound (under crop) from W

I.7 Cruester Burnt Mound

Photograph No. 1 Overhead view, Cruester burnt mound from S

APPENDIX I

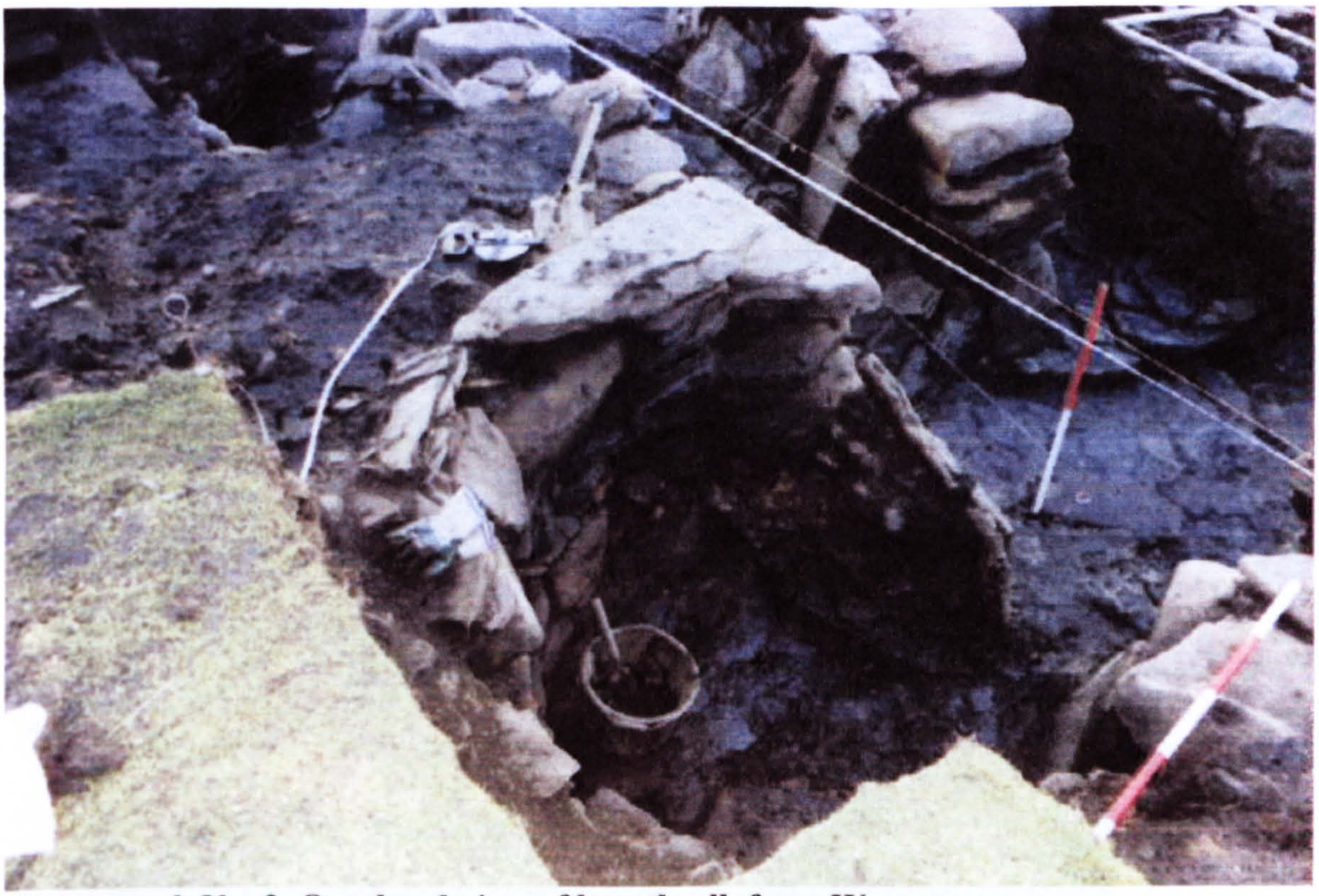

Photograph No. 2 Overhead view of hearthcell, from W

Photograph No. 3 Gamma spectrometry reading (17) at southern edge of cell A

Photograph No. 4 Gamma spectrometry reading (29) at sampling position TL11, above cistern (H) from S

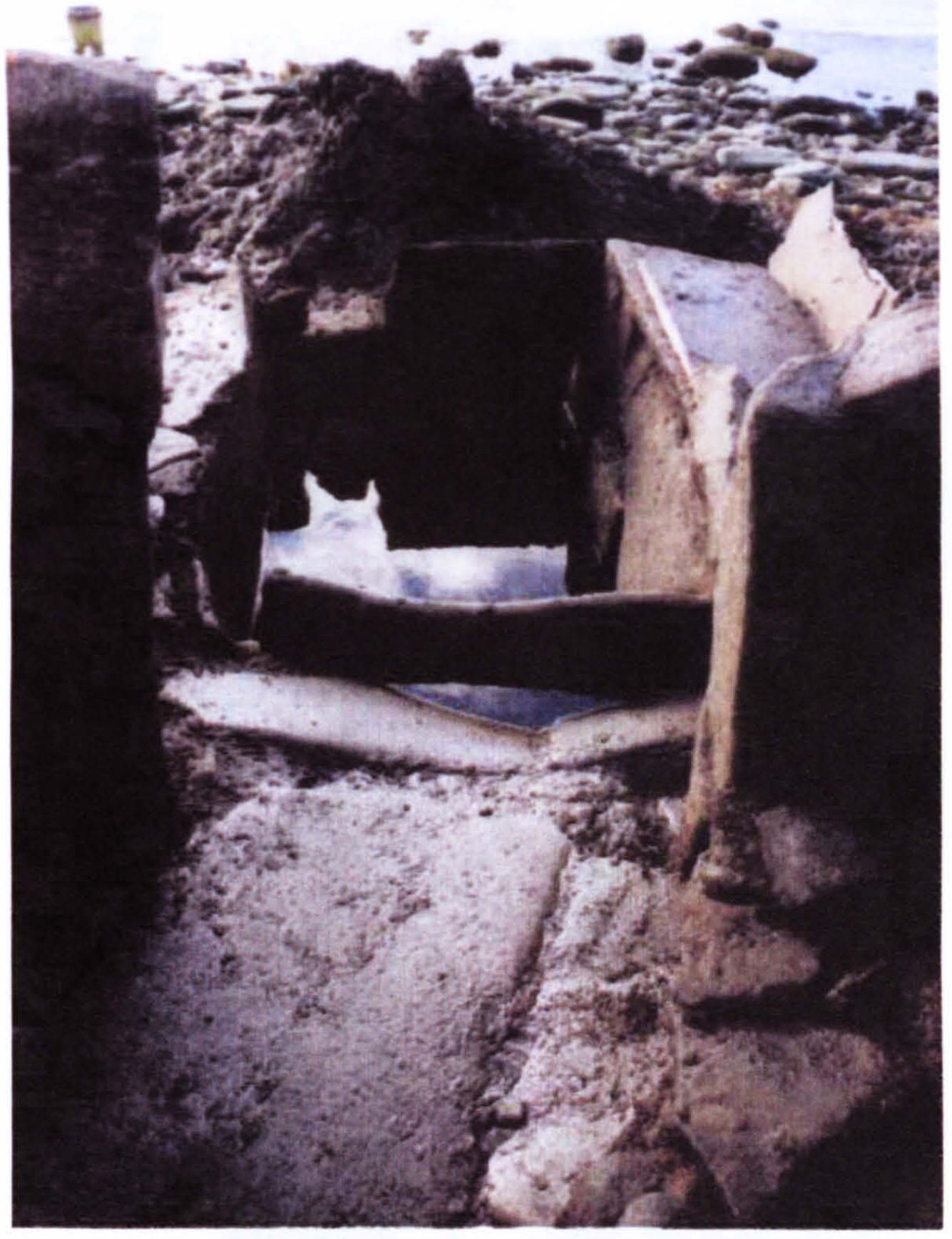

Photograph No. 5 View of tank from N

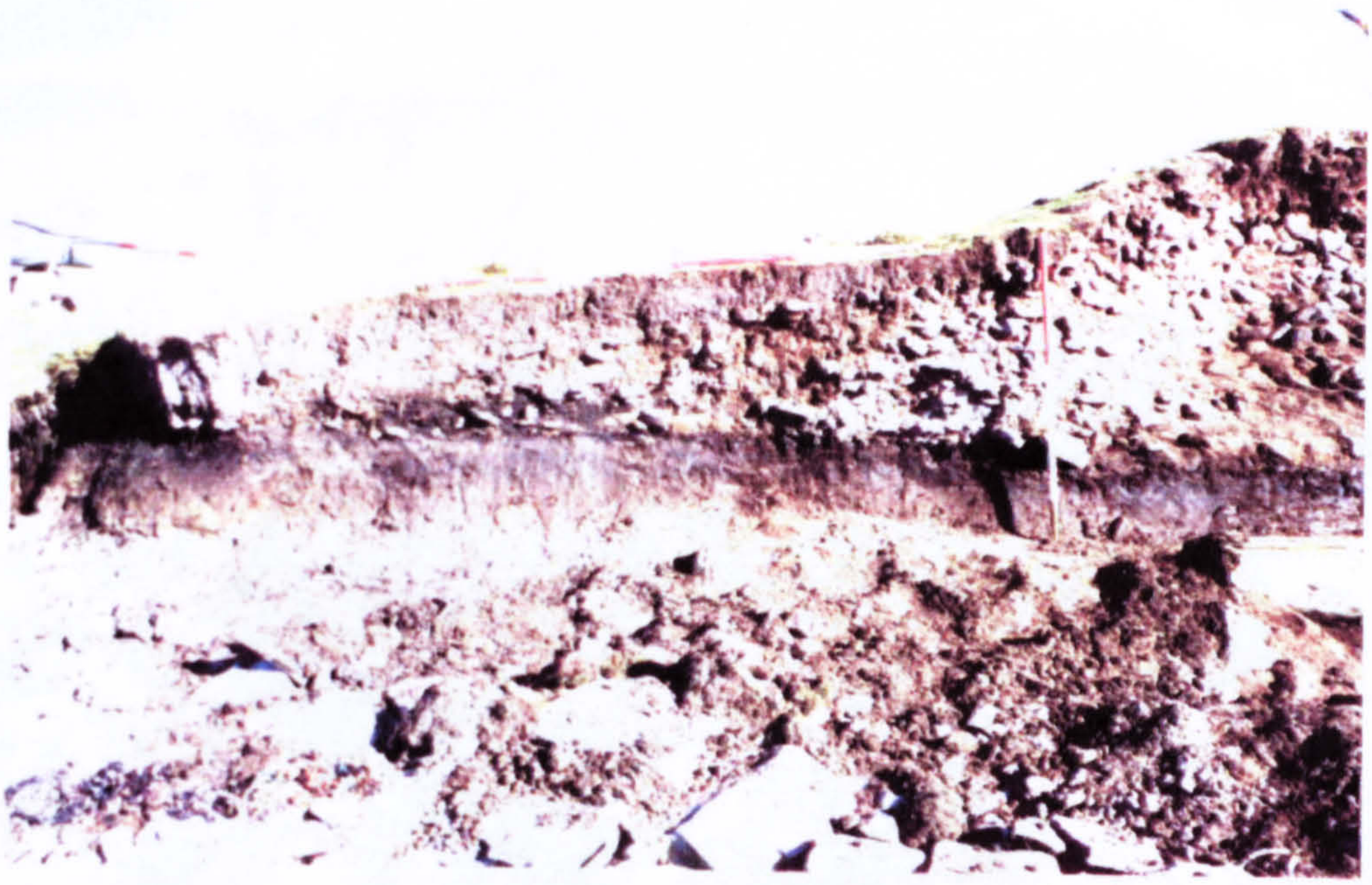

Photograph No. 6 View of coastal mound section from S

I.8 Tangwick burnt mound

Photograph No. 1 View of Tangwick from N

Photograph No. 2 View of Tangwick sampling positions TL1-3

I.9 Houlls burnt mound

Photograph No. 1 View of Houlls from N

Photograph No. 2 View of Houlls coastal section, from SE

I.10 Loch of Garths Burnt Mound

Photograph No. 1 View of Loch of Garths Burnt Mound from S

Photograph No. 2 View of Loch of Garths burnt mound from W

Photograph No. 3 View of Sampling locations TL1-4 during gamma spectrometry measurement, from S